

# Synthesis and Reactivity of Lewis base stabilized pnictogenylboranes



DISSERTATION  
ZUR ERLANGUNG DES  
DOKTORGRADES DER NATURWISSENSCHAFTEN  
(DR. RER. NAT)  
DER FAKULTÄT FÜR CHEMIE UND PHARMAZIE  
DER UNIVERSITÄT REGENSBURG

vorgelegt von  
**Felix Lehnfeld**  
aus Burglengenfeld  
im Jahr 2023



Diese Arbeit wurde angeleitet von Prof. Dr. Manfred Scheer.

Promotionsgesuch eingereicht am: 22. März 2023

Tag der mündlichen Prüfung: 12. Mai 2023

Vorsitzender: Prof. Dr. Rainer Müller

Prüfungsausschuss: Prof. Dr. Manfred Scheer

Prof. Dr. Robert Wolf

Prof. Dr. Frank-Michael Matysik



Universität Regensburg



## Eidesstattliche Erklärung

Ich erkläre hiermit an Eides statt, dass ich die vorliegende Arbeit ohne unzulässige Hilfe Dritter und ohne Benutzung anderer als der angegebenen Hilfsmittel angefertigt habe; die aus anderen Quellen direkt oder indirekt übernommenen Daten und Konzepte sind unter Angabe des Literaturzitats gekennzeichnet.

---

Felix Lehnfeld



This thesis was elaborated within the period from January 2019 until March 2023 in the Institute of Inorganic Chemistry at the University of Regensburg under the supervision of Prof. Dr. Manfred Scheer.

Parts of this work have already been published:

F. Lehnfeld, M. Seidl, A. Y. Timoshkin, M. Scheer, *Eur. J. Inorg. Chem.* **2022**, e202100930.

F. Lehnfeld, O. Hegen, G. Balázs, A. Y. Timoshkin, M. Scheer, *Z. Anorg. Allg. Chem.* **2022**, e202200265.



*“Man merkt nie, was schon getan wurde, man sieht immer nur, was noch zu tun bleibt.”*

**Marie Curie**

*“Je weiter das Experiment von der Theorie entfernt ist, desto näher ist es am Nobelpreis.”*

**Irène Joliot Curie**

*“Wie immer im Leben wollen die Menschen eine einfache Antwort... und es ist immer falsch.”*

**Susan Greenfield**



## **Preface**

Some of the presented results have already been published during the preparation of this work (*vide supra*). The relevant content is reprinted with permission of the respective scientific publisher.

Each chapter includes a list of authors. At the end of each chapter the section “author contributions” is included, describing the individual contribution of each author. Additionally, if some of the presented results have already been partly discussed in other theses, it is stated in the author contributions of the respective chapters.

To ensure a uniform design of this work, all chapters are subdivided into ‘Introduction’, ‘Results and Discussion’, ‘Conclusion’, ‘References’, ‘Supporting Information’ and ‘Author contributions’. Furthermore, all chapters have the same text settings and the compound numeration begins anew. Due to different requirements of the journals and different article types, the presentation of figures for single crystal X-ray structures or the ‘Supporting Information’ may differ. In addition, a general introduction is given at the beginning and a comprehensive conclusion of all chapters is presented at the end of this thesis.



## Table of Contents

1. Introduction .....	15
1.1. Analogy of organic CC-groups/units and group 13/15-compounds: An isovalence-electronic relationship.....	16
1.2. Materials based on group 13/15 compounds: Polymerization and Applications.....	18
1.3. Stabilization and general synthesis of monomers of the type $[R_2EE'R'_2]$ .....	20
1.4. Synthesis and Reactivity of Lewis Base Stabilized Pnictogenyltrielanes.....	21
1.5. References .....	25
2. Coordination chemistry of pnictogenylboranes towards group 6 transition metal Lewis acids .....	29
2.1. Introduction.....	30
2.2. Results and Discussion .....	31
2.3. Conclusions.....	38
2.4. Experimental Section.....	39
2.5. References .....	44
2.6. Supporting Information .....	47
2.7. Author contributions.....	84
3. Synthesis and Reactivity of a Lewis-Base-Stabilized Tert-Butyl Arsanylborane: A Versatile Building Block for Arsenic-Boron Oligomers .....	85
3.1. Introduction.....	86
3.2. Results and Discussion .....	88
3.3. Conclusion.....	97
3.4. Experimental Section.....	97
3.5. References .....	101
3.6. Supporting information .....	105
3.7. Author contributions.....	137
4. On the brink of decomposition: Controlled oxidation of a substituted arsanylborane as a way to labile group 13-15-16 compounds.....	139
4.1. Introduction.....	140
4.2. Results and Discussion .....	141
4.3. Conclusion.....	151
4.4. References .....	151
4.5. Supporting Information .....	156
4.6. Author contributions.....	182

5. Mono alkyl substituted phosphanylboranes (HRP–BH <sub>2</sub> –NMe <sub>3</sub> ) as precursors for poly(alkylphosphinoborane)s: improved synthesis and comparative study .....	183
5.1. Introduction.....	184
5.2. Results and Discussion .....	185
5.3. Conclusion.....	194
5.4. References .....	194
5.5. Supporting information .....	197
5.6. Author contributions.....	221
6. Thesis treasury: Oxidation of a parent arsanylborane as a route to novel mixed main group element compounds .....	223
6.1. Introduction.....	223
6.2. Results and Discussion .....	223
6.3. Experimental section .....	228
6.4. References .....	234
6.5. Author contributions.....	236
7. Conclusion .....	237
7.1. Coordination of pnictogenylboranes towards group 6 Lewis acids .....	237
7.2. Synthesis and reactivity of an alkylsubstituted arsanylborane.....	238
7.3. Controlled oxidation of tBuAsHBH <sub>2</sub> NMe <sub>3</sub> .....	240
7.4. Improved synthesis of alkylsubstituted phosphanylboranes as starting material for poly(alkylphosphinoborane)s.....	242
8. Appendices .....	243
8.1. Alphabetic List of Abbreviations .....	243
8.2. Acknowledgments .....	245

## 1. Introduction

The chemistry of binary group 13/15 compounds goes back over two centuries, when *Gay-Lussac* first reported the ammonia-borane adduct  $\text{H}_3\text{N}\cdot\text{BF}_3$ .<sup>[1]</sup> Since then, a great variety of similar adducts (Fig. 1, I,  $\text{E}' =$  group 13 element,  $\text{E} =$  group 15 element) has been investigated and reported, such as the first ever phosphine-borane adduct by *Besson* in 1890<sup>[2]</sup> and the parent ammonia-borane  $\text{H}_3\text{N}\cdot\text{BH}_3$  by *Shore* and *Perry* in 1955.<sup>[3]</sup> While there is a general high importance of this kind of compounds in material sciences as reflected by numerous publications and review articles,<sup>[4]</sup> especially  $\text{H}_3\text{N}\cdot\text{BH}_3$  has recently received disproportionately more attention mainly due to its potential as hydrogen storage material.<sup>[5]</sup>

Besides simple binary adducts, a broad variety of more complex group 13/15 compounds have been investigated. The reported structural motifs range from hyperconjugated adducts containing a five-coordinate group 13 element center (Fig. 1, II) to heterocyclic and cage-like organometallic group 13/15 compounds (Fig. 1, IV-VII).<sup>[6]</sup>

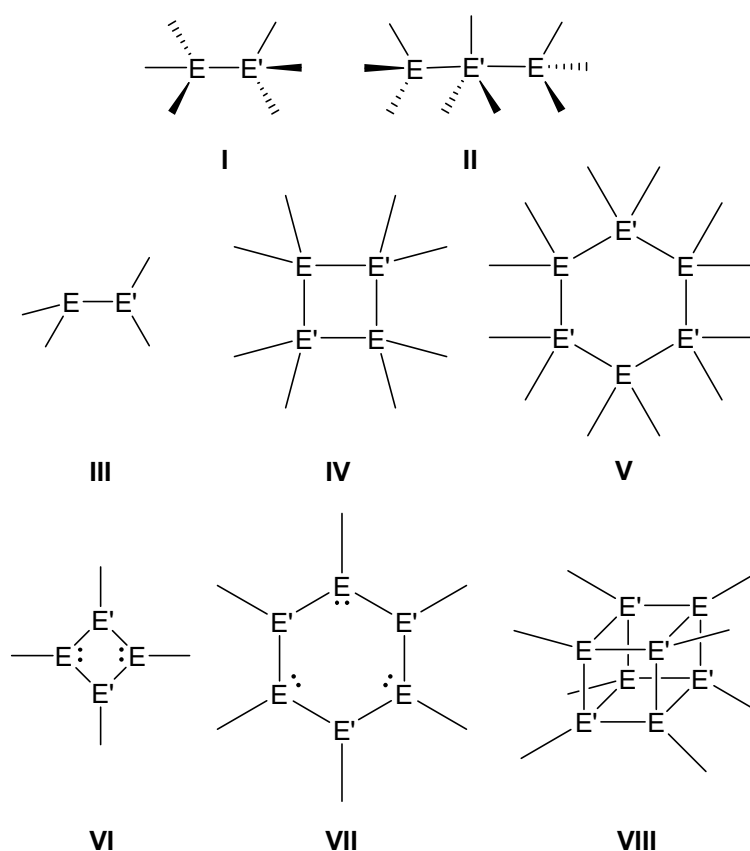


**Figure 1.** Examples for different structural motifs of group 13/15 compounds

## 1.1. Analogy of organic CC-groups/units and group 13/15-compounds: An isovalence-electronic relationship

The combination of a group 13 and a group 15 element is isovalence electronic to two group 14 elements such as two carbon atoms, as both possess eight valence electrons. This isovalence electronic relationship can be observed for multiple examples for structural motifs of group 13/15 compounds similar to hydrocarbons and other organic compounds. As this relationship is most prominently described for boron-nitrogen compounds, they will be used as examples in the following (Fig. 2).<sup>[7]</sup>

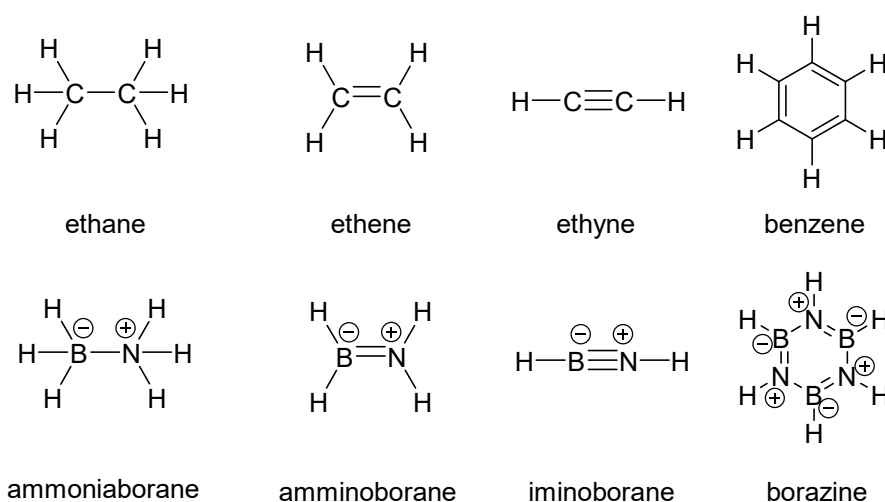


**Figure 2.** Structural and electronic analogy of compounds containing BN- and CC- units.

Applying this analogy, e.g. B-N compounds are essentially isostructural to the corresponding C-C compounds. In all examples, the same structural conformation is observed with only slightly elongated B-N bond lengths compared to the respective C-C compound ( $\Delta r \sim 0.04 \text{ \AA}$ ). However, as similar as the structural properties are, there is a large difference in electronegativities, leading to the B-N compounds exhibiting polar bonds. According to calculations, most of the electron density is localized on the nitrogen atom, leading to a strongly polarized dative bond.<sup>[8]</sup> Despite the isoelectronic and isolobal relationship between B-N compounds and organic compounds, they reveal some important differences in their properties and reactivity due to this very polarization. These differences can be observed, for example, by means of the state of matter of these compounds: Whereas ethane is gaseous at ambient conditions, the corresponding saturated B-N compound, the ammonia borane adduct  $\text{BH}_3\text{-NH}_3$ , is a solid under these conditions.<sup>[7]</sup>

Another example for this analogy is boron-nitride,  $(\text{BN})_x$ , which exists in three different modifications, all structural analogues of carbon modifications.<sup>[7]</sup> The hexagonal  $\alpha$ - $(\text{BN})_x$  is related to graphite, consisting of layers built up by six membered B-N-rings. However, comparing the arrangement of these layers reveals an important difference: Whereas the layers in graphite are shifted, the ones in  $\alpha$ - $(\text{BN})_x$  are stacked eclipsing with alternating B-N atoms. Some properties differ only slightly with e.g.  $\alpha$ - $(\text{BN})_x$  being inflammable and therefore being used as high-temperature lubricant or coating for high-temperature applications analogous to graphite, but there are also important differences:  $\alpha$ - $(\text{BN})_x$  is white and nonconductive, as no delocalization of electrons takes place, in contrast to the dark grey electrical conductor that is graphite.  $\beta$ - $(\text{BN})_x$  has a diamond lattice and is, like actual diamond, one of the hardest known materials. The third modification  $\chi$ - $(\text{BN})_x$  exhibits a hexagonal Wurzit structure and has no common applications. Borazine ( $\text{B}_3\text{N}_3\text{H}_6$ ),<sup>[9]</sup> often referred to as inorganic benzene due to its similarities, is a colorless liquid with aromatic smell at ambient conditions. Nevertheless, the chemical properties differ significantly from its organic counterpart, as it exhibits only weak aromaticity. Therefore, it is much more prone to hydrolysis and addition reactions than its carbon analogue. Furthermore, its coordination behavior towards metal centers differs, with the preferred coordination mode being  $\eta^3$  by rearranging of the planar ring to a chair like conformation in contrast to the  $\eta^6$  complexes usually observed for benzene.

When considering the group 13/15 analogues of unsaturated compounds like ethene, an interesting difference is that in these compounds of the type  $[\text{R}_2\text{E}-\text{E}'\text{R}'_2]$  (E = group 15 element; E' = group 13 element; R, R' = H or small organic substituent, Fig 1, III) the group 15 element possesses a lone pair, whereas the group 13 element has a vacant p-orbital. In contrast to their organic analogue, which is stable under ambient conditions, this type of group 13/15 compounds undergoes rapid head-to-tail oligo- or polymerization. This can be prevented by offering additional stabilization through bulky substituents<sup>[10]</sup> or stabilization via Lewis acids and/or bases,<sup>[11]</sup> which will be discussed in more detail in a later chapter.

## 1.2. Materials based on group 13/15 compounds: Polymerization and Applications

As already stated at the beginning of the introduction, materials consisting of group 13/15 elements are used in a broad field of applications.<sup>[12]</sup> For example, GaAs has several industrial applications such as in opto- and microelectronic devices due to its semiconducting properties. Such materials, often referred to as III-V materials, are usually obtained via the MOCVD (**M**etal**O**rganic **C**hemical **V**apor **D**eposition) process, which was first introduced by *Manasevit* in 1968.<sup>[13]</sup>

Furthermore, the aforementioned hydrogen storage potential of  $\text{NH}_3 \cdot \text{BH}_3$  due to its high hydrogen content is of great scientific interest.<sup>[5]</sup> Therefore, especially the dehydrogenation and dehydrocoupling reactions of binary group 13/15 adducts are heavily researched. The first dehydrocoupling reaction of amine-boranes was mentioned in 1989,<sup>[14]</sup> but it was not until 1999 for the first detailed study of a transition metal catalyzed reaction to be reported by *Manners et al.*<sup>[15]</sup> Applying the Rh(I) based catalysts  $[\text{Rh}(1,5\text{-cod})_2][\text{OTf}]$  and  $[\text{Rh}(1,5\text{-cod})(\mu\text{-Cl})_2]$  (1,5-cod = cycloocta-1,5-diene), the dimerization of the aryl-substituted group 13/15 adduct  $\text{Ph}_2\text{HP} \cdot \text{BH}_3$  was achieved. Further studies revealed Rh(I) and Rh(III) based catalysts to be also very well suited for the dehydrocoupling of amine-boranes.<sup>[16]</sup> The formed products of dehydrocoupling reactions are heavily dependent on the substitution pattern at the pnictogen atom. While secondary amine-boranes tend to form cyclic dimers (Fig. 3, **A**), primary amine-boranes initially form cyclotriborazanes, which upon heating are transformed into borazines under the release of  $\text{H}_2$  (Fig 3, **B**). With two bulky substituents on the nitrogen atom of a secondary amine-borane, also the monomeric aminoborane can be obtained (Fig 3, **C**).

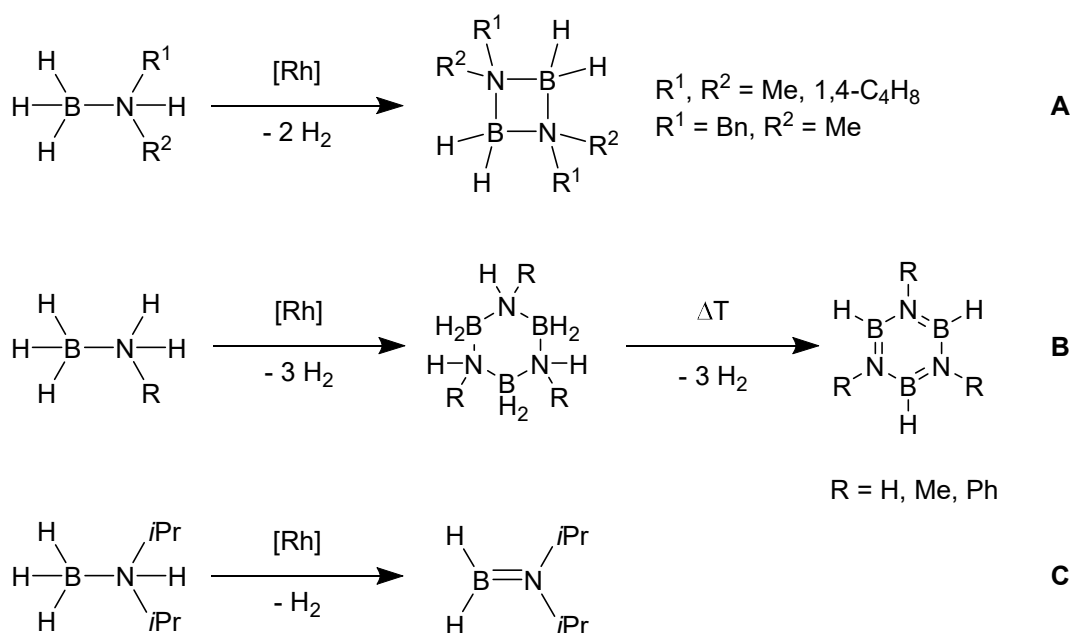


**Figure 3.** Dehydrocoupling of primary and secondary amine-boranes, formal charges omitted for clarity

Since then, not only the rhodium catalysts have been thoroughly investigated, but also various alternative catalysts for dehydrocoupling reactions of group 13/15 adducts have been reported.<sup>[17]</sup> Notable examples include iridium based catalysts such as Brookhart's catalyst [IrH<sub>2</sub>(POCP)] (POCOP = [μ<sub>3</sub>-1,3-(OP*t*Bu)<sub>2</sub>C<sub>6</sub>H<sub>3</sub>])<sup>[17c, 18]</sup> and the use of catalysts based on earth abundant Fe under molecular weight control.<sup>[19]</sup> Furthermore, also the use of catalysts based on early transition metals such as *in situ* generated Cp<sub>2</sub>Ti or its heavier homologue Zr have been reported,<sup>[20]</sup> leading to the formation of the same products as reported for Rh(I) catalysts. However, Ti-based precatalysts were reported to reveal far higher catalytic activity than their Zr derivatives. The application of group 6 metal catalysts as another example of early transition metal catalyzed dehydrocoupling reactions has been reported.<sup>[21]</sup> Overall, even high molecular weight polymers have been reported by the application of transition metal based catalysts in the recent past. However, to avoid transition metals as catalysts in these reactions, also main group catalyzed dehydrocoupling reactions are investigated. The polymerization of *in situ* generated PH<sub>3</sub>·BH<sub>3</sub> was achieved by catalysis with the main group Lewis acid B(C<sub>6</sub>F<sub>5</sub>)<sub>3</sub> by *Denis* and *Gaumont*.<sup>[22]</sup> Very recently, advances on the application of magnesium-based catalysts for dehydrogenation reactions of group 13/15 compounds have been reported.<sup>[23]</sup>

Insights into the P-B bond formation process during the d-block element catalyzed oligo- and polymerization were obtained by recent studies on the coordination

chemistry of phosphine-borane ligands to transition metal centers.<sup>[24]</sup> The P-H group was revealed to play two important roles: Whereas the activation by the metal centers leads to the formation of metal-phosphidoborane intermediate, the dehydrogenative P-B coupling is promoted by the release of hydrogen through the combination of a protic P-H and a hydridic B-H moiety. However, electron withdrawing substituents such as aryl groups are necessary for the reaction to take place in most cases due to the almost non-polar nature of the P-H bond ( $E_N$ : P = 2.19, H = 2.20).<sup>[25]</sup> This results in a rather limited scope of potential substrates, with only few examples of poly(alkylphosphinoborane)s accessible via dehydrogenative coupling of group 13/15 adducts.<sup>[26]</sup> Additionally, all these examples only report moderate molecular masses and polymers with high polydispersity indices due to significant amounts of uncontrollable branching and crosslinking.

### 1.3. Stabilization and general synthesis of monomers of the type $[R_2EE'R'_2]$

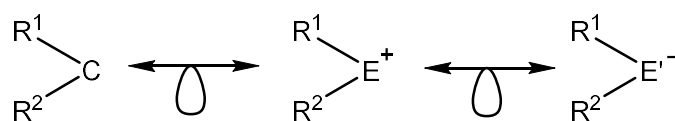


**Figure 4.** Isolobal relationship between  $CR_2$  fragments with cationic  $ER_2$  and anionic  $E'R_2$  fragments ( $E$  = group 15 element,  $E'$  = group 13 element)

Considering the isolobal relationship between  $CR_2$  fragments with cationic  $ER_2$  and anionic  $E'R_2$  fragments ( $E$  = group 15 element,  $E'$  = group 13 element, Fig. 4)<sup>[27]</sup>, pnictogenyltrielane monomers of the type  $[R_2E-E'R'_2]$  can be described. As elucidated in an earlier chapter, they are analogues to unsaturated carbon compounds. However, instead of a double bond, a localized lone pair on the group 15 element is observed, whereas the group 13 element has a vacant p-orbital. Therefore, they are not only prone to rapid head-to-tail-polymerization, but also reveal a vast reactivity deviating from the one established for alkenes. To access this reactivity, stabilization of the otherwise very fragile monomers is necessary, which can be achieved by bulky substituents as in  $Ph_2P-BMes_2$ <sup>[10]</sup> or by Lewis acid/base interactions. Without stabilization, an only hydrogen substituted monomer has only been characterized under cryogenic conditions at liquid nitrogen temperature in the case of  $H_2NBH_2$ ,<sup>[28]</sup> while the heavier homologue  $PH_2BH_2$ <sup>[29]</sup> was only studied computationally so far.

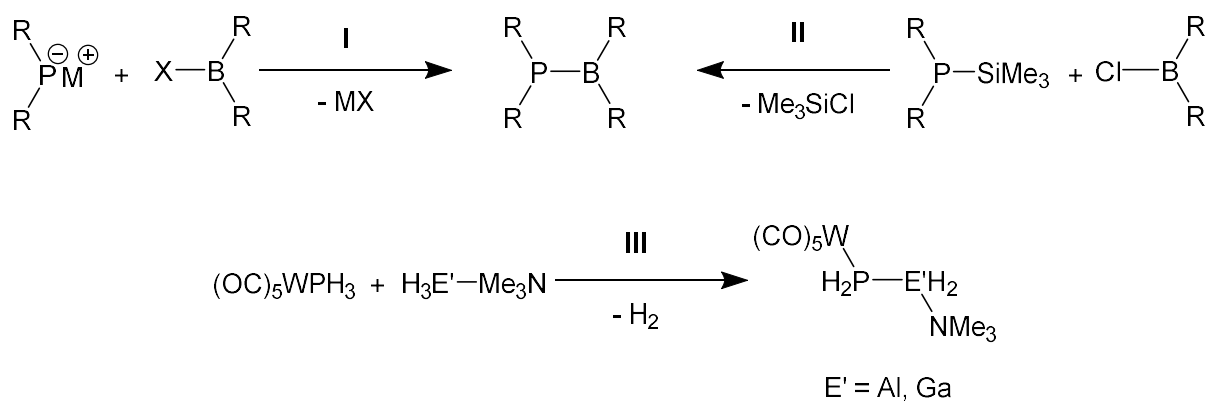


**Figure 5.** Different synthetic pathways to pnictogenyltrielanes

In the case of pnictogenylboranes, the most common synthesis is via salt metathesis starting from halogen boranes of the type  $\text{XBR}_2$  ( $\text{X} = \text{halogen}$ ) and metal pnictogenides  $\text{MER}'_2$  (Fig. 5, I)<sup>[30]</sup> or by the elimination of  $\text{Me}_3\text{SiCl}$  (Fig. 5, II).<sup>[31]</sup> Other, less frequently used synthetic procedures include the reaction of a B-centered nucleophile with a chlorophosphine,<sup>[32]</sup> Pd-based P-B cross-coupling reactions<sup>[33]</sup> and reductive coupling under 1,2-aryl migration.<sup>[34]</sup> For heavier group 13 elements also the formation of E-E' bonds under elimination of small molecules such as  $\text{H}_2$  has been reported (Fig 6. III).<sup>[35]</sup>

#### 1.4. Synthesis and Reactivity of Lewis Base Stabilized Pnictogenyltrielanes

Starting with the synthesis of the LA/LB stabilized phosphanylalanes and -galanes  $(\text{OC})_5\text{W}-\text{PH}_2\text{E}'\text{H}_2-\text{NMe}_3$  ( $\text{E}' = \text{Al, Ga}$ ) in 2001,<sup>[35]</sup> our group has had great success in the synthesis of various pnictogenyltrielanes. Some years later, the synthesis of the monomeric parent phosphanyl- and arsanylboranes  $(\text{OC})_5\text{W}-\text{EH}_2\text{BH}_2-\text{NMe}_3$  ( $\text{E} = \text{P, As}$ , Fig. 6, I) could be achieved by the salt metathesis of  $[(\text{OC})_5\text{W}-\text{EH}_2\text{Li}]$  and  $\text{ClH}_2\text{BNMe}_3$ .<sup>[36]</sup> The isolation of the first only LB stabilized pnictogenylborane was achieved by the photolysis of  $(\text{OC})_5\text{W}-\text{EH}_2\text{BH}_2-\text{NMe}_3$  in the presence of  $\text{P}(\text{OMe})_3$  (Fig. 6, II) in 2006.<sup>[37]</sup> Over the next almost two decades, a wide range of different compounds, both parent only hydrogen substituted pnictogenyltrielanes as well as several substituted derivatives, have been reported. Notable examples include the parent arsanylborane,<sup>[38]</sup> the substituted phosphanylboranes  $t\text{BuPHBH}_2\text{NMe}_3$  and  $\text{Ph}_2\text{PBH}_2\text{NMe}_3$ <sup>[39]</sup> and the NHC stabilized parent stibanylborane  $\text{SbH}_2\text{BH}_2\text{Ime}$  (Fig. 6, II-V,  $\text{Ime} = 1,3,4,5\text{-Tetramethylimidazol-2-yliden}$ ).<sup>[40]</sup>

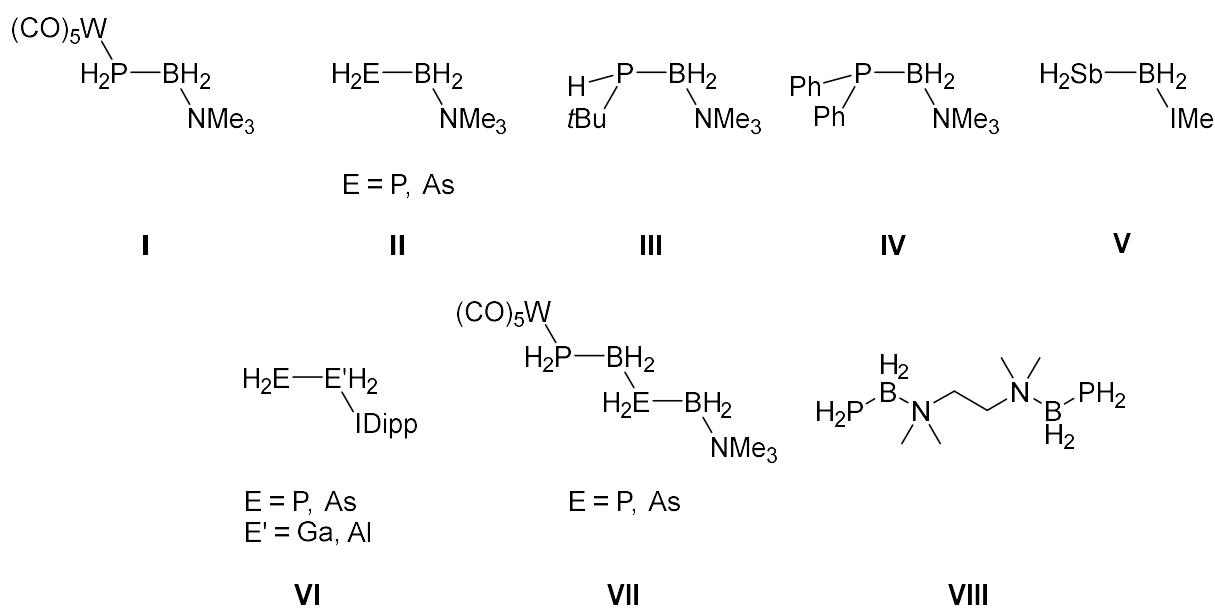


**Figure 6.** Selected examples of pnictogenyltrielanes

Recently, advances on the field of only Lewis base stabilized pnictogenyltrielanes with heavier group 13 atoms have been reported by the application of a bulky NHC as Lewis base, such as the isolation of the only hydrogen substituted  $\text{EH}_2\text{E}'\text{H}_2\text{IDipp}$  ( $\text{E} = \text{P}, \text{As}$ ;  $\text{E}' = \text{Ga}, \text{Al}$ , Fig. 6, **VI**,  $\text{IDipp} = 1,3\text{-Bis}(2,6\text{-diisopropylphenyl})\text{imidazolin-2-yliden}$ ).<sup>[41]</sup> By applying both Lewis acid and Lewis base stabilization it was possible to obtain longer chained mixed pnictogenylboranes of the type  $(\text{OC})_5\text{W}-\text{PH}_2\text{BH}_2-\text{ER}_2\text{BH}_2-\text{LB}$  (Fig. 6, **VII**).<sup>[42]</sup> Bidentate pnictogenylboranes are accessible by stabilization with Lewis bases such as *tmeda* (= tetramethylethylenediamine, Fig. 6, **VIII**).<sup>[43]</sup>

The reactivity of pnictogenyltrielanes was thoroughly investigated over the last years. As the lone pair on the pnictogen atom is available for further reactions, Lewis basic reactivity related to phosphines or arsines has been observed for phosphanyl- and arsanylboranes. Examples for such reactions include the coordination towards either main group Lewis acids like  $\text{BH}_3\text{SMe}_2$  (Fig. 7, **I**) or transition metal Lewis acids such as  $[\text{Fe}(\text{CO})_4]$ .<sup>[37-38,44]</sup> In the context of transition metal chemistry of the parent phosphanylborane also the formation of P-P bridged oligomers with  $[\text{Cp}_2\text{Ti}(\text{btmsa})]$  (*btmsa* = bis(trimethylsilyl)acetylene) has been reported.<sup>[45]</sup> Recently, the formation of luminescent complexes by the coordination of pnictogenylboranes ( $\text{E} = \text{P}, \text{As}$ ) towards Au centers<sup>[46]</sup> and TI-mediated P-P couplings in phosphanylboranes have been reported.<sup>[47]</sup>

By reaction with halogenated group 13 compounds cationic three- and five-membered chain like compounds can be obtained (Fig. 7, **II**).<sup>[37,44b,48]</sup> Similar anionic

chains can be synthesized in the reaction of pnictogenylboranes with phosphanides and arsanides (Fig. 7, **III**).<sup>[49]</sup> They have recently been shown to be good anionic ligands capable of bridging transition metal centers.<sup>[50]</sup> Due to their more fragile nature, the heavier congeners reveal less controllable reactivity therefore no follow up chemistry could be reported so far. However, current results show, that it is possible to include heavier group 14 elements and thereby synthesize novel, cationic group 13/14/15 chains.<sup>[51]</sup> Another way to incorporate different main group elements in the chemistry of pnictogenylboranes is the controlled oxidation with chalcogens or chalcogen reagents like TMSO (TMSO = trimethylsilylperoxide), which can be widely accessed for the phosphorus derivatives (Fig. 7, **IV**).<sup>[37, 52]</sup> However, in the case of arsanylboranes, the number of reported compounds is limited due to the significantly weaker As-B bond compared to the P-B bond.<sup>[44b]</sup> Furthermore, pnictogenylboranes offer an alternative pathway to poly(phosphinoborane)s: By thermal treatment of  $RR'PBH_2NMe_3$  ( $R, R' = H, Me, tBu, Ph$ ) the stabilizing Lewis base can be eliminated and therefore head-to-tail polymerization is induced (Fig 7. **V**).<sup>[39]</sup> Depending on the conditions and the substituents, oligomeric species or even high molecular weight polymers can be obtained. Especially the mild thermolysis of  $tBuPHBH_2NMe_3$  at 40 °C leads to the formation of a high molecular weight polymer  $[tBuPHBH_2]_n$  with a molar mass of up to 35000 g/mol. This represents the rare example of a poly(alkylphosphinoborane), which are difficult to obtain via traditional dehydrocoupling reactions. Due to the aforementioned lability of the E-E' bond in the heavier homologues, such thermal oligo- or polymerization could not be observed for arsanylboranes or stibanylborane up to this point.

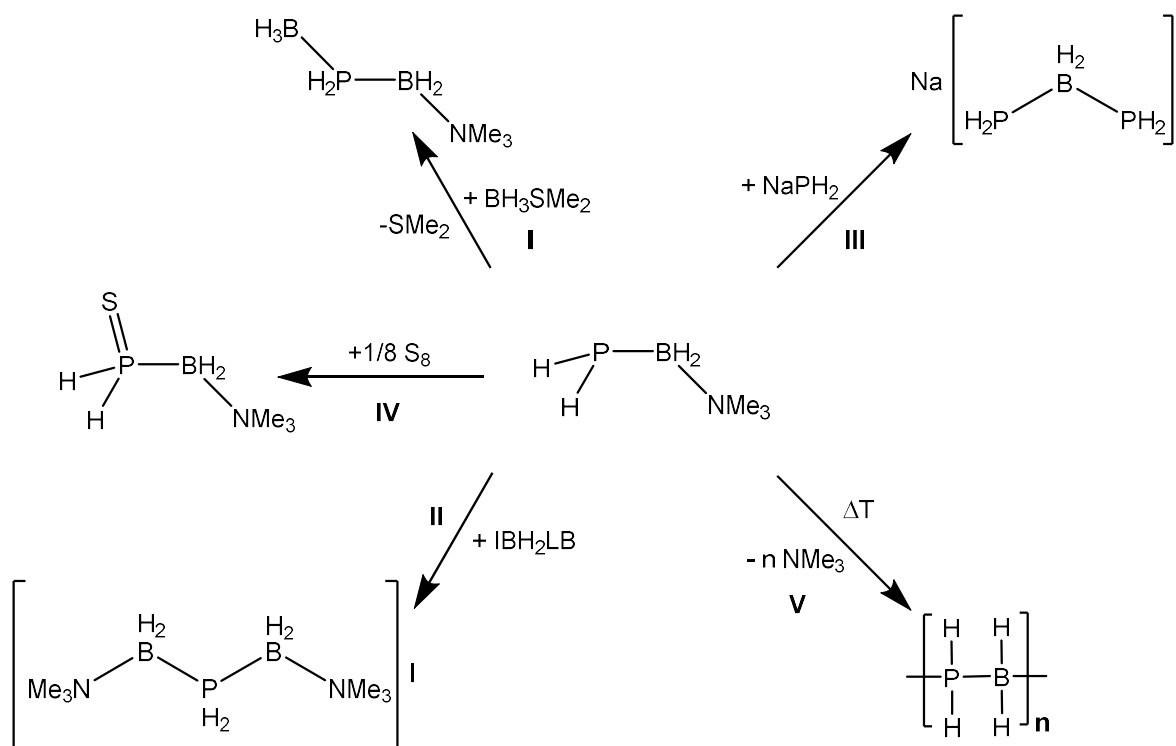


**Figure 7.** Selected examples for the reactivity of phosphanylborane

## 1.5. References

- [1] V. Jonas, G. Frenking, *J. Chem. Soc., Chem. Commun.* **1994**, 1489-1490.
- [2] E. Besson, *Comptes Rendus* **1890**, 516.
- [3] S. G. Shore, R. W. Parry, *J. Am. Chem. Soc.* **1955**, 77, 6084-6085.
- [4] a) A. Staubitz, A. P. M. Robertson, M. E. Sloan, I. Manners, *Chem. Rev.* **2010**, 110, 4023-4078; b) D. Han, F. Anke, M. Trose, T. Beweries, *Coord. Chem. Rev.* **2019**, 380, 260-286; c) J. A. Bailey, P. G. Pringle, *Coord. Chem. Rev.* **2015**, 297-298, 77-90; d) R. T. Paine, H. Noeth, *Chem. Rev.* **1995**, 95, 343-379; e) C. J. Carmalt, *Coord. Chem. Rev.* **2001**, 223, 217-264; f) S. Schulz, *Coord. Chem. Rev.* **2001**, 215, 1-37; g) J. M. Brunel, B. Faure, M. Maffei, *Coord. Chem. Rev.* **1998**, 178-180, 665-698; h) H. Schmidbaur, *J. Organomet. Chem.* **1980**, 200, 287-306.
- [5] a) A. Staubitz, A. P. Robertson, I. Manners, *Chem. Rev.* **2010**, 110, 4079-4124; b) C. W. Hamilton, R. T. Baker, A. Staubitz, I. Manners, *Chem. Soc. Rev.* **2009**, 38, 279-293; c) M. E. Bluhm, M. G. Bradley, R. Butterick, U. Kusari, L. G. Sneddon, *J. Am. Chem. Soc.* **2006**, 128, 7748-7749; d) F. H. Stephens, V. Pons, R. Tom Baker, *Dalton Trans.* **2007**, 2613-2626.
- [6] S. Schulz, in *Adv. Organomet. Chem., Vol. 49*, Academic Press, **2003**, pp. 225-317.
- [7] E. Wiberg, *Lehrbuch der anorganischen Chemie*, Walter de Gruyter GmbH & Co KG, **2019**.
- [8] H. Umeyama, K. Morokuma, *J. Am. Chem. Soc.* **1976**, 98, 7208-7220.
- [9] A. Stock, E. Pohland, *Chem. Ber.* **1926**, 59, 2215-2223.
- [10] X. Feng, M. M. Olmstead, P. P. Power, *Inorg. Chem.* **1986**, 25, 4615-4616.
- [11] U. Vogel, K.-C. Schwan, P. Hoemensch, M. Scheer, *Eur. J. Inorg. Chem.* **2005**, 2005, 1453-1458.
- [12] a) H. R. Allcock, *Chem. Mater.* **1994**, 6, 1476-1491; b) R. H. Neilson, P. Wisian-Neilson, *Chem. Rev.* **1988**, 88, 541-562; c) R. D. Jaeger, M. Gleria, *Prog. Polym. Sci.* **1998**, 23, 179-276; d) M. Liang, I. Manners, *J. Am. Chem. Soc.* **1991**, 113, 4044-4045; e) X. He, T. Baumgartner, *RSC Adv.* **2013**, 3, 11334-11350; f) P. J. Fazen, J. S. Beck, A. T. Lynch, E. E. Remsen, L. G. Sneddon, *Chem. Mater.* **1990**, 2, 96-97; g) R. De Jaeger, M. Gleria, *Prog. Polym. Sci.*

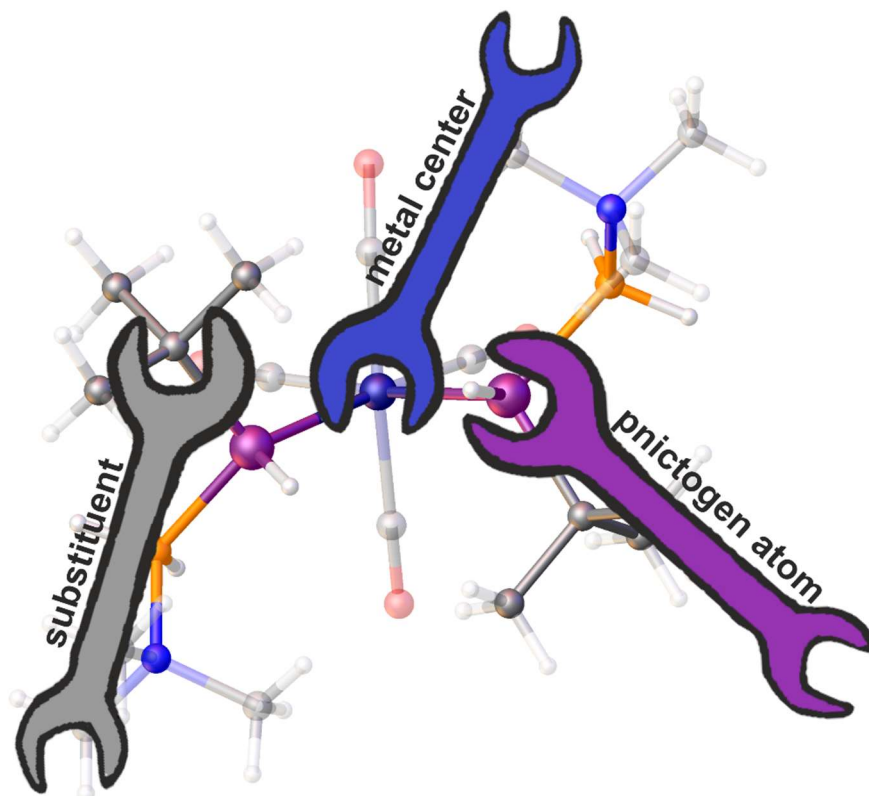
- 1998, 23, 179-276; h) H. Kutz, F. Cheng, S. Schwedler, L. Böhling, A. Brockhinke, L. Weber, K. Parab, F. Jäkle, *ACS Macro Lett.* **2012**, 1, 555-559.
- [13] H. M. Manasevit, *Appl. Phys. Lett.* **1968**, 12, 156-159.
- [14] Y. D. Blum, R. M. Laine, Google Patents, **1989**.
- [15] H. Dorn, R. A. Singh, J. A. Massey, A. J. Lough, I. Manners, *Angew. Chem. Int. Ed.* **1999**, 38, 3321-3323.
- [16] a) C. A. Jaska, K. Temple, A. J. Lough, I. Manners, *Chem. Commun.* **2001**, 962-963; b) C. A. Jaska, K. Temple, A. J. Lough, I. Manners, *J. Am. Chem. Soc.* **2003**, 125, 9424-9434.
- [17] a) H. C. Johnson, E. M. Leitao, G. R. Whittell, I. Manners, G. C. Lloyd-Jones, A. S. Weller, *J. Am. Chem. Soc.* **2014**, 136, 9078-9093; b) A. N. Marziale, A. Friedrich, I. Klopsch, M. Drees, V. R. Celinski, J. Schmedt auf der Günne, S. Schneider, *J. Am. Chem. Soc.* **2013**, 135, 13342-13355; c) A. Staubitz, M. E. Sloan, A. P. M. Robertson, A. Friedrich, S. Schneider, P. J. Gates, J. Schmedt auf der Günne, I. Manners, *J. Am. Chem. Soc.* **2010**, 132, 13332-13345; d) T. J. Clark, J. M. Rodezno, S. B. Clendenning, S. Aouba, P. M. Brodersen, A. J. Lough, H. E. Ruda, I. Manners, *Chem. Eur. J.* **2005**, 11, 4526-4534.
- [18] A. Staubitz, A. Presa Soto, I. Manners, *Angew. Chem. Int. Ed.* **2008**, 47, 6212-6215.
- [19] J. R. Vance, A. P. Robertson, K. Lee, I. Manners, *Chem. Eur. J.* **2011**, 17, 4099-4103.
- [20] M. E. Sloan, A. Staubitz, T. J. Clark, C. A. Russell, G. C. Lloyd-Jones, I. Manners, *J. Am. Chem. Soc.* **2010**, 132, 3831-3841.
- [21] Y. Kawano, M. Uruichi, M. Shimoi, S. Taki, T. Kawaguchi, T. Kakizawa, H. Ogino, *J. Am. Chem. Soc.* **2009**, 131, 14946-14957.
- [22] J.-M. Denis, H. Forintos, H. Szelke, L. Toupet, T.-N. Pham, P.-J. Madec, A.-C. Gaumont, *Chem. Commun.* **2003**, 54-55.
- [23] L. Wirtz, J. Lambert, B. Morgenstern, A. Schäfer, *Organometallics* **2021**, 40, 2108-2117.
- [24] a) M. A. Huertos, A. S. Weller, *Chem. Commun.* **2012**, 48, 7185-7187; b) M. A. Huertos, A. S. Weller, *Chem. Sci.* **2013**, 4, 1881-1888; c) T. N. Hooper, M. A. Huertos, T. Jurca, S. D. Pike, A. S. Weller, I. Manners, *Inorg. Chem.* **2014**, 53, 3716-3729; d) H. C. Johnson, T. N. Hooper, A. S. Weller, *Synthesis and Application of Organoboron Compounds* **2015**, 153-220.

- [25] W. M. Haynes, *CRC handbook of chemistry and physics*, CRC press, **2016**.
- [26] a) S. Pandey, P. Lönnecke, E. Hey-Hawkins, *Eur. J. Inorg. Chem.* **2014**, 2014, 2456-2465; b) H. Dorn, J. M. Rodezno, B. Brunnhöfer, E. Rivard, J. A. Massey, I. Manners, *Macromolecules* **2003**, 36, 291-297.
- [27] R. Hoffmann, *Angew. Chem. Int. Ed.* **1982**, 21, 711-724.
- [28] H. A. McGee Jr, C. Kwon, *Inorg. Chem.* **1970**, 9, 2458-2461.
- [29] a) T. L. Allen, W. H. Fink, *Inorg. Chem.* **1992**, 31, 1703-1705; b) T. L. Allen, A. C. Scheiner, H. F. Schaefer III, *Inorg. Chem.* **1990**, 29, 1930-1936; c) M. B. Coolidge, W. T. Borden, *J. Am. Chem. Soc.* **1990**, 112, 1704-1706.
- [30] a) J. A. Bailey, P. G. Pringle, *Coord. Chem. Rev.* **2015**, 297, 77-90; b) J. M. Breunig, A. Hübner, M. Bolte, M. Wagner, H.-W. Lerner, *Organometallics* **2013**, 32, 6792-6799.
- [31] J. A. Bailey, M. F. Haddow, P. G. Pringle, *Chem. Commun.* **2014**, 50, 1432-1434.
- [32] M. Kaaz, J. Bender, D. Förster, W. Frey, M. Nieger, D. Gudat, *Dalton Trans.* **2014**, 43, 680-689.
- [33] A. M. Spokoiny, C. D. Lewis, G. Teverovskiy, S. L. Buchwald, *Organometallics* **2012**, 31, 8478-8481.
- [34] A. Tsurusaki, T. Sasamori, A. Wakamiya, S. Yamaguchi, K. Nagura, S. Irle, N. Tokitoh, *Angew. Chem. Int. Ed.* **2011**, 50, 10940-10943.
- [35] U. Vogel, A. Y. Timoshkin, M. Scheer, *Angew. Chem. Int. Ed.* **2001**, 40, 4409-4412.
- [36] U. Vogel, P. Hoemensch, K.-C. Schwan, A. Y. Timoshkin, M. Scheer, *Chem. Eur. J.* **2003**, 9, 515-519.
- [37] K.-C. Schwan, A. Y. Timoshkin, M. Zabel, M. Scheer, *Chem. Eur. J.* **2006**, 12, 4900-4908.
- [38] C. Marquardt, A. Adolf, A. Stauber, M. Bodensteiner, A. V. Virovets, A. Y. Timoshkin, M. Scheer, *Chem. Eur. J.* **2013**, 19, 11887-11891.
- [39] C. Marquardt, T. Jurca, K.-C. Schwan, A. Stauber, A. V. Virovets, G. R. Whittell, I. Manners, M. Scheer, *Angew. Chem. Int. Ed.* **2015**, 54, 13782-13786.
- [40] C. Marquardt, O. Hegen, M. Hautmann, G. Balázs, M. Bodensteiner, A. V. Virovets, A. Y. Timoshkin, M. Scheer, *Angew. Chem. Int. Ed.* **2015**, 54, 13122-13125.

- [41] a) M. A. Weinhart, A. S. Lisovenko, A. Y. Timoshkin, M. Scheer, *Angew. Chem. Int. Ed.* **2020**, *59*, 5541-5545; b) M. A. Weinhart, M. Seidl, A. Y. Timoshkin, M. Scheer, *Angew. Chem. Int. Ed.* **2021**, *60*, 3806-3811.
- [42] O. Hegen, C. Marquardt, A. Y. Timoshkin, M. Scheer, *Angew. Chem. Int. Ed.* **2017**, *56*, 12783-12787.
- [43] O. Hegen, J. Braese, A. Y. Timoshkin, M. Scheer, *Chem. Eur. J.* **2019**, *25*, 485-489.
- [44] a) C. Marquardt, T. Kahoun, J. Baumann, A. Y. Timoshkin, M. Scheer, *Z. Anorg. Allg. Chem.* **2017**, *643*, 1326-1330; b) O. Hegen, A. V. Virovets, A. Y. Timoshkin, M. Scheer, *Chem. Eur. J.* **2018**, *24*, 16521-16525.
- [45] C. Thoms, C. Marquardt, A. Y. Timoshkin, M. Bodensteiner, M. Scheer, *Angew. Chem. Int. Ed.* **2013**, *52*, 5150-5154.
- [46] J. Braese, A. Schinabeck, M. Bodensteiner, H. Yersin, A. Y. Timoshkin, M. Scheer, *Chem. Eur. J.* **2018**, *24*, 10073-10077.
- [47] R. Szlosek, M. T. Ackermann, C. Marquardt, M. Seidl, A. Y. Timoshkin, M. Scheer, *Chem. Eur. J.* **2023**, *29*, e202202911.
- [48] a) C. Marquardt, C. Thoms, A. Stauber, G. Balázs, M. Bodensteiner, M. Scheer, *Angew. Chem. Int. Ed.* **2014**, *53*, 3727-3730; b) C. Marquardt, G. Balázs, J. Baumann, A. V. Virovets, M. Scheer, *Chem. Eur. J.* **2017**, *23*, 11423-11429.
- [49] a) C. Marquardt, T. Kahoun, A. Stauber, G. Balázs, M. Bodensteiner, A. Y. Timoshkin, M. Scheer, *Angew. Chem. Int. Ed.* **2016**, *55*, 14828-14832; b) M. E. Moussa, T. Kahoun, C. Marquardt, M. Ackermann, O. Hegen, M. Seidl, A. Y. Timoshkin, A. V. Virovets, M. Bodensteiner, M. Scheer, *Chem. Eur. J.* **2022**.
- [50] M. Elsayed Moussa, T. Kahoun, M. T. Ackermann, M. Seidl, M. Bodensteiner, A. Y. Timoshkin, M. Scheer, *Organometallics* **2022**, *41*, 1572-1578.
- [51] a) M. T. Ackermann, M. Seidl, F. Wen, M. J. Ferguson, A. Y. Timoshkin, E. Rivard, M. Scheer, *Chem. Eur. J.* **2022**, *28*, e202103780; b) M. T. Ackermann, M. Seidl, R. Grande, Y. Zhou, M. J. Ferguson, A. Timoshkin, E. Rivard, M. Scheer, *Chemical Science* **2023**.
- [52] C. Marquardt, O. Hegen, T. Kahoun, M. Scheer, *Chem. Eur. J.* **2017**, *23*, 4397-4404.

## 2. Coordination chemistry of pnictogenylboranes towards group 6 transition metal Lewis acids

Felix Lehnfeld, Oliver Hegen, Gábor Balázs, Alexey Y. Timoshkin and Manfred Scheer



**Abstract:** The systematic coordination of different pnictogenylboranes towards group 6 metal Lewis acids is investigated. The resulting complexes with phosphanylboranes  $[(\text{CO})_4\text{M}(\text{PH}_2\text{BH}_2\cdot\text{NMe}_3)_2]$  ( $\text{M} = \text{Cr}, \text{Mo}, \text{W}$ ; **1-3**), arsanylboranes  $[(\text{CO})_4\text{M}(\text{AsH}_2\text{BH}_2\cdot\text{NMe}_3)_2]$  ( $\text{M} = \text{Cr}, \text{Mo}, \text{W}$ ; **4-6**) and *t*Bu-substituted phosphanylborane  $[(\text{CO})_4\text{M}(\text{tBuPHBH}_2\cdot\text{NMe}_3)_2]$  ( $\text{M} = \text{Cr}, \text{W}$ ; **7-8**) are fully characterized by multinuclear NMR spectroscopy, single crystal X-ray diffraction and IR spectroscopy. The systematic nature of the approach of the synthesis and the high purity of the compounds enables the comparative investigation of the coordination behavior of pnictogenylboranes. The observed trends allow to make qualitative statements concerning the influence of the metal center, the pnictogen atom and the substituent at the pnictogen atom on the coordination behavior of pnictogenylboranes.

## 2.1. Introduction

Transition metal complexes bearing phosphine ligands have been of scientific interest for many years, and still are, due to their broad field of potential applications.<sup>[1]</sup> Important fields of application include antitumor therapies, enantioselective catalysis and luminescence compounds, as reported e.g. for copper-phosphine complexes.<sup>[2]</sup> Also, similar arsine complexes are of interest, even though the number of reported compounds is much smaller, especially for primary arsines.<sup>[3]</sup> Being closely related to phosphines or arsines and also exhibiting interesting reactivity due to their polar bond situation and additional reactive sites, group 13-15 compounds have been spotlighted in current research. E.g., for phosphine-boranes, mostly dehydrocoupling reactions have been investigated.<sup>[4]</sup> Over the last decades, our group has contributed to this field by investigating the group 13-15 analogs to alkenes, stabilized only by a Lewis-base (LB),  $R_2E-BH_2 \cdot LB$  ( $E = P, As$ ;  $R = H, Ph, tBu$ , Figure 1)<sup>[5]</sup> and has reported their reactivity towards main group Lewis acids,<sup>[5e-g,6]</sup> their oxidation with chalcogens<sup>[5a,5e,7]</sup> and their use as building blocks for oligomeric and polymeric compounds.<sup>[5c,5d,5g,8]</sup> In contrast, their reactivity towards transition metal complexes was only investigated on a limited scale.

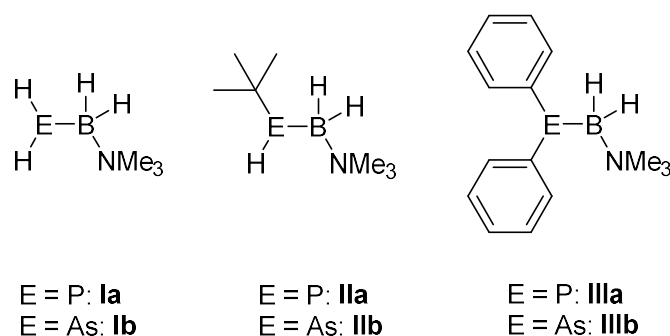


**Figure 1.** Selected examples of pnictogenylboranes reported in recent years

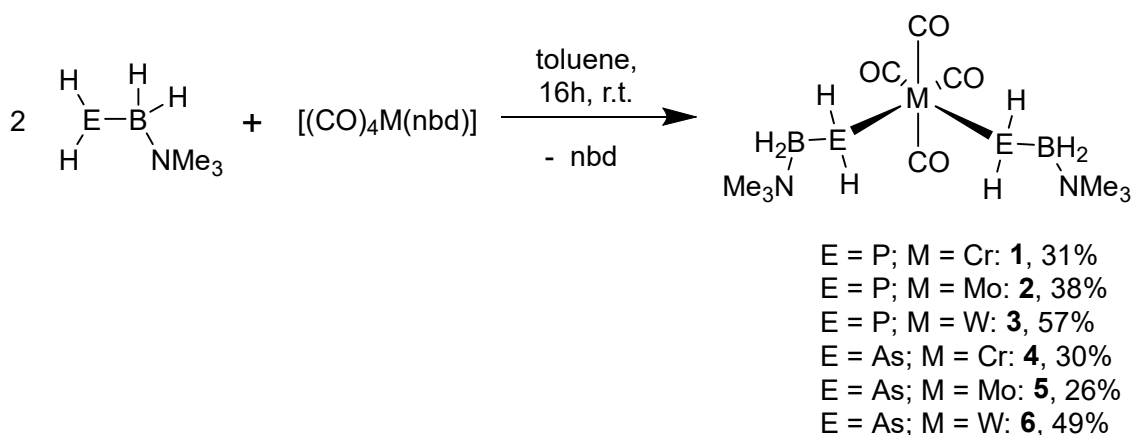
For the reaction of the parent phosphanylborane **Ia** towards the early transition metal complex  $Cp_2Ti(btmsa)$  ( $btmsa = bis(trimethylsilyl)acetylene$ ), adduct formation at low temperature as well as at room temperature by using several equivalents of **Ia** the formation of coordination oligomers incorporating multiple metal centers was observed.<sup>[9]</sup> For late transition metal complexes, the coordination towards  $Cu^I$  centers was reported for the parent compound **Ia**<sup>[10]</sup> as well as for the diphenyl-substituted derivative **IIIa**.<sup>[11]</sup> In a similar manner, the reaction of **IIIa** with  $Ag^I$  salts has been

investigated.<sup>[12]</sup> When reacting **1a** and **1b** with a Pt<sup>0</sup> complex, the reaction proceeds under oxidative addition of the E-H bond to the Pt center.<sup>[13]</sup> When reacting various pnictogenylboranes with (tht)AuCl, the resulting complexes reveal aurophilic interactions resulting in photoluminescent properties.<sup>[14]</sup>

Considering the recently reported bidentate phosphanyl- and arsanylboranes<sup>[15]</sup> as well as the increasing interest in longer or mixed element chain pnictogenylboranes,<sup>[16]</sup> a further investigation of the coordination behavior of pnictogenylboranes was the next step, especially focusing on the less frequently investigated earlier transition metals. We report the coordination behavior of pnictogenylboranes towards group 6 complexes as transition metal Lewis acids. Their accessibility in good yields and high purity enables this system to serve as model system for the coordination behavior of LB-stabilized pnictogenylboranes in general. The influence of the metal center, the pnictogen atom and the substituents on the pnictogen atom have been studied.

## 2.2. Results and Discussion

The reaction of the Lewis acidic group 6 carbonyl complexes [(CO)<sub>4</sub>M(nbd)] (nbd = norbornadiene, M = Cr, Mo, W) with different LB-stabilized pnictogenylboranes of the type RHEBH<sub>2</sub>•NMe<sub>3</sub> (E = P, As, R = H, *t*Bu) leads to the formation of the coordination compounds [M(CO)<sub>4</sub>(HREBH<sub>2</sub>•NMe<sub>3</sub>)<sub>2</sub>] (Scheme 1). After addition of the pnictogenylborane to a toluene solution of the respective norbornadiene complex and stirring for 16h at r.t., yellow to brown precipitate is formed, often already crystalline. In case of the arsenic derivatives **4-6**, a color change from yellow to brown becomes visible. The reactions proceed selectively and almost quantitatively according to <sup>31</sup>P and <sup>11</sup>B NMR spectroscopy of the crude reaction solutions. While being almost insoluble in non-polar solvents, they can be isolated by washing with *n*-hexane and subsequent layering of saturated CH<sub>2</sub>Cl<sub>2</sub> solutions of compounds **1-8** with *n*-hexane at r.t. or 6°C and washing the crystalline solid with *n*-hexane. All compounds can be isolated in moderate to good crystalline yields, although the yields have not been optimized in terms of analytically pure precipitate.



**Scheme 1.** General synthesis of the group 6 coordination starting by the parent pnictogenylboranes (compounds **1-6**)

The coordination compounds of  $\text{PH}_2\text{BH}_2\cdot\text{NMe}_3$  (**1-3**) all reveal a broad singlet in the  $^{31}\text{P}\{^1\text{H}\}$  NMR spectrum due to the coupling with the boron atom. In case of the tungsten compound **3**, a broadening of the signal with a half-height width of about 157 Hz occurs, to be the reason why no coupling with the tungsten nuclear can be observed. In all cases, a downfield shift of the  $^{31}\text{P}$  signal compared to the starting material is observed. A clear trend in the shift can be noted from the W to the Cr complex with a shift for compound **3** at  $\delta = -170.3$  ppm, for **2** at  $\delta = -157.1$  ppm and for the chromium compound **1** at  $\delta = -116.5$  ppm. In the  $^{31}\text{P}\{^1\text{H}\}$  NMR spectra of all three compounds, further splittings are revealed. The P-H coupling constants are also dependent on the metal center, being smaller in the Cr compound **1** ( $^1J_{\text{P,H}} = 265$  Hz), whereas the coordination products of the heavier homologs reveal a similar coupling constant of  $^1J_{\text{P,H}} = 280$  Hz (**2** and **3**). However, in all cases the coupling constants are approx. 80-90 Hz larger than in the starting material  $\text{PH}_2\text{BH}_2\cdot\text{NMe}_3$ .

In the  $^{11}\text{B}\{^1\text{H}\}$  NMR spectra, compounds **1** and **3** show broad multiplets, **2** only a broad singlet, all with very similar chemical shifts, exhibiting an upfield shift of about 1 ppm compared to  $\text{PH}_2\text{BH}_2\cdot\text{NMe}_3$  (**1**:  $\delta = -7.72$  ppm; **2**:  $\delta = -7.75$  ppm; **3**:  $\delta = -7.52$  ppm). For **1** and **3**,  $^1J_{\text{P,B}}$  coupling constants can be determined. (**1**: 66 Hz; **3**: 64 Hz). In the  $^{11}\text{B}$  NMR spectra of **2** and **3**, further splitting into broad triplets can be noticed (**2**:  $^1J_{\text{B,H}} = 132$  Hz; **3**:  $^1J_{\text{B,H}} = 130$  Hz), which for **1**, is only a very strong broadening of the signal.

In the  $^1\text{H}$  NMR spectra of all three compounds **1-3**, the signals for the  $\text{PH}_2$  moiety can be assigned at around  $\delta = 2.7$  ppm. The signals corresponding to the  $\text{BH}_2$  group can only be observed for **3** at  $\delta = 2.34$  ppm. For the other two compounds, the signals show too much broadening but can be allotted in the range between 2 and 2.5 ppm.

The comparison of the different coordination compounds exhibits a clear trend, especially considering the chemical shifts and coupling constants of the phosphorus atom in **1-3**, with the influence of the different metals on the respective data of the BH<sub>2</sub> moiety being minor. This trend matches the electronegativity and polarizability of the group 6 metals nicely, indicating more backbonding in the case of the heavier homologs. This is in accordance with phosphine complexes of group 6 metals in general.<sup>[17]</sup>

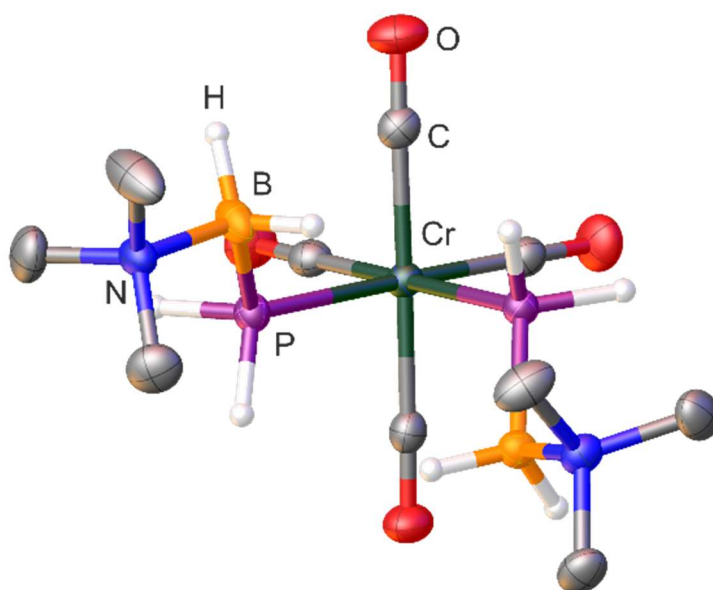


**Figure 2.** Molecular structure of **1**. Thermal ellipsoids displayed at 50 % probability. Carbon-bound hydrogen atoms omitted for clarity. Selected bond distances (Å) and angles [°]: Cr1-P1 2.3979(4), Cr1-P2 2.3998(4), P1-B1 1.9576(17), P2-B2 1.9565(18), N1-B1 1.612(2), N2-B2 1.613(2); P1-Cr1-P2 86.8(1), B1-P1-Cr1 119.0(1), B2-P2-Cr1 119.1(5), N2-B2-P2 115.6(1), N1-B1-P1 115.7(1).

The molecular structure in the solid state of **1-3** have been determined by single crystal X-ray diffraction analysis (**1**: Figure 2; **2-3**: supporting information). All three compounds crystallize in the space group  $P2_1/n$  and reveal a similar molecular structure. In all cases, the phosphanylborane molecules are located at the coordination site in *cis*-position on the  $M(\text{CO})_4$ -fragment. Apart from the CO groups, all bonds are in the range of single bonds. The B-P bond adapts an antiperiplanar arrangement, whereas the BH<sub>2</sub>NMe<sub>3</sub> moieties arrange in a trans position to the P-M-P plane. The P-M-P angles for all three compounds are below 90° (**1**: 86.83°; **2**: 85.68°; **3**: 85.44°) and therefore deviate slightly from the perfect octahedral structure, most likely due to steric effects.

Also, for the parent arsanylborane  $\text{AsH}_2\text{BH}_2\cdot\text{NMe}_3$  the substitution of norbornadiene proceeds in a selective manner. Compounds **4-6** have been characterized by multinuclear NMR spectroscopy. In the  $^{11}\text{B}\{^1\text{H}\}$  NMR spectra, singlets at  $\delta = -7.01$  ppm (**4**),  $\delta = -7.24$  ppm (**5**) and  $\delta = -7.36$  ppm (**6**), respectively, are observed. The  $^{11}\text{B}$  NMR spectra of both compounds reveal additional splitting with similar coupling constants for all three complexes (**4**:  $^1J_{\text{B,H}} = 115$  Hz; **5** and **6**:  $^1J_{\text{B,H}} = 112$  Hz).

In the  $^1\text{H}$  NMR spectra the expected broad multiplet corresponding to the  $\text{BH}_2$  moiety is detected at approx.  $\delta = 2.5$  ppm and in both cases partly overlapped by the signal corresponding to the  $\text{NMe}_3$  at around  $\delta = 2.8$  ppm. The  $\text{AsH}_2$  groups reveal multiplets at  $\delta = 1.15$  ppm (**4**),  $\delta = 1.19$  ppm (**5**) and  $\delta = 1.50$  ppm (**6**), respectively. A trend for a larger upfield shift in compound **4** and **5** can be observed, which correlates with the less electropositive nature of tungsten compared to molybdenum and chromium. This trend is similar to the trend observed for the shifts of the phosphorus atoms in the  $^{31}\text{P}\{^1\text{H}\}$  NMR spectra of **1-3**.

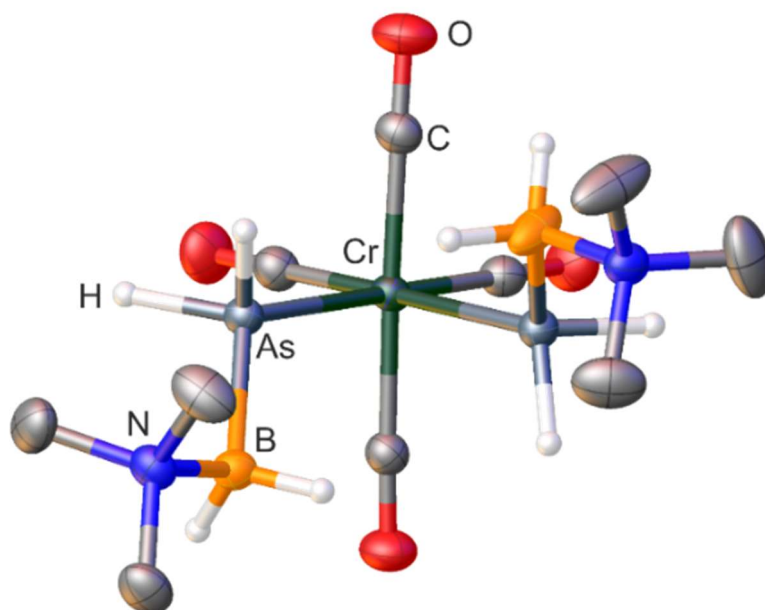
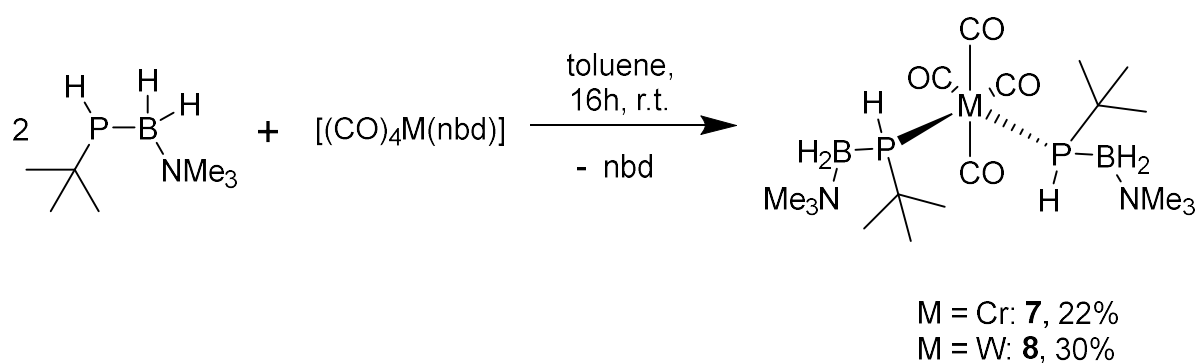


**Figure 3.** Molecular structure of **4**. Thermal ellipsoids displayed at 50 % probability. Carbon-bound hydrogen atoms omitted for clarity. Selected bond distances (Å) and angles [°]: As1-Cr1 2.4968(3), As1-B1 2.0670(19), As2-Cr1 2.4960(3), As2-B2 2.059(2), N1-B1 1.607(2), N2-B2 1.604(3); B1-As1-Cr1 119.70(6), B2-As2-Cr1 119.13(6), As2-Cr1-As1 86.066(10), N1-B1-As1 115.19(12), N2-B2-As2 116.04(14).

For **4-6**, crystals suitable for single crystal X-ray diffraction have been obtained, although for **5** only in poor crystalline yield. All three compounds crystallize in the space

group  $P2_1/n$  and reveal a similar molecular structure (**4**: Figure 3, **5-6**: supporting information). In all cases, the molecular structures are almost identical to the phosphorus analogs **1-3**. All observed bond lengths are in the range of single bonds, except for the CO bonds, which exhibit the expected bond lengths in the range of C-O multiple bonds. The bond angles reveal a similar trend for the As-M-As angle as observed for **1-3**, being slightly below  $90^\circ$  due to steric effects.

To investigate the influence of an organic substituent at the pnictogen atom, the reaction of  $[(CO)_4M(nbd)]$  ( $M = Cr, W$ ) with  $tBuPHBH_2 \cdot NMe_3$  was performed (Scheme 2). In both cases, the products **7-8** are formed selectively and almost quantitatively according to the  $^{31}P$  NMR spectroscopic investigation of the crude reaction mixture. **7** and **8** can be isolated as yellow blocks in moderate yields, which are lower compared to **1-3** due to an increased solubility. Both compounds were characterized by multinuclear NMR spectroscopy and single crystal X-ray diffraction.



**Scheme 2.** Synthesis of the group 6 coordination products of a substituted phosphanylborane (compounds **7-8**)

The  $^{31}P\{^1H\}$  NMR spectra of the two compounds reveals interesting differences compared to the unsubstituted analogs: In both cases, two signals can be observed, at  $\delta = -7.3$  ppm and  $\delta = -15.9$  ppm for **7** and at  $\delta = -46.4$  ppm and  $\delta = -50.7$  ppm for **8**, respectively. All signals appear as broad singlets due to the coupling with the boron atom. Due to the asymmetric nature of  $tBuPHBH_2 \cdot NMe_3$ , two different diastereomers can be formed in these products, the *d/l* and the *meso* isomer, both of which appear in the  $^{31}P$  NMR spectra. In case of the 3d element Cr, the *d/l* isomer is favored due to steric repulsion of the *tBu* groups, which can be observed in a 5:1 ratio of the products according to the  $^{31}P\{^1H\}$  NMR spectroscopy. For the heavier 5d metal tungsten, both signals appear in a 1:1 integral ratio, with no diastereomer being favored during the synthesis. In the  $^{31}P$  NMR spectra, all signals split into doublets, with similar  $^1J_{P,H}$

coupling constants of ca. 260 Hz, which are comparable but slightly lower than in compounds **1-3**. As compared to the starting material, for the complexes incorporating the parent phosphanylborane, a downfield shift is observed which is larger in the case of the chromium complex.

The  $^{11}\text{B}\{^1\text{H}\}$  NMR spectra of **7** and **8** are similar to each other, revealing a broad singlet at  $\delta = -4.7$  ppm, due to the overlap of the signals for the two isomers. Nevertheless, from the  $^{31}\text{P}$  NMR spectra, a similar  $^1J_{\text{P,B}}$  of about 58 Hz can be identified for both compounds. In the  $^{11}\text{B}$  NMR spectra, the signals only show broadening instead of further splitting due to the B-H coupling.

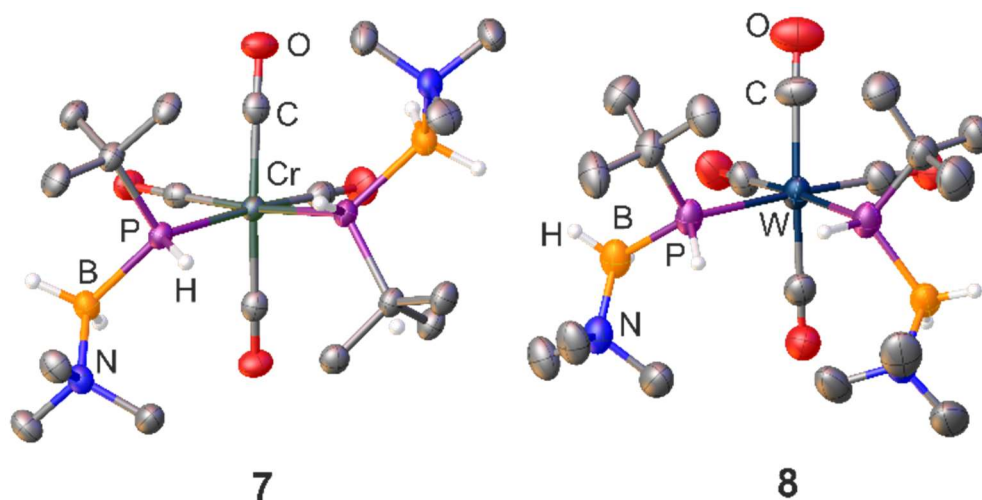


**Figure 4.** Molecular structure of **7** and **8**. Thermal ellipsoids displayed at 50 % probability. Carbon-bound hydrogen atoms omitted for clarity. Selected bond distances (Å) and angles [°] for **7**: Cr1-P1 2.4336(8), Cr1-P2 2.4251(8), N1-B1 1.620(4), P1-C1 1.890(3), N2-B2 1.618(5), P1-B1 2.003(4), P2-C8 1.890(3), P2-B2 1.997(4); P2-Cr1-P1 91.20(3), B1-P1-Cr1 116.44(11), B2-P2-Cr1 114.36(11), N2-B2-P2 115.8(2), N1-B1-P1 116.2(2). Selected bond distances (Å) and angles [°] for **8**: W1-P1 2.579(3), W1-P2 2.576(3), N1-B1 1.618(16), N2-B2 1.626(16), P1-B1 1.980(13), P2-B2 1.993(14); P2-W1-P1 90.11(9), B1-P1-W1 115.7(4), B2-P2-W1 114.6(5), N1-B1-P1 116.2(8), N2-B2-P2 114.4(9).

In the  $^1\text{H}$  NMR spectra, the signals corresponding to the P-H group (**7**:  $\delta = 2.79$  ppm; **8**:  $\delta = 3.15$  ppm) can be assigned. In both cases, the signals corresponding to the  $\text{BH}_2$  group reveal broad signals in the range between 2 and 3 ppm. Due to the mixture of two diastereomers, the signals corresponding to the *t*Bu group appear slightly different: for **7** a doublet at  $\delta = 1.22$  ppm ( $^3J_{\text{P,H}} = 12$  Hz) for the main product as well as a smaller doublet at  $\delta = 1.27$  ppm for the other isomer can be identified. In the case of **8**, the two doublets at  $\delta = 1.25$  ppm and  $\delta = 1.21$  ppm overlap forming a pseudo triplet due to the

almost identical coupling constants ( $^3J_{P,H} = 13$  Hz). In the case of **8**, for both isomers, two almost identical singlets are observed at  $\delta = 2.75$  ppm and  $\delta = 2.74$  ppm, but neither one can be assigned to one specific isomer.

The molecular structure in the solid state of **7** and **8** have been determined by single crystal X-ray diffraction analysis (Figure 4). Again, due to the asymmetric nature of the starting material, there are some differences. Whereas **7**, crystallizing in the acentric spacegroup  $P2_1$ , reveals both the D and L isomer in the unit cell, **8** only crystallizes as *meso*-isomer. This can be explained by the fact that the two bulky *t*Bu groups are able to occupy a *cis*-position relative to the P–W–P plane due to lower steric repulsion in the coordination sphere of the tungsten atom. Apart from these differences, the structures are relatively like the already discussed structures for **1-6** with all bond lengths and bond angles found in the expected ranges.

**Table 1.** Comparison of selected CO stretching frequencies of **1-6**, **8** and  $[(CO)_4M(nbd)]$  <sup>[18]</sup> obtained by IR spectroscopy

Compound	$\nu_1$ [cm <sup>-1</sup> ]	$\nu_2$ [cm <sup>-1</sup> ]	$\nu_3$ [cm <sup>-1</sup> ]
<b>1</b>	1993	1869	1822
<b>2</b>	2006	1876	1827
<b>3</b>	2002	1866	1820
<b>4</b>	1989	1865	1816
<b>5</b>	2004	1874	1820
<b>6</b>	1999	1862	1814
<b>7</b>	1977	1845	1818
<b>8</b>	1986	1854	1816
$[(CO)_4Cr(nbd)]$	2032	1980	1923
$[(CO)_4Mo(nbd)]$	2071	1980	1920
$[(CO)_4W(nbd)]$	2014	1939	1893

In addition to the X-ray diffraction analysis and the NMR spectroscopy, also mass spectrometry was applied for all compounds. ESI-MS in CH<sub>3</sub>CN of **1**, **2**, **4**, **5**, **7** and **8**

reveals the respective molecule ion peak as well as multiple fragmentation peaks for decarbonylation products occurring during ionization. For **3** and **6**, LIFDI-MS has been performed, only revealing the molecular ion peaks.

Additionally, all compounds were investigated in a comparative infrared spectroscopy analysis to obtain further insight into the coordination behavior of the pnictogenylboranes. Selected stretching frequencies are summarized in Table 1.

The CO stretching frequencies of the compounds reveal several trends. All compounds share one common feature, showing significantly lower CO stretching frequencies than the respective starting materials  $[(\text{CO})_4\text{M}(\text{nbd})]$  ( $\text{M} = \text{Cr}, \text{Mo}, \text{W}$ ), indicating the weaker  $\pi$  acceptor property of the pnictogenylboranes compared to the norbornadiene ligand. The most significant differences occur for the highest CO stretching band ( $A_1$ , axial CO), which mainly depends on the nature of the metal, all others are similar across all investigated compounds. Noticeably, there is a significant difference for the chromium complexes, with CO stretching frequencies by up to  $15 \text{ cm}^{-1}$  smaller than the analogue molybdenum complexes.

Considering the donor/acceptor strength, a small but consistent difference between the arsanylborane and the phosphanylborane complexes are observed. However, the difference is small compared to the effect of the introduced *t*Bu group. The tungsten complex of the *t*Bu-substituted phosphanylborane differs the most, pointing to having the strongest effect within the phosphanylboranes as ligands.

Computational studies (see SI for details) indicate that the stability of the  $[\text{M}(\text{CO})_4(\text{HREBH}_2\cdot\text{NMe}_3)_2]$  compounds slightly increase in order  $\text{Cr} < \text{Mo} < \text{W}$ , and decreases in order  $\text{H} > \textit{t}\text{Bu}$ , which is due to steric bulk of *t*Bu substituents and is also consistent with the longer (by  $0.027 - 0.034(1) \text{ \AA}$ ) distances in **7** compared to **1**. Computed CO stretching frequencies shifts are consistent with experimental IR spectra.

### 2.3. Conclusions

In summary, different pnictogenylboranes have been systematically coordinated towards group 6 transition metal Lewis acids. The obtained complexes incorporating phosphanylborane  $[(\text{CO})_4\text{M}(\text{PH}_2\text{BH}_2\cdot\text{NMe}_3)_2]$  ( $\text{M} = \text{Cr}, \text{Mo}, \text{W}$ ; **1-3**), arsanylborane  $[(\text{CO})_4\text{M}(\text{AsH}_2\text{BH}_2\cdot\text{NMe}_3)_2]$  ( $\text{M} = \text{Cr}, \text{Mo}, \text{W}$ ; **4-6**) and *t*Bu-substituted phosphanylborane  $[(\text{CO})_4\text{M}(\textit{t}\text{BuPHBH}_2\cdot\text{NMe}_3)_2]$  ( $\text{M} = \text{Cr}, \text{W}$ ; **7-8**) have been fully characterized by multinuclear NMR spectroscopy, single crystal X-ray diffraction, mass

spectrometry and infrared spectroscopy. The good yields and high purity of the obtained compounds allowed their use as a model system to investigate the coordination behavior of pnictogenylboranes. It was possible to utilize the obtained analytical data to work out systematic trends within this family of compounds and therefore deepen the understanding of the coordination behavior of pnictogenylboranes towards early transition metals. In all cases, the resulting complexes show a similar solid-state structure but reveal significant differences according to multinuclear NMR spectroscopy and IR spectroscopy, most notably for the different metal centers. The effect on the coordination behavior of pnictogenylboranes possessing an organic substituent at the pnictogen atom in comparison to the parent compounds clearly dominates. An influence of the donating pnictogen atom could be observed but appeared to be rather small compared to the effect of the used (organic) substituent.

## 2.4. Experimental Section

### General remarks

All reactions have been performed under Argon or Nitrogen inert gas atmosphere using standard glovebox and Schlenk techniques. All solvents were taken from a solvent purification system of the type MB-SPS-800 of the company MBRAUN and have been degassed by standard procedures.

All NMR spectra were recorded on a Bruker Avance 400 spectrometer ( $^1\text{H}$ : 400.13 MHz,  $^{13}\text{C}\{^1\text{H}\}$ : 100.623 MHz,  $^{11}\text{B}$ : 128.387 MHz) with  $\delta$  [ppm] referenced to external standards ( $^1\text{H}$  and  $^{13}\text{C}\{^1\text{H}\}$ :  $\text{SiMe}_4$ ,  $^{11}\text{B}$ :  $\text{BF}_3\text{-Et}_2\text{O}$ ). The C, H, N analyses were measured on an Elementar Vario EL III apparatus. All ESI-MS measurements have been performed on a Micromass LCT ESI-TOF, all LIFDI-MS measurements on a Jeol AccuTOF GCX spectrometer. IR spectra were recorded as solids using a ThermoFisher Nicolet iS5 FT-IR spectrometer with an iD7 ATR module and an ITX Diamond crystal.

### Synthesis of $[(\text{CO})_4\text{Cr}(\text{PH}_2\text{BH}_2\text{NMe}_3)_2]$ (1)

To a solution of  $[(\text{CO})_4\text{Cr}(\text{nbd})]$  (nbd = norbornadiene, 0.25 mmol, 65 mg) in 2 mL toluene, a solution of  $\text{PH}_2\text{BH}_2\text{NMe}_3$  (0.5 mmol, 53 mg) in 1 mL toluene is added at r.t.. After stirring for 16 h at r.t., the solvent is removed *in vacuo*. The remaining yellow solid

is washed three times with 2 mL *n*-hexane. By layering a saturated CH<sub>2</sub>Cl<sub>2</sub> solution with *n*-hexane at 279 K, compound **1** can be isolated as yellow blocks. Yield: 29 mg (0.078 mmol, 31%); <sup>1</sup>H-NMR (C<sub>6</sub>D<sub>6</sub>, 293 K) δ = 2.65 (4H, dm, <sup>1</sup>J<sub>P,H</sub> = 270 Hz, PH<sub>2</sub>), 2.6-1.8 (4H, br, BH<sub>2</sub>), 1.76 (18H, s, NMe<sub>3</sub>). <sup>31</sup>P NMR (C<sub>6</sub>D<sub>6</sub>, 293 K) δ = -116.5 (t, <sup>1</sup>J<sub>P,H</sub> = 265 Hz, PH<sub>2</sub>). <sup>31</sup>P{<sup>1</sup>H} NMR (C<sub>6</sub>D<sub>6</sub>, 293 K) δ = -116.5 (s (br), PH<sub>2</sub>). <sup>11</sup>B NMR (C<sub>6</sub>D<sub>6</sub>, 293 K) δ = -7.7 (br, BH<sub>2</sub>). <sup>11</sup>B{<sup>1</sup>H} NMR (C<sub>6</sub>D<sub>6</sub>, 293 K) δ = -7.7 (br, BH<sub>2</sub>). IR:  $\tilde{\nu}$  = 3008 vw, 2948 vw, 2393 w, 2373 w, 2304 w, 1992 m, 1869 s, 1822 s, 1481 m, 1461 m, 1406 vw, 1243 w, 1150 m, 1123 m, 1095 m, 1060 w, 1011 w, 978 vw, 853 w, 796 m, 784 m, 688 s, 671 s, 657 s, 623 m; ESI-MS (CH<sub>3</sub>CN) *m/z*: 374.12 (M<sup>+</sup>), 346.13 (M<sup>+</sup>-CO).

### Synthesis of [(CO)<sub>4</sub>Mo(PH<sub>2</sub>BH<sub>2</sub>NMe<sub>3</sub>)<sub>2</sub>] (**2**)

To a solution of [(CO)<sub>4</sub>Mo(nbd)] (nbd = norbornadiene, 0.25 mmol, 75 mg) in 2 mL toluene, a solution of PH<sub>2</sub>BH<sub>2</sub>•NMe<sub>3</sub> (0.5 mmol, 53 mg) in 1 mL toluene is added at r.t.. After stirring for 16 h at r.t., the solvent is removed *in vacuo*. The remaining yellow solid is washed three times with 2 mL *n*-hexane. By layering a saturated CH<sub>2</sub>Cl<sub>2</sub> solution with *n*-hexane at 279 K, compound **2** can be isolated as yellow blocks. Yield: 45 mg (0.095 mmol, 38%); <sup>1</sup>H-NMR (CD<sub>2</sub>Cl<sub>2</sub>, 293 K) δ = 2.73 (18H, s, NMe<sub>3</sub>), 2.6-1.8 (4H, br, BH<sub>2</sub>), 2.45 (4H, dm, <sup>1</sup>J<sub>P,H</sub> = 276 Hz, PH<sub>2</sub>). <sup>31</sup>P NMR (CD<sub>2</sub>Cl<sub>2</sub>, 293 K) δ = -157.2 (t, <sup>1</sup>J<sub>P,H</sub> = 278 Hz, PH<sub>2</sub>). <sup>31</sup>P{<sup>1</sup>H} NMR (CD<sub>2</sub>Cl<sub>2</sub>, 293 K) δ = -157.2 (s (br), PH<sub>2</sub>). <sup>11</sup>B NMR (CD<sub>2</sub>Cl<sub>2</sub>, 293 K) δ = -7.7 (t(br), <sup>1</sup>J<sub>B,H</sub> = 132 Hz, BH<sub>2</sub>). <sup>11</sup>B{<sup>1</sup>H} NMR (CD<sub>2</sub>Cl<sub>2</sub>, 293 K) δ = -7.7 (br, BH<sub>2</sub>). IR:  $\tilde{\nu}$  = 3006 vw, 2948 vw, 2392 w, 2371 w, 2309 w, 2006 m, 1876 s, 1827 s, 1481 m, 1461 m, 1405 vw, 1243 w, 1149 m, 1122 m, 1094 m, 1058 w, 1010 w, 977 vw, 851 w, 780 s, 769 s, 701 w, 648 s, 637 s, 623 m, 611 m; ESI-MS (CH<sub>3</sub>CN) *m/z*: 418.07 (M<sup>+</sup>), 389.07 (M<sup>+</sup>-CO), 360.06 (M<sup>+</sup>-2CO), 333.06 (M<sup>+</sup>-3CO).

### Synthesis of [(CO)<sub>4</sub>W(PH<sub>2</sub>BH<sub>2</sub>NMe<sub>3</sub>)<sub>2</sub>] (**3**)

To a solution of [(CO)<sub>4</sub>W(nbd)] (nbd = norbornadiene, 0.25 mmol, 99 mg) in 2 mL toluene, a solution of PH<sub>2</sub>BH<sub>2</sub>•NMe<sub>3</sub> (0.5 mmol, 53 mg) in 1 mL toluene is added at r.t.. After stirring for 16 h at r.t., the solvent is removed *in vacuo*. The remaining yellow solid is washed three times with 2 mL *n*-hexane. By storing a saturated CH<sub>2</sub>Cl<sub>2</sub> solution at 245 K, compound **3** can be isolated as yellow blocks. Yield: 72 mg (0.143 mmol, 57%); <sup>1</sup>H-NMR (CDCl<sub>3</sub>, 293 K) δ = 2.82 (4H, dm, <sup>1</sup>J<sub>P,H</sub> = 280 Hz, PH<sub>2</sub>), 2.76 (18H, s, NMe<sub>3</sub>), 2.34 (4H, m, <sup>1</sup>J<sub>B,H</sub> = 130 Hz, BH<sub>2</sub>). <sup>31</sup>P NMR (CDCl<sub>3</sub>, 293 K) δ = -170.3 (t, <sup>1</sup>J<sub>P,H</sub> = 278 Hz, PH<sub>2</sub>). <sup>31</sup>P{<sup>1</sup>H} NMR (CDCl<sub>3</sub>, 293 K) δ = -170.3 (m, <sup>1</sup>J<sub>P,B</sub> = 64 Hz, PH<sub>2</sub>). <sup>11</sup>B NMR

(CDCl<sub>3</sub>, 293 K)  $\delta = -7.5$  (t(br),  $^1J_{B,H} = 130$  Hz, BH<sub>2</sub>).  $^{11}B\{^1H\}$  NMR (CDCl<sub>3</sub>, 293 K)  $\delta = -7.5$  (br,  $^1J_{P,B} = 64$  Hz, BH<sub>2</sub>). IR:  $\tilde{\nu} = 3003$  vw, 2948 vw, 2394 w, 2373 w, 2310 w, 2002 m, 1866 s, 1820 s, 1480 m, 1461 m, 1405 vw, 1243 w, 1149 m, 1122 m, 1093 m, 1058 w, 1010 vw, 977 vw, 853 m, 788 s, 777 s, 704 m, 639 w, 624 vw; EA: calculated for C<sub>10</sub>H<sub>26</sub>B<sub>2</sub>N<sub>2</sub>O<sub>4</sub>WP<sub>2</sub>: C: 23.75 %; H: 5.18 %; N: 5.54 %; found: C: 23.99 %; H: 5.13 %; N: 5.43 %; LIFDI-MS (CH<sub>2</sub>Cl<sub>2</sub>)  $m/z$ : 504 (M<sup>+</sup>).

### Synthesis of [(CO)<sub>4</sub>Cr(AsH<sub>2</sub>BH<sub>2</sub>NMe<sub>3</sub>)<sub>2</sub>] (4)

To a solution of [(CO)<sub>4</sub>Cr(nbd)] (nbd = norbornadiene, 0.25 mmol, 65 mg) in 2 mL toluene, a solution of AsH<sub>2</sub>BH<sub>2</sub>·NMe<sub>3</sub> (0.5 mmol, 74 mg) in 1 mL toluene is added at r.t.. After stirring for 16 h at r.t., the solvent is removed *in vacuo*. The remaining brown solid is washed three times with 2 mL *n*-hexane. By layering a saturated CH<sub>2</sub>Cl<sub>2</sub> solution with *n*-hexane at 279 K compound **4** can be isolated as dark yellow blocks. Yield: 35 mg (0.075 mmol, 30%);  $^1H$ -NMR (CD<sub>2</sub>Cl<sub>2</sub>, 293 K)  $\delta = 2.78$  (18H, s, NMe<sub>3</sub>), 2.9-1.9 (4H, m,  $^1J_{B,H} = 112$  Hz, BH<sub>2</sub>), 1.15 (4H, m, AsH<sub>2</sub>).  $^{11}B$  NMR (CD<sub>2</sub>Cl<sub>2</sub>, 293 K)  $\delta = -7.0$  (t,  $^1J_{B,H} = 112$  Hz, BH<sub>2</sub>).  $^{11}B\{^1H\}$  NMR (CD<sub>2</sub>Cl<sub>2</sub>, 293 K)  $\delta = -7.0$  (s, BH<sub>2</sub>). IR:  $\tilde{\nu} = 3007$  vw, 2947 vw, 2414 w, 2382 w, 2112 w, 1989 m, 1865 s, 1816 s, 1480 m, 1460 m, 1406 vw, 1241 w, 1150 m, 1116 m, 1066 m, 1007 w, 979 w, 852 m, 723 m, 681 s, 644 s; EA: calculated for C<sub>18</sub>H<sub>42</sub>B<sub>2</sub>N<sub>2</sub>O<sub>4</sub>CrP<sub>2</sub>: C: 26.01 %; H: 5.68 %; N: 6.07 %; found: C: 25.94 %; H: 5.45 %; N: 5.88 %.

### Synthesis of [(CO)<sub>4</sub>Mo(AsH<sub>2</sub>BH<sub>2</sub>NMe<sub>3</sub>)<sub>2</sub>] (5)

To a solution of [(CO)<sub>4</sub>Mo(nbd)] (nbd = norbornadiene, 0.25 mmol, 75 mg) in 2 mL toluene, a solution of AsH<sub>2</sub>BH<sub>2</sub>·NMe<sub>3</sub> (0.5 mmol, 74 mg) in 1 mL toluene is added at r.t.. After stirring for 16 h at r.t., the solvent is removed *in vacuo*. The remaining brown solid is washed three times with 2 mL *n*-hexane. By layering a saturated CH<sub>2</sub>Cl<sub>2</sub> solution with *n*-hexane at 279 K compound **5** can be isolated as dark yellow blocks. Yield: 33 mg (0.065 mmol, 26%);  $^1H$ -NMR (CDCl<sub>3</sub>, 293 K)  $\delta = 2.79$  (18H, s, NMe<sub>3</sub>), 2.9-1.9 (4H, m,  $^1J_{B,H} = 112$  Hz, BH<sub>2</sub>), 1.19 (4H, m, AsH<sub>2</sub>).  $^{11}B$  NMR (CDCl<sub>3</sub>, 293 K)  $\delta = -7.3$  (t,  $^1J_{B,H} = 112$  Hz, BH<sub>2</sub>).  $^{11}B\{^1H\}$  NMR (CDCl<sub>3</sub>, 293 K)  $\delta = -7.3$  (s, BH<sub>2</sub>). IR:  $\tilde{\nu} = 3006$  vw, 2947 vw, 2413 w, 2381 w, 2115 w, 2004 m, 1874 s, 1820 s, 1480 m, 1460 m, 1449 vw, 1405 vw, 1241 w, 1150 m, 1116 m, 1066 m, 1007 w, 978 w, 958 vw, 851 m, 718 m, 676 m, 629 w; ESI-MS (CH<sub>3</sub>CN)  $m/z$ : 462.20 (M<sup>+</sup>), 434.18 (M<sup>+</sup>-CO); 405.20 (M<sup>+</sup>-2CO).

**Synthesis of  $[(\text{CO})_4\text{W}(\text{AsH}_2\text{BH}_2\text{NMe}_3)_2]$  (6)**

To a solution of  $[(\text{CO})_4\text{W}(\text{nbd})]$  (nbd = norbornadiene, 0.5 mmol, 196 mg) in 20 mL toluene, a solution of  $\text{AsH}_2\text{BH}_2\cdot\text{NMe}_3$  (1 mmol, 149 mg) in 1 mL toluene is added at r.t.. After stirring for 16 h at r.t., the solvent is removed *in vacuo*. The remaining brown solid is washed with 20 mL *n*-hexane. By storing a saturated  $\text{CH}_2\text{Cl}_2$  solution at 245 K compound **6** can be isolated as yellow needles. Yield: 72 mg (0.245 mmol, 49%);  $^1\text{H}$ -NMR ( $\text{CDCl}_3$ , 293 K)  $\delta$  = 2.81 (18H, s,  $\text{NMe}_3$ ), 2.51 (4H, m,  $^1J_{\text{B,H}} = 112$  Hz,  $\text{BH}_2$ ), 1.51 (4H, m,  $\text{AsH}_2$ ).  $^{11}\text{B}$  NMR ( $\text{CDCl}_3$ , 293 K)  $\delta$  = -7.4 (t,  $^1J_{\text{B,H}} = 112$  Hz,  $\text{BH}_2$ ).  $^{11}\text{B}\{^1\text{H}\}$  NMR ( $\text{CDCl}_3$ , 293 K)  $\delta$  = -7.4 (s,  $\text{BH}_2$ ). IR:  $\tilde{\nu}$  = 3006 vw, 2947 vw, 2415 w, 2383 w, 2117 w, 1999 m, 1862 s, 1814 s, 1480 m, 1459 m, 1405 vw, 1241 w, 1150 w, 1116 m, 1065 m, 1006 m, 978 w, 959 vw, 720 m, 678 s, 623 w; EA: calculated for  $\text{C}_{10}\text{H}_{26}\text{As}_2\text{N}_2\text{O}_4\text{WB}_2$ : C: 20.23 %; H: 4.41 %; N: 4.71 %; found: C: 20.52 %; H: 4.49 %; N: 4.54 %; LIFDI-MS ( $\text{CH}_2\text{Cl}_2$ )  $m/z$ : 592 ( $\text{M}^+$ ).

**Synthesis of  $[(\text{CO})_4\text{Cr}(\text{tBuPHBH}_2\text{NMe}_3)_2]$  (7)**

$[(\text{CO})_4\text{Cr}(\text{nbd})]$  (nbd = norbornadiene, 0.2 mmol, 51 mg) and  $\text{tBuPHBH}_2\cdot\text{NMe}_3$  (0.4 mmol, 64 mg) are dissolved in 4 mL toluene at r.t.. After stirring for 16 h at r.t., the solvent is removed *in vacuo*. The remaining yellow solid is washed three times with 2 mL *n*-hexane. By layering a saturated  $\text{CH}_2\text{Cl}_2$  solution with *n*-hexane at 293 K compound **7** can be isolated as yellow needles. Yield: 18 mg (0.040 mmol, 22%);  $^1\text{H}$ -NMR ( $\text{CD}_2\text{Cl}_2$ , 293 K)  $\delta$  = 2.79 (2H, dm,  $^1J_{\text{P,H}} = 266$  Hz, PH), 2.74 (18H, s,  $\text{NMe}_3$ ), 2.8-1.9 (4H, br,  $\text{BH}_2$ ), 1.22 (18H, m, *t*Bu).  $^{31}\text{P}$  NMR ( $\text{CD}_2\text{Cl}_2$ , 293 K)  $\delta$  = -7.3 (d,  $^1J_{\text{P,H}} = 266$  Hz,  $\text{PH}_2$ , *D/L*-isomer), -15.8 (d,  $^1J_{\text{P,H}} = 266$  Hz,  $\text{PH}_2$ , *meso*-isomer).  $^{31}\text{P}\{^1\text{H}\}$  NMR ( $\text{CD}_2\text{Cl}_2$ , 293 K)  $\delta$  = -7.3 (s,  $\text{PH}_2$ , *D/L*-isomer), -15.8 (s,  $\text{PH}_2$ , *meso*-isomer).  $^{11}\text{B}$  NMR ( $\text{CD}_2\text{Cl}_2$ , 293 K)  $\delta$  = -4.9 (br,  $\text{BH}_2$ ).  $^{11}\text{B}\{^1\text{H}\}$  NMR ( $\text{CD}_2\text{Cl}_2$ , 293 K)  $\delta$  = -4.9 (br,  $\text{BH}_2$ ); ESI-MS ( $\text{CH}_3\text{CN}$ )  $m/z$ : 486 ( $\text{M}^+$ ), 458 ( $\text{M}^+-\text{CO}$ ); IR:  $\tilde{\nu}$  = 2940 w, 2860 vw, 2397 w, 2266 w, 1977 m, 1845 s, 1818 s, 1485 m, 1460 m, 1406 vw, 1386 w, 1359 w, 1251 vw, 1164 w, 1127 m, 1083 m, 1018 w, 979 w, 934 vw, 841 m, 816 w, 780 w, 681 s, 647 s;

**Synthesis of  $[(\text{CO})_4\text{W}(\text{tBuPHBH}_2\text{NMe}_3)_2]$  (8)**

$[(\text{CO})_4\text{W}(\text{nbd})]$  (nbd = norbornadiene, 0.2 mmol, 78 mg) and  $\text{tBuPHBH}_2\cdot\text{NMe}_3$  (0.4 mmol, 64 mg) are dissolved in 4 mL toluene at r.t.. After stirring for 16 h at r.t., the solvent is removed *in vacuo*. The remaining yellow solid is washed three times with 2

mL *n*-hexane. By layering a saturated CH<sub>2</sub>Cl<sub>2</sub> solution with *n*-hexane at 293 K compound **8** can be isolated as yellow blocks. Yield: 33 mg (0.059 mmol, 30%); <sup>1</sup>H-NMR (CD<sub>2</sub>Cl<sub>2</sub>, 293 K) δ = 3.16 (2H, dm, <sup>1</sup>J<sub>P,H</sub> = 266 Hz, PH), 2.75 (9H, s, NMe<sub>3</sub>), 2.75 (9H, s NMe<sub>3</sub>), 2.8-1.9 (4H, br, BH<sub>2</sub>), 1.21 (9H, d, *t*Bu). <sup>31</sup>P NMR (CD<sub>2</sub>Cl<sub>2</sub>, 293 K) δ = -46.3 (d, <sup>1</sup>J<sub>P,H</sub> = 266 Hz, PH<sub>2</sub>, *D/L*-isomer), -50.7 (d, <sup>1</sup>J<sub>P,H</sub> = 266 Hz, PH<sub>2</sub>, *meso*-isomer), <sup>31</sup>P{<sup>1</sup>H} NMR (CD<sub>2</sub>Cl<sub>2</sub>, 293 K) δ = -46.3 (s, PH<sub>2</sub>, *D/L*-isomer), -50.7 (s, PH<sub>2</sub>, *meso*-isomer). <sup>11</sup>B NMR (CD<sub>2</sub>Cl<sub>2</sub>, 293 K) δ = -4.8 (br, BH<sub>2</sub>). <sup>11</sup>B{<sup>1</sup>H} NMR (CD<sub>2</sub>Cl<sub>2</sub>, 293 K) δ = -4.8 (br, BH<sub>2</sub>); IR:  $\tilde{\nu}$  = 2948 w, 2861 vw, 2397 w, 2270 w, 1986 w, 1854 m, 1816 vs, 1484 m, 1460 m, 1406 vw, 1359 w, 1253 m, 1188 m, 1126 m, 1081 w, 1020 w, 990 w, 860 m, 842 m, 817 w, 786 m, 696 vw, 609 m; EA: calculated for C<sub>18</sub>H<sub>42</sub>B<sub>2</sub>N<sub>2</sub>O<sub>4</sub>WP<sub>2</sub>: C: 34.99 %; H: 6.85 %; N: 4.53 %; found: C: 34.90 %; H: 6.63 %; N: 4.49 %; ESI-MS (CH<sub>3</sub>CN) *m/z*: 618 (M<sup>+</sup>), 590 (M<sup>+</sup>-CO).

### Crystallographic details

To characterize the products using single crystal X-ray diffraction, a small number of crystals were transferred into dried mineral oil. Thereafter, a suitable crystal was selected and mounted on a Rigaku SuperNova diffractometer with an Atlas detector (**3** and **6**), on a XTaLab Synergy R, DW system with Hy-Pix Arc detector (**7-8**) or a GV1000 with a TitanS2 detector (**1-2**, **4-5**) using MiTeGen loops. All data were collected at 123 K. The software CrysAlisPro (Version 41\_64.93a) was used for data collection and data reduction.<sup>[19]</sup> For structure solution ShelXT<sup>[20]</sup> was used and the subsequent data refinement was carried out with ShelXL.<sup>[21]</sup> Olex2<sup>[22]</sup> was taken for visualization. All atoms are depicted as ellipsoids with a 50% probability level.

Deposition Numbers (for **1**), (for **2**), (for **3**), (for **4**), (for **5**), (for **6**), (for **7**) and (for **8**) contain the supplementary crystallographic data for this paper. These data are provided free of charge by the joint Cambridge Crystallographic Data Centre and Fachinformationszentrum Karlsruhe Access Structures service [www.ccdc.cam.ac.uk/structures](http://www.ccdc.cam.ac.uk/structures).

## 2.5. References

- [1] a) A. Gallen, A. Riera, X. Verdaguer, A. Grabulosa, *Catal. Sci. Technol.* **2019**, *9*, 5504-5561; b) J. T. Fleming, L. J. Higham, *Coord. Chem. Rev.* **2015**, *297-298*, 127-145; c) I. V. Kourkine, S. V. Maslennikov, R. Ditchfield, D. S. Glueck, G. P. A. Yap, L. M. Liable-Sands, A. L. Rheingold, *Inorg. Chem.* **1996**, *35*, 6708-6716; d) P. G. Edwards, B. M. Kariuki, P. D. Newman, H. A. Tallis, C. Williams, *Dalton Trans.* **2014**, *43*, 15532-15545.
- [2] a) K. Tsuge, Y. Chishina, H. Hashiguchi, Y. Sasaki, M. Kato, S. Ishizaka, N. Kitamura, *Coord. Chem. Rev.* **2016**, *306*, 636-651; b) R. Czerwieniec, M. J. Leidl, H. H. H. Homeier, H. Yersin, *Coord. Chem. Rev.* **2016**, *325*, 2-28; c) V. W.-W. Yam, V. K.-M. Au, S. Y.-L. Leung, *Chem. Rev.* **2015**, *115*, 7589-7728; d) C. Marzano, F. Tisato, M. Porchia, M. Pellei, V. Gandin, in *Copper(I) Chemistry of Phosphines, Functionalized Phosphines and Phosphorus Heterocycles* (Ed.: M. S. Balakrishna), Elsevier, **2019**, pp. 83-107; e) R. Narayan, in *Copper(I) Chemistry of Phosphines, Functionalized Phosphines and Phosphorus Heterocycles* (Ed.: M. S. Balakrishna), Elsevier, **2019**, pp. 259-313; f) S. Evariste, A. M. Khalil, M. E. Moussa, A. K.-W. Chan, E. Y.-H. Hong, H.-L. Wong, B. Le Guennic, G. Calvez, K. Costuas, V. W.-W. Yam, C. Lescop, *J. Am. Chem. Soc.* **2018**, *140*, 12521-12526.
- [3] a) O. M. A. Salah, M. I. Bruce, P. J. Lohmeyer, C. L. Raston, B. W. Skelton, A. H. White, *Dalton Trans.* **1981**, 962-967; b) G. A. Bowmaker, Effendy, R. D. Hart, J. D. Kildea, A. H. White, *Aust. J. Chem.* **1997**, *50*, 653-670; c) M. F. Davis, M. Jura, W. Levason, G. Reid, M. Webster, *J. Organomet. Chem.* **2007**, *692*, 5589-5597; d) J. R. Black, W. Levason, M. D. Spicer, M. Webster, *Dalton Trans.* **1993**, 3129-3136.
- [4] a) H. C. Johnson, A. S. Weller, *Angew. Chem. Int. Ed.* **2015**, *54*, 10173-10177; b) H. C. Johnson, E. M. Leitao, G. R. Whittell, I. Manners, G. C. Lloyd-Jones, A. S. Weller, *J. Am. Chem. Soc.* **2014**, *136*, 9078-9093; c) A. N. Marziale, A. Friedrich, I. Klopsch, M. Drees, V. R. Celinski, J. Schmedt auf der Günne, S. Schneider, *J. Am. Chem. Soc.* **2013**, *135*, 13342-13355; d) S. Pandey, P. Lönnecke, E. Hey-Hawkins, *Eur. J. Inorg. Chem.* **2014**, *2014*, 2456-2465; e) D. Han, F. Anke, M. Trose, T. Beweries, *Coord. Chem. Rev.* **2019**, *380*, 260-286; f) J. A. Bailey, P. G. Pringle, *Coord. Chem. Rev.* **2015**, *297-298*, 77-90; g) R. T. Paine, H. Noeth, *Chem. Rev.* **1995**, *95*, 343-379.

- [5] a) K.-C. Schwan, A. Y. Timoskin, M. Zabel, M. Scheer, *Chem. Eur. J.* **2006**, *12*, 4900-4908; b) U. Vogel, P. Hoemensch, K.-C. Schwan, A. Y. Timoshkin, M. Scheer, *Chem. Eur. J.* **2003**, *9*, 515-519; c) C. Marquardt, T. Jurca, K.-C. Schwan, A. Stauber, A. V. Virovets, G. R. Whittell, I. Manners, M. Scheer, *Angew. Chem. Int. Ed.* **2015**, *54*, 13782-13786; d) A. Stauber, T. Jurca, C. Marquardt, M. Fleischmann, M. Seidl, G. R. Whittell, I. Manners, M. Scheer, *Eur. J. Inorg. Chem.* **2016**, 2684-2687; e) O. Hegen, A. V. Virovets, A. Y. Timoshkin, M. Scheer, , *Chem. Eur. J.* **2018**, *24*, 16521-16525; f) C. Marquardt, A. Adolf, A. Stauber, M. Bodensteiner, A. V. Virovets, A. Y. Timoshkin, M. Scheer, , *Chem. Eur. J.* **2013**, *19*, 11887-11891; g) F. Lehnfeld, M. Seidl, A. Y. Timoshkin, M. Scheer, *Eur. J. Inorg. Chem.* **2022**, 2022, e202100930.
- [6] C. Marquardt, T. Kahoun, J. Baumann, A. Y. Timoshkin, M. Scheer, *Z. Anorg. Allg. Chem.* **2017**, *643*, 1326-1330.
- [7] C. Marquardt, O. Hegen, T. Kahoun, M. Scheer, *Chem. Eur. J.* **2017**, *23*, 4397-4404.
- [8] a) C. Marquardt, T. Kahoun, A. Stauber, G. Balázs, M. Bodensteiner, A. Y. Timoshkin, M. Scheer, *Angew. Chem. Int. Ed.* **2016**, *55*, 14828-14832; b) C. Marquardt, G. Balázs, J. Baumann, A. V. Virovets, M. Scheer, *Chem. Eur. J.* **2017**, *23*, 11423-11429; c) C. Marquardt, C. Thoms, A. Stauber, G. Balázs, M. Bodensteiner, M. Scheer, *Angew. Chem. Int. Ed.* **2014**, *53*, 3727-3730.
- [9] C. Thoms, C. Marquardt, A. Y. Timoshkin, M. Bodensteiner, M. Scheer, *Angew. Chem. Int. Ed.* **2013**, *52*, 5150-5154.
- [10] K.-C. Schwan, A. Adolf, M. Bodensteiner, M. Zabel, M. Scheer, *Z. Anorg. Allg. Chem.* **2008**, *634*, 1383-1387
- [11] M. Elsayed Moussa, J. Braese, C. Marquardt, M. Seidl, M. Scheer, *Eur. J. Inorg. Chem.* **2020**, 2020, 2501-2505.
- [12] M. Elsayed Moussa, C. Marquardt, O. Hegen, M. Seidl, M. Scheer, *New J. Chem.* **2021**, *45*, 14916-14919.
- [13] U. Vogel, K.-C. Schwan, P. Hoemensch, M. Scheer, *Eur. J. Inorg. Chem.* **2005**, *2005*, 1453-1458.
- [14] J. Braese, A. Schinabeck, M. Bodensteiner, H. Yersin, A. Y. Timoshkin, M. Scheer, *Chem. Eur. J.* **2018**, *24*, 10073-10077.
- [15] O. Hegen, J. Braese, A. Y. Timoshkin, M. Scheer, *Chem. Eur. J.* **2019**, *25*, 485-489.

- [16] O. Hegen, C. Marquardt, A. Y. Timoshkin, M. Scheer, *Angew. Chem. Int. Ed.* **2017**, *56*, 12783-12787.
- [17] a) W.-L. Su, H.-P. Huang, W.-T. Chen, W.-Y. Hsu, H.-Y. Chang, S.-Y. Ho, S.-P. Wang, S.-G. Shyu, *J. Chin. Chem. Soc.* **2011**, *58*, 163-173; b) T. J. Malosh, S. R. Wilson, J. R. Shapley, *Inorg. Chim. Acta* **2009**, *362*, 2849-2855.
- [18] E. Subasi, S. Karahan, A. Ercag, *Russ. J. Coord. Chem.* **2007**, *33*, 886-890.
- [19] CrysAlisPro Software System, Rigaku Oxford Diffraction, **2020**.
- [20] G. Sheldrick, *Acta Cryst. A71* **2015**, 3-8.
- [21] G. Sheldrick, *Acta Cryst. C71* **2015**, 3-8.
- [22] O. V. Dolomanov, L. J. Bourhis, R. J. Gildea, J. A. K. Howard, H. Puschmann, *J. Appl. Crystallogr.* **2009**, *42*, 339-341.

## 2.6. Supporting Information

### Single crystal X-ray diffraction

Compound	1	2	3
Formula	C <sub>10</sub> H <sub>26</sub> B <sub>2</sub> CrN <sub>2</sub> O <sub>4</sub> P <sub>2</sub>	C <sub>10</sub> H <sub>26</sub> B <sub>2</sub> MoN <sub>2</sub> O <sub>4</sub> P <sub>2</sub>	C <sub>10</sub> H <sub>26</sub> B <sub>2</sub> N <sub>2</sub> O <sub>4</sub> P <sub>2</sub> W
<i>D</i> <sub>calc.</sub> / g cm <sup>-3</sup>	1.303	1.408	1.720
$\mu$ /mm <sup>-1</sup>	5.057	5.248	12.621
Formula Weight	373.89	417.83	505.74
Color	Yellow	Yellow	clear yellow
Shape	Plate	Block	block
Size/mm <sup>3</sup>	0.26×0.18×0.07	0.05x0.05x0.05	0.29×0.11×0.08
<i>T</i> /K	122.98(13)	123.00(10)	123.00(10)
Crystal System	monoclinic	monoclinic	monoclinic
Space Group	<i>P</i> 2 <sub>1</sub> / <i>n</i>	<i>P</i> 2 <sub>1</sub> / <i>n</i>	<i>P</i> 2 <sub>1</sub> / <i>n</i>
<i>a</i> /Å	9.44270(10)	9.61370(10)	9.5756(2)
<i>b</i> /Å	11.94450(10)	11.98250(10)	11.9386(3)
<i>c</i> /Å	16.9150(2)	17.1217(2)	17.0963(5)
$\alpha$ °	90	90	90
$\beta$ °	92.2460(10)	92.1980(10)	92.201(2)
$\gamma$ °	90	90	90
<i>V</i> /Å <sup>3</sup>	1906.35(3)	1970.90(3)	1952.99(9)
<i>Z</i>	4	4	4
<i>Z'</i>	1	1	1
Wavelength/Å	1.39222	1.39222	1.54184
Radiation type	CuK $\beta$	CuK $\beta$	CuK $\alpha$
$\theta$ <sub>min</sub> °	4.092	4.067	4.518
$\theta$ <sub>max</sub> °	60.261	74.57	73.788
Measured Refl's.	13076	17597	6618
Indep't Refl's	3785	5455	3758
<i>R</i> <sub>int</sub>	0.0207	0.0221	0.0158
Parameters	220	228	228
Restraints	0	0	0
Largest Peak	0.38	0.63	0.548
Deepest Hole	-0.20	-0.58	-0.950
GooF	1.025	1.054	1.115
<i>wR</i> <sub>2</sub> (all data)	0.0652	0.0554	0.0522
<i>wR</i> <sub>2</sub>	0.0639	0.0545	0.0514
<i>R</i> <sub>I</sub> (all data)	0.0256	0.0224	0.0212
<i>R</i> <sub>I</sub>	0.0240	0.0212	0.0197

Compound	4	5	6
Formula	C <sub>10</sub> H <sub>26</sub> As <sub>2</sub> B <sub>2</sub> CrN <sub>2</sub> O <sub>4</sub>	C <sub>10</sub> H <sub>26</sub> As <sub>2</sub> B <sub>2</sub> MoN <sub>2</sub> O <sub>4</sub>	C <sub>10</sub> H <sub>26</sub> As <sub>2</sub> B <sub>2</sub> N <sub>2</sub> O <sub>4</sub> W
<i>D</i> <sub>calc.</sub> / g cm <sup>-3</sup>	1.566	1.668	1.964
$\mu$ /mm <sup>-1</sup>	6.551	3.923	14.431
Formula Weight	461.79	505.73	593.64
Color	Yellow	Yellow	colorless
Shape	Block	Block	block
Size/mm <sup>3</sup>	0.2x0.1x0.1	0.15x0.1x0.05	0.30x0.09x0.06
<i>T</i> /K	123.02(13)	293(2)	123.00(10)
Crystal System	Monoclinic	monoclinic	monoclinic
Space Group	P2 <sub>1</sub> /n	P2 <sub>1</sub> /n	P2 <sub>1</sub> /n
<i>a</i> /Å	9.57770(10)	9.7495(2)	9.7332(2)
<i>b</i> /Å	11.9949(2)	12.0007(3)	12.0019(3)
<i>c</i> /Å	17.0539(2)	17.2175(4)	17.1944(5)
$\alpha$ <sup>o</sup>	90	90	90
$\beta$ <sup>o</sup>	91.2580(10)	91.200(2)	91.403(3)
$\gamma$ <sup>o</sup>	90	90	90
<i>V</i> /Å <sup>3</sup>	1958.74(4)	2014.02(8)	2007.99(9)
<i>Z</i>	4	4	4
<i>Z'</i>	1	1	1
Wavelength/Å	1.39222	0.71073	1.54184
Radiation type	CuK <sub>β</sub>	MoK <sub>α</sub>	CuK <sub>α</sub>
$\theta_{min}$ <sup>o</sup>	4.069	3.395	4.493
$\theta_{max}$ <sup>o</sup>	74.057	31.608	73.728
Measured Refl's.	15874	23365	7066
Indep't Refl's	5270	6222	7066
<i>R</i> <sub>int</sub>	0.0286	0.0311	/
Parameters	228	220	218
Restraints	0	0	8
Largest Peak	0.80	0.88	1.827
Deepest Hole	-0.60	-0.74	-1.717
GooF	1.033	1.047	1.043
<i>wR</i> <sub>2</sub> (all data)	0.0660	0.0661	0.1648
<i>wR</i> <sub>2</sub>	0.0640	0.0622	0.1608
<i>R</i> <sub>1</sub> (all data)	0.0273	0.0374	0.0672
<i>R</i> <sub>1</sub>	0.0247	0.0278	0.0630

Compound	7	8
Formula	C <sub>18</sub> H <sub>42</sub> B <sub>2</sub> CrN <sub>2</sub> O <sub>4</sub> P <sub>2</sub>	C <sub>18</sub> H <sub>42</sub> B <sub>2</sub> N <sub>2</sub> O <sub>4</sub> P <sub>2</sub> W
<i>D</i> <sub>calc.</sub> /g cm <sup>-3</sup>	1.198	1.489
$\mu$ /mm <sup>-1</sup>	4.800	9.050
Formula Weight	486.09	617.94
Color	Yellow	Yellow
Shape	Block	Block
Size/mm <sup>3</sup>	0.14x0.1x0.06	0.06x0.08x0.09
<i>T</i> /K	123.01(10)	123.00(10)
Crystal System	monoclinic	monoclinic
Space Group	P2 <sub>1</sub>	P2 <sub>1</sub> /n
<i>a</i> /Å	10.01360(10)	11.4878(2)
<i>b</i> /Å	12.3037(2)	15.7210(3)
<i>c</i> /Å	11.3278(2)	15.2642(3)
$\alpha^\circ$	90	90
$\beta^\circ$	105.016(2)	91.323(2)
$\gamma^\circ$	90	90
<i>V</i> /Å <sup>3</sup>	1347.98(4)	2755.98(9)
<i>Z</i>	2	4
<i>Z'</i>	1	1
Wavelength/Å	1.54184	1.54184
Radiation type	CuK $\alpha$	CuK $\alpha$
$\theta_{min}^\circ$	4.041	4.037
$\theta_{max}^\circ$	73.792	73.376
Measured Refl's.	24251	11354
Indep't Refl's	5277	11354
<i>R</i> <sub>int</sub>	0.0234	\
Parameters	298	299
Restraints	1	0
Largest Peak	0.26	2.49
Deepest Hole	-0.39	-2.76
Flack parameter	-0.010(4)	
GooF	1.116	1.096
<i>wR</i> <sub>2</sub> (all data)	0.0722	0.2135
<i>wR</i> <sub>2</sub>	0.0719	0.2045
<i>R</i> <sub>1</sub> (all data)	0.0279	0.0858
<i>R</i> <sub>1</sub>	0.0273	0.0744

## Solid state structures

### $[(\text{CO})_4\text{Cr}(\text{PH}_2\text{BH}_2\text{NMe}_3)_2]$ (1)

Compound **1** crystallizes from saturated  $\text{CH}_2\text{Cl}_2$  solution layered with *n*-hexane at 277 K as yellow blocks in the monoclinic space group  $P2_1/n$ . A suitable crystal with dimensions  $0.26 \times 0.18 \times 0.07 \text{ mm}^3$  was selected and mounted on a GV1000, TitanS2 diffractometer. The crystal was kept at a steady  $T = 122.98(13)$  K during data collection. The structure was solved with the **ShelXT**<sup>[1]</sup> solution program using dual methods and by using **Olex2 1.5-alpha**<sup>[2]</sup> as the graphical interface. The model was refined with **ShelXL** 2018/3<sup>[3]</sup> using full matrix least squares minimization on  $F^2$ . Figure S1 shows the structure in the solid state.

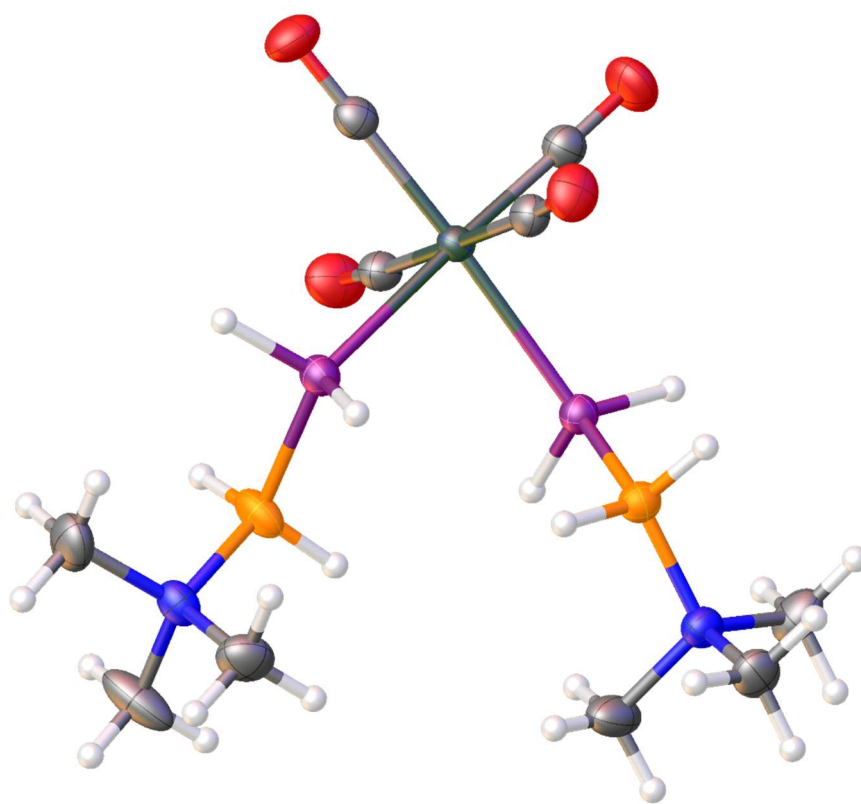


**Figure S1.** Molecular structure of compound **1** in the solid state. The thermal ellipsoids are displayed at 50% probability. Selected bond distances (Å) and angles [°]: Cr1-P1 2.3979(4), Cr1-P2 2.3998(4), P1-B1 1.9576(17), P2-B2 1.9565(18), N1-B1 1.612(2), N2-B2 1.613(2); P1-Cr1-P2 86.8(1), B1-P1-Cr1 119.0(1), B2-P2-Cr1 119.1(5), N2-B2-P2 115.6(1), N1-B1-P1 115.7(1).

**[(CO)<sub>4</sub>Mo(PH<sub>2</sub>BH<sub>2</sub>NMe<sub>3</sub>)<sub>2</sub>] (2)**

Compound **2** crystallizes from saturated CH<sub>2</sub>Cl<sub>2</sub> solution layered with *n*-hexane at 277 K as yellow blocks in the monoclinic space group *P*2<sub>1</sub>/*n*. A suitable crystal with dimensions 0.05×0.05×0.05mm<sup>3</sup> was selected and mounted on a GV1000, TitanS2 diffractometer. The crystal was kept at a steady T = 123.00(10) K during data collection. The structure was solved with the **ShelXT**<sup>[1]</sup> solution program using dual methods and by using **Olex2 1.5-alpha**<sup>[2]</sup> as the graphical interface. The model was refined with **ShelXL** 2018/3<sup>[3]</sup> using full matrix least squares minimization on *F*<sup>2</sup>. Figure S2 shows the structure in the solid state.

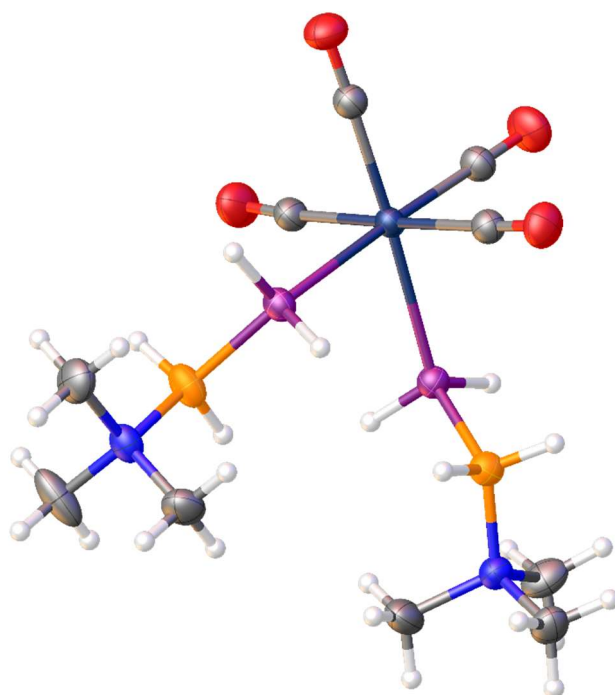


**Figure S2.** Molecular structure of compound **2** in the solid state. The thermal ellipsoids are displayed at 50% probability. Selected bond distances (Å) and angles [°]: Mo1-P1 2.5494(3), Mo1-P2 2.5523(3), P1-B1 1.9630(14), P2-B2 1.9515(17), N2-B2 1.6162(19), N1-B1 1.6156(19); P1-Mo1-P2 85.7(11), B1-P1-Mo1 118.7(5), N1-B1-P1 115.0(9), B2-P2-Mo1 118.4(5), N2-B2-P2 115.9(10).

**$[(\text{CO})_4\text{W}(\text{PH}_2\text{BH}_2\text{NMe}_3)_2]$  (**3**)**

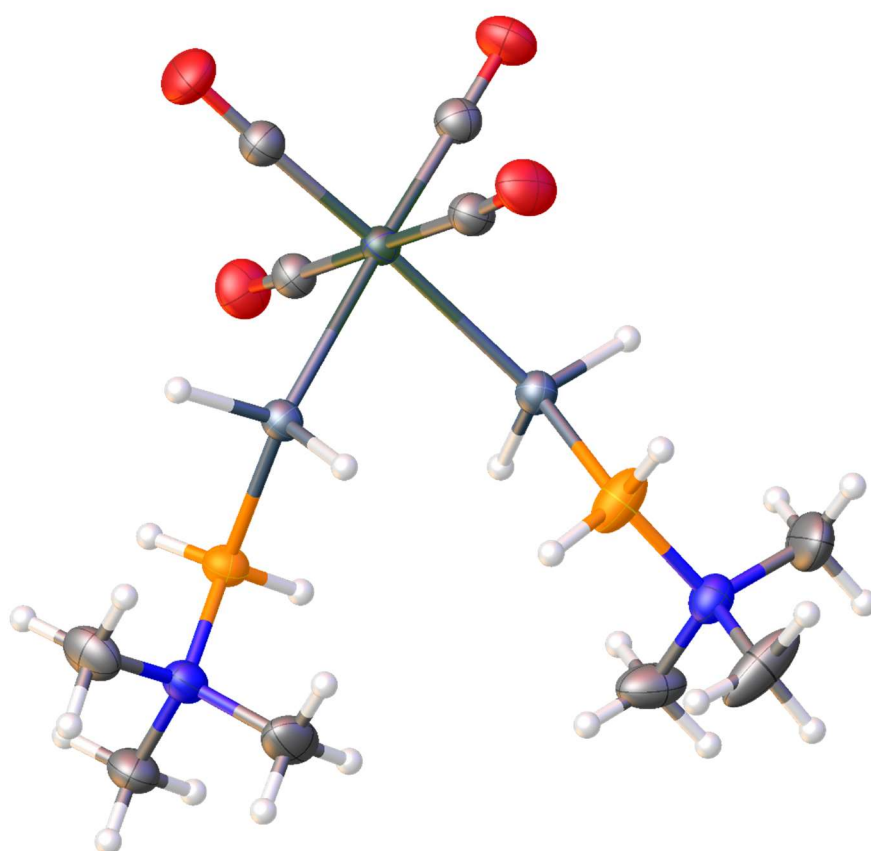
Compound **3** crystallizes from  $\text{CH}_2\text{Cl}_2$  at 243 K as yellow blocks in the monoclinic space group  $P2_1/n$ . A suitable crystal with dimensions  $0.29 \times 0.11 \times 0.08 \text{ mm}^3$  was selected and mounted on Rigaku SuperNova diffractometer. The crystal was kept at a steady  $T = 123.00(10)$  K during data collection. The structure was solved with the **ShelXT**<sup>[1]</sup> solution program using dual methods and by using **Olex2 1.5-alpha**<sup>[2]</sup> as the graphical interface. The model was refined with **ShelXL 2018/3**<sup>[3]</sup> using full matrix least squares minimization on  $F^2$ . Figure S3 shows the structure in the solid state.



**Figure S3.** Molecular structure of compound **3** in the solid state. The thermal ellipsoids are displayed at 50% probability. Selected bond distances (Å) and angles [°]: W1-P1 2.5408(7), W1-P2 2.5363(7), N1-B1 1.615(4), P1-B1 1.951(4), P2-B2 1.962(3), N2-B2 1.605(4); P2-W1-P3 85.44(2), B1-P1-W1 118.44(10), B2-P2-W1 118.70(10), N1-B1-P1 115.7(2), N2-B2-P2 115.4(2).

**$[(\text{CO})_4\text{Cr}(\text{AsH}_2\text{BH}_2\text{NMe}_3)_2]$  (4)**

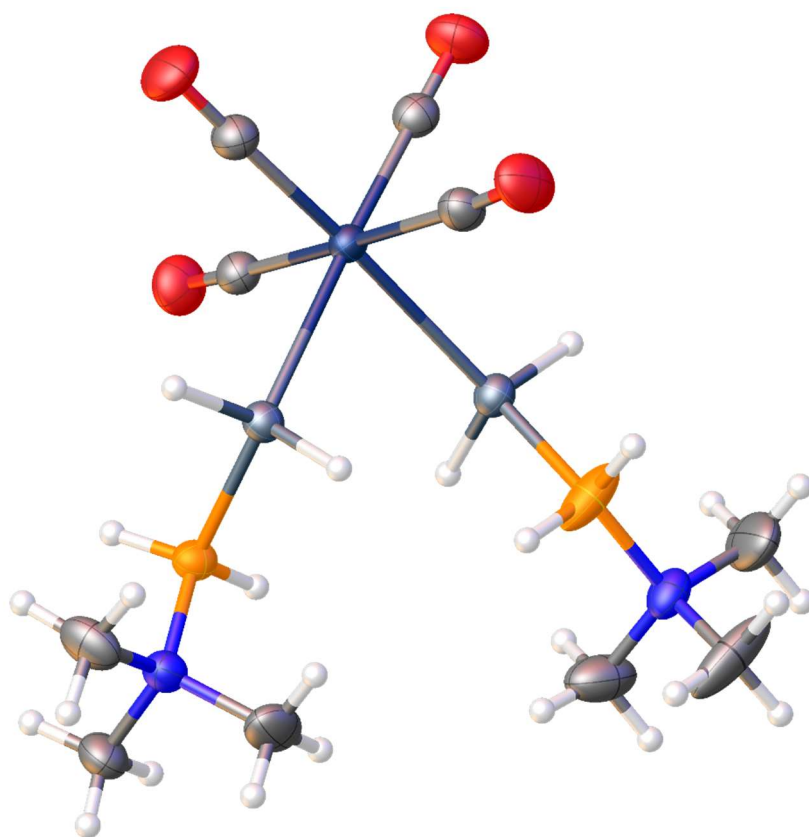
Compound **4** crystallizes from saturated  $\text{CH}_2\text{Cl}_2$  solution layered with *n*-hexane at 277 K as yellow blocks in the monoclinic space group  $P2_1/n$ . A suitable crystal with dimensions  $0.2 \times 0.1 \times 0.1 \text{ mm}^3$  was selected and mounted on a GV1000, TitanS2 diffractometer. The crystal was kept at a steady  $T = 123.00(10)$  K during data collection. The structure was solved with the **ShelXT**<sup>[1]</sup> solution program using dual methods and by using **Olex2 1.5-alpha**<sup>[2]</sup> as the graphical interface. The model was refined with **ShelXL 2018/3**<sup>[3]</sup> using full matrix least squares minimization on  $F^2$ . Figure S4 shows the structure in the solid state.



**Figure S4.** Molecular structure of compound **4** in the solid state. The thermal ellipsoids are displayed at 50% probability. Selected bond distances (Å) and angles [°]: As1-Cr1 2.4968(3), As1-B1 2.0670(19), As2-Cr1 2.4960(3), As2-B2 2.059(2), N1-B1 1.607(2), N2-B2 1.604(3); B1-As1-Cr1 119.70(6), B2-As2-Cr1 119.13(6), As2-Cr1-As1 86.066(10), N1-B1-As1 115.19(12), N2-B2-As2 116.04(14).

**$[(\text{CO})_4\text{Mo}(\text{AsH}_2\text{BH}_2\text{NMe}_3)_2]$  (**5**)**

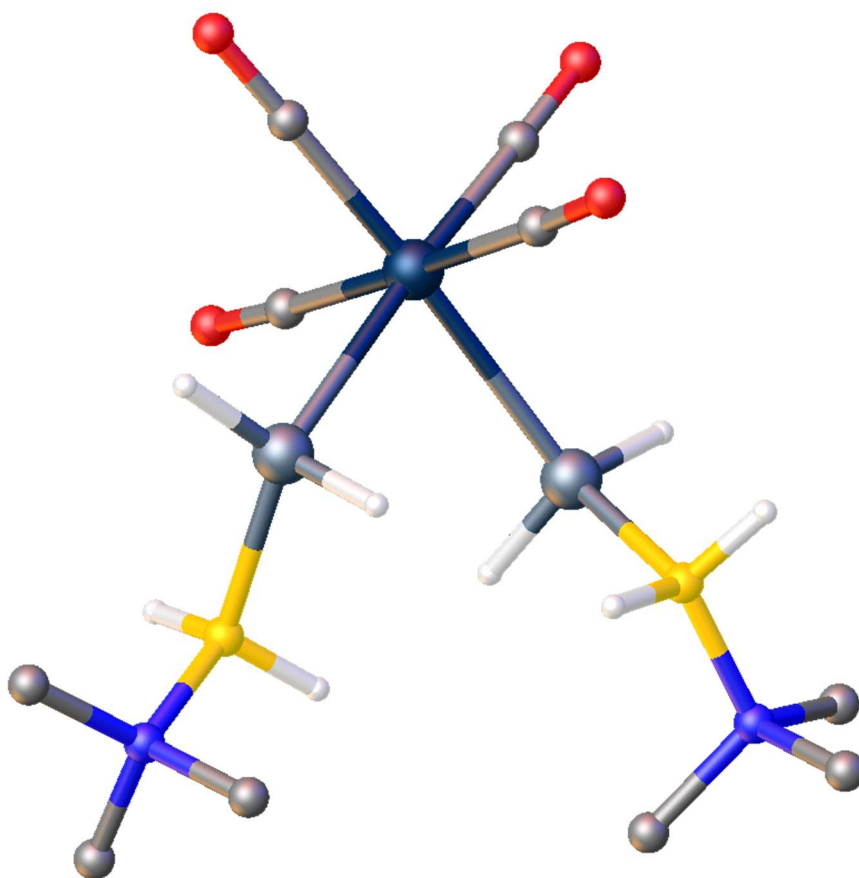
Compound **5** crystallizes from a  $\text{CH}_2\text{Cl}_2/n$ -hexane layering at 273 K as yellow blocks in the monoclinic space group  $P2_1/n$ . A suitable crystal with dimensions  $0.15 \times 0.1 \times 0.05$  mm<sup>3</sup> was selected and mounted on a GV1000, TitanS2 diffractometer. The crystal was kept at a steady  $T = 293(2)$  K during data collection. The structure was solved with the **ShelXT** 2014/5<sup>[1]</sup> solution program using dual methods and by using **Olex2 1.5-alpha**<sup>[2]</sup> as the graphical interface. The model was refined with **ShelXL** 2018/3<sup>[3]</sup> using full matrix least squares minimization on  $F^2$ . Figure S5 shows the structure in the solid state.



**Figure S5.** Molecular structure of compound **5** in the solid state. The thermal ellipsoids are displayed at 50% probability. Selected bond distances (Å) and angles Mo1-As1 2.6391(3), Mo1-As1 2.6403(3), N1-B1 1.603(3), As1-B1 2.062(2), N2-B2 1.597(4), As2-B2 2.058(3); As1-Mo1-As2-84.848(8), B1-As1-Mo1-119.86(7), N1-B1-As1-115.28(15), B2-As2-Mo1-118.75(8), N2-B2-As2-116.19(17).

**$[(\text{CO})_4\text{W}(\text{AsH}_2\text{BH}_2\text{NMe}_3)_2]$  (**6**)**

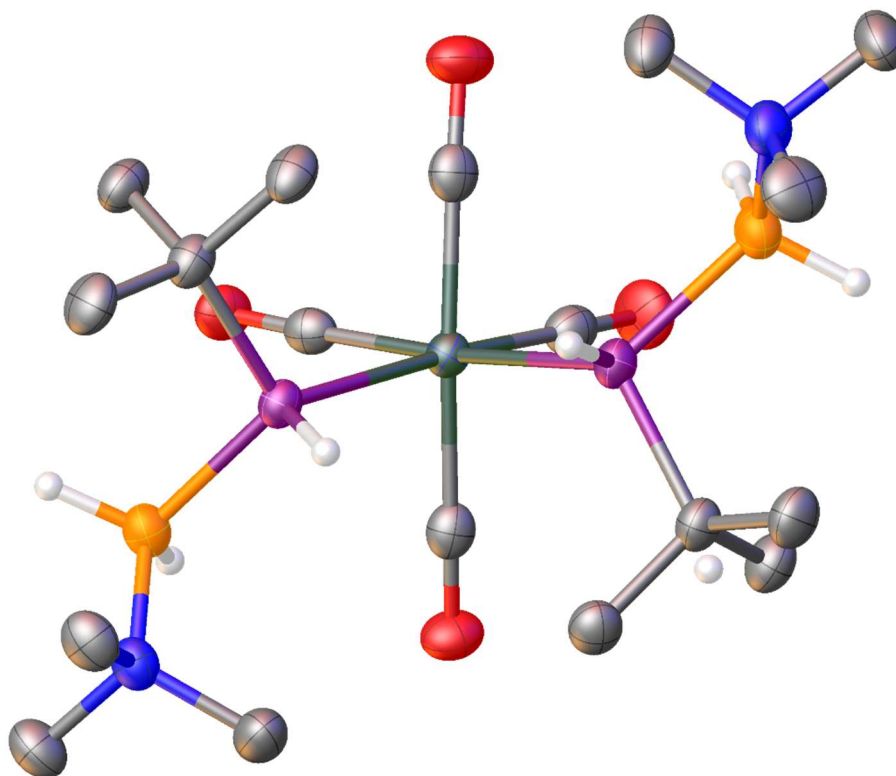
Compound **6** crystallizes from a  $\text{CH}_2\text{Cl}_2$  solution at 243 K as yellow blocks in the monoclinic space group  $P2_1/n$ . A suitable crystal with dimensions  $0.30 \times 0.09 \times 0.06 \text{ mm}^3$  was selected and mounted on a Rigaku SuperNova diffractometer. The crystal was kept at a steady  $T = 123.00(10) \text{ K}$  during data collection. The structure was solved with the **ShelXT 2014/5**<sup>[1]</sup> solution program using dual methods and by using **Olex2 1.5-alpha**<sup>[2]</sup> as the graphical interface. The model was refined with **ShelXL 2018/3**<sup>[3]</sup> using full matrix least squares minimization on  $F^2$ . Figure S6 shows the structure in the solid state. All crystals of **6** showed twinning and were refined applying hklf5 refinement.



**Figure S6.** Molecular structure of compound **6** in the solid state. The thermal ellipsoids are displayed at 50% probability. Selected bond distances (Å) and angles [°]: W1-As1 2.6337(9), W1-As2 2.6353(9), N1-B1 1.602(11), N2-B2 1.62(2), As1-B1 2.072(9), As2-B2 2.07(2); As1-W1-As2 84.56(3), B1-As1-W1 119.5(3), B2-As2-W1 119.4(8), N1-B1-As1 115.0(6), N2-B2-As2 114.5(14).

**$[(\text{CO})_4\text{Cr}(\text{tBuPHBH}_2\text{NMe}_3)_2]$  (7)**

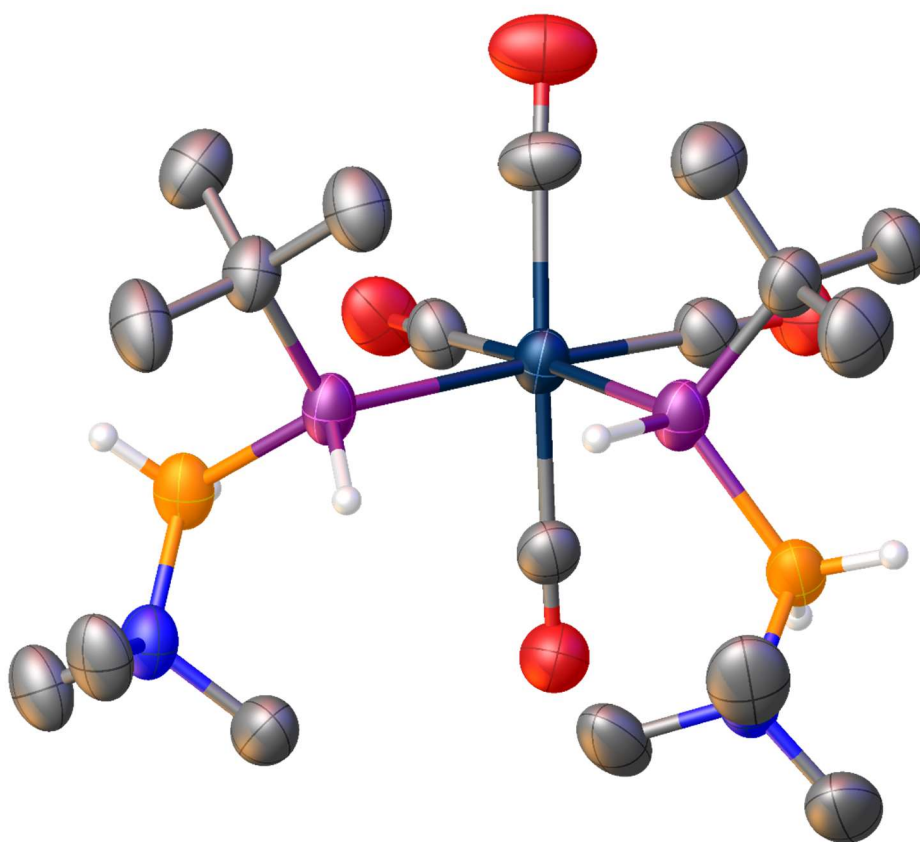
Compound **7** crystallizes from a  $\text{CH}_2\text{Cl}_2/n$ -hexane layering at 277 K as yellow blocks in the monoclinic space group  $P2_1$ . A suitable crystal with dimensions 0.14x0.1x0.06 mm<sup>3</sup> was selected and mounted on a XTaLab Synergy R, DW system with Hy-Pix Arc detector. The crystal was kept at a steady  $T = 123.01(10)$  K during data collection. The structure was solved with the **ShelXT** 2014/5<sup>[1]</sup> solution program using dual methods and by using **Olex2 1.5-alpha**<sup>[2]</sup> as the graphical interface. The model was refined with **ShelXL** 2018/3<sup>[3]</sup> using full matrix least squares minimization on  $F^2$ . Figure S7 shows the structure in the solid state. **7** crystallizes a racemate with both enantiomers present in the unit cell.



**Figure S7.** Molecular structure of compound **7** in the solid state. The thermal ellipsoids are displayed at 50% probability. Selected bond distances (Å) and angles [°]: Cr1-P1 2.4336(8), Cr1-P2 2.4251(8), N1-B1 1.620(4), P1-C1 1.890(3), N2-B2 1.618(5), P1-B1 2.003(4), P2-C8 1.890(3), P2-B2 1.997(4); P2-Cr1-P1 91.20(3), B1-P1-Cr1 116.44(11), B2-P2-Cr1 114.36(11), N2-B2-P2 115.8(2), N1-B1-P1 116.2(2).

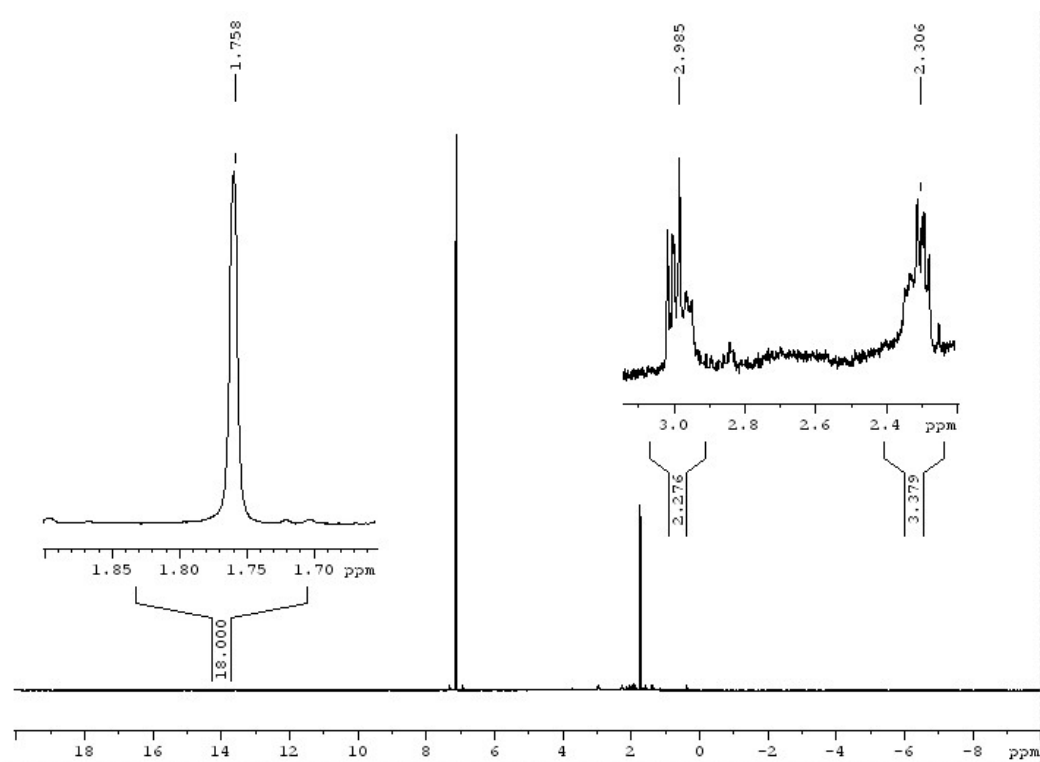
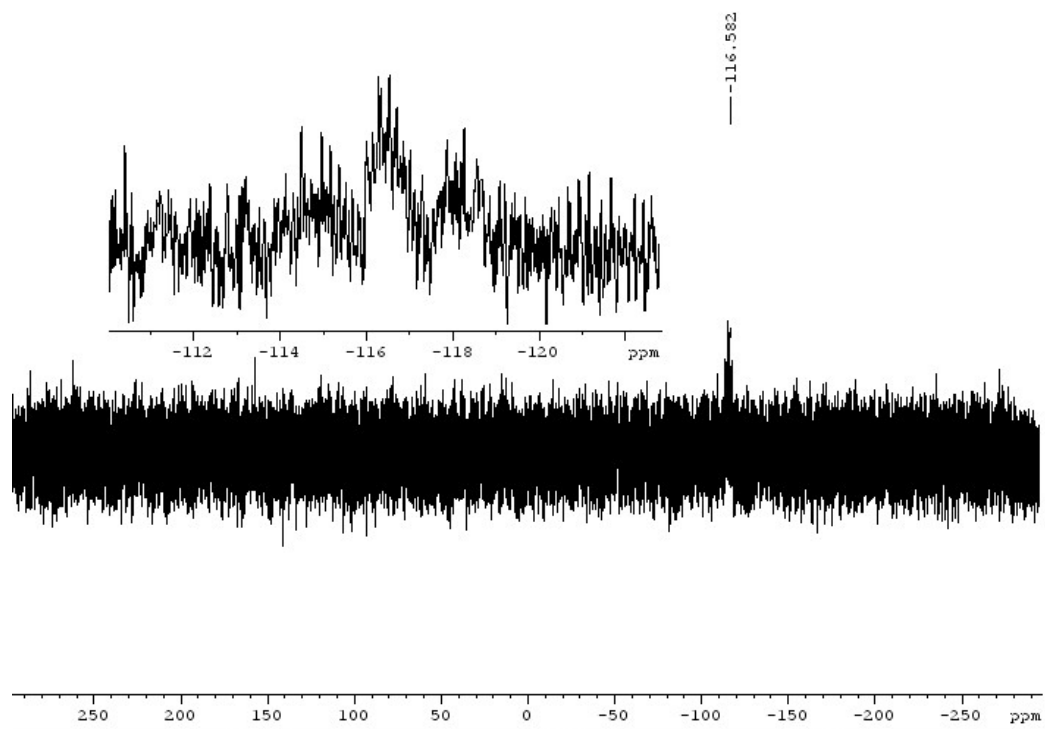
**$[(\text{CO})_4\text{W}(\text{tBuPHBH}_2\text{NMe}_3)_2]$  (**8**)**

Compound **8** crystallizes from a  $\text{CH}_2\text{Cl}_2/n$ -hexane layering at 277 K as yellow blocks in the monoclinic space group  $P2_1/n$ . A suitable crystal with dimensions 0.06x0.08x0.09  $\text{mm}^3$  was selected and mounted on a XTaLab Synergy R, DW system with Hy-Pix Arc detector. The crystal was kept at a steady  $T = 123.01(10)$  K during data collection. The structure was solved with the **ShelXT** 2014/5<sup>[1]</sup> solution program using dual methods and by using **Olex2 1.5-alpha**<sup>[2]</sup> as the graphical interface. The model was refined with **ShelXL** 2018/3<sup>[3]</sup> using full matrix least squares minimization on  $F^2$ . Figure S8 shows the structure in the solid state.



**Figure S8.** Molecular structure of compound **8** in the solid state. The thermal ellipsoids are displayed at 50% probability. Selected bond distances ( $\text{\AA}$ ) and angles [ $^\circ$ ]: W1-P1 2.579(3), W1-P2 2.576(3), N1-B1 1.618(16), N2-B2 1.626(16), P1-B1 1.980(13), P2-B2 1.993(14); P2-W1-P1 90.11(9), B1-P1-W1 115.7(4), B2-P2-W1 114.6(5), N1-B1-P1 116.2(8), N2-B2-P2 114.4(9).

## NMR spectra

 $[(\text{CO})_4\text{Cr}(\text{PH}_2\text{BH}_2\text{NMe}_3)_2]$  (**1**)Figure S9.  $^1\text{H}$  NMR spectrum of **1** in  $\text{C}_6\text{D}_6$ Figure S10.  $^{31}\text{P}$  NMR spectrum of **1** in  $\text{C}_6\text{D}_6$

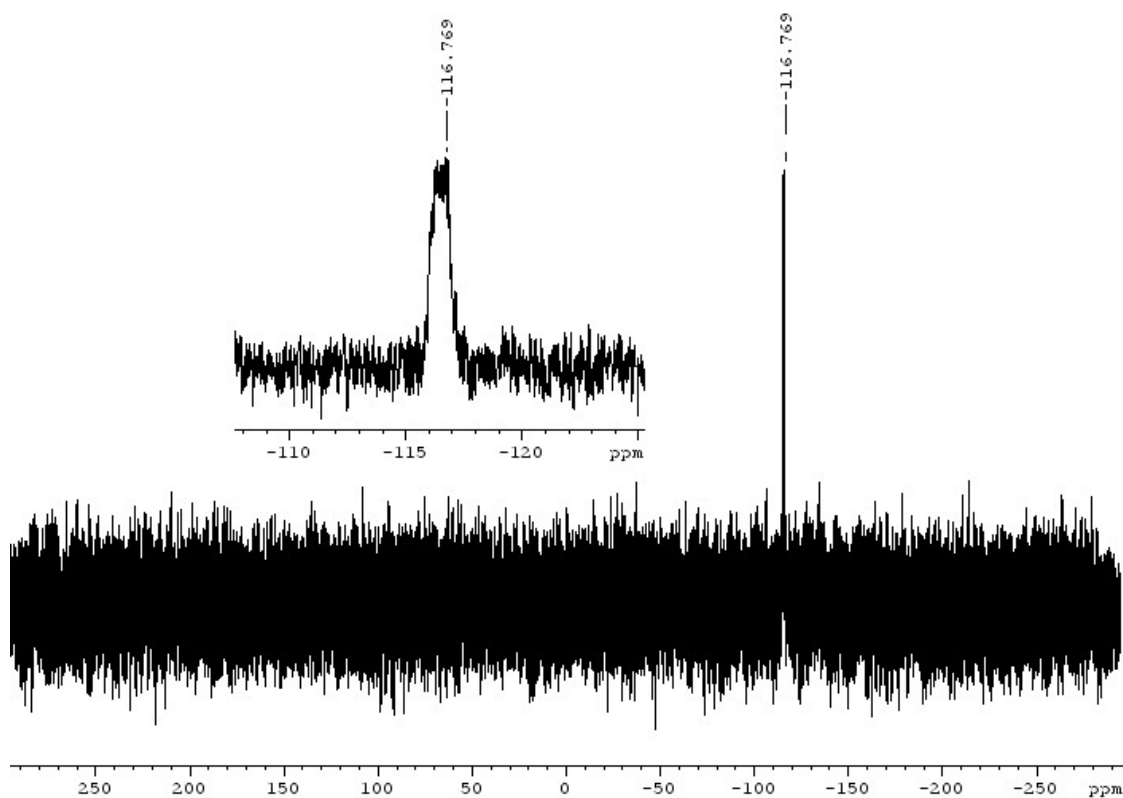


Figure S11.  $^{31}\text{P}\{^1\text{H}\}$  NMR spectrum of **1** in  $\text{C}_6\text{D}_6$

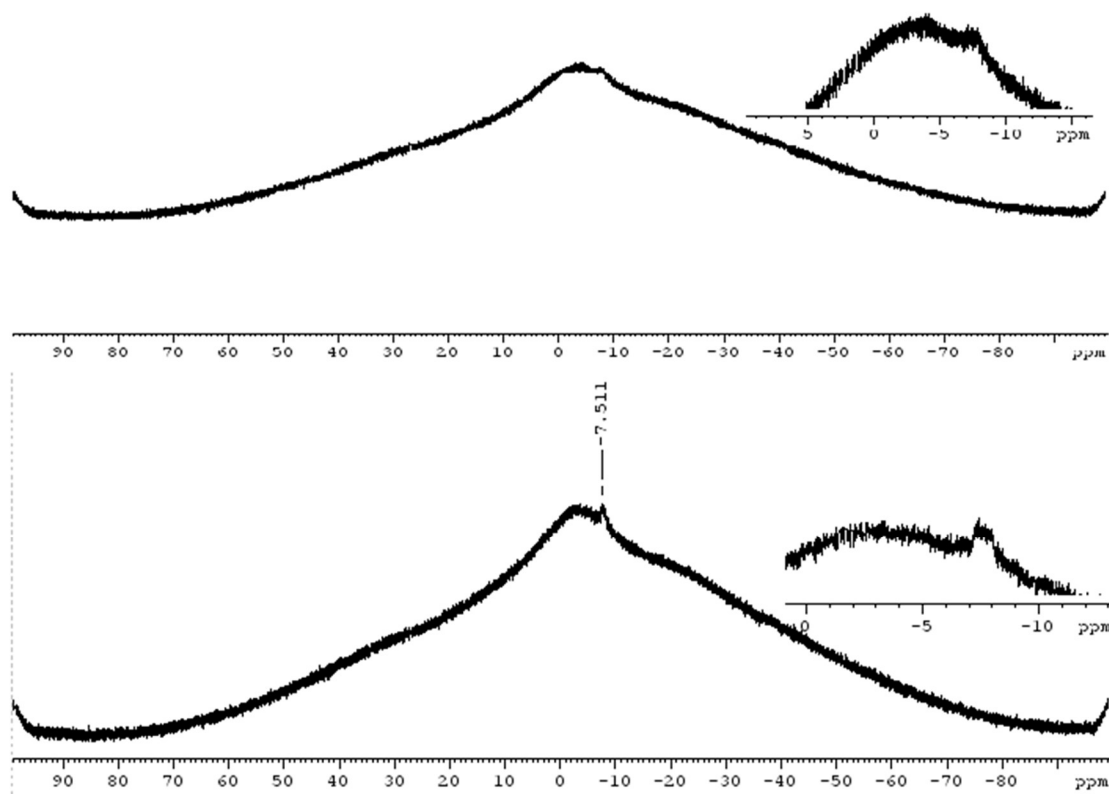
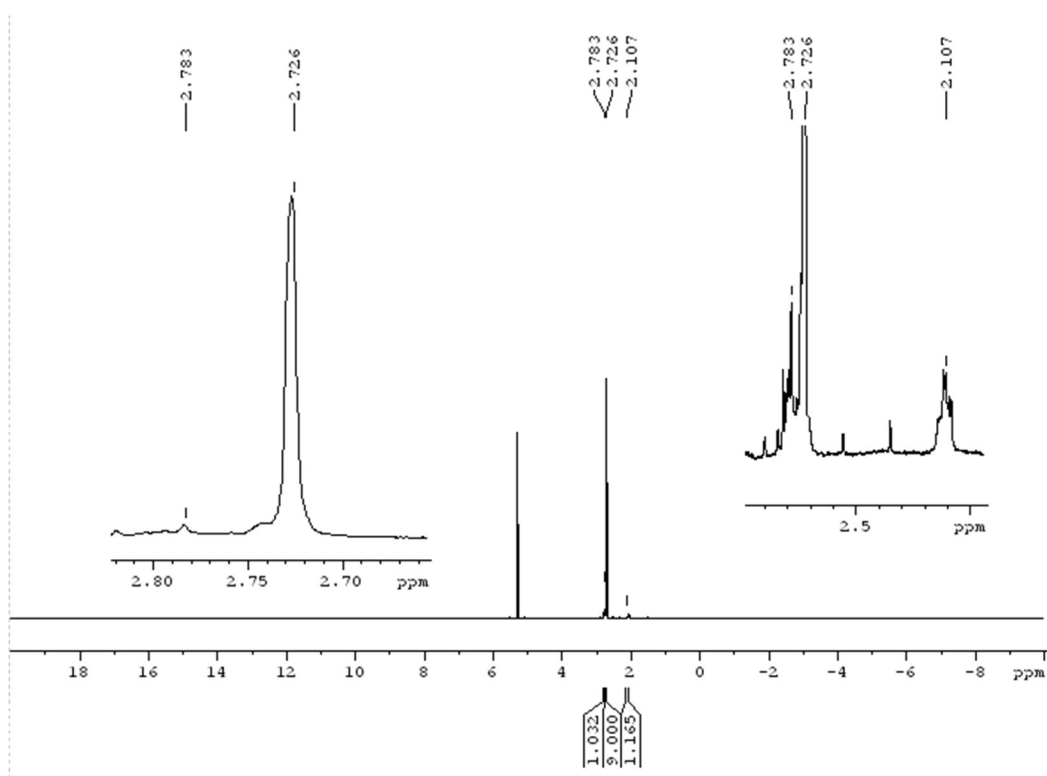
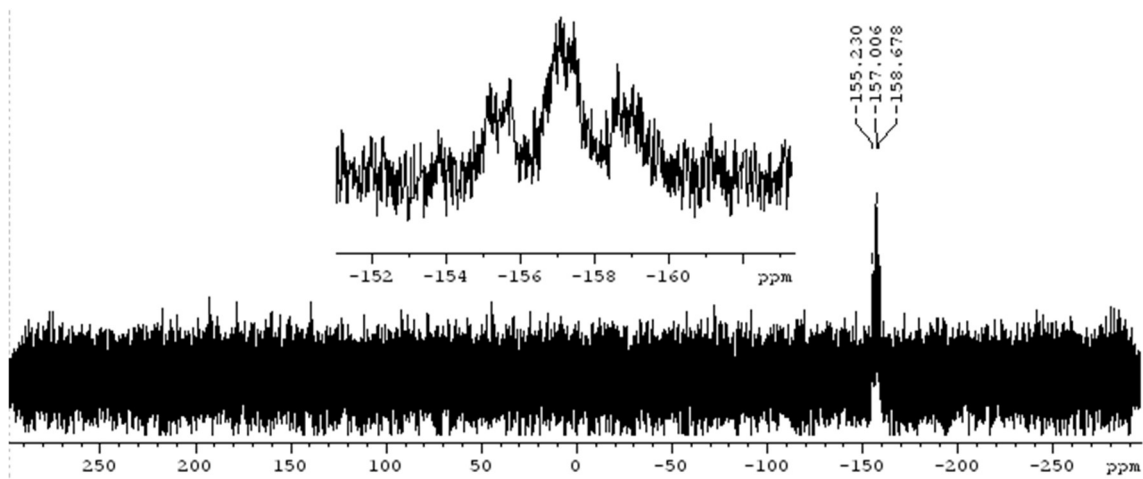


Figure S12.  $^{11}\text{B}\{^1\text{H}\}$  NMR spectrum (bottom) and  $^{11}\text{B}$  NMR spectrum of **1** in  $\text{C}_6\text{D}_6$

$[(\text{CO})_4\text{Mo}(\text{PH}_2\text{BH}_2\text{NMe}_3)_2]$  (**2**)Figure S13.  $^1\text{H}$  NMR spectrum of **2** in  $\text{CD}_2\text{Cl}_2$ Figure S14.  $^{31}\text{P}$  NMR spectrum of **2** in  $\text{CD}_2\text{Cl}_2$

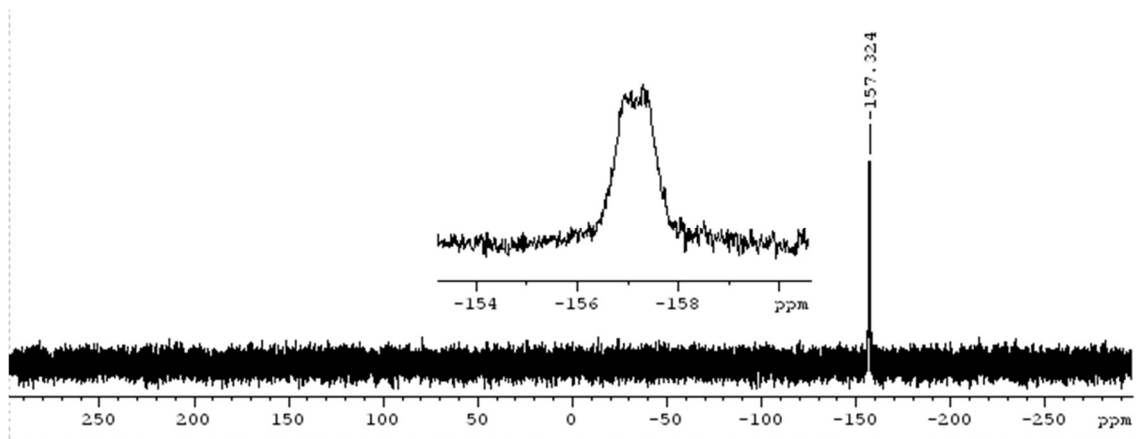


Figure S15.  $^{31}\text{P}\{^1\text{H}\}$  NMR spectrum of **2** in  $\text{CD}_2\text{Cl}_2$

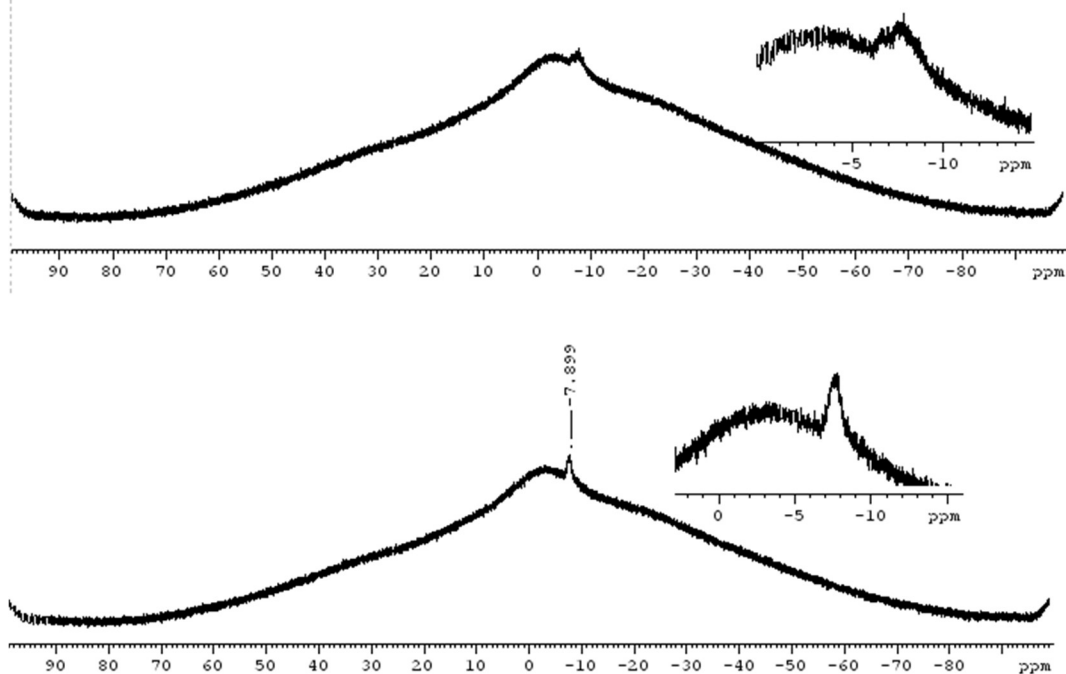
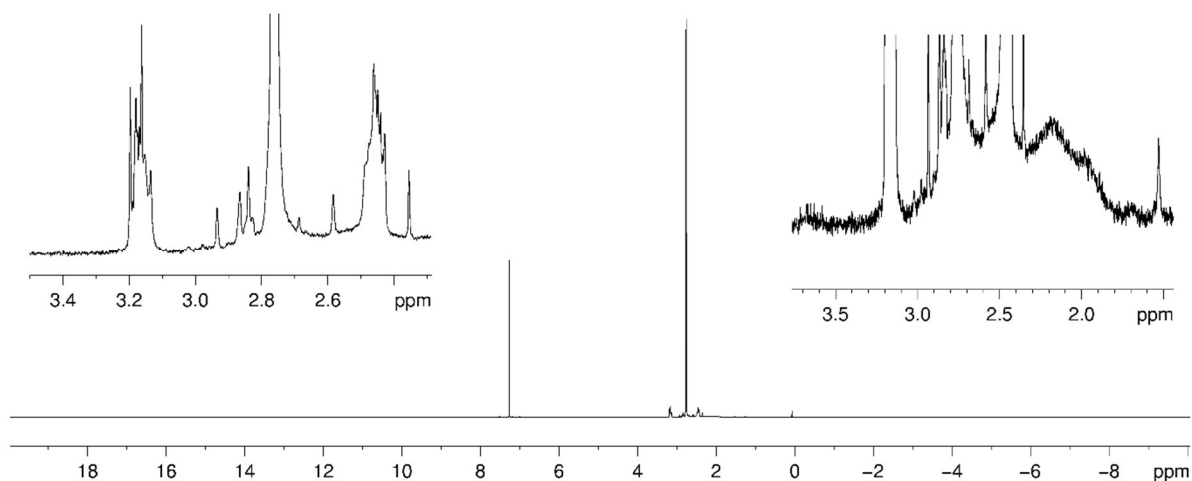
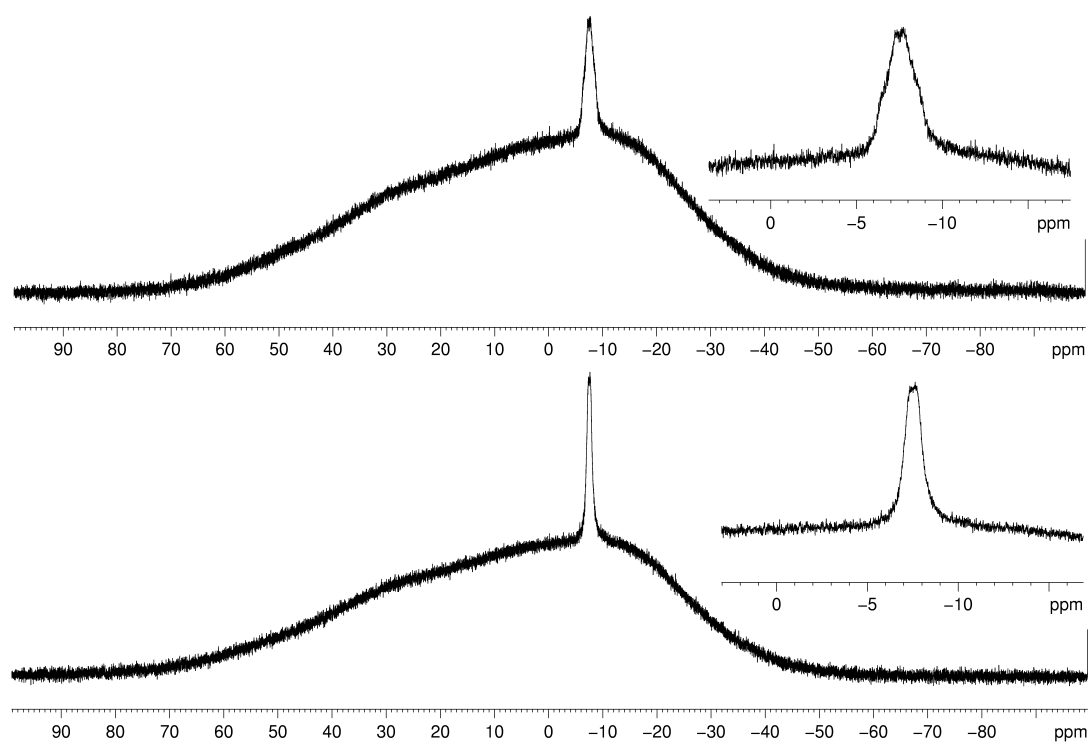


Figure S16.  $^{11}\text{B}\{^1\text{H}\}$  NMR spectrum (bottom) and  $^{11}\text{B}$  NMR spectrum of **2** in  $\text{CD}_2\text{Cl}_2$

**$[(\text{CO})_4\text{W}(\text{PH}_2\text{BH}_2\text{NMe}_3)_2]$  (**3**)****Figure S17.**  $^1\text{H}$  NMR spectrum of **3** in  $\text{CDCl}_3$ **Figure S18.**  $^{11}\text{B}\{^1\text{H}\}$  NMR spectrum (bottom) and  $^{11}\text{B}$  NMR spectrum of **3** in  $\text{CDCl}_3$

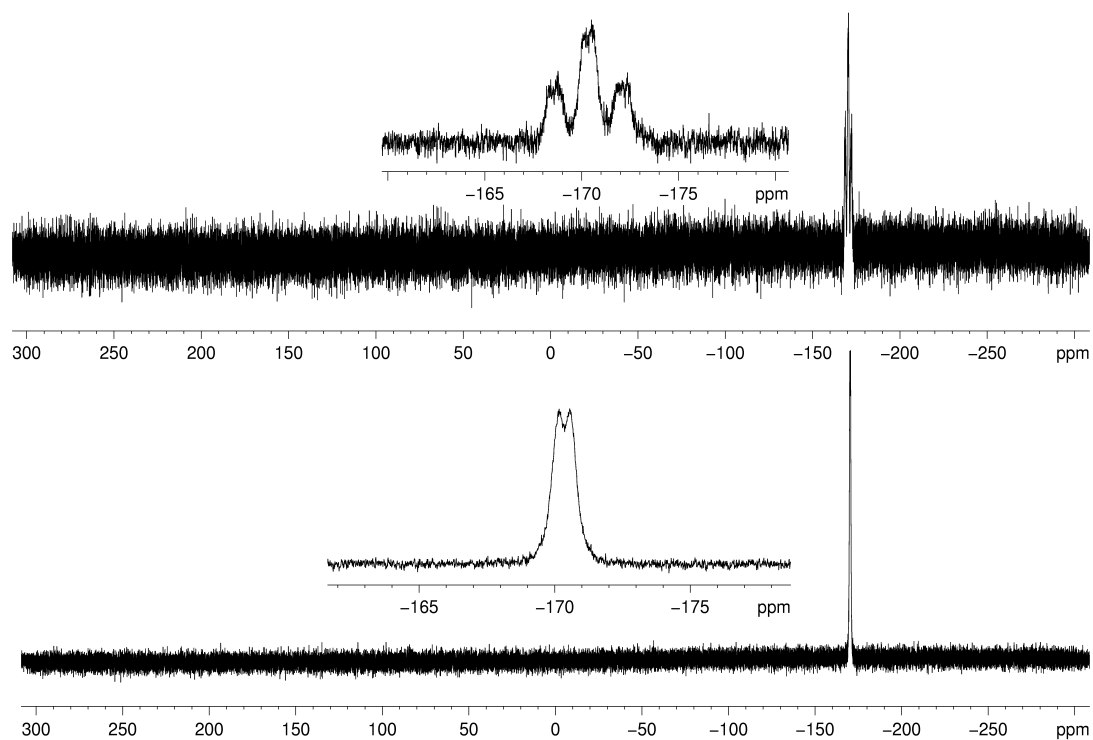


Figure S19.  $^{31}\text{P}$   $\{^1\text{H}\}$  NMR spectrum (bottom) and  $^{31}\text{P}$  NMR spectrum of **3** in  $\text{CDCl}_3$

**$[(\text{CO})_4\text{Cr}(\text{AsH}_2\text{BH}_2\text{NMe}_3)_2]$  (**4**)**

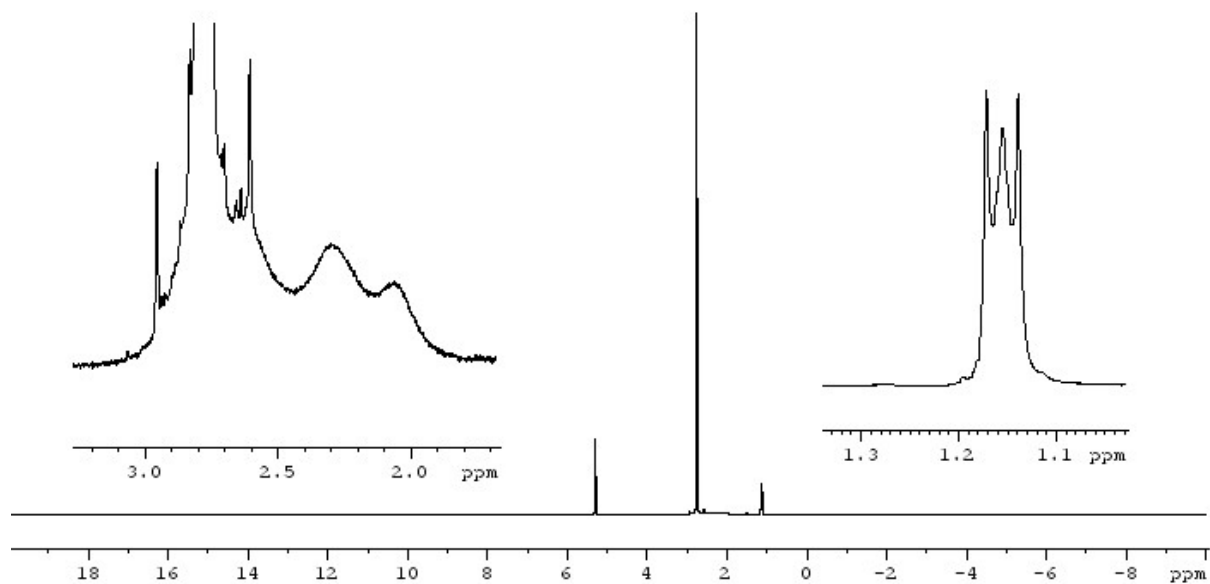


Figure S20.  $^1\text{H}$  NMR spectrum of **4** in  $\text{CD}_2\text{Cl}_2$

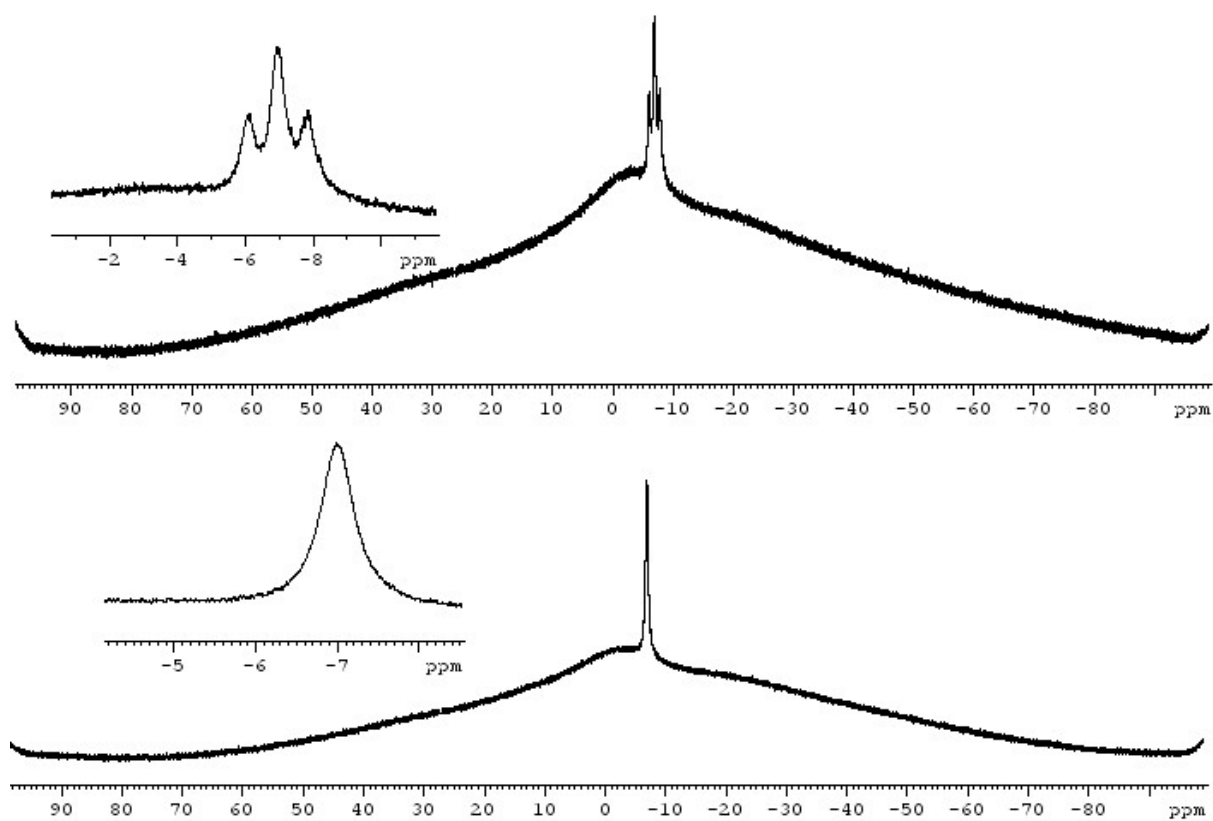


Figure S21. <sup>11</sup>B {<sup>1</sup>H} NMR spectrum (bottom) and <sup>11</sup>B NMR spectrum of 4 in CD<sub>2</sub>Cl<sub>2</sub>

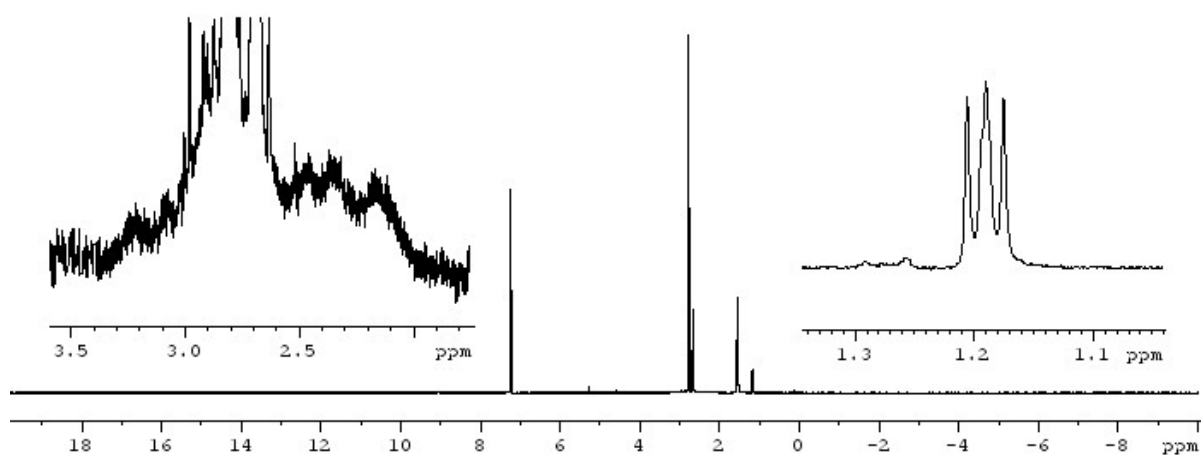


Figure S22.  $^1\text{H}$  NMR spectrum of **5** in  $\text{CDCl}_3$

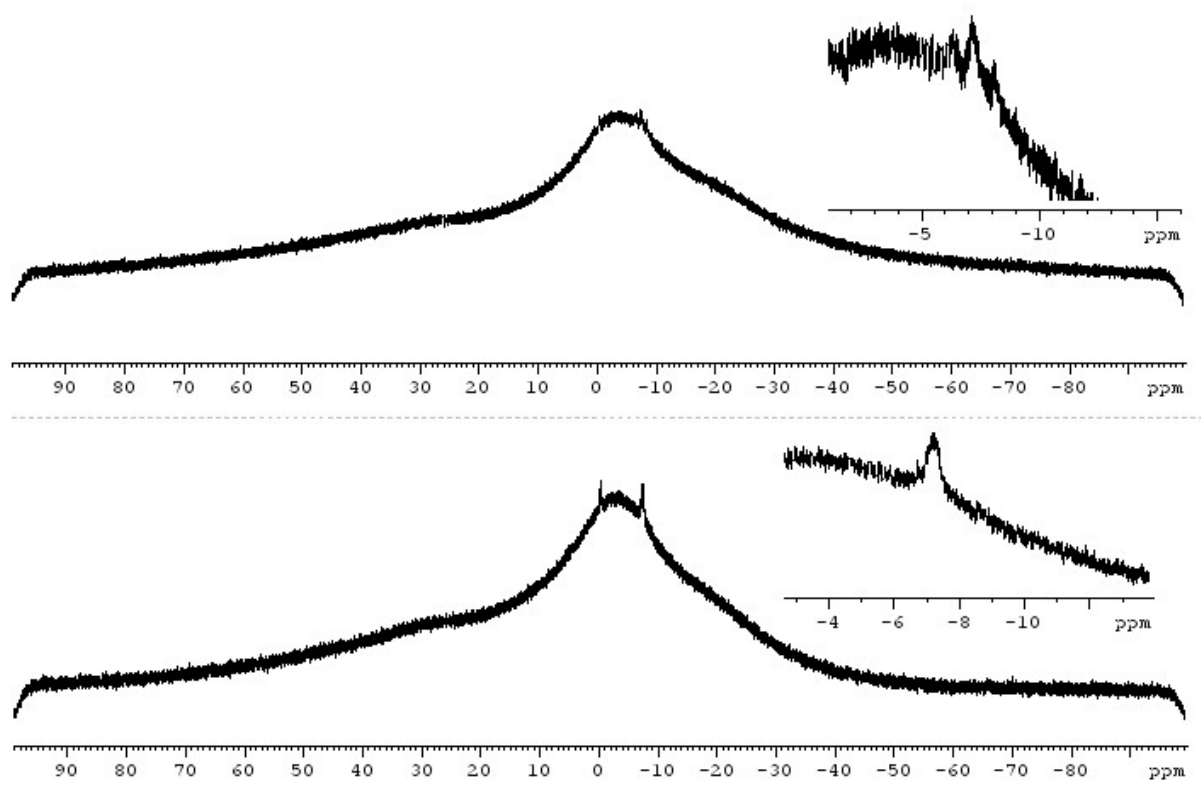
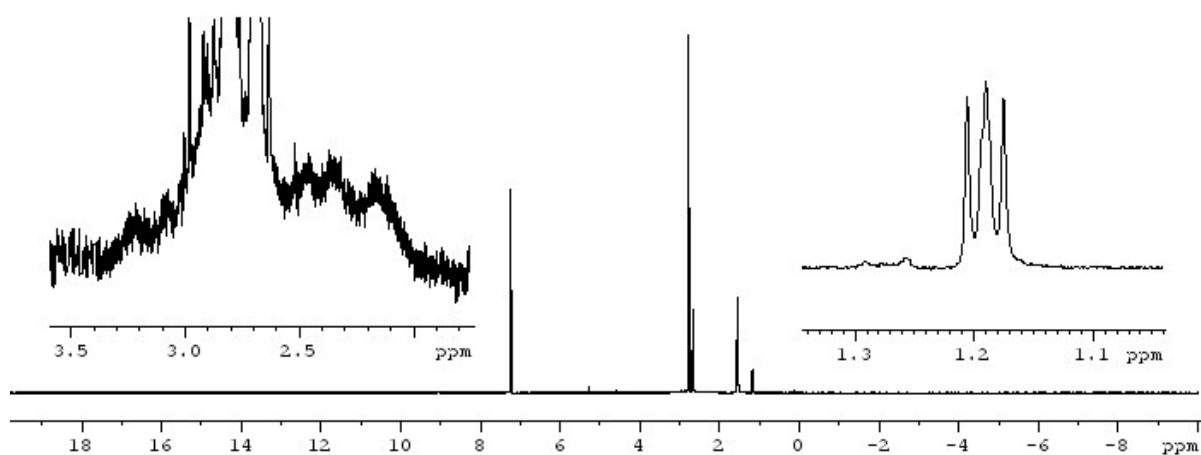
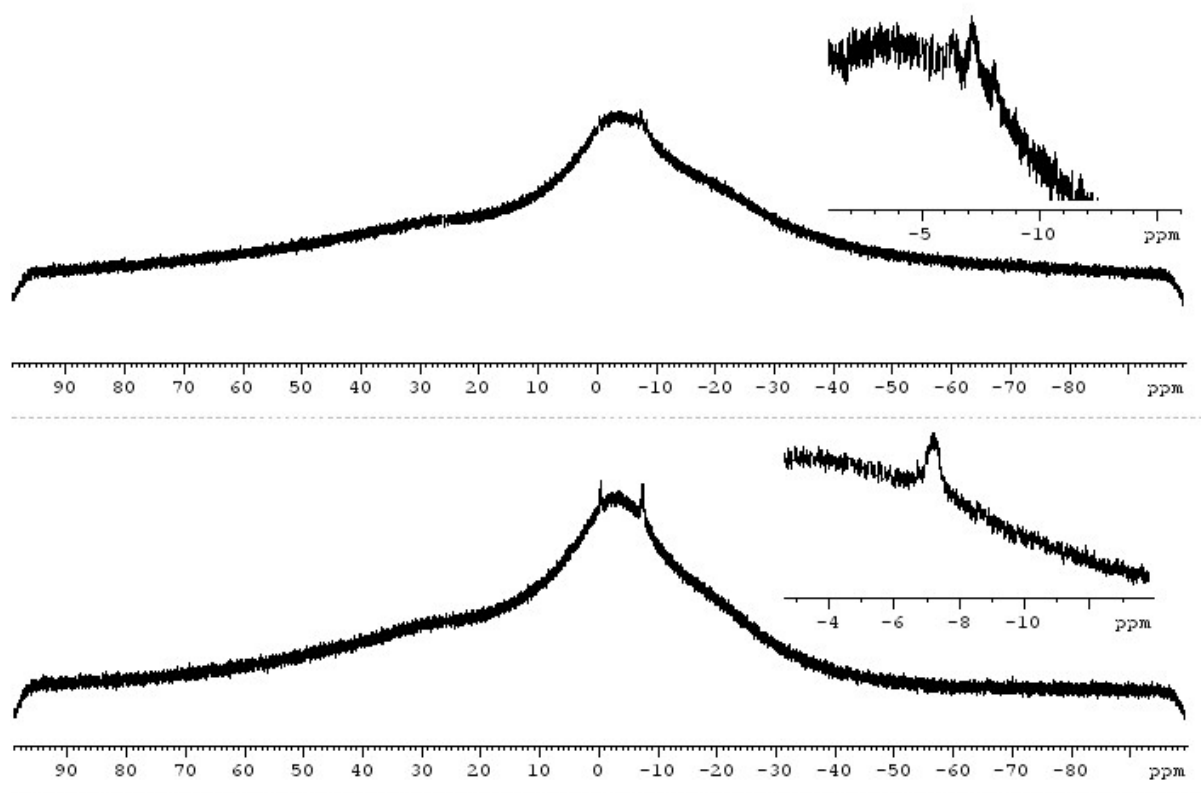


Figure S23.  $^{11}\text{B}$   $\{^1\text{H}\}$  NMR spectrum (bottom) and  $^{11}\text{B}$  NMR spectrum of **5** in  $\text{CDCl}_3$

$[(\text{CO})_4\text{W}(\text{AsH}_2\text{BH}_2\text{NMe}_3)_2]$  (**6**)Figure S24.  $^1\text{H}$  NMR spectrum of **6** in  $\text{CDCl}_3$ Figure S25.  $^{11}\text{B}$   $\{^1\text{H}\}$  NMR spectrum (bottom) and  $^{11}\text{B}$  NMR spectrum of **6** in  $\text{CDCl}_3$

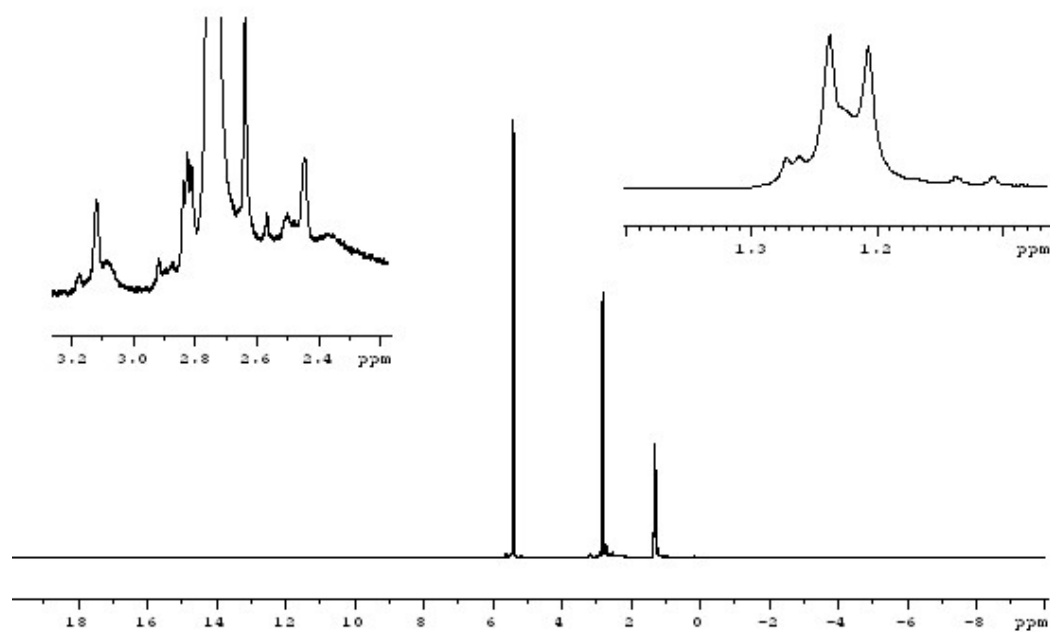


Figure S26.  $^1\text{H}$  NMR spectrum of 7 in  $\text{CD}_2\text{Cl}_2$

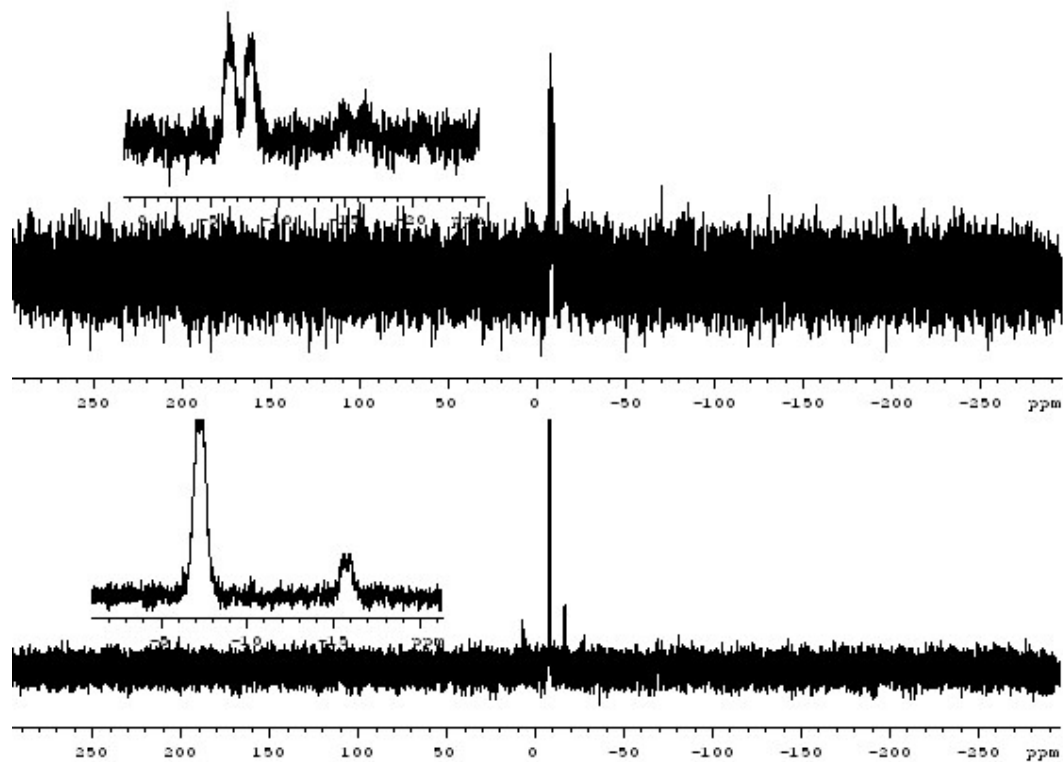


Figure S27.  $^{31}\text{P}\{^1\text{H}\}$  NMR spectrum (bottom) and  $^{31}\text{P}$  NMR spectrum of 7 in  $\text{CD}_2\text{Cl}_2$

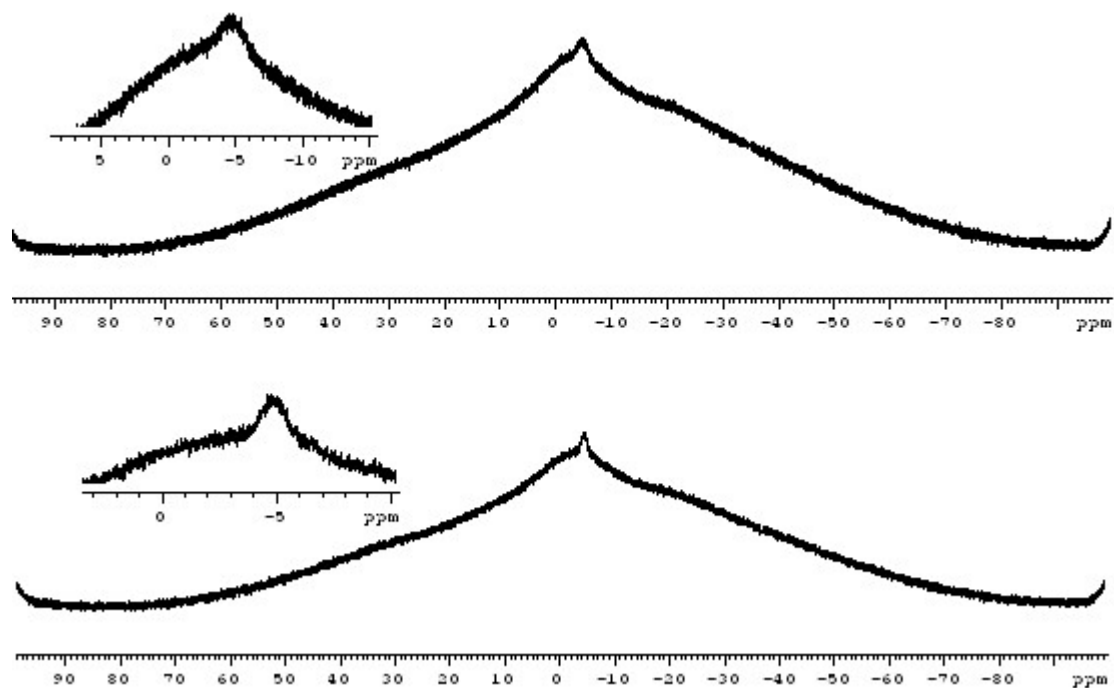


Figure S28. <sup>11</sup>B {<sup>1</sup>H} NMR spectrum (bottom) and <sup>11</sup>B NMR spectrum of 7 in CD<sub>2</sub>Cl<sub>2</sub>

**[(CO)<sub>4</sub>W(*t*BuPHBH<sub>2</sub>NMe<sub>3</sub>)<sub>2</sub>] (8)**

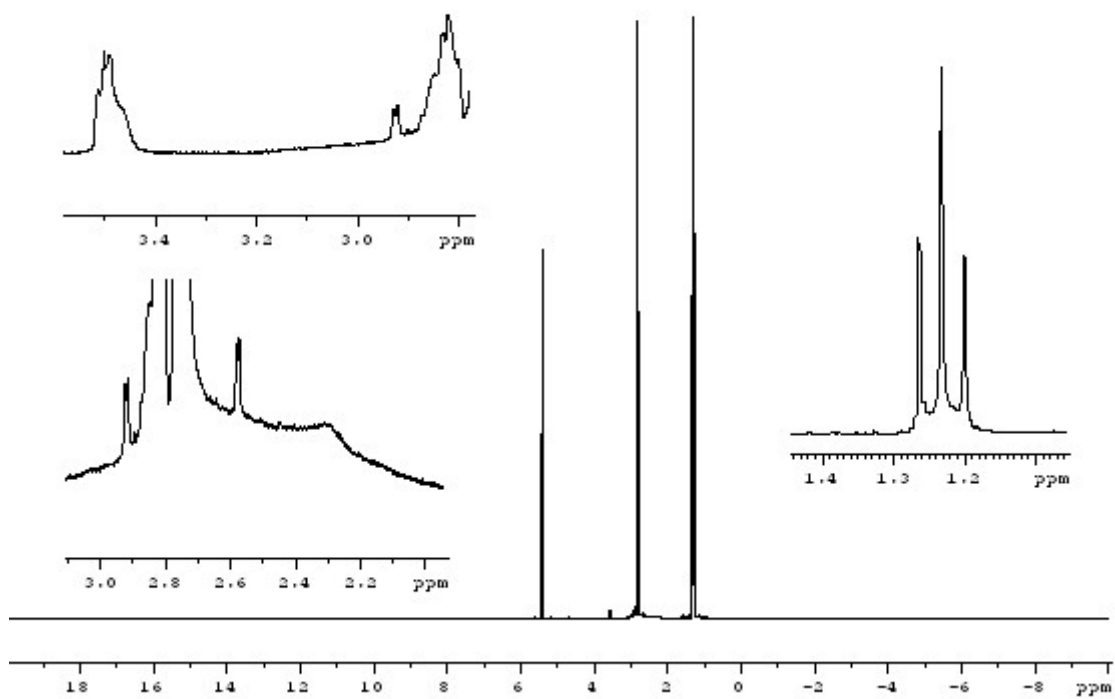


Figure S29. <sup>1</sup>H NMR spectrum of 8 in CD<sub>2</sub>Cl<sub>2</sub>

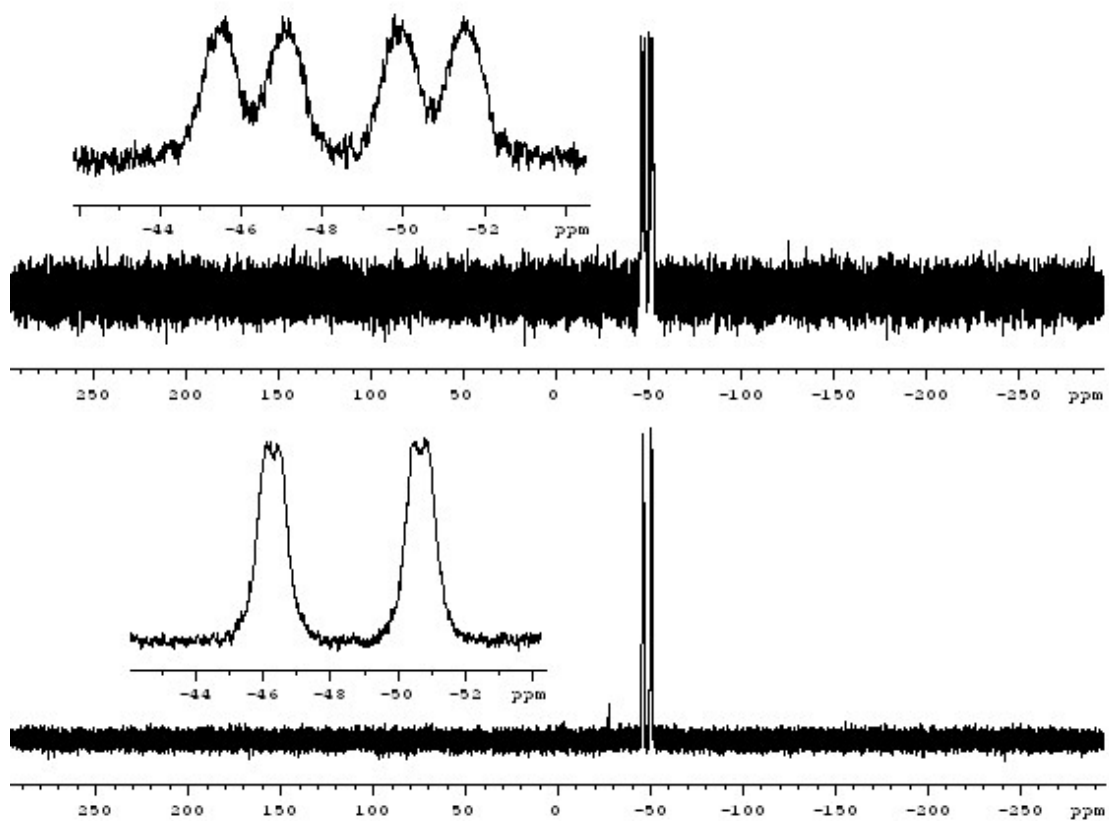


Figure S30.  $^{31}\text{P}\{^1\text{H}\}$  NMR spectrum (bottom) and  $^{31}\text{P}$  NMR spectrum of **8** in  $\text{CD}_2\text{Cl}_2$

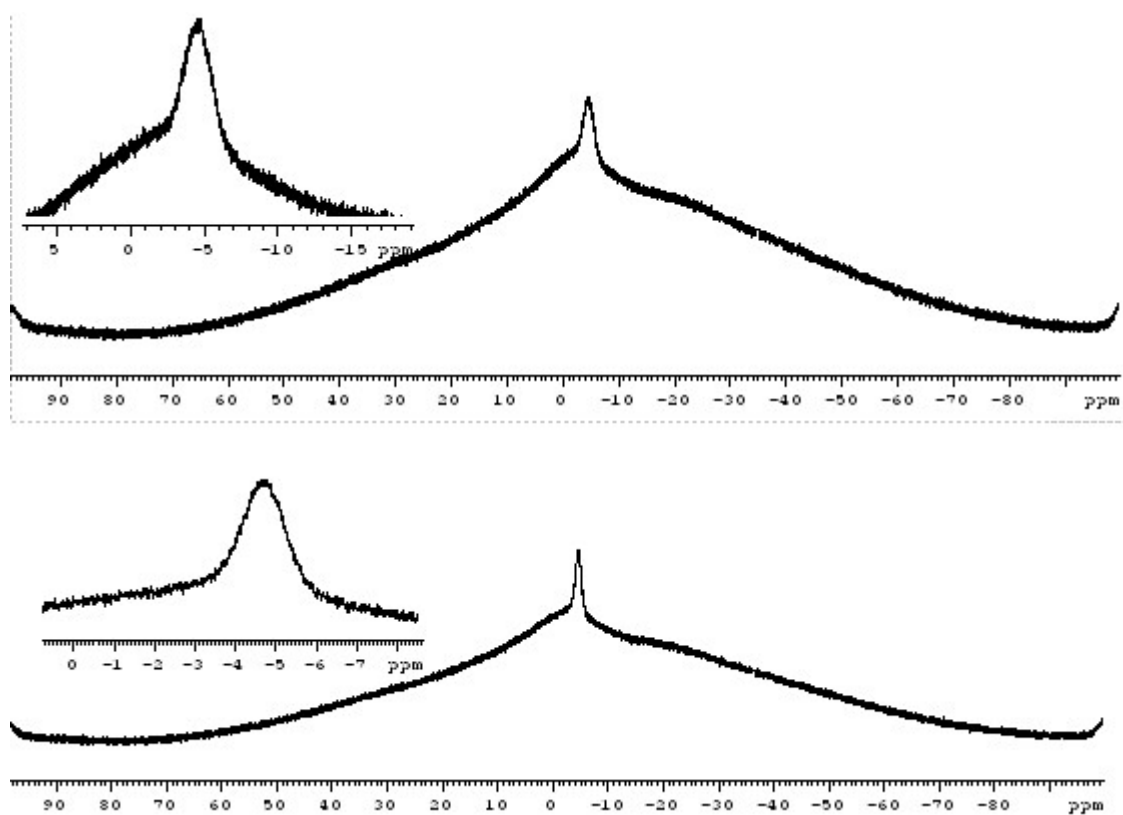


Figure S31.  $^{11}\text{B}\{^1\text{H}\}$  NMR spectrum (bottom) and  $^{11}\text{B}$  NMR spectrum of **8** in  $\text{CD}_2\text{Cl}_2$

### Computational details.

The geometries of the compounds have been fully optimized with gradient-corrected density functional theory (DFT) in form of Becke's three-parameter hybrid method B3LYP<sup>[1]</sup> with def2-SVP all electron basis set (ECP on Mo, W).<sup>[2]</sup> Gaussian 09 program package<sup>[3]</sup> was used throughout. All structures correspond to minima on their respective potential energy surfaces as verified by computation of second derivatives. Basis sets were obtained from the EMSL basis set exchange database.<sup>[4]</sup> Vibrational frequencies are scaled by 0.9603.<sup>[5]</sup>

Computed thermodynamic characteristics for the formation of studied compounds are summarized in Table 4S and computed IR spectra for the valence CO region (1800-2200 cm<sup>-1</sup>) are tabulated in Table 6S and depicted in Figure S33. For the creation of the figure from the computed IR spectra, half-width at half height was set to 2 cm<sup>-1</sup>. The maximal predicted CO frequencies shifts are summarized in Figure S32.

Process	$\Delta E^\circ_0$	$\Delta H^\circ_{298}$	$\Delta S^\circ_{298}$	$\Delta G^\circ_{298}$
$\text{Cr}(\text{CO})_4\text{nb}d + 2 \text{PH}_2\text{BH}_2\text{NMe}_3 = \text{Cr}(\text{CO})_4(\text{PH}_2\text{BH}_2\text{NMe}_3)_2 + \text{nb}d$	-71.1	-61.1	-142.1	-18.7
$\text{Mo}(\text{CO})_4\text{nb}d + 2 \text{PH}_2\text{BH}_2\text{NMe}_3 = \text{Mo}(\text{CO})_4(\text{PH}_2\text{BH}_2\text{NMe}_3)_2 + \text{nb}d$	-84.2	-73.9	-142.9	-31.3
$\text{W}(\text{CO})_4\text{nb}d + 2 \text{PH}_2\text{BH}_2\text{NMe}_3 = \text{W}(\text{CO})_4(\text{PH}_2\text{BH}_2\text{NMe}_3)_2 + \text{nb}d$	-85.9	-75.2	-142.4	-32.7
$\text{Cr}(\text{CO})_4\text{nb}d + 2 \text{AsH}_2\text{BH}_2\text{NMe}_3 = \text{Cr}(\text{CO})_4(\text{AsH}_2\text{BH}_2\text{NMe}_3)_2 + \text{nb}d$	-49.4	-41.2	-138.1	0.0
$\text{Mo}(\text{CO})_4\text{nb}d + 2 \text{AsH}_2\text{BH}_2\text{NMe}_3 = \text{Mo}(\text{CO})_4(\text{AsH}_2\text{BH}_2\text{NMe}_3)_2 + \text{nb}d$	-60.6	-52.3	-137.4	-11.3
$\text{W}(\text{CO})_4\text{nb}d + 2 \text{AsH}_2\text{BH}_2\text{NMe}_3 = \text{W}(\text{CO})_4(\text{AsH}_2\text{BH}_2\text{NMe}_3)_2 + \text{nb}d$	-57.4	-47.5	-141.0	-5.5
$\text{Cr}(\text{CO})_4\text{nb}d + 2 \text{}^t\text{BuPHBH}_2\text{NMe}_3 = \text{Cr}(\text{CO})_4(\text{}^t\text{BuPHBH}_2\text{NMe}_3)_2 + \text{nb}d$	-50.4	-40.3	-198.2	18.7
$\text{Mo}(\text{CO})_4\text{nb}d + 2 \text{}^t\text{BuPHBH}_2\text{NMe}_3 = \text{Mo}(\text{CO})_4(\text{}^t\text{BuPHBH}_2\text{NMe}_3)_2 + \text{nb}d$	-61.9	-49.1	-195.9	9.3
$\text{W}(\text{CO})_4\text{nb}d + 2 \text{}^t\text{BuPHBH}_2\text{NMe}_3 = \text{W}(\text{CO})_4(\text{}^t\text{BuPHBH}_2\text{NMe}_3)_2 + \text{nb}d$	-75.0	-61.5	-197.5	-2.6
$\text{Cr}(\text{CO})_4\text{nb}d + 2 \text{}^t\text{BuAsHBH}_2\text{NMe}_3 = \text{Cr}(\text{CO})_4(\text{}^t\text{BuAsHBH}_2\text{NMe}_3)_2 + \text{nb}d$	-48.4	-40.5	-175.9	12.0
$\text{Mo}(\text{CO})_4\text{nb}d + 2 \text{}^t\text{BuAsHBH}_2\text{NMe}_3 = \text{Mo}(\text{CO})_4(\text{}^t\text{BuAsHBH}_2\text{NMe}_3)_2 + \text{nb}d$	-60.7	-50.0	-189.5	6.5
$\text{W}(\text{CO})_4\text{nb}d + 2 \text{}^t\text{BuAsHBH}_2\text{NMe}_3 = \text{W}(\text{CO})_4(\text{}^t\text{BuAsHBH}_2\text{NMe}_3)_2 + \text{nb}d$	-70.2	-59.5	-182.1	-5.2

**Table 4S.** Reaction energies  $\Delta E^\circ_0$ , standard reaction enthalpies  $\Delta H^\circ_{298}$ , Gibbs energies  $\Delta G^\circ_{298}$  (kJ mol<sup>-1</sup>) and standard reaction entropies  $\Delta S^\circ_{298}$  (J mol<sup>-1</sup> K<sup>-1</sup>) for the considered gas phase processes and estimated values of standard reaction entropies and Gibbs energies in solution (solv). B3LYP/def2-SVP(ECP on Mo, W) level of theory.

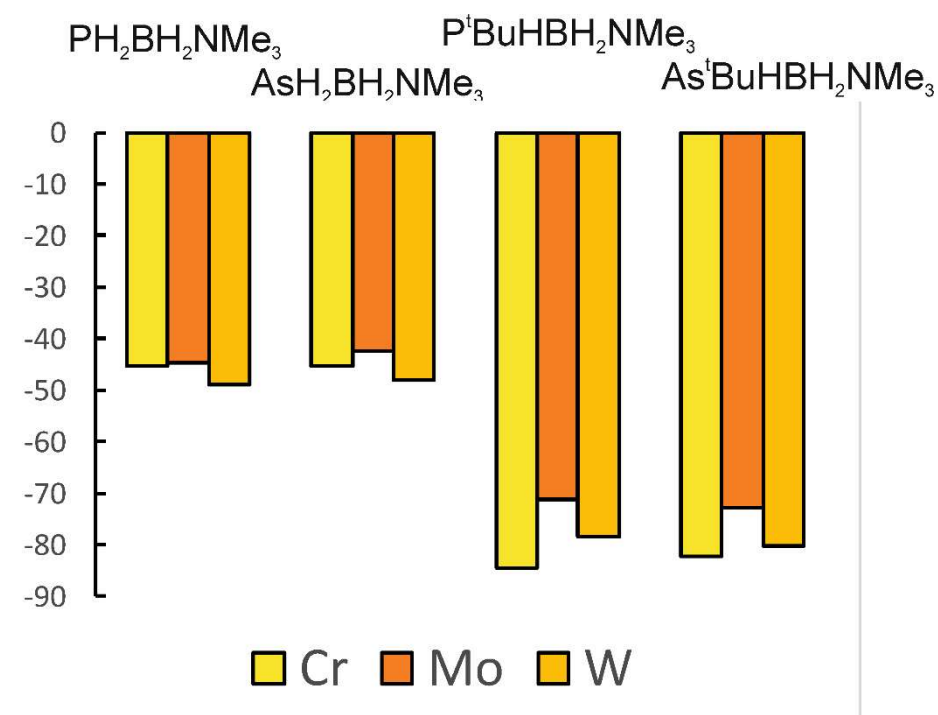
Compound	Point group	$E^{\circ}_0$	$H^{\circ}_{298}$	$S^{\circ}_{298}$
$C_7H_8$ (nbd)	$C_{2v}$	-271.2841677	-271.150122	70.045
$Cr(CO)_4nbd$	$C_{2v}$	-1768.7030135	-1768.522306	119.932
$Mo(CO)_4nbd$	$C_{2v}$	-792.6117983	-792.432171	123.977
$W(CO)_4nbd$	$C_{2v}$	-791.4957838	-791.316480	125.559
$PH_2BH_2NMe_3$	$C_1$	-542.8624678	-542.689005	89.962
$AsH_2BH_2NMe_3$	$C_1$	-2437.237466	-2437.065523	94.255
$^tBuPHBH_2NMe_3$	$C_1$	-700.0005239	-699.708233	115.995
$^tBuAsHBH_2NMe_3$	$C_1$	-2594.374946	-2594.083822	118.809
$Cr(CO)_4(PH_2BH_2NMe_3)_2$	$C_1$	-2583.170861	-2582.773467	195.852
$Mo(CO)_4(PH_2BH_2NMe_3)_2$	$C_1$	-1607.084655	-1606.688216	199.711
$W(CO)_4(PH_2BH_2NMe_3)_2$	$C_1$	-1605.969269	-1605.573002	201.402
$Cr(CO)_4(AsH_2BH_2NMe_3)_2$	$C_1$	-6371.912609	-6371.518925	205.382
$Mo(CO)_4(AsH_2BH_2NMe_3)_2$	$C_1$	-5395.825642	-5395.433007	209.596
$W(CO)_4(AsH_2BH_2NMe_3)_2$	$C_1$	-5394.708414	-5394.315495	210.333
$Cr(CO)_4(^tBuPHBH_2NMe_3)_2$	$C_1$	-2897.439085	-2896.804014	234.514
$Mo(CO)_4(^tBuPHBH_2NMe_3)_2$	$C_1$	-1921.3522481	-1920.7172	239.107
$W(CO)_4(^tBuPHBH_2NMe_3)_2$	$C_1$	-1920.241238	-1919.60623	240.306
$Cr(CO)_4(^tBuAsHBH_2NMe_3)_2$	$C_2$	-6686.1871557	-6685.555247	245.472
$Mo(CO)_4(^tBuAsHBH_2NMe_3)_2$	$C_2$	-5710.1006500	-5709.468743	246.261
$W(CO)_4(^tBuAsHBH_2NMe_3)_2$	$C_1$	-5708.9882386	-5708.356657	249.608

**Table 5S.** Total energies  $E^{\circ}_0$ , sum of electronic and thermal enthalpies  $H^{\circ}_{298}$  (Hartree) and standard entropies  $S^{\circ}_{298}$  ( $\text{cal mol}^{-1}\text{K}^{-1}$ ). B3LYP/def2-SVP (ECP on Mo, W) level of theory.

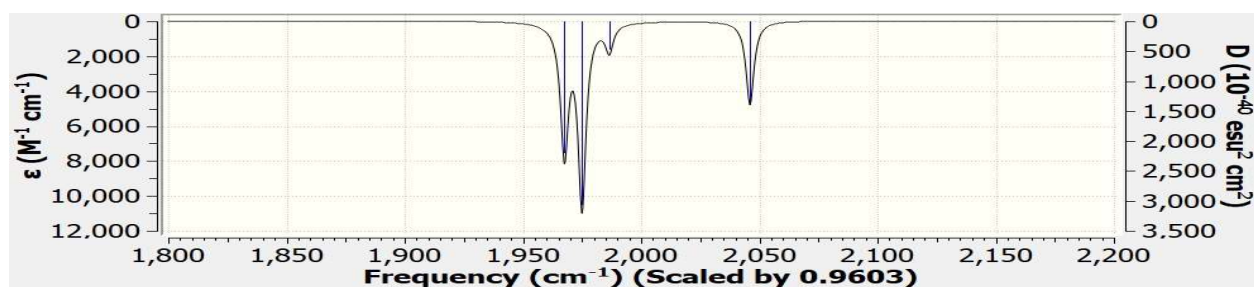
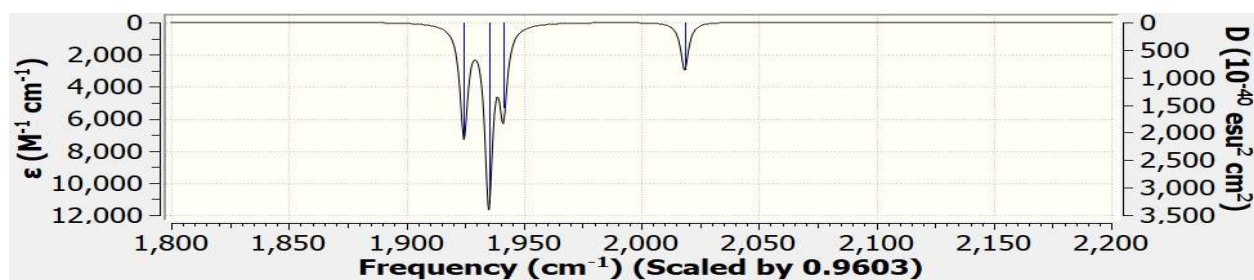
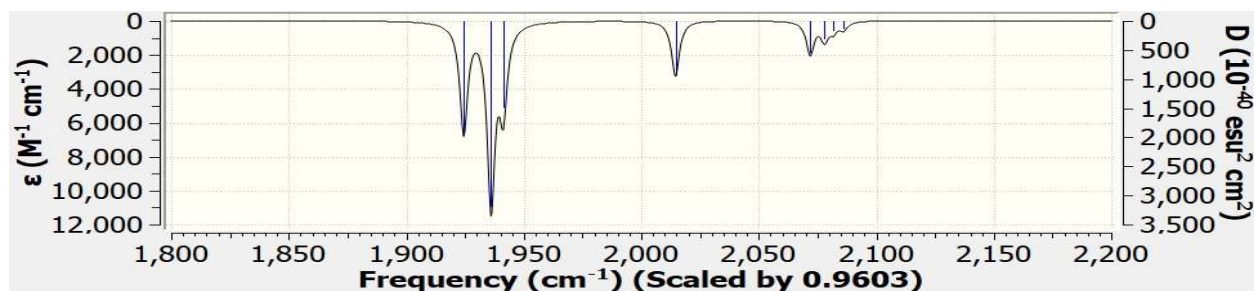
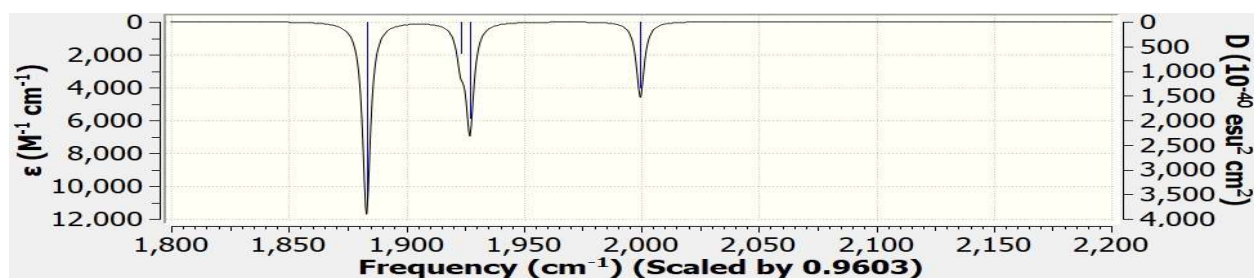
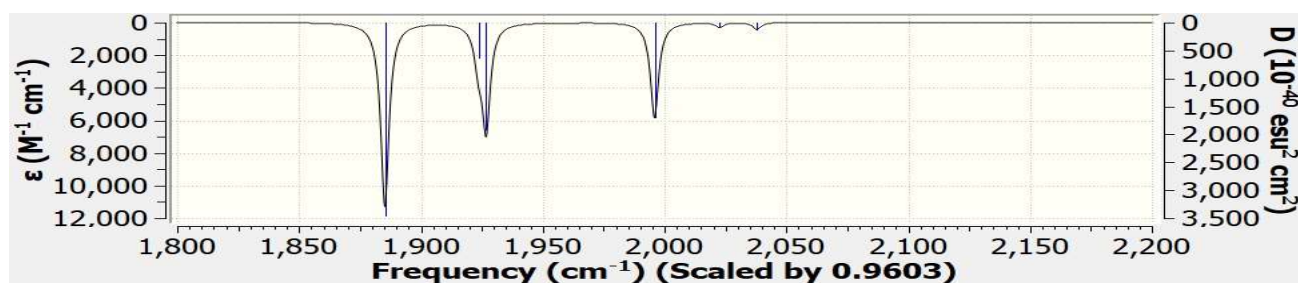
Compound	$\omega$ , $\text{cm}^{-1}$	$\nu$ , $\text{cm}^{-1}$	$I$ , $\text{km mol}^{-1}$	$\Delta\nu$ , $\text{cm}^{-1}$	Comment
$\text{Cr}(\text{CO})_4\text{nbd}$	2048.9	1967.6	1112.2	0	B1 eq antisymm
	2056.7	1975.0	1574.9	0	B2 ax antisymm
	2068.8	1986.7	236.9	0	A1 antisymm
	2130.7	2046.1	720.9	0	A1 symm
$\text{Mo}(\text{CO})_4\text{nbd}$	2030.2	1949.6	1271.5	0	
	2060.3	1978.5	1772.6	0	
	2060.9	1979.1	399.9	0	
	2137.5	2052.6	605.1	0	
$\text{W}(\text{CO})_4\text{nbd}$	2025.8	1945.4	1339.2	0	
	2058.5	1976.8	1829.9	0	
	2058.7	1977.0	398.9	0	
	2137	2052.2	593.8	0	
$\text{Cr}(\text{CO})_4(\text{PH}_2\text{BH}_2\text{NMe}_3)_2$	2004.1	1924.5	1040.7	-43.0	eq
	2015.1	1935.1	1650.6	-39.9	ax
	2021.6	1941.3	780.2	-45.3	eq+ax
	2101.9	2018.5	447.7	-27.7	all stretch
$\text{Mo}(\text{CO})_4(\text{PH}_2\text{BH}_2\text{NMe}_3)_2$	1996.5	1917.2	1147.3	-32.4	
	2013.7	1933.8	1930.7	-44.7	
	2019.3	1939.1	750.6	-39.9	
	2108.9	2025.2	340.8	-27.5	
$\text{W}(\text{CO})_4(\text{PH}_2\text{BH}_2\text{NMe}_3)_2$	1993	1913.9	1192.2	-31.5	
	2007.6	1927.9	2005.8	-48.9	
	2015.7	1935.7	778.7	-41.3	
	2106.2	2022.6	334.7	-29.6	
$\text{Cr}(\text{CO})_4(\text{AsH}_2\text{BH}_2\text{NMe}_3)_2$	2004.0	1924.4	969.8	-43.1	
	2016.2	1936.2	1608.2	-38.9	
	2021.6	1941.3	748.4	-45.3	
	2097.9	2014.6	490.2	-31.5	coupled with As-H
$\text{Mo}(\text{CO})_4(\text{AsH}_2\text{BH}_2\text{NMe}_3)_2$	1994.2	1915.0	1096.4	-34.6	
	2016.2	1936.2	1854.3	-42.3	
	2018.2	1938.1	828.4	-41.0	
	2105.8	2022.2	445.3	-30.4	coupled with As-H
$\text{W}(\text{CO})_4(\text{AsH}_2\text{BH}_2\text{NMe}_3)_2$	1990.2	1911.2	1121.4	-34.2	
	2008.5	1928.8	1938.4	-48.0	
	2014.1	1934.1	884.6	-42.8	
	2103.7	2020.2	407.8	-32.0	coupled with As-H
$\text{Cr}(\text{CO})_4(^t\text{BuPHBH}_2\text{NMe}_3)_2$	1960.9	1883.1	1762.6	-84.5	ax asymm
	2002.7	1923.2	315.2	-51.9	ax-eq asymm
	2006.7	1927.0	980.7	-59.6	eq
	2082.3	1999.6	693.3	-46.5	symm
$\text{Mo}(\text{CO})_4(^t\text{BuPHBH}_2\text{NMe}_3)_2$	1980.1	1901.5	1882.9	-48.1	
	1986.1	1907.3	1147.6	-71.3	
	2002.8	1923.3	603.5	-55.8	
	2091.3	2008.3	516.2	-44.4	
$\text{W}(\text{CO})_4(^t\text{BuPHBH}_2\text{NMe}_3)_2$	1951.5	1874.0	1703	-71.4	
	1976.9	1898.4	1194.8	-78.4	
	2007.2	1927.5	840.7	-49.5	
	2087.9	2005.0	558.5	-47.2	
$\text{Cr}(\text{CO})_4(^t\text{BuAsHBH}_2\text{NMe}_3)_2$	1963.2	1885.3	1700.2	-82.3	

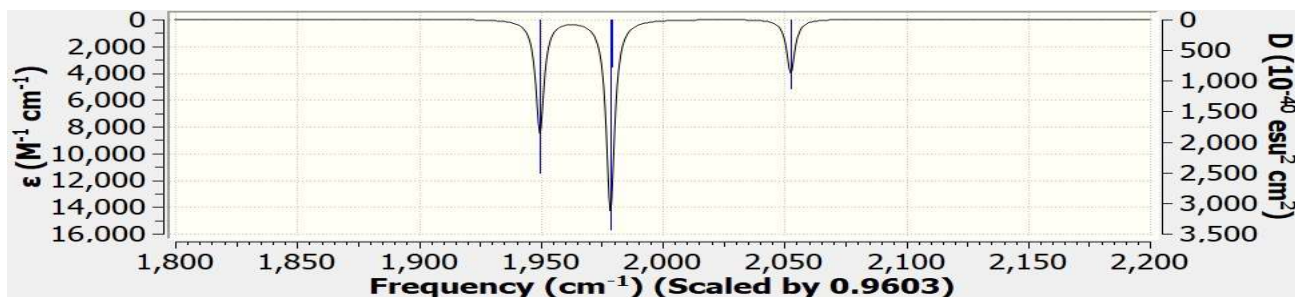
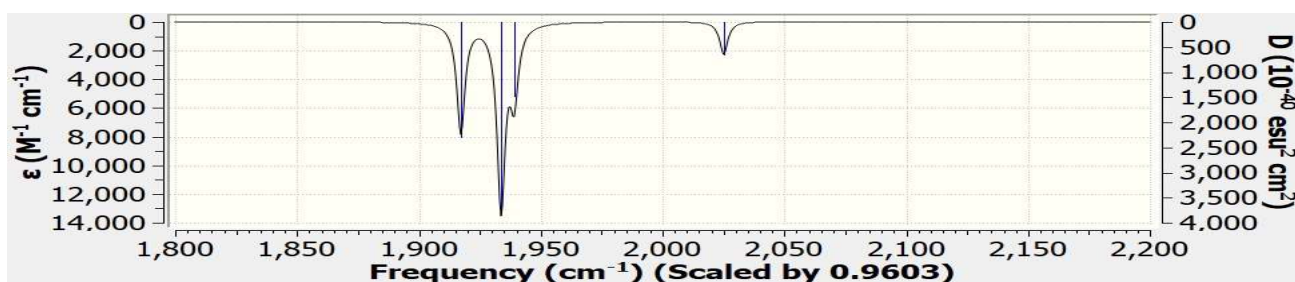
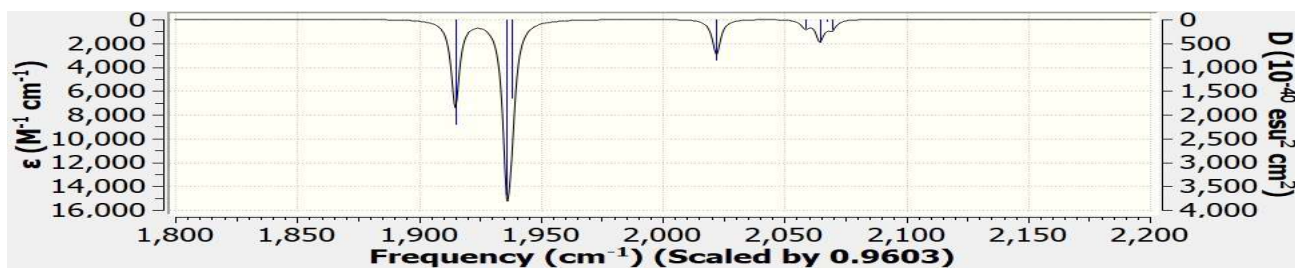
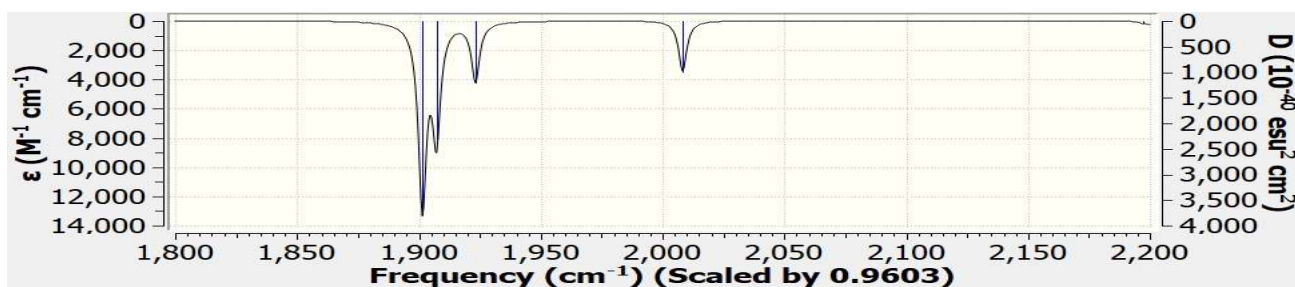
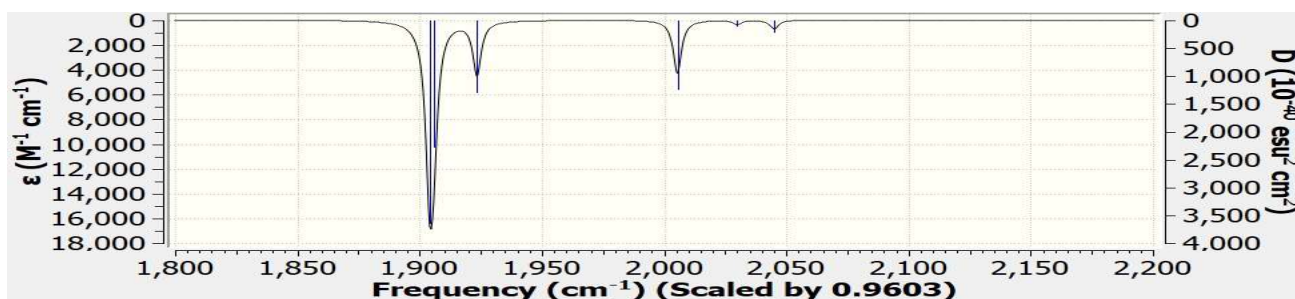
	2003.2	1923.7	318.7	-51.4	
	2006.5	1926.8	962.5	-59.8	
	2078.4	1995.9	879.8	-50.2	coupled with As-H
$\text{Mo}(\text{CO})_4(\text{}^t\text{BuAsHBH}_2\text{NMe}_3)_2$	1982.8	1904.1	1808.1	-45.5	
	1984.6	1905.8	1130.5	-72.7	
	2003	1923.5	648.5	-55.6	
	2088.4	2005.5	643.9	-47.2	coupled with As-H
$\text{W}(\text{CO})_4(\text{}^t\text{BuAsHBH}_2\text{NMe}_3)_2$	1950.3	1872.9	1643.6	-72.5	
	1974.9	1896.5	1193.8	-80.3	
	2007.5	1927.8	890.5	-49.2	
	2084.6	2001.8	666.1	-50.3	coupled with As-H

**Table 6S.** Computed CO stretching vibrations (harmonic vibrational frequencies  $\omega$ ,  $\text{cm}^{-1}$ ; vibrational frequencies  $\nu$ ,  $\text{cm}^{-1}$  scaled by 0.9603<sup>[5]</sup>; IR intensities,  $I$  in  $\text{km mol}^{-1}$ , and the shift with respect to  $\text{M}(\text{CO})_4\text{ndb}$   $\Delta\nu$ ,  $\text{cm}^{-1}$ ).



**Figure S32.** The maximal predicted CO frequencies shifts (in  $\text{cm}^{-1}$ ) from  $\text{M}(\text{CO})_4\text{ndb}$  to  $\text{M}(\text{CO})_4\text{ER}_2\text{BH}_2\text{NMe}_3$ .

**Cr(CO)<sub>4</sub>nbd****Cr(CO)<sub>4</sub>(PH<sub>2</sub>BH<sub>2</sub>NMe<sub>3</sub>)<sub>2</sub>****Cr(CO)<sub>4</sub>(AsH<sub>2</sub>BH<sub>2</sub>NMe<sub>3</sub>)<sub>2</sub>****Cr(CO)<sub>4</sub>(PH<sup>t</sup>BuBH<sub>2</sub>NMe<sub>3</sub>)<sub>2</sub>****Cr(CO)<sub>4</sub>(AsH<sup>t</sup>BuBH<sub>2</sub>NMe<sub>3</sub>)<sub>2</sub>**

 $\text{Mo(CO)}_4\text{nbd}$  $\text{Mo(CO)}_4(\text{PH}_2\text{BH}_2\text{NMe}_3)_2$  $\text{Mo(CO)}_4(\text{AsH}_2\text{BH}_2\text{NMe}_3)_2$  $\text{Mo(CO)}_4(\text{PH}^t\text{BuBH}_2\text{NMe}_3)_2$  $\text{Mo(CO)}_4(\text{AsH}^t\text{BuBH}_2\text{NMe}_3)_2$

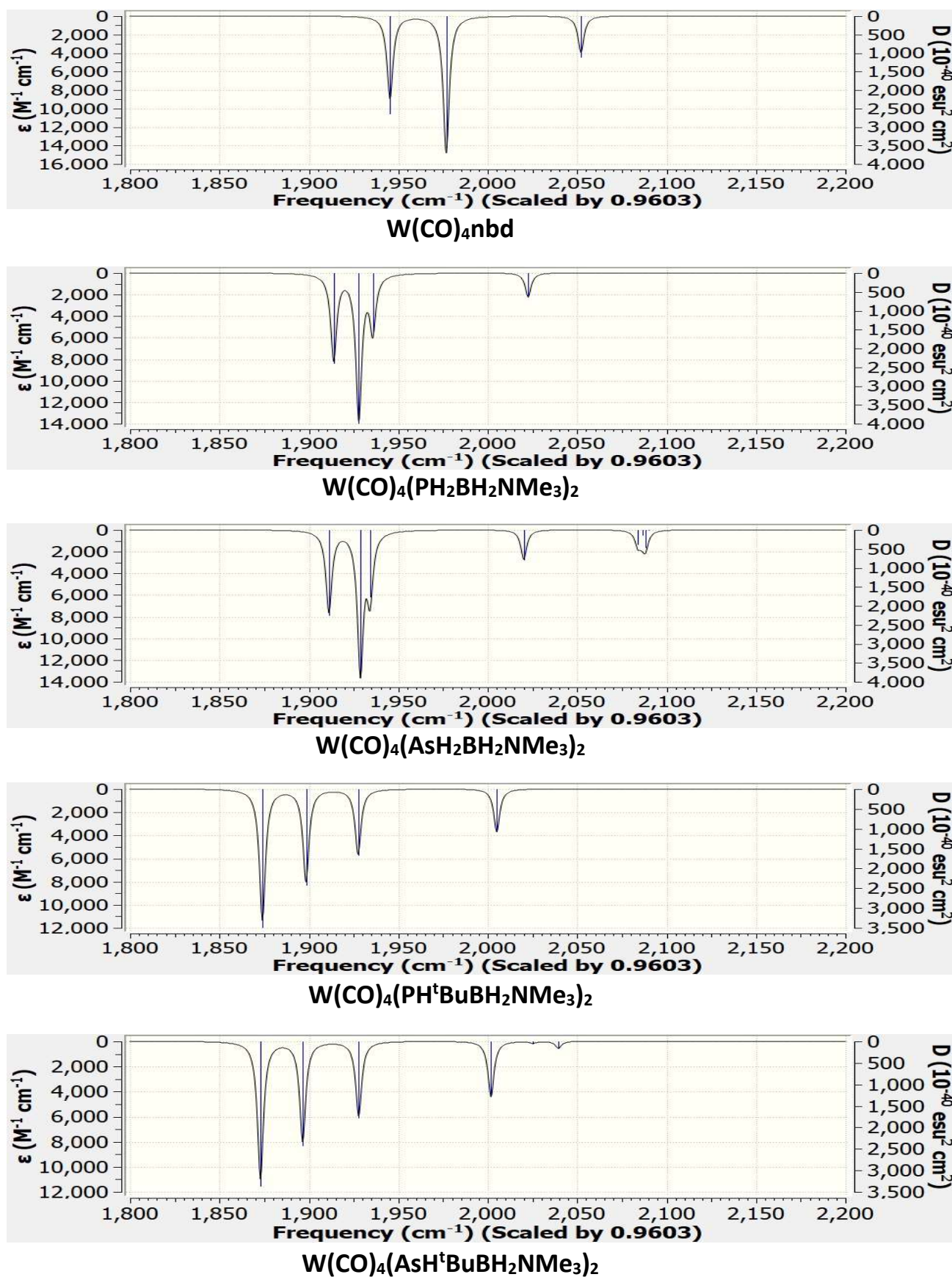


Figure S33. Fragments of the predicted IR spectra at B3LYP/def2-SVP level of theory.

**Table 7S.** Optimized geometries of computationally studied compounds. xyz coordinates in angstroms. B3LYP/def2-SVP (ECP on Mo,W) level of theory.

<b>C<sub>7</sub>H<sub>8</sub>(nbd)</b>				6	0.00000000	-2.06272000	0.62478300
6	-1.24408000	0.66939000	-0.52097500	1	2.04822100	1.34195100	-1.36598900
6	-1.24408000	-0.66939000	-0.52097500	1	2.04822100	-1.34195100	-1.36598900
6	0.00000000	-1.12204400	0.27330500	1	0.00000000	-2.16949300	-2.82325600
6	1.24408000	-0.66939000	-0.52097500	1	-2.04822100	-1.34195100	-1.36598900
6	1.24408000	0.66939000	-0.52097500	1	-2.04822100	1.34195100	-1.36598900
6	0.00000000	1.12204400	0.27330500	1	0.00000000	2.16949300	-2.82325600
6	0.00000000	0.00000000	1.35479000	1	-0.90285900	0.00000000	-4.19078200
1	-1.93969000	1.34183600	-1.02535000	1	0.90285900	0.00000000	-4.19078200
1	-1.93969000	-1.34183600	-1.02535000	<b>PH<sub>2</sub>BH<sub>2</sub>NMe<sub>3</sub></b>			
1	0.00000000	-2.16552800	0.61522500	5	0.48456100	0.76101600	0.66332500
1	1.93969000	-1.34183600	-1.02535000	1	0.38703800	1.92378800	0.30700800
1	1.93969000	1.34183600	-1.02535000	1	0.35953900	0.61471900	1.86695900
1	0.00000000	2.16552800	0.61522500	15	2.14790200	-0.04725000	-0.09588700
1	0.90411000	0.00000000	1.98297100	7	-0.85627300	0.00699400	0.00650000
1	-0.90411000	0.00000000	1.98297100	6	-2.06303700	0.61492700	0.62315800
<b>Cr(CO)<sub>6</sub>nbd</b>				6	-0.83103900	-1.44749300	0.30797900
24	0.00000000	0.00000000	0.49289100	6	-0.90611200	0.20737900	-1.46599900
8	2.28145600	0.00000000	2.46820400	1	-1.74170300	-1.93582800	-0.07539600
8	0.00000000	3.01276600	0.95657200	1	-0.76420200	-1.58535600	1.39453000
8	-2.28145600	0.00000000	2.46820400	1	0.05199200	-1.89711700	-0.16497300
8	0.00000000	-3.01276600	0.95657200	1	-2.97719100	0.15976300	0.20742100
6	1.20600600	0.69070400	-1.35732600	1	-2.05959800	1.69352800	0.42422500
6	1.20600600	-0.69070400	-1.35732600	1	-2.02824500	0.45876000	1.70804000
6	0.00000000	-1.12456500	-2.21845200	1	-1.79120400	-0.29380700	-1.89035300
6	-1.20600600	-0.69070400	-1.35732600	1	0.00863300	-0.20263000	-1.91279900
6	-1.20600600	0.69070400	-1.35732600	1	-0.95143700	1.28304100	-1.67683700
6	0.00000000	1.12456500	-2.21845200	1	2.98930200	1.09489300	0.03956000
6	0.00000000	0.00000000	-3.28649500	1	2.67078700	-0.70792100	1.05796400
6	1.40080700	0.00000000	1.72515700	<b>AsH<sub>2</sub>BH<sub>2</sub>NMe<sub>3</sub></b>			
6	0.00000000	1.88385900	0.73444300	5	-0.10901900	-0.68854600	-0.79526600
6	-1.40080700	0.00000000	1.72515700	1	-0.23257100	-1.88701600	-0.61960700
6	0.00000000	-1.88385900	0.73444300	1	-0.23459300	-0.34696300	-1.95707700
1	2.03136500	1.34087100	-1.06906000	33	1.69853900	0.03638200	0.04505000
1	2.03136500	-1.34087100	-1.06906000	7	-1.41293100	-0.00694700	-0.00813300
1	0.00000000	-2.16794800	-2.55607900	6	-2.64514500	-0.54698900	-0.64083700
1	-2.03136500	-1.34087100	-1.06906000	6	-1.40258200	1.47260100	-0.15006400
1	-2.03136500	1.34087100	-1.06906000	6	-1.40910100	-0.36826900	1.43379000
1	0.00000000	2.16794800	-2.55607900	1	-2.29159400	1.90999100	0.33252000
1	-0.90303500	0.00000000	-3.91819400	1	-1.39572100	1.72723800	-1.21722300
1	0.90303500	0.00000000	-3.91819400	1	-0.49460900	1.87388100	0.31814200
<b>Mo(CO)<sub>6</sub>nbd</b>				1	-3.54109900	-0.12772000	-0.15385200
42	0.00000000	0.00000000	0.46306600	1	-2.64508900	-1.63953800	-0.54654100
8	2.33256100	0.00000000	2.58394700	1	-2.64246100	-0.28699500	-1.70617600
8	0.00000000	3.17512500	0.91198400	1	-2.29529700	0.05187700	1.93649300
8	-2.33256100	0.00000000	2.58394700	1	-0.49786300	0.02566400	1.90175700
8	0.00000000	-3.17512500	0.91198400	1	-1.41266200	-1.46148500	1.52627600
6	1.21897000	0.69064800	-1.55300100	1	2.41940200	-1.30573600	0.13800000
6	1.21897000	-0.69064800	-1.55300100	1	2.38894700	0.41350000	-1.26343800
6	0.00000000	-1.12468400	-2.40008000	<b><sup>t</sup>BuPHBH<sub>2</sub>NMe<sub>3</sub></b>			
6	-1.21897000	-0.69064800	-1.55300100	5	0.80533800	-0.15040900	-0.85542200
6	-1.21897000	0.69064800	-1.55300100	1	1.07974500	0.28980000	-1.95911600
6	0.00000000	1.12468400	-2.40008000	1	0.53488100	-1.34005300	-0.87626600
6	0.00000000	0.00000000	-3.47113500	15	-0.58400000	0.91430800	0.09630700
6	1.46468000	0.00000000	1.82280300	7	2.24730000	-0.07151100	-0.00852300
6	0.00000000	2.04619100	0.69928300	6	3.25528600	-0.86578900	-0.75578200
6	-1.46468000	0.00000000	1.82280300	6	2.09125500	-0.63986900	1.35623300
6	0.00000000	-2.04619100	0.69928300	6	2.71084300	1.33725800	0.09318200
1	2.04406000	1.34301500	-1.26839800	1	3.04749600	-0.59040200	1.90193100
1	2.04406000	-1.34301500	-1.26839800	1	1.76575200	-1.68432600	1.27197700
1	0.00000000	-2.16893100	-2.73511900	1	1.32238700	-0.06918300	1.89310400
1	-2.04406000	-1.34301500	-1.26839800	1	4.22535800	-0.84519200	-0.23209000
1	-2.04406000	1.34301500	-1.26839800	1	3.36574600	-0.44669400	-1.76323100
1	0.00000000	2.16893100	-2.73511900	1	2.90088800	-1.90005300	-0.84363600
1	-0.90309600	0.00000000	-4.10253600	1	3.67638400	1.38541600	0.62265400
1	0.90309600	0.00000000	-4.10253600	1	1.95753700	1.92104000	0.63862300
<b>W(CO)<sub>6</sub>nbd</b>				1	2.81984300	1.74932000	-0.91789200
74	0.00000000	0.00000000	0.38420400	6	-2.19044200	-0.12118600	-0.00497600
8	2.36853800	0.00000000	2.49225200	6	-2.04838000	-1.32297200	0.94476600
8	0.00000000	3.19445300	0.82482800	1	-1.84584200	-0.99880700	1.97910400
8	-2.36853800	0.00000000	2.49225200	1	-2.98138200	-1.91440900	0.95691600
8	0.00000000	-3.19445300	0.82482800	1	-1.23467900	-1.99496900	0.62927400
6	1.21516100	0.69317200	-1.63570600	6	-2.48831400	-0.61229800	-1.43064700
6	1.21516100	-0.69317200	-1.63570600	1	-3.42840500	-1.19505500	-1.45140500
6	0.00000000	-1.12507700	-2.48891900	1	-2.60489800	0.23245200	-2.12844900
6	-1.21516100	-0.69317200	-1.63570600	1	-1.68340400	-1.25678100	-1.81409200
6	0.00000000	1.12507700	-2.48891900	6	-3.34168600	0.77822200	0.48059400
6	0.00000000	0.00000000	-3.55920900	1	-3.46717900	1.65915400	-0.17006100
6	1.48485800	0.00000000	1.74745500	1	-4.29621300	0.22119700	0.47401600
6	0.00000000	2.06272000	0.62478300	1	-3.16650400	1.14072400	1.50610800
6	-1.48485800	0.00000000	1.74745500	1	-0.91667200	1.85463200	-0.92551900
				<b><sup>t</sup>BuAsHBH<sub>2</sub>NMe<sub>3</sub></b>			



1	-3.891328000	0.303851000	-0.496961000
1	-2.170543000	-0.844030000	1.908686000
<hr/>			
Cr(CO) <sub>4</sub> (AsH <sub>2</sub> BH <sub>2</sub> NMe <sub>3</sub> ) <sub>2</sub>			
33	-1.616760000	0.050025000	-0.692363000
33	1.722508000	-0.048719000	0.689432000
24	0.002669000	-1.784310000	-0.004040000
8	-1.114837000	-1.748021000	2.833847000
8	1.928116000	-3.949462000	0.793124000
8	1.143404000	-1.769178000	-2.832412000
8	-2.040172000	-3.826503000	-0.834218000
7	-3.781934000	2.233756000	0.173583000
7	3.711951000	2.306743000	-0.155054000
6	-0.700522000	-1.742621000	1.755696000
6	0.716071000	-1.756556000	-1.758916000
6	1.183341000	-3.114816000	0.486994000
6	-1.251501000	-3.038966000	-0.513301000
6	-4.930405000	1.342018000	-0.145395000
1	-4.648405000	0.665803000	-0.960738000
1	-5.804695000	1.941481000	-0.444380000
1	-5.173270000	0.743642000	0.741073000
5	-2.478399000	1.359598000	0.689351000
6	-4.170067000	3.132244000	1.296443000
1	-5.055994000	3.726247000	1.019535000
1	-3.330538000	3.798622000	1.527646000
1	-4.389839000	2.522187000	2.180787000
6	-3.447983000	3.062561000	-1.014987000
1	-3.181174000	2.408030000	-1.852871000
1	-2.585717000	3.697315000	-0.775736000
1	-4.308715000	3.690758000	-1.294201000
6	3.571211000	2.934028000	1.186015000
1	2.682552000	3.577410000	1.187062000
1	4.465801000	3.531866000	1.421875000
1	3.439204000	2.151639000	1.942374000
5	2.344648000	1.486145000	-0.585012000
6	3.911634000	3.376839000	-1.171559000
1	3.043366000	4.046386000	-1.160991000
1	3.989573000	2.915520000	-2.163343000
1	4.828107000	3.946730000	-0.948805000
6	4.899798000	1.409336000	-0.165273000
1	5.809177000	1.981123000	0.077920000
1	4.997006000	0.958991000	-1.160520000
1	4.756833000	0.609924000	0.570835000
1	1.465802000	0.663057000	2.019037000
1	-1.165842000	0.966909000	-1.830818000
1	-2.805687000	-0.519907000	-1.469763000
1	1.450724000	2.313101000	-0.617926000
1	2.581148000	0.989724000	-1.668890000
1	3.022800000	-0.705319000	1.160760000
1	-2.873627000	0.695576000	1.626919000
1	-1.625263000	2.172222000	0.998436000
<hr/>			
Mo(CO) <sub>4</sub> (AsH <sub>2</sub> BH <sub>2</sub> NMe <sub>3</sub> ) <sub>2</sub>			
Mo	5.8533918469	2.9797484353	7.0259318511
As	4.5170316567	4.7322595454	5.4881272307
As	3.6164327356	2.5259905916	8.4444456708
O	5.0682808338	0.5733532	5.0601042134
O	7.417682456	0.9392583924	8.8411359637
O	8.465769397	3.5019503709	5.3501234221
O	6.6809831992	5.370916455	8.9929248444
N	3.3172996242	5.380756501	2.5922021394
C	5.33606326	1.4508948617	5.7601638286
N	2.1117384494	2.8606888133	11.2498572958
C	6.8369386129	1.6898620183	8.1733526225
C	6.3639471615	4.5111816724	8.2913472918
C	7.5007192064	3.3132943663	5.9663158478
C	2.876743827	4.7262186543	1.3280006168
H	3.7258797172	4.1868661789	0.8915063228
H	2.5070254798	5.4831110874	0.617683074
H	2.0820607733	4.0060078455	1.5562173686
B	3.8759943852	4.1812784131	3.5781322403
C	4.3934615151	6.3588401986	2.2762438098
H	5.2403855131	5.8239903006	1.8296456001
H	4.7289966113	6.8408087178	3.2017585224
H	4.0194564745	7.1210910005	1.5746633055
C	2.159618205	6.0892130057	3.1986712882
H	1.7591609224	6.8366965791	2.4956216213
H	2.4803610319	6.5857940944	4.1219226896
H	1.3820044565	5.3553615727	3.4443471505
B	3.366826979	3.4007431319	10.3246321547
C	0.8076584431	3.0474101412	10.5610368307
H	0.6983256246	4.1037896358	10.2859262865
H	-0.0197087757	2.7461664764	11.2229194203
H	0.7888830313	2.4412710666	9.6477436996
C	2.1202033043	3.6722427191	12.4996625264
H	3.0897533559	3.5500112414	12.9971436372
H	1.3097004176	3.3445630719	13.1703621531
H	1.9883894942	4.7294861478	12.2404956208
<hr/>			
C	2.288434934	1.4270267464	11.6076060231
H	2.2902861839	0.8224135767	10.6933401131
H	1.4719697433	1.0976427725	12.26943065
H	3.2529725236	1.3031802558	12.1146837396
H	4.829714193	3.6951095419	3.0042858476
H	2.9515495277	3.4045856904	3.7294347562
H	5.2590510503	6.0565253833	5.2977955785
H	3.280820917	5.3838358447	6.1170575028
H	4.3742304456	3.173948143	10.9641129793
H	2.2900341587	2.8057700434	7.7297907007
H	3.3233268713	1.0385779444	8.649833001
H	3.1670882255	4.5861315529	10.1356829469
<hr/>			
W(CO) <sub>4</sub> (AsH <sub>2</sub> BH <sub>2</sub> NMe <sub>3</sub> ) <sub>2</sub>			
74	0.000000000	-1.465582000	-0.000011000
33	-1.772950000	0.446966000	-0.736650000
1	-1.304182000	1.416450000	-1.821500000
1	-2.913122000	-0.128621000	-1.577501000
33	1.773265000	0.446707000	0.736706000
1	1.304840000	1.415692000	1.822122000
1	2.913802000	-0.129146000	1.576873000
6	0.774751000	-1.433318000	-1.915305000
8	-1.201307000	-1.421825000	2.989051000
8	1.201062000	-1.422253000	-2.989193000
8	2.084945000	-3.683289000	0.858395000
7	-4.034194000	2.508647000	0.168631000
6	-0.774777000	-1.433052000	1.915253000
7	4.034120000	2.508711000	-0.168654000
8	-2.085456000	-3.682840000	-0.858327000
6	1.314797000	-2.872467000	0.542984000
5	-2.702666000	1.675484000	0.674925000
1	-3.078375000	0.965620000	1.585958000
1	-1.884190000	2.510222000	1.015669000
6	-1.315100000	-2.872227000	-0.542890000
6	-4.470865000	3.358251000	1.312181000
1	-4.671101000	2.714830000	2.177235000
1	-5.379580000	3.920109000	1.042597000
1	-3.663509000	4.054113000	1.569499000
5	2.702347000	1.675847000	-0.674759000
1	3.077645000	0.966337000	-1.586247000
1	1.883768000	2.510753000	-1.014838000
6	-5.141839000	1.579461000	-0.187352000
1	-4.826161000	0.939760000	-1.019696000
1	-6.037504000	2.151038000	-0.477234000
1	-5.367410000	0.945670000	0.678834000
6	-3.723661000	3.383993000	-0.992656000
1	-2.892177000	4.048128000	-0.725872000
1	-4.607372000	3.982834000	-1.264230000
1	-3.421162000	2.765603000	-1.845844000
6	4.470455000	3.358685000	-1.312048000
1	4.669711000	2.715608000	-2.177586000
1	5.379670000	3.919898000	-1.042813000
1	3.663324000	4.055161000	-1.568422000
6	5.141780000	1.579305000	0.186619000
1	4.826291000	0.939298000	1.018797000
1	6.037585000	2.150678000	0.476466000
1	5.367065000	0.945842000	-0.679896000
6	3.724053000	3.383710000	0.993059000
1	2.892290000	4.047732000	0.726902000
1	4.607815000	3.982643000	1.264292000
1	3.422218000	2.765025000	1.846277000
<hr/>			
Cr(CO) <sub>4</sub> ( <sup>t</sup> BuPHBH <sub>2</sub> NMe <sub>3</sub> ) <sub>2</sub>			
15	0.000000000	1.804546000	-0.364472000
15	0.000000000	-1.804546000	-0.364472000
24	0.000000000	0.000000000	1.361631000
8	-0.247317000	2.117096000	3.486339000
8	-3.008691000	-0.349272000	1.585315000
8	3.008691000	0.349272000	1.585315000
8	0.247317000	-2.117096000	3.486339000
7	2.453607000	3.701234000	-0.854537000
6	-0.145973000	1.315175000	2.656203000
7	-2.453607000	-3.701234000	-0.854537000
6	-1.865016000	-0.204269000	1.444328000
6	1.865016000	0.204269000	1.444328000
6	-1.666689000	2.497044000	-1.035120000
6	1.666689000	-2.497044000	-1.035120000
6	2.486838000	-1.339583000	-1.629059000
1	1.960674000	-0.860082000	-2.471486000
1	3.450121000	-1.720533000	-2.012940000
1	2.711198000	-0.571947000	-0.878065000
6	0.145973000	-1.315175000	2.656203000
6	-2.433971000	3.137558000	0.134758000
1	-2.651436000	2.410191000	0.929689000
1	-3.397893000	3.539880000	-0.223894000
1	-1.869141000	3.970079000	0.581623000
6	-2.486838000	1.339583000	-1.629059000
1	-1.960674000	0.860082000	-2.471486000

1	-3.450121000	1.720533000	-2.012940000
1	-2.711198000	0.571947000	-0.878065000
6	1.443402000	-3.545896000	-2.135977000
1	0.886559000	-4.415763000	-1.761523000
1	2.417433000	-3.911159000	-2.507797000
1	0.901648000	-3.124688000	-2.999212000
6	2.433971000	-3.137558000	0.134758000
1	2.651436000	-2.410191000	0.929689000
1	3.397893000	-3.539880000	-0.223894000
1	1.869141000	-3.970079000	0.581623000
6	-1.443402000	3.545896000	-2.135977000
1	-0.886559000	4.415763000	-1.761523000
1	-2.417433000	3.911159000	-2.507797000
1	-0.901648000	3.124688000	-2.999212000
6	3.172490000	4.845944000	-0.226646000
1	3.466275000	4.566950000	0.791714000
1	2.496920000	5.708223000	-0.175915000
1	4.065492000	5.101550000	-0.819498000
6	-2.086809000	-4.076103000	-2.244184000
1	-2.994230000	-4.297739000	-2.828285000
1	-1.437516000	-4.958970000	-2.220834000
1	-1.544531000	-3.247766000	-2.713391000
6	3.369322000	2.528011000	-0.888846000
1	4.283418000	2.781291000	-1.449225000
1	2.865018000	1.687961000	-1.379700000
1	3.622975000	2.232599000	0.135108000
6	-3.369322000	-2.528011000	-0.888846000
1	-2.865018000	-1.687961000	-1.379700000
1	-3.622975000	-2.232599000	0.135108000
1	-4.283418000	-2.781291000	-1.449225000
5	1.125696000	3.409511000	0.095956000
6	2.086809000	4.076103000	-2.244184000
1	1.437516000	4.958970000	-2.220834000
1	1.544531000	3.247766000	-2.713391000
1	2.994230000	4.297739000	-2.828285000
5	-1.125696000	-3.409511000	0.095956000
6	-3.172490000	-4.845944000	-0.226646000
1	-4.065492000	-5.101550000	-0.819498000
1	-3.466275000	-4.566950000	0.791714000
1	-2.496920000	-5.708223000	-0.175915000
1	-0.503592000	-1.358883000	-1.631011000
1	0.503592000	1.358883000	-1.631011000
1	0.456565000	4.424799000	0.032930000
1	-1.581982000	-3.232994000	1.205219000
1	1.581982000	3.232994000	1.205219000
1	-0.456565000	-4.424799000	0.032930000
Mo(CO) <sub>4</sub> ( <sup>t</sup> BuPHBH <sub>2</sub> NMe <sub>3</sub> ) <sub>2</sub>			
42	-0.003098000	-0.040173000	1.449720000
15	1.834553000	-0.475389000	-0.429730000
15	-1.834252000	0.498525000	-0.409367000
8	2.047259000	-0.879112000	3.686381000
8	1.160317000	2.915327000	1.809193000
8	-1.158838000	-3.013671000	1.663785000
7	2.766418000	2.084269000	-1.965800000
7	-2.767501000	-1.983358000	-2.065123000
8	-2.061895000	0.689841000	3.716824000
6	1.307219000	-0.567055000	2.848471000
6	0.730897000	1.857050000	1.619253000
6	2.929867000	-2.062363000	-0.336757000
6	-0.734238000	-1.945519000	1.524389000
6	-1.318733000	0.417807000	2.867711000
6	3.887967000	3.064649000	-2.030432000
1	3.662570000	3.846231000	-2.773628000
1	4.809327000	2.538788000	-2.307675000
1	4.021711000	3.517457000	-1.041177000
6	1.525088000	2.811869000	-1.585213000
1	1.670518000	3.283423000	-0.607533000
1	0.694056000	2.101939000	-1.509754000
1	1.291360000	3.578119000	-2.341427000
6	-2.054096000	3.251996000	0.255533000
1	-1.642795000	3.060595000	1.255074000
1	-2.665468000	4.169742000	0.312789000
1	-1.212718000	3.459174000	-0.425066000
6	-2.920454000	2.084813000	-0.240575000
6	-3.895210000	-2.951321000	-2.185966000
1	-3.665119000	-3.702478000	-2.958440000
1	-4.808791000	-2.406951000	-2.452928000
1	-4.045763000	-3.444194000	-1.218545000
6	-1.535787000	-2.736237000	-1.702869000
1	-1.699585000	-3.257985000	-0.754065000
1	-0.703319000	-2.035375000	-1.574670000
1	-1.292617000	-3.463006000	-2.494237000
6	2.592380000	1.473606000	-3.309538000
1	2.369326000	2.253048000	-4.055162000
1	1.767808000	0.752700000	-3.276691000
1	3.513270000	0.946309000	-3.586629000
6	-2.573860000	-1.315368000	-3.378712000
1	-2.353735000	-2.063789000	-4.156265000
1	-1.740842000	-0.606942000	-3.307710000
1	-3.485747000	-0.764674000	-3.639654000
5	3.195458000	0.953185000	-0.842924000
6	-4.042286000	1.818533000	0.781010000
1	-4.715748000	1.013363000	0.453153000
1	-4.648892000	2.732638000	0.905832000
1	-3.642043000	1.550642000	1.769651000
6	4.044320000	-1.841435000	0.703382000
1	4.714602000	-1.017151000	0.419234000
1	4.655397000	-2.757322000	0.786322000
1	3.637254000	-1.624813000	1.701718000
6	-3.528447000	2.463494000	-1.602086000
1	-2.748299000	2.719301000	-2.338350000
1	-4.175812000	3.351044000	-1.487408000
1	-4.145961000	1.655570000	-2.019403000
6	2.065748000	-3.256408000	0.093979000
1	1.647507000	-3.115914000	1.098921000
1	2.679763000	-4.174047000	0.108717000
1	1.228938000	-3.431059000	-0.601306000
6	3.547730000	-2.366849000	-1.712131000
1	2.773798000	-2.592387000	-2.464579000
1	4.202901000	-3.253101000	-1.638557000
1	4.159872000	-1.533182000	-2.084266000
5	-3.200755000	-0.899681000	-0.898262000
1	3.403922000	1.565400000	0.183880000
1	4.205046000	0.453236000	-1.300489000
1	-1.244228000	0.847907000	-1.671677000
1	-4.203164000	-0.373772000	-1.342656000
1	1.250892000	-0.764257000	-1.710018000
1	-3.422926000	-1.554493000	0.099121000
W(CO) <sub>4</sub> ( <sup>t</sup> BuPHBH <sub>2</sub> NMe <sub>3</sub> ) <sub>2</sub>			
74	-0.070479000	-0.835052000	-0.837054000
15	-1.606256000	0.089917000	1.178340000
15	2.084639000	0.198902000	0.387134000
8	-0.349300000	1.892888000	-2.490781000
8	1.765474000	-1.867172000	-3.200731000
8	-2.585882000	-1.974372000	-2.378268000
8	0.147207000	-3.834732000	0.320917000
7	-3.879881000	1.767335000	-0.236131000
6	1.105760000	-1.483825000	-2.325627000
6	0.089946000	-2.732981000	-0.022760000
7	2.432381000	3.291821000	0.326351000
6	-1.668621000	-1.551834000	-1.798317000
6	-0.238123000	0.919733000	-1.859618000
6	-1.794695000	-1.033137000	2.735905000
6	-0.393024000	-1.418881000	3.234143000
1	0.180805000	-1.958017000	2.469679000
1	-0.481668000	-2.078480000	4.115165000
1	0.188266000	-0.533684000	3.539133000
6	-2.577742000	-2.302323000	2.355788000
1	-3.591460000	-2.066612000	1.999951000
1	-2.677291000	-2.951201000	3.243366000
1	-2.067930000	-2.885611000	1.576675000
6	-5.267080000	2.250791000	0.014950000
1	-5.930080000	1.385258000	0.130319000
1	-5.605802000	2.869949000	-0.830710000
1	-5.285011000	2.837132000	0.941174000
6	3.620724000	-0.900103000	0.763546000
5	-3.464977000	0.855573000	1.067336000
6	-2.982263000	2.944094000	-0.374397000
1	-3.332797000	3.596585000	-1.189528000
1	-1.969127000	2.602026000	-0.608404000
1	-2.977382000	3.500610000	0.571739000
6	-3.878789000	0.982325000	-1.502801000
1	-4.506098000	0.092896000	-1.374908000
1	-2.859539000	0.661854000	-1.729818000
1	-4.264094000	1.601841000	-2.327426000
6	-2.530536000	-0.294345000	3.868403000
1	-2.032684000	0.653829000	4.128889000
1	-2.536652000	-0.927226000	4.773453000
1	-3.573775000	-0.069048000	3.610346000
6	3.170691000	-2.229178000	1.387457000
1	2.599052000	-2.077653000	2.316887000
1	4.057125000	-2.837150000	1.639919000
1	2.553576000	-2.817635000	0.697597000
6	2.942234000	3.375907000	1.721030000
1	2.674975000	4.348456000	2.163742000
1	4.032560000	3.259659000	1.712050000
1	2.504327000	2.568230000	2.318443000
6	4.363318000	-1.179079000	-0.555557000
1	3.719667000	-1.687521000	-1.288195000
1	5.229812000	-1.834967000	-0.360384000
1	4.740911000	-0.255153000	-1.018307000
6	0.956074000	3.473680000	0.325319000
1	0.489167000	2.677142000	0.917214000
1	0.592136000	3.411136000	-0.706458000

1	0.697359000	4.452552000	0.760181000	1	0.616756000	4.550561000	-0.040637000
5	2.874131000	1.875210000	-0.403386000	<hr/>			
6	4.555401000	-0.185114000	1.754650000	Mo(CO) <sub>4</sub> ( <sup>t</sup> BuAsHBH <sub>2</sub> NMe <sub>3</sub> ) <sub>2</sub>			
1	4.912042000	0.778938000	1.365913000	42	0.005506000	-0.232912000	1.525954000
1	5.442936000	-0.813412000	1.947180000	33	-1.915606000	0.386508000	-0.326701000
1	4.060714000	-0.010342000	2.724448000	33	1.916733000	-0.273638000	-0.436943000
6	3.047102000	4.389480000	-0.473039000	8	-2.117628000	-0.029429000	3.836771000
1	2.800230000	5.365688000	-0.025713000	8	-0.811260000	-3.314071000	1.280859000
1	2.665169000	4.339753000	-1.499400000	8	0.827424000	2.793348000	2.161083000
1	4.134607000	4.251211000	-0.492901000	7	-2.586221000	-1.974253000	-2.395274000
1	-0.912604000	1.153985000	1.837658000	7	2.543691000	2.582422000	-1.766343000
1	1.794349000	0.553562000	1.742562000	8	2.135838000	-1.097242000	3.671684000
1	-4.245478000	-0.077372000	1.070207000	6	-1.346086000	-0.105488000	2.972722000
1	-3.618483000	1.602983000	2.014978000	6	-0.506038000	-2.198035000	1.321120000
1	4.086765000	1.857046000	-0.319827000	6	-3.265846000	1.856486000	0.152154000
1	2.495630000	1.968695000	-1.551850000	6	0.519530000	1.711446000	1.888259000
<hr/>				6	1.362950000	-0.774069000	2.867987000
Cr(CO) <sub>4</sub> ( <sup>t</sup> BuAsHBH <sub>2</sub> NMe <sub>3</sub> ) <sub>2</sub>				6	-3.644933000	-2.951156000	-2.780363000
33	0.000000000	-1.853967000	-0.320974000	1	-3.286447000	-3.590574000	-3.602926000
33	0.000000000	1.853967000	-0.320974000	1	-4.541770000	-2.403997000	-3.094666000
24	0.000000000	0.000000000	1.463486000	1	-3.892705000	-3.568898000	-1.909286000
8	0.198129000	-2.118720000	3.589137000	6	-1.377826000	-2.730459000	-1.964148000
8	3.019712000	0.301521000	1.631637000	1	-1.628738000	-3.349151000	-1.095919000
8	-3.019712000	-0.301521000	1.631637000	1	-0.590416000	-2.025549000	-1.673576000
8	-0.198129000	2.118720000	3.589137000	1	-1.019375000	-3.366227000	-2.789089000
7	-2.574516000	-3.692141000	-0.890793000	6	2.584549000	-3.092181000	0.029274000
6	0.118772000	-1.314714000	2.758450000	1	2.148349000	-3.020270000	1.034997000
7	2.574516000	3.692141000	-0.890793000	1	3.311698000	-3.924473000	0.038678000
6	1.871097000	0.174456000	1.518506000	1	1.779004000	-3.368222000	-0.670589000
6	-1.871097000	-0.174456000	1.518506000	6	3.291317000	-1.796066000	-0.384286000
6	1.764587000	-2.678098000	-0.954775000	6	3.575338000	3.656978000	-1.834459000
6	-1.764587000	2.678098000	-0.954775000	1	3.213109000	4.486893000	-2.461849000
6	-2.675952000	1.561412000	-1.483556000	1	4.498234000	3.242114000	-2.256946000
1	-2.208862000	1.015068000	-2.319907000	1	3.780155000	4.018246000	-0.819942000
1	-3.620332000	1.996748000	-1.859748000	6	1.302090000	3.154691000	-1.174999000
1	-2.940909000	0.840095000	-0.699093000	1	1.512476000	3.497727000	-0.156259000
6	-0.118772000	1.314714000	2.758450000	1	0.525885000	2.381621000	-1.131473000
6	2.415863000	-3.369426000	0.251803000	1	0.948606000	3.996716000	-1.790841000
1	2.611515000	-2.662727000	1.072323000	6	-2.253278000	-1.140870000	-3.580840000
1	3.384298000	-3.813002000	-0.043493000	1	-1.903149000	-1.779644000	-4.406917000
1	1.784692000	-4.180982000	0.646426000	1	-1.467621000	-0.425705000	-3.311657000
6	2.675952000	-1.561412000	-1.483556000	1	-3.147093000	-0.586385000	-3.891842000
1	2.208862000	-1.015068000	-2.319907000	6	2.261764000	2.103609000	-3.145461000
1	3.620332000	-1.996748000	-1.859748000	1	1.894785000	2.934610000	-3.768230000
1	2.940909000	-0.840095000	-0.699093000	1	1.504963000	1.311853000	-3.105112000
6	-1.516075000	3.695400000	-2.075349000	1	3.182245000	1.692343000	-3.577465000
1	-0.872697000	4.521779000	-1.741508000	5	-3.210427000	-1.059574000	-1.177776000
1	-2.476555000	4.135581000	-2.401962000	6	4.364029000	-1.433050000	0.654418000
1	-1.054226000	3.226906000	-2.960391000	1	4.911017000	-0.519054000	0.379509000
6	-2.415863000	3.369426000	0.251803000	1	5.100318000	-2.253992000	0.726711000
1	-2.611515000	2.662727000	1.072323000	1	3.934822000	-1.289246000	1.657186000
1	-3.384298000	3.813002000	-0.043493000	6	-4.356654000	1.232836000	1.037356000
1	-1.784692000	4.180982000	0.646426000	1	-4.922041000	0.451352000	0.507595000
6	1.516075000	-3.695400000	-2.075349000	1	-5.075163000	2.014845000	1.343293000
1	0.872697000	-4.521779000	-1.741508000	1	-3.939963000	0.793359000	1.956173000
1	2.476555000	-4.135581000	-2.401962000	6	3.927010000	-1.977241000	-1.769379000
1	1.054226000	-3.226906000	-2.960391000	1	3.181765000	-2.277838000	-2.524082000
6	-3.358971000	-4.832201000	-0.336074000	1	4.692164000	-2.774037000	-1.726083000
1	-3.652276000	-4.595226000	0.693145000	1	4.423467000	-1.061477000	-2.121804000
1	-2.728685000	-5.729589000	-0.327202000	6	-2.540063000	2.964778000	0.922755000
1	-4.255871000	-5.008450000	-0.951432000	2	-2.113631000	2.596932000	1.866023000
6	2.199419000	4.008598000	-2.293794000	1	-3.251354000	3.774248000	1.168170000
1	3.104658000	4.158897000	-2.903247000	1	-1.722685000	3.412115000	0.334173000
1	1.589154000	4.919385000	-2.306522000	6	-3.882547000	2.437008000	-1.127596000
1	1.612590000	3.180149000	-2.706561000	1	-3.125676000	2.935197000	-1.755297000
6	-3.430371000	-2.472887000	-0.871528000	1	-4.642578000	3.195059000	-0.863251000
1	-4.350022000	-2.651107000	-1.451010000	1	-4.379873000	1.666544000	-1.734413000
1	-2.879752000	-1.634686000	-1.313783000	5	3.178450000	1.381758000	-0.838060000
1	-3.679576000	-2.218556000	0.164724000	1	-3.505255000	-1.829735000	-0.286339000
6	3.430371000	2.472887000	-0.871528000	1	-4.172570000	-0.501026000	-1.667516000
1	2.879752000	1.634686000	-1.313783000	1	1.363841000	-0.624265000	-1.831033000
1	3.679576000	2.218556000	0.164724000	4	4.162163000	1.005366000	-1.445129000
1	4.350022000	2.651107000	-1.451010000	1	-1.359615000	1.103876000	-1.569127000
5	-1.250555000	-3.519000000	0.077396000	1	3.440978000	1.882068000	0.236575000
6	-2.199419000	-4.008598000	-2.293794000	<hr/>			
1	-1.589154000	-4.919385000	-2.306522000	W(CO) <sub>4</sub> ( <sup>t</sup> BuAsHBH <sub>2</sub> NMe <sub>3</sub> ) <sub>2</sub>			
1	-1.612590000	-3.180149000	-2.706561000	74	0.100526000	-0.809529000	0.996005000
1	-3.104658000	-4.158897000	-2.903247000	33	1.712691000	0.073811000	-1.080969000
5	1.250555000	3.519000000	0.077396000	33	-2.108758000	0.136929000	-0.363649000
6	3.358971000	4.832201000	-0.336074000	8	0.323815000	2.062396000	2.397834000
1	4.255871000	5.008450000	-0.951432000	8	-1.780344000	-1.728468000	3.366583000
1	3.652276000	4.595226000	0.693145000	8	2.587230000	-1.809144000	2.666990000
1	2.728685000	5.729589000	-0.327202000	8	-0.055302000	-3.836314000	-0.103508000
1	0.432225000	1.371978000	-1.717213000	7	4.040618000	1.822138000	0.319268000
1	-0.432225000	-1.371978000	-1.717213000	6	-1.099945000	-1.388410000	2.489304000
1	-0.616756000	-4.550561000	-0.040637000	6	-0.017370000	-2.732321000	0.234958000
1	1.687620000	3.361446000	1.197695000	7	-2.638365000	3.289286000	-0.377232000
1	-1.687620000	-3.361446000	1.197695000	<hr/>			

6	1.677982000	-1.440407000	2.038855000
6	0.230959000	1.026331000	1.872525000
6	1.963663000	-1.181539000	-2.680442000
6	0.576153000	-1.580390000	-3.198260000
1	-0.027843000	-2.073889000	-2.424564000
1	0.682334000	-2.287941000	-4.040675000
1	0.012073000	-0.708353000	-3.566622000
6	2.732023000	-2.421828000	-2.203026000
1	3.724045000	-2.160103000	-1.804765000
1	2.885840000	-3.111844000	-3.052214000
1	2.184901000	-2.974977000	-1.426498000
6	5.437755000	2.297432000	0.110274000
1	6.101306000	1.428404000	0.029440000
1	5.749866000	2.927868000	0.957904000
1	5.489049000	2.870898000	-0.822898000
6	-3.682113000	-1.106314000	-0.765115000
5	3.666110000	0.892281000	-0.978859000
6	3.142921000	3.004499000	0.414618000
1	3.477380000	3.668865000	1.226784000
1	2.121935000	2.672173000	0.630952000
1	3.162544000	3.544233000	-0.540510000
6	3.987261000	1.051191000	1.593932000
1	4.617850000	0.159443000	1.502784000
1	2.958346000	0.734488000	1.783063000
1	4.339430000	1.679224000	2.426789000
6	2.742384000	-0.476259000	-3.800029000
1	2.244634000	0.451950000	-4.124160000
1	2.805912000	-1.143900000	-4.678848000
1	3.768694000	-0.223364000	-3.499537000
6	-3.147086000	-2.418420000	-1.349273000
1	-2.576085000	-2.255170000	-2.277488000
1	-3.991357000	-3.087968000	-1.594906000
1	-2.500504000	-2.952342000	-0.640668000
6	-3.110210000	3.321520000	-1.788017000
1	-2.855956000	4.288552000	-2.249991000
1	-4.197038000	3.176108000	-1.805620000
1	-2.634256000	2.509074000	-2.349105000
6	-4.418043000	-1.376327000	0.555810000
1	-3.756959000	-1.828693000	1.310362000
1	-5.253315000	-2.078304000	0.380483000
1	-4.842537000	-0.455917000	0.985253000
6	-1.167290000	3.513387000	-0.338579000
1	-0.661383000	2.721458000	-0.904507000
1	-0.827823000	3.476145000	0.702810000
1	-0.925099000	4.492284000	-0.782405000
5	-3.058448000	1.882383000	0.370697000
6	-4.625227000	-0.443454000	-1.778046000
1	-5.027382000	0.510626000	-1.407142000
1	-5.485118000	-1.109347000	-1.975796000
1	-4.124498000	-0.259968000	-2.742886000
6	-3.308038000	4.388025000	0.375893000
1	-3.081797000	5.359364000	-0.092422000
1	-2.950576000	4.379127000	1.412167000
1	-4.390755000	4.214499000	0.372779000
1	0.992916000	1.173232000	-1.873799000
1	-1.799813000	0.476326000	-1.828055000
1	4.440220000	-0.045248000	-0.951443000
1	3.817299000	1.615544000	-1.944190000
1	-4.261838000	1.790812000	0.229019000
1	-2.725227000	2.006032000	1.530269000

## References

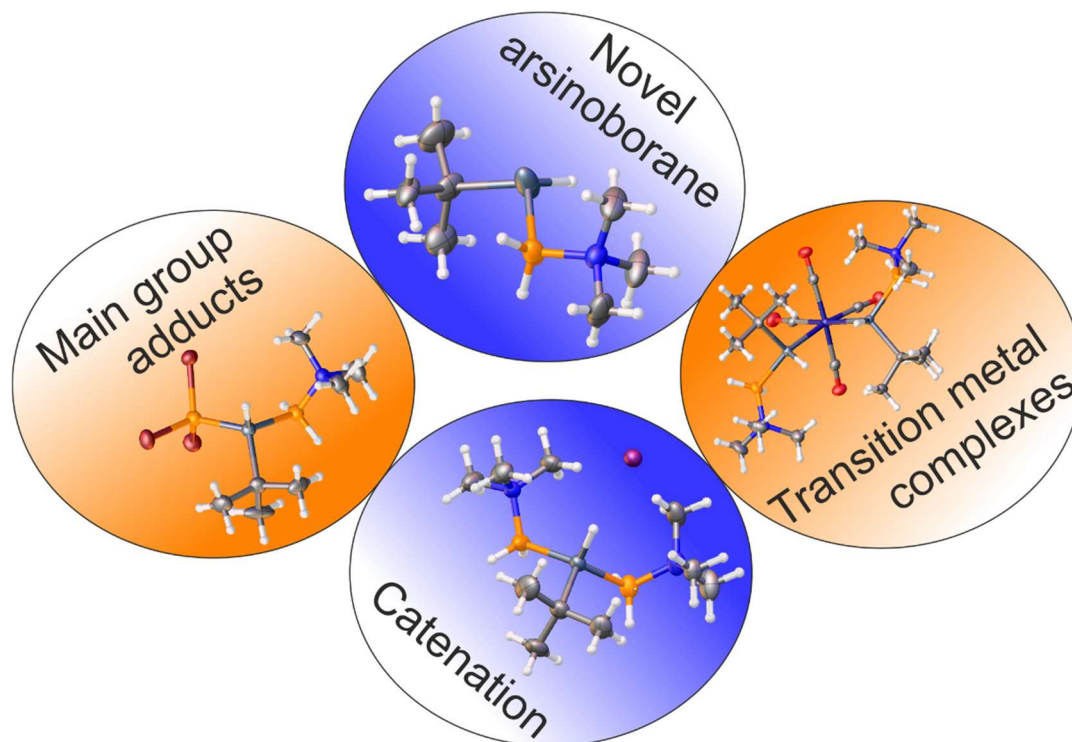
- [1] a) A. D. Becke, *J. Chem. Phys.* **1993**, *98*, 5648; b) Lee, Yang, Parr, *Phys. rev. B, Condensed matter* **1988**, *37*, 785.
- [2] a) F. Weigend, R. Ahlrichs, *Phys. Chem. Chem. Phys.* **2005**, *7*, 3297; b) K. A. Peterson, D. Figgen, E. Goll, H. Stoll, M. Dolg, *J. Chem. Phys.* **2003**, *119*, 11113.
- [3] M. J. Frisch, G. W. Trucks, H. B. Schlegel, G. E. Scuseria, M. A. Robb, J. R. Cheeseman, G. Scalmani, V. Barone, B. Mennucci, G. A. Petersson, H. Nakatsuji, M. Caricato, X. Li, H. P. Hratchian, A. F. Izmaylov, J. Bloino, G. Zheng, J. L. Sonnenberg, M. Hada, M. Ehara, K. Toyota, R. Fukuda, J. Hasegawa, M. Ishida, T. Nakajima, Y. Honda, O. Kitao, H. Nakai, T. Vreven, J. A. Montgomery, Jr., J. E. Peralta, F. Ogliaro, M. Bearpark, J. J. Heyd, E. Brothers, K. N. Kudin, V. N. Staroverov, T. Keith, R. Kobayashi, J. Normand, K. Raghavachari, A. Rendell, J. C. Burant, S. S. Iyengar, J. Tomasi, M. Cossi, N. Rega, J. M. Millam, M. Klene, J. E. Knox, J. B. Cross, V. Bakken, C. Adamo, J. Jaramillo, R. Gomperts, R. E. Stratmann, O. Yazyev, A. J. Austin, R. Cammi, C. Pomelli, J. W. Ochterski, R. L. Martin, K. Morokuma, V. G. Zakrzewski, G. A. Voth, P. Salvador, J. J. Dannenberg, S. Dapprich, A. D. Daniels, O. Farkas, J. B. Foresman, J. V. Ortiz, J. Cioslowski, and D. J. Fox, Gaussian 09, Revision E.01, Gaussian, Inc., Wallingford CT, 2013.
- [4] a) K. L. Schuchardt, B. T. Didier, T. Elsethagen, L. Sun, V. Gurumoorthi, J. Chase, J. Li, T. L. Windus, *J. Chem. Inform. Model.* **2007**, *47*, 1045; b) D. Feller, *J. Comput. Chem.* **1996**, *17*, 1571.
- [5] Computational Chemistry Comparison and Benchmark DataBase, Standard Reference Database 101 National Institute of Standards and Technology Release 22 (May 2022), Internet: <https://cccbdb.nist.gov/vsfx.asp>.

## 2.7. Author contributions

- The synthesis and characterization of compounds **1**, **2**, **4**, **5**, **7**, **8** have been performed by Felix Lehnfeld
- X-ray structural analysis of compounds **1**, **2**, **4**, **5**, **7**, **8** have been performed by Felix Lehnfeld with help from Dr. Michael Seidl.
- The synthesis and characterization of compounds **3** and **6** have been performed by Dr. Oliver Hegen (reported in his PhD-thesis, Regensburg, **2018**), the IR spectroscopy measurements of **3** and **6** used in this chapter have been performed by Felix Lehnfeld.
- The DFT calculations have been performed by Prof. Dr. Alexey Timoshkin
- The manuscript (including supporting information, figures, schemes and graphical abstract) was written by Felix Lehnfeld, with Dr. Gábor Balázs contributing to the interpretation of the IR spectroscopy and NMR spectroscopy data and Prof. Dr. Alexey Timoshkin contributing the segments concerning the theoretical data.

### 3. Synthesis and Reactivity of a Lewis-Base-Stabilized *tert*-Butyl Arsanylborane: A Versatile Building Block for Arsenic-Boron Oligomers

Felix Lehnfeld, Michael Seidl, Alexey Y. Timoshkin, and Manfred Scheer



**Abstract:** The synthesis and reactivity of the *tert*-butyl-substituted arsanylborane  $t\text{BuAsHBH}_2\cdot\text{NMe}_3$  (**1**) stabilized by a Lewis base (LB) are reported. Compound **1** is obtained by the reaction of *in situ* generated  $\text{Na}t\text{BuAsH}$  with  $\text{IBH}_2\cdot\text{NMe}_3$ . By the reaction of **1** with Lewis acids the neutral compounds  $\text{BBr}_3\cdot t\text{BuAsHBH}_2\cdot\text{NMe}_3$  (**2**) and  $\text{BH}_3\cdot t\text{BuAsHBH}_2\cdot\text{NMe}_3$  (**3**) as well as the coordination products towards Group 6 metal complexes  $[\text{M}(\text{CO})_4(t\text{BuAsHBH}_2\cdot\text{NMe}_3)_2]$  ( $\text{M} = \text{Cr}, \text{Mo}, \text{W}$ ; **4a-c**) are obtained. Upon reaction with  $\text{IBH}_2\cdot\text{LB}$  ( $\text{LB} = \text{SMe}_2, \text{NMe}_3$ ), the cationic oligomeric arsanylboranes  $[(\text{Me}_3\text{NBH}_2t\text{BuAsHBH}_2\cdot\text{NMe}_3)]\text{I}$  (**5**) and  $[\text{H}_2\text{B}(t\text{BuAsHBH}_2\cdot\text{NMe}_3)_2]\text{I}$  (**6**) were isolated. Compound **1** was also used as starting material for the synthesis of oligomeric arsanylboranes obtained by thermal oligomerization under different conditions. DFT calculations support the experimental observations.

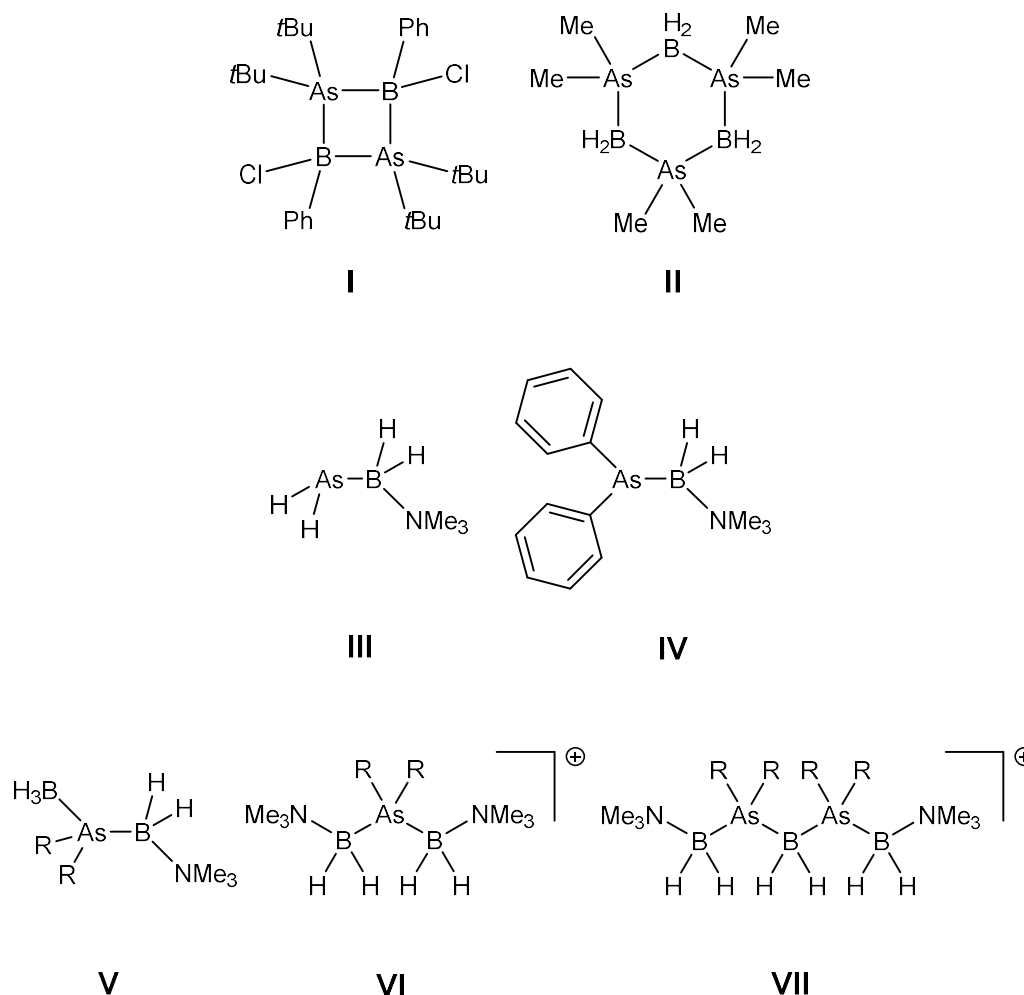
### 3.1. Introduction

Inorganic main-group-based polymers are attractive materials for many different applications, e.g. as ceramic precursors, polyelectrolytes or in optoelectronics due to their broad variety of properties.<sup>[1]</sup> Therefore, the targeted catenation of non-carbon elements has been receiving increasing attention. In the case of phosphorus, not only several chains of polyphosphines and polyphosphorus anions are known,<sup>[2]</sup> but also different *catena*-phosphorus cations, as reported by Burford and Weigand et al.<sup>[3]</sup> On the other hand, for boron, mainly the formation of higher aggregated clusters is known with only few exceptions.<sup>[4]</sup> Besides some references to a linear  $B_8(NMe_2)_{10}$ ,<sup>[5]</sup> only  $B_4(NMe_2)_6$ <sup>[6]</sup> and cyclic  $B_6(NMe_2)_6$ <sup>[7]</sup> have structurally been characterized. Additionally,  $B_4R_4$  was reported as a ligand in the coordination sphere of a transition metal complex,<sup>[8]</sup> but, as for all other examples, organic substituents are necessary for their stabilization.

Due to the isoelectronic relation between carbon compounds and compounds consisting of group 13 and 15 elements, such compounds possess great potential as starting material for main group-based *catena* compounds. In addition to poly(amino)- and poly(phosphinoborane)s based on Lewis acid/base adducts of the type  $R_3E \cdot E'R_3$  ( $E =$  group 15 element;  $E' =$  group 13 element) obtained by dehydrogenation/dehydrocoupling reactions,<sup>[9]</sup> recently the polymerization of Zintl type anions of the type  $[BP_2]^{3-}$  to 1D boron-phosphorus chains, composed of pentagonal  $B_2P_3$  rings, has been reported. Similar arsenic based Zintl anions are known, but no similar polymerizations have been reported to date.<sup>[10]</sup> Especially Lewis base-stabilized pnictogenylboranes of the type  $R_2EBH_2 \cdot LB$  ( $E =$  group 15 element;  $LB =$  Lewis base) exhibit a very promising reactivity owing to their lone pair. Our group has reported numerous different compounds of this type over the past years, including the only hydrogen-substituted parent pnictogenylboranes  $H_2PBH_2 \cdot LB$  and  $H_2AsBH_2 \cdot LB$  in addition to organosubstituted derivatives.<sup>[11]</sup>

For Lewis base-stabilized phosphanylboranes, a very rich chemistry was observed. Among the reported results are Lewis acid adducts resulting in neutral *catena* compounds,<sup>[11a,b,12]</sup> anionic chains obtained by the substitution of the Lewis base by phosphanides<sup>[11a,13]</sup> as well as cationic group 13/15 *catena* compounds by the reaction with  $IBH_2 \cdot LB$ .<sup>[11a,14]</sup> By reaction of  $(OC)_5W \cdot PH_2BH_2 \cdot SMe_2$  with  $LB$ -stabilized pnictogenylboranes, neutral mixed pnictogenylborane chains are accessible.<sup>[15]</sup> For

the parent phosphanylborane  $\text{PH}_2\text{BH}_2\cdot\text{NMe}_3$ , oligomeric compounds can be obtained by reaction with  $[\text{Cp}_2\text{Ti}(\text{btmsa})]$  (btmsa = bis(trimethylsilyl)acetylene)<sup>[16]</sup> as well as polymeric materials under thermolytic conditions.<sup>[11c]</sup>



**Scheme 1.** Selected examples of cyclic arsenanylboranes, monomeric arsenanylboranes and derived *catena* compounds. R = H, Ph. Counterions are omitted for clarity.

The mono tert-butyl-substituted phosphanylborane,  $t\text{BuPHBH}_2\text{NMe}_3$ , exhibits a good combination of steric bulk and donor strength, making it an excellent starting material for the generation of stable high-molecular weight polymers by metal-free head-to-tail polymerization.<sup>[11c]</sup>

In contrast to the variety of phosphorus-boron *catena* compounds, there are very few examples known for oligomeric compounds based on the heavier pnictogen homologue arsenic. Reported examples require bulky organic substituents on both the B and As atoms (I) or the stabilization by thermodynamically favorable ring systems (II) (Scheme 1).<sup>[17]</sup> Only few *catena* compounds based on Lewis-base-stabilized

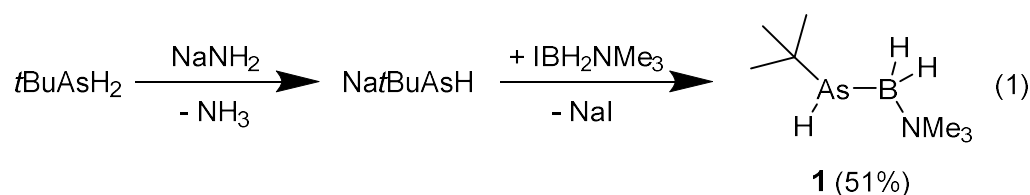
arsanylboranes (**III** and **IV**) have been reported recently. Noteworthy examples include the neutral LA adducts  $\text{BH}_3 \cdot \text{AsR}_2\text{BH}_2 \cdot \text{NMe}_3$  ( $\text{R} = \text{Ph}$  or  $\text{H}$ ; **V**)<sup>[11a,b]</sup> as well as the cationic chain compounds  $[\text{BH}_2(\text{R}_2\text{AsBH}_2 \cdot \text{NMe}_3)_2]^+$  ( $\text{R} = \text{Ph}, \text{H}$ ; **VI**) and  $[\text{Me}_3\text{N} \cdot \text{BH}_2\text{AsR}_2\text{BH}_2 \cdot \text{NMe}_3]^+$  ( $\text{R} = \text{Ph}, \text{H}$ ; **VII**).<sup>[11a,14]</sup> But neither the parent arsanylborane  $\text{H}_2\text{AsBH}_2 \cdot \text{NMe}_3$  nor the diphenyl-substituted arsanylborane  $\text{Ph}_2\text{AsBH}_2 \cdot \text{NMe}_3$  are suitable as precursors for neutral oligo- or poly(arsinoborane)s due to thermal cleavage of the As-B bond in case of **III** or insufficient donor strength of the arsenic atom in case of **IV**.

Therefore, transferring the very versatile reactivity of  $t\text{BuPHBH}_2\text{NMe}_3$  to the corresponding arsanylborane chemistry should allow for a relatively stable, while reactive arsanylborane. Therefore, we targeted the synthesis of a similar, monoalkyl-substituted arsanylborane as model compound to be used as potential precursor for the generation of oligomers.

Herein, we report the synthesis of  $t\text{BuAsHBH}_2\text{NMe}_3$ , which represents the first monoalkyl-substituted arsanylborane only stabilized by a LB. The successful synthesis allows to investigate the reactivity of this new compound as a potential starting material for both neutral and cationic arsenic-boron-based *catena* compounds and oligomers.

### 3.2. Results and Discussion

The one-pot reaction of *in situ* generated  $\text{Na}t\text{BuAsH}$  with  $\text{IBH}_2 \cdot \text{NMe}_3$  in THF leads to the LB-stabilized arsanylborane  $t\text{BuAsHBH}_2 \cdot \text{NMe}_3$  (**1**) in 51% yield. After metalation of  $t\text{BuAsH}_2$ , the dark brown suspension undergoes a color change to colorless upon addition of  $\text{IBH}_2 \cdot \text{NMe}_3$  and stirring overnight, while showing full conversion to **1** according to  $^{11}\text{B}$  NMR spectroscopy (Equation 1). In the  $^{11}\text{B}$  NMR spectrum of isolated **1**, a triplet at  $\delta = -5.26$  ppm with a coupling constant of  $^1J_{\text{B,H}} = 109$  Hz is observed, which is similar to already reported arsanylboranes.<sup>[11a,b]</sup>



In the  $^1\text{H}$  NMR spectrum among the signals corresponding to the  $\text{NMe}_3$  and the  $t\text{Bu}$  groups at  $\delta = 1.92$  ppm and  $\delta = 1.62$  ppm, respectively, two overlapping broad pseudo-quartets for the diastereotopic hydrogen atoms bound to the boron atom can be

detected. In the  $^1\text{H}\{^{11}\text{B}\}$  NMR spectrum, the signals appear as two pseudo-triplets at  $\delta = 2.99$  ppm and  $\delta = 2.50$  ppm with two very similar  $^{2/3}J_{\text{H,H}}$  coupling constants of about 8 Hz. The resonance signal corresponding to the As-H is observed as a triplet at  $\delta = 1.89$  ppm with a  $^3J_{\text{H,H}}$  coupling constant of 7.4 Hz, but the signal is partly overlapped by the signal of the  $\text{NMe}_3$  group.

In contrast to the already reported arsanylboranes such as  $\text{AsH}_2\text{BH}_2\text{NMe}_3$  and  $\text{Ph}_2\text{AsBH}_2\text{NMe}_3$ , compound **1** is asymmetrically substituted on the arsenic atom and therefore occurs as two enantiomers. In the solid-state structure (Figure 1), both enantiomers are incurred as a racemate. The As-B bond length of 2.079(5) Å is in the range of a single bond. The boron atom shows a nearly tetrahedral environment, whereas the arsenic atom possesses a distorted trigonal pyramidal arrangement, with a B-As-C bond angle of 101.0(4)° which is slightly more distorted in comparison to the phosphorus analogue  $t\text{BuPHBH}_2\text{NMe}_3$ .<sup>[11c]</sup>

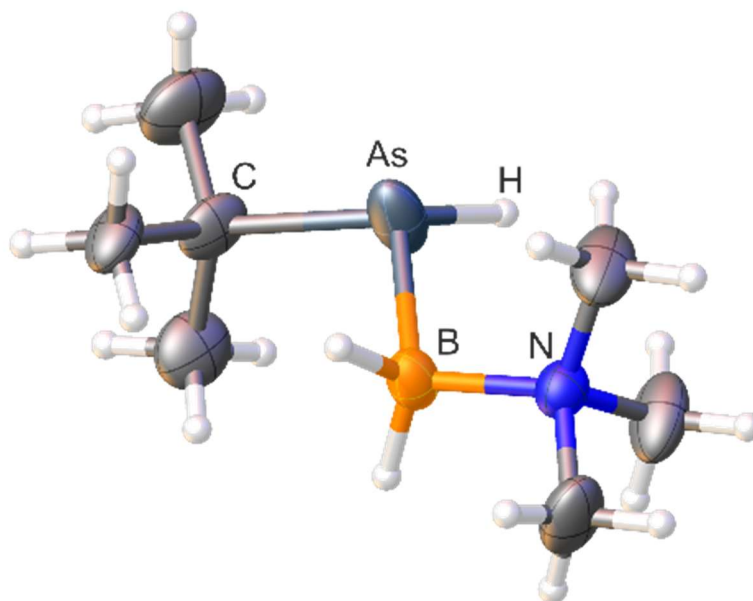
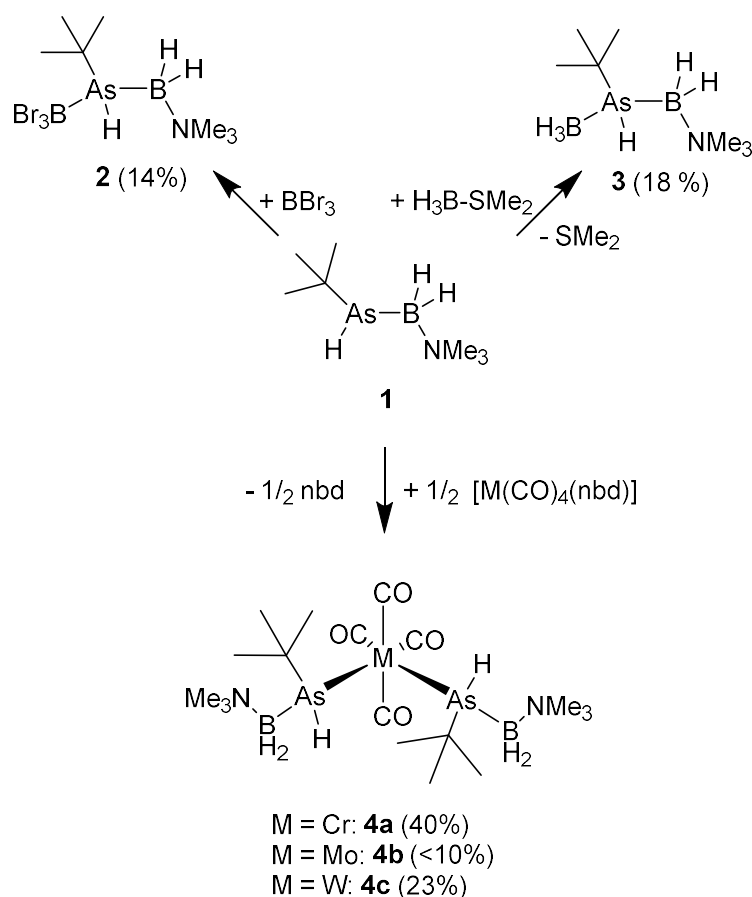


**Figure 1.** Molecular structure of **1**. Only the S enantiomer is shown for clarity. Thermal ellipsoids displayed at 50% probability. Selected bond distances (Å) and angles [°]: N-B 1.619(3), B-As 2.079(5), As-C 1.941(18); N-B-As 109.7(2), C-As-B 101.0(4).

As the donor strength of the As atom is essential for its potential use as building block for oligomeric compounds, its reactivity towards Lewis acids (LAs) was investigated (Scheme 2). The reactions with the main group LAs  $\text{BBr}_3$  and  $\text{BH}_3\cdot\text{SMe}_2$  lead to the formation of the LA-LB-stabilized *tert*-butylarsanylboranes  $\text{BBr}_3\cdot t\text{BuAsHBH}_2\cdot\text{NMe}_3$  (**2**) and  $\text{BH}_3\cdot t\text{BuAsHBH}_2\cdot\text{NMe}_3$  (**3**), respectively. Both reactions proceed almost

quantitatively according to the  $^{11}\text{B}$  NMR spectroscopy, but the products are only accessible in lower crystalline yields due to the good solubility of **2** and **3**. The signals corresponding to the  $\text{BBr}_3$  and  $\text{BH}_3$  moiety in **2** and **3** can be observed at  $\delta = -15.77$  ppm and  $\delta = -35.87$  ppm, respectively. In comparison to the starting material **1**, the signals for the  $\text{BH}_2$  groups are slightly high-field shifted at  $\delta = -7.55$  ppm and  $\delta = -8.60$  ppm for **2** and **3**, respectively. For compound **2**, the  $^1\text{H}$  NMR spectrum exhibits low field shifts both for the signal corresponding to the As-H to 3.88 ppm and for the *t*Bu-group to 2.82 ppm. The  $^1\text{H}$  NMR spectrum of **3** exhibits two broad pseudo quartets for the  $\text{BH}_2$ - and  $\text{BH}_3$ -groups in the range of 1.7-2.7 ppm and 0.4-1.2 ppm, respectively. In addition to multinuclear NMR spectroscopy, both compounds have been characterized by X-ray structure analysis (Figure 2).



**Scheme 2.** Reaction of **1** with main group and transition metal Lewis acids; isolated crystalline yields in parentheses; (nbd = norbornadiene, thf = tetrahydrofuran)

The inner As-B distances in **2** (2.093(5)) and **3** (2.070(6)) are in the range of an As-B single bond and only slightly elongated in **3** in comparison to the starting material **1**

due to the stronger Lewis acidity and steric bulk of  $\text{BBr}_3$ . The As-B distances towards the LA are in both cases very similar (2.064(5) (**2**) and 2.070(6) (**3**)) and in the range of an As-B single bond.

For **2** and **3**, two enantiomers are present in the solid state due to the chirality of the arsenic atom. Whereas **3** crystallizes in the space group  $P2_1/n$  with both enantiomers in the unit cell, **2** crystallizes in the acentric space group  $P2_12_12_1$ , but represents inversion twins.

Computed thermodynamic characteristics for the formation of **2** and **3** are summarized in Table S4. Reactions of  $t\text{BuAsHBH}_2\text{NMe}_3$  with  $\text{BBr}_3$  and  $\text{BH}_3\cdot\text{SMe}_2$  are predicted to be exergonic in solution, in agreement with experimental observations.

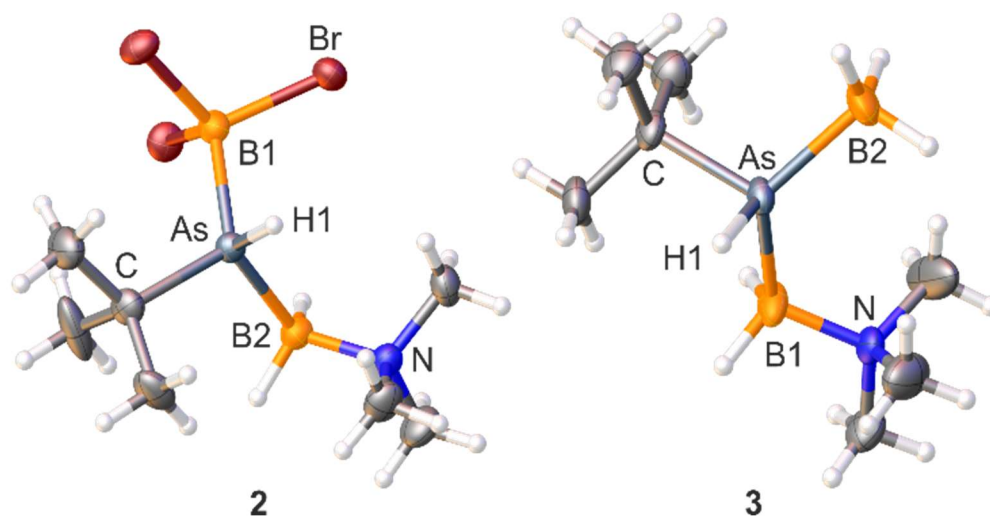


**Figure 2.** Molecular structure of **2** and **3**. Thermal ellipsoids displayed at 50% probability. Selected bond distances (Å) and angles [°]: **2** As-B1 2.064(5), As-B2 2.093(5), As-C 1.986(5), N-B2 1.597(7); C-As-B1 116.1(2), C-As-B2 108.8(2), B1-As-B2 111.9(2), N-B2-As 114.9(3); **3** As-C 1.976(5), As-B1 2.075(6), As-B2 2.070(6), N-B1 1.583(7); C-As-B1 104.1(2), C-As-B2 111.7(3), B2-As-B1 123.6(3), N-B1-As 115.0(4).

In addition to the reactivity towards main group LAs, also the coordination chemistry towards Lewis acidic transition metal complexes of group 6 metals was investigated. The reaction of **1** with *in situ* prepared  $[\text{W}(\text{CO})_5(\text{thf})]$  leads to a slight color change to darker yellow, but no solid product could be isolated (only an oily product).

To yield crystalline products, the group 6 complexes  $[\text{M}(\text{CO})_4(\text{nbd})]$  (M = Cr, Mo, W; nbd = norbornadiene) were used as transition metal LAs instead. In all three cases, the elimination of nbd and the coordination of two equivalents of **1** to the metal center are observed in a quantitative reaction according to  $^{11}\text{B}$  NMR spectra of the reaction

solutions. In the  $^{11}\text{B}$  NMR spectra of **4a** and **4c**, only a slight change in the chemical shift to  $\delta = -4.6$  ppm could be observed, but it was possible to obtain crystals of **4a-c** suitable for X-ray diffraction analysis, with moderate yields for **4a** and **4c**, but only few single crystals for **4b** (Figure 3). Also, the DFT computations reveal that these reactions are exergonic in solution (Table S4).

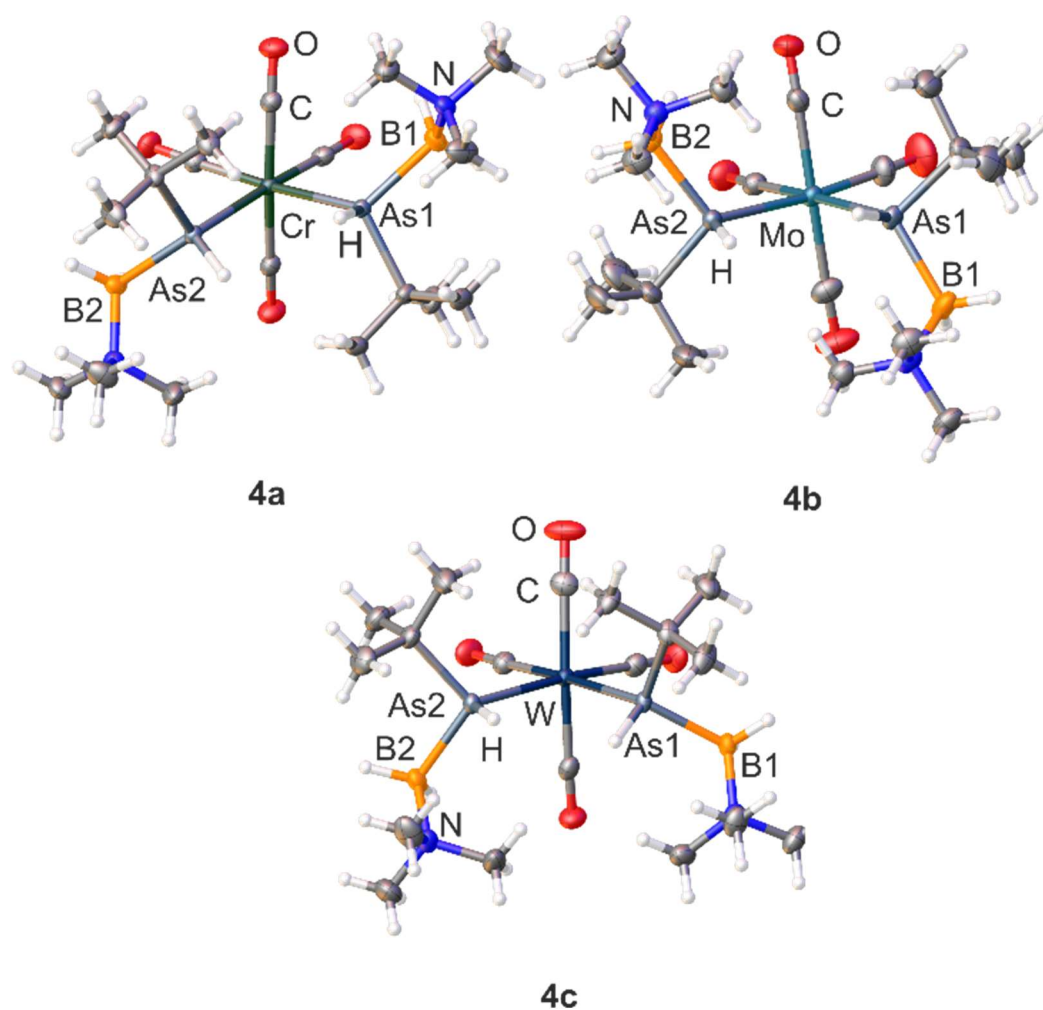


**Figure 3.** Molecular structure of **4a-c**. Thermal ellipsoids displayed at 50% probability. Selected bond distances (Å) and angles [°] are found in table 1.

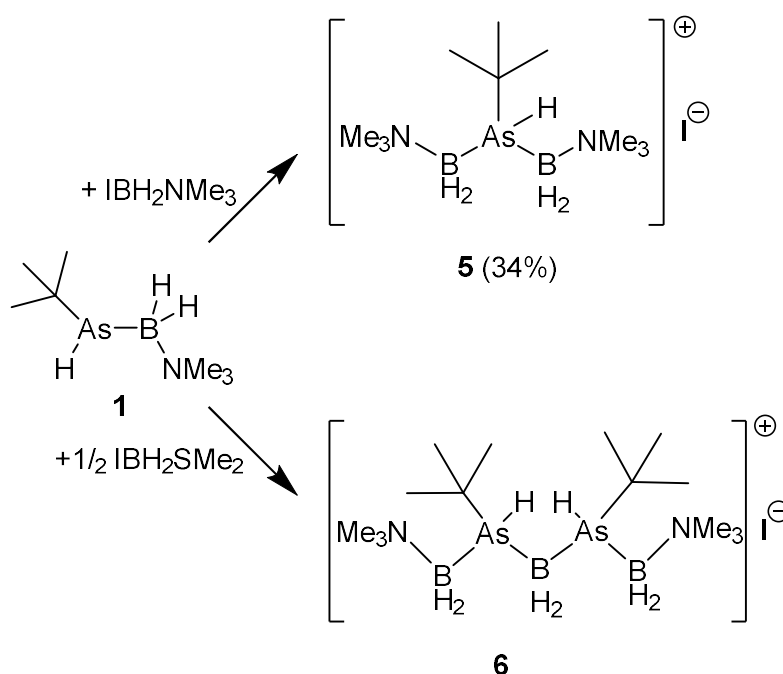
**4a-c** crystallize in the triclinic space group  $P2_1/n$ . All relevant bond lengths and bond angles are depicted in table 1. Whereas **4b** and **4c** show very similar structural features, the Cr-As distance and bond angles such as the As1-Cr-As2 one differ slightly for **4a** due to the smaller atom radius compared to **4b** and **4c**. Concerning the stereochemistry of **4a-c**, one important difference was observed: Whereas in **4a** and **4b**, two molecules of **1** with the same configuration coordinate to the metal center,

leading to RR or SS configuration with both enantiomers found in the unit cell, the tungsten derivative **4c** exists as a *meso*-isomer.

**Table 1.** Selected bond distances (Å) and angles [°] of compounds **4a-c**

	<b>4a</b>	<b>4b</b>	<b>4c</b>
M-As1/	2.5168(2)/	2.6666(3)/	2.6513(4)/
M-As2 [Å]	2.5163(2)	2.6595(3)	2.6501(5)
As1-M-As1 [°]	90.417(7)	88.895(8)	88.719(14)
C-As1-M/	117.35(4)/	119.34(8)/	118.36(12)/
C-As2-M [°]	117.92(4)	118.05(7)	119.16(12)

Having established that the donor strength of the As atom in the *tert*-butyl-substituted arsanylborane is sufficient, we were furthermore interested in the formation of cationic oligomeric chain-like compounds by reacting **1** with  $\text{IBH}_2\cdot\text{LB}$  (LB =  $\text{NMe}_3$ ,  $\text{SMe}_2$ ). Depending on the substituted LB, the formation of  $[\text{Me}_3\text{N}\cdot\text{BH}_2\text{tBuAsHBH}_2\cdot\text{NMe}_3]\text{I}$  (**5**) or  $[\text{H}_2\text{B}(\text{tBuAsHBH}_2\cdot\text{NMe}_3)_2]\text{I}$  (**6**) is observed (Scheme 3).



**Scheme 3.** Synthesis of three- and five-membered cationic chain-like compounds starting from **1**; yields of isolated product in parentheses.

Both reactions show full conversion according to the  $^{11}\text{B}$  NMR spectroscopy of the reaction mixture, with **5** and **6** as the only products. Whereas **5** could be isolated in a crystalline yield of 34%, **6** could only be obtained in solution. All attempts to grow single crystals of **6** suitable for X-ray diffraction analysis or precipitation of **6** failed due to decomposition. Both **5** and **6** were characterized by multinuclear NMR spectroscopy and **5** also by single crystal X-ray structure analysis.

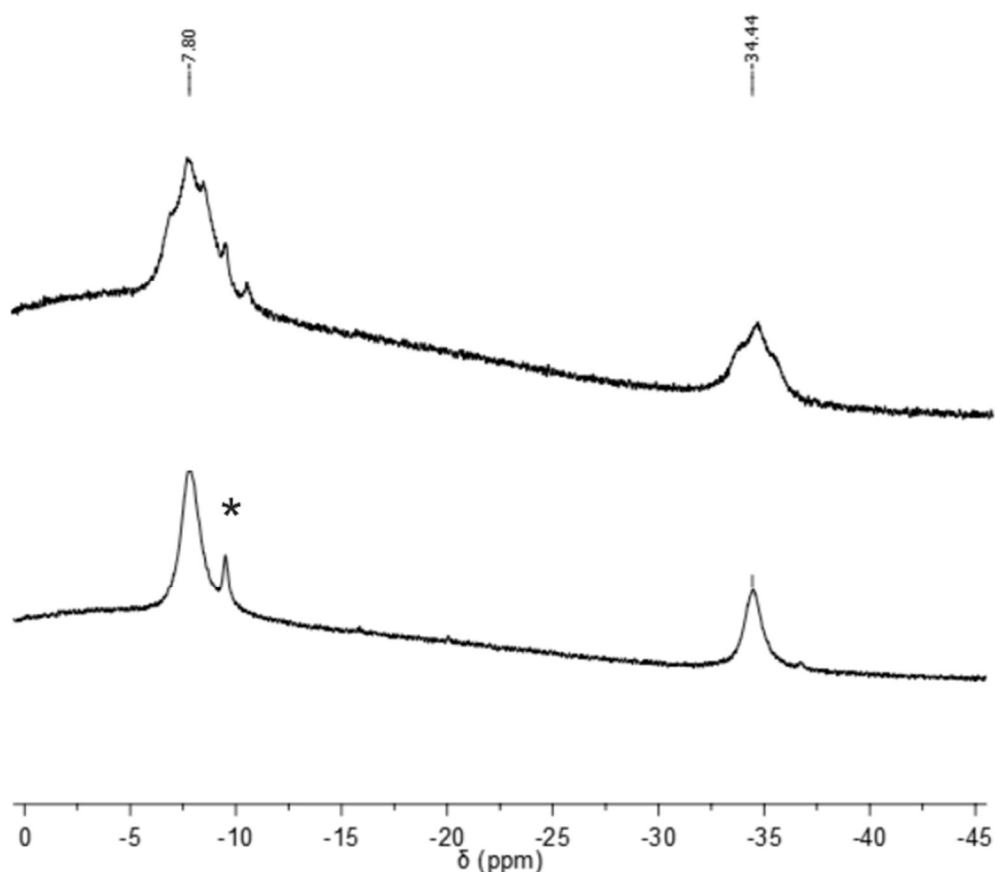


**Figure 4.**  $^{11}\text{B}\{^1\text{H}\}$  NMR spectrum (bottom) and  $^{11}\text{B}$  NMR spectrum (top) of **6** in  $\text{CD}_2\text{Cl}_2$ . (\* = impurity of  $\text{IBH}_2\text{SMe}_2$ )

Both compounds **5** and **6** show a very similar high field shifted signals for the  $\text{NMe}_3$ -bonded  $\text{BH}_2$  groups at  $\delta = -7.7$  ppm (**5**) and  $\delta = -7.8$  ppm (**6**), respectively. The signal for the  $\text{BH}_2$  moiety between the two As centers in **6** is observed as a broadened triplet at  $\delta = -34.4$  ppm (Fig. 4).<sup>[11a,14a]</sup> In the  $^1\text{H}$  NMR spectra of **5**, the As-H signal is shifted to lower field as opposed to those of **1** where it is found at around  $\delta = 4.0$  ppm. The signals corresponding to the  $\text{BH}_2$ -groups appear as a broad overlapping signal in the

range between 2 and 3 ppm. The signals corresponding to the NMe<sub>3</sub> and *t*Bu groups are shifted by about 1 ppm to lower field compared to **1**.

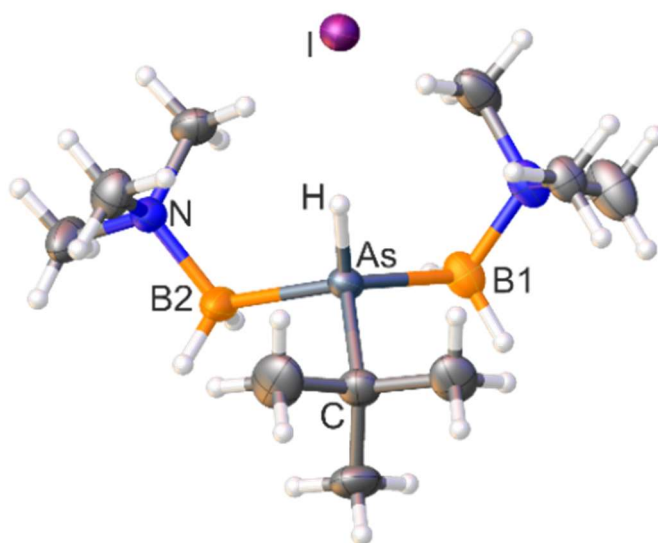


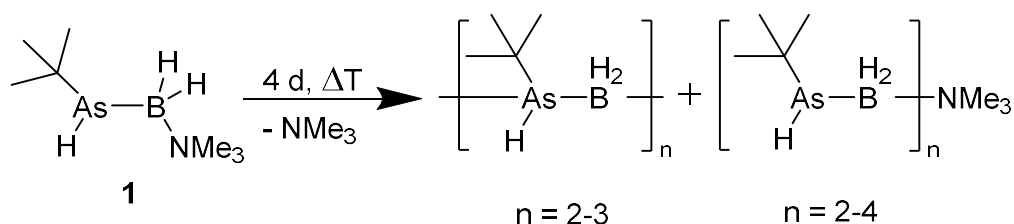
**Figure 5.** Molecular structure of **5**. The thermal ellipsoids are displayed at 50% probability. Selected bond distances (Å) and angles [°]: As-C 1.978(5), As-B1 2.074(5), As-B2 2.070(5), N-B1 1.591(6), C-As1-B1 110.8(2), C-As1-B2 107.6(2), B2-As1-B1 114.2(2), N1-B1-As 114.2(3), N2-B2-As 114.3(3).

**5** crystallizes as colorless blocks in the space group *Pca*2<sub>1</sub>. The solid-state structure reveals a central *tert*-butyl-substituted As-H moiety that is connected to two BH<sub>2</sub>NMe<sub>3</sub> groups via As-B single bonds (Figure 5). The conformation of both As-B bonds is almost eclipsed, leading to an overall almost symmetric arrangement, as both As-B distances are very similar (As-B1 2.074(5), As-B2 2.070(5)). The arsenic atom reveals a distorted tetrahedral arrangement, with all non-hydrogen-substituents exhibiting bond angles of approximately 114° around the As atom.

According to DFT calculations, the reaction of *t*BuAsHBH<sub>2</sub>•NMe<sub>3</sub> with IBH<sub>2</sub>•SMe<sub>2</sub> is predicted to be exergonic in solution, in agreement with experimental observations. The reaction with IBH<sub>2</sub>•NMe<sub>3</sub> under formation of **5** is predicted to be slightly endergonic, but the crystal lattice energy favors the formation of a solid product (Table S4).

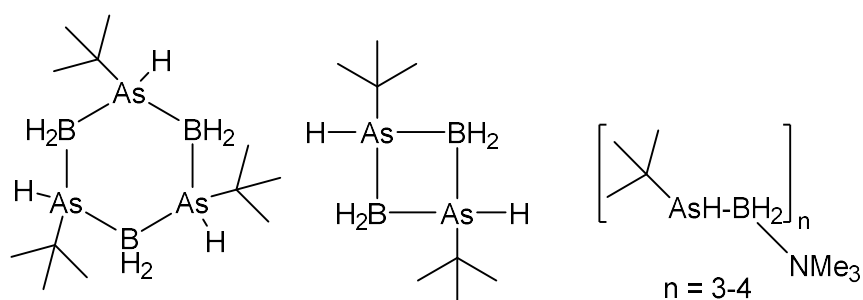
Having established **1** as a suitable starting material for the targeted synthesis of cationic oligomeric compounds, the next step was the synthesis of neutral oligomers. As in the case of *t*BuPHBH<sub>2</sub>•NMe<sub>3</sub>, this was achieved by thermolysis (Scheme 4).<sup>[11c]</sup> After already 40 h stirring at 80°C, about 50% conversion was detected in the <sup>11</sup>B NMR spectrum, indicated by a broad multiplet at  $\delta = -36.8$  ppm. The conversion can be increased by longer reaction times as well as higher temperatures. However, the

thermolysis is always accompanied by decomposition, visible in the precipitation of an insoluble orange solid, which increases over time and with more elevated temperatures.



**Scheme 4.** Thermal oligomerization of **1**

Besides the insoluble orange solid, the obtained oil is very soluble in polar and nonpolar organic solvents and was characterized by ESI mass spectrometry. Hereby, it was possible to identify NMe<sub>3</sub>-capped oligomeric fragments with up to  $n = 4$  as well as oligomers missing the NMe<sub>3</sub> group with up to  $n = 3$ . This indicates that, very probably, cyclic oligomers are formed among presumably NMe<sub>3</sub>-capped linear oligomers. To investigate the nature of the formed oligomers and their relative stability, DFT computations were performed. According to the calculations, the oligomerization processes of **1** to form *catena*-(*t*BuAsHBH<sub>2</sub>)<sub>*n*</sub> oligomers are thermodynamically unfavorable and therefore highly unlikely even at 373 K, while the formation of *catena*-(*t*BuAsHBH<sub>2</sub>)<sub>*n*</sub>NMe<sub>3</sub> oligomers is exergonic for  $n = 3, 4$  and *cyclo*-(*t*BuAsHBH<sub>2</sub>)<sub>*n*</sub> is exergonic for  $n = 2, 3, 4$ .



**Scheme 5.** Structures of the most likely formed oligomers according to ESI-MS results and DFT calculations. Reaction Gibbs energies  $\Delta G^\circ_{373}$  for the formation of oligomer compounds from **1** (in kJ per mole of **1**) (-53 (left), -21 (middle), -5 (right,  $n = 3$ ), -20.5 (right,  $n = 4$ )).

For the oligomerization of *t*BuAsHBH<sub>2</sub>•NMe<sub>3</sub> per one mole of starting material, the formation of the trimeric *cyclo*-(*t*BuAsHBH<sub>2</sub>)<sub>3</sub> is predicted to be the most thermodynamically favorable product both at 298 and at 373 K, followed by the ring

tetramer *cyclo*-(*t*BuAsHBH<sub>2</sub>)<sub>4</sub>, the ring dimer *cyclo*-(*t*BuAsHBH<sub>2</sub>)<sub>2</sub>, the NMe<sub>3</sub>-stabilized chain tetramer *catena*-(*t*BuAsHBH<sub>2</sub>)<sub>4</sub>NMe<sub>3</sub> and the NMe<sub>3</sub>-stabilized chain trimer *catena*-(*t*BuAsHBH<sub>2</sub>)<sub>3</sub>NMe<sub>3</sub>. Taking all information into account, the most likely formed oligomers are summarized in Scheme 5.

### 3.3. Conclusion

In summary, a straightforward synthesis of an alkyl-substituted monomeric arsanylborane *t*BuAsHBH<sub>2</sub>•NMe<sub>3</sub> (**1**) stabilized only by a Lewis base was developed. It was isolated in good yields and showed high thermal stability. Using **1** as starting material, it was possible to access numerous new products. In addition to the neutral arsanylborane chain compounds BBr<sub>3</sub>•*t*BuAsHBH<sub>2</sub>•NMe<sub>3</sub> (**2**) and BH<sub>3</sub>•*t*BuAsHBH<sub>2</sub>•NMe<sub>3</sub> (**3**) obtained by the reaction with main group Lewis acids, also coordination products with transition metal centers were obtained. Taking into account the asymmetric nature of **1**, these coordination products as well as the crystallization of **2** in the chiral space group *P*<sub>2</sub><sub>1</sub><sub>2</sub><sub>1</sub><sub>2</sub><sub>1</sub> allow for some fascinating insights into the stereochemistry of **1** and its products. It was also shown that **1** is a suitable precursor for larger arsanylborane oligomers. Not only the cationic group 13/15-based oligomers [Me<sub>3</sub>N•BH<sub>2</sub>*t*BuAsHBH<sub>2</sub>•NMe<sub>3</sub>]<sup>+</sup>I<sup>-</sup> (**5**) or [H<sub>2</sub>B(*t*BuAsHBH<sub>2</sub>•NMe<sub>3</sub>)<sub>2</sub>]<sup>+</sup>I<sup>-</sup> (**6**) are accessible via reactions with IBH<sub>2</sub>•LB (LB = NMe<sub>3</sub>, SMe<sub>2</sub>), but it is also possible to obtain neutral oligo(arsanylborane)s through thermolysis of **1**. This makes **1** not only the first asymmetrically substituted arsanylborane only stabilized by an LB, but also the first isolable arsanylborane to undergo metal-free head-to-tail oligomerization under thermolytic conditions.

### 3.4. Experimental Section

#### Synthesis of *t*BuAsHBH<sub>2</sub>•NMe<sub>3</sub> (**1**)

A solution of *t*BuAsH<sub>2</sub> (5 mmol, 670 mg) in 5 mL toluene is added to a suspension of NaNH<sub>2</sub> (5 mmol, 195 mg) in 10 mL thf at 193 K. After stirring for 16 h while slowly warming up to r.t., a deep brown solution is obtained. A suspension of IBH<sub>2</sub>•NMe<sub>3</sub> (5 mmol, 994 mg) in 5 mL thf is added to this solution cooled to 193 K. After stirring for 16 h while slowly warming up to r.t., a colorless solution and a white precipitate are obtained. After carefully removing the solvent under reduced pressure at 253 K, compound **1** is extracted with *n*-hexane (3x 10 mL) and filtrated over diatomaceous

earth. After carefully removing the solvent, compound **1** can be obtained as a colorless liquid. **1** can be isolated as colorless blocks by storing a saturated solution of **1** in *n*-hexane at 243 K. Yield: 523 mg (2.55 mmol, 51%).  $^1\text{H}$  NMR ( $\text{C}_6\text{D}_6$ , 293 K)  $\delta$  = 3.5-2.0 (2H, br,  $^1J_{\text{H,B}}$  = 109 Hz,  $\text{BH}_2$ ), 1.92 (9H, s,  $\text{NMe}_3$ ), 1.85 (1H, d,  $^3J_{\text{H,H}}$  = 7.4 Hz), 1.62 (9H, s, *t*Bu).  $^{11}\text{B}$  NMR ( $\text{C}_6\text{D}_6$ , 293 K)  $\delta$  = -5.26 (t,  $^1J_{\text{H,B}}$  = 109 Hz,  $\text{BH}_2$ ).  $^{11}\text{B}\{^1\text{H}\}$  NMR ( $\text{C}_6\text{D}_6$ , 293 K)  $\delta$  = -5.26 (s,  $\text{BH}_2$ ).  $^{13}\text{C}\{^1\text{H}\}$  NMR ( $\text{C}_6\text{D}_6$ , 293 K)  $\delta$  = 27.18 (s,  $(\text{CH}_3)_3\text{C}$ ), 34.10 (s,  $(\text{CH}_3)_3\text{C}$ ), 52.74 (s,  $\text{NMe}_3$ ). ESI-MS ( $\text{CH}_2\text{Cl}_2$ ):  $m/z$  = 205.98. Elemental analysis (%) calculated for  $\text{C}_7\text{H}_{21}\text{AsBN}$ : C: 41.02, H: 10.33, N: 6.83; found: C: 41.16, H: 10.01, N: 6.72.

### Synthesis of $\text{BBr}_3 \cdot t\text{BuAsHBH}_2 \cdot \text{NMe}_3$ (**2**)

To a solution of  $t\text{BuAsHBH}_2 \cdot \text{NMe}_3$  (0.2 mmol, 41 mg) in 4 mL toluene,  $\text{BBr}_3$  (0.2 mmol, 50 mg) is added at 273 K. After stirring at 273 K for 1h, the solution is slowly warmed up to r.t. and continued to be stirred for 16 h hours at r.t.. All volatiles are removed under reduced pressure and the obtained white, oily solid is washed with two times 2 ml of *n*-hexane. **2** can be isolated as colorless blocks by storing a saturated solution in  $\text{CH}_3\text{CN}$  at 243 K. Yield: 13 mg (0.03 mmol, 14%).  $^1\text{H}$  NMR ( $\text{CD}_3\text{CN}$ , 293 K)  $\delta$  = 3.89 (1H, br, AsH), 2.83 (9H, s,  $\text{NMe}_3$ ) 3.0-2.0 (br, 2H,  $\text{BH}_2$ ), 1.48 (9H, s, *t*Bu).  $^{11}\text{B}$  NMR ( $\text{CD}_3\text{CN}$ , 293 K)  $\delta$  = -15.77 (s,  $\text{BBr}_3$ ), -7.55 (t,  $^1J_{\text{H,B}}$  = 117 Hz,  $\text{BH}_2$ ).  $^{11}\text{B}\{^1\text{H}\}$  NMR ( $\text{CD}_3\text{CN}$ , 293 K)  $\delta$  = -15.77 (s,  $\text{BBr}_3$ ), -7.55 (s,  $\text{BH}_2$ ). ESI-MS ( $\text{CH}_3\text{CN}$ ):  $m/z$  = 375.9 (M-Br). Elemental analysis (%) calculated for  $\text{C}_7\text{H}_{21}\text{AsB}_2\text{Br}_3\text{N}$ : C: 18.46, H: 4.65, N: 3.08; found: C: 19.26, H: 4.44, N: 3.09; containing 1/12 *n*-hexane.

### Synthesis of $\text{BH}_3 \cdot t\text{BuAsHBH}_2 \cdot \text{NMe}_3$ (**3**)

To a solution of  $t\text{BuAsHBH}_2 \cdot \text{NMe}_3$  (0.2 mmol, 41 mg) in 3 ml toluene, a solution of  $\text{BH}_3 \cdot \text{SMe}_2$  (0.2 mmol, 15 mg) in 0.4 mL toluene is added at r.t. After stirring for 16 h at r.t., all volatiles are removed under reduced pressure. The remaining solid is dissolved in 5 mL *n*-hexane and filtrated of diatomaceous earth. **3** can be isolated as colorless needles by storing a saturated solution in *n*-hexane at 243 K. Yield: 8 mg (0.04 mmol, 18%).  $^1\text{H}$  NMR ( $\text{C}_6\text{D}_6$ , 293 K)  $\delta$  = 2.78 (9H, s,  $\text{NMe}_3$ ), 2.73-1.73 (2H, br,  $^1J_{\text{H,B}}$  = 112 Hz,  $\text{BH}_2$ ), 2.28 (1H, m, AsH), 1.2 (9H, s, *t*Bu), 1.2-0.4 (3H, brq,  $^1J_{\text{H,B}}$  = 103 Hz,  $\text{BH}_3$ ).  $^{11}\text{B}$  NMR ( $\text{C}_6\text{D}_6$ , 293 K)  $\delta$  = -35.87 (q,  $^1J_{\text{H,B}}$  = 103 Hz,  $\text{BH}_3$ ), -8.60 (t,  $^1J_{\text{H,B}}$  = 112 Hz,  $\text{BH}_2$ ).  $^{11}\text{B}\{^1\text{H}\}$  NMR ( $\text{CD}_3\text{CN}$ , 293 K)  $\delta$  = -35.87 (s,  $\text{BH}_3$ ), -8.60 (s,  $\text{BH}_2$ ). ESI-MS ( $\text{CH}_3\text{CN}$ ):

$m/z = 217.9$  ( $M-H^+$ ). Elemental analysis (%) calculated for  $C_7H_{24}AsB_2N$ : C: 38.42, H: 11.06, N: 6.40; found: C: 39.53, H: 10.61, N: 6.45; containing 1/8 *n*-hexane.

#### Synthesis of $[Cr(CO)_4(tBuAsHBH_2 \cdot NMe_3)_2]$ (**4a**)

To a solution of  $[Cr(CO)_4(nbd)]$  (*nbd* = norbornadiene, 0.1 mmol, 26 mg) in 2 mL  $CH_2Cl_2$ , a solution of  $tBuAsHBH_2 \cdot NMe_3$  (0.2 mmol, 41 mg) in 2 mL toluene is added at r.t.. After stirring for 16 h at r.t., the solution is filtrated. **4a** can be isolated as yellow blocks by layering a saturated  $CH_2Cl_2$ /toluene solution with *n*-hexane at 273 K. Yield: 23 mg (0.04 mmol, 40%).  $^1H$  NMR ( $CD_2Cl_2$ , 293 K)  $\delta = 3.0$ -2.0 (4H, br,  $BH_2$ ), 2.78 (18H, s,  $NMe_3$ ), 1.68 (2H, s, AsH), 1.29 (18H, s, *t*Bu).  $^{11}B$  NMR ( $CD_2Cl_2$ , 293 K)  $\delta = -4.51$  (t (br),  $^1J_{H,B} = 114$  Hz,  $BH_2$ ).  $^{11}B\{^1H\}$  NMR ( $CD_2Cl_2$ , 293 K)  $\delta = -4.51$  (br,  $BH_2$ ).  $^{13}C\{^1H\}$  NMR ( $CD_2Cl_2$ , 293 K)  $\delta = 231.4$  (s,  $(CH_3)_3C$ ), 231.2 (s,  $(CH_3)_3C$ ), 225.9 (s,  $NMe_3$ ), 32.54 (s, CO), 32.19 (s, CO), 31.87 (s, CO), 31.58 (s, CO).

#### Synthesis of $[Mo(CO)_4(tBuAsHBH_2 \cdot NMe_3)_2]$ (**4b**)

To a solution of  $[Mo(CO)_4(nbd)]$  (*nbd* = norbornadiene, 0.1 mmol, 30 mg) in 2 mL  $CH_2Cl_2$ , a solution of  $tBuAsHBH_2 \cdot NMe_3$  (0.2 mmol, 41 mg) in 2 mL toluene is added at r.t.. After stirring for 16 h at r.t., the solution is filtrated. **4b** can be isolated as yellow blocks by layering a saturated  $CH_2Cl_2$ /toluene solution with *n*-hexane at 273 K. Yield: few crystals (<10%).

#### Synthesis of $[W(CO)_4(tBuAsHBH_2 \cdot NMe_3)_2]$ (**4c**)

To a solution of  $[W(CO)_4(nbd)]$  (*nbd* = norbornadiene, 0.1 mmol, 39 mg) in 2 mL  $CH_2Cl_2$ , a solution of  $tBuAsHBH_2 \cdot NMe_3$  (0.2 mmol, 41 mg) in 2 mL toluene is added at r.t.. After stirring for 16 h at r.t., the solution is filtrated. **4c** can be isolated as yellow blocks by layering a saturated  $CH_2Cl_2$ /toluene solution with *n*-hexane at 273 K. Yield: 16 mg (0.023 mmol, 23%).  $^1H$  NMR ( $CD_2Cl_2$ , 293 K)  $\delta = 3.0$ -2.0 (4H, br,  $BH_2$ ), 2.78 (18H, s,  $NMe_3$ ), 1.68 (2H, m, AsH), 1.30 (18H, s, *t*Bu).  $^{11}B$  NMR ( $CD_2Cl_2$ , 293 K)  $\delta = -4.96$  (t (br),  $^1J_{H,B} = 105$  Hz,  $BH_2$ ).  $^{11}B\{^1H\}$  NMR ( $CD_2Cl_2$ , 293 K)  $\delta = -4.96$  (br,  $BH_2$ ).

#### Synthesis of $[Me_3N \cdot BH_2 \cdot tBuAsH \cdot BH_2 \cdot NMe_3]^+I^-$ (**5**)

To a solution of  $\text{IBH}_2\cdot\text{NMe}_3$  (0.2 mmol, 40 mg) in 3 mL  $\text{CH}_2\text{Cl}_2$ , a solution of  $t\text{BuAsHBH}_2\cdot\text{NMe}_3$  (0.2 mmol, 41 mg) in 2 mL toluene is added dropwise at 243 K. The solution is stirred for 16 h while allowed to reach r.t.. After removing all volatiles under reduced pressure, the obtained yellowish oil is suspended in benzene. Benzene is removed under reduced pressure and the oil is dried in vacuo. **5** can be isolated as colorless blocks by layering a saturated  $\text{CH}_2\text{Cl}_2$  solution with *n*-hexane at 273 K. Yield: 28 mg (0.07 mmol, 34%).  $^1\text{H}$  NMR ( $\text{CD}_2\text{Cl}_2$ , 293 K)  $\delta$  = 4.01 (1H, s, AsH), 3.1-1.8 (4H, br,  $\text{BH}_2$ ), 2.91 (18H, s,  $\text{NMe}_3$ ), 1.32 (9H, s, *t*Bu).  $^{11}\text{B}$  NMR ( $\text{CD}_2\text{Cl}_2$ , 293 K)  $\delta$  = -7.72 (t,  $^1J_{\text{H,B}}$  = 116 Hz,  $\text{BH}_2$ ).  $^{11}\text{B}\{^1\text{H}\}$  NMR ( $\text{CD}_2\text{Cl}_2$ , 293 K)  $\delta$  = -7.72 (s,  $\text{BH}_2$ ).  $^{13}\text{C}\{^1\text{H}\}$  NMR ( $\text{CD}_2\text{Cl}_2$ , 293 K)  $\delta$  = 45.1 (s,  $(\text{CH}_3)_3\text{C}$ ), 32.3 (s,  $(\text{CH}_3)_3\text{C}$ ), 29.6 (s,  $\text{NMe}_3$ ). ESI-MS ( $\text{CH}_3\text{CN}$ ):  $m/z$  = 277.3 ( $\text{M}^+$ ). Elemental analysis (%) calculated for  $\text{C}_{10}\text{H}_{32}\text{AsB}_2\text{N}_2$ : C: 29.74, H: 7.99, N: 6.94; found: C: 30.08, H: 7.77, N: 7.04.

### Synthesis of $[\text{Me}_3\text{N}\cdot\text{BH}_2\text{-}t\text{BuAsH-BH}_2\text{-}t\text{BuAsH-BH}_2\cdot\text{NMe}_3]^+\text{I}^-$ (**6**)

To a solution of  $\text{IBH}_2\text{SMe}_2$  (0.2 mmol, 40 mg) in 1 mL  $\text{CH}_2\text{Cl}_2$ , a solution of  $t\text{BuAsHBH}_2\text{NMe}_3$  (0.4 mmol, 82 mg) in 2 mL toluene is added dropwise at 243 K. The solution is stirred for 16 h while allowed to reach r.t.. All attempts to isolate **6** as solid failed due to decomposition, but it can be characterized in solution.

### Thermolytic oligomerization of $t\text{BuAsHBH}_2\cdot\text{NMe}_3$

A solution of  $t\text{BuAsHBH}_2\cdot\text{NMe}_3$  (0.2 mmol, 40 mg) in 1 mL toluene is stirred at 80 °C for 40 h, the colorless solution turns slightly yellow during that time. According to the  $^{11}\text{B}$  NMR, the reaction shows 50% conversion to oligomeric species. Increasing the reaction time to 65 h or the temperature to 100 °C, augments conversion to 70%, but more decomposition product is formed as an orange precipitate.  $^{11}\text{B}$  NMR ( $\text{CD}_2\text{Cl}_2$ , 293 K)  $\delta$  = -36.75 (t (br),  $^1J_{\text{H,B}}$  = 109 Hz).  $^{11}\text{B}\{^1\text{H}\}$  NMR ( $\text{CD}_2\text{Cl}_2$ , 293 K)  $\delta$  = -36.75 (m (br))

### DFT computations

The geometries of the compounds have been fully optimized with gradient-corrected density functional theory (DFT) in form of Becke's three-parameter hybrid method B3LYP<sup>[17]</sup> with def2-SVP<sup>[18]</sup> all electron basis set (ECP on Mo, W). Gaussian 09 program package<sup>[19]</sup> was used throughout. All structures correspond to minima on their respective potential energy surfaces as verified by computation of second derivatives.

Basis sets were obtained from the EMSL basis set exchange database.<sup>[20]</sup> Standard entropies of the reactions in solution were estimated by taking into account the loss of translational degrees of freedom upon solvation of one gaseous mole in the inert solvent ( $90 \text{ J mol}^{-1} \text{ K}^{-1}$ ).<sup>[21]</sup>

### 3.5. References

- [1] a) J. Linshoef, E. J. Baum, A. Hussain, P. J. Gates, C. Näther, A. Staubitz, *Angew. Chem. Int. Ed.* **2014**, *53*, 12916-12920; b) A. Hübner, Z.-W. Qu, U. Englert, M. Bolte, H.-W. Lerner, M. C. Holthausen, M. Wagner, *J. Am. Chem. Soc.* **2011**, *133*, 4596-4609; c) R. H. Neilson, P. Wisian-Neilson, *Chem. Rev.* **1988**, *88*, 541-562; d) R. D. Jaeger, M. Gleria, *Prog. Polym. Sci.* **1998**, *23*, 179-276; e) M. Liang, I. Manners, *J. Am. Chem. Soc.* **1991**, *113*, 4044-4045; f) A. M. Priegert, B. W. Rawe, S. C. Serin, D. P. Gates, *Chem. Soc. Rev.* **2016**, *45*, 922-953; g) I. Manners, *Angew. Chem. Int. Ed.* **1996**, *35*, 1602-1621; h) R. D. Miller, J. Michl, *Chem. Rev.* **1989**, *89*, 1359-1410; i) F. Choffat, S. Käser, P. Wolfer, D. Schmid, R. Mezzenga, P. Smith, W. Caseri, *Macromolecules* **2007**, *40*, 7878-7889; j) F. Jäkle, *Chem. Rev.* **2010**, *110*, 3985-4022; k) B. W. Rawe, C. P. Chun, D. P. Gates, *Chem. Sci.* **2014**, *5*, 4928-4938; l) Z. M. Hudson, D. J. Lunn, M. A. Winnik, I. Manners, *Nat. Commun.* **2014**, *5*; m) X. He, T. Baumgartner, *RSC Adv.* **2013**, *3*, 11334-11350; n) H. R. Allcock, *Chem. Mater.* **1994**, *6*, 1476-1491; o) G. Zhang, G. M. Palmer, M. W. Dewhurst, C. L. Fraser, *Nat. Mater.* **2009**, *8*, 747-751; p) P. J. Fazen, J. S. Beck, A. T. Lynch, E. E. Remsen, L. G. Sneddon, *Chem. Mater.* **1990**, *2*, 96-97.
- [2] a) M. Baudler, K. Glinka, *Chem. Rev.* **1993**, *93*, 1623-1667; b) M. Baudler, K. Glinka, *Chem. Rev.* **1994**, *94*, 1273-1297; c) M. Baudler, *Angew. Chem. Int. Ed.* **1982**, *21*, 492-512; d) M. Baudler, *Angew. Chem. Int. Ed.* **1987**, *26*, 419-441; e) H. G. Von Schnering, W. Hoenle, *Chem. Rev.* **1988**, *88*, 243-273; f) I. Jevtovic, P. Lönnecke, E. Hey-Hawkins, *Chem. Commun.* **2013**, *49*, 7355-7357.
- [3] C. A. Dyker, N. Burford, *Chem. Asian J.* **2008**, *3*, 28-36; b) M. Donath, E. Conrad, P. Jerabek, G. Frenking, R. Fröhlich, N. Burford, J. J. Weigand, *Angew. Chem. Int. Ed.* **2012**, *51*, 2964-2967; c) J. J. Weigand, N. Burford, M. D. Lumsden, A. Decken, *Angew. Chem. Int. Ed.* **2006**, *45*, 6733-6737; d) C. Taube, K. Schwedtmann, M. Noikham, E. Somsook, F. Hennersdorf, R. Wolf, J. J. Weigand, *Angew. Chem. Int. Ed.* **2020**, *59*, 3585-3591; e) J. J. Weigand, M.

- Holthausen, R. Fröhlich, *Angew. Chem. Int. Ed.* **2009**, *48*, 295-298; f) M. H. Holthausen, C. Richter, A. Hepp, J. J. Weigand, *Chem. Commun.* **2010**, *46*, 6921-6923; g) K.-O. Feldmann, J. J. Weigand, *Angew. Chem. Int. Ed.* **2012**, *51*, 7545-7549; h) J. J. Weigand, N. Burford, R. J. Davidson, T. S. Cameron, P. Seelheim, *J. Am. Chem. Soc.* **2009**, *131*, 17943-17953.
- [4] a) H. Braunschweig, R. D. Dewhurst, *Angew. Chem. Int. Ed.* **2013**, *52*, 3574-3583; b) E. Osorio, J. K. Olson, W. Tiznado, A. I. Boldyrev, *Chem. Eur. J.* **2012**, *18*, 9677-9681.
- [5] K. H. Hermannsdörfer, E. M. Und, H. Nöth, *Chem. Ber.* **1970**, *103*, 516-527.
- [6] G. Linti, D. Loderer, H. Nöth, K. Polborn, W. Rattay, *Chem. Ber.* **1994**, *127*, 1909-1922.
- [7] H. Nöth, H. Pommerening, *Angew. Chem. Int. Ed.*, **1980**, *19*, 482-483.
- [8] H. Braunschweig, Q. Ye, A. Vargas, R. D. Dewhurst, K. Radacki, A. Damme, *Nat. Chem.* **2012**, *4*, 563-567.
- [9] a) H. C. Johnson, A. S. Weller, *Angew. Chem. Int. Ed.* **2015**, *54*, 10173-10177; b) H. C. Johnson, E. M. Leitao, G. R. Whittell, I. Manners, G. C. Lloyd-Jones, A. S. Weller, *J. Am. Chem. Soc.* **2014**, *136*, 9078-9093; c) A. N. Marziale, A. Friedrich, I. Klopsch, M. Drees, V. R. Celinski, J. Schmedt auf der Günne, S. Schneider, *J. Am. Chem. Soc.* **2013**, *135*, 13342-13355; d) A. Staubitz, A. P. M. Robertson, M. E. Sloan, I. Manners, *Chem. Rev.* **2010**, *110*, 4023-4078; e) A. Staubitz, M. E. Sloan, A. P. M. Robertson, A. Friedrich, S. Schneider, P. J. Gates, J. Schmedt auf der Günne, I. Manners, *J. Am. Chem. Soc.* **2010**, *132*, 13332-13345; f) R. T. Baker, J. C. Gordon, C. W. Hamilton, N. J. Henson, P.-H. Lin, S. Maguire, M. Murugesu, B. L. Scott, N. C. Smythe, *J. Am. Chem. Soc.* **2012**, *134*, 5598-5609; g) J.-M. Denis, H. Forintos, H. Szelke, L. Toupet, T.-N. Pham, P.-J. Madec, A.-C. Gaumont, *Chem. Commun.* **2003**, 54-55; h) H. Dorn, J. M. Rodezno, B. Brunnhöfer, E. Rivard, J. A. Massey, I. Manners, *Macromolecules* **2003**, *36*, 291-297; i) A. Kumar, N. A. Beattie, S. D. Pike, S. A. Macgregor, A. S. Weller, *Angew. Chem. Int. Ed.* **2016**, *55*, 6651-6656; j) S. Pandey, P. Lönnecke, E. Hey-Hawkins, *Eur. J. Inorg. Chem.* **2014**, *2014*, 2456-2465; k) H. Dorn, R. A. Singh, J. A. Massey, J. M. Nelson, C. A. Jaska, A. J. Lough, I. Manners, *J. Am. Chem. Soc.* **2000**, *122*, 6669-6678.

- [10] a) K. E. Woo, J. Wang, J. Mark, K. Kovnir, *J. Am. Chem. Soc.* **2019**, *141*, 13017-13021; b) H.-G. von Schnering, M. Somer, M. Hartweg, K. Peters, *Angew. Chem. Int. Ed.* **1990**, *29*, 65-67.
- [11] a) O. Hegen, A. V. Virovets, A. Y. Timoshkin, M. Scheer, *Chem. Eur J.* **2018**, *24*, 16521-16525; b) C. Marquardt, A. Adolf, A. Stauber, M. Bodensteiner, A. V. Virovets, A. Y. Timoshkin, M. Scheer, *Chem. Eur J.* **2013**, *19*, 11887-11891; c) C. Marquardt, T. Jurca, K.-C. Schwan, A. Stauber, A. V. Virovets, G. R. Whittell, I. Manners, M. Scheer, *Angew. Chem. Int. Ed.* **2015**, *54*, 13782-13786; d) A. Stauber, T. Jurca, C. Marquardt, M. Fleischmann, M. Seidl, G. R. Whittell, I. Manners, M. Scheer, *Eur. J. Inorg. Chem.* **2016**, 2684-2687; e) U. Vogel, P. Hoemensch, K.-C. Schwan, A. Y. Timoshkin, M. Scheer, *Chem. Eur. J.* **2003**, *9*, 515-519.
- [12] C. Marquardt, T. Kahoun, J. Baumann, A. Y. Timoshkin, M. Scheer, *Z. Anorg. Allg. Chem.* **2017**, *643*, 1326-1330.
- [13] C. Marquardt, T. Kahoun, A. Stauber, G. Balázs, M. Bodensteiner, A. Y. Timoshkin, M. Scheer, *Angew. Chem. Int. Ed.* **2016**, *55*, 14828-14832.
- [14] a) C. Marquardt, G. Balázs, J. Baumann, A. V. Virovets, M. Scheer, *Chem. Eur. J.* **2017**, *23*, 11423-11429; b) C. Marquardt, C. Thoms, A. Stauber, G. Balázs, M. Bodensteiner, M. Scheer, *Angew. Chem. Int. Ed.* **2014**, *53*, 3727-3730.
- [15] O. Hegen, C. Marquardt, A. Y. Timoshkin, M. Scheer, *Angew. Chem. Int. Ed.* **2017**, *56*, 12783-12787.
- [16] C. Thoms, C. Marquardt, A. Y. Timoshkin, M. Bodensteiner, M. Scheer, *Angew. Chem. Int. Ed.* **2013**, *52*, 5150-5154.
- [17] a) M. A. Petrie, M. M. Olmstead, H. Hope, R. A. Bartlett, P. P. Power, *J. Am. Chem. Soc.* **1993**, *115*, 3221-3226; b) J. Burt, J. W. Emsley, W. Levason, G. Reid, I. S. Tinkler, *Inorg. Chem.* **2016**, *55*, 8852-8864; c) M. A. Mardones, A. H. Cowley, L. Contreras, R. A. Jones, C. J. Carrano, *J. Organomet. Chem.* **1993**, *455*, C1-C2.
- [18] a) A. D. Becke, *J. Chem. Phys.* **1993**, *98*, 5648-5652; b) C. Lee, W. Yang, R. G. Parr, *Phys. Rev. B*, **1988**, *37*, 785-789.
- [19] a) F. Weigend, R. Ahlrichs, *Phys. Chem. Chem. Phys.* **2005**, *7*, 3297-3305; b) K. A. Peterson, D. Figgen, E. Goll, H. Stoll, M. Dolg, *J. Chem. Phys.* **2003**, *119*, 11113.

- [20] M. J. Frisch, G. W. Trucks, H. B. Schlegel, G. E. Scuseria, M. A. Robb, J. R. Cheeseman, G. Scalmani, V. Barone, B. Mennucci, G. A. Petersson, H. Nakatsuji, M. Caricato, X. Li, H. P. Hratchian, A. F. Izmaylov, J. Bloino, G. Zheng, J. L. Sonnenberg, M. Hada, M. Ehara, K. Toyota, R. Fukuda, J. Hasegawa, M. Ishida, T. Nakajima, Y. Honda, O. Kitao, H. Nakai, T. Vreven, J. A. Montgomery, Jr., J. E. Peralta, F. Ogliaro, M. Bearpark, J. J. Heyd, E. Brothers, K. N. Kudin, V. N. Staroverov, T. Keith, R. Kobayashi, J. Normand, K. Raghavachari, A. Rendell, J. C. Burant, S. S. Iyengar, J. Tomasi, M. Cossi, N. Rega, J. M. Millam, M. Klene, J. E. Knox, J. B. Cross, V. Bakken, C. Adamo, J. Jaramillo, R. Gomperts, R. E. Stratmann, O. Yazyev, A. J. Austin, R. Cammi, C. Pomelli, J. W. Ochterski, R. L. Martin, K. Morokuma, V. G. Zakrzewski, G. A. Voth, P. Salvador, J. J. Dannenberg, S. Dapprich, A. D. Daniels, O. Farkas, J. B. Foresman, J. V. Ortiz, J. Cioslowski, D. J. Fox, Gaussian 09, Revision E.01, Gaussian, Inc., Wallingford CT, 2013.
- [21] a) K. L. Schuchardt, B. T. Didier, T. Elsethagen, L. Sun, V. Gurumoorthi, J. Chase, J. Li, T. L. Windus, *J. Chem. Inform. Model.* **2007**, *47*, 1045-1052; b) D. Feller, *J. Comput. Chem.* **1996**, *17*, 1571-1586.
- [22] A. S. Lisovenko, A. Y. Timoshkin, *Inorg. Chem.* **2010**, *49*, 10357-10369.

### 3.6. Supporting information

#### Crystallographic Details

CCDC-2117548 (1), CCDC-2117549 (2), CCDC-2117530 (3), CCDC-2117531 (4a), CCDC-2117532 (4b), CCDC-2117533 (4c) and CCDC-2117534 (5) contain the supplementary crystallographic data for this paper. These data can be obtained free of charge at [www.ccdc.cam.ac.uk/conts/retrieving.html](http://www.ccdc.cam.ac.uk/conts/retrieving.html) (or from the Cambridge Crystallographic Data Centre, 12 Union Road, Cambridge CB2 1EZ, UK; Fax: + 44-1223-336-033; e-mail: [deposit@ccdc.cam.ac.uk](mailto:deposit@ccdc.cam.ac.uk)).

**Table S1.** Crystallographic data for compounds **1**, **2** and **3**.

Compound	1	2	3
Data set (internal naming)	<b>LeF180</b>	<b>LeF099</b>	<b>LeF098</b>
CCDC number	2117548	2117549	2117530
Formula	C <sub>7</sub> H <sub>21</sub> AsBN	C <sub>7</sub> H <sub>21</sub> AsB <sub>2</sub> Br <sub>3</sub> N	C <sub>7</sub> H <sub>24</sub> AsB <sub>2</sub> N
<i>D</i> <sub>calc.</sub> /g cm <sup>-3</sup>	1.165	1.944	1.140
$\mu$ /mm <sup>-1</sup>	3.474	8.609	3.198
Formula Weight	204.98	455.52	218.81
Color	clear colorless	clear colorless	clear colorless
Shape	block	block-shaped	needle-shaped
Size/mm <sup>3</sup>	0.17×0.13×0.08	0.14×0.08×0.05	0.46×0.03×0.03
<i>T</i> /K	123.00(10)	123.00(10)	122.97(13)
Crystal System	orthorhombic	orthorhombic	monoclinic
Space Group	<i>Pnma</i>	<i>P2<sub>1</sub>2<sub>1</sub>2<sub>1</sub></i>	<i>P2<sub>1</sub>/n</i>
<i>a</i> /Å	10.2186(2)	9.0046(2)	6.2175(2)
<i>b</i> /Å	10.0900(4)	11.1740(2)	13.5705(4)
<i>c</i> /Å	11.3316(3)	15.4697(3)	15.2033(6)
$\alpha$ <sup>o</sup>	90	90	90
$\beta$ <sup>o</sup>	90	90	96.486(4)
$\gamma$ <sup>o</sup>	90	90	90
<i>V</i> /Å <sup>3</sup>	1168.35(6)	1556.52(5)	1274.56(8)
<i>Z</i>	4	4	4
<i>Z'</i>	0.5	1	1
Wavelength/Å	1.54184	1.39222	1.54184
Radiation type	Cu K $\alpha$	Cu K $\beta$	Cu K $\alpha$
$\theta$ <sub>min</sub> <sup>o</sup>	5.831	4.407	4.380
$\theta$ <sub>max</sub> <sup>o</sup>	74.923	74.567	73.887
Measured Refl's.	6910	13084	7090
Indep't Refl's	1249	4225	2489
Refl's I $\geq$ 2 $\sigma$ (I)	1027	4090	2297
<i>R</i> <sub>int</sub>	0.0217	0.0329	0.0465
Parameters	136	156	123
Restraints	131	19	14
Largest Peak	0.193	0.496	1.304
Deepest Hole	-0.163	-0.694	-1.129
GooF	1.119	1.022	1.139
<i>wR</i> <sub>2</sub> (all data)	0.0866	0.0623	0.1525
<i>wR</i> <sub>2</sub>	0.0828	0.0615	0.1505
<i>R</i> <sub>1</sub> (all data)	0.0343	0.0272	0.0645
<i>R</i> <sub>1</sub>	0.0280	0.0261	0.0608

Table S2. Crystallographic data for compounds **4a**, **4b** and **4c**.

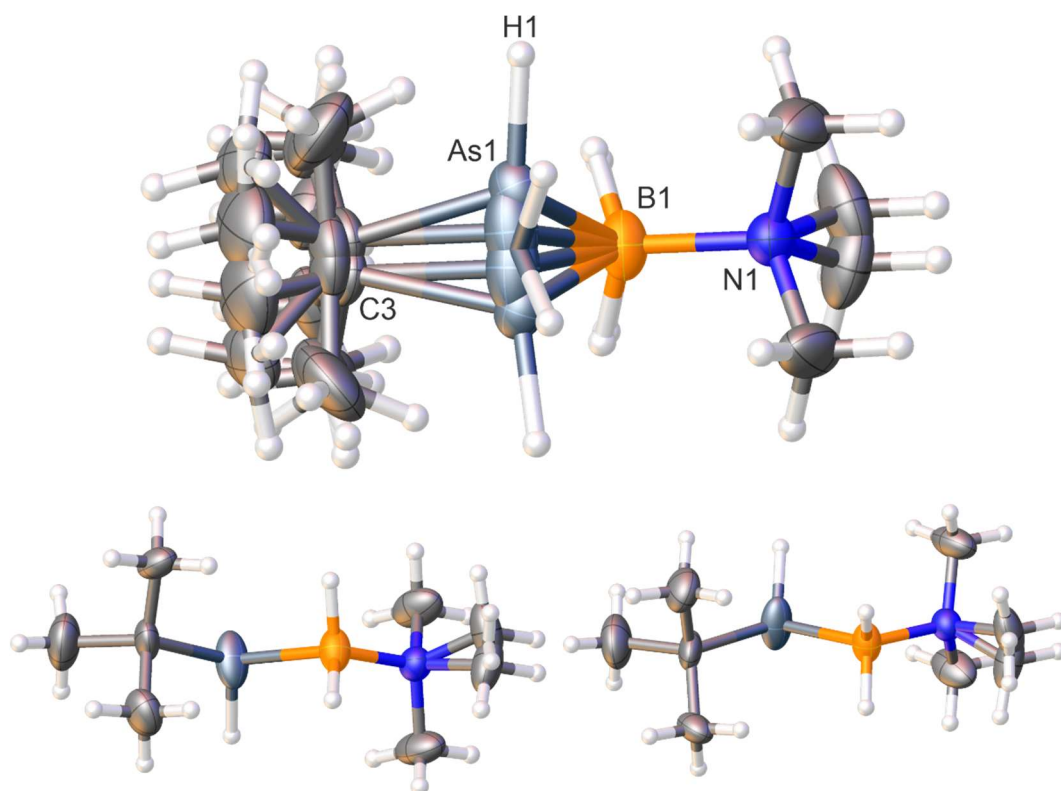
Compound	4a	4b	4c
Data set (internal naming)	LeF108	LeF106	LeF106m
CCDC number	2117531	2117532	2117533
Formula	C <sub>18</sub> H <sub>42</sub> As <sub>2</sub> B <sub>2</sub> CrN <sub>2</sub> O <sub>4</sub>	C <sub>18</sub> H <sub>42</sub> As <sub>2</sub> B <sub>2</sub> MoN <sub>2</sub> O <sub>4</sub>	C <sub>18</sub> H <sub>42</sub> As <sub>2</sub> B <sub>2</sub> N <sub>2</sub> O <sub>4</sub> W
<i>D</i> <sub>calc.</sub> / g cm <sup>-3</sup>	1.388	1.480	1.670
$\mu$ /mm <sup>-1</sup>	2.831	6.704	10.422
Formula Weight	573.99	617.93	705.84
Color	clear yellow	clear yellow	clear yellow
Shape	block-shaped	block-shaped	block-shaped
Size/mm <sup>3</sup>	0.378×0.282×0.25	0.1×0.147×0.193	0.26×0.18×0.12
<i>T</i> /K	123(1)	123(1)	123.00(10)
Crystal System	monoclinic	monoclinic	monoclinic
Space Group	P21/n	P21/n	<i>P</i> 2 <sub>1</sub> / <i>n</i>
<i>a</i> /Å	11.82250(10)	10.83870(10)	11.6127(2)
<i>b</i> /Å	14.6402(2)	15.6686(2)	15.7876(2)
<i>c</i> /Å	15.8954(2)	16.6715(2)	15.3205(2)
$\alpha$ <sup>o</sup>	90	90	90
$\beta$ <sup>o</sup>	93.5810(10)	101.6730(10)	91.2070(10)
$\gamma$ <sup>o</sup>	90	90	90
<i>V</i> /Å <sup>3</sup>	2745.86(6)	2772.72(6)	2808.19(7)
<i>Z</i>	4	4	4
<i>Z'</i>	1	1	1
Wavelength/Å	0.71073	1.54184	1.54184
Radiation type	Mo K $\alpha$	Cu K $\alpha$	Cu K $\alpha$
$\theta$ <sub>min</sub> <sup>o</sup>	3.311	3.910	4.021
$\theta$ <sub>max</sub> <sup>o</sup>	37.635	74.169	74.055
Measured Refl's.	50647	16306	15763
Indep't Refl's	13956	5527	5488
Refl's I $\geq$ 2 $\sigma$ (I)	11185	5237	5470
<i>R</i> <sub>int</sub>	0.0302	0.0201	0.0165
Parameters	298	292	325
Restraints	1	0	66
Largest Peak	1.24	1.13	0.789
Deepest Hole	-0.41	-0.53	-1.025
GooF	1.024	1.059	1.290
<i>wR</i> <sub>2</sub> (all data)	0.0651	0.0584	0.0565
<i>wR</i> <sub>2</sub>	0.0605	0.0575	0.0564
<i>R</i> <sub>I</sub> (all data)	0.0464	0.0251	0.0264
<i>R</i> <sub>I</sub>	0.0305	0.0233	0.0262

**Table S3.** Crystallographic data for compound 5

Compound	5
Data set (internal naming)	<b>LeF103</b>
CCDC number	2117534
Formula	C <sub>10</sub> H <sub>32</sub> AsB <sub>2</sub> IN <sub>2</sub>
<i>D</i> <sub>calc.</sub> / g cm <sup>-3</sup>	1.400
$\mu$ /mm <sup>-1</sup>	11.244
Formula Weight	403.81
Color	clear colorless
Shape	block-shaped
Size/mm <sup>3</sup>	0.25×0.10×0.06
<i>T</i> /K	123.00(10)
Crystal System	orthorhombic
Flack Parameter	-0.011(5)
Hoofit Parameter	-0.018(3)
Space Group	<i>Pca</i> 2 <sub>1</sub>
<i>a</i> /Å	11.7851(2)
<i>b</i> /Å	13.6028(2)
<i>c</i> /Å	11.9503(2)
$\alpha$ <sup>o</sup>	90
$\beta$ <sup>o</sup>	90
$\gamma$ <sup>o</sup>	90
<i>V</i> /Å <sup>3</sup>	1915.76(5)
<i>Z</i>	4
<i>Z</i> '	1
Wavelength/Å	1.39222
Radiation type	Cu K $\beta$
$\theta$ <sub>min</sub> <sup>o</sup>	2.933
$\theta$ <sub>max</sub> <sup>o</sup>	74.023
Measured Refl's.	8882
Indep't Refl's	4236
Refl's I $\geq$ 2 $\sigma$ (I)	4041
<i>R</i> <sub>int</sub>	0.0230
Parameters	174
Restraints	7
Largest Peak	0.531
Deepest Hole	-0.988
GooF	1.026
<i>wR</i> <sub>2</sub> (all data)	0.0731
<i>wR</i> <sub>2</sub>	0.0721
<i>R</i> <sub>1</sub> (all data)	0.0291
<i>R</i> <sub>1</sub>	0.0278

***t*BuAsHBH<sub>2</sub>NMe<sub>3</sub> (1)**

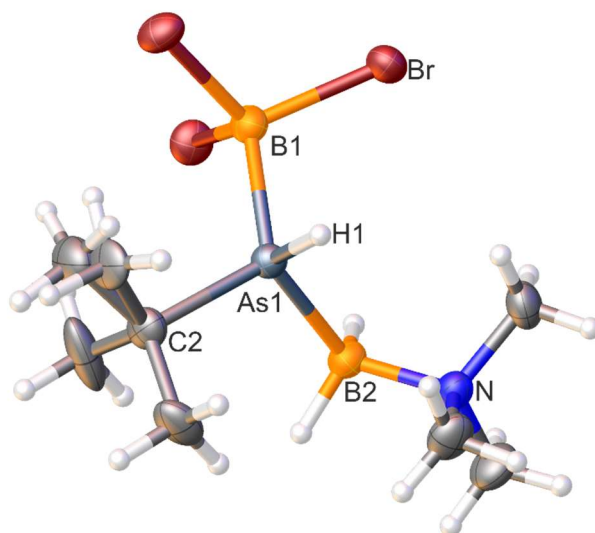
Compound **1** crystallizes from *n*-hexane at 243 K as colorless blocks in the orthorhombic space group *Pnma*. A suitable crystal with the dimensions 0.17 × 0.13 × 0.08 mm<sup>3</sup> was selected and mounted on a XtaLAB Synergy R, DW system equipped with a HyPix-Arc 150 detector. The crystal was kept at a steady temperature of 123.00(10) K during data collection. Data collection, data reduction and the absorption correction were done with CrysAlisPro.<sup>[1]</sup> Using **Olex2**<sup>[2]</sup> as a graphical interface, the structure was solved with **ShelXT**<sup>[3]</sup> using dual methods. The model was refined with **ShelXL**<sup>[4]</sup> using full matrix least squares minimization on *F*<sup>2</sup>. The *t*BuAsH unit is disordered over four positions with refined occupancies of approximately 0.34 : 0.34 : 0.16 : 0.16. Two of these positions are symmetry generated, due to the location near the mirror plane through the B-N bond. The restraints SADI and SIMU were used to describe this disorder. The hydrogen atoms at the As atoms were located from the difference-Fourier map and the As-H distance and the bond angles were fixed. The hydrogen atom positions on the carbon atoms and on the boron atom were calculated geometrically and refined using the riding model. Figure S1 shows the structure in the solid state.



**Figure S1.** Molecular structure of compound **1** in the solid state. The thermal ellipsoids are displayed at 50% probability level. (top) heavily disordered structure, (bottom) the two enantiomers present. Selected bond distances (Å) and angles [°]: N1-B1 1.619(3), B1-As1A 2.079(5), B1-As1B 2.099(8), As1A-C3A 1.941(18), As1B-C3B 2.12(4); N1-B1-As1A 109.7(2), N1-B1-As1B 108.3(4), C3A-As1A-B1 101.0(4), C3B-As1B-B1 103.1(7).

**BBr<sub>3</sub>-*t*BuAsHBH<sub>2</sub>NMe<sub>3</sub> (2)**

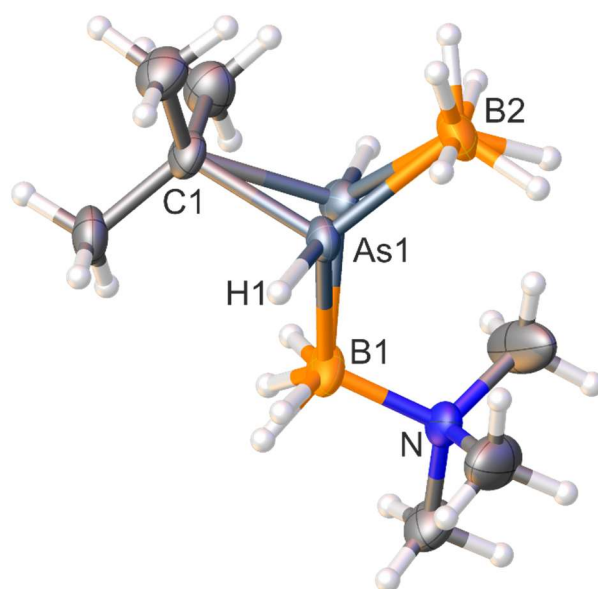
Compound **2** crystallizes from CH<sub>3</sub>CN at 243 K as colorless blocks in the orthorhombic space group *P*2<sub>1</sub>2<sub>1</sub>2<sub>1</sub>. A suitable crystal with dimensions 0.14 × 0.08 × 0.05 mm<sup>3</sup> was selected and mounted on a GV50 diffractometer equipped with a TitanS2 CCD detector. The crystal was kept at a steady temperature of 123.00(10) K during data collection. Data collection, data reduction and the absorption correction were done with **CrysAlisPro**.<sup>[1]</sup> Using **Olex2**<sup>[2]</sup> as a graphical interface, the structure was solved with **ShelXT**<sup>[3]</sup> using dual methods. The model was refined with **ShelXL**<sup>[4]</sup> using full matrix least squares minimization on *F*<sup>2</sup>. One methyl group at the *t*Bu substituent is disordered over two positions (0.53 : 0.47). The restraints SADI and SIMU were used to describe this disorder. Further was compound **2** refined as a 2-component inversion twin with a BASF refined to 0.25(5). The hydrogen atoms at the As atom and the boron atom were located from the difference-Fourier map and refined freely. The hydrogen atom positions on the carbon atoms were calculated geometrically and refined using the riding model. Figure S2 shows the structure in the solid state.



**Figure S2.** Molecular structure of compound **2** in the solid state. The thermal ellipsoids are displayed at 50% probability level. Selected bond distances (Å) and angles [°]: As1-B1 2.064(5), As1-B2 2.093(5), As1-C2 1.986(5), N1-B2 1.597(7); C2-As1-B1 116.1(2), C2-As1-B2 108.8(2), B1-As1-B2 111.9(2), N1-B2-As1 114.9(3).

**BH<sub>3</sub>-*t*BuAsHBH<sub>2</sub>NMe<sub>3</sub> (3)**

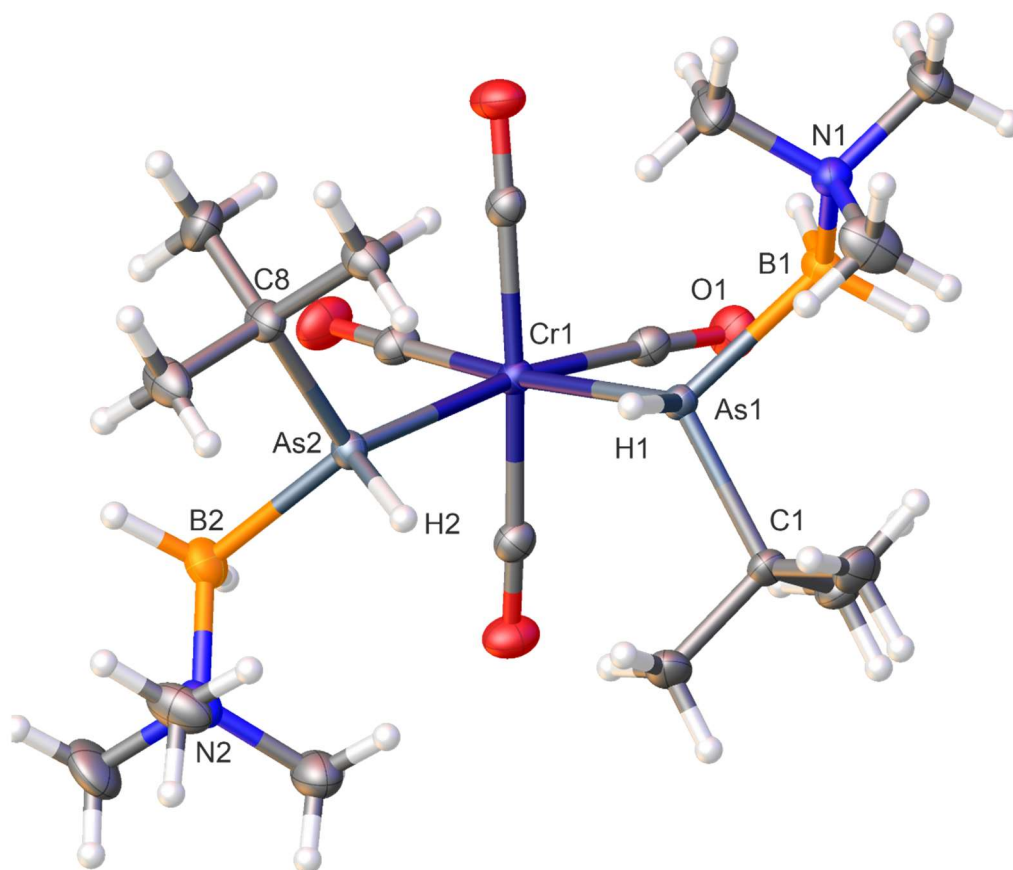
Compound **3** crystallizes from *n*-hexane at 243 K as colorless needles in the monoclinic space group *P*2<sub>1</sub>/*n*. A suitable crystal with dimensions 0.46 × 0.03 × 0.03 mm<sup>3</sup> was selected and mounted on a GV50 diffractometer equipped with a TitanS2 CCD detector. The crystal was kept at a steady temperature of 122.97(13) K during data collection. Data collection, data reduction and the absorption correction were done with **CrysAlisPro**.<sup>[1]</sup> Using **Olex2**<sup>[2]</sup> as a graphical interface, the structure was solved with **ShelXT**<sup>[3]</sup> using dual methods. The model was refined with **ShelXL**<sup>[4]</sup> using full matrix least squares minimization on *F*<sup>2</sup>. The As atom is disordered over two positions with refined occupancies of 0.98 and 0.02. The restraints SADI and SIMU were applied to model this disorder. The hydrogen atoms at the As atoms were located from the difference-Fourier map and the As-H distance and the bond angles were fixed. The hydrogen atom positions on the carbon atoms and on the boron atoms were calculated geometrically and refined using the riding model. Figure S3 shows the structure in the solid state.



**Figure S3.** Molecular structure of compound **3** in the solid state. The thermal ellipsoids are displayed at 50% probability level. Selected bond distances (Å) and angles [°]: As1-C1 1.976(5), As1-B1 2.075(6), As1-B2 2.070(6), N1-B1 1.583(7); C1-As1-B1 104.1(2), C1-As1-B2 111.7(3), B2-As1-B1 123.6(3), N1-B1-As1 115.0(4).

**[Cr(CO)<sub>4</sub>(tBuAsHBH<sub>2</sub>NMe<sub>3</sub>)<sub>2</sub>] (4a)**

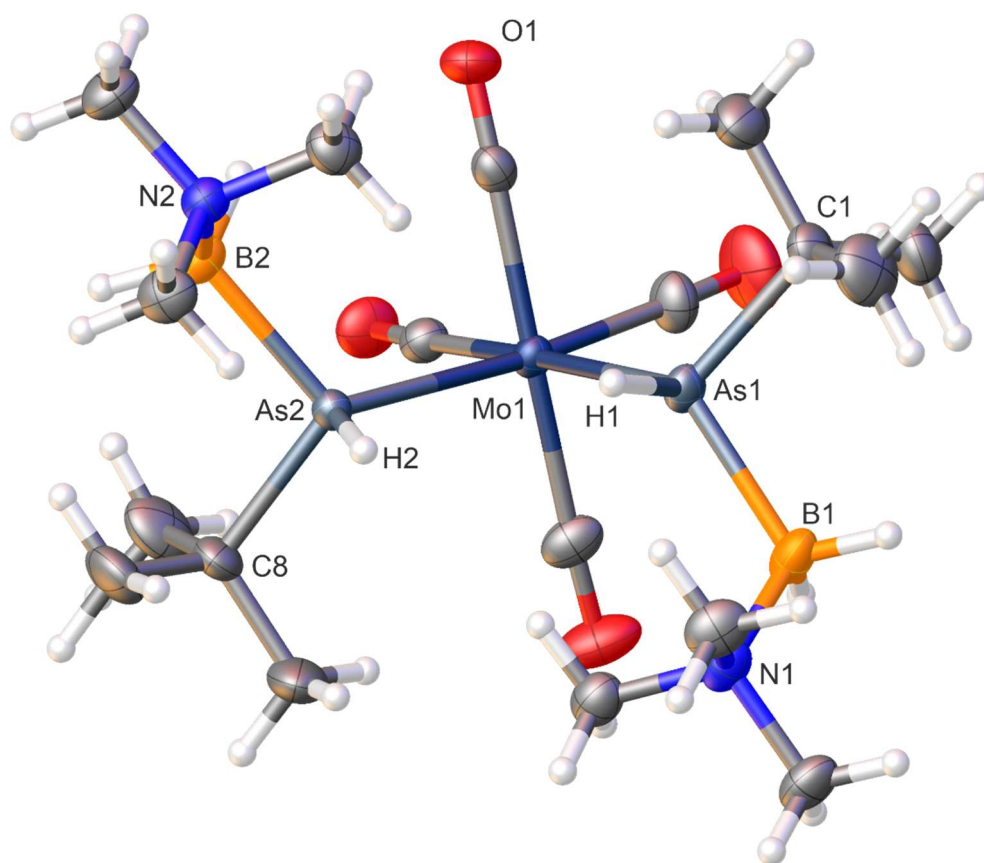
Compound **4a** crystallizes from a CH<sub>2</sub>Cl<sub>2</sub>/*n*-hexane layering at 273 K as yellow blocks in the monoclinic space group *P*2<sub>1</sub>/*n*. A suitable crystal with dimensions 0.378 × 0.282 × 0.25 mm<sup>3</sup> was selected and mounted on a Xcalibur Gemini Ultra diffractometer equipped with an AtlasS2 CCD detector. The crystal was kept at a steady temperature of 123.00(10) K during data collection. Data collection, data reduction and the absorption correction were done with **CrysAlisPro**.<sup>[1]</sup> Using **Olex2**<sup>[2]</sup> as a graphical interface, the structure was solved with **ShelXT**<sup>[3]</sup> using dual methods. The model was refined with **ShelXL**<sup>[4]</sup> using full matrix least squares minimization on *F*<sup>2</sup>. The hydrogen atoms at the As atoms and the boron atoms were located from the difference-Fourier map and the As-H distances were restraint using SADI. The hydrogen atom positions on the carbon atoms were calculated geometrically and refined using the riding model. Figure S4 shows the structure in the solid state.



**Figure S4.** Molecular structure of compound **4a** in the solid state. The thermal ellipsoids are displayed at 50% probability level. Selected bond distances (Å) and angles [°]: As1-Cr1 2.5168(2), As2-Cr1 2.5163(2), As2-B2 2.0942(14), As1-B1 2.0963(13), N1-B1 1.6114(17), N2-B2 1.623(2), As1-C1 2.0001(11), As2-C8 2.0068(12); As2-Cr1-As1 90.417(7), C1-As1-Cr1 117.35(4), C1-As1-B1 105.44(5), B1-As1-Cr1 115.00(4), C8-As2-Cr1 117.92(4), C8-As2-B2 106.11(6), B2-As2-Cr1 117.54(4), N1-B1-As1 115.95(8), N2-B2-As2 115.36(9)

**[Mo(CO)<sub>4</sub>(tBuAsHBH<sub>2</sub>NMe<sub>3</sub>)<sub>2</sub>] (4b)**

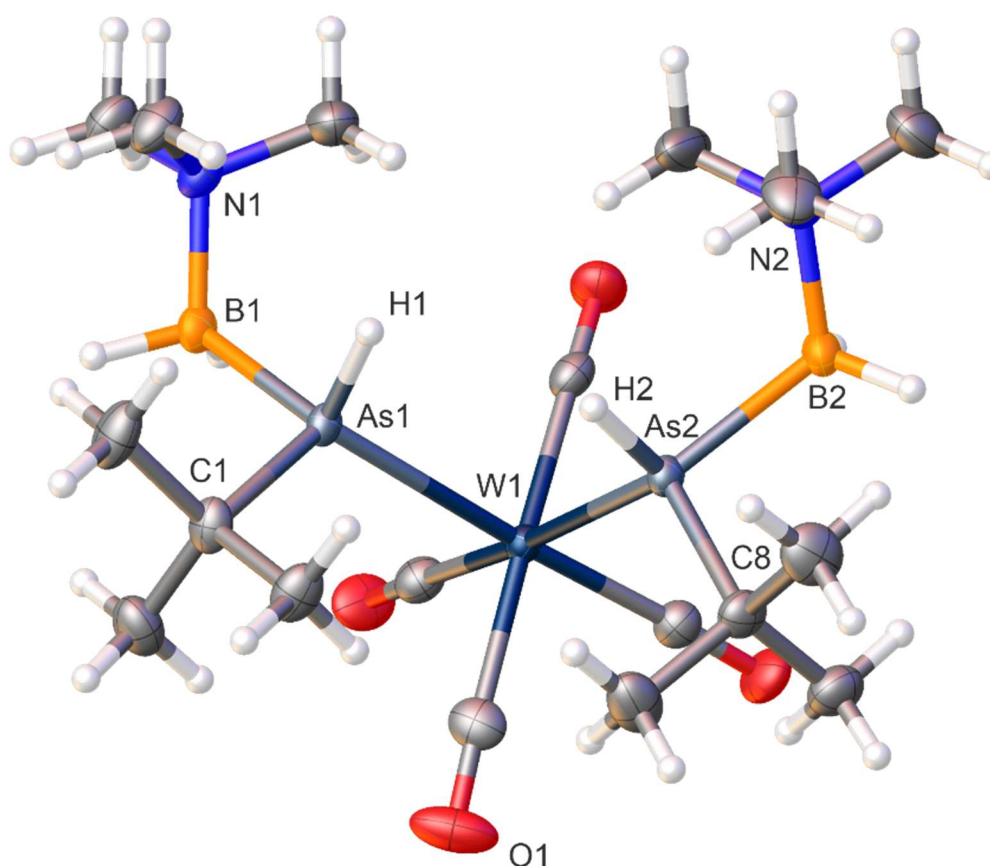
Compound **4b** crystallizes from a CH<sub>2</sub>Cl<sub>2</sub>/*n*-hexane layering at 273 K as yellow blocks in the monoclinic space group *P*2<sub>1</sub>/*n*. A suitable crystal with dimensions 0.1 × 0.15 × 0.19 mm<sup>3</sup> was selected and mounted on a Xcalibur Gemini Ultra diffractometer equipped with an AtlasS2 CCD detector. The crystal was kept at a steady temperature of 123 (1) K during data collection. Data collection, data reduction and the absorption correction were done with **CrysAlisPro**.<sup>[1]</sup> Using **Olex2**<sup>[2]</sup> as a graphical interface, the structure was solved with **ShelXT**<sup>[3]</sup> using dual methods. The model was refined with **ShelXL**<sup>[4]</sup> using full matrix least squares minimization on *F*<sup>2</sup>. The hydrogen atoms at the As atoms and the boron atoms were located from the difference-Fourier map and refined freely. The hydrogen atom positions on the carbon atoms were calculated geometrically and refined using the riding model. Figure S5 shows the structure in the solid state.



**Figure S5.** Molecular structure of compound **4b** in the solid state. The thermal ellipsoids are displayed at 50% probability level. Selected bond distances (Å) and angles [°]: Mo1-As1 2.6666(3), Mo1-As2 2.6595(3), As1-C1 2.010(2), As1-B1 2.098(2), As2-C8 2.006(2), As2-B2 2.096(3), N1-B1 1.612(3), N2-B2 1.615(3); As2-Mo1-As1 88.895(8), C1-As1-Mo1 119.34(8), C1-As1-B1 103.62(10), B1-As1-Mo1 116.14(7), N1-B1-As1 114.62(14), C8-As2-Mo1 118.05(7), C8-As2-B2 103.44(11), B2-As2-Mo1 119.82(9), N2-B2-As2 114.13(16).

**[W(CO)<sub>4</sub>(tBuAsHBH<sub>2</sub>NMe<sub>3</sub>)<sub>2</sub>] (4c)**

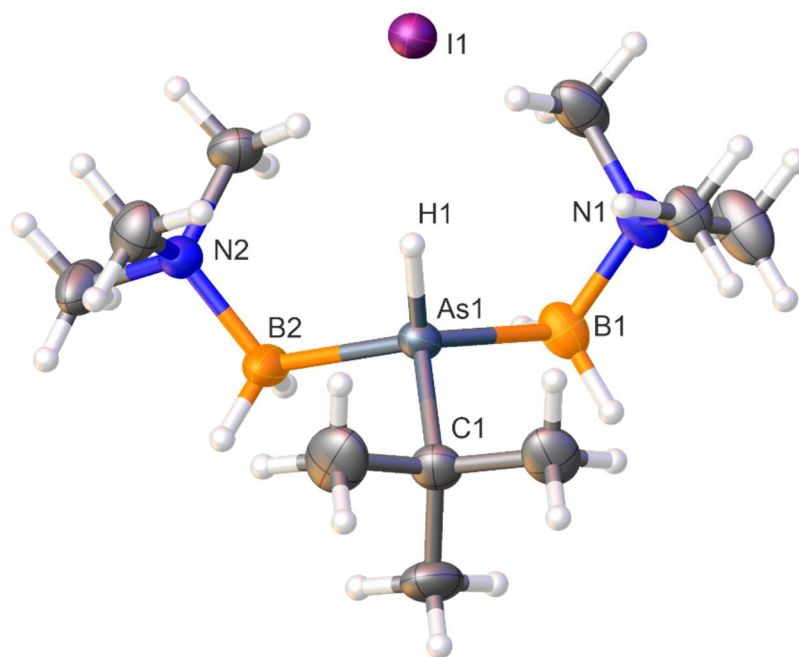
Compound **4c** crystallizes from a CH<sub>2</sub>Cl<sub>2</sub>/*n*-hexane layering at 273 K as yellow blocks in the monoclinic space group *P*2<sub>1</sub>/*n*. A suitable crystal with dimensions 0.26 × 0.18 × 0.12 mm<sup>3</sup> was selected and mounted on a SuperNova diffractometer equipped with an Atlas CCD detector. The crystal was kept at a steady temperature of 123.00(10) K during data collection. Data collection, data reduction and the absorption correction were done with **CrysAlisPro**.<sup>[1]</sup> Using **Olex2**<sup>[2]</sup> as a graphical interface, the structure was solved with **ShelXT**<sup>[3]</sup> using dual methods. The model was refined with **ShelXL**<sup>[4]</sup> using full matrix least squares minimization on *F*<sup>2</sup>. The hole molecule is disordered over two positions with an occupancy of 0.97 and 0.03. However, due to the low occupancy of the minor part (0.03), only the heavy atom framework, consisting of an As<sub>2</sub>W unit, could be properly modelled. The hydrogen atoms at the As atoms and the boron atoms were located from the difference-Fourier map and refined freely. The hydrogen atom positions on the carbon atoms were calculated geometrically and refined using the riding model. Figure S6 shows the structure in the solid state.



**Figure S6.** Molecular structure of compound **4c** in the solid state. The thermal ellipsoids are displayed at 50% probability level. Selected bond distances (Å) and angles [°]: W1-As1 2.6513(4), W1-As2 2.6501(5), As1-C1 2.003(4), As1-B1 2.088(4), As2-C8 2.008(4), As2-B2 2.101(4), N1-B1 1.601(6), N2-B2 1.605(6); As2-W1-As1 88.719(14), C1-As1-W1 118.36(12), C1-As1-B1 105.03(17), B1-As1-W1 116.95(13), C8-As2-W1 119.16(12), C8-As2-B2 104.26(18), B2-As2-W1 115.30(13), N1-B1-As1 115.1(3), N2-B2-As2 114.2(3).

**[Me<sub>3</sub>N-BH<sub>2</sub>-*t*BuAsH-BH<sub>2</sub>-NMe<sub>3</sub>]<sup>+</sup>I<sup>-</sup> (5)**

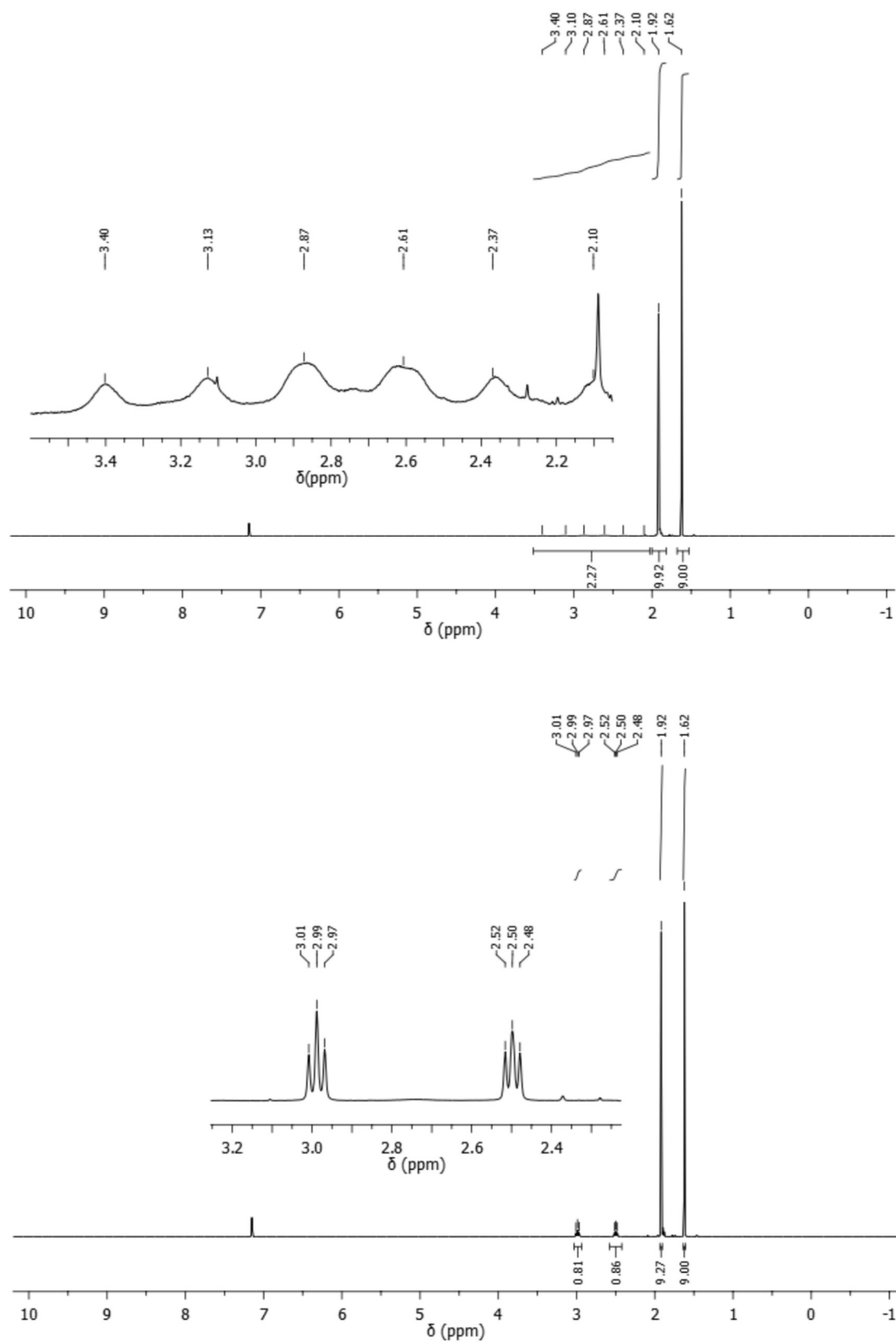
Compound **5** crystallizes from a CH<sub>2</sub>Cl<sub>2</sub>/*n*-hexane layering at 273 K as colorless blocks in the orthorhombic space group *Pca*2<sub>1</sub>. A suitable crystal with dimensions 0.25 × 0.10 × 0.06 mm<sup>3</sup> was selected and mounted on a GV50 diffractometer equipped with an TitanS2 CCD detector. The crystal was kept at a steady temperature of 123.00(10) K during data collection. Data collection, data reduction and the absorption correction were done with **CrysAlisPro**.<sup>[1]</sup> Using **Olex2**<sup>[2]</sup> as a graphical interface, the structure was solved with **ShelXT**<sup>[3]</sup> using dual methods. The model was refined with **ShelXL**<sup>[4]</sup> using full matrix least squares minimization on *F*<sup>2</sup>. The hydrogen atoms at the As atoms and the boron atoms were located from the difference-Fourier map and in the case of the hydrogen located at the As atom refined freely, whereas the B-H distance was restrained (SADI). The hydrogen atom positions on the carbon atoms were calculated geometrically and refined using the riding model. Figure S7 shows the structure in the solid state.



**Figure S7.** Molecular structure of compound **5** in the solid state. The thermal ellipsoids are displayed at 50% probability level. Selected bond distances (Å) and angles [°]: As1-C1 1.978(5), As1-B1 2.074(5), As1-B2 2.070(5), N1-B1 1.591(6), C1-As1-B1 110.8(2), C1-As1-B2 107.6(2), B2-As1-B1 114.2(2), N1-B1-As1 114.2(3), N2-B2-As1 114.3(3).

## NMR spectra

## Compound 1

**Figure S8.**  $^1H$  NMR (top) and  $^1H\{^{11}B\}$  (bottom) spectra of **1** in  $C_6D_6$

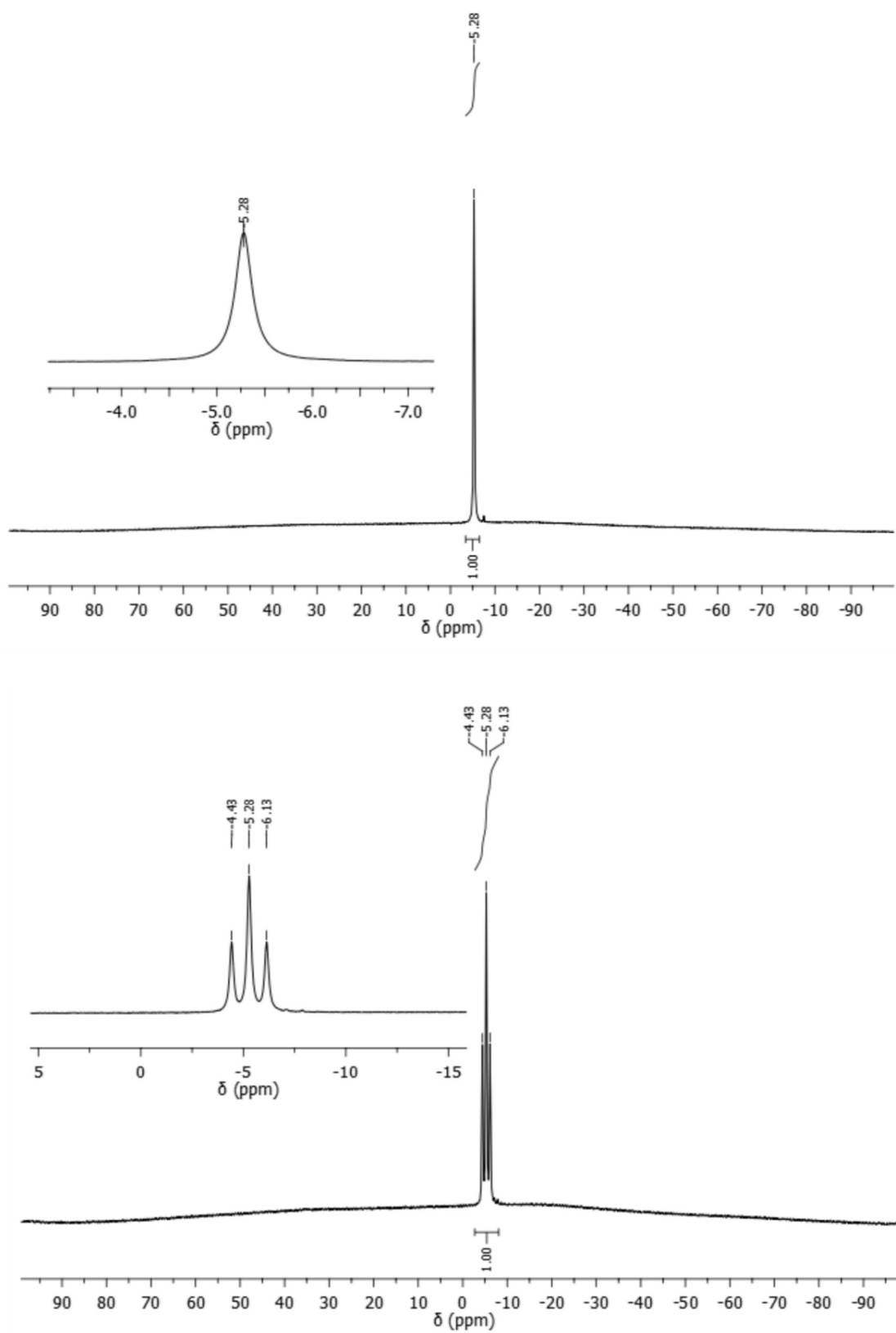


Figure S9.  $^{11}B$  NMR (bottom) and  $^{11}B\{^1H\}$  (top) spectra of **1** in  $C_6D_6$

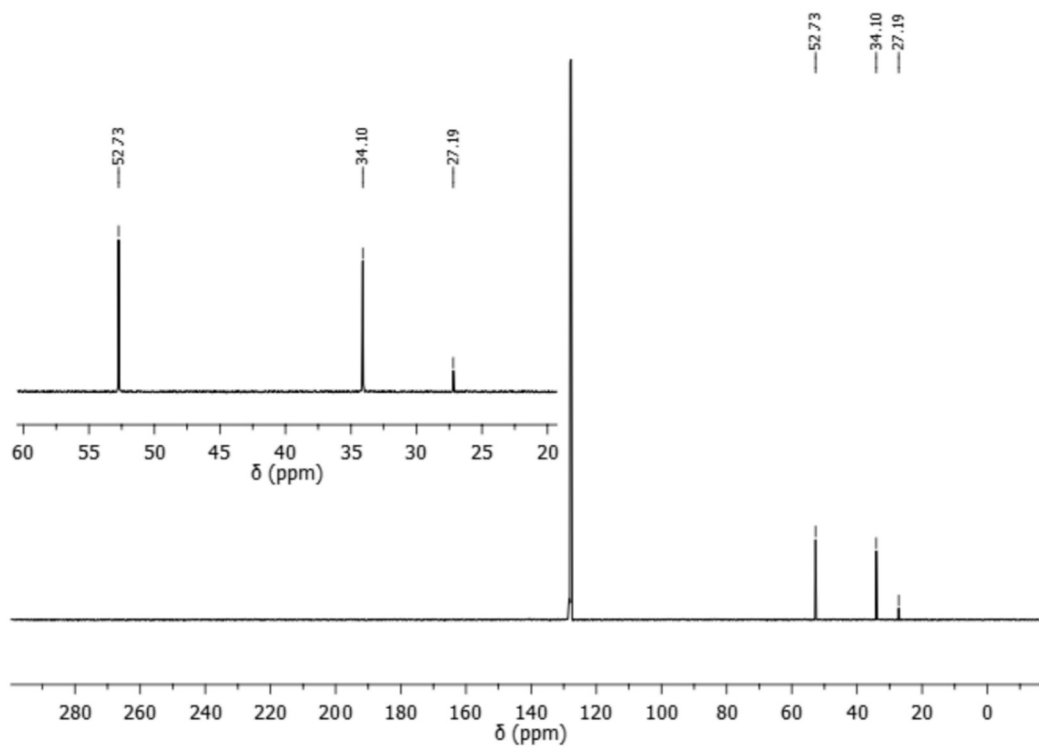


Figure S10.  $^{13}\text{C}\{^1\text{H}\}$  NMR spectrum of **1** in  $\text{C}_6\text{D}_6$

## Compound 2

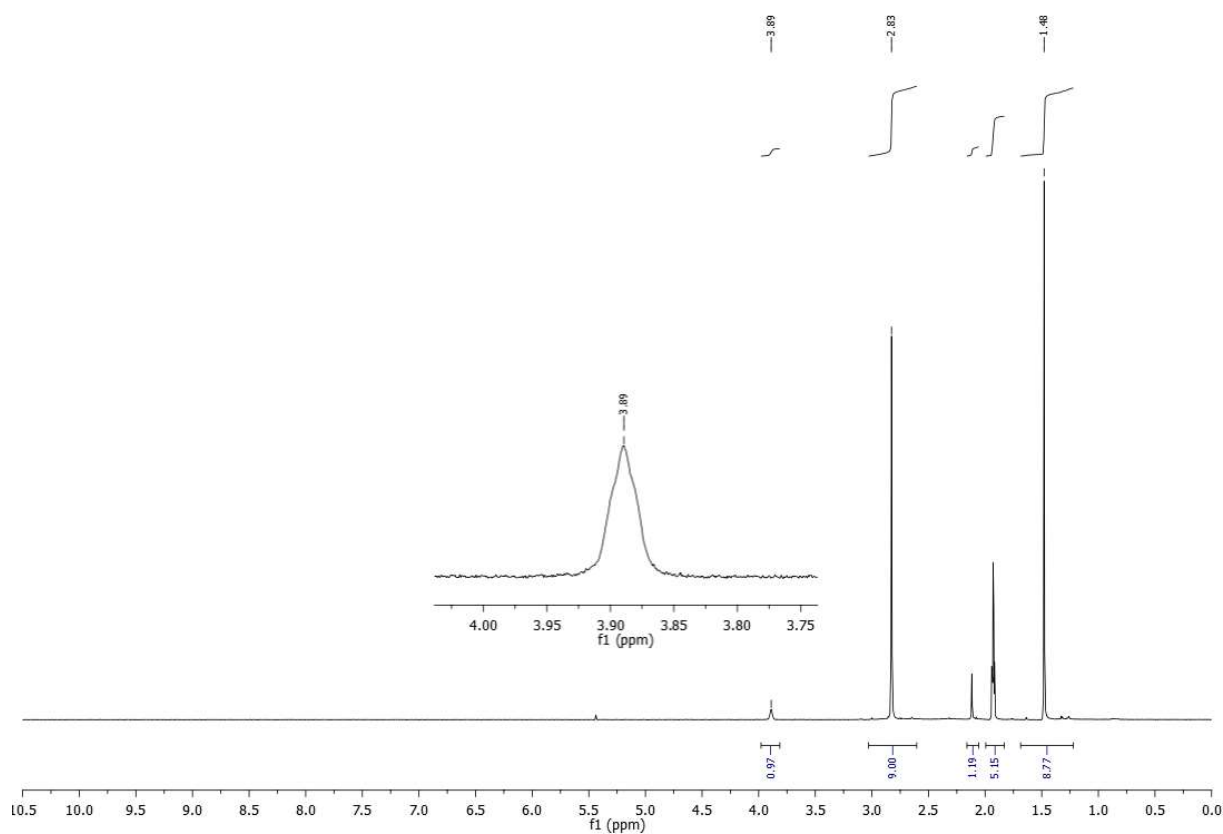


Figure S11.  $^1\text{H}$  NMR and spectrum of **2** in  $\text{CD}_3\text{CN}$

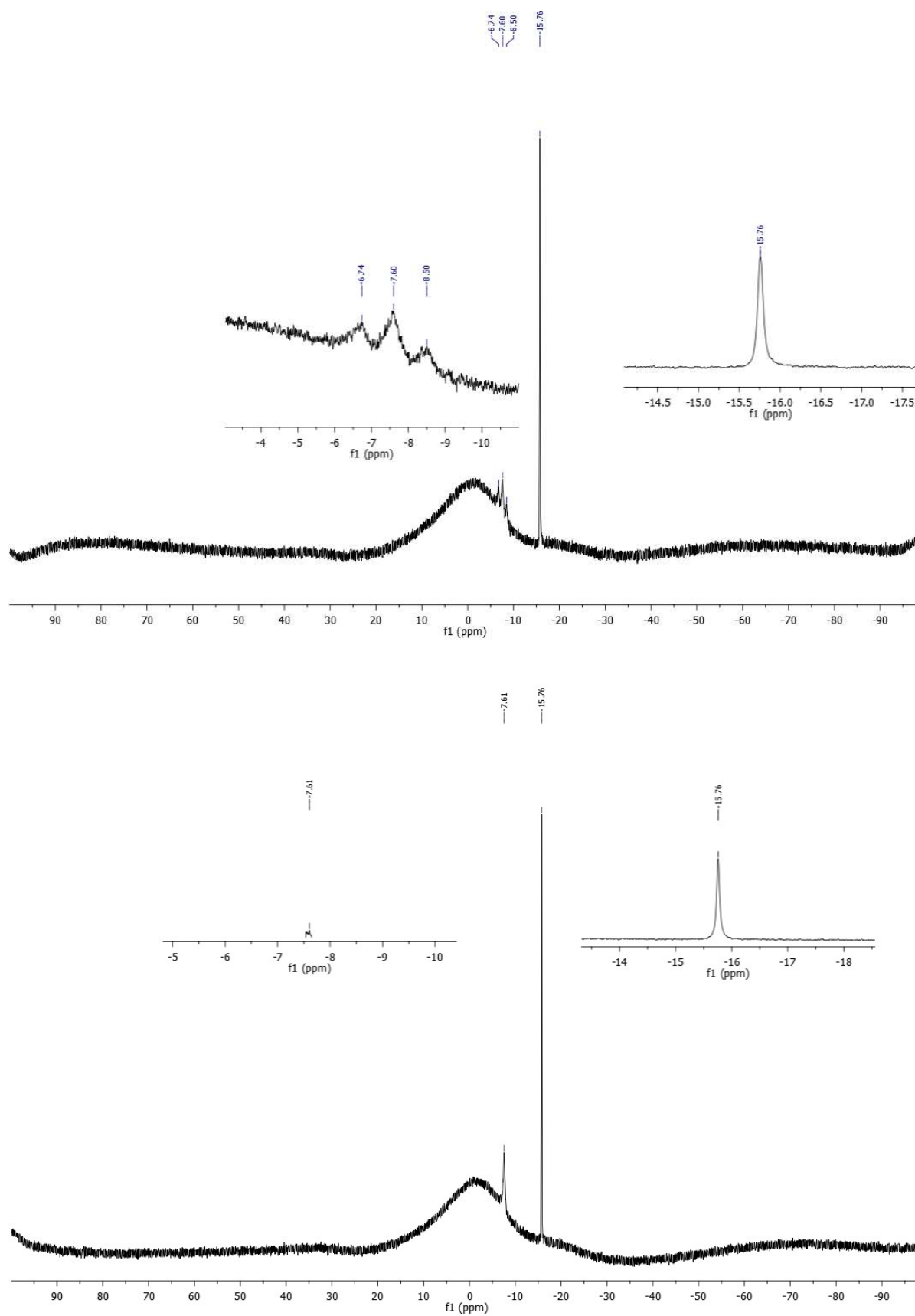
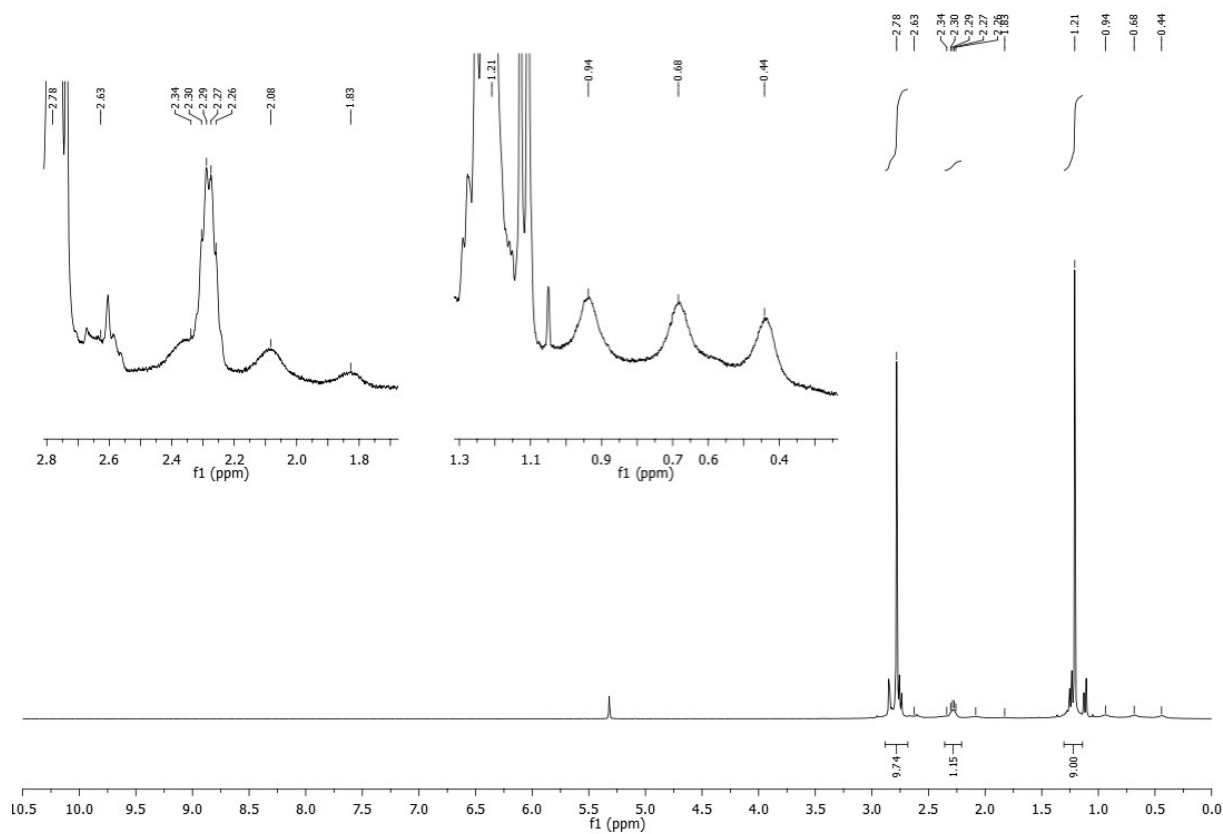


Figure S12.  $^{11}\text{B}$  NMR (top) and  $^{11}\text{B}\{^1\text{H}\}$  (bottom) spectra of **2** in  $\text{CD}_3\text{CN}$

## Compound 3

Figure S13.  $^1\text{H}$  NMR spectrum of 3 in  $\text{CD}_2\text{Cl}_2$

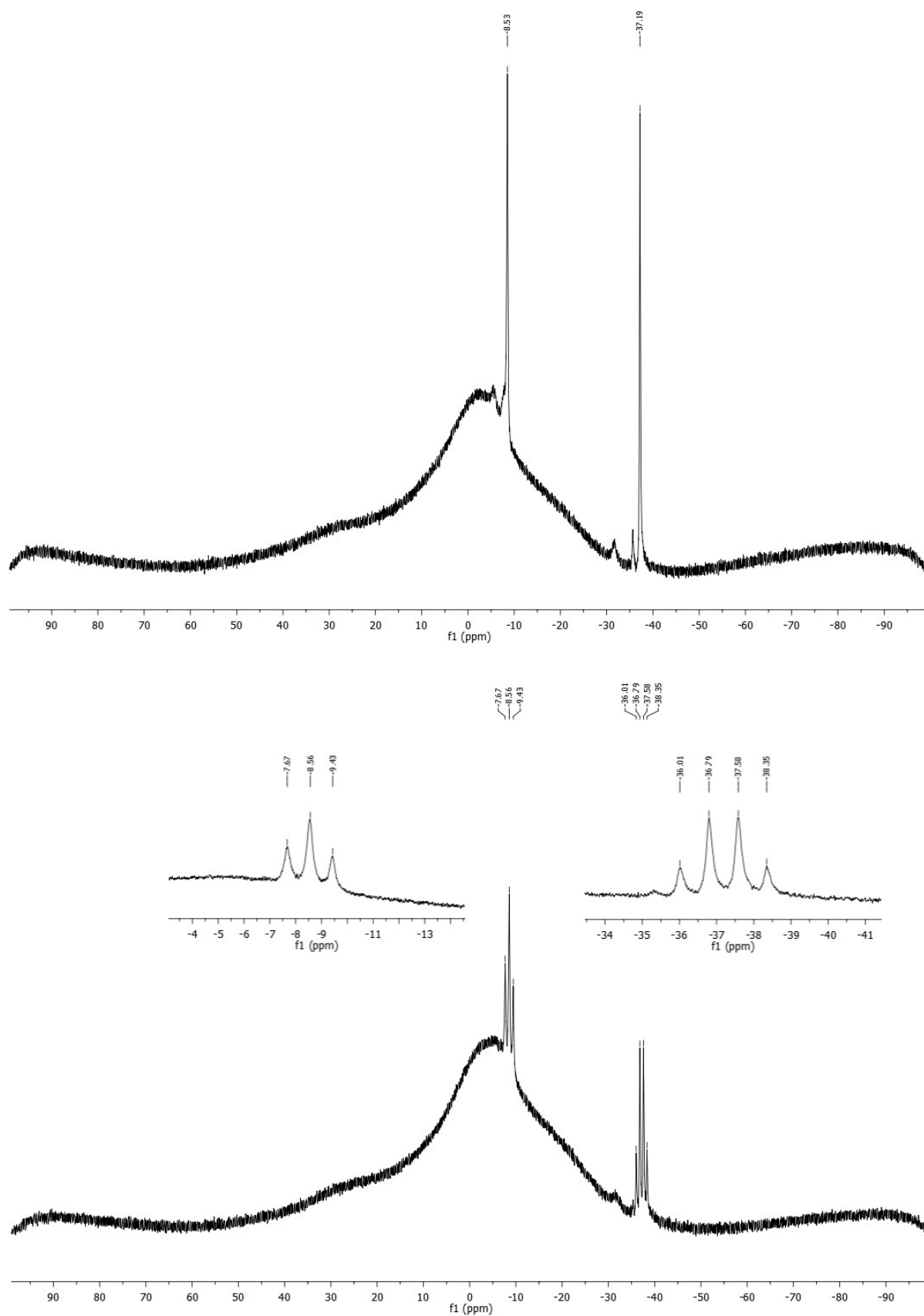
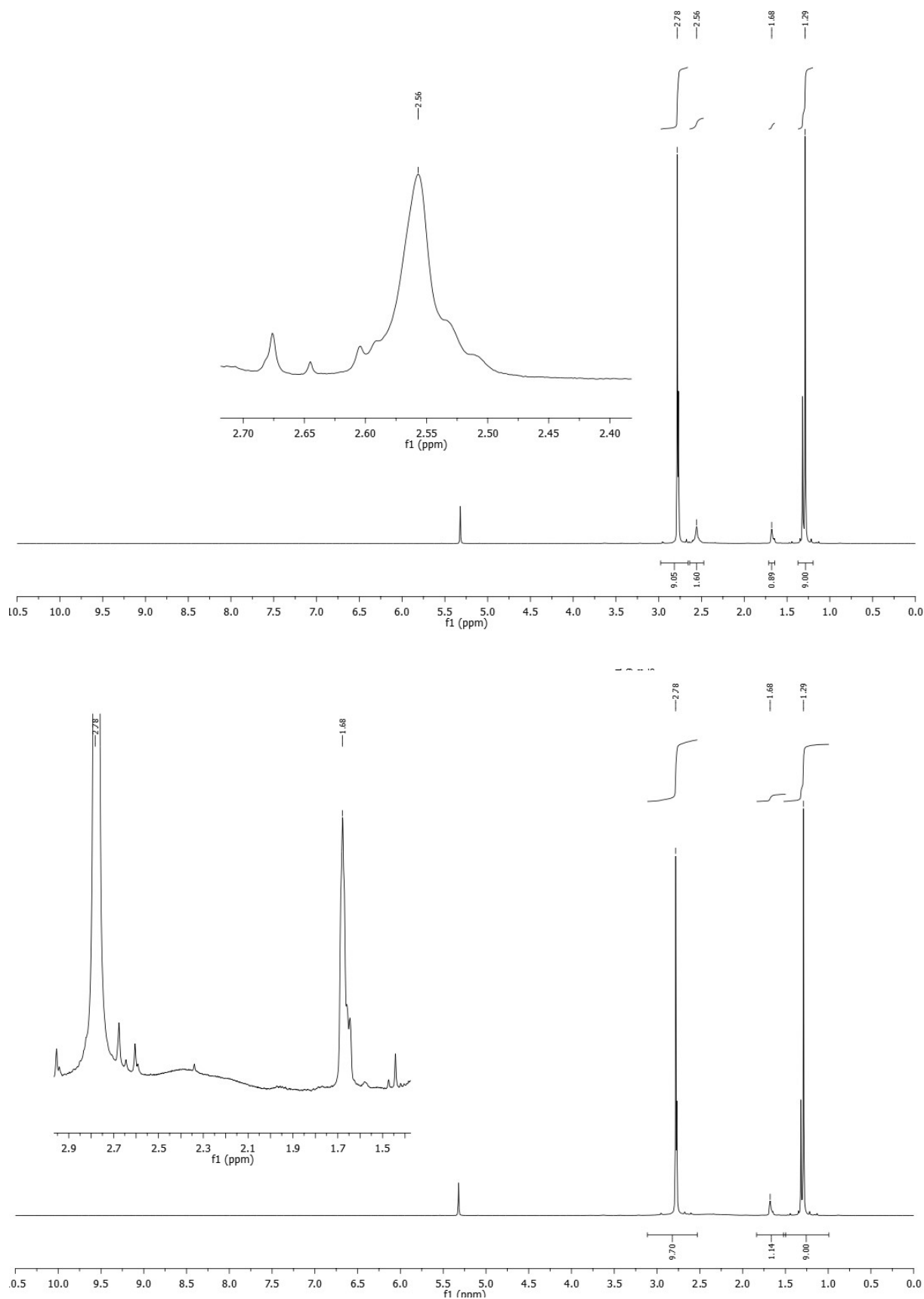


Figure S14.  $^{11}\text{B}$  NMR (top) and  $^{11}\text{B}\{^1\text{H}\}$  (bottom) spectra of **3** in  $\text{CD}_2\text{Cl}_2$

## Compound 4a

Figure S16. <sup>1</sup>H{<sup>11</sup>B} NMR (top) and <sup>1</sup>H NMR (bottom) spectra of 4a in CD<sub>2</sub>Cl<sub>2</sub>

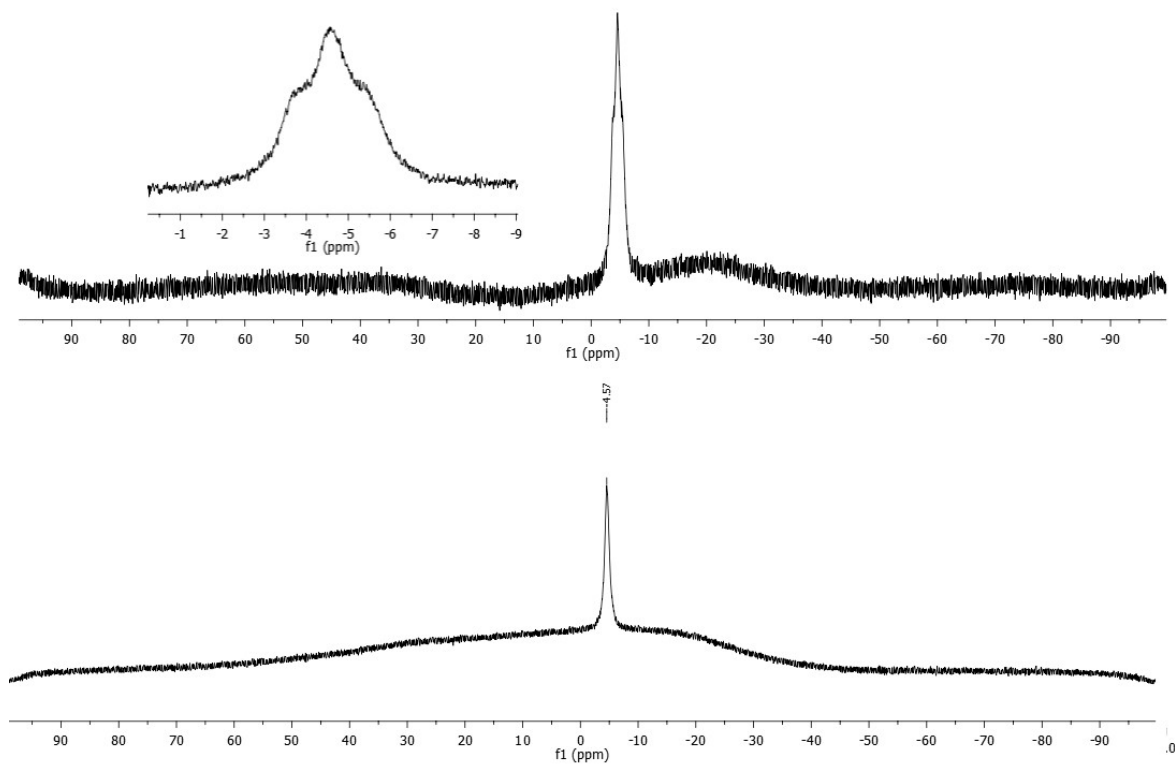


Figure S17.  $^1\text{H}\{^{11}\text{B}\}$  NMR (top) and  $^1\text{H}$  (bottom) spectra of **4a** in  $\text{CD}_2\text{Cl}_2$

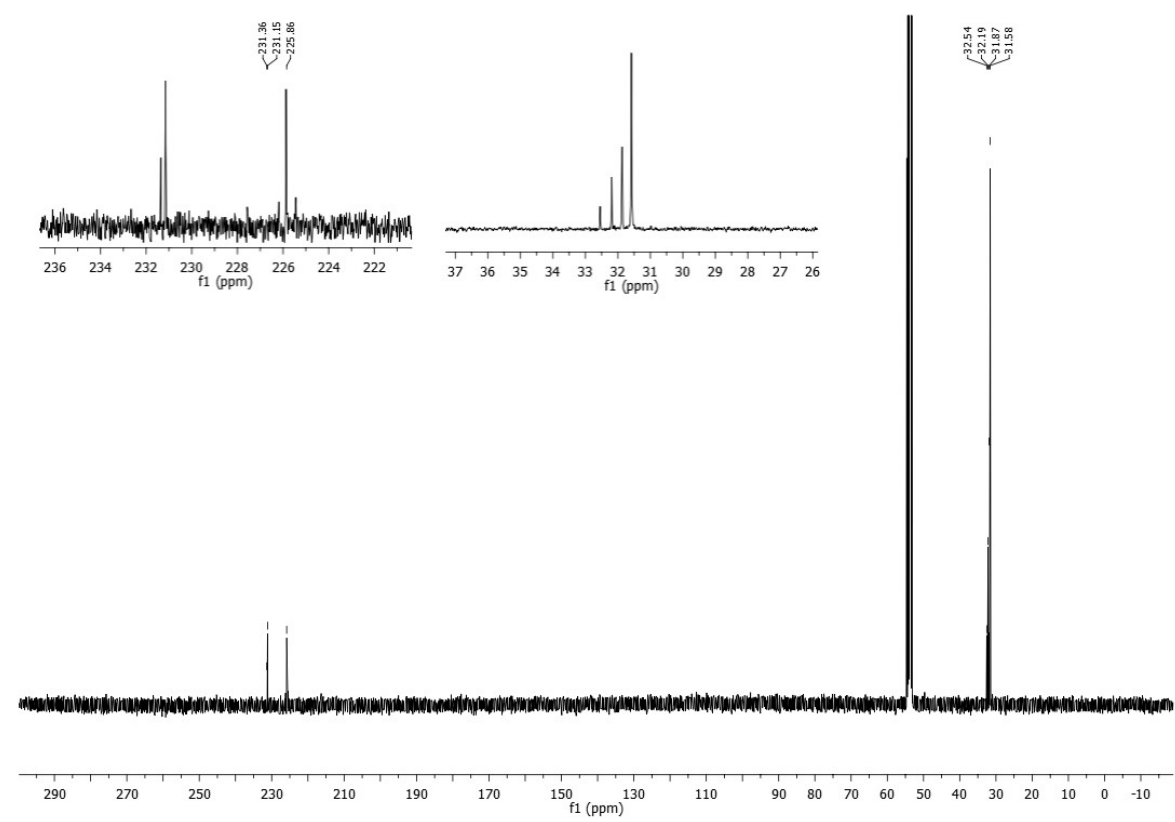
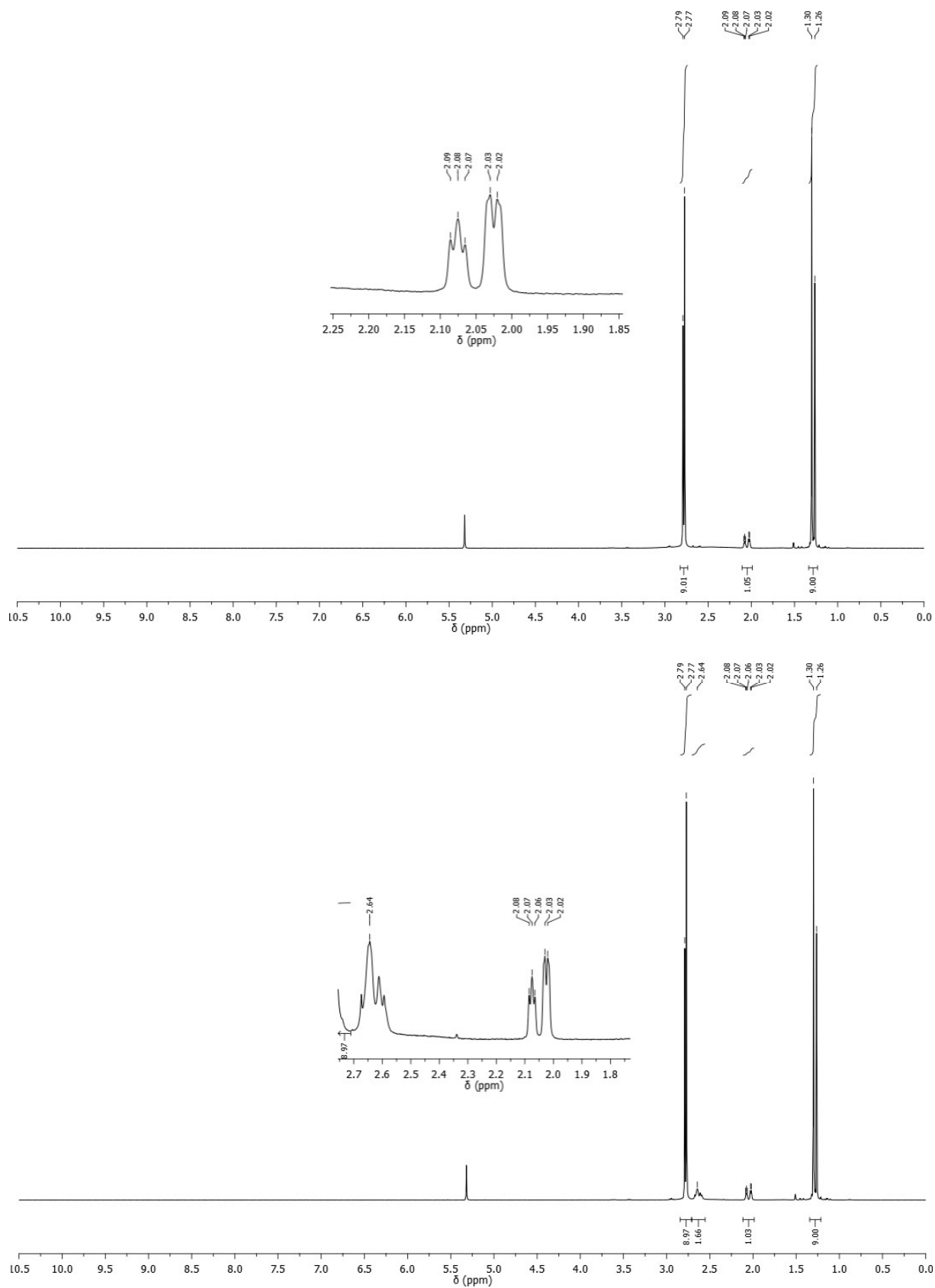


Figure S18.  $^{13}\text{C}\{^1\text{H}\}$  NMR spectrum of **4a** in  $\text{CD}_2\text{Cl}_2$

## Compound 4c

Figure S22. <sup>1</sup>H{<sup>11</sup>B} NMR (top) and <sup>1</sup>H (bottom) spectra of **4c** in CD<sub>2</sub>Cl<sub>2</sub>

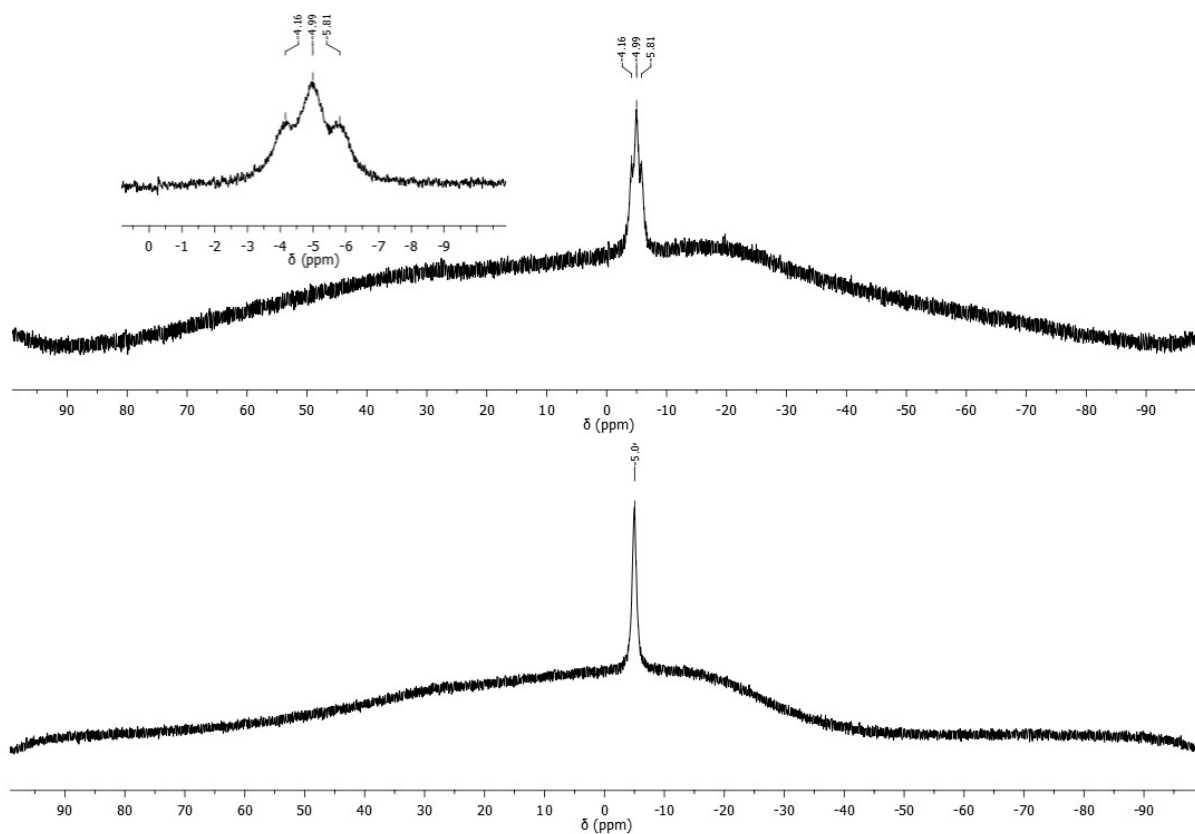
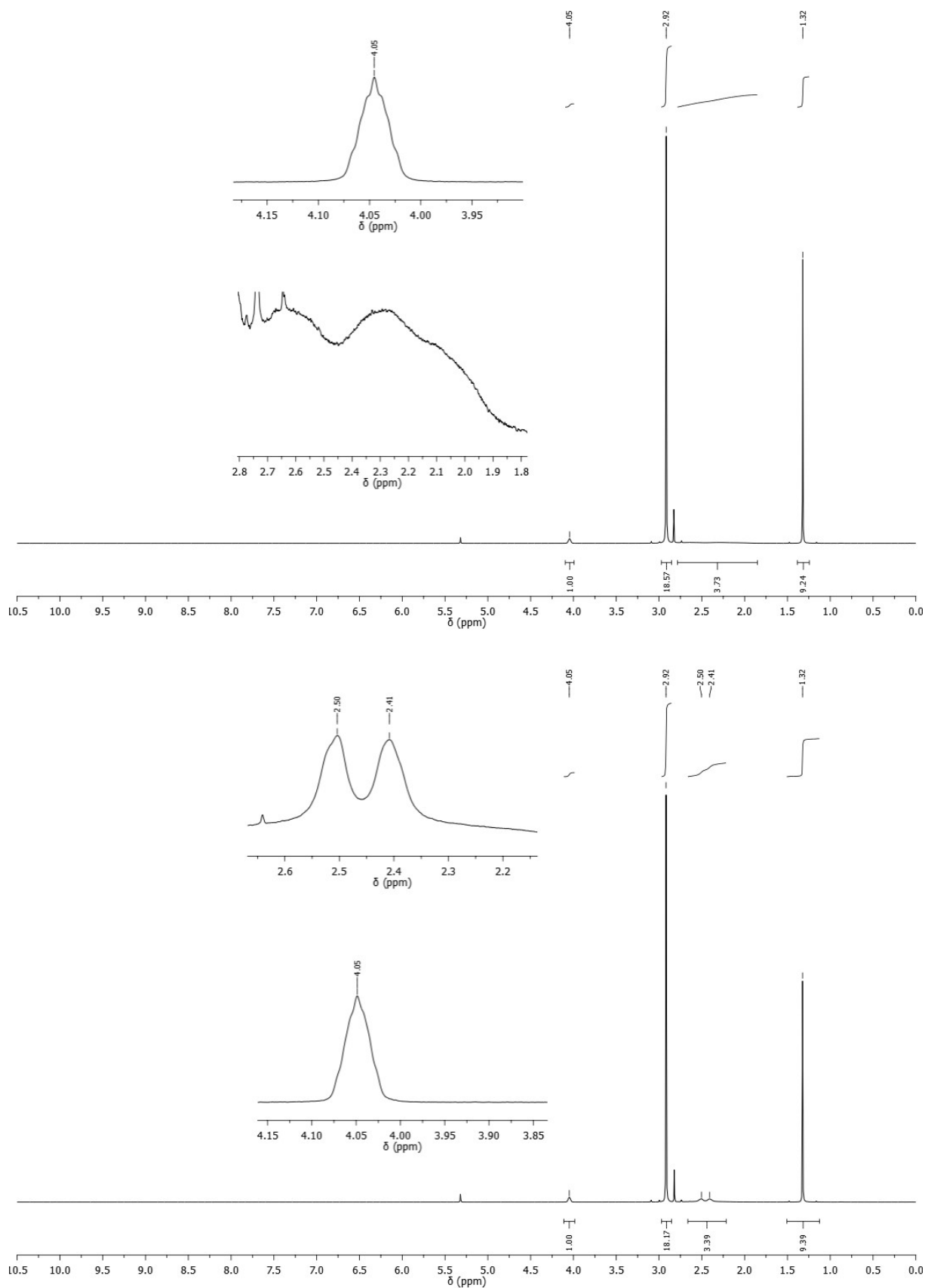


Figure S23.  $^{11}\text{B}$  NMR (top) and  $^{11}\text{B}\{^1\text{H}\}$  (bottom) spectra of **4c** in  $\text{CD}_2\text{Cl}_2$

## Compound 5

Figure S24. <sup>1</sup>H{<sup>11</sup>B} NMR (bottom) and <sup>1</sup>H (top) spectra of **5** in CD<sub>2</sub>Cl<sub>2</sub>

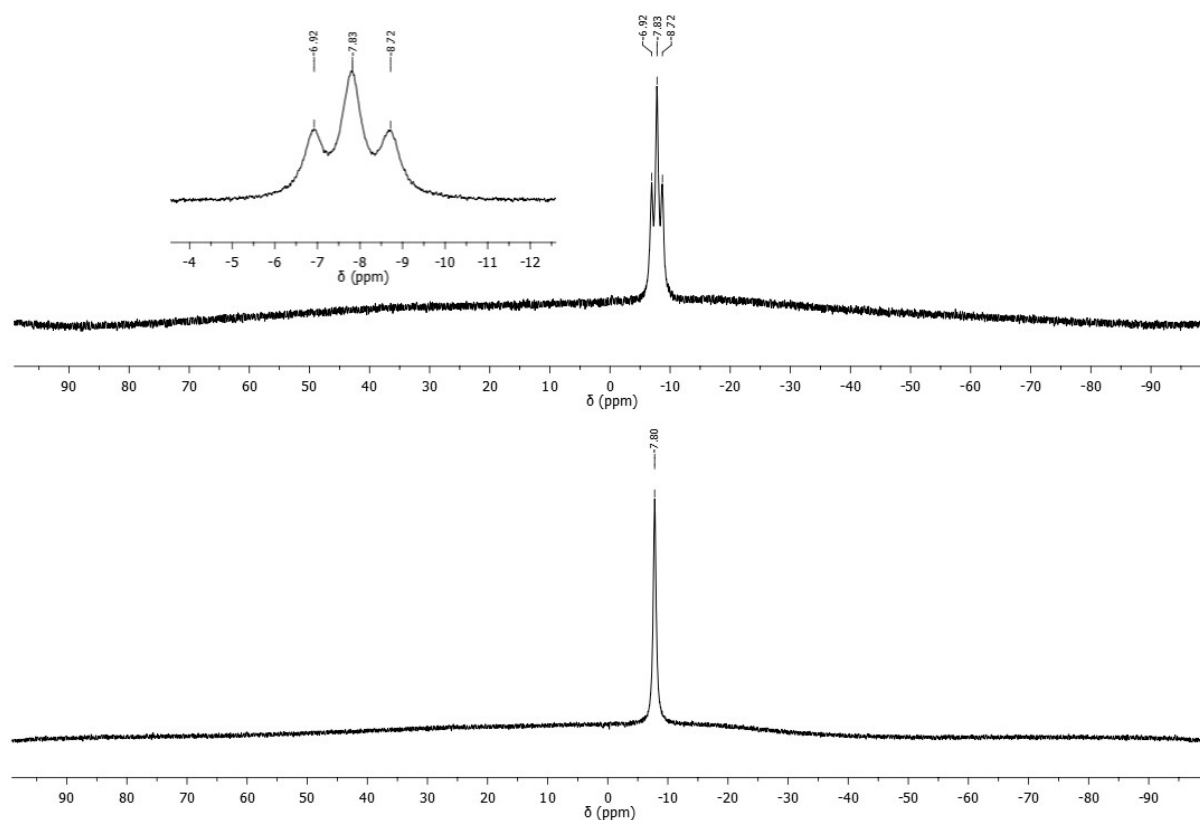


Figure S25.  $^{11}\text{B}$  NMR (top) and  $^{11}\text{B}\{^1\text{H}\}$  (bottom) spectra of **5** in  $\text{CD}_2\text{Cl}_2$

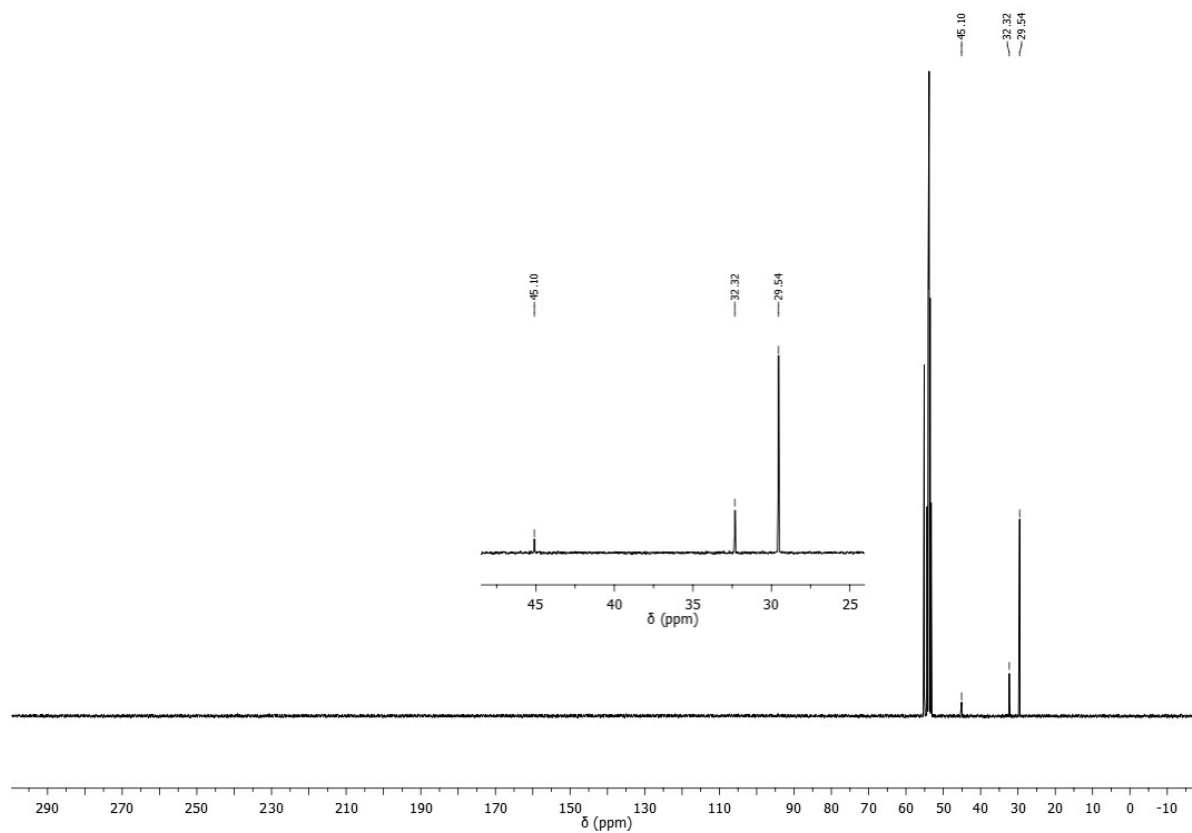


Figure S26.  $^{13}\text{C}\{^1\text{H}\}$  spectra of **5** in  $\text{CD}_2\text{Cl}_2$

## Compound 6

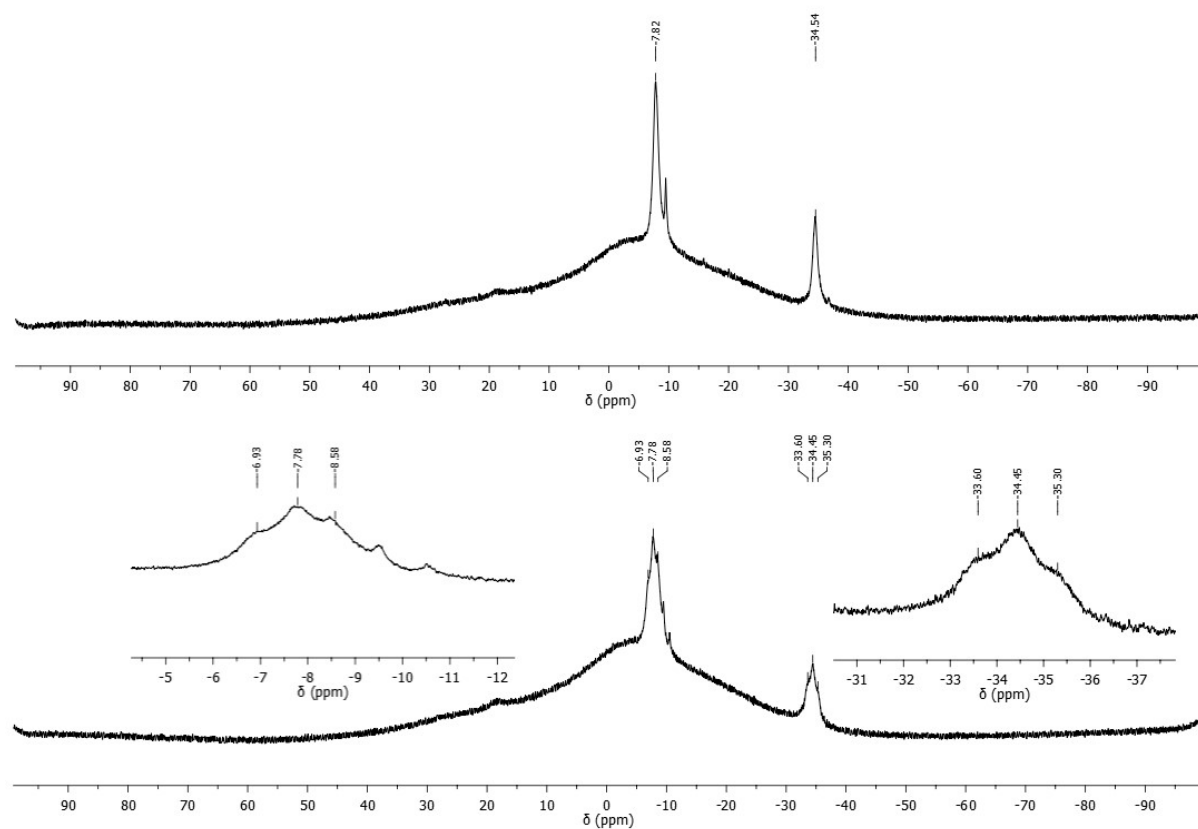
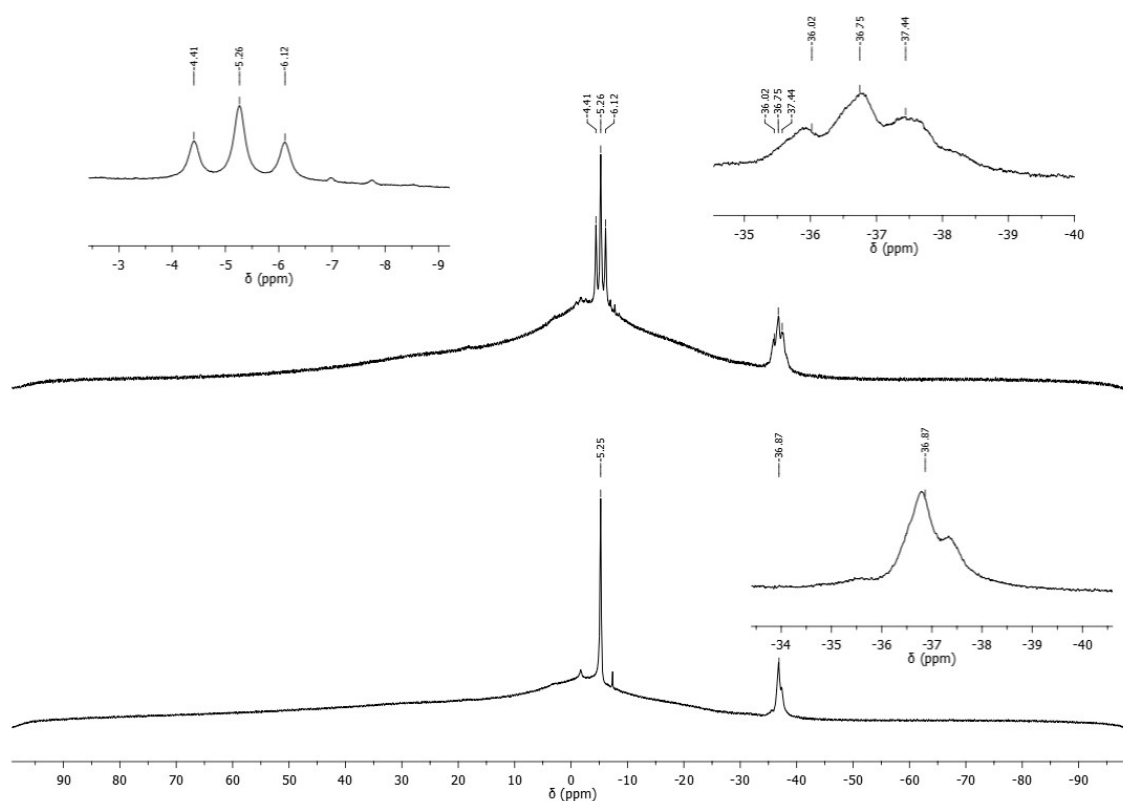
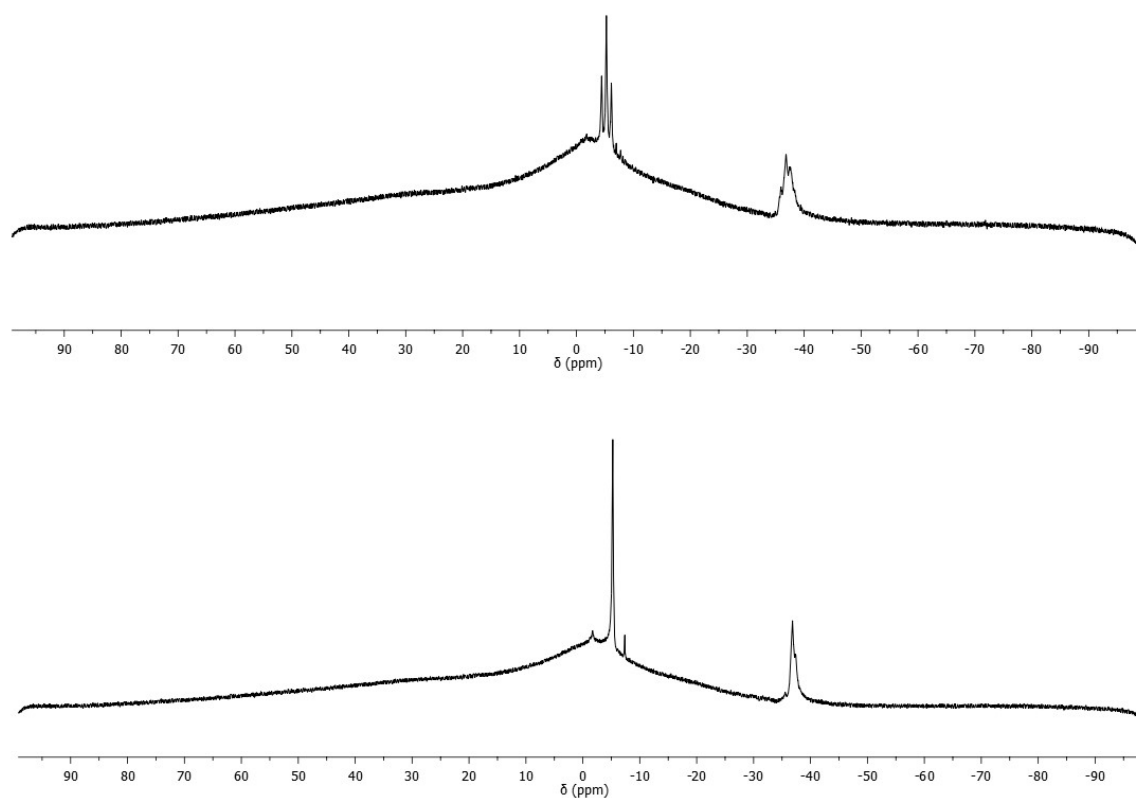


Figure S27.  $^{11}\text{B}$  NMR (top) and  $^{11}\text{B}\{^1\text{H}\}$  (bottom) spectra of 6 in  $\text{CH}_2\text{Cl}_2$

## Thermal Oligomerization



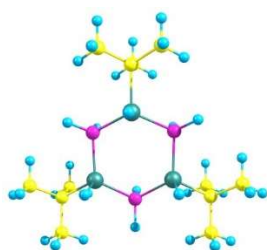
**Figure S28.**  $^{11}\text{B}$  NMR (top) and  $^{11}\text{B}\{^1\text{H}\}$  (bottom) spectra of thermal oligomerization of **1** in  $\text{CD}_2\text{Cl}_2$  after 40h at  $80^\circ\text{C}$



**Figure S29.**  $^{11}\text{B}$  NMR (top) and  $^{11}\text{B}\{^1\text{H}\}$  (bottom) spectra of thermal oligomerization of **1** in  $\text{CD}_2\text{Cl}_2$  after 65h at  $80^\circ\text{C}$

## Quantum chemical calculations

The geometries of the compounds have been fully optimized with gradient-corrected density functional theory (DFT) in form of Becke's three-parameter hybrid method B3LYP<sup>[1]</sup> with def2-SVP all electron basis set (ECP on Mo, W).<sup>[2]</sup> Gaussian 09 program package<sup>[3]</sup> was used throughout. All structures correspond to minima on their respective potential energy surfaces as verified by computation of second derivatives. Basis sets were obtained from the EMSL basis set exchange database.<sup>[4]</sup> Standard entropies of the reactions in solution were estimated by taking into account the loss of translational degrees of freedom upon solvation of one gaseous mole in the inert solvent (90 J mol<sup>-1</sup> K<sup>-1</sup>).<sup>[5]</sup>



Optimized structure of *ring*(*t*BuAsHBH<sub>2</sub>)<sub>3</sub>.

**Table S4** . Reaction energies  $\Delta E^\circ$ , standard reaction enthalpies  $\Delta H^\circ_{298}$ , Gibbs energies  $\Delta G^\circ_{298}$  (kJ mol<sup>-1</sup>) and standard reaction entropies  $\Delta S^\circ_{298}$  (J mol<sup>-1</sup> K<sup>-1</sup>) for the considered gas phase processes and estimated values of standard reaction entropies and Gibbs energies in solution (solv). B3LYP/def2-SVP(ECP on Mo, W) level of theory.

N	Process	$\Delta E^\circ$	$\Delta H^\circ_{298}$	$\Delta S^\circ_{298}$	$\Delta G^\circ_{298}$	$\Delta G^\circ_{373}$	$\Delta S^\circ_{298}$ (solv)	$\Delta G^\circ_{298}$ (solv)	$\Delta G^\circ_{373}$ (solv)
1	${}^t\text{BuAsHBH}_2\text{NMe}_3 + \text{BBr}_3 = \text{BBr}_3 \cdot {}^t\text{BuAsHBH}_2\text{NMe}_3$	-66.4	-58.7	-149.2	-14.3	-3.1	-59.2	-41.1	-36.6
2	${}^t\text{BuAsHBH}_2\text{NMe}_3 + \text{BH}_3 \cdot \text{SMe}_2 = \text{BH}_3 \cdot {}^t\text{BuAsHBH}_2\text{NMe}_3 + \text{SMe}_2$	-31.3	-31.3	-5.4	-29.7	-29.3	-5.4	-29.7	-29.3
3	$2 {}^t\text{BuAsHBH}_2\text{NMe}_3 + \text{Cr}(\text{CO})_4\text{nbnd} = \text{Cr}(\text{CO})_4({}^t\text{BuAsHBH}_2\text{NMe}_3)_2 + \text{nbnd}$	-48.4	-40.5	-175.9	12.0	25.1	-85.9	-14.9	-8.4
4	$2 {}^t\text{BuAsHBH}_2\text{NMe}_3 + \text{Mo}(\text{CO})_4\text{nbnd} = \text{Mo}(\text{CO})_4({}^t\text{BuAsHBH}_2\text{NMe}_3)_2 + \text{nbnd}$	-60.7	-50.0	-189.5	6.5	20.7	-99.5	-20.4	-12.9
5	$2 {}^t\text{BuAsHBH}_2\text{NMe}_3 + \text{W}(\text{CO})_4\text{nbnd} = \text{W}(\text{CO})_4({}^t\text{BuAsHBH}_2\text{NMe}_3)_2 + \text{nbnd}$	-70.2	-59.5	-182.1	-5.2	8.5	-92.1	-32.0	-25.1
6	${}^t\text{BuAsHBH}_2\text{NMe}_3 + \text{tBH}_2 \cdot \text{NMe}_3 = [{}^t\text{BuAsH}(\text{BH}_2\text{NMe}_3)_2]^+ \text{t}^-$	-25.5	-17.6	-171.8	33.7	46.6	-81.8	6.8	13.0
7	$2 {}^t\text{BuAsHBH}_2\text{NMe}_3 + \text{tBH}_2 \cdot \text{SMe}_2 = [\text{BH}_2({}^t\text{BuAsHBH}_2\text{NMe}_3)_2]^+ \text{t}^- + \text{SMe}_2$	-50.6	-41.5	-178.1	11.6	24.9	-88.1	-15.3	-8.7
8	$2 {}^t\text{BuAsHBH}_2\text{NMe}_3 = \text{chain}({}^t\text{BuAsHBH}_2)_2\text{NMe}_3 + \text{NMe}_3$	46.4	39.9	2.2	39.3	39.1	92.2	12.5	5.5
9	$2 {}^t\text{BuAsHBH}_2\text{NMe}_3 = \text{chain}({}^t\text{BuAsHBH}_2)_2 + 2 \text{NMe}_3$	185.1	162.4	192.2	105.1	90.6	282.2	78.2	57.1
10	$2 {}^t\text{BuAsHBH}_2\text{NMe}_3 = \text{ring}({}^t\text{BuAsHBH}_2)_2 + 2 \text{NMe}_3$	75.2	55.0	168.5	4.8	-7.9	258.5	-22.1	-41.5
11	$3 {}^t\text{BuAsHBH}_2\text{NMe}_3 = \text{chain}({}^t\text{BuAsHBH}_2)_3\text{NMe}_3 + 2 \text{NMe}_3$	64.2	52.4	-1.0	52.7	52.8	179.0	-0.9	-14.4
12	$3 {}^t\text{BuAsHBH}_2\text{NMe}_3 = \text{chain}({}^t\text{BuAsHBH}_2)_3 + 3 \text{NMe}_3$	218.7	189.8	212.4	126.5	110.5	392.4	72.8	43.4
13	$3 {}^t\text{BuAsHBH}_2\text{NMe}_3 = \text{ring}({}^t\text{BuAsHBH}_2)_3 + 3 \text{NMe}_3$	-9.5	-33.5	155.9	-80.0	-91.7	335.9	-133.7	-158.8
14	$4 {}^t\text{BuAsHBH}_2\text{NMe}_3 = \text{chain}({}^t\text{BuAsHBH}_2)_4\text{NMe}_3 + 3 \text{NMe}_3$	33.2	17.0	-4.6	18.4	18.7	265.4	-62.1	-82.0
15	$4 {}^t\text{BuAsHBH}_2\text{NMe}_3 = \text{chain}({}^t\text{BuAsHBH}_2)_4 + 4 \text{NMe}_3$	231.4	194.2	167.2	144.4	131.8	437.2	63.9	31.1
16	$4 {}^t\text{BuAsHBH}_2\text{NMe}_3 = \text{ring}({}^t\text{BuAsHBH}_2)_4 + 4 \text{NMe}_3$	6.6	-21.4	141.8	-63.7	-74.3	411.8	-144.2	-175.1

## Cartesian coordinates of the optimized structures

Table S5. Optimized geometries of computationally studied compounds. xyz coordinates in angstroms. B3LYP/def2-SVP (ECP on Mo,W) level of theory.

NMe <sub>3</sub>			
7	0.00000000	0.00000000	0.34593100
6	0.00000000	1.39081900	-0.05556400
6	-1.20448400	-0.69540900	-0.05556400
6	1.20448400	-0.69540900	-0.05556400
1	-2.09267700	-0.18015300	0.34469900
1	-1.20235600	-1.72223500	0.34469900
1	-1.32788000	-0.76665200	-1.16318500
1	-0.89032100	1.90238800	0.34469900
1	0.00000000	1.53330400	-1.16318500
1	0.89032100	1.90238800	0.34469900
1	2.09267700	-0.18015300	0.34469900
1	1.32788000	-0.76665200	-1.16318500
1	1.20235600	-1.72223500	0.34469900
SMe <sub>2</sub>			
6	0.00000000	-1.39170500	-0.51204900
16	0.00000000	0.00000000	0.66041900
6	0.00000000	1.39170500	-0.51204900
1	0.89937300	-1.38485500	-1.14837100
1	-0.89937300	-1.38485500	-1.14837100
1	0.00000000	-2.31476200	0.08568700
1	0.89937300	1.38485500	-1.14837100
1	0.00000000	2.31476200	0.08568700
1	-0.89937300	1.38485500	-1.14837100
BH <sub>3</sub> SMe <sub>2</sub>			
5	0.27932700	1.82108700	0.00000000
16	-0.52872200	0.01717100	0.00000000
6	0.27932700	-0.81884300	1.39638400
6	0.27932700	-0.81884300	-1.39638400
1	-0.17098200	2.30924300	1.02172700
1	-0.17098200	2.30924300	-1.02172700
1	1.48452000	1.62876000	0.00000000
1	0.00406100	-1.88276800	-1.40817900
1	1.36870300	-0.68913900	-1.32616400
1	-0.08854800	-0.32874200	-2.30768800
1	-0.08854800	-0.32874200	2.30768800
1	1.36870300	-0.68913900	1.32616400
1	0.00406100	-1.88276800	1.40817900
IBH <sub>2</sub> NMe <sub>3</sub>			
5	-0.19179900	1.19720600	0.00000000
1	-0.50314200	1.75471500	1.02788800
1	-0.50314200	1.75471500	-1.02788800
7	1.44692600	1.08207800	0.00000000
6	1.95003400	0.38607700	-1.21736700
6	1.95003400	0.38607700	1.21736700
6	1.95003400	2.48513300	0.00000000
1	3.05110100	0.37688400	1.21595100
1	1.56041000	-0.63895900	1.22767500
1	1.58108900	0.91296000	2.10595100
1	3.05117500	2.49057400	0.00000000
1	1.57433700	3.00066800	0.89214100
1	1.57433700	3.00066800	-0.89214100
1	3.05110100	0.37688400	-1.21595100
1	1.58108900	0.91296000	-2.10595100
1	1.56041000	-0.63895900	-1.22767500
53	-1.16696000	-0.87561100	0.00000000
IBH <sub>2</sub> SMe <sub>2</sub>			
5	-1.41942600	-0.10747600	0.00000000
16	-0.81511500	-1.98166600	0.00000000
6	0.32418800	-2.14938700	1.40527900
6	0.32418800	-2.14938700	-1.40527900
1	-2.04623300	-0.02235100	1.02980400
1	-2.04623300	-0.02235100	-1.02980400
1	0.77557300	-3.15042100	-1.38029300
1	1.08560800	-1.35766100	-1.36217300
1	-0.28157100	-2.03517800	-2.31421800
1	-0.28157100	-2.03517800	2.31421800
1	1.08560800	-1.35766100	1.36217300
1	0.77557300	-3.15042100	1.38029300
53	0.32418800	1.34279100	0.00000000
C <sub>7</sub> H <sub>8</sub> (nbd)			
6	-1.24408000	0.66939000	-0.52097500
6	-1.24408000	-0.66939000	-0.52097500
6	0.00000000	-1.12204400	0.27330500
6	1.24408000	-0.66939000	-0.52097500
6	1.24408000	0.66939000	-0.52097500
6			
6	0.00000000	1.12204400	0.27330500
6	0.00000000	0.00000000	1.35479000
1	-1.93969000	1.34183600	-1.02535000
1	-1.93969000	-1.34183600	-1.02535000
1	0.00000000	-2.16552800	0.61522500
1	1.93969000	-1.34183600	-1.02535000
1	1.93969000	1.34183600	-1.02535000
1	0.00000000	2.16552800	0.61522500
1	0.90411000	0.00000000	1.98297100
1	-0.90411000	0.00000000	1.98297100
BBR <sub>3</sub>			
5	0.00000000	0.00000000	0.00000000
35	0.00000000	1.91194200	0.00000000
35	1.65579000	-0.95597100	0.00000000
35	-1.65579000	-0.95597100	0.00000000
BBR <sub>3</sub> <sup>-</sup> BuAsHBH <sub>2</sub> NMe <sub>3</sub>			
33	0.61737300	0.63446100	-0.25514500
35	-0.67862000	-2.41175100	-0.30734800
35	-1.78286300	-0.16209600	1.92484500
35	-2.56078300	0.12763200	-1.33659500
7	3.44076100	-0.82924600	-0.00711900
6	0.50236200	2.65102100	-0.04629100
6	4.05660400	0.02353200	-1.06062100
1	4.87229400	-0.52239700	-1.55922700
1	4.44994100	0.93779700	-0.60018000
1	3.29614200	0.29320600	-1.80269500
6	2.91224400	-2.07893700	-0.62741100
1	2.14998700	-1.83031500	-1.37410400
1	2.43721300	-2.69128700	0.14690800
1	3.73604900	-2.63259300	-1.10392900
5	-1.18135700	-0.45877700	0.01677600
6	4.49548400	-1.20292200	0.98232300
1	5.30614100	-1.74903100	0.47543500
1	4.04755000	-1.83498300	1.75797600
1	4.89093100	-0.29261200	1.44841600
6	1.78671900	3.25011900	-0.63865300
1	2.69039600	2.88210500	-0.12955700
1	1.76559300	4.34761200	-0.51716900
1	1.87982100	3.04240900	-1.71719300
5	2.29693300	-0.02116600	0.84066800
6	0.39823500	2.98199100	1.45060700
1	-0.50758200	2.55059300	1.90029300
1	0.35337400	4.07825600	1.57548300
1	1.26853700	2.61681400	2.01654500
1	2.84193000	0.96712900	1.28750200
1	1.87578500	-0.77185800	1.69009100
1	0.89908300	0.55388300	-1.74811300
6	-0.72082200	3.19203700	-0.79789700
1	-0.68965000	2.95189300	-1.87206600
1	-0.74259400	4.29217200	-0.69913000
1	-1.66309700	2.79494300	-0.39680200
BH <sub>3</sub> <sup>-</sup> BuAsHBH <sub>2</sub> NMe <sub>3</sub>			
33	0.50562100	0.45248000	-0.37733900
7	-2.49946600	-0.30008700	0.05847100
6	2.22033500	-0.48298400	0.11992800
6	-3.48080400	-1.42038900	0.09696200
1	-3.44600900	-1.96403300	-0.85467300
1	-4.49520700	-1.02627300	0.26677400
1	-3.20772400	-2.10636200	0.90796500
6	2.26135100	-0.60976500	1.65033700
1	2.21194600	0.37427700	2.14153400
1	3.20511600	-1.09409000	1.95848600
1	1.43263700	-1.22607100	2.03305400
6	2.27021700	-1.86822000	-0.53918000
1	1.44868500	-2.51700400	-0.19987900
1	3.22121000	-2.36973700	-0.28296500
1	2.21801500	-1.79979400	-1.63780300
6	3.38867900	0.38402600	-0.37191800
1	3.38610500	0.48779700	-1.46908300
1	4.34717800	-0.08481200	-0.08498300
1	3.36115200	1.39393700	0.06390600
5	-1.01685900	-0.96868900	-0.14333500
5	0.33667400	2.37034500	0.43022400
6	-2.84375300	0.60553200	-1.07482800
1	-2.72465100	0.05747400	-2.01807900
1	-2.17188000	1.47292200	-1.06216300
1	-3.88426500	0.95231800	-0.97559000
6	-2.58430200	0.45785600	1.34242300
1	-3.60011000	0.86418100	1.46700300

1	-1.854834000	1.276719000	1.336655000
1	-2.354583000	-0.224537000	2.169765000
1	-1.078871000	-1.658424000	-1.142401000
1	-0.788239000	-1.606277000	0.867098000
1	0.187773000	2.202350000	1.633647000
1	-0.663190000	2.839214000	-0.106396000
1	1.354275000	2.972793000	0.135065000
1	0.716832000	0.547571000	-1.880837000

<sup>t</sup>BuAsHBH<sub>2</sub>NMe<sub>3</sub>

5	0.939378000	0.613201000	0.590837000
1	1.076846000	0.659241000	1.800047000
1	0.704692000	1.701813000	0.092355000
33	-0.506606000	-0.790096000	-0.043857000
7	2.442087000	0.195741000	0.006890000
6	3.413580000	1.207447000	0.499695000
6	2.457079000	0.193342000	-1.480323000
6	2.839625000	-1.145481000	0.510198000
1	3.462331000	-0.063663000	-1.851646000
1	2.172680000	1.190142000	-1.839550000
1	1.724623000	-0.537299000	-1.846095000
1	4.427339000	0.975947000	0.133030000
1	3.403238000	1.208126000	1.596211000
1	3.105702000	2.198666000	0.145490000
1	3.858498000	-1.395706000	0.172548000
1	2.132612000	-1.895846000	0.133074000
1	2.801652000	-1.139084000	1.606675000
6	-2.209487000	0.334169000	0.005228000
6	-2.197396000	1.250771000	-1.226659000
1	-2.139508000	0.672031000	-2.163396000
1	-3.124150000	1.852626000	-1.264675000
1	-1.348128000	1.951911000	-1.204791000
6	-2.310307000	1.168830000	1.287959000
1	-3.248902000	1.756089000	1.290340000
1	-2.315162000	0.530688000	2.185969000
1	-1.472522000	1.875512000	1.382583000
6	-3.395174000	-0.638092000	-0.082223000
1	-3.426742000	-1.319057000	0.783842000
1	-4.349910000	-0.079687000	-0.100589000
1	-3.349975000	-1.255549000	-0.993837000
1	-0.756216000	-1.475850000	1.304024000

Cr(CO)<sub>4</sub>mbd

24	0.000000000	0.000000000	0.492891000
8	2.281456000	0.000000000	2.468204000
8	0.000000000	3.012766000	0.956572000
8	-2.281456000	0.000000000	2.468204000
8	0.000000000	-3.012766000	0.956572000
6	1.206006000	0.690704000	-1.357326000
6	1.206006000	-0.690704000	-1.357326000
6	0.000000000	-1.124565000	-2.218452000
6	-1.206006000	-0.690704000	-1.357326000
6	-1.206006000	0.690704000	-1.357326000
6	0.000000000	1.124565000	-2.218452000
6	0.000000000	0.000000000	-3.286495000
6	1.400807000	0.000000000	1.725157000
6	0.000000000	1.883859000	0.734443000
6	-1.400807000	0.000000000	1.725157000
6	0.000000000	-1.883859000	0.734443000
1	2.031365000	1.340871000	-1.069060000
1	2.031365000	-1.340871000	-1.069060000
1	0.000000000	-2.167948000	-2.556079000
1	-2.031365000	-1.340871000	-1.069060000
1	-2.031365000	1.340871000	-1.069060000
1	0.000000000	2.167948000	-2.556079000
1	-0.903035000	0.000000000	-3.918194000
1	0.903035000	0.000000000	-3.918194000

Mo(CO)<sub>4</sub>mbd

42	0.000000000	0.000000000	0.463066000
8	2.332561000	0.000000000	2.583947000
8	0.000000000	3.175125000	0.911984000
8	-2.332561000	0.000000000	2.583947000
8	0.000000000	-3.175125000	0.911984000
6	1.218970000	0.690648000	-1.553001000
6	1.218970000	-0.690648000	-1.553001000
6	0.000000000	-1.124684000	-2.400080000
6	-1.218970000	-0.690648000	-1.553001000
6	-1.218970000	0.690648000	-1.553001000
6	0.000000000	1.124684000	-2.400080000
6	0.000000000	0.000000000	-3.471135000
6	1.464680000	0.000000000	1.822803000
6	0.000000000	2.046191000	0.699283000
6	-1.464680000	0.000000000	1.822803000
6	0.000000000	-2.046191000	0.699283000
1	2.044060000	1.343015000	-1.268398000
1	2.044060000	-1.343015000	-1.268398000
1	0.000000000	-2.168931000	-2.735119000

1	-2.044060000	-1.343015000	-1.268398000
1	-2.044060000	1.343015000	-1.268398000
1	0.000000000	2.168931000	-2.735119000
1	-0.903096000	0.000000000	-4.102536000
1	0.903096000	0.000000000	-4.102536000

W(CO)<sub>4</sub>mbd

74	0.000000000	0.000000000	0.384204000
8	2.368538000	0.000000000	2.492252000
8	0.000000000	3.194453000	0.824828000
8	-2.368538000	0.000000000	2.492252000
8	0.000000000	-3.194453000	0.824828000
6	1.215161000	0.693172000	-1.635706000
6	1.215161000	-0.693172000	-1.635706000
6	0.000000000	-1.125077000	-2.488919000
6	-1.215161000	-0.693172000	-1.635706000
6	-1.215161000	0.693172000	-1.635706000
6	0.000000000	1.125077000	-2.488919000
6	0.000000000	0.000000000	-3.559209000
6	1.484858000	0.000000000	1.747455000
6	0.000000000	2.062720000	0.624783000
6	-1.484858000	0.000000000	1.747455000
6	0.000000000	-2.062720000	0.624783000
1	2.048221000	1.341951000	-1.365989000
1	2.048221000	-1.341951000	-1.365989000
1	0.000000000	-2.169493000	-2.823256000
1	-2.048221000	-1.341951000	-1.365989000
1	-2.048221000	1.341951000	-1.365989000
1	0.000000000	2.169493000	-2.823256000
1	-0.902859000	0.000000000	-4.190782000
1	0.902859000	0.000000000	-4.190782000

Cr(CO)<sub>4</sub>(<sup>t</sup>BuAsHBH<sub>2</sub>NMe<sub>3</sub>)<sub>2</sub>

33	0.000000000	-1.853967000	-0.320974000
33	0.000000000	1.853967000	-0.320974000
24	0.000000000	0.000000000	1.463486000
8	0.198129000	-2.118720000	3.589137000
8	3.019712000	0.301521000	1.631637000
8	-3.019712000	-0.301521000	1.631637000
8	-0.198129000	2.118720000	3.589137000
7	-2.574516000	-3.692141000	-0.890793000
6	0.118772000	-1.314714000	2.758450000
7	2.574516000	3.692141000	-0.890793000
6	1.871097000	0.174456000	1.518506000
6	-1.871097000	-0.174456000	1.518506000
6	1.764587000	-2.678098000	-0.954775000
6	-1.764587000	2.678098000	-0.954775000
6	-2.675952000	1.561412000	-1.483556000
1	-2.208862000	1.015068000	-2.319907000
1	-3.620332000	1.996748000	-1.859748000
1	-2.940909000	0.840095000	-0.699093000
6	-0.118772000	1.314714000	2.758450000
6	2.415863000	-3.369426000	0.251803000
1	2.611515000	-2.662727000	1.072323000
1	3.384298000	-3.813002000	-0.043493000
1	1.784692000	-4.180982000	0.646426000
6	2.675952000	-1.561412000	-1.483556000
1	2.208862000	-1.015068000	-2.319907000
1	3.620332000	-1.996748000	-1.859748000
1	2.940909000	-0.840095000	-0.699093000
6	-1.516075000	3.695400000	-2.075349000
1	-0.872697000	4.521779000	-1.741508000
1	-2.476555000	4.135581000	-2.401962000
1	-1.054226000	3.226906000	-2.960391000
6	-2.415863000	3.369426000	0.251803000
1	-2.611515000	2.662727000	1.072323000
1	-3.384298000	3.813002000	-0.043493000
1	-1.784692000	4.180982000	0.646426000
6	1.516075000	-3.695400000	-2.075349000
1	0.872697000	-4.521779000	-1.741508000
1	2.476555000	-4.135581000	-2.401962000
1	1.054226000	-3.226906000	-2.960391000
6	-3.358971000	-4.832201000	-0.336074000
1	-3.652276000	-4.595226000	0.693145000
1	-2.728685000	-5.729589000	-0.327202000
1	-4.255871000	-5.008450000	-0.951432000
6	2.199419000	4.008598000	-2.293794000
1	3.104658000	4.158897000	-2.903247000
1	1.589154000	4.919385000	-2.306522000
1	1.612590000	3.180149000	-2.706561000
6	-3.430371000	-2.472887000	-0.871528000
1	-4.350022000	-2.651107000	-1.451010000
1	-2.879752000	-1.634686000	-1.313783000
1	-3.679576000	-2.218556000	0.164724000
6	3.430371000	2.472887000	-0.871528000
1	2.879752000	1.634686000	-1.313783000
1	3.679576000	2.218556000	0.164724000
1	4.350022000	2.651107000	-1.451010000

5	-1.250555000	-3.519000000	0.077396000
6	-2.199419000	-4.008598000	-2.293794000
1	-1.589154000	-4.919385000	-2.306522000
1	-1.612590000	-3.180149000	-2.706561000
1	-3.104658000	-4.158897000	-2.903247000
5	1.250555000	3.519000000	0.077396000
6	3.358971000	4.832201000	-0.336074000
1	4.255871000	5.008450000	-0.951432000
1	3.652276000	4.595226000	0.693145000
1	2.728685000	5.729589000	-0.327202000
1	0.432225000	1.371978000	-1.717213000
1	-0.432225000	-1.371978000	-1.717213000
1	-0.616756000	-4.550561000	-0.040637000
1	1.687620000	-3.361446000	1.197695000
1	-1.687620000	-3.361446000	1.197695000
1	0.616756000	4.550561000	-0.040637000

Mo(CO)<sub>4</sub>(<sup>t</sup>BuAsHBH<sub>2</sub>NMe<sub>3</sub>)<sub>2</sub>

42	0.005506000	-0.232912000	1.525954000
33	-1.915606000	0.386508000	-0.326701000
33	1.916733000	-0.273638000	-0.436943000
8	-2.117628000	-0.029429000	3.836771000
8	-0.811260000	-3.314071000	1.280859000
8	0.827424000	2.793348000	2.161083000
7	-2.586221000	-1.974253000	-2.395274000
7	2.543691000	2.582422000	-1.766343000
8	2.135838000	-1.097242000	3.671684000
6	-1.346086000	-0.105488000	2.972722000
6	-0.506038000	-2.198035000	1.321120000
6	-3.265846000	1.856486000	0.152154000
6	0.519530000	1.711446000	1.888259000
6	1.362950000	-0.774069000	2.867987000
6	-3.644933000	-2.951156000	-2.780363000
1	-3.286447000	-3.590574000	-3.602926000
1	-4.541770000	-2.403997000	-3.094666000
1	-3.892705000	-3.568898000	-1.909286000
6	-1.377826000	-2.730459000	-1.964148000
1	-1.628738000	-3.349151000	-1.095919000
1	-0.590416000	-2.025549000	-1.673576000
1	-1.019375000	-3.366227000	-2.789089000
6	2.584549000	-3.092181000	0.029274000
1	2.148349000	-3.020270000	1.034997000
1	3.311698000	-3.924473000	0.038678000
1	1.779004000	-3.368222000	-0.670589000
6	3.291317000	-1.796066000	-0.384286000
6	3.575338000	3.656978000	-1.834459000
1	3.213109000	4.486893000	-2.461849000
1	4.498234000	3.242114000	-2.256946000
1	3.780155000	4.018246000	-0.819942000
6	1.302090000	3.154691000	-1.174999000
1	1.512476000	3.497727000	-0.156259000
1	0.525885000	2.381621000	-1.131473000
1	0.948606000	3.996716000	-1.790841000
6	-2.253278000	-1.140870000	-3.580840000
1	-1.903149000	-1.779644000	-4.406917000
1	-1.467621000	-0.425705000	-3.311657000
1	-3.147093000	-0.586385000	-3.891842000
6	2.261764000	2.103609000	-3.145461000
1	1.894785000	2.934610000	-3.768230000
1	1.504963000	1.311853000	-3.105112000
1	3.182245000	1.692343000	-3.577465000
5	-3.210427000	-1.059574000	-1.177776000
6	4.364029000	-1.433050000	0.654418000
1	4.911017000	-0.519054000	0.379509000
1	5.100318000	-2.253992000	0.726711000
1	3.934822000	-1.289246000	1.657186000
6	-4.356654000	1.232836000	1.037356000
1	-4.922041000	0.451352000	0.507595000
1	-5.075163000	2.014845000	1.343293000
1	-3.939963000	0.793359000	1.956173000
6	3.927010000	-1.977241000	-1.769379000
1	3.181765000	-2.277838000	-2.524082000
1	4.692164000	-2.774037000	-1.726083000
1	4.423467000	-1.061477000	-2.121804000
6	-2.540063000	2.964778000	0.922755000
1	-2.113631000	2.596932000	1.866023000
1	-3.251354000	3.774248000	1.168170000
1	-1.722685000	3.412115000	0.334173000
6	-3.882547000	2.437008000	-1.127596000
1	-3.125676000	2.935197000	-1.755297000
1	-4.642578000	3.195059000	-0.863251000
1	-4.379873000	1.666544000	-1.734413000
5	3.178450000	1.381758000	-0.838060000
1	-3.505255000	-1.829735000	-0.286339000
1	-4.172570000	-0.501026000	-1.667516000
1	1.363841000	-0.624265000	-1.831033000
1	4.162163000	1.005366000	-1.445129000
1	-1.359615000	1.103876000	-1.569127000

1 3.440978000 1.882068000 0.236575000

W(CO)<sub>4</sub>(<sup>t</sup>BuAsHBH<sub>2</sub>NMe<sub>3</sub>)<sub>2</sub>

74	0.100526000	-0.809529000	0.996005000
33	1.712691000	0.073811000	-1.080969000
33	-2.108758000	0.136929000	-0.363649000
8	0.323815000	2.062396000	2.397834000
8	-1.780344000	-1.728468000	3.366583000
8	2.587230000	-1.809144000	2.666990000
8	-0.055302000	-3.836314000	-0.103508000
7	4.040618000	1.822138000	0.319268000
6	-1.099945000	-1.388410000	2.489304000
6	-0.017370000	-2.732321000	0.234958000
7	-2.638365000	3.289286000	-0.377232000
6	1.677982000	-1.440407000	2.038855000
6	0.230959000	1.026331000	1.872525000
6	1.963663000	-1.181539000	-2.680442000
6	0.576153000	-1.580390000	-3.198260000
1	-0.027843000	-2.073889000	-2.424564000
1	0.682334000	-2.287941000	-4.040675000
1	0.012073000	-0.708353000	-3.566622000
6	2.732023000	-2.421828000	-2.203026000
1	3.724045000	-2.160103000	-1.804765000
1	2.885840000	-3.111844000	-3.052214000
1	2.184901000	-2.974977000	-1.426498000
6	5.437755000	2.297432000	0.110274000
1	6.101306000	1.428404000	0.029440000
1	5.749866000	2.927868000	0.957904000
1	5.489049000	2.870898000	-0.822898000
6	-3.682113000	-1.106314000	-0.765115000
5	3.666110000	0.892281000	-0.978859000
6	3.142921000	3.004499000	0.414618000
1	3.477380000	3.668865000	1.226784000
1	2.121935000	2.672173000	0.630952000
1	3.162544000	3.544233000	-0.540510000
6	3.987261000	1.051191000	1.593932000
1	4.617850000	0.159443000	1.502784000
1	2.958346000	0.734488000	1.783063000
1	4.339430000	1.679224000	2.426789000
6	2.742384000	-0.476259000	-3.800029000
1	2.244634000	0.451950000	-4.124160000
1	2.805912000	-1.143900000	-4.678848000
1	3.768694000	-0.223364000	-3.499537000
6	-3.147086000	-2.418420000	-1.349273000
1	-2.576085000	-2.255170000	-2.277488000
1	-3.991357000	-3.087968000	-1.594906000
1	-2.500504000	-2.952342000	-0.640668000
6	-3.110210000	3.321520000	-1.788017000
1	-2.855956000	4.288552000	-2.249991000
1	-4.197038000	3.176108000	-1.805620000
1	-2.634256000	2.509074000	-2.349105000
6	-4.418043000	-1.376327000	0.555810000
1	-3.756959000	-1.828693000	1.310362000
1	-5.253315000	-2.078304000	0.380483000
1	-4.842537000	-0.455917000	0.985253000
6	-1.167290000	3.513387000	-0.338579000
1	-0.661383000	2.721458000	-0.904507000
1	-0.827823000	3.476145000	0.702810000
1	-0.925099000	4.492284000	-0.782405000
5	-3.058448000	1.882383000	0.370697000
6	-4.625227000	-0.443454000	-1.778046000
1	-5.027382000	0.510626000	-1.407142000
1	-5.485118000	-1.109347000	-1.975796000
1	-4.124498000	-0.259968000	-2.742886000
6	-3.308038000	4.388025000	0.375893000
1	-3.081797000	5.359364000	-0.092422000
1	-2.950576000	4.379127000	1.412167000
1	-4.390755000	4.214499000	0.372779000
1	0.992916000	1.173232000	-1.873799000
1	-1.799813000	0.476326000	-1.828055000
1	4.440220000	-0.045248000	-0.951443000
1	3.817299000	1.615544000	-1.944190000
1	-4.261838000	1.790812000	0.229019000
1	-2.725227000	2.006032000	1.530269000

[<sup>t</sup>BuAsH(BH<sub>2</sub>NMe<sub>3</sub>)]<sup>+</sup>T<sup>-</sup>

53	-0.830223000	2.750303000	0.000000000
33	0.065528000	-1.236148000	0.000000000
7	1.296024000	-0.292187000	2.744870000
7	1.296024000	-0.292187000	-2.744870000
6	-2.457248000	-1.931916000	1.255011000
1	-1.918800000	-2.193033000	2.178621000
1	-3.408929000	-2.492686000	1.259818000
1	-2.703502000	-0.858648000	1.283013000
6	-1.652451000	-2.300018000	0.000000000
6	-0.016710000	0.257755000	3.200403000
1	-0.542936000	0.715247000	2.350790000

1	0.155641000	1.037790000	3.957378000	1	-3.641267000	1.021053000	-2.879153000
1	-0.613204000	-0.554173000	3.633725000	1	-2.988924000	4.013720000	-0.635585000
6	2.057722000	-0.766047000	-3.936811000	1	-3.902791000	3.395558000	0.771676000
1	1.491547000	-1.563299000	-4.433517000	1	-4.759900000	3.894633000	-0.700741000
1	3.025328000	-1.166607000	-3.610762000	6	-1.211371000	-1.991650000	2.710253000
1	2.215685000	0.070406000	-4.634794000	6	-1.396134000	-4.359871000	1.869364000
6	-2.457248000	-1.931916000	-1.255011000	6	-3.311319000	-2.764189000	1.542465000
1	-2.703502000	-0.858648000	-1.283013000	1	-1.480297000	-0.934761000	2.554597000
1	-3.408929000	-2.492686000	-1.259818000	1	-0.115425000	-2.060119000	2.774895000
1	-1.918800000	-2.193033000	-2.178621000	1	-1.626453000	-2.293027000	3.687974000
5	1.130116000	-1.595593000	1.773253000	1	-3.633447000	-1.724031000	1.385502000
6	-0.016710000	0.257755000	-3.200403000	1	-3.751485000	-3.110310000	2.494587000
1	0.155641000	1.037790000	-3.957378000	1	-3.743915000	-3.375649000	0.734830000
1	-0.542936000	0.715247000	-2.350790000	1	-0.306147000	-4.499124000	1.903268000
1	-0.613204000	-0.554173000	-3.633725000	1	-1.806704000	-5.035068000	1.101685000
6	2.070108000	0.801127000	-2.083343000	1	-1.805600000	-4.679478000	2.843957000
1	2.998180000	0.382805000	-1.673847000	53	4.247249000	1.065493000	0.189939000
1	1.459455000	1.258492000	-1.290686000	<i>chain</i> ("BuAsHBH <sub>2</sub> ) <sub>2</sub> NMe <sub>3</sub>			
1	2.306734000	1.582672000	-2.821252000	5	0.989495000	0.427837000	-1.268233000
6	2.070108000	0.801127000	2.083343000	33	-0.755323000	0.330804000	-0.104657000
1	1.459455000	1.258492000	1.290686000	5	-1.927695000	-1.249615000	-0.806726000
1	2.998180000	0.382805000	1.673847000	6	-1.596737000	2.160343000	0.151376000
1	2.306734000	1.582672000	2.821252000	1	0.815073000	1.403947000	-1.978888000
5	1.130116000	-1.595593000	-1.773253000	1	0.986926000	-0.615361000	-1.892026000
6	2.057722000	-0.766047000	3.936811000	33	2.648181000	0.752267000	-0.015619000
1	2.215685000	0.070406000	4.634794000	1	-2.285540000	-0.987730000	-1.936527000
1	3.025328000	-1.166607000	3.610762000	7	-3.260906000	-1.766824000	0.007421000
1	1.491547000	-1.563299000	4.433517000	1	-1.133818000	-2.168220000	-0.757020000
6	-1.308325000	-3.796262000	0.000000000	6	3.497972000	-1.105223000	0.153713000
1	-0.729593000	-4.083281000	-0.891794000	1	3.594652000	1.218295000	-1.129530000
1	-2.238861000	-4.391913000	0.000000000	6	-4.430469000	-0.880554000	-0.238090000
1	-0.729593000	-4.083281000	0.891794000	6	-3.009719000	-1.878619000	1.469796000
1	-0.469909000	0.206176000	0.000000000	6	-3.580902000	-3.122372000	-0.530577000
1	0.525776000	-2.437474000	2.407614000	1	-3.700194000	-3.054318000	-1.618767000
1	0.525776000	-2.437474000	-2.407614000	1	-4.510115000	-3.497993000	-0.073612000
1	2.249052000	-1.945329000	-1.456744000	1	-2.751576000	-3.803248000	-0.308027000
1	2.249052000	-1.945329000	1.456744000	1	-3.875262000	-2.341921000	1.968844000
<i>[BH<sub>2</sub>(BuAsHBH<sub>2</sub>NMe<sub>3</sub>)<sub>2</sub>]<sup>+</sup>T<sup>-</sup></i>				1	-2.835631000	-0.880878000	1.888200000
1	-3.215971000	-1.221426000	-1.201955000	1	-2.115399000	-2.493030000	1.632481000
5	-2.074149000	-0.823366000	-1.115955000	1	-4.627149000	-0.840200000	-1.315935000
1	-1.542103000	-0.667478000	-2.198280000	1	-4.205245000	0.129958000	0.117699000
33	-0.999804000	-2.331969000	-0.170732000	1	-5.317042000	-1.266348000	0.289259000
33	-2.097197000	1.053495000	-0.228404000	1	-0.429300000	0.028863000	1.353221000
5	1.090033000	-2.414055000	0.075921000	6	-2.371281000	2.517866000	-1.125275000
1	-1.442392000	-3.535061000	-0.988208000	6	-0.451674000	3.163451000	0.367729000
6	-1.783565000	-2.896627000	1.607817000	6	-2.517669000	2.181764000	1.379420000
5	-0.388749000	2.272782000	-0.506402000	1	-0.870936000	4.173436000	0.527120000
1	-2.479449000	0.919853000	1.239747000	1	0.219809000	3.207260000	-0.500903000
6	-3.770030000	1.976890000	-0.904292000	1	0.160721000	2.909511000	1.247189000
1	1.290536000	-3.463758000	0.653357000	1	-2.931885000	3.196270000	1.521368000
1	1.389191000	-1.434672000	0.717364000	1	-1.975210000	1.917728000	2.301233000
7	1.955673000	-2.433499000	-1.288308000	1	-3.376629000	1.499047000	1.284317000
1	0.433445000	1.543137000	-1.003456000	1	-2.770245000	3.545167000	-1.049325000
7	0.252034000	2.931356000	0.824353000	1	-3.223485000	1.842368000	-1.301874000
1	-0.755272000	3.168993000	-1.240100000	1	-1.722095000	2.477615000	-2.013734000
6	3.388276000	-2.605723000	-0.873550000	6	3.817710000	-1.725417000	-1.210863000
6	1.840559000	-1.147676000	-2.046466000	6	2.519411000	-2.004207000	0.923254000
6	1.571497000	-3.568848000	-2.168073000	6	4.791308000	-0.934354000	0.964756000
6	1.419890000	3.757026000	0.363778000	1	4.550630000	-1.118755000	-1.766581000
6	0.763151000	1.888536000	1.768430000	1	2.917422000	-1.819769000	-1.836219000
6	-0.708032000	3.817411000	1.532454000	1	4.250462000	-2.737431000	-1.085001000
1	2.176325000	3.095343000	-0.084970000	1	1.589694000	-2.170476000	0.355116000
1	1.867575000	4.261293000	1.233046000	1	2.251469000	-1.572038000	1.902631000
1	1.064209000	4.498166000	-0.362513000	1	2.971691000	-2.996038000	1.113258000
1	-1.074393000	4.585168000	0.840036000	1	5.505644000	-0.269010000	0.452411000
1	-0.209072000	4.300430000	2.385923000	1	5.293093000	-1.910455000	1.108691000
1	-1.557054000	3.227363000	1.899882000	1	4.594820000	-0.506989000	1.961485000
1	1.564911000	-1.315111000	1.276669000	<i>chain</i> ("BuAsHBH <sub>2</sub> ) <sub>2</sub>			
1	-0.064710000	1.233478000	2.068955000	5	0.111190000	-0.937233000	0.696329000
1	1.183327000	2.378316000	2.659395000	33	-1.362637000	0.036305000	-0.468327000
1	2.243224000	-0.330527000	-1.428204000	5	-0.936753000	1.950549000	-0.959800000
1	0.788487000	-0.963939000	-2.296037000	6	-3.217250000	-0.013940000	0.328546000
1	2.432858000	-1.218448000	-2.971263000	1	-0.371129000	-2.049724000	0.806272000
1	1.621090000	-4.504683000	-1.596617000	0	0.123271000	-0.282815000	1.720411000
1	2.258644000	-3.623983000	-3.025633000	33	1.888823000	-1.032515000	-0.417894000
1	0.549046000	-3.424459000	-2.539686000	1	-1.196502000	2.825785000	-0.178934000
1	3.482477000	-3.537357000	-0.302192000	1	-0.405960000	2.189795000	-2.008413000
1	3.691732000	-1.739643000	-0.265104000	6	2.987079000	0.529363000	0.321464000
1	4.019865000	-2.648428000	-1.773745000	1	2.524865000	-2.090788000	0.488827000
6	-3.677435000	2.028159000	-2.437142000	1	-1.581806000	-0.648331000	-1.802850000
6	-3.846679000	3.397079000	-0.329142000	6	-3.153616000	0.645109000	1.713454000
6	-4.998243000	1.168340000	-0.463559000	6	-3.618345000	-1.490932000	0.448597000
1	-4.971688000	0.136997000	-0.843678000	6	-4.190032000	0.735872000	-0.592734000
1	-5.913967000	1.646010000	-0.854730000	1	-4.620468000	-1.562651000	0.906343000
1	-5.090520000	1.128888000	0.634074000	1	-2.916883000	-2.056240000	1.080237000
1	-2.788263000	2.583248000	-2.775026000	1	-3.668074000	-1.984667000	-0.535301000
1	-4.565902000	2.542242000	-2.843942000				

1	-5.213787000	0.672303000	-0.182986000	1	6.742662000	-1.601967000	0.445936000
1	-4.214205000	0.305433000	-1.606643000	1	6.085882000	-2.809447000	1.578655000
1	-3.937836000	1.805419000	-0.678302000	1	6.008518000	-1.071000000	1.976091000
1	-4.153567000	0.613270000	2.180189000	5	-0.917588000	0.723220000	-1.223994000
1	-2.850068000	1.702485000	1.656355000	1	-1.400618000	1.801008000	-1.502196000
1	-2.452410000	0.123204000	2.381815000	33	-2.350768000	-0.245292000	-0.071331000
6	3.150058000	0.467840000	1.843771000	1	-0.757877000	0.010650000	-2.194615000
6	2.279436000	1.829728000	-0.084896000	5	-4.182509000	0.649879000	-0.531246000
6	4.365329000	0.462839000	-0.355184000	1	-2.102737000	-0.036869000	1.415885000
1	3.685655000	-0.443415000	2.153942000	6	-2.117801000	-2.255527000	-0.169482000
1	2.179115000	0.477623000	2.361496000	1	-3.952161000	1.804969000	-0.233608000
1	3.734268000	1.335927000	2.205568000	7	-5.559398000	0.238110000	0.258292000
1	1.293577000	1.924714000	0.407017000	1	-4.385273000	0.488820000	-1.715972000
1	2.139889000	1.896704000	-1.176509000	6	-6.546979000	1.321439000	-0.030921000
1	2.868272000	2.712762000	0.224756000	6	-5.355729000	0.156552000	1.730792000
1	4.892225000	-0.472544000	-0.105055000	6	-6.115617000	-1.046869000	-0.247630000
1	5.004042000	1.301776000	-0.020851000	1	-6.179331000	2.265431000	0.386971000
1	4.28524000	0.517063000	-1.452838000	1	-7.521658000	1.066785000	0.413728000
<i>ring</i> (BuAsHBH <sub>2</sub> ) <sub>2</sub>				1	-6.648425000	1.430525000	-1.117455000
1	-0.342604000	-2.389289000	-0.383824000	1	-6.302453000	-0.955592000	-1.324025000
5	-0.000226000	-1.518010000	0.384416000	1	-7.054383000	-1.285626000	0.275786000
33	-1.410944000	-0.000094000	0.768018000	1	-5.390539000	-1.850138000	-0.081960000
33	1.227921000	0.000268000	-0.411426000	1	-4.899299000	1.090845000	2.080914000
5	-0.000639000	1.518165000	0.384791000	1	-4.683192000	-0.677378000	1.962245000
1	-0.343023000	2.389382000	-0.383528000	1	-6.320517000	0.001670000	2.238153000
1	0.466281000	1.896133000	1.440617000	6	-2.625142000	-2.731707000	-1.539014000
1	0.466637000	-1.895876000	1.440319000	6	-2.868664000	-2.955947000	0.971763000
6	3.199094000	-0.000096000	-0.015441000	6	-0.615080000	-2.548179000	-0.035814000
1	1.235161000	0.000341000	-1.930322000	1	-3.959784000	-2.816304000	0.919773000
1	-2.009765000	-0.000170000	2.163919000	1	-2.526702000	-2.611001000	1.960761000
6	-3.066041000	-0.000038000	-0.369140000	1	-2.685759000	-4.044002000	0.924419000
6	3.368015000	-0.000623000	1.510266000	1	-0.024756000	-2.071246000	-0.831150000
6	3.815267000	1.264702000	-0.628965000	1	-0.445470000	-3.637456000	-0.100935000
6	3.814878000	-1.264663000	-0.629824000	1	-0.215519000	-2.212385000	0.934182000
1	3.363277000	2.180621000	-0.217078000	1	-2.104918000	-2.219933000	-2.363038000
1	3.698450000	1.288934000	-1.724373000	1	-3.706960000	-2.567544000	-1.669149000
1	4.897720000	1.297251000	-0.410409000	1	-2.438173000	-3.814219000	-1.649309000
1	2.915100000	-0.892064000	1.971500000	<i>chain</i> (BuAsHBH <sub>2</sub> ) <sub>3</sub>			
1	2.915494000	0.890728000	1.972078000	5	1.852479000	0.473808000	-1.250388000
1	4.442495000	-0.000922000	1.764852000	33	0.104760000	1.041411000	-0.240714000
1	3.362550000	-2.180733000	-0.218647000	6	0.044878000	2.966074000	0.370059000
1	4.897303000	-1.297730000	-0.411202000	1	2.089549000	1.428710000	-1.968787000
1	3.698144000	-1.288057000	-1.725258000	1	1.499677000	-0.510611000	-1.873370000
6	-3.876071000	-1.264534000	-0.049929000	33	3.405211000	0.149902000	0.136658000
6	-2.625022000	-0.000107000	-1.840152000	6	3.728994000	-1.868499000	0.000350000
6	-3.875949000	1.264551000	-0.050007000	1	4.544622000	0.523810000	-0.818612000
1	-4.202959000	1.287894000	1.002122000	1	-0.001430000	0.361099000	1.119552000
1	-4.783423000	1.297446000	-0.679267000	6	0.130117000	3.855459000	-0.879340000
1	-3.297289000	2.180330000	-0.248128000	6	1.249733000	3.219227000	1.288375000
1	-4.203049000	-1.287797000	1.002208000	6	-1.261606000	3.234282000	1.129036000
1	-3.297511000	-2.180378000	-0.248033000	1	1.249767000	4.274725000	1.615302000
1	-4.783561000	-1.297348000	-0.679169000	1	2.205919000	3.023037000	0.781354000
1	-3.514458000	-0.000137000	-2.494502000	1	1.220804000	2.589594000	2.191724000
1	-2.030954000	-0.893581000	-2.089099000	1	-1.284759000	4.283962000	1.473359000
1	-2.030969000	0.893352000	-2.089188000	1	-1.356346000	2.595622000	2.022737000
<i>chain</i> (BuAsHBH <sub>2</sub> ) <sub>3</sub> NMe <sub>3</sub>				1	-2.148198000	3.080947000	0.493577000
5	2.536856000	0.173532000	-1.304558000	1	0.122148000	4.918254000	-0.579223000
33	0.914043000	0.984863000	-0.266633000	1	-0.722113000	3.694497000	-1.558145000
6	1.060914000	2.929974000	0.269347000	1	1.055725000	3.672372000	-1.445637000
1	2.634613000	0.908595000	-2.273947000	6	4.014898000	-2.314727000	-1.437787000
1	2.121740000	-0.932780000	-1.611386000	6	2.479605000	-2.581974000	0.535392000
33	4.348607000	0.196687000	-0.237567000	6	4.934472000	-2.189754000	0.896593000
6	4.550544000	-1.717704000	0.466150000	1	4.928631000	-1.841544000	-1.831422000
1	5.234711000	-0.032445000	-1.468359000	1	3.186487000	-2.060316000	-2.115802000
1	0.785151000	0.392373000	1.133029000	1	4.162794000	-3.411632000	-1.480678000
6	1.257648000	3.754097000	-1.011805000	1	1.600607000	-2.382082000	-0.099015000
6	2.264394000	3.102042000	1.207119000	1	2.239541000	-2.268592000	1.565692000
6	-0.225900000	3.358190000	0.988733000	1	2.634945000	-3.677126000	0.550602000
1	2.364041000	4.165746000	1.491318000	1	5.844646000	-1.672221000	0.551490000
1	3.207907000	2.783059000	0.740191000	1	5.147573000	-3.275754000	0.887187000
1	2.143471000	2.521416000	2.136279000	1	4.757015000	-1.890479000	1.942260000
1	-0.151664000	4.420374000	1.285818000	5	-1.658368000	0.608968000	-1.250886000
1	-0.392484000	2.771702000	1.907707000	1	-2.117884000	1.609033000	-1.766226000
1	-1.112876000	3.252990000	0.345973000	33	-3.169843000	-0.130144000	0.005758000
1	1.338009000	4.826326000	-0.757550000	1	-1.489968000	-0.299457000	-2.035249000
1	0.411576000	3.638768000	-1.707887000	5	-4.845159000	0.557906000	-0.864591000
1	2.177249000	3.464804000	-1.542888000	1	-3.151471000	0.422925000	1.414027000
6	4.466722000	-2.762088000	-0.652323000	6	-3.196791000	-2.119294000	0.298132000
6	3.439817000	-1.961109000	1.497324000	1	-5.249794000	1.641018000	-0.542076000
6	5.921416000	-1.800191000	1.154310000	1	-5.331472000	-0.056942000	-1.773407000
1	5.280783000	-2.635027000	-1.383967000	6	-3.338916000	-2.800285000	-1.069917000
1	3.514026000	-2.696686000	-1.199035000	6	-4.384809000	-2.461525000	1.209366000
1	4.550393000	-3.785633000	-0.236006000	6	-1.870502000	-2.510526000	0.966071000
1	2.442455000	-1.933944000	1.029826000	1	-5.35012000	-2.198453000	0.747859000
1	3.458257000	-1.207847000	2.303095000	1	-4.318930000	-1.954145000	2.185069000
1	3.558712000	-2.954684000	1.969865000	1	-4.396562000	-3.548128000	1.403168000
				1	-1.000522000	-2.272572000	0.335778000

1	-1.861256000	-3.599439000	1.144954000	1	-3.689040000	3.137009000	0.924700000
1	-1.734671000	-2.016468000	1.941356000	1	-4.799130000	3.482878000	2.279378000
1	-2.507799000	-2.545538000	-1.744138000	1	-3.322760000	0.799114000	1.966417000
1	-4.283767000	-2.536081000	-1.569899000	1	-4.711955000	-0.294735000	2.208522000
1	-3.332804000	-3.894735000	-0.930155000	1	-4.509641000	1.135385000	3.249221000
<i>ring</i> (BuAsHBH <sub>2</sub> ) <sub>3</sub>							
1	-2.712491000	1.566057000	-0.315058000	1	-7.340029000	2.139235000	0.954123000
5	-1.774411000	1.024456000	0.230472000	1	-6.851831000	1.987363000	2.660309000
5	0.000000000	-2.048913000	0.230472000	1	-7.092951000	0.527269000	1.663458000
5	1.774411000	1.024456000	0.230472000	5	-0.103009000	-0.278301000	-0.051083000
33	1.674450000	-0.966744000	-0.329438000	1	0.487467000	0.224381000	-0.990667000
33	0.000000000	1.933488000	-0.329438000	33	1.281472000	-1.599647000	0.728687000
33	-1.674450000	-0.966744000	-0.329438000	1	-0.284098000	0.524354000	0.846211000
1	0.000000000	-2.087169000	1.445991000	1	1.626719000	-2.703635000	-0.256433000
1	1.807542000	1.043585000	1.445991000	6	0.697655000	-2.699031000	2.316756000
1	1.801247000	-1.039950000	-1.843294000	6	0.169675000	-1.732832000	3.388019000
1	0.000000000	2.079900000	-1.843294000	6	1.906804000	-3.482201000	2.847024000
1	-1.801247000	-1.039950000	-1.843294000	6	-0.409379000	-3.667695000	1.878181000
1	-1.807542000	1.043585000	1.445991000	1	2.714847000	-2.815474000	3.181975000
1	0.000000000	-3.132115000	-0.315058000	1	2.321467000	-4.161903000	2.084931000
1	2.712491000	1.566057000	-0.315058000	1	1.597343000	-4.100297000	3.708562000
6	3.360597000	-1.940241000	0.199878000	1	-1.291830000	-3.138198000	1.489860000
6	0.000000000	3.880483000	0.199878000	1	-0.737334000	-4.270209000	2.743904000
6	-3.360597000	-1.940241000	0.199878000	1	-0.061628000	-4.367849000	1.102072000
6	0.000000000	3.953216000	1.733873000	1	-0.702880000	-1.162650000	3.033511000
6	-1.261911000	4.540496000	-0.371832000	1	0.941602000	-1.016300000	3.709433000
6	1.261911000	4.540496000	-0.371832000	1	-0.145432000	-2.304987000	4.278259000
1	-0.891621000	3.474012000	2.167055000	5	3.046891000	-0.635270000	1.229739000
1	0.000000000	5.010475000	2.052899000	1	2.817975000	0.061898000	2.198344000
1	0.891621000	3.474012000	2.167055000	33	3.709448000	0.623544000	-0.302042000
1	-2.180466000	4.072193000	0.012432000	1	3.919761000	-1.453661000	1.427753000
1	-1.288720000	4.490201000	-1.472358000	1	3.017904000	0.283652000	-1.610124000
1	-1.282547000	5.607915000	-0.088112000	6	5.597678000	0.100919000	-0.806264000
1	1.282547000	5.607915000	-0.088112000	5	3.747048000	2.714997000	-0.101590000
1	1.288720000	4.490201000	-1.472358000	1	4.144317000	3.160115000	-1.157557000
1	2.180466000	4.072193000	0.012432000	1	4.495659000	2.929426000	0.831368000
6	3.423586000	-1.976608000	1.733873000	7	2.335464000	3.449381000	0.221450000
6	4.563140000	-1.177401000	-0.371832000	6	2.639378000	4.906439000	0.341587000
6	3.301229000	-3.363095000	-0.371832000	6	1.739177000	2.979689000	1.506335000
1	2.562772000	-2.509172000	2.167055000	6	1.346022000	3.257508000	-0.882128000
1	3.454393000	-0.964840000	2.167055000	1	1.799127000	3.582688000	-1.826468000
1	4.339199000	-2.505238000	2.052899000	1	0.439310000	3.845969000	-0.678559000
1	5.497870000	-1.693239000	-0.088112000	1	1.066836000	2.199637000	-0.945792000
1	4.616856000	-0.147757000	0.012432000	1	2.481625000	3.089307000	2.306019000
1	4.532988000	-1.129037000	-1.472358000	1	1.454062000	1.926787000	1.413909000
1	2.436389000	-3.924436000	0.012432000	1	0.842977000	3.573823000	1.739089000
1	4.215323000	-3.914676000	-0.088112000	1	3.081896000	5.260497000	-0.597149000
1	3.244269000	-3.361165000	-1.472358000	1	3.357590000	5.059279000	1.156145000
6	-3.423586000	-1.976608000	1.733873000	1	1.712716000	5.461959000	0.550831000
6	-3.301229000	-3.363095000	-0.371832000	6	6.071782000	0.958740000	-1.987814000
6	-4.563140000	-1.177401000	-0.371832000	6	5.583224000	-1.381918000	-1.205980000
1	-4.339199000	-2.505238000	2.052899000	6	6.501757000	0.317167000	0.416543000
1	-3.454393000	-0.964840000	2.167055000	1	4.949629000	-1.562389000	-2.089321000
1	-2.562772000	-2.509172000	2.167055000	1	5.227518000	-2.026081000	-0.388231000
1	-5.497870000	-1.693239000	-0.088112000	1	6.608280000	-1.702650000	-1.462927000
1	-4.532988000	-1.129037000	-1.472358000	1	5.408437000	0.858594000	-2.862049000
1	-4.616856000	-0.147757000	0.012432000	1	7.078895000	0.628480000	-2.298279000
1	-4.215323000	-3.914676000	-0.088112000	1	6.135042000	2.025102000	-1.728196000
1	-2.436389000	-3.924436000	0.012432000	1	6.538786000	1.375127000	0.718210000
1	-3.244269000	-3.361165000	-1.472358000	1	7.531942000	0.003635000	0.172291000
<i>chain</i> (BuAsHBH <sub>2</sub> ) <sub>4</sub> NMe <sub>3</sub>							
5	-3.072784000	1.006146000	-1.143635000	1	6.169037000	-0.277118000	1.281357000
33	-1.987614000	-0.743343000	-0.752575000	<i>chain</i> (BuAsHBH <sub>2</sub> ) <sub>4</sub>			
6	-1.978250000	-2.000818000	-2.334003000	5	-2.816845000	-1.314119000	-1.109152000
1	-2.994970000	1.138186000	-2.355471000	33	-1.532970000	-0.860352000	0.485126000
1	-2.466605000	1.875775000	-0.540178000	6	-1.415031000	-2.372525000	1.821694000
33	-5.092522000	0.759217000	-0.618186000	1	-2.864227000	-2.533751000	-1.122523000
6	-5.229092000	1.609999000	1.241437000	1	-2.263609000	-0.850382000	-2.088631000
1	-5.598978000	2.006221000	-1.356480000	33	-4.737068000	-0.565456000	-0.693446000
1	-2.684490000	-1.634282000	0.265661000	6	-4.803595000	1.205206000	-1.725396000
6	-1.123219000	-1.361856000	-3.438191000	1	-5.455476000	-1.371773000	-1.783976000
6	-3.428284000	-2.164945000	-2.813841000	1	-2.146893000	0.197964000	1.391152000
6	-1.401794000	-3.366101000	-1.935938000	6	-0.715617000	-3.555960000	1.137446000
1	-3.456249000	-2.835707000	-3.691772000	6	-2.850478000	-2.756776000	2.212302000
1	-3.873600000	-1.203374000	-3.107765000	6	-0.630815000	-1.936822000	3.065936000
1	-4.072401000	-2.605156000	-2.036170000	1	-2.829723000	-3.598487000	2.928155000
1	-1.420761000	-4.047855000	-2.805775000	1	-3.441693000	-3.068427000	1.338888000
1	-1.988465000	-3.841636000	-1.133827000	1	-3.383130000	-1.921085000	2.693472000
1	-0.356147000	-3.295357000	-1.598869000	1	-0.595310000	-2.765960000	3.796106000
1	-1.139275000	-2.000276000	-4.339577000	1	-1.101454000	-1.077193000	3.569275000
1	-0.072340000	-1.247106000	-3.128581000	1	0.409482000	-1.666559000	2.826711000
1	-1.505756000	-0.369747000	-3.723546000	1	-0.683400000	-4.419846000	1.825311000
6	-4.735533000	3.060929000	1.256691000	1	0.322041000	-3.312671000	0.858102000
6	-4.396355000	0.762326000	2.213622000	1	-1.249440000	-3.870364000	0.227704000
6	-6.709404000	1.560315000	1.648943000	6	-4.513596000	1.019763000	-3.218981000
1	-5.344117000	3.699754000	0.596604000	6	-3.768169000	2.154906000	-1.105293000
				6	-6.214163000	1.783468000	-1.535873000
				1	-5.265560000	0.371648000	-3.697123000
				1	-3.524722000	0.567697000	-3.388169000

1	-4.534619000	1.996149000	-3.742392000	1	5.860827000	-2.444521000	1.187354000
1	-2.740135000	1.785672000	-1.254641000	1	5.123859000	-2.207872000	-0.414847000
1	-3.932210000	2.288761000	-0.022340000	1	3.271927000	-1.848744000	2.884828000
1	-3.830074000	3.155515000	-1.573728000	1	3.542980000	-0.095287000	3.059785000
1	-6.985630000	1.113145000	-1.949423000	1	4.902261000	-1.231786000	3.242595000
1	-6.309937000	2.757411000	-2.053171000	1	5.523263000	0.321282000	-0.156758000
1	-6.449168000	1.943197000	-0.471018000	1	6.208860000	0.071873000	1.465504000
5	0.323890000	-0.185922000	-0.128391000	1	4.848184000	1.197353000	1.243148000
1	0.977779000	-1.155790000	-0.469081000	6	1.226212000	4.783450000	0.028646000
33	1.612324000	0.884430000	1.089543000	6	0.360926000	4.310887000	-2.295554000
1	0.125883000	0.570895000	-1.060346000	6	2.661966000	3.533067000	-1.631019000
1	2.124845000	0.072163000	2.266323000	1	-0.678263000	4.486599000	-1.981038000
6	0.885863000	2.506446000	2.049782000	1	0.346730000	3.610103000	-3.146035000
6	0.146750000	3.367413000	1.015032000	1	0.768734000	5.269367000	-2.663343000
6	2.054506000	3.285173000	2.670125000	1	3.308634000	3.150685000	-0.827238000
6	-0.075912000	2.037574000	3.150577000	1	3.105105000	4.476947000	-1.995919000
1	2.756350000	3.657530000	1.909450000	1	2.686775000	2.813067000	-2.465231000
1	2.621978000	2.671923000	3.388753000	1	1.829823000	4.419729000	0.874893000
1	1.660946000	4.158811000	3.219169000	1	0.206109000	4.979185000	0.394039000
1	-0.924514000	1.468981000	2.744276000	1	1.655960000	5.746619000	-0.298866000
1	-0.486356000	2.916924000	3.677546000	6	-5.267615000	-0.234691000	0.911925000
1	0.431234000	1.409858000	3.900530000	6	-4.907372000	2.247285000	0.665249000
1	-0.706213000	2.835012000	0.567344000	6	-3.977255000	1.030770000	2.673319000
1	0.812425000	3.693797000	0.200756000	1	-4.848787000	-1.196585000	1.243339000
1	-0.246280000	4.274919000	1.505591000	1	-5.523918000	-0.320374000	-0.156449000
5	3.296055000	1.537747000	0.064495000	1	-6.209077000	-0.070685000	1.465954000
1	3.007671000	2.566770000	-0.513687000	1	-5.123880000	2.208672000	-0.414705000
33	3.823436000	0.221596000	-1.478916000	1	-4.239808000	3.102486000	0.846513000
1	4.279875000	1.625734000	0.766169000	1	-5.860412000	2.445543000	1.187664000
1	2.634899000	-0.358435000	-2.202799000	1	-3.542816000	0.095750000	3.059640000
6	4.939526000	-1.379838000	-0.998079000	1	-4.901710000	1.232679000	3.242691000
5	4.771371000	1.411529000	-2.804339000	1	-3.271267000	1.849116000	2.884544000
1	4.104927000	1.996851000	-3.612259000				
1	5.953859000	1.592957000	-2.706529000				
6	5.225650000	-2.171722000	-2.282978000				
6	4.139061000	-2.234608000	-0.004233000				
6	6.241522000	-0.877810000	-0.359310000				
1	3.181666000	-2.576257000	-0.426835000				
1	3.926419000	-1.690949000	0.929165000				
1	4.727021000	-3.130290000	0.260498000				
1	4.300176000	-2.513486000	-2.772721000				
1	5.819932000	-3.068905000	-2.037390000				
1	5.805855000	-1.583526000	-3.012313000				
1	6.836283000	-0.264036000	-1.053461000				
1	6.861204000	-1.743815000	-0.070173000				
1	6.052834000	-0.284991000	0.548605000				
<hr/>							
ring(BuAsHBH <sub>2</sub> ) <sub>4</sub>							
6	4.305399000	-0.930665000	1.175992000				
33	2.575243000	-0.578780000	0.194940000				
33	-0.451315000	-2.050756000	-0.474362000				
33	-2.575511000	0.578938000	0.194566000				
5	-1.729150000	-1.168660000	0.912994000				
5	1.727973000	1.168233000	0.913600000				
5	1.513289000	-2.354698000	0.102583000				
1	-0.475546000	-1.278773000	-1.786860000				
1	-3.121964000	0.306462000	-1.198483000				
1	-1.064632000	-0.883410000	1.884503000				
1	1.062491000	0.882055000	1.884185000				
1	1.456032000	-2.794995000	1.233978000				
1	3.121355000	-0.306246000	-1.198232000				
6	-1.229403000	-3.791079000	-1.142472000				
6	-4.305394000	0.931274000	1.175973000				
1	-2.617483000	-1.963886000	1.144386000				
1	2.615680000	1.963726000	1.146503000				
1	2.066919000	-3.084964000	-0.692381000				
5	-1.513524000	2.354879000	0.101682000				
1	-2.067005000	3.084622000	-0.693860000				
33	0.451194000	2.050559000	-0.474527000				
1	-1.456610000	2.795830000	1.232837000				
6	1.229957000	3.790542000	-1.142677000				
1	0.475683000	1.278248000	-1.786825000				
6	-0.359568000	-4.311673000	-2.294629000				
6	-2.661124000	-3.533954000	-1.631848000				
6	-1.226288000	-4.783625000	0.029157000				
1	-3.103894000	-4.478028000	-1.996694000				
1	-2.685463000	-2.814265000	-2.466343000				
1	-3.308374000	-3.151366000	-0.828639000				
1	-0.767120000	-5.270235000	-2.662487000				
1	0.679402000	-4.487303000	-1.979351000				
1	-0.344779000	-3.611080000	-3.145259000				
1	-1.655585000	-5.746992000	-0.298364000				
1	-1.830589000	-4.419773000	0.874854000				
1	-0.206407000	-4.979029000	0.395351000				
6	4.907612000	-2.246523000	0.665159000				
6	3.977620000	-1.030195000	2.673413000				
6	5.267224000	0.235568000	0.911678000				
1	4.240315000	-3.101897000	0.846594000				

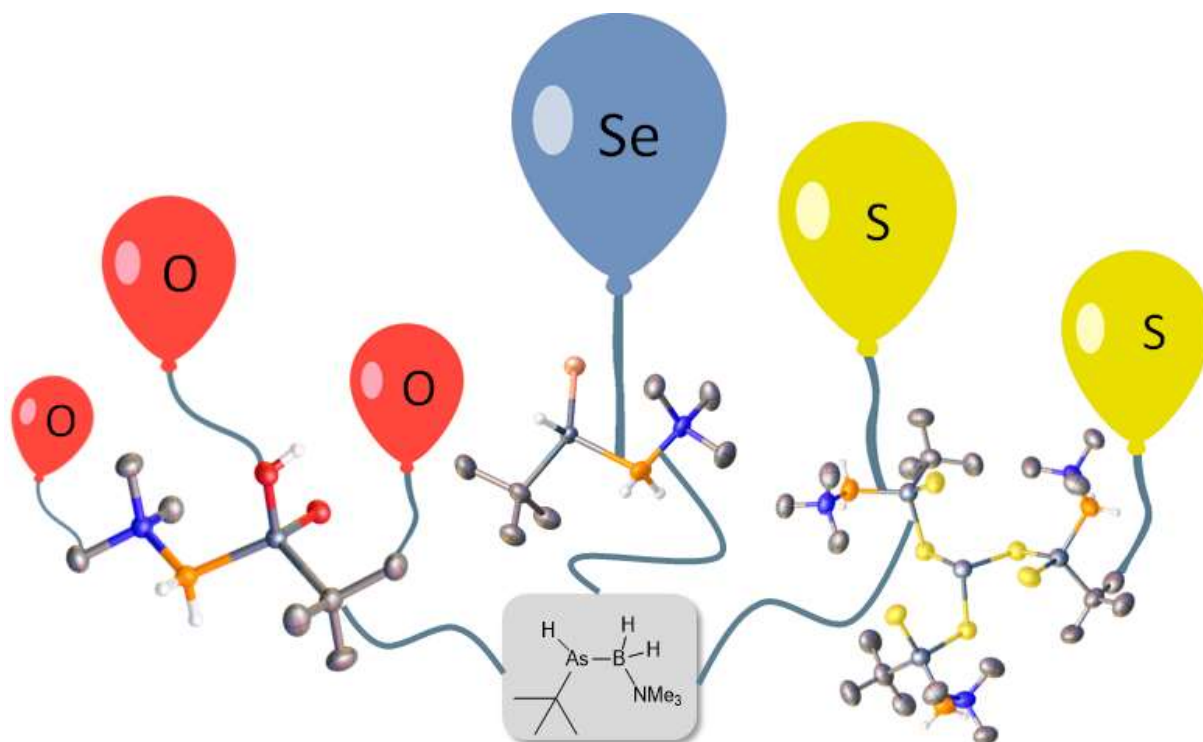
### 3.7. Author contributions

- Compound **1** has been first isolated by Dr. Tobias Kahoun
- The synthesis and characterization of compounds **1-6** have been performed by Felix Lehnfeld
- X-ray structural analysis of compounds **1-6** have been performed by Felix Lehnfeld and Dr. Michael Seidl.
- The thermal oligomerization of **1** has been performed and characterized by Felix Lehnfeld
- The DFT calculations have been performed by Prof. Dr. Alexey Timoshkin
- The manuscript (including supporting information, figures, schemes and graphical abstract) was written by Felix Lehnfeld with Prof. Dr. Alexey Timoshkin contributing the segments concerning the theoretical data and Dr. Michael Seidl contributing to the X-ray part in the supporting information.



## 4. On the brink of decomposition: Controlled oxidation of a substituted arsanylborane as a way to labile group 13-15-16 compounds

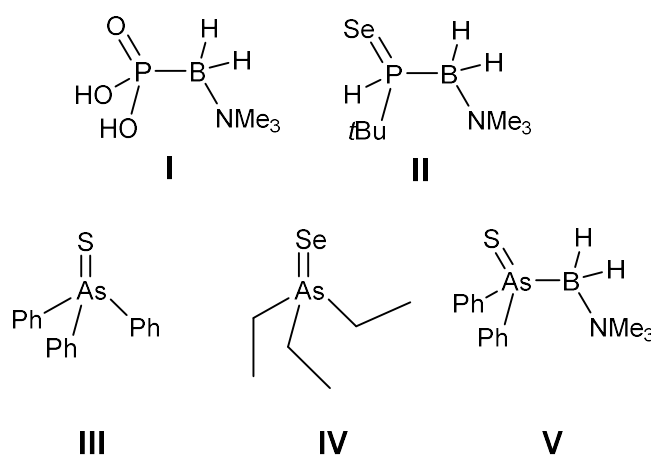
Felix Lehnfeld, Michael Seidl, Alexey Y. Timoshkin and Manfred Scheer



**Abstract:** The reactivity of the substituted arsanylborane  $t\text{BuAsHBH}_2\cdot\text{NMe}_3$  (**1**) towards different elemental chalcogens as well as organic oxidants such as  $\text{O}\cdot\text{NMe}_3$ ,  $\text{Me}_3\text{Si-O-O-SiMe}_3$ ,  $\text{Me}_3\text{CNO}$  and cyclohexene sulfide is reported. By reaction of **1** with grey selenium the selenium oxidation product  $t\text{BuAs}(\text{Se})\text{HBH}_2\cdot\text{NMe}_3$  (**2**) was isolated and fully characterized. For the oxidation with sulfur two oxidation products  $t\text{BuAs}(\text{S})\text{HBH}_2\cdot\text{NMe}_3$  (**3a**) and  $t\text{BuAs}(\text{S})\text{SHBH}_2\cdot\text{NMe}_3$  (**3b**) could be isolated as oils and fully characterized. The structural investigation of  $\text{As}(t\text{BuAs}(\text{S})\text{SHBH}_2\cdot\text{NMe}_3)_3$  (**3c**) as well as DFT calculations allow preliminary insights in the decomposition behavior of **3a** and **3b** in solution. For the reaction of  $\text{Me}_3\text{CNO}$  the formation of an unusual As-H activation product  $\text{Me}_3\text{-C}(\text{NOH})\text{-As}t\text{Bu-BH}_2\text{NMe}_3$  (**4a**) is reported. In the case of  $\text{Me}_3\text{N}\cdot\text{O}$ , the first isolatable oxo-arsanylboranes  $t\text{BuAs}(\text{O})\text{HBH}_2\cdot\text{NMe}_3$  (**4c**) and  $t\text{BuAs}(\text{O})\text{OHBH}_2\cdot\text{NMe}_3$  (**4c**) are reported, with **4c** also being accessible via the controlled reaction of **1** with air. Both compounds were fully characterized.

## 4.1. Introduction

In recent years, the investigation of mixed main group element compounds has been of great interest due to their increasing number of applications. Binary group 13-15 compounds are for example used as materials for micro- and nanoelectronics, in light emitting diodes, photodetectors and in semiconductors.<sup>[1]</sup> Therefore, suitable precursors, for example for chemical vapor deposition, have been heavily researched in the last decades.<sup>[2]</sup> Saturated adducts like ammonia borane are a well investigated class of monomeric compounds,<sup>[3]</sup> as potential hydrogen storage materials<sup>[4]</sup> and as starting materials in dehydrocoupling reactions.<sup>[5]</sup> Similar reactivity has been reported also for the heavier homologues, the phosphine-borane adducts.<sup>[3a, 3c, 6]</sup>



**Scheme 1.** Selected examples of chalcogenated pnictogenylboranes (**I**, **II**, **V**) and organic arsenic chalcogenides (**III**, **IV**).

With respect to a potential application in semiconductors, the reactivity of group 13/15 compounds towards chalcogens is of interest, considering the importance of selenium and tellurium in semiconductor applications.<sup>[7]</sup> When only looking at group 15, there are many examples of phosphorus-chalcogen containing compounds as important reagents in organic synthesis, usually achieved via oxidation with elemental chalcogens or organic oxidants.<sup>[8]</sup> Important examples include e.g. Lawesson's reagent<sup>[9]</sup> and Woolins' reagent.<sup>[10]</sup> Moreover, organophosphorus-chalcogen compounds are used in a broad variety of applications, such as pesticides, as precursors for metal-chalcogenide thin films or nanoparticles and as lubricant additives.<sup>[11]</sup>

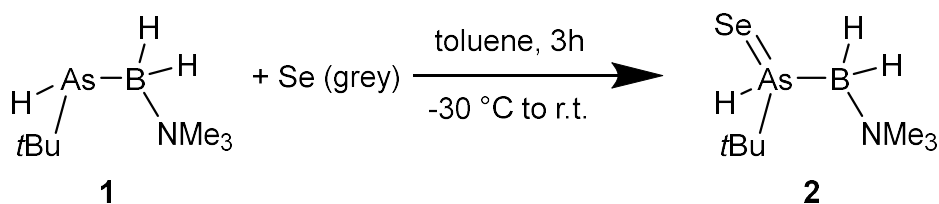
On the oxidation chemistry of phosphino-borane adducts or phosphanylboranes only limited studies have been performed so far. Known examples include boranylphosphines oxides and sulfides as well as some very rare selenide and tellurides derivatives (Scheme 1, I-II).<sup>[12]</sup>

To deepen the understanding on this topic, our group has great interest in the oxidation of pnictogenylboranes of the type  $RR'EBH_2NMe_3$  ( $E = P, As$ ;  $R = H, tBu, Ph$ ;  $R' = H, tBu, Ph$ ). We were able to report about the oxidation of the parent phosphanylborane as well as substituted derivatives in recent years.<sup>[13]</sup> However, when regarding the heavier homologue, only little is known about arsenic chalcogen compounds: In addition to rather well investigated arsine-oxides<sup>[14]</sup> a limited number of known arsine sulfides and selenides (Scheme 1, III-IV).<sup>[15]</sup> Furthermore, we were able to report the oxidation of  $Ph_2AsBH_2NMe_3$  with chalcogens recently (Scheme 1, V).<sup>[16]</sup> However, regardless of many attempts, isolating an arsanylborane oxide was still an open topic. Having recently published the relatively stable although reactive substituted arsanylborane  $tBuAsHBH_2NMe_3$  (**1**),<sup>[17]</sup> we used this compound as a starting material for controlled chalcogenation by applying the knowledge of the oxidation of the corresponding P compound. Herein, the results of the controlled oxidation of **1** using various chalcogens and organic oxidants are presented. Moreover, the formation of the first ever isolatable oxo-arsanylborane is reported.

## 4.2. Results and Discussion

### Reactivity towards selenium

As previous reactions with similar compounds have revealed the reactivity of the oxidizing agent being the key for controlling the reaction, as unwanted side products and decomposition need to be reduced to a minimum. Firstly, the reactivity of the weaker oxidants selenium and tellurium towards **1** was investigated. Tellurium did not show any reactivity towards **1**, which could additionally be supported by DFT calculations revealing the corresponding reaction to be endergonic by 6.6 kJ/mol. Grey selenium however did reveal a rather controlled reactivity. After stirring a stoichiometric mixture of grey selenium and **1** for 3 h in toluene at  $-30\text{ }^\circ\text{C}$  while slowly increasing to r.t., the complete dissolution of the selenium and a color change from colorless to yellow could be observed (Scheme 2).



**Scheme 2.** Reaction of **1** with one equivalent of grey selenium

The obtained product  $t\text{BuAs(Se)HBH}_2\cdot\text{NMe}_3$  (**2**) was characterized by multinuclear NMR spectroscopy. The  $^{11}\text{B}\{^1\text{H}\}$  NMR spectrum of **2** reveals a broad singlet at  $\delta = -3.9$  ppm, which shows further splitting with a  $^1J_{\text{B,H}}$  of 109 Hz in the  $^{11}\text{B}$  NMR spectrum. Exhibiting rapid decomposition in solution even at low temperatures, small signals of decomposition products are observed. In the  $^1\text{H}$  NMR spectrum of **2**, the signals for the  $t\text{Bu}$  group at  $\delta = 2.67$  ppm and for the As-H at  $\delta = 2.34$  ppm can be assigned, both shifted to lower field compared to **1**. The signal corresponding to the  $\text{NMe}_3$  group at  $\delta = 2.97$  ppm is in a similar range as for  $\text{PH}_2\text{As(Se)BH}_2\cdot\text{NMe}_3$ .

After workup, compound **2** could be isolated as a yellow oil in good yields. By storing a saturated solution of **2** in toluene at  $-30^\circ\text{C}$ , some small crystals of **2** suitable for X-ray diffraction analysis were obtained (Fig. 1).

The solid-state structure of **2** exhibits the structural motif of a B-As-Se chain, as it has been observed for the diphenyl substituted derivative. The differences regarding the substitution pattern on the arsenic atom are small. The As-Se and As-B bonds with 2.259 Å and 2.094 Å, respectively, are both in the expected range and slightly elongated compared to  $\text{Ph}_2\text{As(Se)BH}_2\cdot\text{NMe}_3$ . The bond angles around the arsenic atom reveal a distorted tetrahedral environment with a B-As-Se bond angle of  $119.86^\circ$  and a B-As-C bond angle of  $108.99^\circ$ . Due to the asymmetric substitution on the arsenic atom, two enantiomers are formed during the reaction. As a racemic mixture of **1** is used as starting material also both enantiomers are present in the unit cell as a racemic mixture, which are disordered on the same position in the solid state.

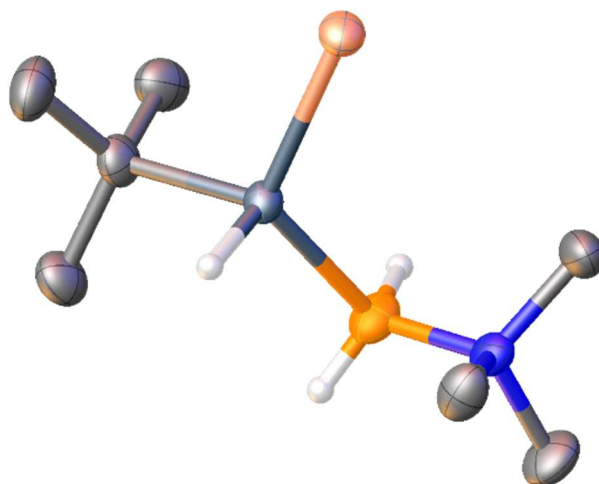


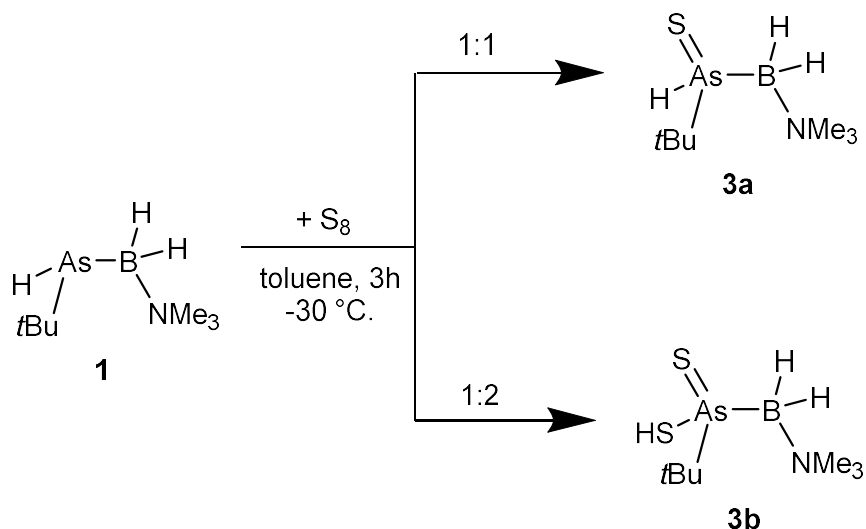
**Figure 1.** Molecular structure of **2**. Only the R enantiomer is depicted for clarity. Thermal ellipsoids displayed at 50% probability. Selected bond distances [Å] and angles [°]: As-Se 2.2592(3), As-B 2.094(3), As-C 1.989(2), N-B 1.586(3); C-As-Se 110.17(7), C-As-B 108.99(11), B-As-Se 119.86(8).

DFT calculations have confirmed the exergonic nature of the reaction with one equivalent selenium, which is favored by 21.3 kJ/mol. The reaction with a second equivalent of selenium is also favored according to the computational data by about 45.6 kJ/mol. However, the experimental findings show that no respective product can be isolated due to rapid decomposition, regardless of the conditions.

### Reactivity towards sulfur

In the case of sulfur, two different reagents have been used. Whereas the reaction with cyclohexene sulfide only leads to inseparable mixtures of products accompanied by immediate decomposition (for further information: SI, section 3), the reaction with elemental sulfur leads to full conversion both for a 1:1 and a 1:2 stoichiometry with negligible amounts of unwanted side reactions (Scheme 3).

The compounds  $t\text{BuAs}(\text{S})\text{HBH}_2\cdot\text{NMe}_3$  (**3a**) and  $t\text{BuAs}(\text{S})\text{SHBH}_2\cdot\text{NMe}_3$  (**3b**) are obtained as yellow oils and are characterized by multinuclear NMR spectroscopy, as no crystals suitable for X-ray diffraction analysis could be obtained. **3a** and **3b** both exhibit a broad singlet in the  $^{11}\text{B}\{^1\text{H}\}$  NMR spectrum at  $\delta = -0.7$  ppm and  $\delta = -5.8$  ppm. Further splitting in the  $^{11}\text{B}$  NMR with a similar  $^1J_{\text{B,H}}$  of about 114 Hz is observed for both compounds. The  $^1\text{H}$  NMR spectra of both compounds reveal the signals for the  $t\text{Bu}$  group at around  $\delta = 1.2$  ppm and for the  $\text{NMe}_3$  at  $\delta = 2.98$  ppm.



**Scheme 3.** Reaction of **1** with elemental sulfur

The broadened and partly overlapped signal corresponding to the BH<sub>2</sub> moiety can be assigned in the region of  $\delta = 2\text{--}3$  ppm. For **3b** a broad singlet for the S-H unit can be assigned at  $\delta = 2.84$  ppm, whereas the spectrum of **3a** exhibits a signal at  $\delta = 2.17$  ppm, which can be assigned to the As-H moiety. ESI-TOF mass spectra of **3a** and **3b** reveal a peak at  $m/z = 236$  and  $m/z = 268$  Da, respectively, which correspond to the release of H<sub>2</sub> from the compounds during the ionization process. After storing a solution of **3a** at  $-30^\circ\text{C}$  for a week, additional signals corresponding to **3b**, **1** and BH<sub>3</sub>NMe<sub>3</sub> can be observed in the NMR and mass spectra. This indicates an intermolecular sulfur transfer between two equivalents of **3a** accompanied by decomposition in solution.

Both the formation of **3a** and **3b** were additionally investigated by DFT calculations. In agreement with experimental findings, the reactions are both exergonic by  $-42.0$  kJ/mol and  $-98.4$  kJ/mol, respectively.

Regardless of numerous attempts to crystallize **3a** or **3b** it was not possible to obtain crystals suitable for X-ray diffraction analysis. However, it was possible to isolate crystals of one of the decomposition products (Fig. 2) from a saturated CH<sub>2</sub>Cl<sub>2</sub> solution of **3a** at  $-30^\circ\text{C}$ .

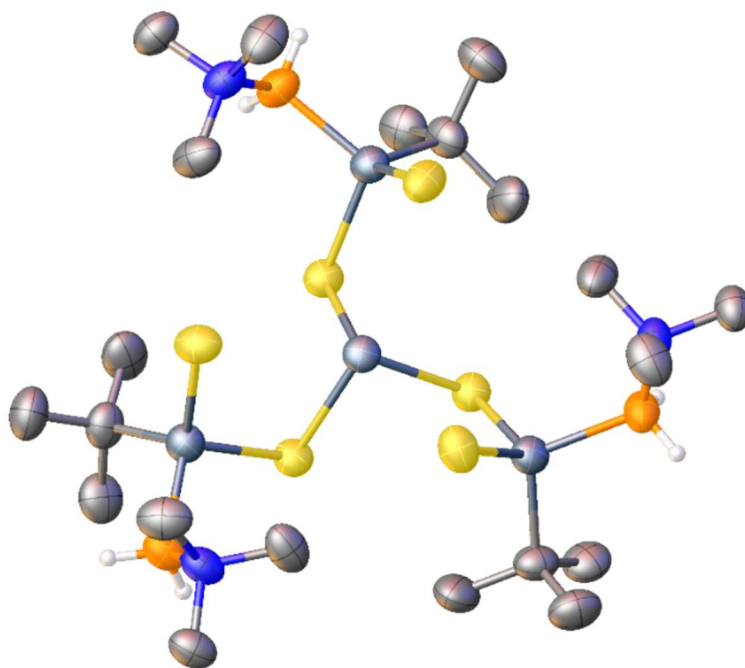
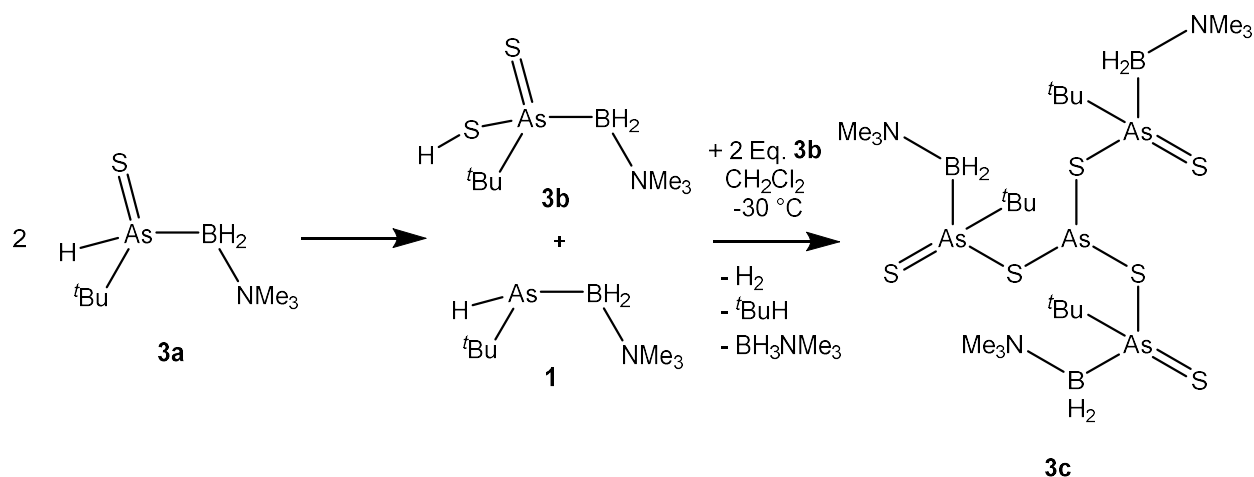


**Figure 2.** Molecular structure of **3c** in the solid state. Solvent molecules in the cell are not depicted for clarity. Thermal ellipsoids displayed at 50% probability. Selected bond distances [Å] and angles [°]: As1-S1 2.2394(13), As1-S2 2.1130(14), As2-S1 2.2822(13), As1-C 1.987(5), As1-B 2.077(6), B-N 1.579(7); S1<sup>1</sup>-As2-S1<sup>2</sup> 92.54(5), S2-As1-S1 108.24(6), C-As1-S1 103.33(18), C-As1-S2 110.5(2), B-As1-S1 105.0(2), B-As1-S2 121.26(18), As1-S1-As2 99.52(5)

Compound **3c** crystallizes in the spacegroup  $P\bar{3}$  as colorless blocks and consists of three deprotonated moieties of **3b**, which are connected via a central threefold coordinate arsenic atom. The As-S bond lengths around the central arsenic atom are in the range of As-S single bonds with 2.282 Å, slightly longer than the ones connected with the arsanylborane moiety with 2.239 Å. They both are notably longer than the terminal As-S bonds present in the molecule with 2.113 Å. This is in agreement with the more double bond character of these bonds and is comparable to the already known  $\text{Ph}_2\text{As}(\text{S})\text{BH}_2\text{NMe}_3$ . The central arsenic atom reveals a trigonal pyramidal arrangement with symmetric S-As-S bond angles of about 92.54°. All other bond angles and bond lengths are in the range of single bonds.



**Scheme 4.** Proposed formation of **3c** from a solution of **3a** as indicated by DFT calculations and analytical data.

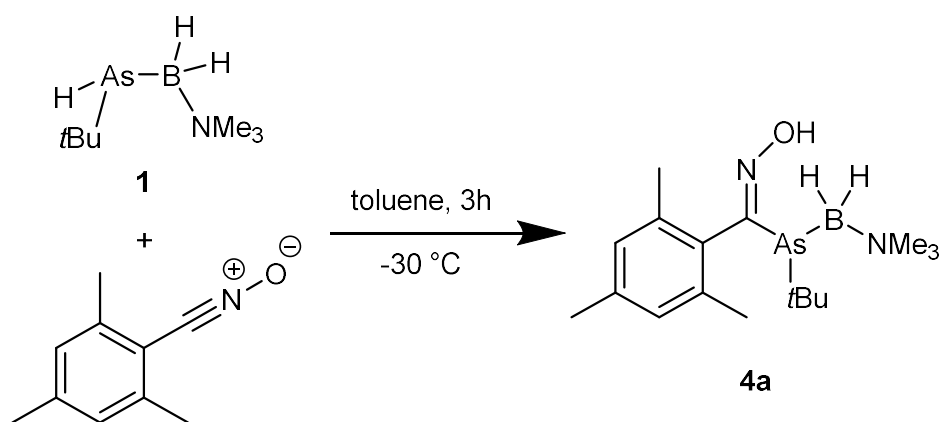
As the formation for **3c** is not obvious, DFT calculations were applied to identify a potential pathway (Scheme 4). The proposed reaction is not only thermodynamically very favored, it also is in good agreement with some experimental observations: **3c** was crystallized from a solution of **3a**, so the already described transformation of **3a** to **3b** under elimination of **1** would yield the necessary starting materials for its synthesis. In addition, NMR data of **3a** solutions after several days indicate a decomposition pathway involving the formation of BH<sub>3</sub>NMe<sub>3</sub>. However, any attempts to synthesize **3c** either from a 3:1 mixture of **3b** and **1** or by reproducing the conditions from the initial synthesis from a solution of **3a** have not been successful up to this point.

### Reactivity towards oxygen sources

The formation of pnictogenylborane-oxo compounds has been successful in the case of the phosphorus derivatives, but for both the parent arsanylborane AsH<sub>2</sub>BH<sub>2</sub>•NMe<sub>3</sub> as well as the substituted Ph<sub>2</sub>AsBH<sub>2</sub>•NMe<sub>3</sub> no oxo species could be isolated so far due to rapid decomposition. In the case of the latter, the resulting species Ph<sub>2</sub>As(O)BH<sub>2</sub>•NMe<sub>3</sub> could only be characterized in solution at low temperature. To obtain an isolatable oxidation product for the *t*Bu derivative, four different oxidizing agents have been applied. While successful for the oxidation of phosphanylboranes, Me<sub>3</sub>Si-O-O-SiMe<sub>3</sub> did not lead to a controllable reaction in the case of **1**, but only to decomposition even at low temperatures.

When reacting one equivalent of MesCNO with **1** in toluene at -30°C, a rapid formation of a white precipitate was observed. The analytical pure powder obtained this way, although very instable in solution, can be recrystallized to get single crystals suitable

for X-ray diffraction analysis. The solid-state structure of the product **4a** (Fig. 3) reveals not to be the oxo-arsanylborane, but the product of a hydroarsination of the nitrile-N-oxide group (Scheme 5).



**Scheme 5.** Reaction of **1** with mesityl nitrile-N-oxide

In the solid-state structure of **4a** the new C-As bond is with 1.9799(15) Å in the range of a single bond. The arrangement around the originally sp-hybridized carbon atom in the N-oxide group changes to a distorted trigonal planar arrangement with a C-C-As bond angle of 124.53(10)° and a N-C-As bond angle of 121.59(11)°. Compared to the starting material, the C-N bond is elongated with 1.281(2) Å, whereas the N-O bond is slightly shortened to 1.4218(16) Å. The bond length of this O-H group is in the expected range for a O-H single bond. This new -OH group allows for the formation of hydrogen bonds and leads to the formation of a dimer in the solid state.

DFT calculations have revealed that the formation of **4a** is slightly endergonic with 20 kJ/mol, but due to the additional stabilization by dimerization the formation is energetically favored in the solid state.

Despite to the very rapid decomposition of **4a** in solution, it was possible to characterize **4a** by multinuclear NMR spectroscopy.

In the  $^{11}\text{B}\{^1\text{H}\}$  NMR spectrum, **4a** reveals a singlet at  $\delta = -2.5$  ppm, which in the  $^{11}\text{B}$  NMR spectrum shows broadening without a clear coupling pattern. In the  $^1\text{H}$  NMR spectrum, in addition to the signals for the NMe<sub>3</sub> group at  $\delta = 2.77$  ppm and the *t*Bu group at  $\delta = 0.90$  ppm especially the absence of an As-H signal, but instead the broad singlet representing the O-H at  $\delta = 7.70$  ppm is noteworthy. The signal corresponding to the BH<sub>2</sub> group cannot be assigned due to being heavily overlapped by signals corresponding to the CH<sub>3</sub> groups at the mesityl group as well as the *t*Bu and the NMe<sub>3</sub> group. The ESI-TOF mass spectrum of **4a** in CH<sub>3</sub>CN shows a peak at  $m/z = 350$  Da.

This fits **4a** with the [M-OH]<sup>+</sup> moiety which forms during the ionization by cleavage of H<sub>2</sub>O.

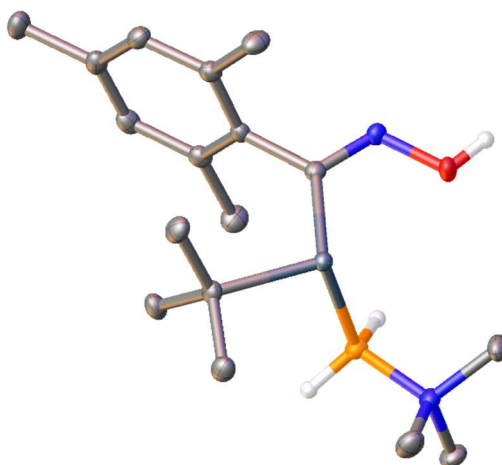
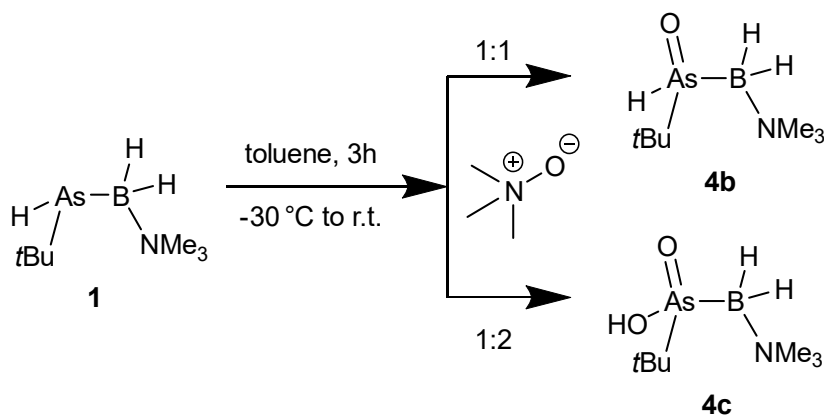


**Figure 3.** Molecular structure of **4a** in the solid state. Thermal ellipsoids displayed at 50% probability. Selected bond distances [Å] and angles [°]: As-C<sub>tBu</sub> 2.0255(15), As-C<sub>CNO</sub> 1.9799(15), As-B 2.1056(17), N-O 1.4218(16), N-C<sub>CNO</sub> 1.281(2), B-N 1.625(2); C<sub>tBu</sub>-As-B 103.25(7), C<sub>CNO</sub>-As-C<sub>tBu</sub> 106.43(6), C<sub>CNO</sub>-As-B 98.98(6), C<sub>CNO</sub>-N-O 113.36(12), N-B-As 110.61(10), C<sub>Mes</sub>-C<sub>CNO</sub>-As 124.53(10), N-C<sub>CNO</sub>-As 121.59(11).

Since **4a** still was not the desired oxo-arsanylborane, so a different oxidizing agent was needed. Therefore, the reaction with one or two equivalents of trimethylamine-N-oxide was performed. For both cases, reactivity of **1** towards the oxidizing agent is significantly lower than towards the previously used oxidizing agents. Nevertheless, full conversion to two different oxidized compounds *t*BuAs(O)HBH<sub>2</sub>•NMe<sub>3</sub> (**4b**) and *t*BuAs(O)OHBH<sub>2</sub>•NMe<sub>3</sub> (**4c**) is observed after 16h at room temperature according to NMR spectroscopy of the reaction solution (Scheme 6).



**Scheme 6.** Reaction of **1** with trimethylamine-N-oxide

In the  $^{11}\text{B}\{^1\text{H}\}$  NMR spectrum of **4b**, a slight low field shift compared to **1** can be observed, revealing a singlet at  $\delta = -0.4$  ppm. For **4c**, the singlet signal is observed at  $\delta = -5.7$  ppm, although a 1:2 mixture of **4b** and **4c** is formed accompanied by an unknown side product. In the  $^{11}\text{B}$  NMR spectrum for both compounds further splitting into broad triplets with very similar  $^1J_{\text{B,H}}$  coupling constants of ca. 115 Hz is observed. Also, the  $^1\text{H}$  NMR spectra of the two compounds are rather similar. Both show singlets for the  $\text{NMe}_3$  and the  $t\text{Bu}$  group at  $\delta = 2.7$  ppm and  $\delta = 1.1$  ppm, respectively. In both cases, signals corresponding to the  $\text{BH}_2$  can be observed in the range of  $\delta = 2\text{--}3$  ppm but they are heavily broadened and superimposed. The most significant difference is the signal corresponding to the As-H group at  $\delta = 1.73$  ppm in the spectrum for **4b**, which is replaced by a low field shifted and very broad signal for the OH-group at  $\delta = 5.50$  ppm in the case of **4c**.

No crystals suitable for X-ray diffraction analysis could be obtained for **4b**, as either complete decomposition or transformation into **4c** and **1** takes place during the crystallization process. In the case of **4c**, it was possible to obtain single crystals suitable for X-ray diffraction analysis by storing a saturated solution in a 9:1 mixture of toluene and methanol at  $-30^\circ\text{C}$  (Fig. 4).

**4c** crystallizes as colorless blocks in the space group  $\text{P}2_1/\text{c}$ . In the solid-state structure, two units of **4c** are stabilized by hydrogen bonds, arranging as a dimer.

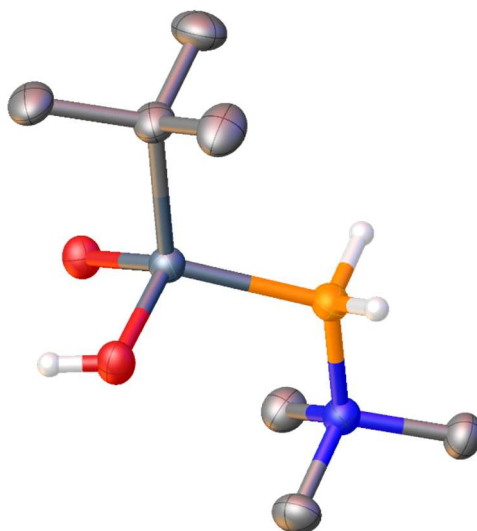


**Figure 4.** Molecular structure of **4c** in the solid state. Thermal ellipsoids displayed at 50% probability. Selected bond distances [ $\text{\AA}$ ] and angles [ $^\circ$ ]: As-O1 1.683(16), As-O2 1.7441(15), As-C 1.971(2), As-B 2.056(3), B-N 1.600(3); O1-As-O2 109.26(7), O1-As-C 107.39(9), O1-As-B 115.03(10), O2-As-C 103.81(9), O2-As-B 108.96(9), C-As-B 111.79(10), N-B-As 112.22(14).

The As-B and As-*t*Bu bond in **4c** are slightly elongated compared to **1**, but still in the range of a single bond. The newformed As-O bonds are in the expected ranges: With 1.683(16) Å, the terminal As-O bond is in the range of a double bond, whereas the bond to the OH group is longer with 1.7441(15) Å and therefore in the expected range for a single bond. The intramolecular O-H interaction is rather short with about 0.794 Å and therefore a bond, whereas the intermolecular interaction is clearly a hydrogen bond with about 1.775 Å. All other bond lengths are in the expected range.

For compound **4c** in solution, some unusual behavior was observed: In the <sup>1</sup>H NMR spectrum of **4c** an additional signal corresponding to about 1 equivalent of NMe<sub>3</sub> is observed, which can't be removed by applying reduced pressure or washing the compound with non-polar solvents. The mass spectrum reveals a strong peak at *m/z* = 313 Da, which correlates to [M+NMe<sub>3</sub>]<sup>+</sup>. Therefore, it is likely, that in solution the NMe<sub>3</sub> forms a strong hydrogen bond to the -OH group of **4c**. The formation of this adduct is additionally supported by elemental analysis of precipitated **4c**, which exhibits increased C and N values. However, this adduct could not be crystallized, and the NMe<sub>3</sub> free compound could only be crystallized in the presence of methanol in small yields, as cleaving the hydrogen bond between the As-OH group and the trimethylamine-N-oxide is necessary for the dimerization and thus crystallization.

Compound **4c** is also accessible by exposing the air sensitive compound **1** to a controlled amount of air. By opening a flask containing a 0.5 M solution of **1** in toluene for 30s without stirring, and then storing it at -30 °C for three days, a large number of colorless crystals of **4c** can be isolated. X-ray diffraction analysis reveals that these temperature sensitive crystals consist of **4c**, which forms additional hydrogen bonds to 0.7 to 1 equivalents of water. The interactions towards the H<sub>2</sub>O are longer than the hydrogen bonds responsible for the dimer formation with a distance of 1.94 Å. Overall, the arrangement of dimeric units bridged by water forming three-dimensional network in the solid state is observed.

DFT calculations on both the water-free **4c** as well as **4c x H<sub>2</sub>O** have shown, that in both cases the hydrogen bonds are essential for the stabilization for the compound in the solid state, stabilizing by about 50 kJ/mol in the case of **4c** and 70 kJ/mol in the case of **4c x H<sub>2</sub>O**. However, the experimental results show that even though the additional hydrogen bonds offered by the presence of water lead to thermodynamical stabilization, the further degradation by the cleavage of the As-B bond is heavily

avored in the presence of water. Therefore, **4c** x **H<sub>2</sub>O** is very instable at room temperature in solution and in the solid state.

### 4.3. Conclusion

In summary, *t*BuAsHBH<sub>2</sub>•NMe<sub>3</sub> can serve as a promising starting material for the synthesis of new compounds containing a group 13-15-16 structural motif. The reaction with grey selenium leads to the selective formation of *t*BuAs(Se)HBH<sub>2</sub>•NMe<sub>3</sub> (**2**), which was isolated and fully characterized. In the case of sulfur, two different compounds *t*BuAs(S)HBH<sub>2</sub>•NMe<sub>3</sub> (**3a**) and *t*BuAs(S)SHBH<sub>2</sub>•NMe<sub>3</sub> (**3b**) were isolated as oils and were exhaustively characterized in solution. Additionally, the larger aggregate **3c**, a decomposition product of **3a** could be isolated and structurally characterized. In addition to the novel example of an As-H activation by MesCNO leading to **4a**, also the first oxo-arsanylboranes **4b** and **4c** could be synthesized, isolated and fully characterized, in the case of **4c**, also the structure in the solid state. This is the first ever example of an isolated oxo-arsanylborane in the solid state, making **1** the so far best arsanylborane to build up arsenic based labile 13-15-16 compounds.

### 4.4. References

- [1] a) J. Linshoef, E. J. Baum, A. Hussain, P. J. Gates, C. Näther, A. Staubitz, *Angew. Chem. Int. Ed.* **2014**, *53*, 12916-12920; b) A. Hübner, Z.-W. Qu, U. Englert, M. Bolte, H.-W. Lerner, M. C. Holthausen, M. Wagner, *J. Am. Chem. Soc.* **2011**, *133*, 4596-4609; c) R. H. Neilson, P. Wisian-Neilson, *Chem. Rev.* **1988**, *88*, 541-562; d) R. De Jaeger, M. Gleria, *Prog. Polym. Sci.* **1998**, *23*, 179-276; e) M. Liang, I. Manners, *J. Am. Chem. Soc.* **1991**, *113*, 4044-4045; f) A. M. Priegert, B. W. Rawe, S. C. Serin, D. P. Gates, *Chem. Soc. Rev.* **2016**, *45*, 922-953; g) I. Manners, *Angew. Chem. Int. Ed.* **1996**, *35*, 1602-1621; h) R. D. Miller, J. Michl, *Chem. Rev.* **1989**, *89*, 1359-1410; i) F. Choffat, S. Käser, P. Wolfer, D. Schmid, R. Mezzenga, P. Smith, W. Caseri, *Macromolecules* **2007**, *40*, 7878-7889; j) F. Jäkle, *Chem. Rev.* **2010**, *110*, 3985-4022; k) B. W. Rawe, C. P. Chun, D. P. Gates, *Chem. Sci* **2014**, *5*, 4928-4938; l) X. He, T. Baumgartner, *RSC Adv.* **2013**, *3*, 11334-11350; m) H. R. Allcock, *Chem. Mater.* **1994**, *6*, 1476-1491; n) G. Zhang, G. M. Palmer, M. W.

- Dewhirst, C. L. Fraser, *Nat. Mater.* **2009**, *8*, 747-751; o) P. J. Fazen, J. S. Beck, A. T. Lynch, E. E. Remsen, L. G. Sneddon, *Chem. Mater.* **1990**, *2*, 96-97; p) R. West, *J. Organomet. Chem.* **1986**, *300*, 327-346; q) F. Vidal, F. Jäkle, *Angew. Chem. Int. Ed.* **2019**, *58*, 5846-5870; r) C. H. Honeyman, I. Manners, C. T. Morrissey, H. R. Allcock, *J. Am. Chem. Soc.* **1995**, *117*, 7035-7036; s) T. Wideman, P. J. Fazen, K. Su, E. E. Remsen, G. A. Zank, L. G. Sneddon, *Appl. Organomet. Chem.* **1998**, *12*, 681-693.
- [2] a) A. C. Jones, P. O'Brien, *CVD of compound semiconductors: Precursor synthesis, developmeny and applications*, John Wiley & Sons, **2008**; b) F. C. Sauls, L. V. Interrante, *Coord. Chem. Rev.* **1993**, *128*, 193-207; c) S. Schulz, in *Adv. Organomet. Chem., Vol. 49*, Academic Press, **2003**, pp. 225-317; d) S. Schulz, *Coord. Chem. Rev.* **2001**, *215*, 1-37; e) R. L. Wells, W. L. Gladfelter, *J. Cluster Sci.* **1997**, *8*, 217-238.
- [3] a) A. Staubitz, A. P. M. Robertson, M. E. Sloan, I. Manners, *Chem. Rev.* **2010**, *110*, 4023-4078; b) K. Takrouri, V. M. Dembitsky, M. Srebnik, in *Studies in Inorganic Chemistry, Vol. 22* (Eds.: H. A. Ali, V. M. Dembitsky, M. Srebnik), Elsevier, **2005**, pp. 495-549; c) B. Carboni, L. Monnier, *Tetrahedron* **1999**, *55*, 1197-1248; d) G. Pawelke, H. Bürger, *Appl. Organomet. Chem.* **1996**, *10*, 147-174; e) J. M. Brunel, B. Faure, M. Maffei, *Coord. Chem. Rev.* **1998**, *178-180*, 665-698.
- [4] a) A. Staubitz, A. P. Robertson, I. Manners, *Chem. Rev.* **2010**, *110*, 4079-4124; b) C. W. Hamilton, R. T. Baker, A. Staubitz, I. Manners, *Chem. Soc. Rev.* **2009**, *38*, 279-293; c) F. H. Stephens, V. Pons, R. Tom Baker, *Dalton Trans.* **2007**, 2613-2626; d) A. Gutowska, L. Li, Y. Shin, C. M. Wang, X. S. Li, J. C. Linehan, R. S. Smith, B. D. Kay, B. Schmid, W. Shaw, M. Gutowski, T. Autrey, *Angew. Chem. Int. Ed.* **2005**, *44*, 3578-3582; e) R. J. Keaton, J. M. Blacquiere, R. T. Baker, *J. Am. Chem. Soc.* **2007**, *129*, 1844-1845; f) M. C. Denney, V. Pons, T. J. Hebden, D. M. Heinekey, K. I. Goldberg, *J. Am. Chem. Soc.* **2006**, *128*, 12048-12049; g) Z. Liu, T. B. Marder, *Angew. Chem. Int. Ed.* **2008**, *47*, 242-244; h) V. Pons, R. T. Baker, *Angew. Chem. Int. Ed.* **2008**, *47*, 9600-9602; i) G. Alcaraz, S. Sabo-Etienne, *Angew. Chem. Int. Ed.* **2010**, *49*, 7170-7179; j) M. E. Sloan, A. Staubitz, T. J. Clark, C. A. Russell, G. C. Lloyd-Jones, I. Manners, *J. Am. Chem. Soc.* **2010**, *132*, 3831-3841.

- [5] a) C. A. Jaska, K. Temple, A. J. Lough, I. Manners, *J. Am. Chem. Soc.* **2003**, *125*, 9424-9434; b) A. Staubitz, A. Presa Soto, I. Manners, *Angew. Chem. Int. Ed.* **2008**, *47*, 6212-6215; c) J. R. Vance, A. P. Robertson, K. Lee, I. Manners, *Chem. Eur. J.* **2011**, *17*, 4099-4103; d) R. Dallanegra, A. P. Robertson, A. B. Chaplin, I. Manners, A. S. Weller, *Chem. Commun.* **2011**, *47*, 3763-3765; e) A. Staubitz, M. E. Sloan, A. P. M. Robertson, A. Friedrich, S. Schneider, P. J. Gates, J. Schmedt auf der Günne, I. Manners, *J. Am. Chem. Soc.* **2010**, *132*, 13332-13345; f) B. L. Dietrich, K. I. Goldberg, D. M. Heinekey, T. Autrey, J. C. Linehan, *Inorg. Chem.* **2008**, *47*, 8583-8585; g) H. C. Johnson, A. P. Robertson, A. B. Chaplin, L. J. Sewell, A. L. Thompson, M. F. Haddow, I. Manners, A. S. Weller, *J. Am. Chem. Soc.* **2011**, *133*, 11076-11079; h) A. L. Colebatch, A. S. Weller, *Chem. Eur. J.* **2019**, *25*, 1379-1390; i) D. Han, F. Anke, M. Trose, T. Beweries, *Coord. Chem. Rev.* **2019**, *380*, 260-286; j) L. J. Morris, N. A. Rajabi, M. S. Hill, I. Manners, C. L. McMullin, M. F. Mahon, *Dalton Trans.* **2020**, *49*, 14584-14591; k) L. Wirtz, J. Lambert, B. Morgenstern, A. Schäfer, *Organometallics* **2021**, *40*, 2108-2117; l) A. N. Marziale, A. Friedrich, I. Klopsch, M. Drees, V. R. Celinski, J. Schmedt auf der Günne, S. Schneider, *J. Am. Chem. Soc.* **2013**, *135*, 13342-13355; m) H. C. Johnson, E. M. Leitao, G. R. Whittell, I. Manners, G. C. Lloyd-Jones, A. S. Weller, *J. Am. Chem. Soc.* **2014**, *136*, 9078-9093; n) H. C. Johnson, A. S. Weller, *Angew. Chem. Int. Ed.* **2015**, *54*, 10173-10177; o) M. E. Bluhm, M. G. Bradley, R. Butterick, U. Kusari, L. G. Sneddon, *J. Am. Chem. Soc.* **2006**, *128*, 7748-7749.
- [6] a) D. W. Himmelberger, C. W. Yoon, M. E. Bluhm, P. J. Carroll, L. G. Sneddon, *J. Am. Chem. Soc.* **2009**, *131*, 14101-14110; b) H. Dorn, R. A. Singh, J. A. Massey, J. M. Nelson, C. A. Jaska, A. J. Lough, I. Manners, *J. Am. Chem. Soc.* **2000**, *122*, 6669-6678; c) H. Dorn, J. M. Rodezno, B. Brunnhöfer, E. Rivard, J. A. Massey, I. Manners, *Macromolecules* **2003**, *36*, 291-297; d) T. J. Clark, J. M. Rodezno, S. B. Clendenning, S. Aouba, P. M. Brodersen, A. J. Lough, H. E. Ruda, I. Manners, *Chem. Eur. J.* **2005**, *11*, 4526-4534; e) S. Pandey, P. Lönnecke, E. Hey-Hawkins, *Eur. J. Inorg. Chem.* **2014**, *2014*, 2456-2465; f) D. Jacquemin, C. Lambert, E. A. Perpète, *Macromolecules* **2004**, *37*, 1009-1015; g) A. Schäfer, T. Jurca, J. Turner, J. R. Vance, K. Lee, V. A. Du, M. F. Haddow, G. R. Whittell, I. Manners, *Angew. Chem. Int. Ed.* **2015**, *54*, 4836-4841; h) J.-M. Denis, H. Forintos, H. Szelke, L. Toupet, T.-N. Pham, P.-J. Madec, A.-C. Gaumont, *Chem. Commun.* **2003**, 54-55; i) H. Dorn, R. A. Singh, J. A. Massey, A. J. Lough, I. Manners, *Angew. Chem. Int.*

- Ed.* **1999**, *38*, 3321-3323; j) M. A. Huertos, A. S. Weller, *Chem. Commun.* **2012**, *48*, 7185-7187; k) M. A. Huertos, A. S. Weller, *Chem. Sci* **2013**, *4*, 1881-1888; l) N. Hooper, M. A. Huertos, T. Jurca, S. D. Pike, A. S. Weller, I. Manners, *Inorg. Chem.* **2014**, *53*, 3716-3729; m) L. Barton, O. Volkov, M. Hata, P. McQuade, N. P. Rath, *Pure Appl. Chem.* **2003**, *75*, 1165-1173; n) H. Schmidbaur, *J. Organomet. Chem.* **1980**, *200*, 287-306.
- [7] a) R. Woods-Robinson, Y. Han, H. Zhang, T. Ablekim, I. Khan, K. A. Persson, A. Zakutayev, *Chem. Rev.* **2020**, *120*, 4007-4055; b) L. Zhang, S. M. Fakhouri, F. Liu, J. C. Timmons, N. A. Ran, A. L. Briseno, *J. Mater. Chem.* **2011**, *21*, 1329-1337; c) M. Jeffries-El, B. M. Kobilka, B. J. Hale, *Macromolecules* **2014**, *47*, 7253-7271; d) R. L. Brutchey, *Acc. Chem. Res.* **2015**, *48*, 2918-2926; e) N. Tohge, T. Minami, M. Tanaka, *J. Non-Cryst. Solids* **1980**, *37*, 23-30; f) J. Zhou, G.-Q. Bian, Q.-Y. Zhu, Y. Zhang, C.-Y. Li, J. Dai, *J. Solid State Chem.* **2009**, *182*, 259-264; g) M. Huang, P. Xu, D. Han, J. Tang, S. Chen, *ACS Appl. Mater. Interfaces* **2019**, *11*, 15564-15572.
- [8] a) M. Brynda, *Coord. Chem. Rev.* **2005**, *249*, 2013-2034; b) F. Uhlig, E. Herrmann, D. Schädler, G. Ohms, G. Großmann, S. Besser, R. Herbst-Irmer, *Z. Anorg. Allg. Chem.* **1993**, *619*, 1962-1970.
- [9] a) M. Jesberger, T. P. Davis, L. Barner, *Synthesis* **2003**, *2003*, 1929-1958; b) M. St. John Foreman, J. D. Woollins, *Dalton Trans.* **2000**, 1533-1543; c) M. P. Cava, M. I. Levinson, *Tetrahedron* **1985**, *41*, 5061-5087; d) R. A. Cherkasov, G. A. Kutyrev, A. N. Pudovik, *Tetrahedron* **1985**, *41*, 2567-2624.
- [10] a) J. D. Woollins, *Synlett* **2012**, *2012*, 1154-1169; b) G. Hua, J. D. Woollins, *Selenium and Tellurium Chemistry* **2011**, 1-39; c) L. Ascherl, A. Nordheider, K. S. A. Arachchige, D. B. Cordes, K. Karaghiosoff, M. Bühl, A. M. Z. Slawin, J. D. Woollins, *Chem. Commun.* **2014**, *50*, 6214-6216.
- [11] R. Davies, L. Patel, *Selenium and Tellurium 2nd ed.*, RSC **2013**, *1*, 238-306.
- [12] a) B. Wrackmeyer, E. V. Klimkina, W. Milius, *Eur. J. Inorg. Chem.* **2014**, *2014*, 4865-4876; b) B. Bildstein, F. Sladky, *Phosphorus Sulfur Silicon Relat. Elem.* **1990**, *47*, 341-347; c) F. Dornhaus, M. Bolte, H.-W. Lerner, M. Wagner, *Eur. J. Inorg. Chem.* **2006**, *2006*, 5138-5147.
- [13] a) K.-C. Schwan, A. Y. Timoskin, M. Zabel, M. Scheer, *Chem. Eur. J.* **2006**, *12*, 4900-4908; b) C. Marquardt, O. Hegen, T. Kahoun, M. Scheer, *Chem. Eur. J.* **2017**, *23*, 4397-4404.

- [14]a) R. F. de Ketelaere, F. T. Delbeke, G. P. Van Der Kelen, *J. Organomet. Chem.* **1971**, *28*, 217-223; b) A. Merijanjan, R. A. Zingaro, *Inorg. Chem.* **1966**, *5*, 187-191.
- [15]a) V. Krishnan, A. Datta, S. V. L. Narayana, *J. inorg. nucl. chem.* **1977**, *13*, 517-522; b) S. V. L. Narayana, H. N. Shrivastava, *Acta Cryst. Sect. B* **1981**, *37*, 1186-1189; c) D. H. Brown, A. F. Cameron, R. J. Cross, M. McLaren, *Dalton Trans.* **1981**, 1459-1462; d) G. Sakane, T. Shibahara, H. Hou, Y. Liu, X. Xin, *Transition Met. Chem.* **1996**, *21*, 398-400.
- [16]O. Hegen, A. V. Virovets, A. Y. Timoshkin, M. Scheer, *Chem. Eur. J.* **2018**, *24*, 16521-16525.
- [17]F. Lehnfeld, M. Seidl, A. Y. Timoshkin, M. Scheer, *Eur. J. Inorg. Chem.* **2022**, *2022*, e202100930.

## 4.5. Supporting Information

### Experimental section

#### General remarks

All reactions have been performed under Argon or Nitrogen inert gas atmosphere using standard glove-box and Schlenk techniques. All solvents have been taken from a solvent purification system of the type MB-SPS-800 of the company MBRAUN and have been degassed by standard procedures. All NMR spectra were recorded on a Bruker Avance 400 spectrometer ( $^1\text{H}$ : 400.13 MHz,  $^{13}\text{C}\{^1\text{H}\}$ : 100.623 MHz,  $^{11}\text{B}$ : 128.387 MHz) with  $\delta$  [ppm] referenced to external standards ( $^1\text{H}$  and  $^{13}\text{C}\{^1\text{H}\}$ :  $\text{SiMe}_4$ ,  $^{11}\text{B}$ :  $\text{BF}_3\text{-Et}_2\text{O}$ ). All mass spectra were recorded on a Micromass LCT ESI-TOF.

#### Synthesis of $t\text{BuAs}(\text{Se})\text{HBH}_2\text{NMe}_3$ (**2**)

A solution of  $t\text{BuAsHBH}_2\text{NMe}_3$  (0.31 mmol, 64 mg) in 0.5 mL toluene is added to a suspension of grey selenium (0.31 mmol, 24 mg) in 3 mL toluene at 243 K. After stirring for 2.5 h at 243 K, the grey selenium has completely dissolved and a light yellow solution has formed. After removing the solvent under reduced pressure, compound **2** is washed with cold hexane and extracted with 2 mL  $\text{Et}_2\text{O}$ . After removing the solvent *in vacuo*, compound **2** can be obtained as a light yellow oil. Compound **1** can be isolated as light yellow blocks by storing a saturated solution of **2** in  $\text{CH}_2\text{Cl}_2$  at 243 K.

Yield:  $m = 32$  mg (0.11 mmol, 37%).  $^1\text{H-NMR}$  ( $\text{CD}_2\text{Cl}_2$ , 293 K)  $\delta = 3.2\text{-}2.0$  (2H, br,  $^1J_{\text{H,B}} = 109$  Hz,  $\text{BH}_2$ ), 2.97 (9H, s,  $\text{NMe}_3$ ), 2.67 (9H, s,  $t\text{Bu}$ ), 2.34 (1H, s,  $\text{AsH}$ ).  $^{11}\text{B-NMR}$  ( $\text{CD}_2\text{Cl}_2$ , 293 K)  $\delta = -3.94$  (t,  $^1J_{\text{H,B}} = 109$  Hz,  $\text{BH}_2$ ).  $^{11}\text{B}\{^1\text{H}\}\text{-NMR}$  ( $\text{CD}_2\text{Cl}_2$ , 293 K)  $\delta = -3.94$  (s,  $\text{BH}_2$ ).

#### Synthesis of $t\text{BuAs}(\text{S})\text{HBH}_2\text{NMe}_3$ (**3a**)

A solution of  $t\text{BuAsHBH}_2\text{NMe}_3$  (0.4 mmol, 81 mg) in 0.5 mL toluene is added to a solution of  $\text{S}_8$  (0.4 mmol, 13 mg) in 2 mL toluene is added at 243 K. After stirring at 243 K for 3 h, all volatiles are removed under reduced pressure. Compound **3a** is isolated as yellowish oil by washing the residue with three times 2 mL of *n*-hexane.

Yield:  $m = 34$  mg (0.14 mmol, 36%).  $^1\text{H-NMR}$  ( $\text{CD}_3\text{CN}$ , 293 K)  $\delta = 2.98$  (9H, s,  $\text{NMe}_3$ ) 3.0-2.0 (br, 2H,  $\text{BH}_2$ ), 2.17 (1H, s,  $\text{AsH}$ ), 1.20 (9H, s,  $t\text{Bu}$ ).  $^{11}\text{B-NMR}$  (toluene, 293 K)  $\delta = -0.7$  (t,  $^1J_{\text{H,B}} = 114$  Hz,  $\text{BH}_2$ ).  $^{11}\text{B}\{^1\text{H}\}\text{-NMR}$  (toluene, 293 K)  $\delta = -0.7$  (s,  $\text{BH}_2$ ). ESI-MS ( $\text{CH}_3\text{CN}$ ):  $m/z = 236$  ( $\text{M}^+ - \text{H}_2$ ).

### Synthesis of **tBuAs(S)SHBH<sub>2</sub>NMe<sub>3</sub> (3b)**

A solution of **tBuAsHBH<sub>2</sub>NMe<sub>3</sub>** (0.31 mmol, 63 mg) in 0.5 mL toluene is added to a solution of S<sub>8</sub> (0.6 mmol, 19 mg) in 2 mL toluene is added at 243 K. After stirring at 243 K for 4 h, all volatiles are removed under reduced pressure. Compound **3b** is isolated as yellowish oil by washing the residue with three times 2 ml of *n*-hexane.

Yield: *m* = 67 mg (0.26 mmol, 42%). <sup>1</sup>H-NMR (CD<sub>3</sub>CN, 293 K) δ = 2.98 (9H, s, NMe<sub>3</sub>) 3.0-2.0 (br, 2H, BH<sub>2</sub>), 2.84 (1H, s, SH), 1.20 (9H, s, *t*Bu). <sup>11</sup>B-NMR (toluene, 293 K) δ = -5.8 (t, <sup>1</sup>J<sub>H,B</sub> = 114 Hz, BH<sub>2</sub>). <sup>11</sup>B{<sup>1</sup>H}-NMR (toluene, 293 K) δ = -5.8 (s, BH<sub>2</sub>). ESI-MS (CH<sub>3</sub>CN): *m/z* = 268 (M<sup>+</sup>-H<sub>2</sub>).

### Isolation of **(tBuAs(S)SHBH<sub>2</sub>NMe<sub>3</sub>)<sub>3</sub>As (3c)**

By storing a solution of **3a** (0.2 mmol, 47 mg) in 0.5 mL CH<sub>2</sub>Cl<sub>2</sub> at 243 K for 14 days, compound **3c** was crystallized as colorless blocks.

Yield: few crystals (< 10%).

### Synthesis of **1-(Me<sub>3</sub>NBH<sub>2</sub>tBuAs-C-NOH)-2,4,6-methylbenzene (4a)**

To a solution of 1-nitril-N-oxide-2,4,6-methylbenzene (0.62 mmol, 100 mg) in 2 mL toluene a solution of **tBuAsHBH<sub>2</sub>NMe<sub>3</sub>** (0.62 mmol, 127 mg) in 1 mL toluene is added at r.t.. After stirring for 3 h at 243 K, the solvent is decanted of and the remaining white precipitate is washed with two times 2 mL of *n*-hexane. After drying analytically pure powder is obtained. Compound **4a** can be isolated as colorless blocks by storing a saturated CH<sub>2</sub>Cl<sub>2</sub> solution at 243 K.

Yield: *m* = 184 mg (0.5 mmol, 80%). <sup>1</sup>H-NMR (CD<sub>2</sub>Cl<sub>2</sub>, 293 K) δ = 7.70 (1H, brs, OH), 7.00-6.71 (2H, m, mesityl-H), 2.77 (9H, s, NMe<sub>3</sub>), 2.26-2.22 (6H, m, *o*-CH<sub>3</sub>), 2.12 (3H, s, *p*-CH<sub>3</sub>) 0.90 (9H, s, *t*Bu). <sup>11</sup>B-NMR (CD<sub>2</sub>Cl<sub>2</sub>, 293 K) δ = -2.5 (br, BH<sub>2</sub>). <sup>11</sup>B{<sup>1</sup>H}-NMR (CD<sub>2</sub>Cl<sub>2</sub>, 293 K) δ = -2.5 (s, BH<sub>2</sub>). <sup>13</sup>C{<sup>1</sup>H} NMR (CD<sub>2</sub>Cl<sub>2</sub>, 293 K) δ = 143.29 (s, CN), 142.28 (s, aromatic system C-H) 128.52 (s, aromatic system C-CH<sub>3</sub>) 49.52 (s, NMe<sub>3</sub>), 32.10 (s, *o*-CH<sub>3</sub>), 31.38 (s, *p*-CH<sub>3</sub>) 21.67 (s, (CH<sub>3</sub>)<sub>3</sub>C), 20.78 (s, (CH<sub>3</sub>)<sub>3</sub>C). ESI-MS (CH<sub>3</sub>CN): *m/z* = 350 (M<sup>+</sup>-OH).

### Synthesis of **tBuAs(O)HBH<sub>2</sub>NMe<sub>3</sub> (4b)**

To a solution of Trimethylamine-N-oxide (0.3 mmol, 23 mg) in 2 mL toluene a solution of **tBuAsHBH<sub>2</sub>NMe<sub>3</sub>** (0.3 mmol, 62 mg) in 0.5 mL toluene is added at r.t.. After stirring for 16 h at r.t., all solvents are removed under reduced pressure. The remaining white

solid is washed three times with 2 mL *n*-pentane. Compound **4b** can be isolated as microcrystalline white solid by layering a saturated solution of **4b** with *n*-pentane at 243K.

Yield:  $m = 26$  mg (0.12 mmol, 39%).  $^1\text{H-NMR}$  ( $\text{CD}_2\text{Cl}_2$ , 293 K)  $\delta = 5.92$  (1H, s, AsH), 3.37 (coordinated  $\text{NMe}_3$ ), 3.0-2.0 (2H, br,  $\text{BH}_2$ ), 2.64 (9H, s,  $\text{NMe}_3$ ), 1.05 (9H, s, *t*Bu).  $^{11}\text{B-NMR}$  ( $\text{CD}_2\text{Cl}_2$ , 293 K)  $\delta = -0.40$  (t,  $^1J_{\text{H,B}} = 120$  Hz,  $\text{BH}_2$ ).  $^{11}\text{B}\{^1\text{H}\}$ -NMR ( $\text{CD}_2\text{Cl}_2$ , 293 K)  $\delta = -0.40$  (s,  $\text{BH}_2$ ).

#### Synthesis of ***t*BuAs(O)OHBH<sub>2</sub>NMe<sub>3</sub> (4c)**

To a solution of Trimethylamine-N-oxide (0.6 mmol, 45 mg) in 2 mL toluene a solution of *t*BuAsHBH<sub>2</sub>NMe<sub>3</sub> (0.3 mmol, 62 mg) in 0.5 mL toluene is added at r.t.. After stirring for 16 h at r.t., all solvents are removed under reduced pressure. The remaining white solid is washed two times with 2 mL *n*-pentane. Compound **4c** can be obtained as microcrystalline white solid by layering a saturated solution of **4c** with *n*-pentane at 243K. Compound **4c** can be isolated as colorless blocks by storing a saturated solution in a 1:1 mixture of toluene and methanol at 243K.

Yield:  $m = 32$  mg (0.135 mmol, 45%).  $^1\text{H-NMR}$  ( $\text{CD}_2\text{Cl}_2$ , 293 K)  $\delta = 5.50$  (1H, s, OH), 2.94 (coordinated  $\text{NMe}_3$ ), 2.8-2.0 (2H, br,  $\text{BH}_2$ ), 2.67 (9H, s,  $\text{NMe}_3$ ), 1.21 (9H, s, *t*Bu).  $^{11}\text{B-NMR}$  ( $\text{CD}_2\text{Cl}_2$ , 293 K)  $\delta = -5.72$  (t,  $^1J_{\text{H,B}} = 109$  Hz,  $\text{BH}_2$ ).  $^{11}\text{B}\{^1\text{H}\}$ -NMR ( $\text{CD}_2\text{Cl}_2$ , 293 K)  $\delta = -5.72$  (s,  $\text{BH}_2$ ). ESI-MS ( $\text{CH}_3\text{CN}$ ):  $m/z = 313$  ( $\text{M}^+ + \text{NMe}_3$ ).

#### Synthesis of ***t*BuAs(O)OHBH<sub>2</sub>NMe<sub>3</sub> (4c)** by controlled exposure to air

A solution of *t*BuAsHBH<sub>2</sub>NMe<sub>3</sub> (0.62 mmol, 127 mg) in 1 mL toluene is exposed to air for 10s under stirring. After storing the solution at 243K, compound **4c x H<sub>2</sub>O** is obtained as colorless blocks by decanting the solvent and washing the crystals with *n*-hexane.

Yield:  $m = 75$  mg (0.31 mmol, 50%).

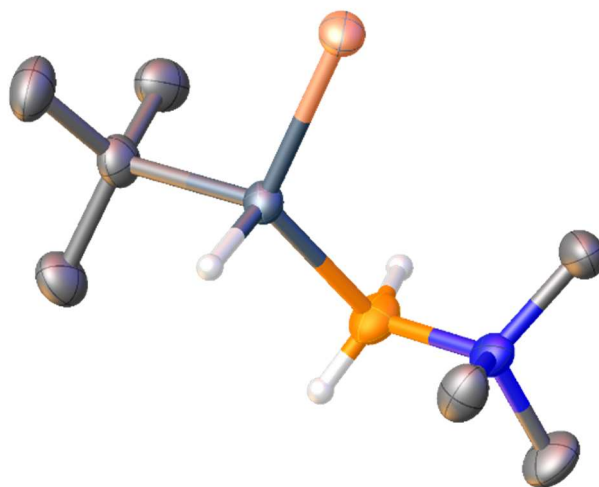
## Crystallographic Details

Table S 4. Crystallographic data for compounds **2**, **3c**, **4a**, **4c** and **4cxH<sub>2</sub>O**

Compound	<b>2</b>	<b>3c</b>	<b>4a</b>	<b>4c</b>	<b>4cxH<sub>2</sub>O</b>
Data set	<b>LeF125</b>	<b>LeF142</b>	<b>LeF157</b>	<b>LeF270</b>	<b>LeF262_2</b>
Formula	C <sub>7</sub> H <sub>21</sub> AsBNSe	C <sub>24</sub> H <sub>66</sub> As <sub>4</sub> B <sub>3</sub> Cl <sub>6</sub> N <sub>3</sub> S <sub>6</sub>	C <sub>17</sub> H <sub>32</sub> AsBN <sub>2</sub> O	C <sub>7</sub> H <sub>21</sub> AsBNO <sub>2</sub>	C <sub>7</sub> H <sub>22.39</sub> AsBNO <sub>2.69</sub>
<i>D</i> <sub>calc.</sub> / g cm <sup>-3</sup>	1.504	1.490	1.278	1.321	1.348
$\mu$ /mm <sup>-1</sup>	6.585	8.489	2.424	3.612	3.568
Formula Weight	283.94	1133.96	366.17	236.98	249.50
Color	clear colorless	clear colorless	clear colorless	clear colorless	Clear colorless
Shape	block-shaped	block	block-shaped	block-shaped	block-shaped
Size/mm <sup>3</sup>	0.18×0.15×0.09	0.33×0.31×0.18	0.18×0.17×0.11	0.09×0.07×0.06	0.18×0.04×0.02
<i>T</i> /K	123(1)	123.01(10)	123.00(10)	123.00(10)	123.01(10)
Crystal System	monoclinic	trigonal	monoclinic	monoclinic	monoclinic
Space Group	<i>P</i> 2 <sub>1</sub> / <i>c</i>	<i>P</i> -3	<i>P</i> 2 <sub>1</sub> / <i>c</i>	<i>P</i> 2 <sub>1</sub> / <i>c</i>	<i>P</i> 2 <sub>1</sub> / <i>c</i>
<i>a</i> /Å	14.3862(2)	15.3037(2)	10.06720(10)	11.2063(2)	11.6001(5)
<i>b</i> /Å	7.64830(10)	15.3037(2)	11.24480(10)	10.1683(2)	9.5023(3)
<i>c</i> /Å	11.4219(2)	12.4591(2)	17.0088(2)	11.4197(2)	11.8938(5)
$\alpha$ <sup>o</sup>	90	90	90	90	90
$\beta$ <sup>o</sup>	93.694(2)	90	98.7600(10)	113.738(2)	110.296(5)
$\gamma$ <sup>o</sup>	90	120	90	90	90
<i>V</i> /Å <sup>3</sup>	1254.14(3)	2527.03(8)	1903.00(3)	1191.17(4)	1229.63(9)
<i>Z</i>	4	2	4	4	4
<i>Z</i> '	1	0.333333	1	1	1
Wavelength/Å	1.54184	1.54184	1.54184	1.54184	1.54184
Radiation type	Cu K $\alpha$	Cu K $\alpha$	Cu K $\alpha$	Cu K $\alpha$	Cu K $\alpha$
$\theta$ <sub>min</sub> <sup>o</sup>	6.165	3.335	4.444	4.310	4.063
$\theta$ <sub>max</sub> <sup>o</sup>	71.863	75.971	73.952	72.938	73.211
Measured Refl's.	8320	38315	11924	11601	7154
Indep't Refl's	2397	3482	3826	2278	2402
Refl's I $\geq$ 2 $\sigma$ (I)	2192	3287	3705	2092	2216
<i>R</i> <sub>int</sub>	0.0286	0.0743	0.0202	0.0271	0.0229
Parameters	131	226	217	127	140
Restraints	9	39	0	0	1
Largest Peak	0.495	1.181	0.377	0.456	0.932
Deepest Hole	-0.326	-0.950	-0.529	-0.731	-0.728
GooF	1.060	1.102	1.071	1.120	1.053
<i>wR</i> <sub>2</sub> (all data)	0.0609	0.1634	0.0689	0.0800	0.1254
<i>wR</i> <sub>2</sub>	0.0594	0.1620	0.0682	0.0787	0.1231
<i>R</i> <sub>I</sub> (all data)	0.0269	0.0634	0.0266	0.0311	0.0447
<i>R</i> <sub>I</sub>	0.0239	0.0612	0.0259	0.0283	0.0424

## Compound 2

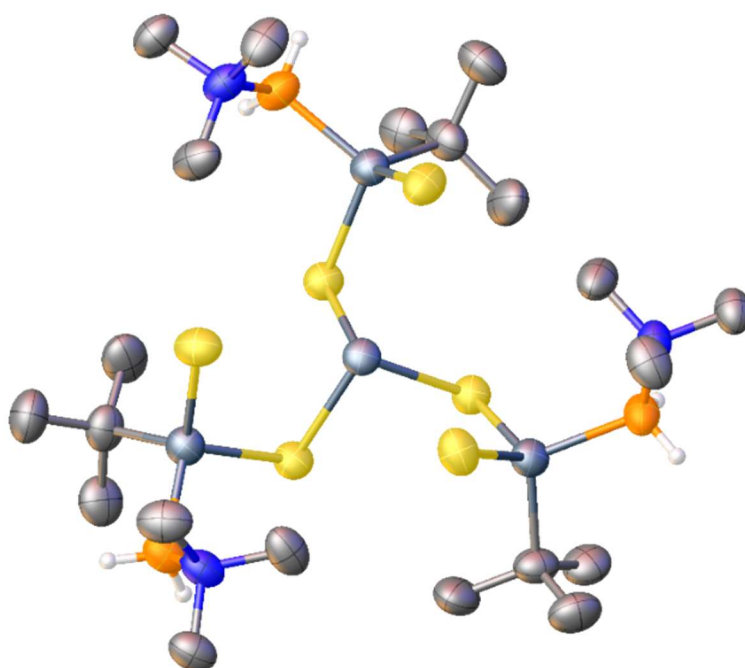
Compound **2** crystallizes from a saturated solution in toluene as colorless blocks. A suitable crystal with dimensions  $0.18 \times 0.15 \times 0.09 \text{ mm}^3$  was selected and mounted on a Xcalibur, AtlasS2, Gemini ultra diffractometer. The crystal was kept at a steady  $T = 123(1) \text{ K}$  during data collection. The structure was solved with the **SheIXT** 2014/5 (Sheldrick, 2014) solution program using dual methods and by using **Olex2** 1.5-alpha (Dolomanov et al., 2009) as the graphical interface. The model was refined with **SheIXL** 2018/3 (Sheldrick, 2015) using full matrix least squares minimization on  $F^2$ .



**Figure S1.** Molecular structure of **2**. Only the R enantiomer is depicted for clarity. Thermal ellipsoids displayed at 50% probability. Selected bond distances [ $\text{\AA}$ ] and angles [ $^\circ$ ]: As-Se 2.2592(3), As-B 2.094(3), As-C 1.989(2), N-B 1.586(3); C-As-Se 110.17(7), C-As-B 108.99(11), B-As-Se 119.86(8).

### Compound 3c

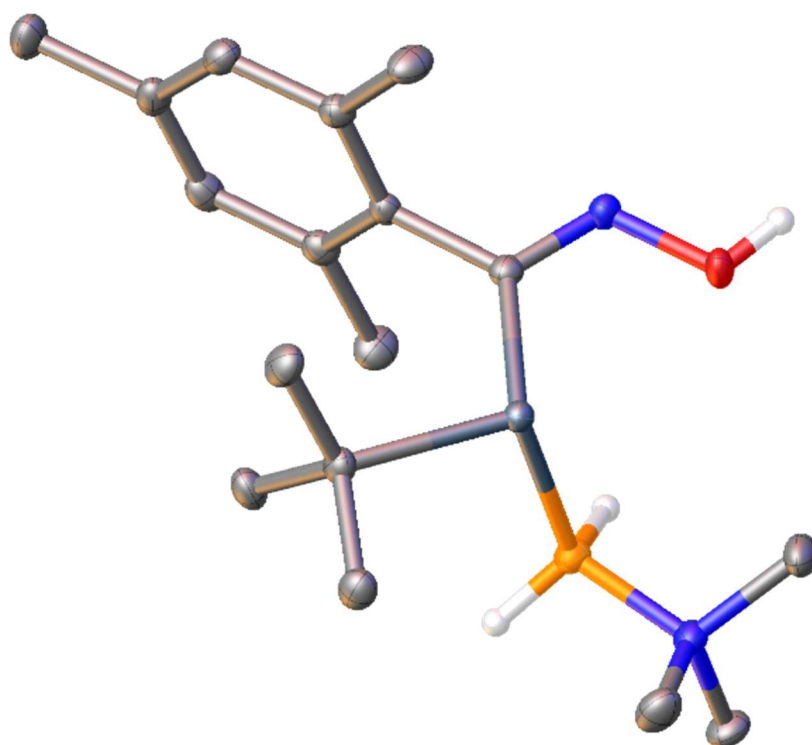
Compound **3c** crystallizes from a saturated solution of **3a** in CH<sub>2</sub>Cl<sub>2</sub> as colorless blocks. A suitable crystal with dimensions 0.33 × 0.31 × 0.18 mm<sup>3</sup> was selected and mounted on a XtaLAB Synergy R, DW system, HyPix-Arc 150 diffractometer. The crystal was kept at a steady  $T = 123.01(10)$  K during data collection. The structure was solved with the **ShelXT** 2018/2 (Sheldrick, 2018) solution program using dual methods and by using **Olex2** 1.3-alpha (Dolomanov et al., 2009) as the graphical interface. The model was refined with **ShelXL** 2018/3 (Sheldrick, 2015) using full matrix least squares minimization on  $F^2$ .



**Figure 2.** Molecular structure of **3c** in the solid state. Solvent molecules in the cell are not depicted for clarity. Thermal ellipsoids displayed at 50% probability. Selected bond distances [Å] and angles [°]: As1-S1 2.2394(13), As1-S2 2.1130(14), As2-S1 2.2822(13), As1-C 1.987(5), As1-B 2.077(6), B-N 1.579(7); S1<sup>1</sup>-As2-S1<sup>2</sup> 92.54(5), S2-As1-S1 108.24(6), C-As1-S1 103.33(18), C-As1-S2 110.5(2), B-As1-S1 105.0(2), B-As1-S2 121.26(18), As1-S1-As2 99.52(5)

**Compound 4a**

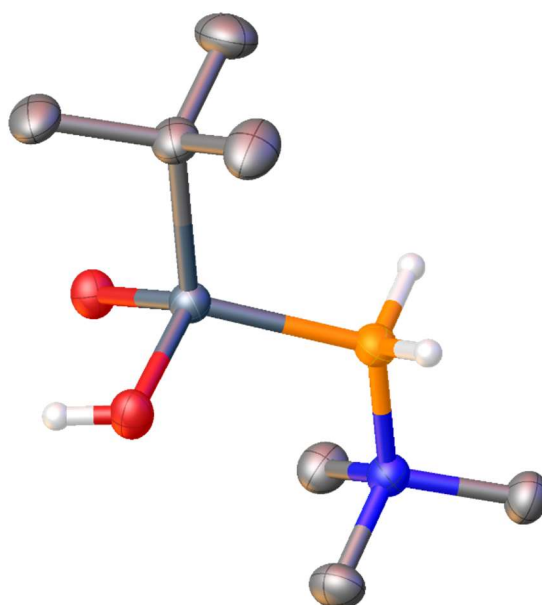
Compound **4a** crystallizes from a saturated solution in CH<sub>2</sub>Cl<sub>2</sub> as colorless blocks. A suitable crystal with dimensions 0.18 × 0.17 × 0.11 mm<sup>3</sup> was selected and mounted on a GV50, TitanS2 diffractometer. The crystal was kept at a steady  $T = 123.00(10)$  K during data collection. The structure was solved with the **ShelXT** (Sheldrick, 2015) solution program using dual methods and by using **Olex2** 1.5-alpha (Dolomanov et al., 2009) as the graphical interface. The model was refined with **ShelXL** 2018/3 (Sheldrick, 2015) using full matrix least squares minimization on  $F^2$ .



**Figure S3.** Molecular structure of **4a** in the solid state. Thermal ellipsoids displayed at 50% probability. Selected bond distances [Å] and angles [°]: As-C<sub>tBu</sub> 2.0255(15), As-C<sub>CNO</sub> 1.9799(15), As-B 2.1056(17), N-O 1.4218(16), N-C<sub>CNO</sub> 1.281(2), B-N 1.625(2); C<sub>tBu</sub>-As-B 103.25(7), C<sub>CNO</sub>-As-C<sub>tBu</sub> 106.43(6), C<sub>CNO</sub>-As-B 98.98(6), C<sub>CNO</sub>-N-O 113.36(12), N-B-As 110.61(10), C<sub>Mes</sub>-C<sub>CNO</sub>-As 124.53(10), N-C<sub>CNO</sub>-As 121.59(11).

### Compound 4c

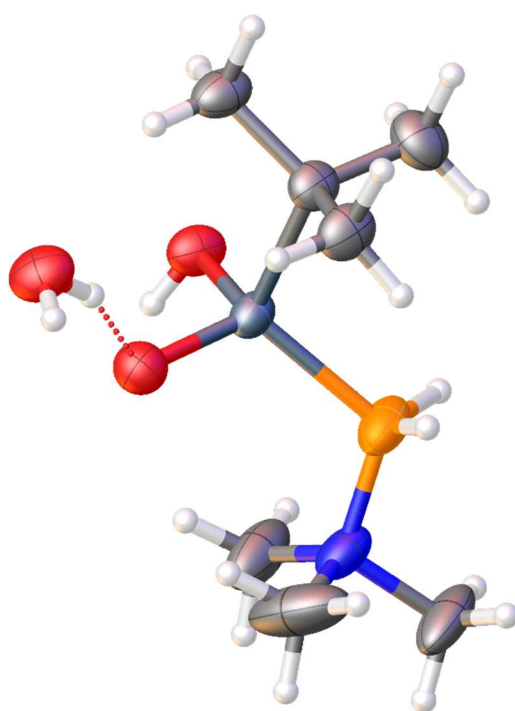
Compound **4c** crystallizes from a saturated solution in CH<sub>2</sub>Cl<sub>2</sub> as colorless blocks. A suitable crystal with dimensions 0.09 × 0.07 × 0.06 mm<sup>3</sup> was selected and mounted on a XtaLAB Synergy R, DW system, HyPix-Arc 150 diffractometer. The crystal was kept at a steady  $T = 123.00(10)$  K during data collection. The structure was solved with the **ShelXT** 2018/2 (Sheldrick, 2018) solution program using iterative methods and by using **Olex2** 1.5-alpha (Dolomanov et al., 2009) as the graphical interface. The model was refined with **ShelXL** 2018/3 (Sheldrick, 2015) using full matrix least squares minimization on  $F^2$



**Figure S4.** Molecular structure of **4c** in the solid state. Thermal ellipsoids displayed at 50% probability. Selected bond distances [Å] and angles [°]: As-O1 1.683(16), As-O2 1.7441(15), As-C 1.971(2), As-B 2.056(3), B-N 1.600(3); O1-As-O2 109.26(7), O1-As-C 107.39(9), O1-As-B 115.03(10), O2-As-C 103.81(9), O2-As-B 108.96(9), C-As-B 111.79(10), N-B-As 112.22(14).

**Compound 4cxH<sub>2</sub>O**

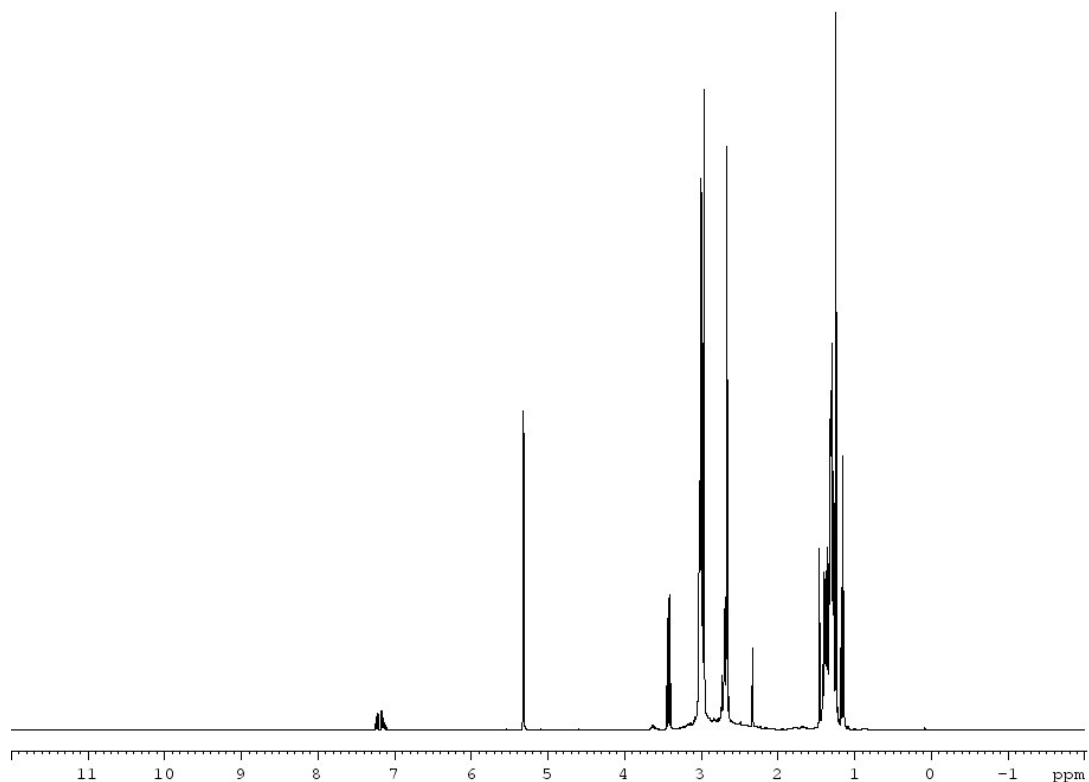
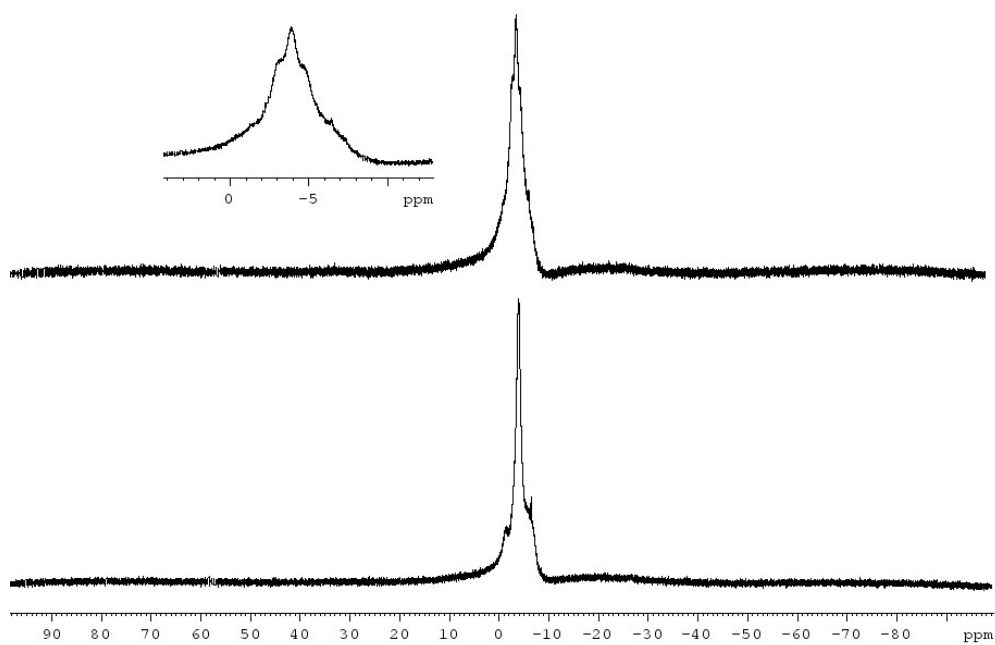
Compound **4cxH<sub>2</sub>O** crystallizes from a saturated solution of **1** in toluene after exposing it to air for 10s as colorless blocks. A suitable crystal with dimensions 0.18 × 0.04 × 0.02 mm<sup>3</sup> was selected and mounted on a XtaLAB Synergy R, DW system, HyPix-Arc 150 diffractometer. The crystal was kept at a steady  $T = 123.01(10)$  K during data collection. The structure was solved with the **ShelXT** 2018/2 (Sheldrick, 2018) solution program using dual methods and by using **Olex2** 1.5 (Dolomanov et al., 2009) as the graphical interface. The model was refined with **ShelXL** 2018/3 (Sheldrick, 2015) using full matrix least squares minimization on  $F^2$ .



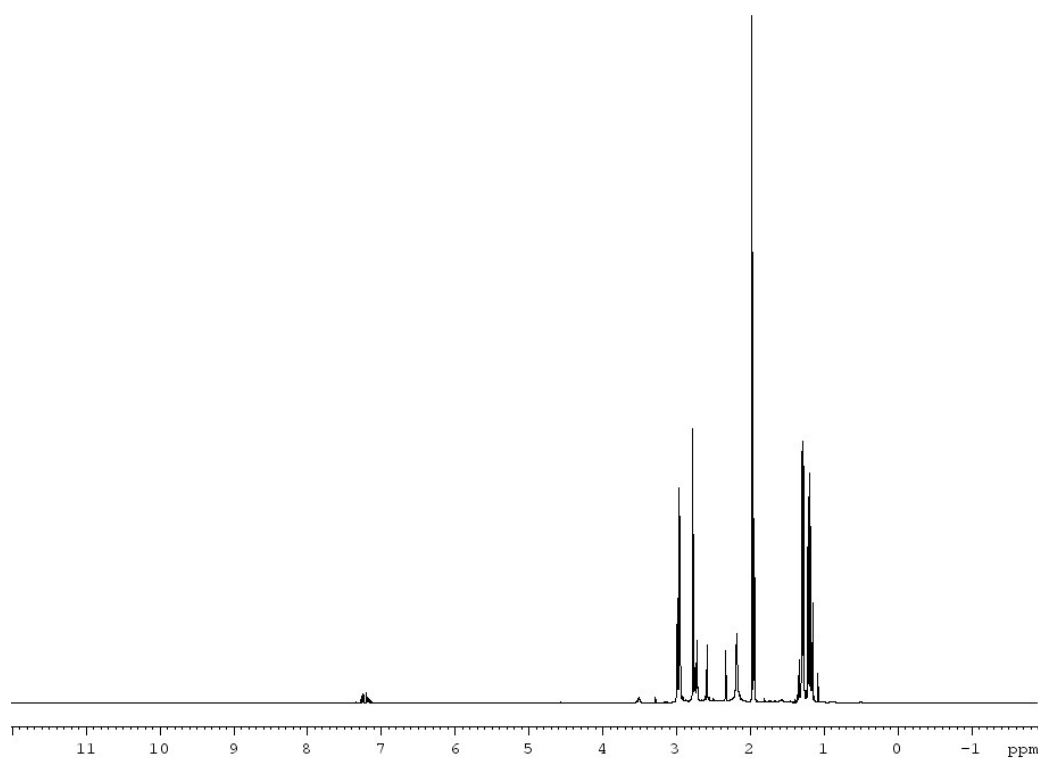
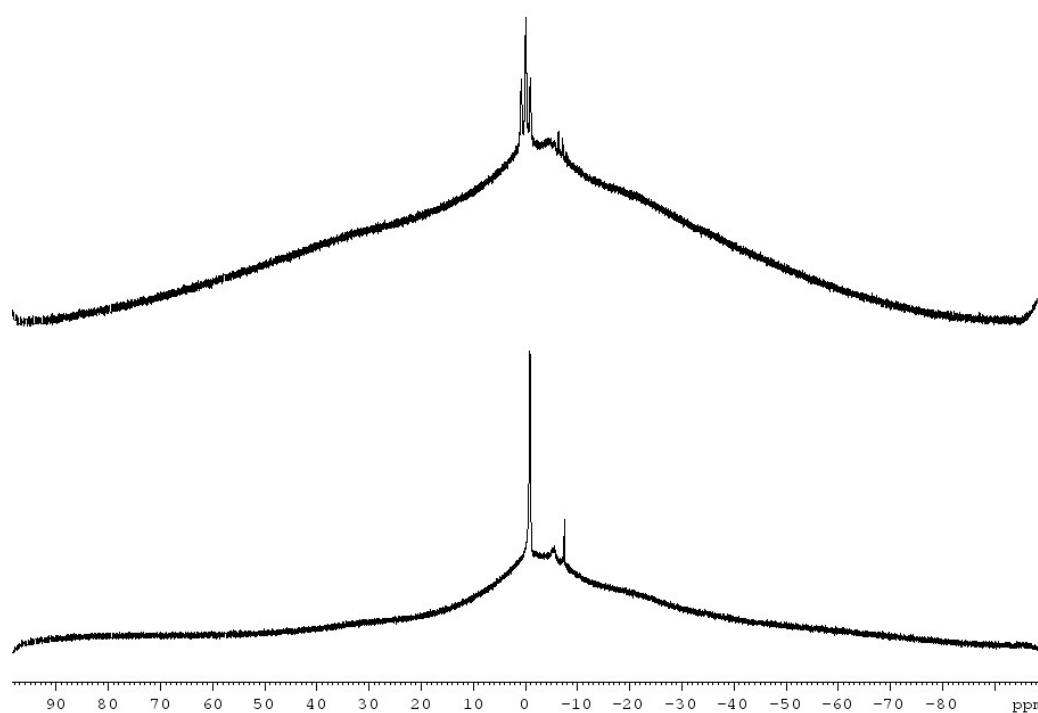
**Figure S5.** Molecular structure of **4cxH<sub>2</sub>O** in the solid state. Thermal ellipsoids displayed at 50% probability. Selected bond distances [Å] and angles [°]: As-O1 1.706(2), As-O2 1.719(2), As-C 1.971(3), As-B 2.066(4), B-N 1.587(5); O1-As-O2 107.84(11), O1-As-C 105.44(11), O1-As-B 117.79(16), O2-As-C 104.14(11), O2-As-B 111.25(16), C-As-B 109.39(14), N-B-As 11.1(2).

## NMR spectra

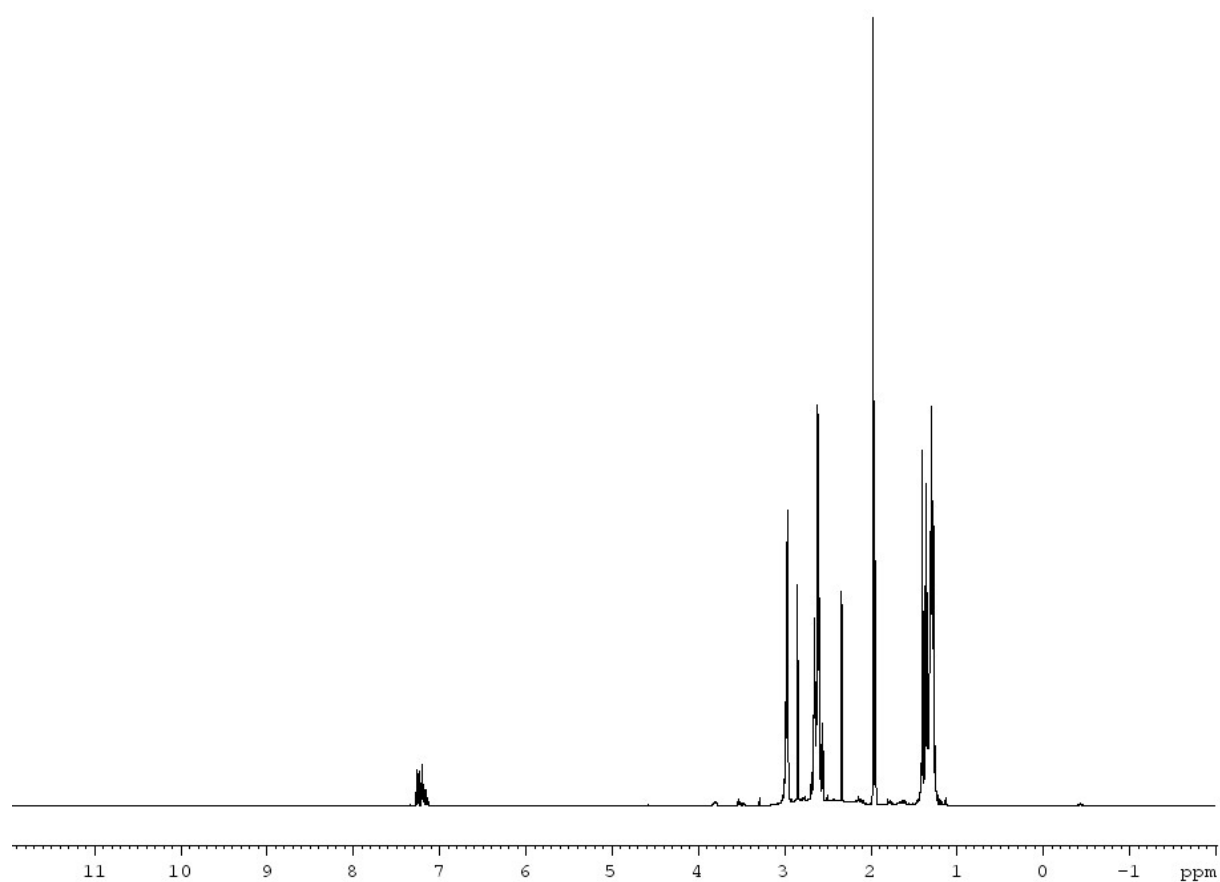
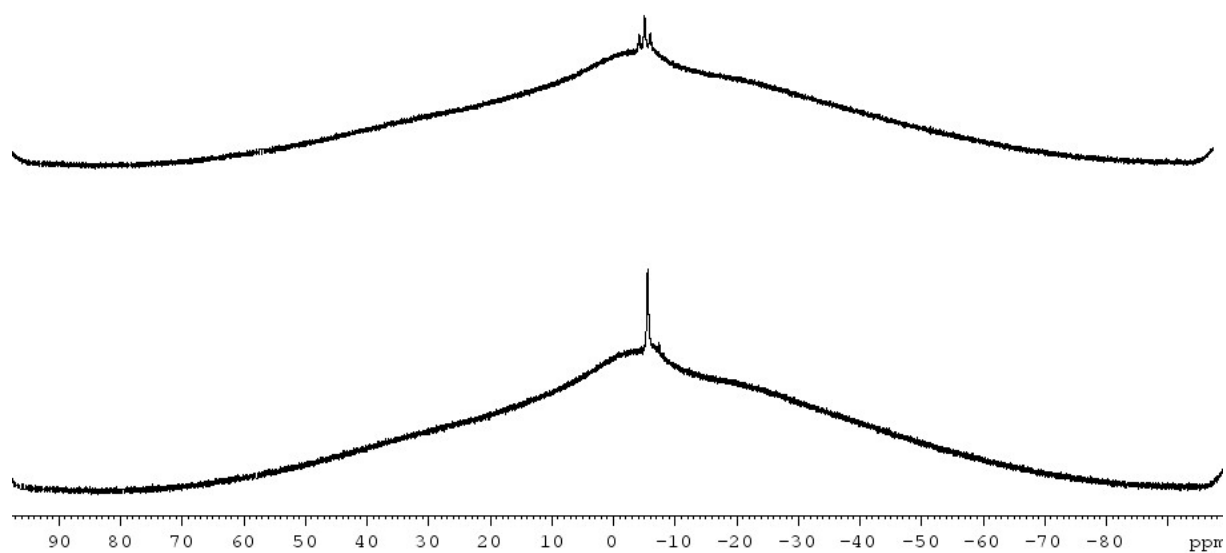
## Compound 2

Figure S6.  $^1\text{H}$  NMR spectrum of 2 in  $\text{CD}_2\text{Cl}_2$ Figure S7.  $^{11}\text{B}$  NMR (top) and  $^{11}\text{B}\{^1\text{H}\}$  NMR (bottom) spectra of 2 in  $\text{CD}_2\text{Cl}_2$

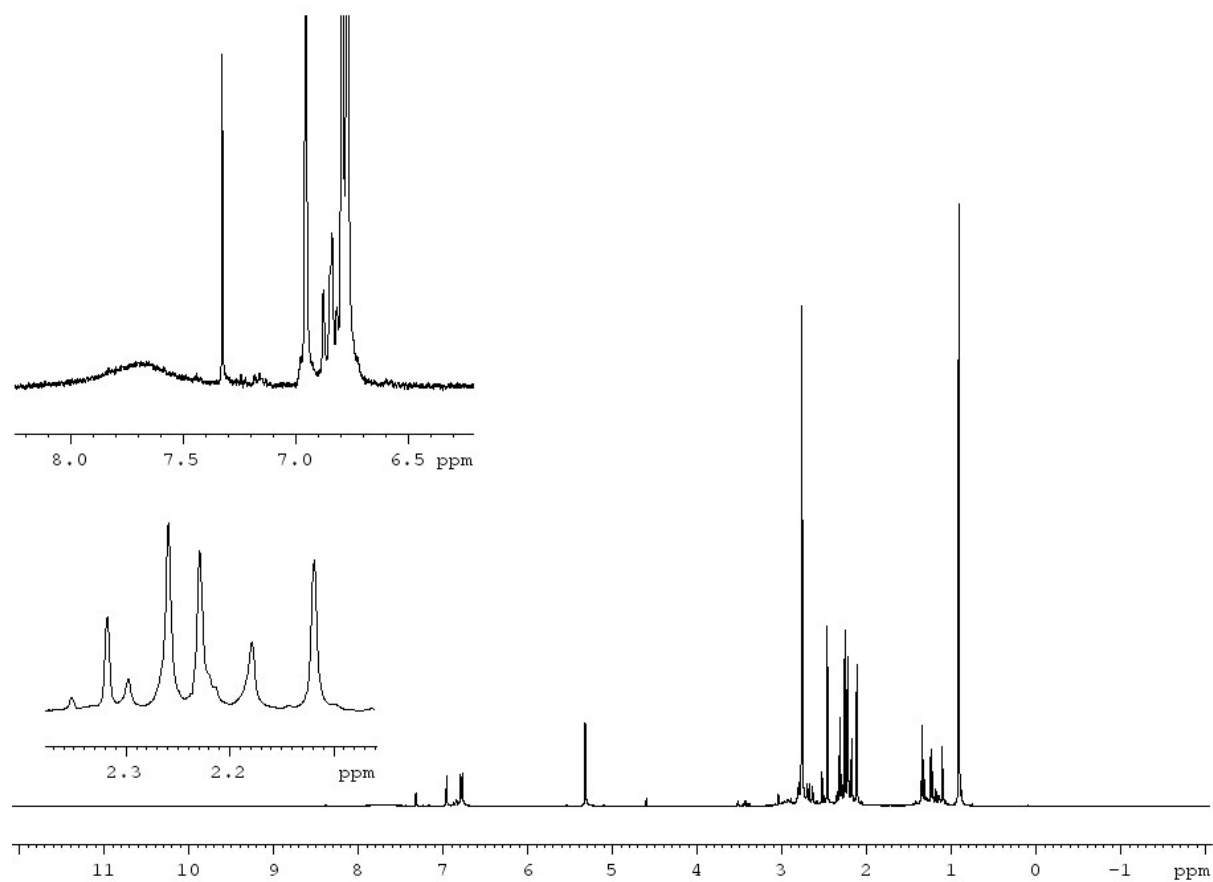
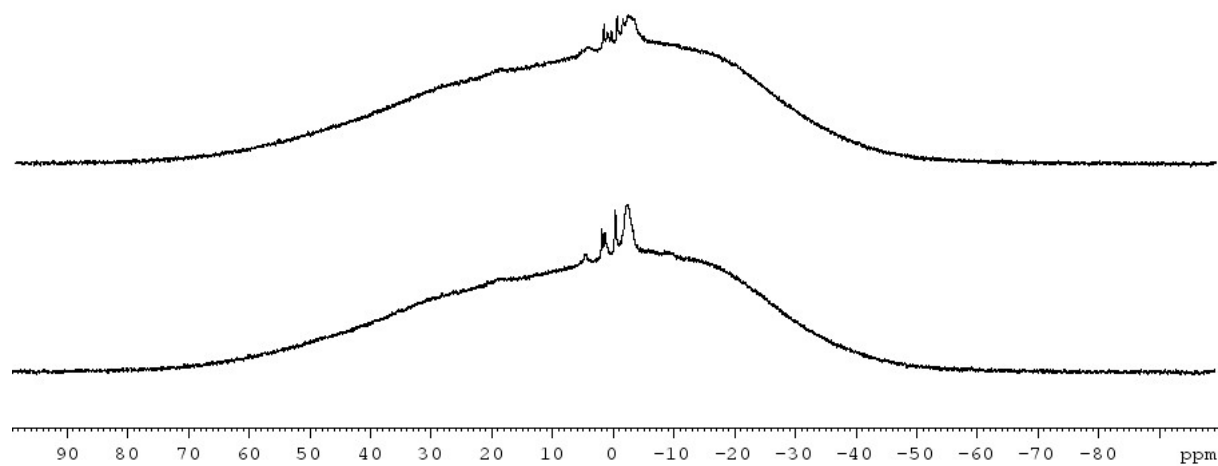
## Compound 3a

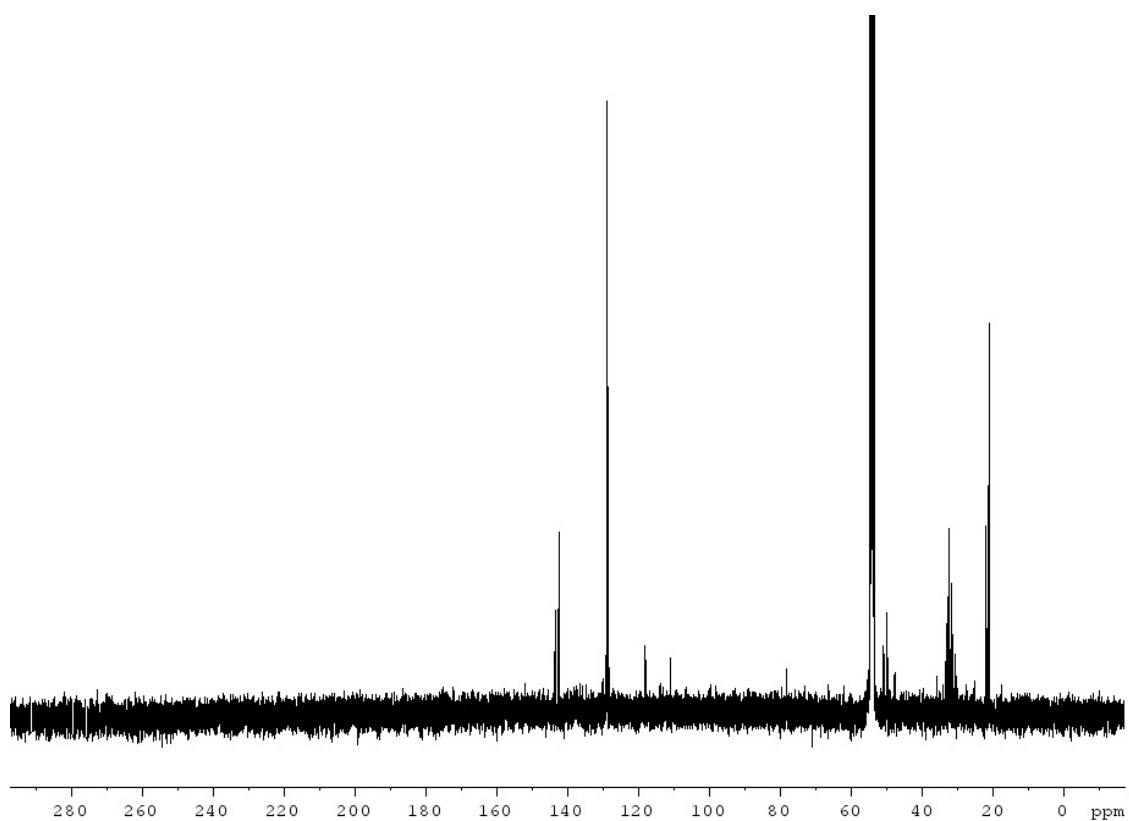
Figure S8.  $^1\text{H}$  NMR spectrum of 3a in  $\text{CD}_3\text{CN}$ Figure S9.  $^{11}\text{B}$  NMR (top) and  $^{11}\text{B}\{^1\text{H}\}$  NMR (bottom) spectra of 3a in toluene

## Compound 3b

Figure S10.  $^1\text{H}$  NMR spectrum of 3b in  $\text{CD}_3\text{CN}$ Figure S11.  $^{11}\text{B}$  NMR (top) and  $^{11}\text{B}\{^1\text{H}\}$  NMR (bottom) spectra of 3b in toluene

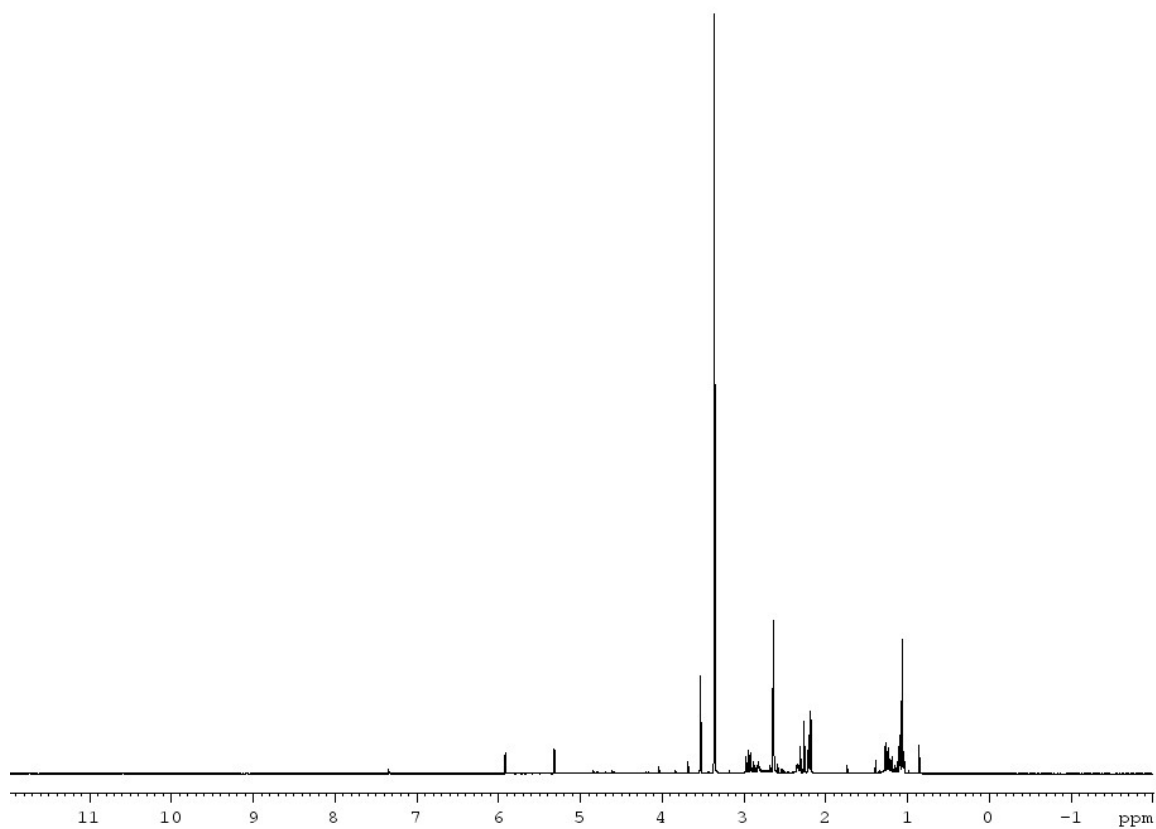
## Compound 4a

Figure S12.  $^1\text{H}$  NMR spectrum of 4a in  $\text{CD}_2\text{Cl}_2$ Figure S13.  $^{11}\text{B}$  NMR (top) and  $^{11}\text{B}\{^1\text{H}\}$  NMR (bottom) spectra of 4a in  $\text{CD}_2\text{Cl}_2$



**Figure S14.**  $^{13}\text{C}\{^1\text{H}\}$  NMR spectrum of **4a** in  $\text{CD}_2\text{Cl}_2$

### Compound **4b**



**Figure S15.**  $^1\text{H}$  NMR spectrum of **4b** in  $\text{CD}_2\text{Cl}_2$

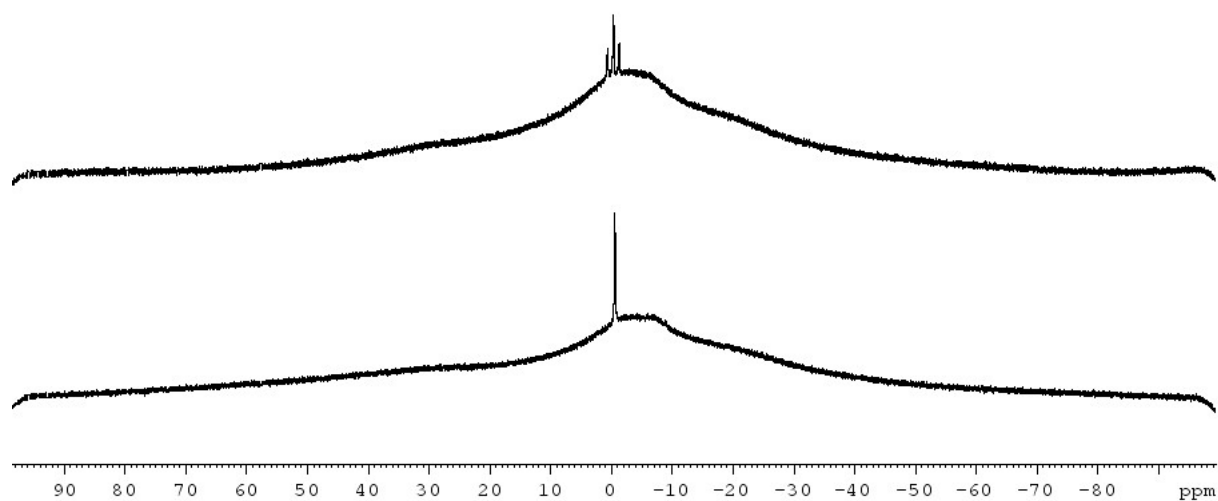


Figure S16.  $^{11}\text{B}$  NMR (top) and  $^{11}\text{B}\{^1\text{H}\}$  NMR (bottom) spectra of **4b** in  $\text{CD}_2\text{Cl}_2$

### Compound 4c

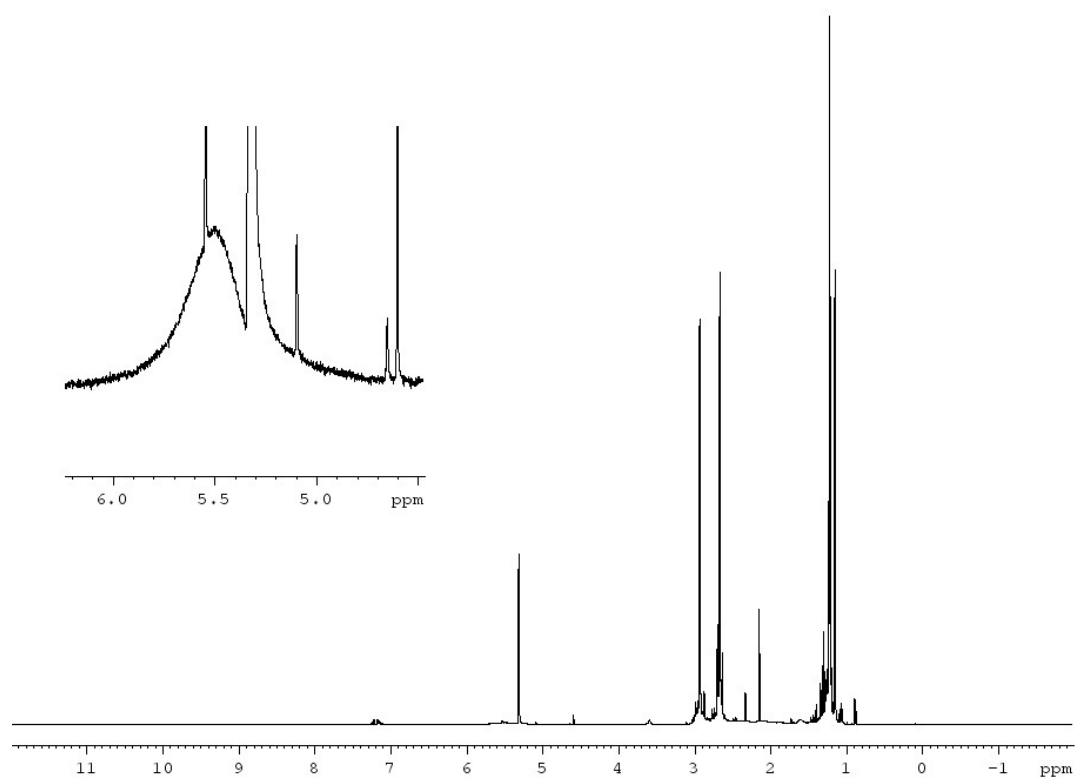
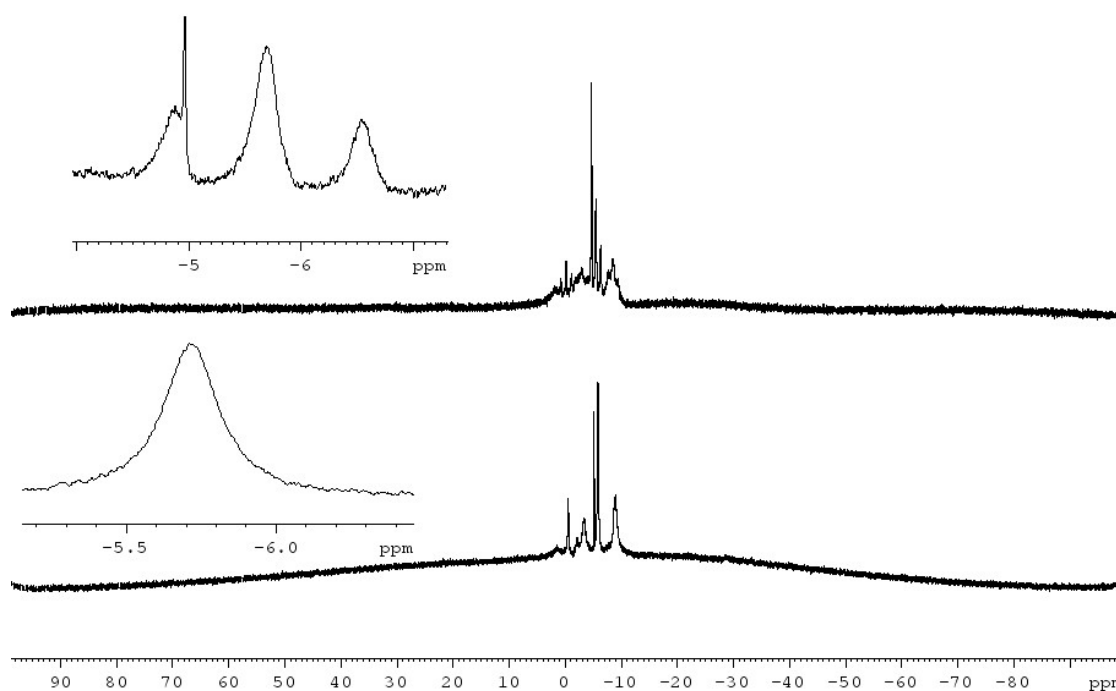


Figure S17.  $^1\text{H}$  NMR spectrum of **4c** in  $\text{CD}_2\text{Cl}_2$



**Figure S18.**  $^{11}\text{B}$  NMR (top) and  $^{11}\text{B}\{^1\text{H}\}$  NMR (bottom) spectra of **4c** in  $\text{CD}_2\text{Cl}_2$

### Computational details.

The geometries of the compounds have been fully optimized with gradient-corrected density functional theory (DFT) in form of Becke's three-parameter hybrid method B3LYP<sup>[1]</sup> with def2-SVP all electron basis set (ECP on Te).<sup>[2]</sup> Gaussian 09 program package<sup>[3]</sup> was used throughout. All structures correspond to minima on their respective potential energy surfaces as verified by computation of second derivatives. Basis sets were obtained from the EMSL basis set exchange database.<sup>[4]</sup> Standard entropies of the reactions in solution were estimated by taking into account the loss of translational degrees of freedom upon solvation of one gaseous mole in the inert solvent ( $90 \text{ J mol}^{-1} \text{ K}^{-1}$ ).<sup>[5]</sup>

Gas phase IR spectra for  ${}^t\text{BuAsOHOBH}_2\text{NMe}_3$  and  ${}^t\text{BuAsSHSBH}_2\text{NMe}_3$  (Fig. 2S) were computed at B3LYP/TZVP level of theory. Obtained harmonic vibrational frequencies are scaled by 0.965 as recommended in ref. [6].

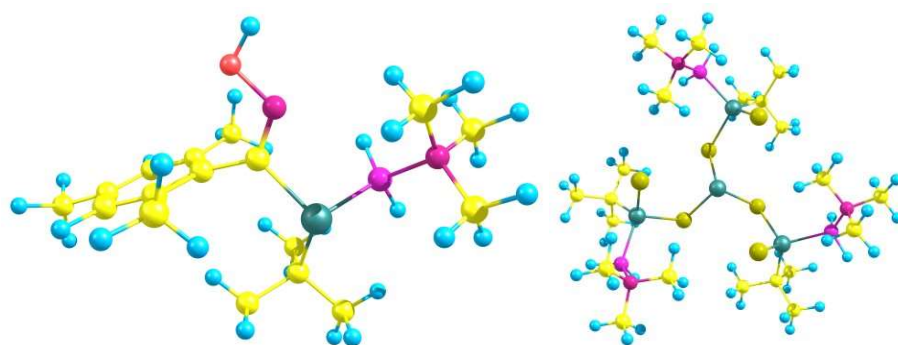
Computed thermodynamic characteristics for the formation of 13-15-16 compounds are summarized in Table S2.

As expected, oxidation reactions by  $\text{O}_2$ ,  $\text{S}_8$ ,  $\text{Se}_8$  are exothermic and exergonic, synthesis is thermodynamically allowed both in case of formation of  ${}^t\text{BuAsHEBH}_2\text{NMe}_3$  (reactions 1-3) and  ${}^t\text{BuAsEHEBH}_2\text{NMe}_3$  (reactions 7, 9; **E** = O, S, Se). In contrast,

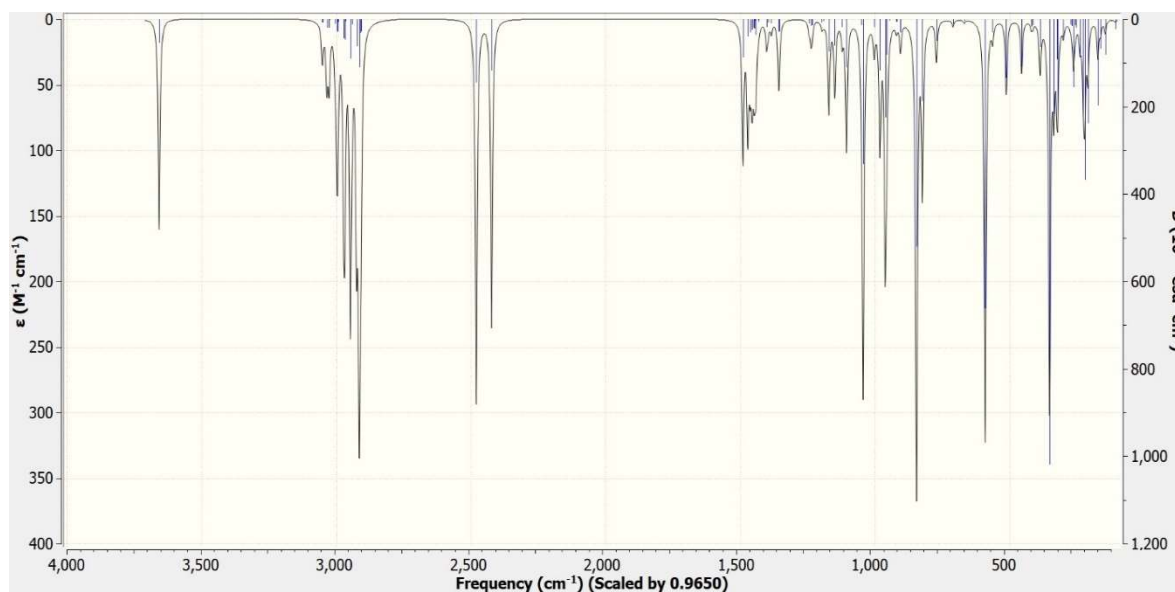
oxidation by  $\text{Te}_8$  (used as a model for the solid tellurium) and  $\text{TePEt}_3$  are endergonic and thermodynamically unfavorable (processes 4, 6, 10) which qualitatively agrees with experimental observations.

Oxidation by  $\text{ONMe}_3$ ,  $\text{Me}_3\text{SiOOSiMe}_3$ ,  $\text{MesCNO}$  (reactions 11-13) and  $\text{C}_6\text{H}_{10}\text{S}$  (reaction 5) are also exergonic and thermodynamically allowed. Reaction 14 with  $\text{MesCNO}$  with formation of  $\text{MesCNOHAs}^t\text{BuBH}_2\text{NMe}_3$  (Fig. S19) is predicted to be endergonic in the gas phase, but slightly exergonic in solution.

Formation of  $\text{As}(\text{SAsS}^t\text{BuBH}_2\text{NMe}_3)_3$  can be rationalized as formal reaction of  $^t\text{BuAsHBH}_2\text{NMe}_3$  with three  $^t\text{BuAsSHSBH}_2\text{NMe}_3$  molecules, with evolution of  $\text{H}_2$ ,  $t\text{Bu}$  and  $\text{BH}_3\text{NMe}_3$  (process 15) or  $\frac{1}{2} \text{B}_2\text{H}_6$  and  $\text{NMe}_3$  (process 16), both reactions are exergonic and thermodynamically allowed both in the gas phase and in solution.



**Figure S19.** Optimized structures of  $\text{MesCNOHAs}^t\text{BuBH}_2\text{NMe}_3$  and  $\text{As}(\text{SAsS}^t\text{BuBH}_2\text{NMe}_3)_3$ .



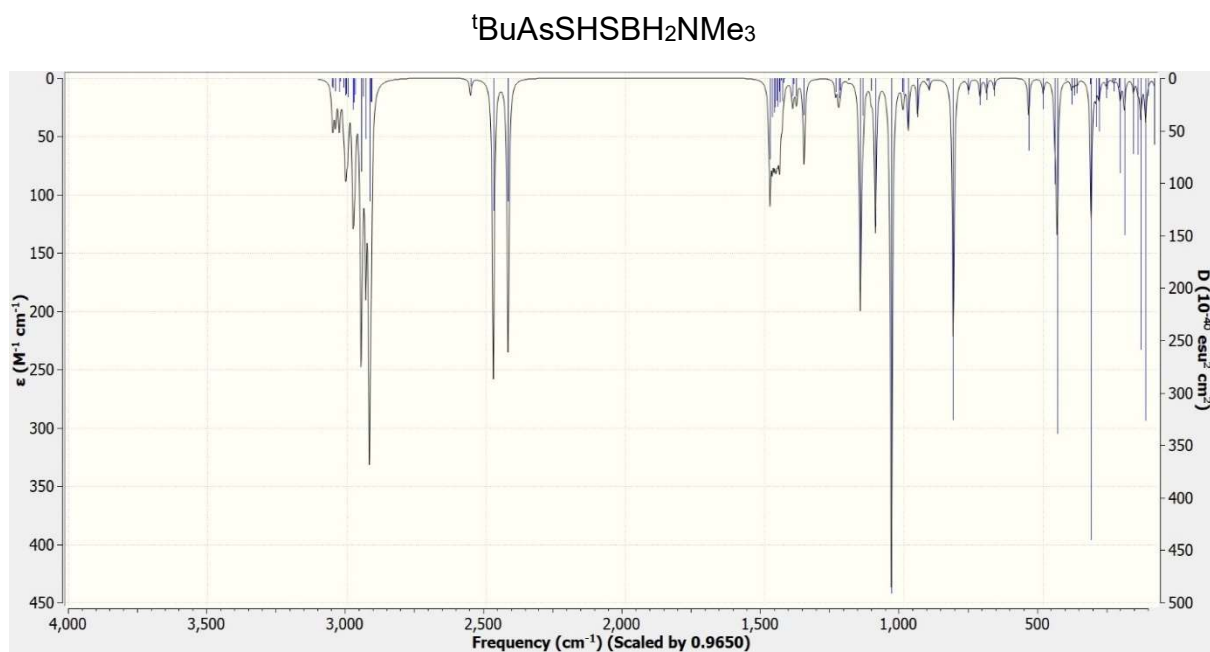


**Figure S20.** Gas phase IR spectra of  ${}^t\text{BuAsOHOBH}_2\text{NMe}_3$  (top) and  ${}^t\text{BuAsSHSBH}_2\text{NMe}_3$  (bottom). Harmonic frequencies are scaled by 0.965. Blue: computed frequencies and their IR-intensities, black: simulated spectra using peak half-width at half-height  $4.18848\text{ cm}^{-1}$ . B3LYP/TZVP level of theory.

**Table S2.** Reaction energies  $\Delta E^\circ$ , standard reaction enthalpies  $\Delta H^\circ_{298}$ , Gibbs energies  $\Delta G^\circ_{298}$  (kJ mol<sup>-1</sup>) and standard reaction entropies  $\Delta S^\circ_{298}$  (J mol<sup>-1</sup> K<sup>-1</sup>) for the considered gas phase processes and estimated values of standard reaction entropies and Gibbs energies in solution (solv). B3LYP/def2-SVP level of theory.

N	Process	$\Delta E^\circ$	$\Delta H^\circ_{298}$	$\Delta S^\circ_{298}$	$\Delta G^\circ_{298}$	$\Delta S^\circ_{298(\text{solv})}$	$\Delta G^\circ_{298(\text{solv})}$
1	<sup>t</sup> BuAsHBH <sub>2</sub> NMe <sub>3</sub> + 1/2 O <sub>2</sub> = <sup>t</sup> BuAsHOBH <sub>2</sub> NMe <sub>3</sub>	-133.0	-129.5	-89.0	-103.0	-89.0	-103.0
2	<sup>t</sup> BuAsHBH <sub>2</sub> NMe <sub>3</sub> + 1/8 S <sub>8</sub> = <sup>t</sup> BuAsHSBH <sub>2</sub> NMe <sub>3</sub>	-50.4	-47.3	-29.1	-38.6	-17.8	-42.0
3	<sup>t</sup> BuAsHBH <sub>2</sub> NMe <sub>3</sub> + 1/8 Se <sub>8</sub> = <sup>t</sup> BuAsHSeBH <sub>2</sub> NMe <sub>3</sub>	-30.2	-27.0	-30.2	-18.0	-18.9	-21.3
4	<sup>t</sup> BuAsHBH <sub>2</sub> NMe <sub>3</sub> + 1/8 Te <sub>8</sub> = <sup>t</sup> BuAsHTeBH <sub>2</sub> NMe <sub>3</sub>	-1.5	1.6	-27.9	9.9	-16.7	6.6
5	<sup>t</sup> BuAsHBH <sub>2</sub> NMe <sub>3</sub> + C <sub>6</sub> H <sub>10</sub> S = <sup>t</sup> BuAsHSBH <sub>2</sub> NMe <sub>3</sub> + C <sub>6</sub> H <sub>10</sub>	-68.2	-67.6	0.3	-67.7	0.3	-67.7
6	<sup>t</sup> BuAsHBH <sub>2</sub> NMe <sub>3</sub> + TePEt <sub>3</sub> = <sup>t</sup> BuAsHTeBH <sub>2</sub> NMe <sub>3</sub> + PEt <sub>3</sub>	0.4	0.3	-8.4	2.8	-8.4	2.8
7	<sup>t</sup> BuAsHBH <sub>2</sub> NMe <sub>3</sub> + O <sub>2</sub> = <sup>t</sup> BuAsOHOBH <sub>2</sub> NMe <sub>3</sub>	-368.0	-354.6	-158.5	-307.4	-158.5	-307.4
8	<sup>t</sup> BuAsHBH <sub>2</sub> NMe <sub>3</sub> + 1/4 S <sub>8</sub> = <sup>t</sup> BuAsSHSBH <sub>2</sub> NMe <sub>3</sub>	-110.9	-106.0	-48.0	-91.7	-25.5	-98.4
9	<sup>t</sup> BuAsHBH <sub>2</sub> NMe <sub>3</sub> + 1/4 Se <sub>8</sub> = <sup>t</sup> BuAsSeHSeBH <sub>2</sub> NMe <sub>3</sub>	-54.5	-52.1	-44.4	-38.8	-21.9	-45.6
10	<sup>t</sup> BuAsHBH <sub>2</sub> NMe <sub>3</sub> + 1/4 Te <sub>8</sub> = <sup>t</sup> BuAsTeHTeBH <sub>2</sub> NMe <sub>3</sub>	20.9	20.9	-44.7	34.2	-22.2	27.5
11	<sup>t</sup> BuAsHBH <sub>2</sub> NMe <sub>3</sub> + ONMe <sub>3</sub> = <sup>t</sup> BuAsHOBH <sub>2</sub> NMe <sub>3</sub> + NMe <sub>3</sub>	-188.9	-190.4	-0.3	-190.3	-0.3	-190.3
12	<sup>t</sup> BuAsHBH <sub>2</sub> NMe <sub>3</sub> + Me <sub>3</sub> SiOOSiMe <sub>3</sub> = <sup>t</sup> BuAsHOBH <sub>2</sub> NMe <sub>3</sub> + Me <sub>3</sub> SiOSiMe <sub>3</sub>	-256.9	-255.0	-20.9	-248.8	-20.9	-248.8
13	<sup>t</sup> BuAsHBH <sub>2</sub> NMe <sub>3</sub> + MesCNO = <sup>t</sup> BuAsHOBH <sub>2</sub> NMe <sub>3</sub> + MesCN	-151.5	-152.7	-14.3	-148.4	-14.3	-148.4
14	<sup>t</sup> BuAsHBH <sub>2</sub> NMe <sub>3</sub> + MesCNO = MesCNOHAs <sup>t</sup> BuBH <sub>2</sub> NMe <sub>3</sub>	-51.6	-37.4	-208.2	24.7	-118.2	-2.2
15	<sup>t</sup> BuAsHBH <sub>2</sub> NMe <sub>3</sub> + 3 <sup>t</sup> BuAsSHSBH <sub>2</sub> NMe <sub>3</sub> = As(SAsS <sup>t</sup> BuBH <sub>2</sub> NMe <sub>3</sub> ) <sub>3</sub> + <sup>t</sup> BuH + H <sub>2</sub> + BH <sub>3</sub> NMe <sub>3</sub>	-142.3	-137.0	-83.5	-112.1	6.5	-139.0
16	<sup>t</sup> BuAsHBH <sub>2</sub> NMe <sub>3</sub> + 3 <sup>t</sup> BuAsSHSBH <sub>2</sub> NMe <sub>3</sub> = As(SAsS <sup>t</sup> BuBH <sub>2</sub> NMe <sub>3</sub> ) <sub>3</sub> + <sup>t</sup> BuH + H <sub>2</sub> + 1/2 B <sub>2</sub> H <sub>6</sub> + NMe <sub>3</sub>	-81.7	-83.2	-4.4	-81.9	175.6	-135.5

**Table S3.** Total energies  $E^0$ , sum of electronic and thermal enthalpies  $H^0_{298}$  (Hartree) and standard entropies  $S^0_{298}$  (cal mol<sup>-1</sup>K<sup>-1</sup>). B3LYP/def2-SVP level of theory.

Compound	Point group	$E^0$	$H^0_{298}$	$S^0_{298}$
H <sub>2</sub>	D <sub>∞h</sub>	-1.1737901	-1.160528	31.227
O <sub>2</sub>	D <sub>∞h</sub>	-150.2047989	-150.197625	48.961
S <sub>8</sub>	D <sub>4d</sub>	-3184.691874	-3184.668126	103.978
Se <sub>8</sub>	D <sub>4d</sub>	-19210.50315	-19210.48134	129.865
Te <sub>8</sub>	D <sub>4d</sub>	-2145.076521	-2145.055273	149.258
NMe <sub>3</sub>	C <sub>3v</sub>	-174.3458754	-174.219985	68.868
ONMe <sub>3</sub>	C <sub>3v</sub>	-249.4270063	-249.295605	72.148
BH <sub>3</sub> NMe <sub>3</sub>	C <sub>3v</sub>	-200.9916903	-200.829922	77.797
MesCN	C <sub>1</sub>	-442.1257855	-441.93255	107.509
MesCNO	C <sub>s</sub>	-517.221159	-517.022543	114.134
Me <sub>3</sub> SiOSiMe <sub>3</sub>	C <sub>2</sub>	-893.482484	-893.239745	130.681
Me <sub>3</sub> SiOOSiMe <sub>3</sub>	C <sub>1</sub>	-968.5376879	-968.290739	138.867
C <sub>6</sub> H <sub>10</sub>	C <sub>1</sub>	-234.4809502	-234.328908	73.858
C <sub>6</sub> H <sub>10</sub> S	C <sub>1</sub>	-632.5606731	-632.40467	79.833
PEt <sub>3</sub>	C <sub>3</sub>	-578.7712182	-578.561935	98.264
TePEt <sub>3</sub>	C <sub>3</sub>	-846.9065055	-846.693342	112.259
<sup>t</sup> BuAsHBH <sub>2</sub> NMe <sub>3</sub>	C <sub>1</sub>	-2594.374946	-2594.083822	118.809
<sup>t</sup> BuAsHOBH <sub>2</sub> NMe <sub>3</sub>	C <sub>1</sub>	-2669.528008	-2669.231957	122.011
<sup>t</sup> BuAsHSBH <sub>2</sub> NMe <sub>3</sub>	C <sub>1</sub>	-2992.480629	-2992.185344	124.859
<sup>t</sup> BuAsHSeBH <sub>2</sub> NMe <sub>3</sub>	C <sub>1</sub>	-4995.699332	-4995.404258	127.832
<sup>t</sup> BuAsHTeBH <sub>2</sub> NMe <sub>3</sub>	C <sub>1</sub>	-2862.510086	-2862.215118	130.792
<sup>t</sup> BuAsOHOBH <sub>2</sub> NMe <sub>3</sub>	C <sub>1</sub>	-2744.719904	-2744.416507	129.898
<sup>t</sup> BuAsSHSBH <sub>2</sub> NMe <sub>3</sub>	C <sub>1</sub>	-3390.59017	-3390.291245	133.322
<sup>t</sup> BuAsSeHSeBH <sub>2</sub> NMe <sub>3</sub>	C <sub>1</sub>	-7397.021499	-7396.723993	140.668
<sup>t</sup> BuAsTeHTeBH <sub>2</sub> NMe <sub>3</sub>	C <sub>1</sub>	-3130.636102	-3130.339687	145.449
MesCNOHAs <sup>t</sup> BuBH <sub>2</sub> NMe <sub>3</sub>	C <sub>1</sub>	-3111.6157502	-3111.120604	183.19
As(SAs <sup>t</sup> BuBH <sub>2</sub> NMe <sub>3</sub> ) <sub>3</sub>	C <sub>3</sub>	-12405.690708	-12404.81323	319.91

**Table S4.** Optimized geometries of theoretically studied compounds. xyz coordinates in angstroms. B3LYP/def2-SVP level of theory

<hr/>			
H <sub>2</sub>			
1	0.000000000	0.000000000	0.380387000
1	0.000000000	0.000000000	-0.380387000
<hr/>			
O <sub>2</sub>			
8	0.000000000	0.000000000	0.599970000
8	0.000000000	0.000000000	-0.599970000
<hr/>			
S <sub>8</sub>			
16	0.000000000	2.406107000	0.504468000
16	-1.701375000	1.701375000	-0.504468000
16	1.701375000	1.701375000	-0.504468000
16	-2.406107000	0.000000000	0.504468000
16	2.406107000	0.000000000	0.504468000
16	1.701375000	-1.701375000	-0.504468000
16	-1.701375000	-1.701375000	-0.504468000
16	0.000000000	-2.406107000	0.504468000
<hr/>			
Se <sub>8</sub>			
34	0.000000000	2.696428000	0.579350000
34	-1.906663000	1.906663000	-0.579350000
34	1.906663000	1.906663000	-0.579350000
34	-2.696428000	0.000000000	0.579350000
34	2.696428000	0.000000000	0.579350000
34	1.906663000	-1.906663000	-0.579350000
34	-1.906663000	-1.906663000	-0.579350000
34	0.000000000	-2.696428000	0.579350000
<hr/>			
Te <sub>8</sub>			
52	0.000000000	3.137716000	0.687136000
52	-2.218700000	2.218700000	-0.687136000
52	2.218700000	2.218700000	-0.687136000
52	-3.137716000	0.000000000	0.687136000
52	3.137716000	0.000000000	0.687136000
52	2.218700000	-2.218700000	-0.687136000
52	-2.218700000	-2.218700000	-0.687136000
52	0.000000000	-3.137716000	0.687136000
<hr/>			
NMe <sub>3</sub>			
7	0.000000000	0.000000000	0.345931000
6	0.000000000	1.390819000	-0.055564000
6	-1.204484000	-0.695409000	-0.055564000
6	1.204484000	-0.695409000	-0.055564000
1	-2.092677000	-0.180153000	0.344699000
1	-1.202356000	-1.722235000	0.344699000
1	-1.327880000	-0.766652000	-1.163185000
1	-0.890321000	1.902388000	0.344699000
1	0.000000000	1.533304000	-1.163185000
1	0.890321000	1.902388000	0.344699000
1	2.092677000	-0.180153000	0.344699000
1	1.327880000	-0.766652000	-1.163185000
1	1.202356000	-1.722235000	0.344699000
<hr/>			
ONMe <sub>3</sub>			
8	0.000000000	0.000000000	1.433054000
7	0.000000000	0.000000000	0.085811000
6	0.000000000	1.414095000	-0.417631000
6	-1.224643000	-0.707048000	-0.417631000
6	1.224643000	-0.707048000	-0.417631000
1	0.000000000	1.467168000	-1.518546000
1	0.891438000	1.894860000	0.001313000
1	-0.891438000	1.894860000	0.001313000
1	-1.270605000	-0.733584000	-1.518546000
1	-2.086716000	-0.175422000	0.001313000
1	-1.195278000	-1.719438000	0.001313000
1	1.270605000	-0.733584000	-1.518546000
1	1.195278000	-1.719438000	0.001313000
1	2.086716000	-0.175422000	0.001313000
<hr/>			
BH <sub>3</sub> NMe <sub>3</sub>			
1	-1.990904000	0.425984000	-1.094620000
5	-1.659867000	-0.007088000	0.001102000
7	0.000766000	0.000028000	-0.000068000
1	-1.983853000	-1.174721000	0.173070000
1	-1.991305000	0.723488000	0.925350000
6	0.484817000	1.387117000	-0.203012000
6	0.494316000	-0.866016000	-1.098092000
6	0.494440000	-0.514832000	1.300177000
1	1.597037000	-0.878269000	-1.119107000
1	0.107780000	-0.486867000	-2.052104000
1	0.113184000	-1.883437000	-0.947038000
1	1.597178000	-0.520608000	1.323739000
1	0.113289000	-1.532789000	1.447443000
1	0.107917000	0.122318000	2.105066000
<hr/>			
1	1.587323000	1.418556000	-0.208255000
1	0.097878000	2.020550000	0.604606000
1	0.097015000	1.763422000	-1.157625000
<hr/>			
MesCN			
6	-2.288049000	0.005993000	0.000002000
7	-3.450356000	0.010127000	0.000003000
6	-0.852669000	0.000676000	0.000001000
6	-0.164226000	-1.235096000	0.000000000
6	-0.153982000	1.233997000	0.000000000
6	1.234845000	-1.210326000	-0.000003000
6	1.241815000	1.199516000	-0.000003000
6	1.955848000	-0.009228000	-0.000003000
1	1.777879000	-2.159595000	-0.000006000
1	1.791727000	2.145303000	-0.000006000
6	-0.902682000	2.542188000	-0.000001000
1	-1.557298000	2.628986000	-0.882553000
1	-1.557299000	2.628985000	0.882549000
1	-0.211166000	3.396453000	0.000000000
6	-0.919353000	-2.539557000	-0.000001000
1	-1.574326000	-2.623298000	-0.882586000
1	-0.231949000	-3.397120000	-0.000001000
1	-1.574328000	-2.623298000	0.882582000
6	3.464287000	-0.002947000	0.000004000
1	3.875306000	-1.022752000	-0.000129000
1	3.859477000	0.522202000	-0.885544000
1	3.859466000	0.521959000	0.885702000
<hr/>			
MesCNO			
6	-0.000477000	1.856669000	0.000000000
7	0.000133000	3.027924000	0.000000000
8	0.000892000	4.232414000	0.000000000
6	-0.000275000	0.425968000	0.000000000
6	-0.003328000	-0.275937000	1.233191000
6	-0.003328000	-0.275937000	-1.233191000
6	-0.006614000	-1.673011000	1.203293000
6	-0.006614000	-1.673011000	-1.203293000
6	-0.005135000	-2.393031000	0.000000000
1	-0.012223000	-2.218128000	2.151806000
1	-0.012223000	-2.218128000	-2.151806000
6	-0.006614000	0.472959000	-2.540839000
1	-0.890631000	1.126292000	-2.627992000
1	0.876935000	1.126384000	-2.631993000
1	-0.008219000	-0.217455000	-3.396088000
6	-0.006614000	0.472959000	2.540839000
1	-0.890631000	1.126292000	2.627992000
1	-0.008219000	-0.217455000	3.396088000
1	0.876935000	1.126384000	2.631993000
6	0.026766000	-3.901213000	0.000000000
1	-0.466552000	-4.317142000	0.891664000
1	-0.466552000	-4.317142000	-0.891664000
1	1.066721000	-4.273163000	0.000000000
<hr/>			
Me <sub>3</sub> SiOSiMe <sub>3</sub>			
6	0.000000000	2.744273000	-0.678310000
14	-1.003661000	1.311379000	0.025368000
6	-1.709235000	1.773483000	1.709215000
8	0.000000000	0.000000000	0.235156000
6	-2.394294000	0.847223000	-1.160953000
1	0.825563000	3.018762000	-0.000988000
1	-0.627754000	3.639754000	-0.823015000
1	0.440111000	2.481721000	-1.654616000
1	-0.903275000	2.019871000	2.419943000
1	-2.289545000	0.939527000	2.137345000
1	-2.377018000	2.648578000	1.639270000
1	-2.968524000	-0.014048000	-0.781382000
1	-1.999619000	0.576404000	-2.154368000
1	-3.097543000	1.686034000	-1.297676000
14	1.003661000	-1.311379000	0.025368000
6	1.709235000	-1.773483000	1.709215000
6	2.394294000	-0.847223000	-1.160953000
6	0.000000000	-2.744273000	-0.678310000
1	2.377018000	-2.648578000	1.639270000
1	0.903275000	-2.019871000	2.419943000
1	2.289545000	-0.939527000	2.137345000
1	3.097543000	-1.686034000	-1.297676000
1	2.968524000	0.014048000	-0.781382000
1	1.999619000	-0.576404000	-2.154368000
1	0.627754000	-3.639754000	-0.823015000
1	-0.440111000	-2.481721000	-1.654616000
1	-0.825563000	-3.018762000	-0.000988000
<hr/>			
Me <sub>3</sub> SiOOSiMe <sub>3</sub>			
6	-2.335109000	1.055605000	-1.551828000
14	-2.056143000	0.033593000	0.000000000

6	-2.334478000	1.051493000	1.554642000
8	-0.450068000	-0.581154000	-0.001191000
6	-3.077399000	-1.544636000	-0.001812000
1	-1.632779000	1.903135000	-1.583484000
1	-3.361075000	1.458649000	-1.589427000
1	-2.173780000	0.447573000	-2.456773000
1	-1.632552000	1.899293000	1.588098000
1	-2.172311000	0.441176000	2.457899000
1	-3.360615000	1.453948000	1.593952000
1	-2.868345000	-2.158438000	0.889045000
1	-2.868362000	-2.156330000	-0.894118000
1	-4.154217000	-1.305531000	-0.001519000
8	0.450070000	0.581165000	-0.000653000
14	2.056143000	-0.033591000	-0.000015000
6	3.077408000	1.544632000	-0.000234000
6	2.335193000	-1.054053000	-1.552845000
6	2.334383000	-1.053051000	1.553625000
1	4.154225000	1.305518000	-0.000258000
1	2.868415000	2.157515000	0.891267000
1	2.868320000	2.157249000	-0.891897000
1	3.361134000	-1.457138000	-1.590725000
1	2.174028000	-0.445091000	-2.457193000
1	1.632806000	-1.901501000	-1.585452000
1	3.360555000	-1.455440000	1.592673000
1	1.632534000	-1.900952000	1.586105000
1	2.172016000	-0.443676000	2.457483000

C<sub>6</sub>H<sub>10</sub>

6	1.497968000	0.048206000	0.109323000
6	0.699471000	-1.192797000	-0.314685000
6	-0.698989000	-1.193047000	0.314633000
6	-1.497989000	0.047703000	-0.109265000
6	-0.668135000	1.306413000	-0.055550000
6	0.667580000	1.306661000	0.055589000
1	2.391757000	0.165084000	-0.529056000
1	1.893212000	-0.084454000	1.135905000
1	1.248144000	-2.110317000	-0.045022000
1	0.598768000	-1.200551000	-1.415188000
1	-1.247397000	-2.110708000	0.044963000
1	-0.598249000	-1.200750000	1.415139000
1	-2.391812000	0.163998000	0.529173000
1	-1.893231000	-0.085166000	-1.135829000
1	-1.202405000	2.261877000	-0.111093000
1	1.201770000	2.262156000	0.110738000

C<sub>6</sub>H<sub>10</sub>S

6	0.541483000	1.502797000	0.360249000
6	1.479868000	0.791119000	-0.619863000
6	1.862948000	-0.590907000	-0.080161000
6	0.646265000	-1.521793000	0.069593000
6	-0.597658000	-0.826751000	0.634018000
6	-0.654047000	0.656608000	0.764857000
1	0.195132000	2.467052000	-0.046826000
1	1.100382000	1.741000000	1.285792000
1	2.381426000	1.405372000	-0.777056000
1	0.985563000	0.688955000	-1.600795000
1	2.611009000	-1.071115000	-0.731867000
1	2.350284000	-0.460626000	0.903771000
1	0.904605000	-2.365018000	0.732077000
1	0.396360000	-1.967500000	-0.906130000
1	-1.130109000	-1.395103000	1.404921000
1	-1.210594000	1.048981000	1.624561000
16	-1.766076000	-0.009902000	-0.541288000

PEt<sub>3</sub>

15	0.000000000	0.000000000	0.494111000
6	1.614427000	0.357286000	-0.394152000
6	-1.116633000	1.219492000	-0.394152000
6	-0.497795000	-1.576778000	-0.394152000
1	-1.011101000	2.652498000	0.135455000
1	-2.147988000	0.851317000	-0.259129000
1	-0.912187000	1.187044000	-1.480038000
6	2.802681000	-0.450610000	0.135455000
1	1.811256000	1.434554000	-0.259129000
1	1.484104000	0.196455000	-1.480038000
1	0.336732000	-2.285871000	-0.259129000
1	-0.571917000	-1.383499000	-1.480038000
6	-1.791581000	-2.201888000	0.135455000
1	0.000000000	3.069188000	-0.003327000
1	-1.241085000	2.699387000	1.212112000
1	-1.712791000	3.322660000	-0.387986000
1	3.733903000	-0.178009000	-0.387986000
1	2.657995000	-1.534594000	-0.003327000
1	2.958281000	-0.274883000	1.212112000
1	-1.717196000	-2.424505000	1.212112000
1	-2.021112000	-3.144651000	-0.387986000
1	-2.657995000	-1.534594000	-0.003327000

TePEt<sub>3</sub>

52	1.582729000	0.002604000	0.000462000
15	-0.804118000	-0.000964000	-0.000142000
6	-1.575684000	0.558759000	-1.593690000
6	-1.575555000	1.095717000	1.284462000
6	-1.573568000	-1.661334000	0.310735000
6	-1.156368000	2.564408000	1.222806000
1	-1.286444000	0.657954000	2.253954000
1	-2.670808000	0.984546000	1.189157000
6	-1.144909000	-0.224267000	-2.834362000
1	-1.296515000	1.619590000	-1.696375000
1	-2.670902000	0.521608000	-1.451758000
1	-1.295248000	-2.280643000	-0.556635000
1	-2.669204000	-1.520818000	0.272019000
6	-1.141081000	-2.347074000	1.607307000
1	-1.491880000	3.052751000	0.294227000
1	-0.061655000	2.659888000	1.280765000
1	-1.596359000	3.121382000	2.065327000
1	-1.588358000	0.221712000	-3.738702000
1	-1.468038000	-1.276554000	-2.793060000
1	-0.049682000	-0.209524000	-2.942708000
1	-0.045034000	-2.441939000	1.651253000
1	-1.576694000	-3.356959000	1.667663000
1	-1.470313000	-1.791214000	2.499407000

<sup>1</sup>BuAsHBBH<sub>2</sub>NMe<sub>3</sub>

5	0.939378000	0.613201000	0.590837000
1	1.076846000	0.659241000	1.800047000
1	0.704692000	1.701813000	0.092355000
33	-0.506606000	-0.790096000	-0.043857000
7	2.442087000	0.195741000	0.006890000
6	3.413580000	1.207447000	0.499695000
6	2.457079000	0.193342000	-1.480323000
6	2.839625000	-1.145481000	0.510198000
1	3.462331000	-0.063663000	-1.851646000
1	2.172680000	1.190142000	-1.839550000
1	1.724623000	-0.537299000	-1.846095000
1	4.427339000	0.975947000	0.133030000
1	3.403238000	1.208126000	1.596211000
1	3.105702000	2.198666000	0.145490000
1	3.858498000	-1.395706000	0.172548000
1	2.132612000	-1.895846000	0.133074000
1	2.801652000	-1.139084000	1.606675000
6	-2.209487000	0.334169000	0.005228000
6	-2.197396000	1.250771000	-1.226659000
1	-2.139508000	0.672031000	-2.163396000
1	-3.124150000	1.852626000	-1.264675000
1	-1.348128000	1.951911000	-1.204791000
6	-2.310307000	1.168830000	1.287959000
1	-3.248902000	1.756089000	1.290340000
1	-2.315162000	0.530688000	2.185969000
1	-1.472522000	1.875512000	1.382583000
6	-3.395174000	-0.638092000	-0.082223000
1	-3.426742000	-1.319057000	0.783842000
1	-4.349910000	-0.079687000	-0.100589000
1	-3.349975000	-1.255549000	-0.993837000
1	-0.756216000	-1.475850000	1.304024000

<sup>1</sup>BuAsHOBH<sub>2</sub>NMe<sub>3</sub>

5	1.100787000	-0.846973000	-0.718821000
1	1.350233000	-0.909995000	-1.907298000
1	0.833593000	-1.923948000	-0.220424000
33	-0.487973000	0.483773000	-0.422774000
7	2.427289000	-0.274583000	0.040111000
6	3.540413000	-1.222493000	-0.234498000
6	2.199267000	-0.184639000	1.516167000
6	2.795506000	1.083877000	-0.465883000
1	3.126409000	0.143837000	2.011810000
1	1.911651000	-1.175251000	1.890663000
1	1.391609000	0.545035000	1.684028000
1	4.457454000	-0.880407000	0.270738000
1	3.710661000	-1.276775000	-1.316955000
1	3.264629000	-2.218923000	0.132543000
1	3.745895000	1.401967000	-0.009371000
1	1.989899000	1.778573000	-0.185402000
1	2.907480000	1.038863000	-1.556909000
6	-2.200977000	-0.409091000	0.120541000
8	-0.112769000	1.716077000	0.652711000
1	-0.927136000	1.051011000	-1.784860000
6	-1.978928000	-1.014908000	1.512523000
1	-1.652548000	-0.243918000	2.228175000
1	-2.918333000	-1.456052000	1.890667000
1	-1.220022000	-1.813999000	1.495147000
6	-2.563217000	-1.484884000	-0.908723000
1	-3.516741000	-1.971328000	-0.634013000
1	-2.692905000	-1.059265000	-1.917847000
1	-1.794842000	-2.272817000	-0.967167000
6	-3.264673000	0.695370000	0.182857000
1	-3.473370000	1.116158000	-0.814603000

1	-4.213246000	0.292821000	0.581078000
1	-2.934421000	1.518839000	0.835278000
<sup>1</sup> BuAsHSBH <sub>2</sub> NMe <sub>3</sub>			
5	1.105027000	-1.103888000	-0.367452000
1	1.265830000	-1.582212000	-1.473183000
1	0.829106000	-1.925790000	0.483977000
33	-0.504817000	0.242594000	-0.516663000
7	2.504592000	-0.403919000	0.078612000
6	3.552659000	-1.461460000	0.025254000
6	2.420242000	0.126953000	1.474564000
6	2.886856000	0.705326000	-0.847372000
1	3.394787000	0.547970000	1.767026000
1	2.154639000	-0.696791000	2.148817000
1	1.645537000	0.907989000	1.509142000
1	4.519621000	-1.044275000	0.347384000
1	3.633591000	-1.839399000	-1.001261000
1	3.265359000	-2.287349000	0.687652000
1	3.884866000	1.084034000	-0.577345000
1	2.145506000	1.512924000	-0.757537000
1	2.903687000	0.318987000	-1.874588000
6	-2.189390000	-0.631406000	0.178511000
16	-0.275710000	2.208811000	0.274518000
1	-0.872010000	0.302770000	-2.000337000
6	-2.049580000	-0.759147000	1.699959000
1	-1.860668000	0.223347000	2.160321000
1	-2.980115000	-1.168802000	2.130909000
1	-1.226377000	-1.436077000	1.979494000
6	-2.342779000	-2.003824000	-0.488836000
1	-3.271897000	-2.488603000	-0.138860000
1	-2.410517000	-1.921308000	-1.586340000
1	-1.506182000	-2.677950000	-0.247276000
6	-3.361478000	0.290905000	-0.177823000
1	-3.504392000	0.364926000	-1.268418000
1	-4.297097000	-0.105158000	0.255423000
1	-3.199568000	1.306989000	0.214043000
<sup>1</sup> BuAsHSeBH <sub>2</sub> NMe <sub>3</sub>			
5	1.202534000	-1.378219000	-0.239294000
1	1.354204000	-1.982834000	-1.282684000
1	0.962333000	-2.097052000	0.709974000
33	-0.461489000	-0.118811000	-0.526988000
7	2.592740000	-0.599232000	0.086853000
6	3.664759000	-1.633945000	0.124115000
6	2.531254000	0.082758000	1.416248000
6	2.924654000	0.405212000	-0.967963000
1	3.501626000	0.556514000	1.631636000
1	2.303819000	-0.665359000	2.185691000
1	1.738198000	0.845656000	1.388726000
1	4.626840000	-1.164116000	0.381564000
1	3.736754000	-2.116906000	-0.857982000
1	3.408243000	-2.390719000	0.875666000
1	3.921120000	0.830832000	-0.772664000
1	2.170658000	1.205487000	-0.948022000
1	2.920205000	-0.092965000	-1.945941000
6	-2.109348000	-1.053350000	0.188771000
34	-0.366833000	2.063868000	0.119511000
1	-0.786447000	-0.203737000	-2.017060000
6	-2.019633000	-1.062416000	1.718898000
1	-1.923444000	-0.039573000	2.115731000
1	-2.934497000	-1.511347000	2.144223000
1	-1.161777000	-1.654194000	2.076110000
6	-2.136813000	-2.478827000	-0.378484000
1	-3.040635000	-3.004344000	-0.021114000
1	-2.171116000	-2.481594000	-1.480448000
1	-1.262743000	-3.068400000	-0.061189000
6	-3.332595000	-0.253823000	-0.274452000
1	-3.429491000	-0.255378000	-1.372464000
1	-4.251787000	-0.702212000	0.142832000
1	-3.276121000	0.793562000	0.060335000
<sup>1</sup> BuAsHTeBH <sub>2</sub> NMe <sub>3</sub>			
5	-1.469563000	1.489265000	-0.109056000
1	-1.673246000	2.191680000	-1.079522000
1	-1.319830000	2.108909000	0.924176000
33	0.341299000	0.482575000	-0.504192000
7	-2.770934000	0.534774000	0.088330000
6	-3.953363000	1.439508000	0.170989000
6	-2.678703000	-0.253290000	1.355677000
6	-2.956984000	-0.397682000	-1.063491000
1	-3.591702000	-0.855511000	1.482192000
1	-2.572225000	0.442960000	2.196507000
1	-1.800895000	-0.915141000	1.307782000
1	-4.863291000	0.846076000	0.350811000
1	-4.050496000	1.995604000	-0.769252000
1	-3.805538000	2.150859000	0.992888000
1	-3.910036000	-0.937499000	-0.952937000
1	-2.128051000	-1.119735000	-1.080891000
5	-2.966782000	0.184237000	-1.994026000
6	1.842275000	1.662168000	0.184808000
52	0.651641000	-1.952702000	0.070141000
1	0.583085000	0.670845000	-1.997476000
6	1.829783000	1.606887000	1.716384000
1	1.959061000	0.575580000	2.080626000
1	2.659530000	2.216155000	2.116036000
1	0.892279000	2.006031000	2.134572000
6	1.593760000	3.089674000	-0.322516000
1	2.416354000	3.747864000	0.010380000
1	1.562455000	3.134983000	-1.423439000
1	0.653560000	3.511128000	0.064610000
6	3.161896000	1.109892000	-0.365058000
1	3.200346000	1.162136000	-1.465236000
1	4.005451000	1.705091000	0.027620000
1	3.314131000	0.060632000	-0.068224000
<sup>1</sup> BuAsOHOBH <sub>2</sub> NMe <sub>3</sub>			
5	-1.139247000	0.664348000	-0.868359000
1	-1.220690000	0.284971000	-2.017620000
1	-0.965856000	1.861668000	-0.751368000
33	0.420978000	-0.347493000	0.055317000
7	-2.528323000	0.287859000	-0.099103000
6	-3.642404000	0.885576000	-0.884106000
6	-2.535167000	0.850383000	1.287709000
6	-2.718951000	-1.193063000	-0.015002000
1	-3.491265000	0.608438000	1.777907000
1	-2.416218000	1.939394000	1.227665000
1	-1.694772000	0.403030000	1.840074000
1	-4.601687000	0.699618000	-0.375735000
1	-3.658856000	0.438353000	-1.885595000
1	-3.476100000	1.965940000	-0.979225000
1	-3.731422000	-1.414667000	0.356626000
1	-1.968633000	-1.595758000	0.678937000
1	-2.576726000	-1.630639000	-1.010966000
6	2.215573000	0.528273000	-0.076753000
8	0.119898000	-0.842612000	1.615724000
6	2.162488000	1.798497000	0.783456000
1	1.894579000	1.560281000	1.824863000
1	3.149555000	2.294163000	0.788992000
1	1.429343000	2.525781000	0.397765000
6	2.506021000	0.850135000	-1.547523000
1	3.509877000	1.300769000	-1.647678000
1	2.477697000	-0.059524000	-2.167193000
1	1.778822000	1.567513000	-1.961946000
6	3.234791000	-0.467917000	0.491036000
1	3.290547000	-1.377200000	-0.127948000
1	4.240844000	-0.013120000	0.513810000
1	2.964743000	-0.765681000	1.516391000
8	0.667024000	-1.836877000	-0.951027000
1	0.938942000	-2.538218000	-0.338185000
<sup>1</sup> BuAsSHSBH <sub>2</sub> NMe <sub>3</sub>			
5	-1.199916000	0.528213000	-1.029122000
1	-1.204327000	-0.122927000	-2.054073000
1	-1.034713000	1.718522000	-1.205113000
33	0.414328000	-0.165148000	0.128705000
7	-2.639469000	0.332504000	-0.299301000
6	-3.682411000	0.623905000	-1.323415000
6	-2.795689000	1.289746000	0.839568000
6	-2.826959000	-1.063010000	0.204794000
1	-3.782824000	1.147078000	1.305911000
1	-2.710472000	2.313415000	0.454837000
1	-1.998919000	1.097580000	1.572803000
1	-4.680593000	0.579700000	-0.860629000
1	-3.613075000	-0.115175000	-2.130606000
1	-3.509929000	1.624725000	-1.738725000
1	-3.866948000	-1.195433000	0.540555000
1	-2.139628000	-1.231605000	1.045037000
1	-2.597373000	-1.770983000	-0.601051000
6	2.114224000	0.820168000	-0.392043000
16	0.205892000	-0.213942000	2.232748000
6	1.932398000	2.268737000	0.084100000
1	1.728004000	2.308992000	1.164918000
1	2.857879000	2.838431000	-0.112247000
1	1.110490000	2.777540000	-0.443837000
6	2.288925000	0.752490000	-1.913202000
1	3.202256000	1.300407000	-2.205924000
1	2.402238000	-0.285692000	-2.262059000
1	1.442520000	1.210352000	-2.449786000
6	3.285979000	0.155287000	0.335359000
1	3.425383000	-0.886009000	0.006953000
1	4.216585000	0.710231000	0.121935000
1	3.125597000	0.152507000	1.424419000
16	0.795226000	-2.330089000	-0.589133000
1	0.514212000	-2.069806000	-1.888654000
<sup>1</sup> BuAsSeHSBH <sub>2</sub> NMe <sub>3</sub>			

5	1.37888000	0.248975000	-1.362258000	6	1.571039000	3.269459000	0.118436000
1	1.271426000	1.385301000	-1.774582000	1	1.852699000	3.366786000	-0.943503000
1	1.349854000	-0.597356000	-2.232423000	1	1.253375000	4.268595000	0.468073000
33	-0.297159000	-0.094781000	-0.127719000	1	2.468446000	2.988386000	0.689352000
7	2.806244000	0.120166000	-0.597031000	6	0.076675000	2.152135000	1.802484000
6	3.841413000	0.635585000	-1.538300000	1	-0.187306000	3.148755000	2.205217000
6	3.115319000	-1.307022000	-0.273565000	1	-0.789829000	1.496862000	1.968637000
6	2.846119000	0.929036000	0.659538000	1	0.922150000	1.767343000	2.392093000
1	4.092659000	-1.365730000	0.229754000	6	-0.798849000	2.758459000	-0.478137000
1	3.141470000	-1.882912000	-1.206606000	1	-1.663467000	2.087964000	-0.375685000
1	2.327787000	-1.700980000	0.385317000	1	-1.106067000	3.753904000	-0.106521000
1	4.842219000	0.503109000	-1.098742000	1	-0.571554000	2.862529000	-1.551407000
1	3.657418000	1.699130000	-1.732058000	6	-0.248353000	-0.898402000	-0.164405000
1	3.775352000	0.082742000	-2.483722000	7	0.263475000	-2.074226000	-0.140340000
1	3.869891000	0.927706000	1.064214000	8	-0.699629000	-3.097597000	-0.059845000
1	2.157677000	0.485713000	1.391920000	1	-0.151369000	-3.892285000	-0.027354000
1	2.530201000	1.955787000	0.437604000	6	-1.720674000	-0.646754000	-0.086955000
6	-1.847375000	-0.707011000	-1.306384000	6	-2.458944000	-0.353275000	-1.255429000
34	-0.091710000	-1.427545000	1.690986000	6	-2.378570000	-0.738131000	1.160962000
6	-1.478038000	-2.112712000	-1.802333000	6	-3.829775000	-0.088337000	-1.143613000
1	-1.312080000	-2.802748000	-0.961032000	6	-3.749576000	-0.455446000	1.225640000
1	-2.306546000	-2.511294000	-2.414347000	6	-4.493456000	-0.114441000	0.089588000
1	-0.573893000	-2.106611000	-2.430995000	1	-4.396946000	0.138215000	-2.051958000
6	-1.997021000	0.271245000	-2.476778000	1	-4.253234000	-0.517808000	2.195490000
1	-2.823383000	-0.061105000	-3.130130000	6	-1.644653000	-1.201792000	2.396381000
1	-2.241059000	1.287143000	-2.129382000	1	-1.396932000	-2.271345000	2.299612000
1	-1.086860000	0.323395000	-3.094832000	1	-0.692301000	-0.670819000	2.542668000
6	-3.116101000	-0.753187000	-0.452109000	1	-2.258192000	-1.068254000	3.299712000
1	-3.400217000	0.247737000	-0.092838000	6	-1.800432000	-0.370969000	-2.614294000
1	-3.951471000	-1.148803000	-1.056422000	1	-1.378438000	-1.366756000	-2.828933000
1	-2.983474000	-1.408040000	0.422834000	1	-2.521319000	-0.127010000	-3.408589000
34	-0.983446000	2.109526000	0.686633000	1	-0.963450000	0.342316000	-2.674928000
1	-0.699437000	2.806623000	-0.587776000	6	-5.961693000	0.222524000	0.190980000
<b><sup>1</sup>BuAsTeHTeBH<sub>2</sub>NMe<sub>3</sub></b>				1	-6.505538000	-0.056560000	-0.724979000
5	-1.411844000	1.108471000	1.292115000	1	-6.437481000	-0.291346000	1.040613000
1	-0.927714000	2.214586000	1.405976000	1	-6.113503000	1.306395000	0.340480000
1	-1.706994000	0.584761000	2.346523000	<b>As(SAsS<sup>1</sup>BuBH<sub>2</sub>NMe<sub>3</sub>)<sub>3</sub></b>			
33	0.104794000	-0.099760000	0.437128000	33	0.000000000	0.000000000	0.178944000
7	-2.774474000	1.242422000	0.418137000	33	-1.204427000	3.382188000	0.172461000
6	-3.582038000	2.318523000	1.062866000	16	0.068014000	1.944446000	1.446880000
6	-3.561566000	-0.028609000	0.444166000	16	-1.959788000	2.379130000	-1.550619000
6	-2.503193000	1.626832000	-1.000132000	7	0.884847000	5.039757000	-1.469942000
1	-4.90663000	0.102599000	-0.131450000	6	-2.708827000	3.892890000	1.444890000
1	-3.800159000	-0.275675000	1.485747000	6	1.862487000	6.160579000	-1.379473000
1	-2.959843000	-0.835433000	0.001648000	1	2.537695000	5.982111000	-0.534145000
1	-4.554005000	2.408185000	0.553488000	1	1.321248000	7.100974000	-1.214707000
1	-3.037617000	3.268078000	0.997507000	1	2.443069000	6.222867000	-2.313029000
1	-3.738444000	2.067367000	2.119375000	6	1.634690000	3.750631000	-1.604246000
1	-3.454223000	1.842753000	-1.510789000	1	2.358617000	3.825847000	-2.428871000
1	-1.994129000	0.796596000	-1.508169000	1	0.926767000	2.940331000	-1.814036000
1	-1.858713000	2.514321000	-1.016294000	1	2.157956000	3.531753000	-0.667475000
6	1.267743000	-0.755145000	1.997789000	6	-2.086224000	4.533753000	2.691119000
52	-0.462690000	-1.975312000	-1.132261000	1	-1.419787000	3.832184000	3.216784000
6	0.405614000	-1.748622000	2.789795000	1	-2.886167000	4.824877000	3.395359000
1	0.093492000	-2.599041000	2.164392000	1	-1.511346000	5.440565000	2.446829000
1	0.998140000	-2.145220000	3.633435000	6	-3.599421000	4.888349000	0.687994000
1	-0.495316000	-1.276189000	3.210180000	1	-3.065580000	5.818795000	0.440583000
6	1.652582000	0.452789000	2.858774000	1	-4.466116000	5.157273000	1.317812000
1	2.263656000	0.110978000	3.713076000	1	-3.979660000	4.448711000	-0.247280000
1	2.255188000	1.181015000	2.294125000	6	-3.499456000	2.634044000	1.804865000
1	0.771519000	0.971536000	3.266718000	1	-3.917910000	2.160356000	0.904057000
6	2.506342000	-1.452071000	1.433475000	1	-4.336599000	2.903815000	2.473234000
1	3.138380000	-0.758374000	0.857937000	1	-2.874894000	1.889302000	2.319158000
1	3.111995000	-1.850129000	2.266835000	6	0.027269000	5.239118000	-2.676937000
1	2.230957000	-2.293054000	0.778477000	1	-0.472402000	6.213088000	-2.601383000
52	1.663873000	1.547120000	-0.952692000	1	-0.724681000	4.438020000	-2.713086000
1	1.602408000	2.806880000	0.155670000	1	0.653887000	5.210210000	-3.581765000
<b>MesCNOHAs<sup>1</sup>BuBH<sub>2</sub>NMe<sub>3</sub></b>				5	0.000000000	5.083370000	-0.113511000
5	2.615219000	-0.036099000	0.871288000	1	-0.748831000	6.037238000	-0.187215000
1	2.218200000	-0.884630000	1.642932000	1	0.751983000	5.117441000	0.837286000
1	3.061986000	0.956066000	1.418772000	33	3.531274000	-0.648030000	0.172461000
33	1.125040000	0.523984000	-0.517288000	16	1.649933000	-1.031125000	1.446880000
7	3.922850000	-0.705066000	0.094588000	16	3.040281000	0.507661000	-1.550619000
6	4.886770000	-1.125221000	1.146454000	7	3.922134000	-3.286179000	-1.469942000
6	4.578413000	0.290049000	-0.794725000	6	4.725755000	0.399468000	1.444890000
6	3.530208000	-1.897573000	-0.704959000	6	4.403975000	-4.693251000	-1.379473000
1	5.452447000	-0.160906000	-1.291772000	1	3.911813000	-5.188764000	-0.534145000
1	4.896553000	1.152216000	-0.195649000	1	5.489000000	-4.694722000	-1.214707000
1	3.855237000	0.626811000	-1.548413000	1	4.167626000	-5.227194000	-2.313029000
1	5.795637000	-1.545836000	0.685580000	6	2.430797000	-3.290998000	-1.604246000
1	4.410231000	-1.877656000	1.785865000	1	2.133972000	-3.955546000	-2.428871000
1	5.148099000	-0.255100000	1.761063000	1	2.083018000	-2.272770000	-1.814036000
1	4.428296000	-2.383696000	-1.119467000	1	1.979610000	-3.634722000	-0.667475000
1	2.865394000	-1.584275000	-1.518710000	6	4.969457000	-0.460154000	2.691119000
1	2.969894000	-2.588024000	-0.065471000	1	4.028662000	-0.686520000	3.216784000
6	0.421639000	2.265050000	0.313304000	1	5.621549000	0.087056000	3.395359000
				1	5.467341000	-1.411419000	2.446829000

6	6.033145000	0.673016000	0.687994000
1	6.572014000	-0.254527000	0.440583000
1	6.699388000	1.289134000	1.317812000
1	5.842527000	1.222132000	-0.247280000
6	4.030877000	1.713595000	1.804865000
1	3.829878000	2.312832000	0.904057000
1	4.683077000	2.303698000	2.473234000
1	3.073630000	1.545080000	2.319158000
6	4.523575000	-2.643175000	-2.676937000
1	5.616893000	-2.697432000	-2.601383000
1	4.205778000	-1.591418000	-2.713086000
1	4.185231000	-3.171388000	-3.581765000
5	4.402327000	-2.541685000	-0.113511000
1	5.602817000	-2.370112000	-0.187215000
1	4.055843000	-3.209957000	0.837286000
33	-2.326848000	-2.734158000	0.172461000
16	-1.717947000	-0.913321000	1.446880000
16	-1.080493000	-2.886791000	-1.550619000
7	-4.806981000	-1.753579000	-1.469942000
6	-2.016928000	-4.292358000	1.444890000
6	-6.266462000	-1.467329000	-1.379473000
1	-6.449508000	-0.793347000	-0.534145000
1	-6.810248000	-2.406252000	-1.214707000
1	-6.610695000	-0.995673000	-2.313029000
6	-4.065487000	-0.459633000	-1.604246000
1	-4.492589000	0.129699000	-2.428871000
1	-3.009785000	-0.667562000	-1.814036000
1	-4.137566000	0.102968000	-0.667475000
6	-2.883234000	-4.073599000	2.691119000
1	-2.608875000	-3.145664000	3.216784000
1	-2.735382000	-4.911932000	3.395359000
1	-3.955995000	-4.029146000	2.446829000
6	-2.433724000	-5.561365000	0.687994000
1	-3.506434000	-5.564268000	0.440583000
1	-2.233271000	-6.446407000	1.317812000
1	-1.862866000	-5.670842000	-0.247280000
6	-0.531421000	-4.347640000	1.804865000
1	0.088032000	-4.473188000	0.904057000
1	-0.346478000	-5.207512000	2.473234000
1	-0.198736000	-3.434382000	2.319158000
6	-4.550844000	-2.595943000	-2.676937000
1	-5.144491000	-3.515656000	-2.601383000
1	-3.481098000	-2.846602000	-2.713086000
1	-4.839118000	-2.038822000	-3.581765000
5	-4.402327000	-2.541685000	-0.113511000
1	-4.853986000	-3.667126000	-0.187215000
1	-4.807825000	-1.907484000	0.837286000

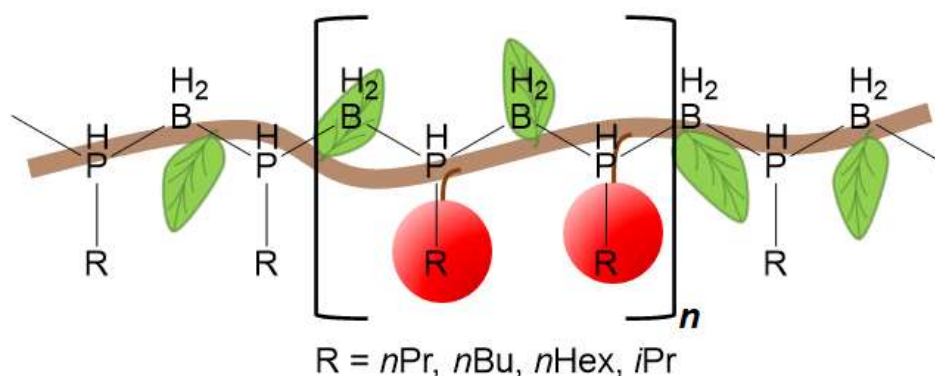
**References.**

- [1] a) A. D. Becke, *J. Chem. Phys.* **1993**, *98*, 5648; b) Lee, Yang, Parr, *Phys. rev. B, Condensed matter* **1988**, *37*, 785.
- [2] a) F. Weigend, R. Ahlrichs, *Phys. Chem. Chem. Phys.* **2005**, *7*, 3297; b) K. A. Peterson, D. Figgen, E. Goll, H. Stoll, M. Dolg, *J. Chem. Phys.* **2003**, *119*, 11113.
- [3] M. J. Frisch, G. W. Trucks, H. B. Schlegel, G. E. Scuseria, M. A. Robb, J. R. Cheeseman, G. Scalmani, V. Barone, B. Mennucci, G. A. Petersson, H. Nakatsuji, M. Caricato, X. Li, H. P. Hratchian, A. F. Izmaylov, J. Bloino, G. Zheng, J. L. Sonnenberg, M. Hada, M. Ehara, K. Toyota, R. Fukuda, J. Hasegawa, M. Ishida, T. Nakajima, Y. Honda, O. Kitao, H. Nakai, T. Vreven, J. A. Montgomery, Jr., J. E. Peralta, F. Ogliaro, M. Bearpark, J. J. Heyd, E. Brothers, K. N. Kudin, V. N. Staroverov, T. Keith, R. Kobayashi, J. Normand, K. Raghavachari, A. Rendell, J. C. Burant, S. S. Iyengar, J. Tomasi, M. Cossi, N. Rega, J. M. Millam, M. Klene, J. E. Knox, J. B. Cross, V. Bakken, C. Adamo, J. Jaramillo, R. Gomperts, R. E. Stratmann, O. Yazyev, A. J. Austin, R. Cammi, C. Pomelli, J. W. Ochterski, R. L. Martin, K. Morokuma, V. G. Zakrzewski, G. A. Voth, P. Salvador, J. J. Dannenberg, S. Dapprich, A. D. Daniels, O. Farkas, J. B. Foresman, J. V. Ortiz, J. Cioslowski, and D. J. Fox, Gaussian 09, Revision E.01, Gaussian, Inc., Wallingford CT, 2013.
- [4] a) K. L. Schuchardt, B. T. Didier, T. Elsethagen, L. Sun, V. Gurumoorthi, J. Chase, J. Li, T. L. Windus, *J. Chem. Inform. Model.* **2007**, *47*, 1045; b) D. Feller, *J. Comput. Chem.* **1996**, *17*, 1571.
- [5] A. S. Lisovento, A. Y. Timoshkin, *Inorg. Chem.* **2010**, *49*, 10357.
- [6] Computational Chemistry Comparison and Benchmark DataBase, Release 21, August 2020, NIST Standard Reference Database 101, <https://cccbdb.nist.gov/vibscale.asp>.

#### 4.6. Author contributions

- The synthesis and characterization of compounds **2-4c** have been performed by Felix Lehnfeld
- X-ray structural analysis of compounds **2**, **3c** and **4a** have been performed by Felix Lehnfeld and Dr. Michael Seidl, of **4c** and **4c x H<sub>2</sub>O** by Felix Lehnfeld.
- The DFT calculations have been performed by Prof. Dr. Alexey Timoshkin
- The manuscript (including supporting information, figures, schemes and graphical abstract) was written by Felix Lehnfeld with Prof. Dr. Alexey Timoshkin contributing the segments concerning the theoretical data and Dr. Michael Seidl contributing to the X-ray part in the supporting information.
- Lorenz Dittrich is gratefully acknowledged for contributions to the syntheses of **2**, **3a-b** and **4a** during his bachelor thesis (Regensburg, **2020**)

## 5. Mono alkyl substituted phosphanylboranes (HRP–BH<sub>2</sub>–NMe<sub>3</sub>) as precursors for poly(alkylphosphinoborane)s: improved synthesis and comparative study



A new synthetic pathway to various mono-alkyl substituted phosphanylborane HRP–BH<sub>2</sub>•NMe<sub>3</sub> has been developed. The new synthetic route starting from alkyl halides and NaPH<sub>2</sub> followed by metalation and salt metathesis is performed in a one-pot procedure and leads to higher yields and purity of the resulting phosphanylboranes compared to previously reported routes. Additionally, the scope of accessible compounds could be expanded from short-chained linear alkyl substituents to longer chained linear alkyl substituents as well as secondary or functionalized alkyl substituents. The reported examples include primary alkyl substituted phosphanylboranes RHP–BH<sub>2</sub>•NMe<sub>3</sub> (R = *n*-butyl, *n*-pentyl, *n*-hexyl; **1a-c**), the secondary alkyl substituted *i*PrPH–BH<sub>2</sub>•NMe<sub>3</sub> (**2**) and the alkyl bridged diphosphanylborane Me<sub>3</sub>N•BH<sub>2</sub>PHC<sub>4</sub>H<sub>8</sub>PH–BH<sub>2</sub>•NMe<sub>3</sub> (**3a**). Compounds **1a**, **1c** and **2** have additionally been used for preliminary polymerization reactions via a thermal and a transition metal catalyzed pathway, revealing the formation of high molecular weight polymers under certain conditions. Detailed investigations on the influence of temperature, concentration, substituents and reaction time on the respective polymerization reactions have been performed.



leads to the formation of high molecular weight polymers.<sup>[6]</sup> Via this pathway also the formation of alkyl substituted arsenic-boron oligomers was reported recently.<sup>[7]</sup> Recently, a titanium catalyzed polymerization of **I** under very mild conditions and by shorter reaction times has been achieved (Scheme 1).<sup>[8]</sup> So far, the scope of accessible polymers was very limited by the range of suitable starting materials, as only a few mono-alkyl substituted phosphanylboranes have been reported so far. Therefore, the search for a more generally applicable and improved synthetic route to alkyl substituted phosphanylboranes was still open.

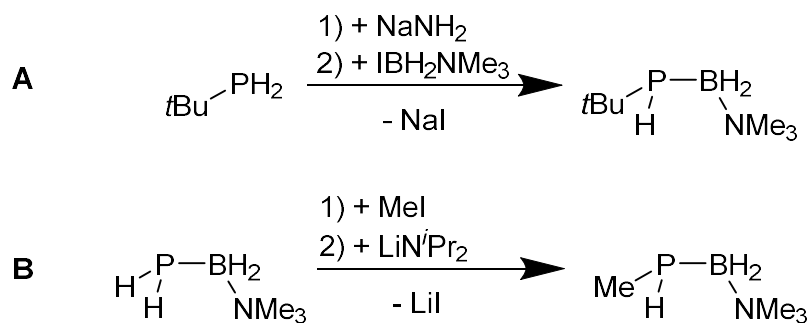
Herein we report on a synthetic procedure which is applicable for a variety of primary alkyl substituents as well as for secondary and even functionalized alkyl residues. Furthermore, the obtained monomers have been used as starting materials for polymerization reactions, which have been thoroughly studied. Especially the influence of various conditions has been investigated in detail.

## 5.2. Results and Discussion

### General synthetic procedure

So far, alkyl substituted phosphanylboranes can be synthesized via two different synthetic routes. Either by metalation of a phosphine and subsequent salt metathesis reaction (path **A**)<sup>[6b]</sup> or by the formation of a phosphonium-borane salt by reaction of  $\text{PH}_2\text{-BH}_2\text{-NMe}_3$  with alkyl halides and subsequent deprotonation (path **B**).<sup>[6a]</sup> However, both methods have some disadvantages. Path **A** works very well for commercially available phosphines such as *t*BuPH<sub>2</sub>, but otherwise a prior synthesis of the phosphine is necessary. The established laboratory scale synthesis of monoalkylated phosphines can be considered as elaborate, time intensive and expensive. Additionally, the overall reaction is rather waste intensive and has low atom efficiency.

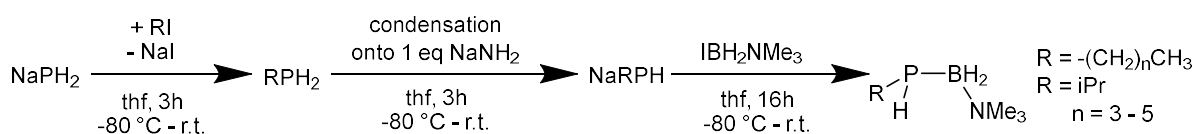
Method **B**, however, so far only has been reported for short chained, primary alkyl substituents ( $\text{R} = \text{Me}, \text{Et}, n\text{Pr}$ ) and is therefore rather limited in scope. Furthermore, the yield of resulting phosphanylboranes is mediocre at best when moving beyond the methyl substituted derivative (Scheme 2).



**Scheme 2.** Previously reported syntheses of monoalkyl substituted phosphanylboranes

In view of further possible reaction pathways, the synthesis of several monoalkyl phosphines from PH<sub>3</sub> and alkyl halides has been reported.<sup>[10]</sup> However, the challenge of handling the highly toxic phosphine gas in the laboratory makes this method difficult for the synthesis of substituted phosphines as starting material for phosphanylboranes on a day-to-day basis. By replacing the phosphine gas with NaPH<sub>2</sub> and performing the alkyl phosphine synthesis and the subsequent metalation of the phosphine by NaNH<sub>2</sub> in a one pot procedure, the release of toxic gases can be reduced to a minimum. This step can be followed up by a simple salt metathesis of the resulting phosphanide NaRHP with IBH<sub>2</sub>NMe<sub>3</sub>, leading directly to the desired phosphanylborane. (Scheme 3). With all starting materials readily available in gram scale and good yields, the products are accessible on a new scale (for further information, see SI).

Via this route different phosphanylboranes can be obtained in medium to good yields as colorless oils. In some cases, lower temperature and careful workup are necessary to reduce unwanted side-reactions to a minimum, such as the formation of the dialkylsubstituted phosphanylborane or unwanted thermal polymerization.



**Scheme 3.** General synthetic route for monoalkyl substituted phosphanylboranes starting from NaPH<sub>2</sub>, alkyl halides and IBH<sub>2</sub>NMe<sub>3</sub>

All obtained compounds reveal a broad singlet or pseudo-quartet in the <sup>31</sup>P{<sup>1</sup>H} NMR spectra, which show further splitting into a triplet in the <sup>31</sup>P NMR spectra. The chemical shifts for phosphanylboranes with primary alkyl substituents are about δ = -130 ppm, for an *i*Pr substituent at δ = -92 ppm. Independent of the substituents, all compounds

reveal similar  $^1J_{P,H}$  coupling constants of about 200 Hz. In the  $^{11}B\{^1H\}$  NMR spectra a doublet for all compounds is observed with very similar chemical shifts around  $\delta = -3$  ppm and a  $^1J_{P,B}$  coupling constant of about 50 Hz. In the  $^{11}B$  NMR spectra, all products reveal further splitting into a triplet of doublets with a  $^1J_{B,H}$  coupling of ca. 100 Hz. All the observed chemical shifts are in good agreement with values for already reported phosphanylboranes.<sup>[6,9]</sup>

Some general trends can be observed: The synthesis of primary alkyl phosphanylboranes proceeds with good yields, with the *n*-hexyl substituted compounds being the best with up to 66%. Longer chained alkyl substituents lead to higher yields due to less losses during condensation. Furthermore, the formation of the most prominent side product, dialkylsubstituted phosphanylborane, is not observed for primary alkyl substituted phosphanylboranes, but a significant decrease in yield and purity has been observed for formation of a butyl bridged phosphanylborane.

### Phosphanylboranes with primary alkyl substituents

Expanding on the already reported MeHP-BH<sub>2</sub>-NMe<sub>3</sub> further phosphanylboranes with primary alkyl substituents have been investigated. To cover a variety of different features within this type of substituents, three different phosphanylboranes have been prepared: the rather short-chained *n*PrHP-BH<sub>2</sub>•NMe<sub>3</sub> (**1a**), the longer chained *n*HexHP-BH<sub>2</sub>•NMe<sub>3</sub> (*n*Hex = *n*-hexyl; **1c**) and the linear isomer to the very well investigated *t*Bu derivative, *n*BuHP-BH<sub>2</sub>•NMe<sub>3</sub> (**1b**). All compounds are accessible via adjusted synthetic procedures of method **B** starting from the unsubstituted H<sub>2</sub>P-BH<sub>2</sub>•NMe<sub>3</sub>, but yields are moderate at best (for details, refer to SI). Using the new method reported herein, yields can be heavily increased, especially considering the phosphorus-based atom efficiency. Additionally, the reaction can be scaled up significantly compared to previous reports, offering an improved access to these monomers as precursors for poly(phosphinoborane)s. The chemical shifts as well as the yields of compounds **1a-c** obtained by this method and by adjusted literature methods are summarized in table 1.

**Table 1.** Chemical shifts and yields of compounds **1a-c** obtained by adjusted literature procedures and as reported in this work

Compound	substituent	$\delta$ ( <sup>31</sup> P) [a]	$\delta$ ( <sup>11</sup> B) [a]	yield [b]
<b>1a</b>	<i>n</i> -propyl	-130.4	-3.2	28%/29%
<b>1b</b>	<i>n</i> -butyl	-127.6	-4.0	13%/54%
<b>1c</b>	<i>n</i> -hexyl	-128.7	-3.3	38%/66%

[a] in ppm in toluene solution; [b] adjusted literature procedure<sup>[6b]</sup>/this work; both referred to NaPH<sub>2</sub>

Polymerization experiments with compounds **1a-c** have been performed under varying conditions, both via thermal elimination of the stabilizing NMe<sub>3</sub> Lewis base as well as catalytic conditions using the recently reported bispentafulvene [Ti] catalyst.<sup>[8,11]</sup> Overall, the influence of temperature, reaction time, concentration and solvent as well as the presence and concentration of the catalyst have been investigated and will be discussed in the following.

For all three compounds, thermal polymerization at room temperature reveals comparably long reaction times. Under these conditions several days of stirring are necessary to achieve conversion of >50% of the starting material. Reaction times over 14 days lead to increasing amounts of decomposition as observed by new signals in the <sup>11</sup>B and <sup>31</sup>P NMR spectra, without any noteworthy increase in conversion rates. Already slightly elevated temperatures (323 K) lead to a significant decrease in the necessary reaction times, resulting in similar conversion rates in solution after only three to five days.

The concentration of the phosphanylborane has strong influence on its polymerization behavior. In all cases, already noticeably shorter reaction times lead to full conversion for more concentrated systems. The best results have been reached, when almost no solvent is used. Due to the increasing viscosity of the formed polymers, traces of toluene are always necessary to still achieve full conversion, therefore a completely neat approach is not feasible. When heating **1c** in the presence of traces of toluene to 323K, full conversion is achieved within only two days of stirring. However, these conditions reveal small amounts of side products that could not be further identified but are most likely formed in competing thermal induced decomposition reactions. A clear trend emerged during the studies: The chain length of the substitute directly influences the reaction times, with increasing chain length also reaction times increased.

When the polymerization reaction is performed in the presence of the recently reported bispentafulvene [Ti] catalyst,<sup>[8]</sup> significant differences can be observed: The presence of the [Ti] catalyst leads to drastically reduced reaction times in the frame of hours, but in all cases, the reaction stopped at around 80% conversion. In this case, neither increased temperature nor longer reaction times lead to an improvement. Changing the solvent to more polar solvents like THF or using mixtures of toluene and THF did not impact the reaction in a meaningful way. Catalyst loading, which has been identified as an important factor in the [Ti] catalyzed polymerization of *t*BuHPBH<sub>2</sub>•NMe<sub>3</sub>, did not lead to any observable differences for the investigated reactions with compounds **1a-c**. In analogy to the thermal polymerization, the concentration of the phosphanylborane seems to be crucial to good conversion and fast reactions. The most significant reduction of reaction time accompanied by higher conversion was observed when only traces of toluene are used as solvent. In contrast to thermal polymerization of **1-c** or catalytic polymerization of *t*BuPHBH<sub>2</sub>•NMe<sub>3</sub>, however, complete conversion was not observed for **1a-c** under the applied conditions in the presence of the [Ti] catalyst.

**Table 2.** Overview over results from polymerization experiments under varying conditions using **1c** as starting material.

Catalyst loading	Reaction time	Temperature	Concentration <b>1c</b> [mol/L]	Conversion
-	16 h	r.t.	0.1	18%
-	16 h	323 K	Neat <sup>[a]</sup>	84%
-	40 h	323 K	Neat <sup>[a]</sup>	100% <sup>[b]</sup>
10 mol%	3 h	r.t.	0.1	17%
10 mol%	3 h	r.t.	0.2	27%
4 mol%	30 min	r.t.	0.4	18%
4 mol%	90 min	r.t.	0.4	22%
4 mol%	7 d	r.t.	0.4	41%
4 mol%	21 d	r.t.	0.4	65%

[a] traces of toluene/*n*-hexane are necessary to provide suitable viscosity during the reaction; [b] accompanied by small amounts of unidentified side products

From the primary alkyl substituted monomers, **1c** was selected to be characterized by ESI mass spectrometry in addition to multinuclear NMR spectroscopy. Whereas for the catalytic polymerization only aggregates with a molar mass of up to 1700 Da ( $n = 12$ )

could be observed, it was possible to observe peaks for polymers with up to 2700 Da ( $n = 20$ ) for polymerization under thermal conditions (323 K, traces of toluene). In both cases, polymers with three different end groups could be identified (Fig. 1). Further investigation on the nature of these polymers considering polydispersity, tacticity and more detailed data on the end groups and chain lengths of the resulting polymers will be the focus of future work and will give valuable insight in the nature of the resulting polymers.

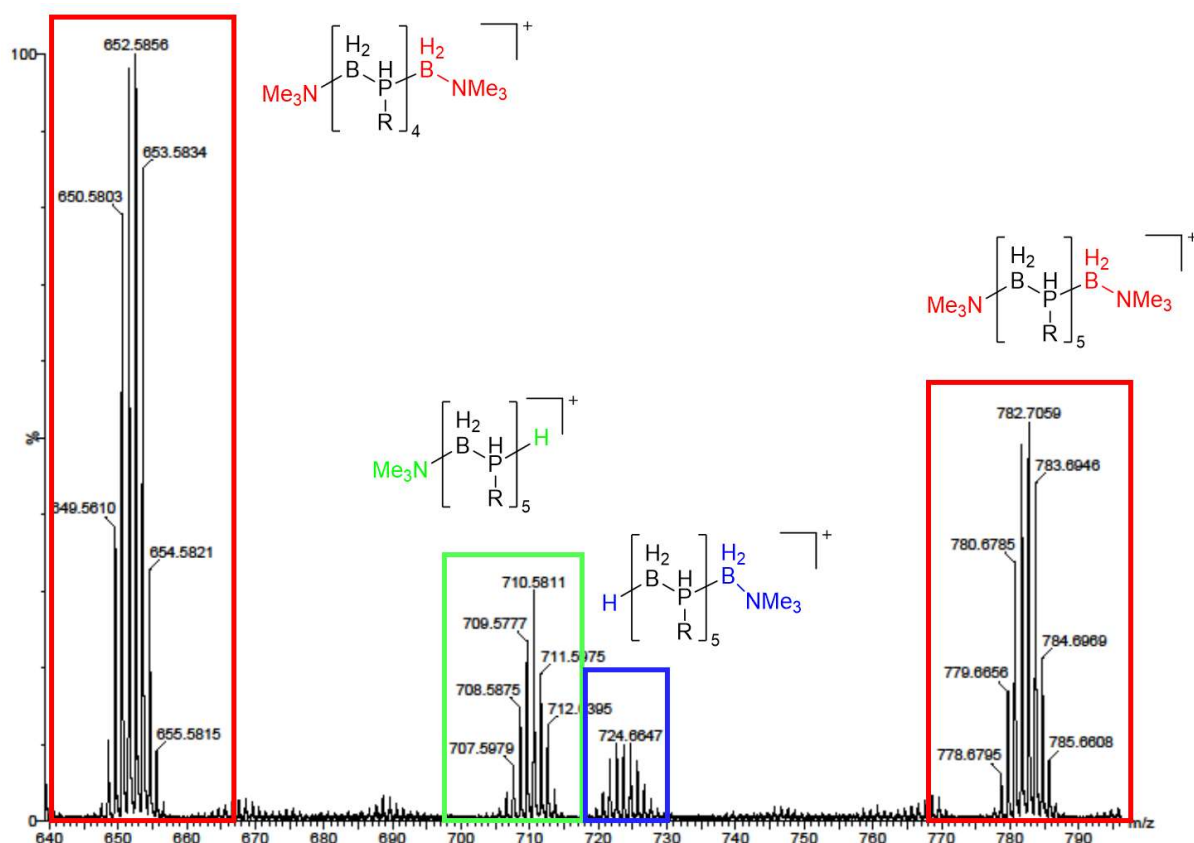


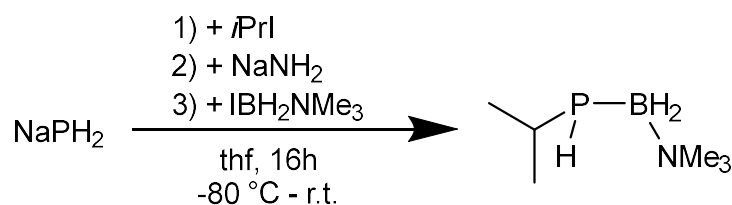
Figure 1. End groups observed in the ESI mass spectra of poly-1c

### Phosphanylboranes with secondary alkyl substituents

Secondary alkyl substituents position themselves as a promising starting material in terms of solubility, reactivity and steric hinderance between primary alkyl substituents like *n*Pr and tertiary alkyl substituents like *t*Bu. Therefore, the quest for a suitable phosphanylborane with a secondary alkyl substituent was still open, as the synthesis via method **B** for such substituents is not applicable as reported. Adapting the reported method **B** by using one equivalent of the Lewis acid AlCl<sub>3</sub> to activate the iso-propyl halide led to both the formation of the phosphonium borane salt and the corresponding phosphanylborane after a secondary deprotonation step (Scheme 4).

Applying the synthetic procedure presented in this work allowed for a significant improvement, not needing the additional Lewis acid while providing improved purity and good yields. The obtained phosphanylborane was investigated by multinuclear NMR spectroscopy, as discussed in the first part of the results and discussion. The reaction showed almost no side reactions or decomposition, even less than observed for **1a-c** (Scheme 3, **D**).

In contrast to other phosphanylboranes, the *i*Pr substituted phosphanylborane **2** revealed a way lower tendency to polymerization. Thermal polymerization at r.t. did only lead to minimal conversion, while [Ti] based catalytic polymerization revealed an unexpected behavior: Similar as reported for the parent phosphanylborane,<sup>[8]</sup> the formation of polymeric species is not observed. Instead, a significant broadening of the signal corresponding to **2** in the <sup>31</sup>P NMR spectra is observed, which increased with higher catalyst load without any new signals emerging (Fig. 2). Simultaneously an unusual color change to a deep purple is observed, indicating the potential formation of a paramagnetic species. In the case of a stoichiometric reaction with the [Ti] complex, the signal for compound **2** disappears completely from the NMR spectra, but no product could be isolated regardless of numerous attempts.



**Scheme 4.** Synthesis of an *i*Pr substituted-phosphanylborane **2**

The unusual behavior in both thermal and catalytic polymerization experiments makes **2** a very interesting compound for future investigations, as both isolating a product from the reaction with the [Ti] catalyst as well as applying different conditions for the thermal polymerization such as more concentrated systems as well as elevated temperatures could lead to interesting insights.

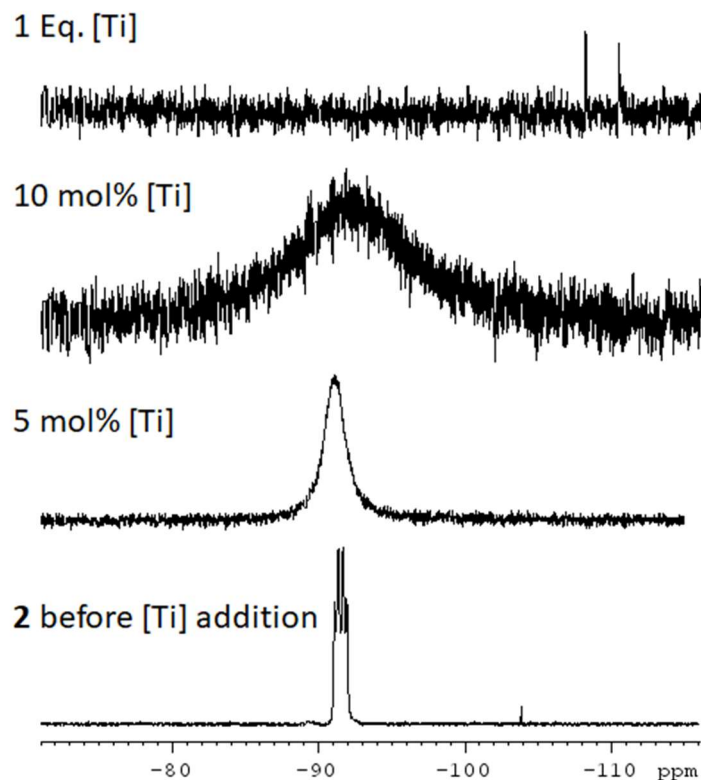


**Figure 2.** Signal broadening in the <sup>31</sup>P{<sup>1</sup>H} NMR spectra of the reaction solution of **2** in the presence of different amounts of [Ti]

### Alkyl-bridged diphosphanylborane

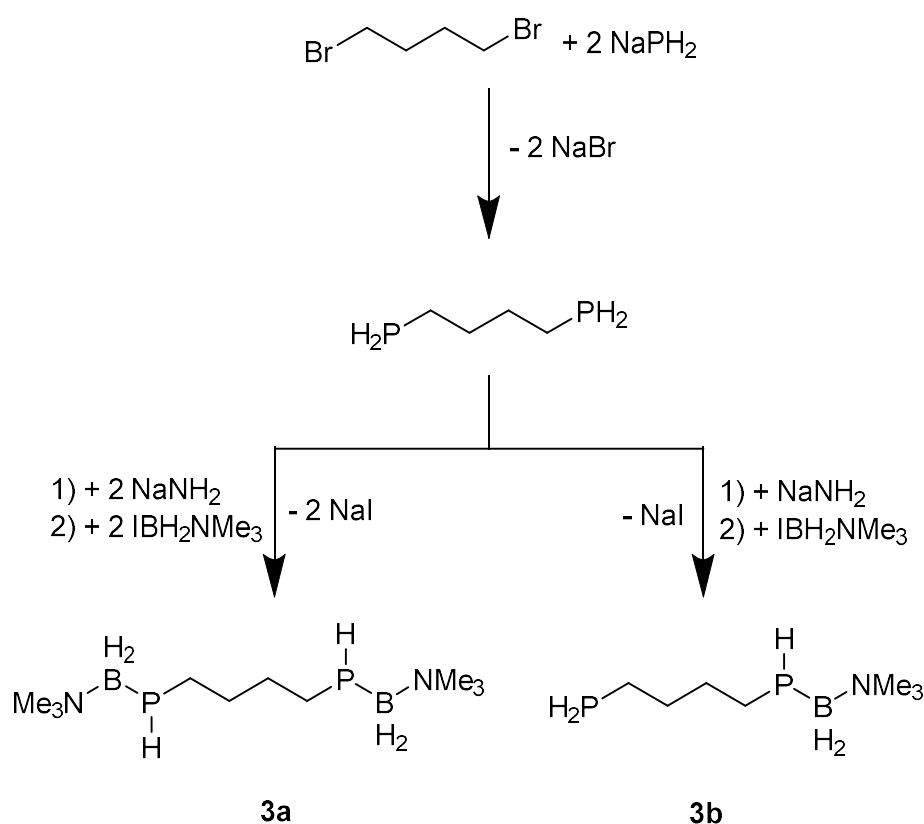
In the industrial application of polymers, crosslinking and other linked networks play an important role. Therefore, the investigation of a phosphanylborane with additional functionalized groups is of great interest.

Using the well-developed access to phosphanylboranes with primary alkyl substituents allows to access this kind of chemistry. A crosslinking should be possible by preforming the linkage in the monomer. By the reaction of NaPH<sub>2</sub> with an alkyl dihalide with suitable chain length a diphosphine and a subsequent diphosphanylborane is accessible (Scheme 5).

The first step of the reaction yields the corresponding diphosphine. The reaction proceeds under full conversion according to <sup>31</sup>P NMR spectroscopy of the crude reaction mixture. In addition to the diphosphine, revealing a triplet at  $\delta = -137.3$  ppm in the <sup>31</sup>P NMR spectrum ( $^1J_{P,H} = 189$  Hz), the bromobutylphosphine BrC<sub>4</sub>H<sub>8</sub>PH<sub>2</sub> is formed as a minor side product. Upon metalation and reaction with IBH<sub>2</sub>NMe<sub>3</sub>, a very unselective reaction is observed, but in addition to unreacted diphosphine, two promising products can be identified: the bridged diphosphanylborane **3a** and the

phosphinebutylphosphanylborane **3b**, which has only reacted with one equivalent of  $\text{NaNH}_2$ . A product ratio of 1:1 was observed.

The two products have been investigated by NMR spectroscopy: Compound **3a** reveals a pseudo-quartet at  $\delta = -68.8$  ppm in the  $^{31}\text{P}\{^1\text{H}\}$  NMR spectrum, whereas for **3b** a similar signal is observed at  $\delta = -128.1$  ppm. In both cases coupling to the boron atom is observed with  $^1J_{\text{P,B}}$  coupling constants of 51 Hz. Both show further splitting as a doublet of multiplets in the  $^{31}\text{P}$  NMR spectrum with  $^1J_{\text{P,H}}$  coupling constants of around 200 Hz. In the case of **3b**, the signal for the unreacted  $\text{PH}_2$  is observed as a triplet at  $\delta = -138.7$  ppm with a  $^1J_{\text{P,H}}$  coupling constant of 189 Hz. In the  $^{11}\text{B}\{^1\text{H}\}$  NMR spectrum **3a** reveals a broad doublet at  $\delta = -3.9$  ppm, **3b** a strongly broadened signal at  $\delta = 4.5$  ppm. In the  $^{11}\text{B}$  NMR spectrum, both reveal further splitting with respective  $^1J_{\text{B,H}}$  coupling constants of 120 Hz (**3a**) and 112 Hz (**3b**). In addition, multiple decomposition products can be observed in the  $^{11}\text{B}$  NMR spectrum. Therefore, further investigation of the reaction conditions is necessary to isolate clean diphosphanylborane from this reaction system, as purification of this reaction mixture was not possible in the scope of this work.



**Scheme 5.** Synthesis of a butyl-bridged diphosphanylborane **3a** and most the most prominent side product **3b**

### 5.3. Conclusion

With substituted phosphanylboranes as an important precursor for functionalized inorganic polymers, having a flexible synthetic route for different substituents is of great value. With the approach presented in this work, various primary alkyl substituted phosphanylboranes are accessible in high purity and yields. The resulting compounds **1a-c** have been used as starting materials for thermal and [Ti] catalyzed polymerization reactions. All three compounds revealed good properties in these reactions, leading to the formation of polymers with up to 30 repetition units. This system allowed to investigate in detail the influence of various factors such as concentration, temperature, reaction time or catalyst loading. It was possible to identify the best conditions for these polymerizations to be at elevated temperatures in very concentrated solutions.

Furthermore, two new phosphanylborane system were investigated. In addition to being inaccessible by established synthetic routes up to this day, both the *i*Pr substituted phosphanylborane **2** and the butyl bridged diphosphanylborane **3a** reveal surprising and interesting properties, that distinguish them from already reported compounds. The detailed investigation of these compounds as well as their potential as polymer precursors will be the focus of future work.

### 5.4. References

- [1] a) M. Chanda, S. K. Roy, *Industrial polymers, specialty polymers, and their applications*, CRC press, **2008**; b) M. R. Aguilar, J. San Román, *Smart polymers and their applications*, Woodhead publishing, **2019**.
- [2] a) M. A. Gauthier, M. I. Gibson, H. A. Klok, *Angew. Chem. Int. Ed.* **2009**, *48*, 48-58; b) C. E. Carraher, J. A. Moore, *Modification of polymers, Vol. 21*, Springer Science & Business Media, **2012**.
- [3] a) M. Liang, I. Manners, *J. Am. Chem. Soc.* **1991**, *113*, 4044-4045; b) H. R. Allcock, *Chem. Mater.* **1994**, *6*, 1476-1491; c) C. H. Honeyman, I. Manners, C. T. Morrissey, H. R. Allcock, *J. Am. Chem. Soc.* **1995**, *117*, 7035-7036; d) R. D. Archer, *Inorganic and Organometallic Polymers*, Wiley VCH, New York, **2001**; e) I. Manners, *Angew. Chem. Int. Ed.* **1996**, *35*, 1602-1621; f) S. J. Clarson, J. A. Semlyen, *Siloxane polymers*, Prentice Hall, **1993**; g) R. H. Neilson, P. Wisian-Neilson, *Chem. Rev.* **1988**, *88*, 541-562; h) R. D. Miller, J. Michl, *Chem. Rev.* **1989**,

- 89, 1359-1410; i) R. D. Jaeger, M. Gleria, *Prog. Polym. Sci.* **1998**, *23*, 179-276; j) X. He, T. Baumgartner, *RSC Adv.* **2013**, *3*, 11334-11350; k) S. Wilfert, H. Henke, W. Schoefberger, O. Brüggemann, I. Teasdale, *Macromol. Rapid Commun.* **2014**, *35*, 1135-1141; l) B. W. Rawe, C. P. Chun, D. P. Gates, *Chem. Sci.* **2014**, *5*, 4928-4938; m) P. J. Fazen, J. S. Beck, A. T. Lynch, E. E. Remsen, L. G. Sneddon, *Chem. Mater.* **1990**, *2*, 96-97; n) F. Jäkle, *Chem. Rev.* **2010**, *110*, 3985-4022; o) H. Kutz, F. Cheng, S. Schwedler, L. Böhring, A. Brockhinke, L. Weber, K. Parab, F. Jäkle, *ACS Macro Lett.* **2012**, *1*, 555-559; p) Z. M. Hudson, D. J. Lunn, M. A. Winnik, I. Manners, *Nat. Commun.* **2014**, *5*; q) A. Lorbach, M. Bolte, H. Li, H. W. Lerner, M. C. Holthausen, F. Jäkle, M. Wagner, *Angew. Chem. Int. Ed.* **2009**, *48*, 4584-4588; r) H. R. Allcock, C. Chen, *J. Org. Chem.* **2020**, *85*, 14286-14297; s) F. Vidal, F. Jäkle, *Angew. Chem. Int. Ed.* **2019**, *58*, 5846-5870.
- [4] a) A. Hübner, Z.-W. Qu, U. Englert, M. Bolte, H.-W. Lerner, M. C. Holthausen, M. Wagner, *J. Am. Chem. Soc.* **2011**, *133*, 4596-4609; b) T. Imori, V. Lu, H. Cai, T. D. Tilley, *J. Am. Chem. Soc.* **1995**, *117*, 9931-9940; c) A. Staubitz, A. Presa Soto, I. Manners, *Angew. Chem. Int. Ed.* **2008**, *47*, 6212-6215; d) J. R. Vance, A. P. Robertson, K. Lee, I. Manners, *Eur. J. Chem.* **2011**, *17*, 4099-4103; e) A. Staubitz, M. E. Sloan, A. P. M. Robertson, A. Friedrich, S. Schneider, P. J. Gates, J. Schmedt auf der Günne, I. Manners, *J. Am. Chem. Soc.* **2010**, *132*, 13332-13345; f) B. L. Dietrich, K. I. Goldberg, D. M. Heinekey, T. Autrey, J. C. Linehan, *Inorg. Chem.* **2008**, *47*, 8583-8585; g) H. C. Johnson, A. P. Robertson, A. B. Chaplin, L. J. Sewell, A. L. Thompson, M. F. Haddow, I. Manners, A. S. Weller, *J. Am. Chem. Soc.* **2011**, *133*, 11076-11079; h) H. C. Johnson, A. S. Weller, *Angew. Chem. Int. Ed.* **2015**, *54*, 10173-10177; i) H. C. Johnson, E. M. Leitao, G. R. Whittell, I. Manners, G. C. Lloyd-Jones, A. S. Weller, *J. Am. Chem. Soc.* **2014**, *136*, 9078-9093; j) A. L. Colebatch, A. S. Weller, *Eur. J. Chem.* **2019**, *25*, 1379-1390; k) D. Han, F. Anke, M. Trose, T. Beweries, *Coord. Chem. Rev.* **2019**, *380*, 260-286; l) L. Wirtz, J. Lambert, B. Morgenstern, A. Schäfer, *Organometallics* **2021**, *40*, 2108-2117.
- [5] a) J.-M. Denis, H. Forintos, H. Szelke, L. Toupet, T.-N. Pham, P.-J. Madec, A.-C. Gaumont, *Chem. Commun.* **2003**, 54-55; b) H. Dorn, R. A. Singh, J. A. Massey, J. M. Nelson, C. A. Jaska, A. J. Lough, I. Manners, *J. Am. Chem. Soc.* **2000**, *122*, 6669-6678; c) H. Dorn, R. A. Singh, J. A. Massey, A. J. Lough, I. Manners, *Angew. Chem. Int. Ed.* **1999**, *38*, 3321-3323; d) H. Dorn, J. M. Rodezno, B. Brunnhöfer, E.

- Rivard, J. A. Massey, I. Manners, *Macromolecules* **2003**, *36*, 291-297; e) T. J. Clark, J. M. Rodezno, S. B. Clendenning, S. Aouba, P. M. Brodersen, A. J. Lough, H. E. Ruda, I. Manners, *Eur. J. Chem.* **2005**, *11*, 4526-4534; f) S. Pandey, P. Lönnecke, E. Hey-Hawkins, *Eur. J. Inorg. Chem.* **2014**, *2014*, 2456-2465; g) D. Jacquemin, C. Lambert, E. A. Perpète, *Macromolecules* **2004**, *37*, 1009-1015; h) A. Schäfer, T. Jurca, J. Turner, J. R. Vance, K. Lee, V. A. Du, M. F. Haddow, G. R. Whittell, I. Manners, *Angew. Chem. Int. Ed.* **2015**, *54*, 4836-4841; i) H. Cavaye, F. Clegg, P. J. Gould, M. K. Ladyman, T. Temple, E. Dossi, *Macromolecules* **2017**, *50*, 9239-9248.
- [6] a) C. Marquardt, T. Jurca, K.-C. Schwan, A. Stauber, A. V. Virovets, G. R. Whittell, I. Manners, M. Scheer, *Angew. Chem. Int. Ed.* **2015**, *54*, 13782-13786; b) A. Stauber, T. Jurca, C. Marquardt, M. Fleischmann, M. Seidl, G. R. Whittell, I. Manners, M. Scheer, *Eur. J. Inorg. Chem.* **2016**, 2684-2687.
- [7] F. Lehnfeld, M. Seidl, A. Y. Timoshkin, M. Scheer, *Eur. J. Inorg. Chem.* **2022**, *2022*, e202100930.
- [8] a) Dissertation Jens Braese, Universität Regensburg; b) Manuscript in preparation
- [9] K. P. Langhans, O. Stelzer, J. Svara, N. Weferling, *Z. Naturforsch. B* **1990**, *45*, 203-211.
- [10] U. Vogel, P. Hoemensch, K.-C. Schwan, A. Y. Timoshkin, M. Scheer, *Eur. J. Chem* **2003**, *9*, 515-519.
- [11] M. Diekmann, G. Bockstiegel, A. Lützen, M. Friedemann, W. Saak, D. Haase, R. Beckhaus, *Organometallics* **2006**, *25*, 339-348.

## 5.5. Supporting information

### Experimental section

#### General remarks

All reactions have been performed under Argon or Nitrogen inert gas atmosphere using standard glove-box and Schlenk techniques. All solvents have been taken from a solvent purification system of the type MB-SPS-800 of the company MBRAUN and have been degassed by standard procedures. All NMR spectra were recorded on a Bruker Avance 400 spectrometer ( $^1\text{H}$ : 400.13 MHz,  $^{13}\text{C}\{^1\text{H}\}$ : 100.623 MHz,  $^{11}\text{B}$ : 128.387 MHz,  $^{31}\text{P}$ : 161.976 Hz) with  $\delta$  [ppm] referenced to external standards ( $^1\text{H}$  and  $^{13}\text{C}\{^1\text{H}\}$ :  $\text{SiMe}_4$ ,  $^{11}\text{B}$ :  $\text{BF}_3\text{-Et}_2\text{O}$ ,  $^{31}\text{P}$ :  $\text{H}_3\text{PO}_4$ ). All mass spectra were recorded on a Micromass LCT ESI-TOF.

#### Synthesis of *n*PrPHBH<sub>2</sub>NMe<sub>3</sub> (**1a**), *n*BuPHBH<sub>2</sub>NMe<sub>3</sub> (**1b**), *n*HexPHBH<sub>2</sub>NMe<sub>3</sub> (**1c**) by adjusted literature procedures.

Following the literature procedure for  $\text{MePHBH}_2\text{NMe}_3$ ,<sup>[1]</sup> Compounds **1a-1c** were prepared by using *n*PrI, *n*BuI and *n*HexI as replacement for MeI.

Yields (referred to  $\text{NaPH}_2$ )

**1a**:  $m = 72$  mg (0.49 mmol, 28%).

**1b**:  $m = 57$  mg (0.46 mmol, 13%).

**1c**:  $m = 125$  mg (0.67 mmol, 38%).

#### One-pot synthesis of *n*PrPHBH<sub>2</sub>NMe<sub>3</sub> (**1a**), *n*BuPHBH<sub>2</sub>NMe<sub>3</sub> (**1b**), *n*HexPHBH<sub>2</sub>NMe<sub>3</sub> (**1c**)

For the preparation of **1b**, a H-shaped Schlenk flask for condensation is filled with  $\text{NaPH}_2$  (0.99 g, 17.6 mmol) on one side and  $\text{NaNH}_2$  (700 mg, 17.9 mmol) on the other side.  $\text{NaPH}_2$  is suspended in 5 mL THF and the suspension cooled to 213 K. *n*BuI (2 mL, 3.24 g, 17.6 mmol) is added to the suspension and the mixture stirred for 16 h, while the solution is allowed to reach r.t. The formation of white precipitate is observed. The resulting THF solution of *n*BuPH<sub>2</sub> is then condensed onto the solid  $\text{NaNH}_2$  in the other half of the flask. The mixture is allowed to reach room temperature under stirring. After stirring overnight, a yellow solution is obtained. A solution of  $\text{IBH}_2\text{NMe}_3$  (3.8 g, 17.6 mmol) in THF is added to the yellow solution and the mixture is stirred overnight. A color change from yellow to colorless and the formation of white precipitate is observed. After removing the solvent *in vacuo*, compound **1b** is extracted with *n*-

hexane and filtered over diatomaceous earth. After removing the solvent *in vacuo*, compound **1b** is obtained as a colorless oil.

Compounds **1a** and **1c** are obtained by the same procedure, using *n*PrI, and *n*HexI instead of *n*Bul and with different sample sizes.

Yield:

**1a**: *m* = 0.414 g (2.82 mmol, 29%)

**1b**: *m* = 1.537 g (9.5 mmol, 54%)

**1c**: *m* = 1.256 g (6.6 mmol, 66%)

**1a**: <sup>31</sup>P{<sup>1</sup>H} NMR (crude, 293 K): δ [ppm] = -130.4 (q, <sup>1</sup>J<sub>P;B</sub> = 46 Hz); <sup>31</sup>P NMR (crude, 293 K): δ [ppm] = -130.4 (dq, <sup>1</sup>J<sub>P;H</sub> = 206 Hz, <sup>1</sup>J<sub>P;B</sub> = 48 Hz); <sup>11</sup>B {<sup>1</sup>H} NMR (C<sub>6</sub>D<sub>6</sub>, 293 K): δ [ppm] = -3.2 (d, <sup>1</sup>J<sub>P;B</sub> = 48 Hz); <sup>11</sup>B NMR (C<sub>6</sub>D<sub>6</sub>, 293 K): δ [ppm] = -3.2 (td, <sup>1</sup>J<sub>B;H</sub> = 107 Hz, <sup>1</sup>J<sub>P;B</sub> = 48 Hz).

**1b**: <sup>1</sup>H NMR (C<sub>6</sub>D<sub>6</sub>, 293 K): δ [ppm] = 0.96 (t, <sup>3</sup>J<sub>H;H</sub> = 7 Hz, 3H, *n*Bu-CH<sub>3</sub>), 1.53 (m, 2H, *n*Bu-CH<sub>2</sub>), 1.63-1.88 (m, 4H, *n*Bu-CH<sub>2</sub>), 1.94 (s, 9H, NMe<sub>3</sub>), 2.43 (m, <sup>1</sup>J<sub>P;H</sub> = 196 Hz, 1H, PH), 2.25-3.10 (q, 2H, <sup>1</sup>J<sub>B;H</sub> = 105 Hz, BH<sub>2</sub>); <sup>31</sup>P{<sup>1</sup>H} NMR (C<sub>6</sub>D<sub>6</sub>, 293 K): δ [ppm] = -127.7 (q, <sup>1</sup>J<sub>P;B</sub> = 46 Hz); <sup>31</sup>P NMR (C<sub>6</sub>D<sub>6</sub>, 293 K): δ [ppm] = -127.7 (dq, <sup>1</sup>J<sub>P;H</sub> = 196 Hz, <sup>1</sup>J<sub>P;B</sub> = 46 Hz); <sup>11</sup>B {<sup>1</sup>H} NMR (C<sub>6</sub>D<sub>6</sub>, 293 K): δ [ppm] = -3.9 (d, <sup>1</sup>J<sub>P;B</sub> = 46 Hz); <sup>11</sup>B NMR (C<sub>6</sub>D<sub>6</sub>, 293 K): δ [ppm] = -3.9 (td, <sup>1</sup>J<sub>B;H</sub> = 105 Hz, <sup>1</sup>J<sub>P;B</sub> = 46 Hz).

**1c**: <sup>1</sup>H NMR (C<sub>6</sub>D<sub>6</sub>, 293 K): δ [ppm] = 0.88 (t, <sup>3</sup>J<sub>H;H</sub> = 7 Hz, 3H, *n*Hex-CH<sub>3</sub>), 1.33 (m, 2H, *n*Hex-CH<sub>2</sub>), 1.54 (pent, 2H, *n*Hex-CH<sub>2</sub>), 1.64-1.90 (m, 4H, *n*Hex-CH<sub>2</sub>), 1.95 (s, 9H, NMe<sub>3</sub>), 2.47 (m, <sup>1</sup>J<sub>P;H</sub> = 198 Hz, 1H, PH), 2.25-3.10 (q, 2H, <sup>1</sup>J<sub>B;H</sub> = 105 Hz, BH<sub>2</sub>); <sup>31</sup>P{<sup>1</sup>H} NMR (C<sub>6</sub>D<sub>6</sub>, 293 K): δ [ppm] = -128.2 (q, <sup>1</sup>J<sub>P;B</sub> = 48 Hz); <sup>31</sup>P NMR (C<sub>6</sub>D<sub>6</sub>, 293 K): δ [ppm] = -128.2 (dq, <sup>1</sup>J<sub>P;H</sub> = 198 Hz, <sup>1</sup>J<sub>P;B</sub> = 48 Hz); <sup>11</sup>B {<sup>1</sup>H} NMR (C<sub>6</sub>D<sub>6</sub>, 293 K): δ [ppm] = -4.1 (d, <sup>1</sup>J<sub>P;B</sub> = 48 Hz); <sup>11</sup>B NMR (C<sub>6</sub>D<sub>6</sub>, 293 K): δ [ppm] = -4.1 (td, <sup>1</sup>J<sub>B;H</sub> = 105 Hz, <sup>1</sup>J<sub>P;B</sub> = 48 Hz).

### Synthesis of [*i*PrPH<sub>2</sub>BH<sub>2</sub>NMe<sub>3</sub>]AlCl<sub>3</sub>I

To a solution of 253 mg (1.9 mmol) AlCl<sub>3</sub> in 10 mL Et<sub>2</sub>O a solution of 199 mg (1.9 mmol) PH<sub>2</sub>BH<sub>2</sub>NMe<sub>3</sub> in 4 mL toluene is added. After stirring for 15 min at r.t. 0.19 mL (1.9 mmol) *i*PrI is added and the mixture is stirred for 40 h. All volatiles are removed *in vacuo* and a colorless oil is obtained. The product is washed with toluene (2 x 5 mL) at -30 °C and extracted with 2 x 5 mL THF and filtrated over diatomaceous earth. After

removing the solvent *in vacuo* a colorless oil is obtained containing [*i*PrPHBH<sub>2</sub>NMe<sub>3</sub>]AlCl<sub>3</sub>l among two impurities. Further purification was not possible, therefore no yield could be determined.

<sup>31</sup>P{<sup>1</sup>H} NMR (crude, THF, 293 K): δ [ppm] = -64.4 (q, <sup>1</sup>J<sub>P;B</sub> = 65 Hz); <sup>31</sup>P NMR (crude, THF, 293 K): δ [ppm] = -64.4 (t, <sup>1</sup>J<sub>P;H</sub> = 416 Hz); <sup>11</sup>B{<sup>1</sup>H} NMR (crude, THF, 293 K): δ [ppm] = -11.6 (m); <sup>11</sup>B NMR (crude, THF, 293 K): δ [ppm] = -11.6 (m).

### Synthesis of *i*PrPHBH<sub>2</sub>NMe<sub>3</sub> (**2**)

#### from [*i*PrPHBH<sub>2</sub>NMe<sub>3</sub>]AlCl<sub>3</sub>l

To a solution of 51 mg (0.475 mmol) lithiumdiisopropylamide (LDA) in 5 mL THF a solution of the product mixture of [*i*PrPHBH<sub>2</sub>NMe<sub>3</sub>]l in 3 mL CH<sub>3</sub>CN is added at -243 K. After stirring for 30 min at 243 K, all volatiles are removed *in vacuo* at 243 K. The product is extracted with 3 x 4 mL *n*-hexane and filtrated over diatomaceous earth. **2** has been obtained as a colorless oil after removing the solvent. The oil could not be further purified, thus no yield could be determined.

#### from a one pot synthesis

For the preparation of **2**, a H-shaped Schlenk flask for condensation is filled with NaPH<sub>2</sub> (560 mg, 10 mmol) on one side and NaNH<sub>2</sub> (390 mg, 10 mmol) on the other side. NaPH<sub>2</sub> is suspended in 5 mL THF and the suspension cooled to 213 K. *i*PrI (2 mL, 760 mg, 10 mmol) is added to the suspension and the mixture stirred for 16 h, while the solution is allowed to reach r.t. The formation of white precipitate is observed. The resulting THF solution of *i*PrPH<sub>2</sub> is then condensed onto the solid NaNH<sub>2</sub> in the other half of the flask. The mixture is allowed to reach room temperature under stirring. After stirring overnight, a yellow solution is obtained. A solution of IBH<sub>2</sub>NMe<sub>3</sub> (2.0 g, 10 mmol) in THF is added to the yellow solution and the mixture is stirred overnight. A color change from yellow to colorless and the formation of white precipitate is observed. After removing the solvent *in vacuo*, compound **2** is extracted with *n*-hexane and filtered over diatomaceous earth. After removing the solvent *in vacuo*, compound **2** is obtained as a colorless oil.

Yield: m = 529 mg (3.6 mmol, 36%). <sup>31</sup>P{<sup>1</sup>H} NMR (crude, 293 K): δ [ppm] = -92.5 (q, <sup>1</sup>J<sub>P;B</sub> = 49 Hz); <sup>31</sup>P NMR (crude, 293 K): δ [ppm] = -92.5 (dq, <sup>1</sup>J<sub>P;H</sub> = 203 Hz, <sup>1</sup>J<sub>P;B</sub> = 49

Hz); <sup>11</sup>B{<sup>1</sup>H}-NMR (crude, 293 K)  $\delta$  = -4.3 (d, <sup>1</sup>J<sub>P,B</sub> = 49 Hz); <sup>11</sup>B-NMR (crude, 293 K)  $\delta$  = -4.3 (td, <sup>1</sup>J<sub>P;H</sub> = 203 Hz, <sup>1</sup>J<sub>P,B</sub> = 49 Hz).

### Synthesis of Me<sub>3</sub>NBH<sub>2</sub>PH<sub>2</sub>C<sub>4</sub>H<sub>8</sub>PH<sub>2</sub>BH<sub>2</sub>NMe<sub>3</sub> (**3a**) and H<sub>2</sub>PC<sub>4</sub>H<sub>8</sub>PH<sub>2</sub>BH<sub>2</sub>NMe<sub>3</sub> (**3b**)

For the preparation of **3a** and **3b**, a H-shaped Schlenk flask for condensation is filled with NaPH<sub>2</sub> (560 mg, 10 mmol) on one side and NaNH<sub>2</sub> (390 mg, 10 mmol) on the other side. NaPH<sub>2</sub> is suspended in 20 mL THF and the suspension cooled to 213 K. 1,4-dibrombutane (0.59 mL, 1.1 g, 5 mmol) is added to the suspension and the mixture stirred for 16 h, while the solution is allowed to reach r.t. The formation of white precipitate is observed. The resulting THF solution is then condensed onto the solid NaNH<sub>2</sub> in the other half of the flask. The mixture is allowed to reach room temperature under stirring. After stirring for 4 h while slowly warming up to room temperature, a yellow solution is obtained. A solution of IBH<sub>2</sub>NMe<sub>3</sub> (2.0 g, 10 mmol) in THF is added to the yellow solution and the mixture is stirred overnight. A color change from yellow to colorless and the formation of white precipitate is observed. After removing the solvent *in vacuo*, compounds **3a** and **3b** are extracted with *n*-hexane and filtered over diatomaceous earth. After removing the solvent *in vacuo*, the mixture of **3a** and **3b** is obtained as a colorless oil.

**3a**: <sup>31</sup>P{<sup>1</sup>H} NMR (crude, 293 K):  $\delta$  [ppm] = -68.8 (q, <sup>1</sup>J<sub>P;B</sub> = 51 Hz); <sup>31</sup>P NMR (crude, 293 K):  $\delta$  [ppm] = -68.8 (dq, <sup>1</sup>J<sub>P;H</sub> = 192 Hz, <sup>1</sup>J<sub>P,B</sub> = 51 Hz); <sup>11</sup>B{<sup>1</sup>H}-NMR (crude, 293 K)  $\delta$  = -3.9 (d, <sup>1</sup>J<sub>P,B</sub> = 51 Hz); <sup>11</sup>B-NMR (crude, 293 K)  $\delta$  = -3.9 (t, <sup>1</sup>J<sub>H,B</sub> = 120 Hz).

**3b**: <sup>31</sup>P{<sup>1</sup>H} NMR (crude, 293 K):  $\delta$  [ppm] = -128.1 (q, <sup>1</sup>J<sub>P;B</sub> = 51 Hz, PH<sub>2</sub>BH<sub>2</sub>), -138.7 (s, PH<sub>2</sub>CH<sub>2</sub>); <sup>31</sup>P NMR (crude, 293 K):  $\delta$  [ppm] = -128.1 (dq, <sup>1</sup>J<sub>P;H</sub> = 203 Hz, <sup>1</sup>J<sub>P,B</sub> = 51 Hz), -138.7 (t, <sup>1</sup>J<sub>P;H</sub> = 189 Hz, PH<sub>2</sub>CH<sub>2</sub>); <sup>11</sup>B{<sup>1</sup>H}-NMR (crude, 293 K)  $\delta$  = 4.5 (br); <sup>11</sup>B-NMR (crude, 293 K)  $\delta$  = -4.5 (brt, <sup>1</sup>J<sub>H,B</sub> = 112 Hz).

### Polymerization experiments of **1a**

A solution of **1a** in toluene was stirred under different conditions, in the presence or absence of a  $[(\eta^5:\eta^1\text{-C}_5\text{H}_4\text{C}_{10}\text{H}_{14})_2\text{Ti}]$ . Details are summarized in Table S1.

**Table S1.** Conditions used in polymerization experiments of **1a**

Catalyst loading	Reaction time	Temperature	Concentration <b>1c</b> [mol/L]	Conversion
-	90 min	r.t.	0.089	19%
-	24 h	r.t.	0.089	23%
<b>5 mol%</b>	90 min	r.t.	0.089	41%
5 mol%	24 h	r.t.	0.089	51%
10 mol%	24 h	r.t.	0.089	64%
10 mol%	210 min	r.t.	0.03	54%
10 mol%	42 h	r.t.	0.03	76%

### Polymerization experiments of **1b** under catalytic conditions

A solution of **1b** (9.5 mmol, 1.54 g) in 19 mL toluene is added to  $[(\eta^5:\eta^1\text{-C}_5\text{H}_4\text{C}_{10}\text{H}_{14})_2\text{Ti}]$  (0.475 mmol, 211 mg, 5 mol%) and stirred for 21 d at r.t. In the presence of [Ti], a color change to first green, then brown is observed. The solvent is removed *in vacuo*, the remaining highly viscous dark brown oil is washed three times with cold *n*-pentane

Conversion: 90%.

$^{31}\text{P}\{^1\text{H}\}$  NMR (crude, 293 K):  $\delta$  [ppm] = -63.3 (br, poly-**1b**);  $^{31}\text{P}$  NMR (crude, 293 K):  $\delta$  [ppm] = -63.3 (br, poly-**1b**);  $^{11}\text{B}\{^1\text{H}\}$ -NMR (crude, 293 K)  $\delta$  = -38.0 (br, poly-**1b**);  $^{11}\text{B}$ -NMR (crude, 293 K)  $\delta$  = -38.0 (br, poly-**1b**).

### Polymerization experiments of **1c** under thermal and catalytical conditions

A solution of **1c** in toluene was stirred under different conditions, in the presence or absence of a  $[(\eta^5:\eta^1\text{-C}_5\text{H}_4\text{C}_{10}\text{H}_{14})_2\text{Ti}]$ . Details are summarized in Table S2. In the presence of [Ti], a color change to first green, then brown is observed.

**Table S2.** Conditions used in polymerization experiments of **1c**

Catalyst loading	Reaction time	Temperature	Concentration <b>1c</b> [mol/L]	Conversion
-	16 h	r.t.	0.1	18%
-	16 h	323 K	Neat <sup>[a]</sup>	84%
-	40 h	323 K	Neat <sup>[a]</sup>	100% <sup>[b]</sup>
10 mol%	3 h	r.t.	0.1	17%
10 mol%	3 h	r.t.	0.2	27%
4 mol%	30 min	r.t.	0.4	18%
4 mol%	90 min	r.t.	0.4	22%
4 mol%	7 d	r.t.	0.4	41%
4 mol%	21 d	r.t.	0.4	65%

[a] traces of toluene/*n*-hexane are necessary to provide suitable viscosity during the reaction; [b] accompanied by unidentified side reactions

### Polymerization experiments of **2** under thermal and catalytic conditions

A solution of **2** in toluene (*c*= 0.2 mol/L) was stirred for 90 min either in the absence or in the presence of a [(η<sup>5</sup>:η<sup>1</sup>-C<sub>5</sub>H<sub>4</sub>C<sub>10</sub>H<sub>14</sub>)<sub>2</sub>Ti] (5 mol% or 10 mol%) and monitored by <sup>31</sup>P NMR spectroscopy. In the presence of [Ti], an unusual color change to purple is observed, which turns to brown after several days.

### Reaction of **2** with stoichiometric amounts of [(η<sup>5</sup>:η<sup>1</sup>-C<sub>5</sub>H<sub>4</sub>C<sub>10</sub>H<sub>14</sub>)<sub>2</sub>Ti]

To a solution of [(η<sup>5</sup>:η<sup>1</sup>-C<sub>5</sub>H<sub>4</sub>C<sub>10</sub>H<sub>14</sub>)<sub>2</sub>Ti] (90 mg, 0.2 mmol) in 3 mL toluene a solution of *i*PrPHBH<sub>2</sub>NMe<sub>3</sub> (29 mg, 0.2 mmol) in 0.27 mL toluene is added. A color change from blue-green over a green-purple color to a red-brown color is observed. The solution is stirred for 16 h at r.t. and reduced to 0.75 mL. By precipitating in 40 mL CH<sub>3</sub>CN a gray-green solid is obtained. The solvent is removed *in vacuo* and the obtained powder used for multinuclear NMR spectroscopy, which reveals empty <sup>31</sup>P and <sup>11</sup>B NMR spectra, indicating paramagnetism.

## NMR spectra

## Compound 1a

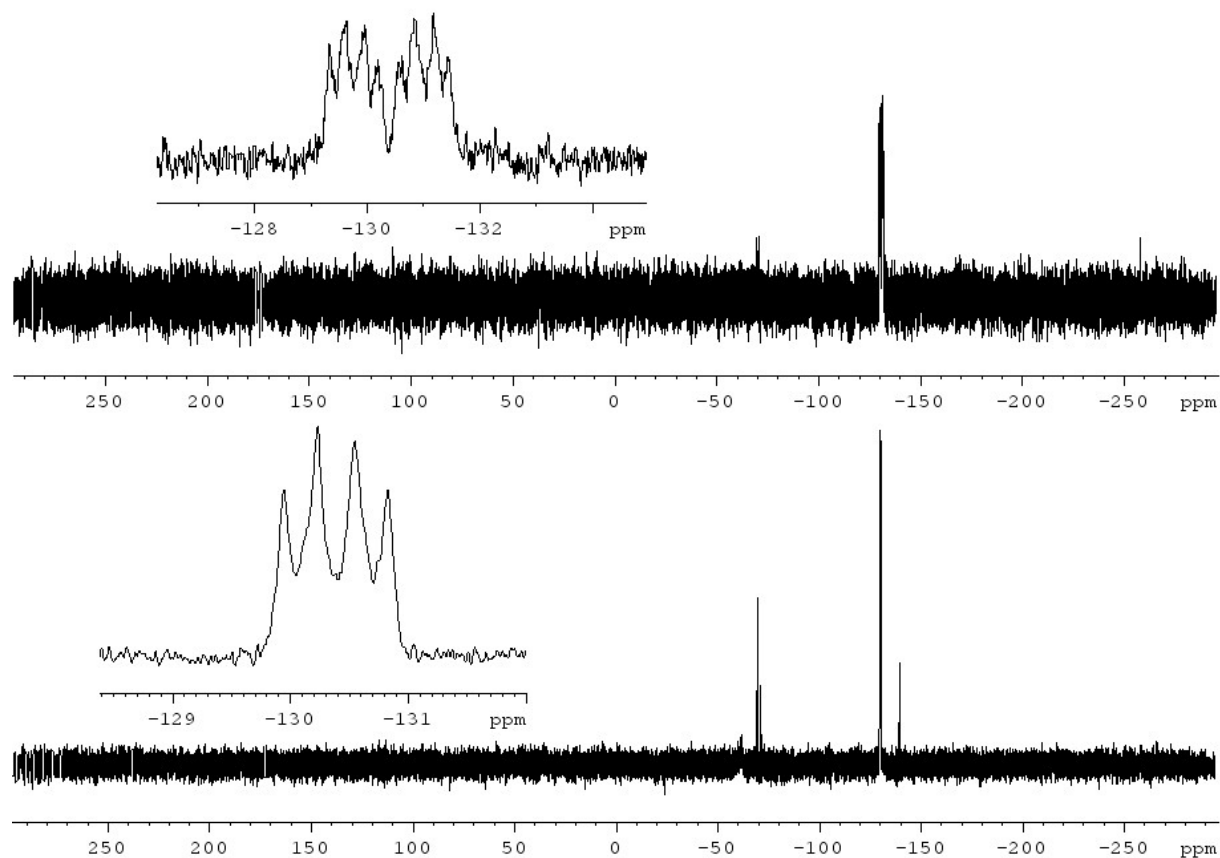


Figure S1.  $^{31}\text{P}$  NMR (top) and  $^{31}\text{P}\{^1\text{H}\}$  NMR (bottom) spectra of 1a in *n*-hexane

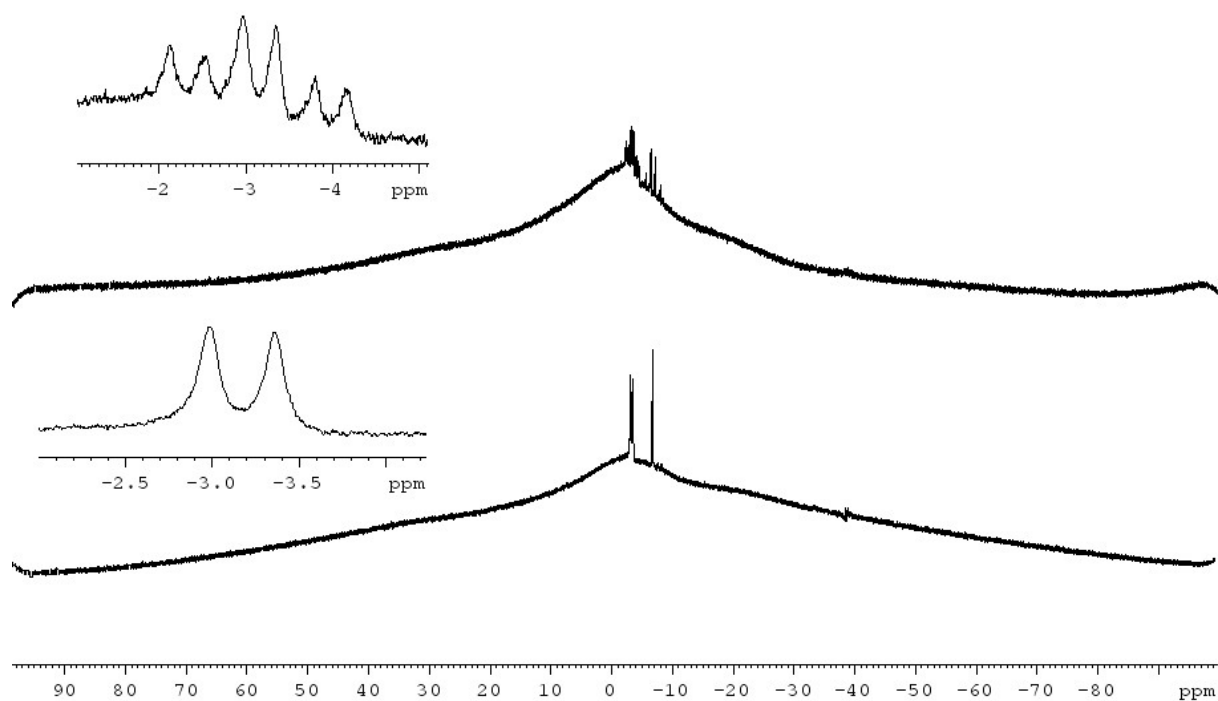
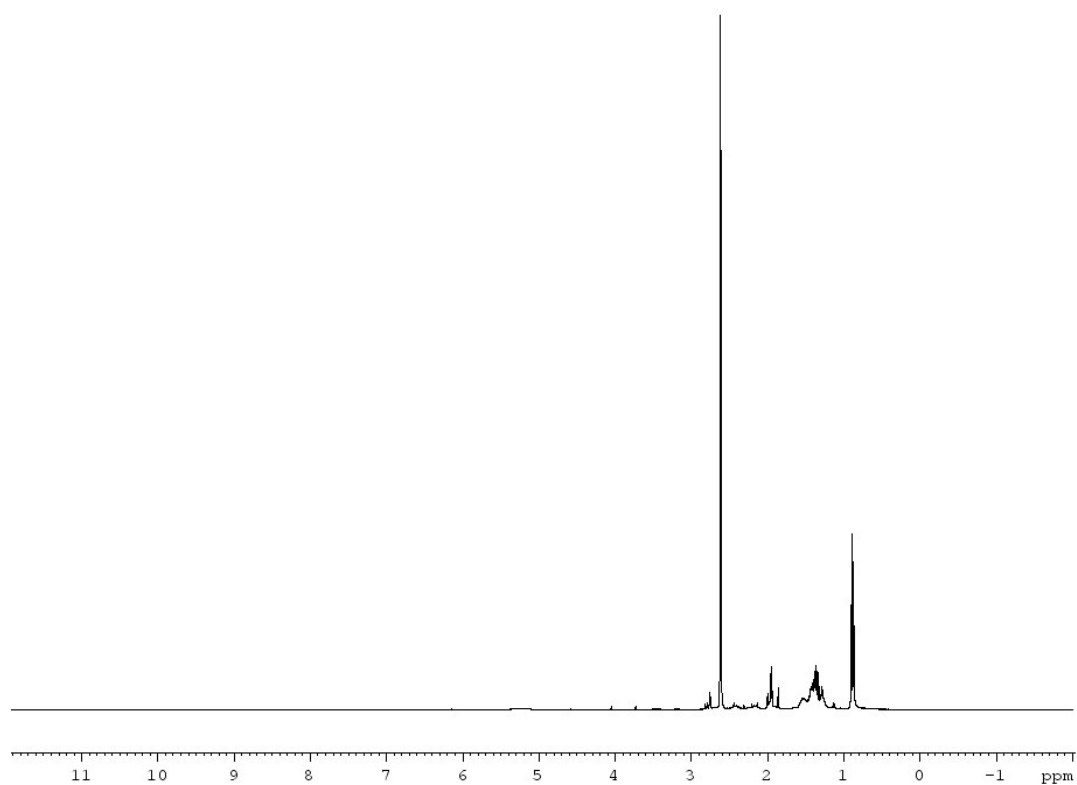
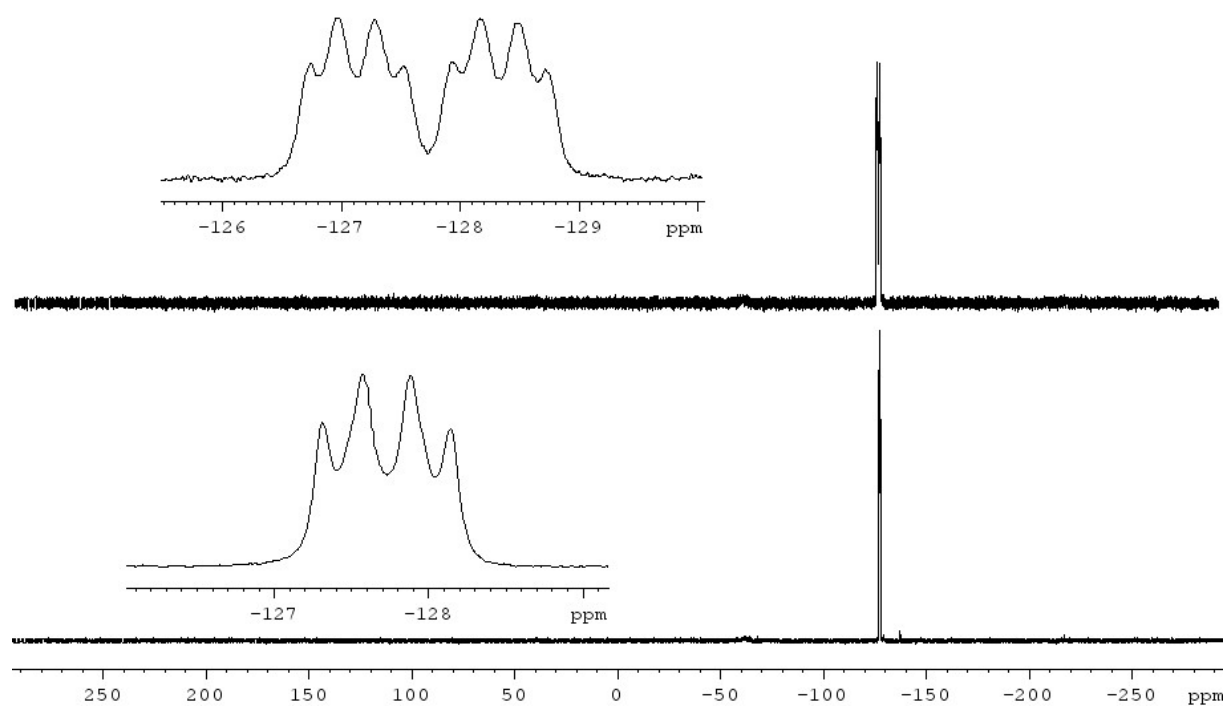
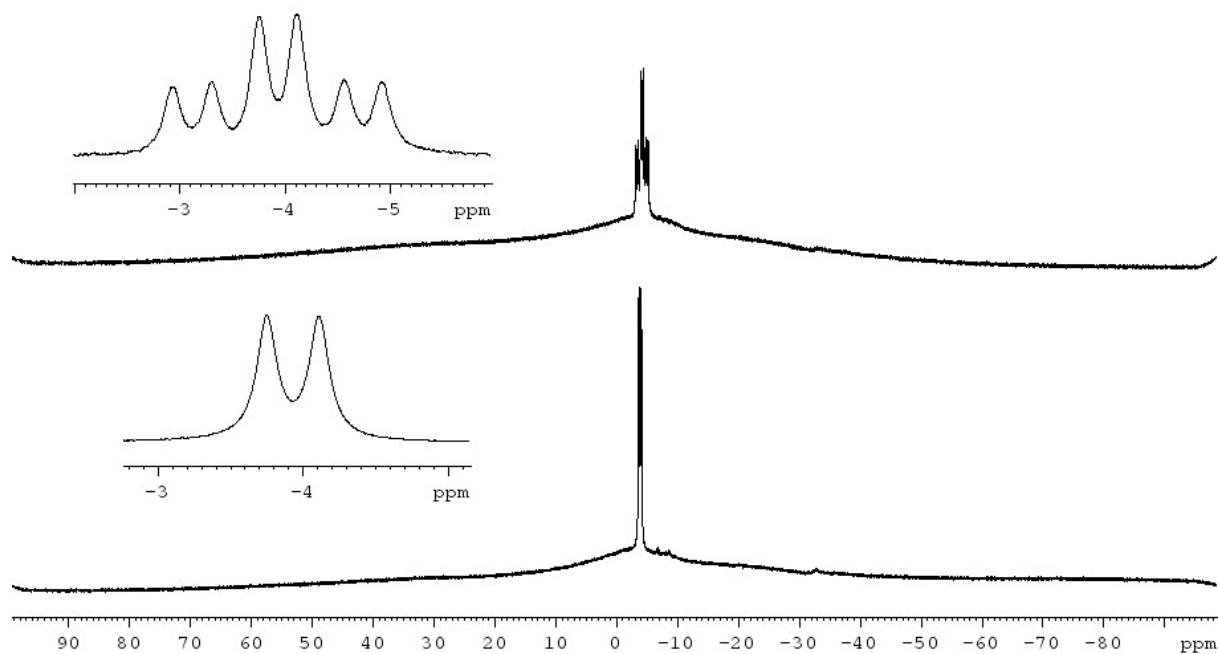


Figure S2.  $^{11}\text{B}$  NMR (top) and  $^{11}\text{B}\{^1\text{H}\}$  NMR (bottom) spectra of 1a in *n*-hexane

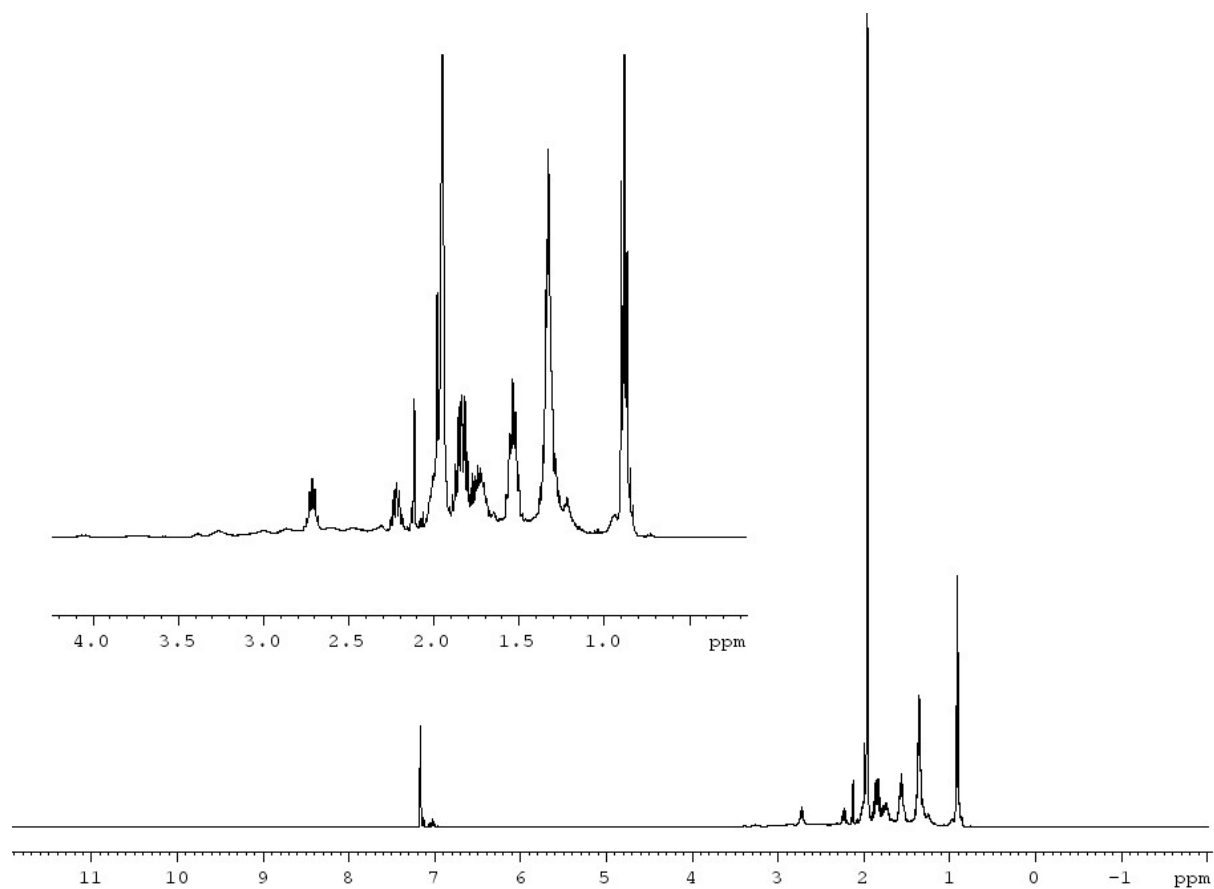
## Compound 1b

Figure S3. <sup>1</sup>H NMR spectrum of 1b in CD<sub>3</sub>CNFigure S4. <sup>31</sup>P NMR (top) and <sup>31</sup>P{<sup>1</sup>H} NMR (bottom) spectra of 1b in CD<sub>3</sub>CN



**Figure S5.**  $^{11}\text{B}$  NMR (top) and  $^{11}\text{B}\{^1\text{H}\}$  NMR (bottom) spectra of **1b** in  $\text{CD}_3\text{CN}$

### Compound **1c**



**Figure S6.**  $^1\text{H}$  NMR spectrum of **1c** in  $\text{C}_6\text{D}_6$

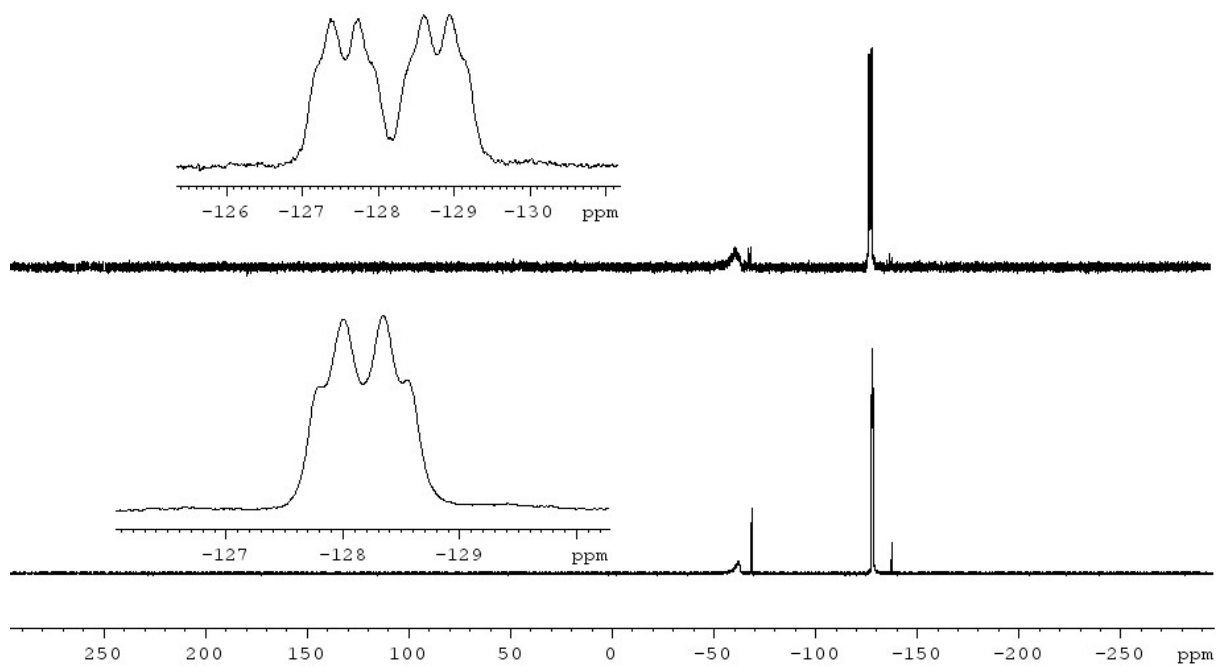


**Figure S7.** <sup>31</sup>P NMR (top) and <sup>31</sup>P{<sup>1</sup>H} NMR (bottom) spectra of **1c** in C<sub>6</sub>D<sub>6</sub>

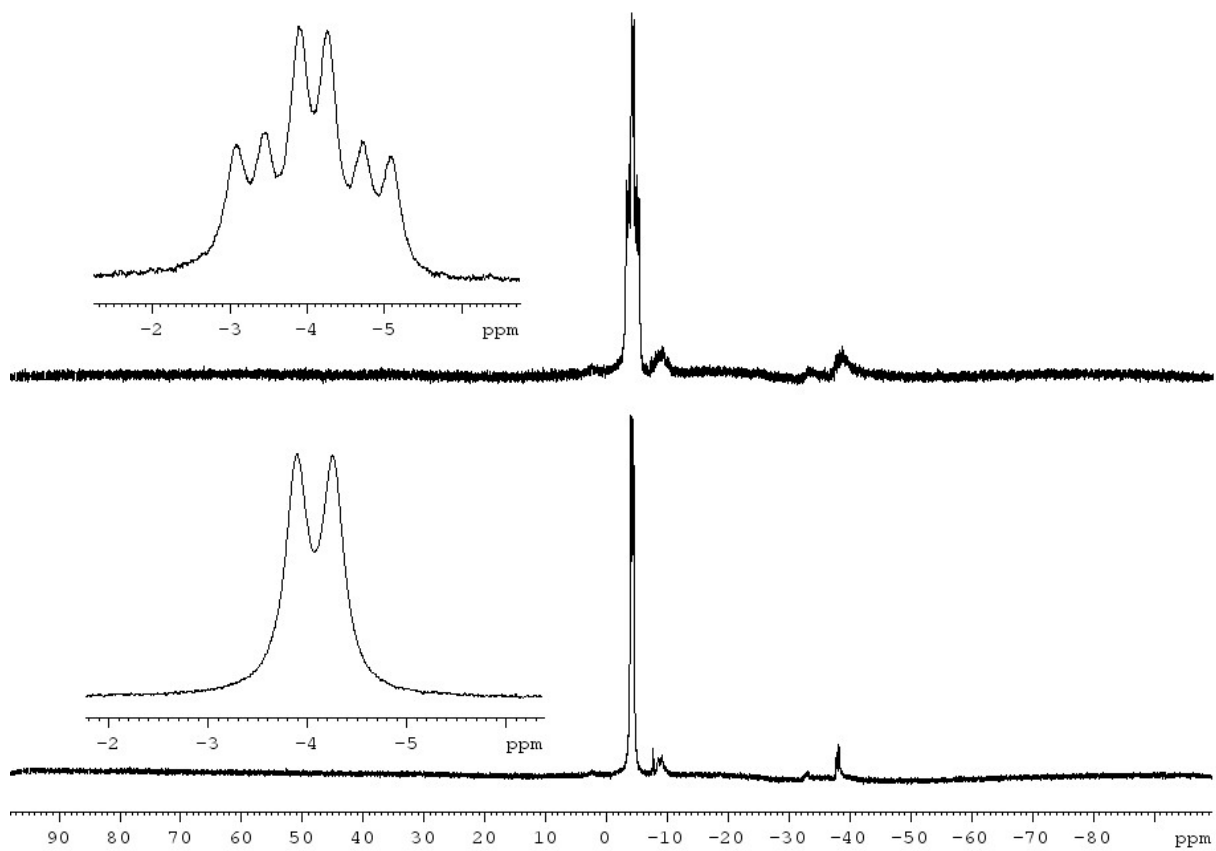


**Figure S8.** <sup>11</sup>B NMR (top) and <sup>11</sup>B{<sup>1</sup>H} NMR (bottom) spectra of **1c** in C<sub>6</sub>D<sub>6</sub>

## Compound 2

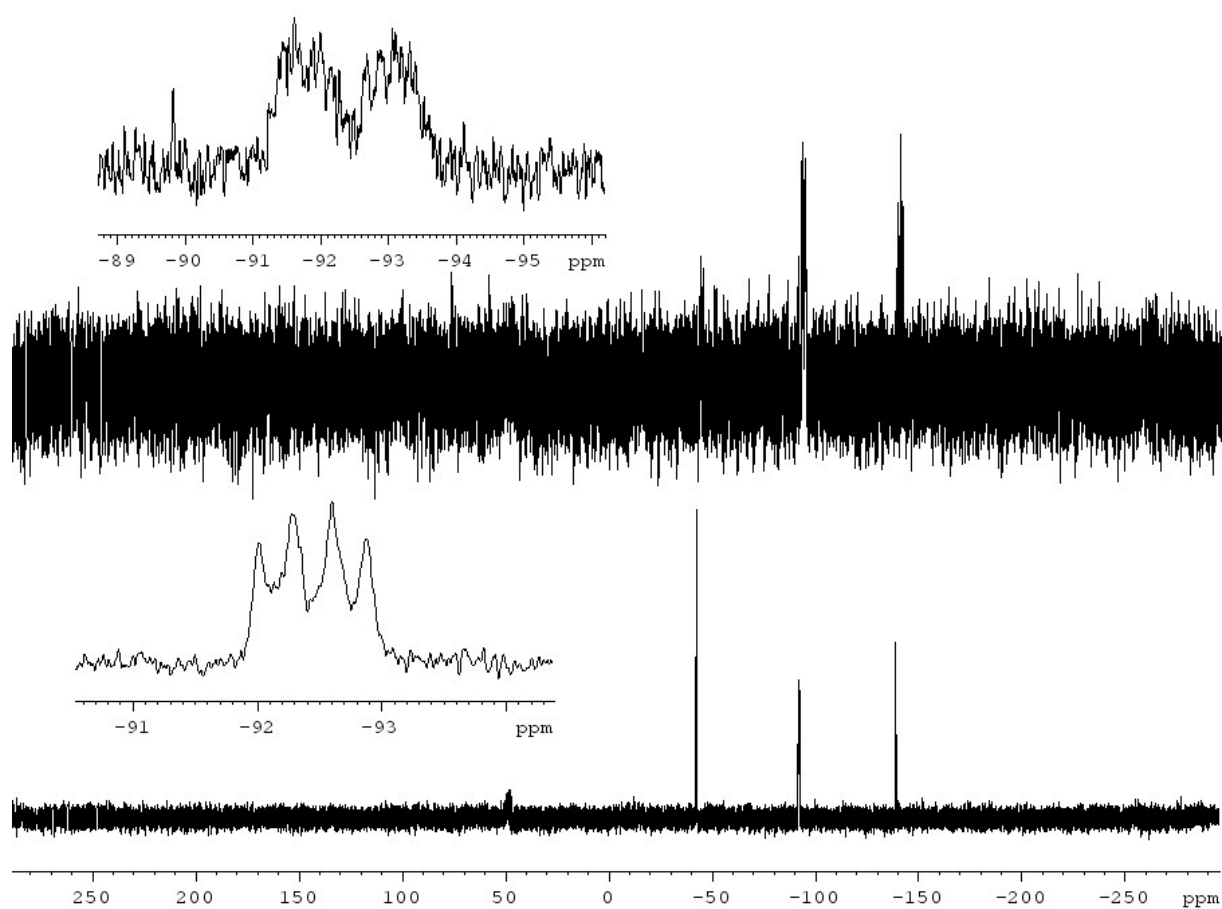


Figure S9.  $^{31}\text{P}$  NMR (top) and  $^{31}\text{P}\{^1\text{H}\}$  NMR (bottom) spectra of 2 in *n*-hexane

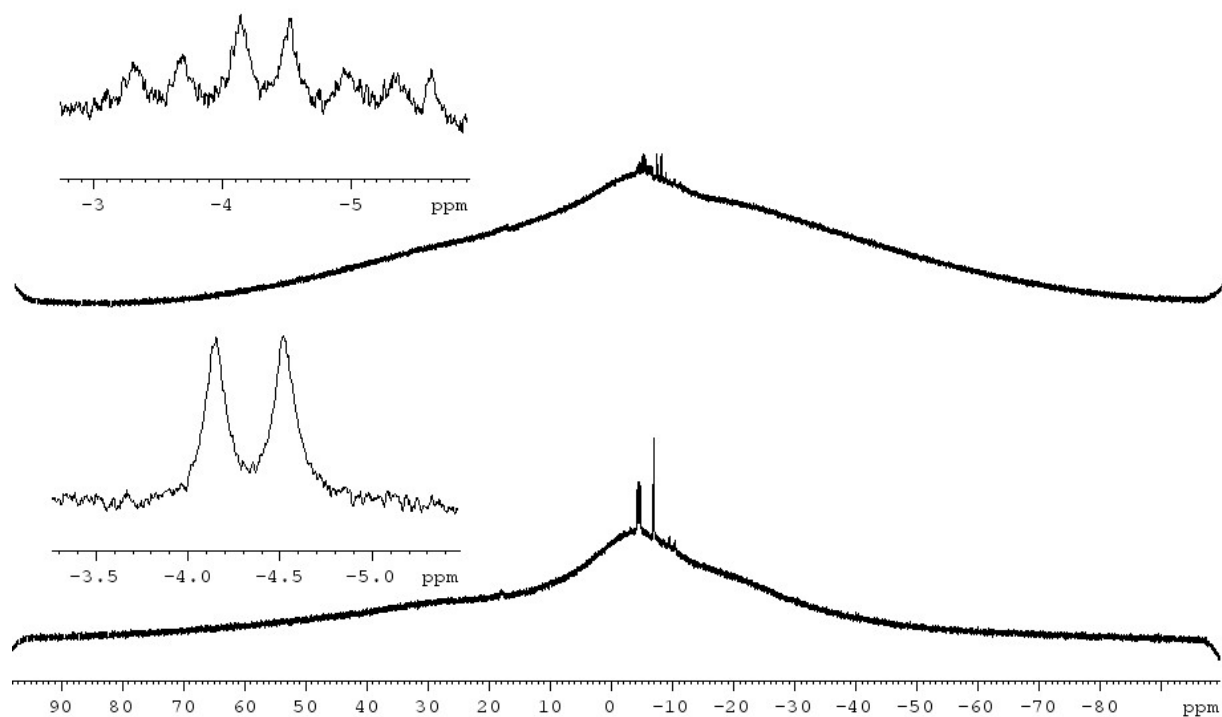
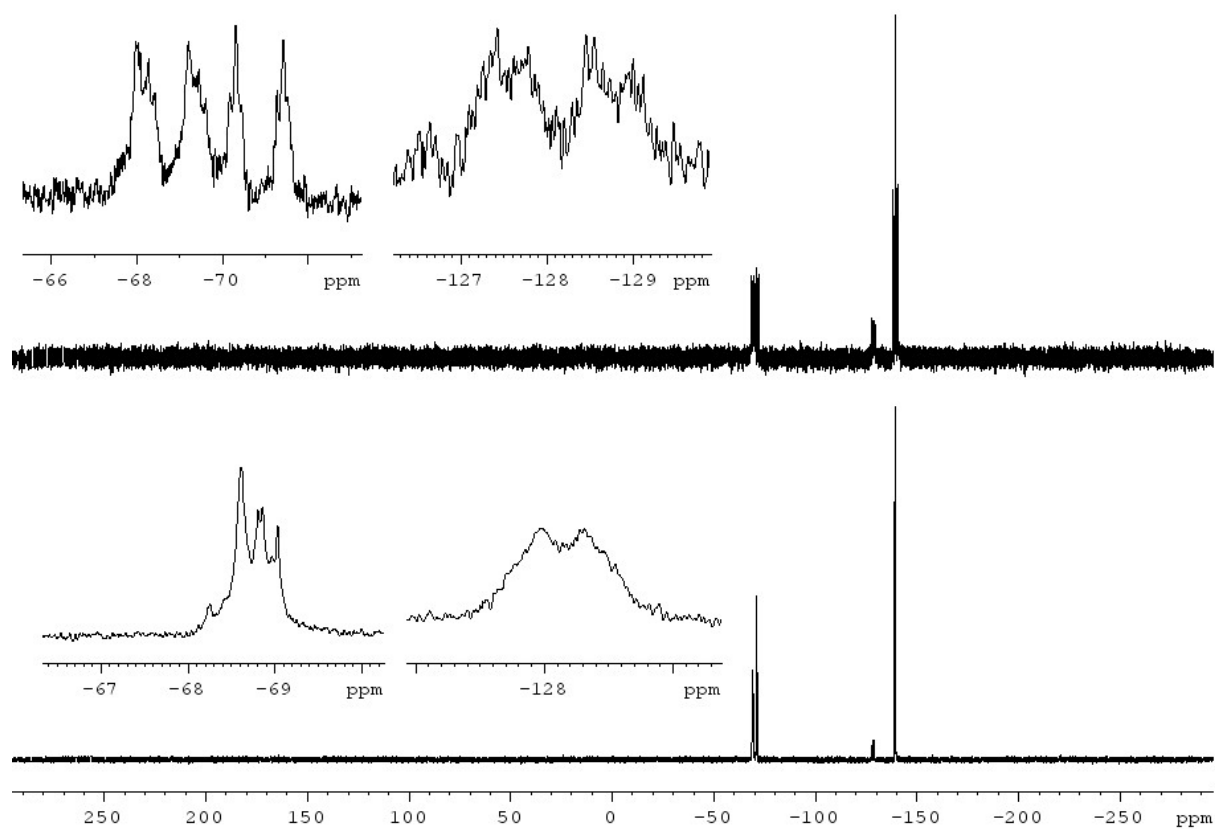
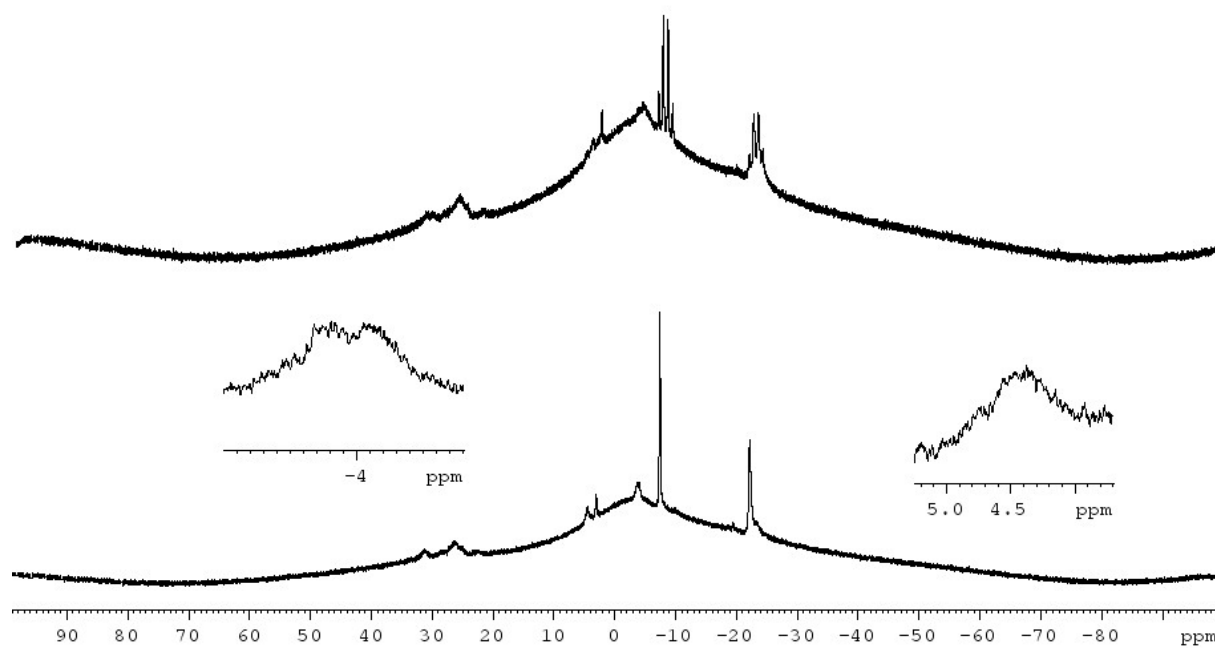
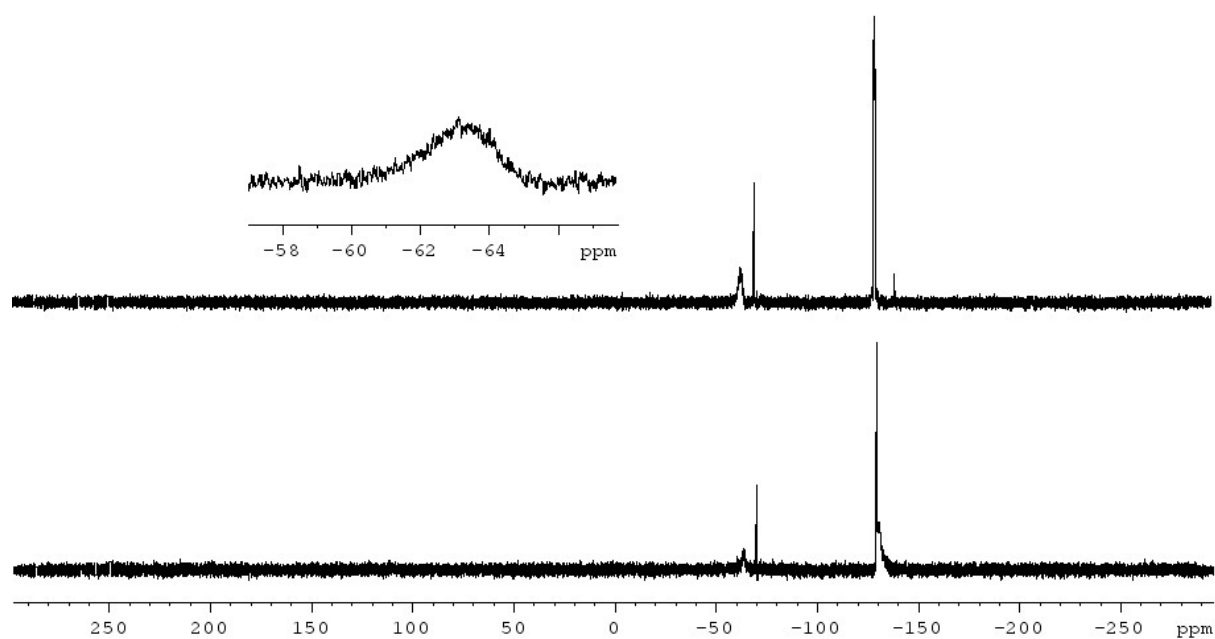


Figure S10.  $^{11}\text{B}$  NMR (top) and  $^{11}\text{B}\{^1\text{H}\}$  NMR (bottom) spectra of 2 in *n*-hexane

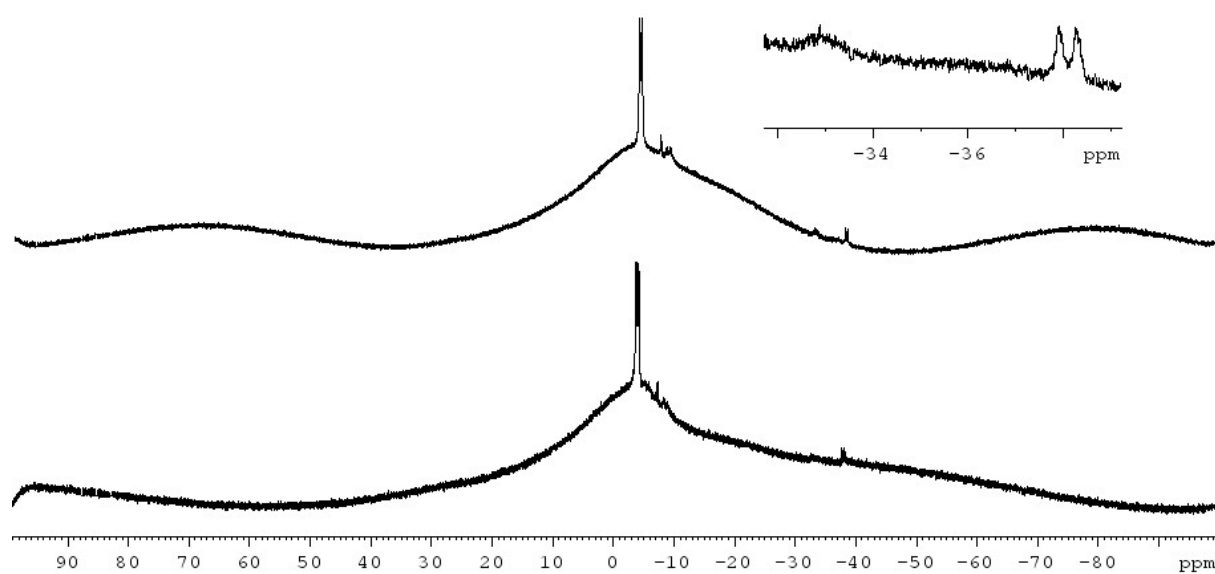
## Compound 3a und 3b

Figure S11. <sup>31</sup>P NMR (top) and <sup>31</sup>P{<sup>1</sup>H} NMR (bottom) spectra of 3a and 3b in THFFigure S12. <sup>11</sup>B NMR (top) and <sup>11</sup>B{<sup>1</sup>H} NMR (bottom) spectra of 3a and 3b in THF

## Polymerization reactions



**Figure S13.**  $^{31}\text{P}\{^1\text{H}\}$  NMR spectra of **1a** ( $c = 0.089$  mol/L) after stirring at r.t. for 90 min (bottom) and 24 h (top)



**Figure S14.**  $^{11}\text{B}\{^1\text{H}\}$  NMR spectra of **1a** ( $c = 0.089$  mol/L) after stirring at r.t. for 90 min (bottom) and 24 h (top)

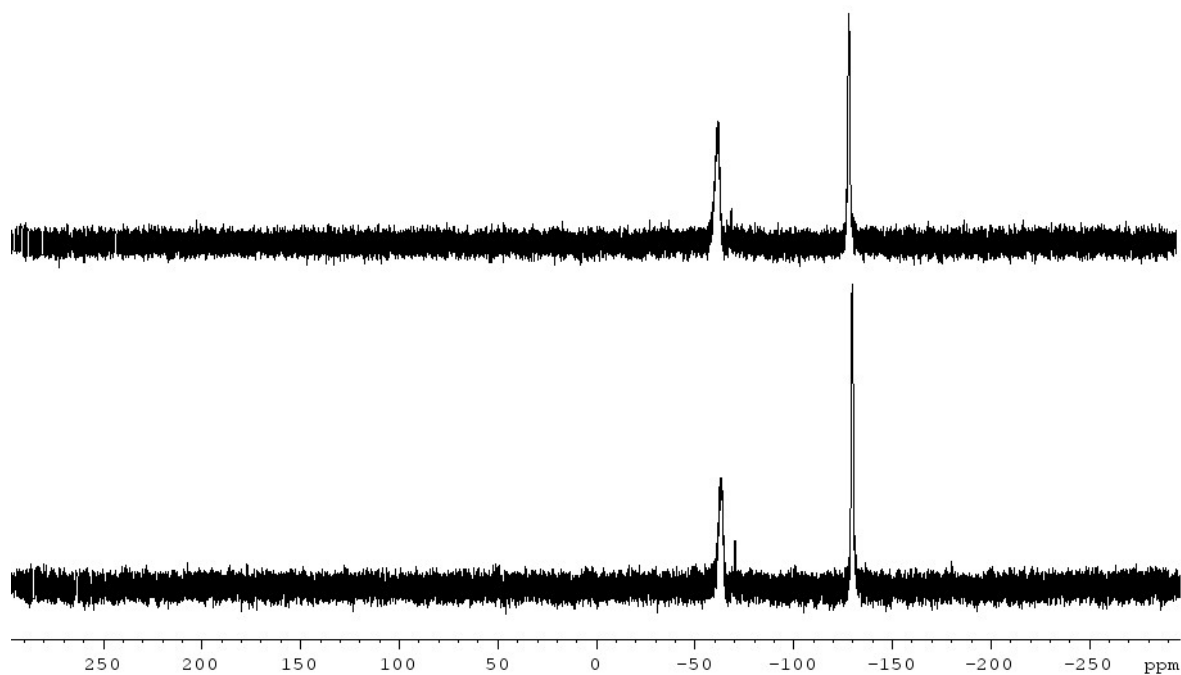


**Figure S15.**  $^{31}\text{P}\{^1\text{H}\}$  NMR spectra of **1a** ( $c = 0.089$  mol/L) after stirring at r.t. for 90 min (bottom) and 24 h (top) in the presence of 5 mol% of  $[(\eta^5\text{-}\eta^1\text{-C}_5\text{H}_4\text{C}_{10}\text{H}_{14})_2\text{Ti}]$ .

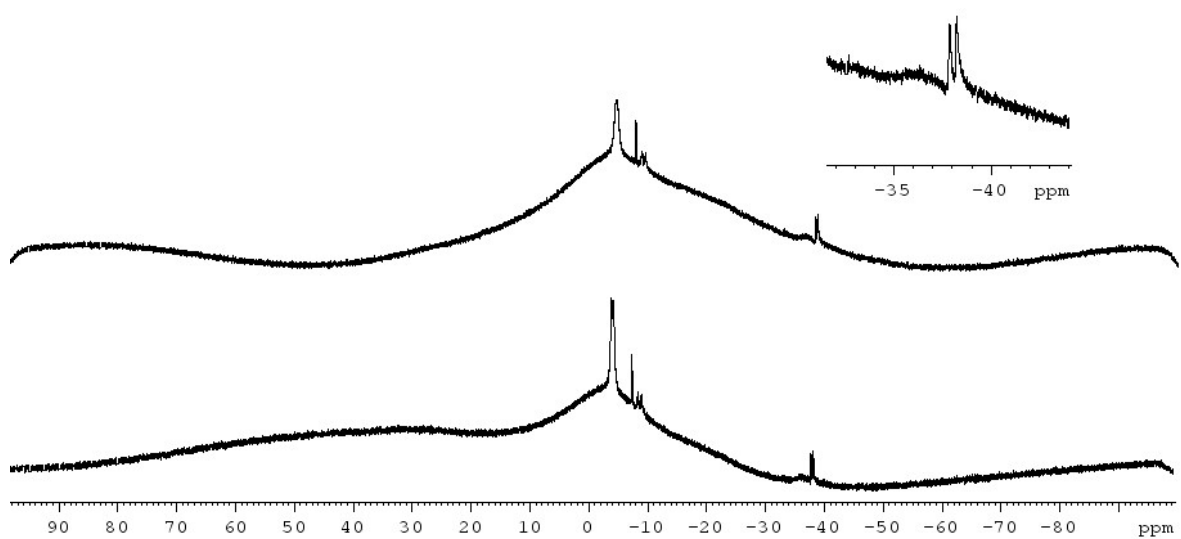


**Figure S16.**  $^{11}\text{B}\{^1\text{H}\}$  NMR spectra of **1a** ( $c = 0.089$  mol/L) after stirring at r.t. for 90 min (bottom) and 24 h (top) in the presence of 5 mol% of  $[(\eta^5\text{-}\eta^1\text{-C}_5\text{H}_4\text{C}_{10}\text{H}_{14})_2\text{Ti}]$ .

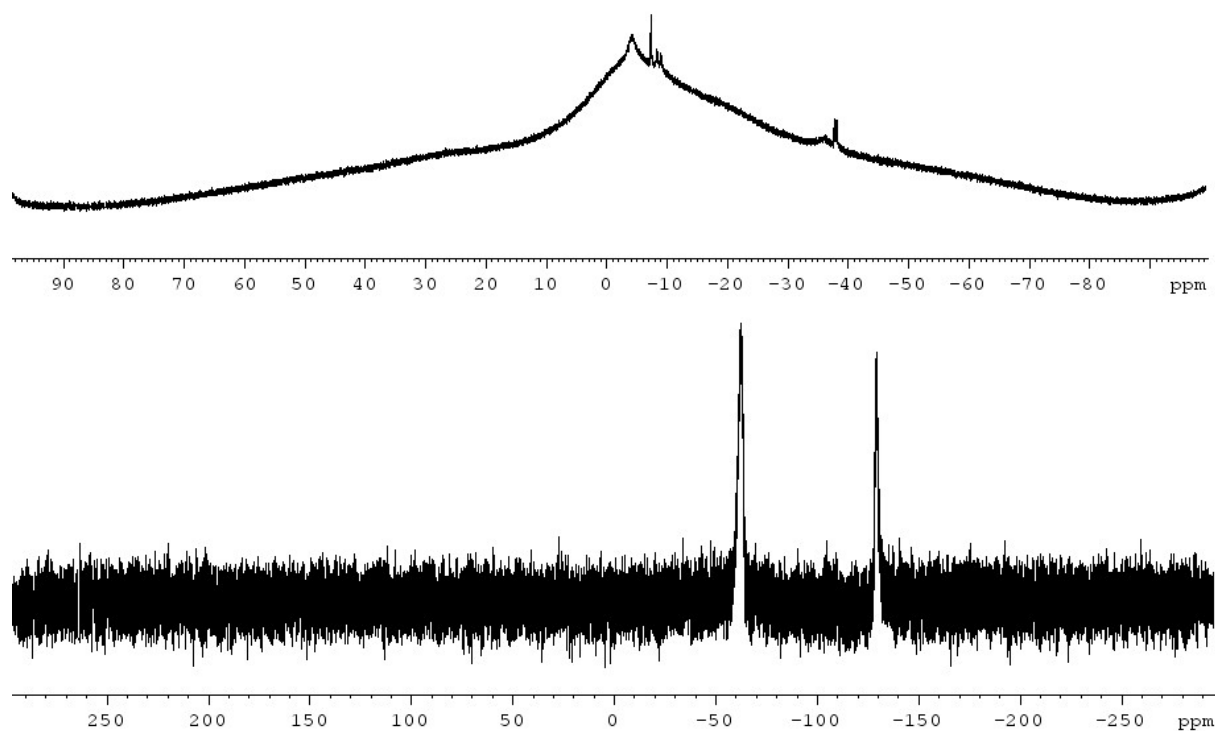


**Figure S16.**  $^{31}\text{P}\{^1\text{H}\}$  NMR and  $^{11}\text{B}\{^1\text{H}\}$  NMR (top) spectra of **1a** ( $c = 0.089$  mol/L) after stirring at r.t. for 24 h in the presence of 10 mol% of  $[(\eta^5\text{-}\eta^1\text{-C}_5\text{H}_4\text{C}_{10}\text{H}_{14})_2\text{Ti}]$ .

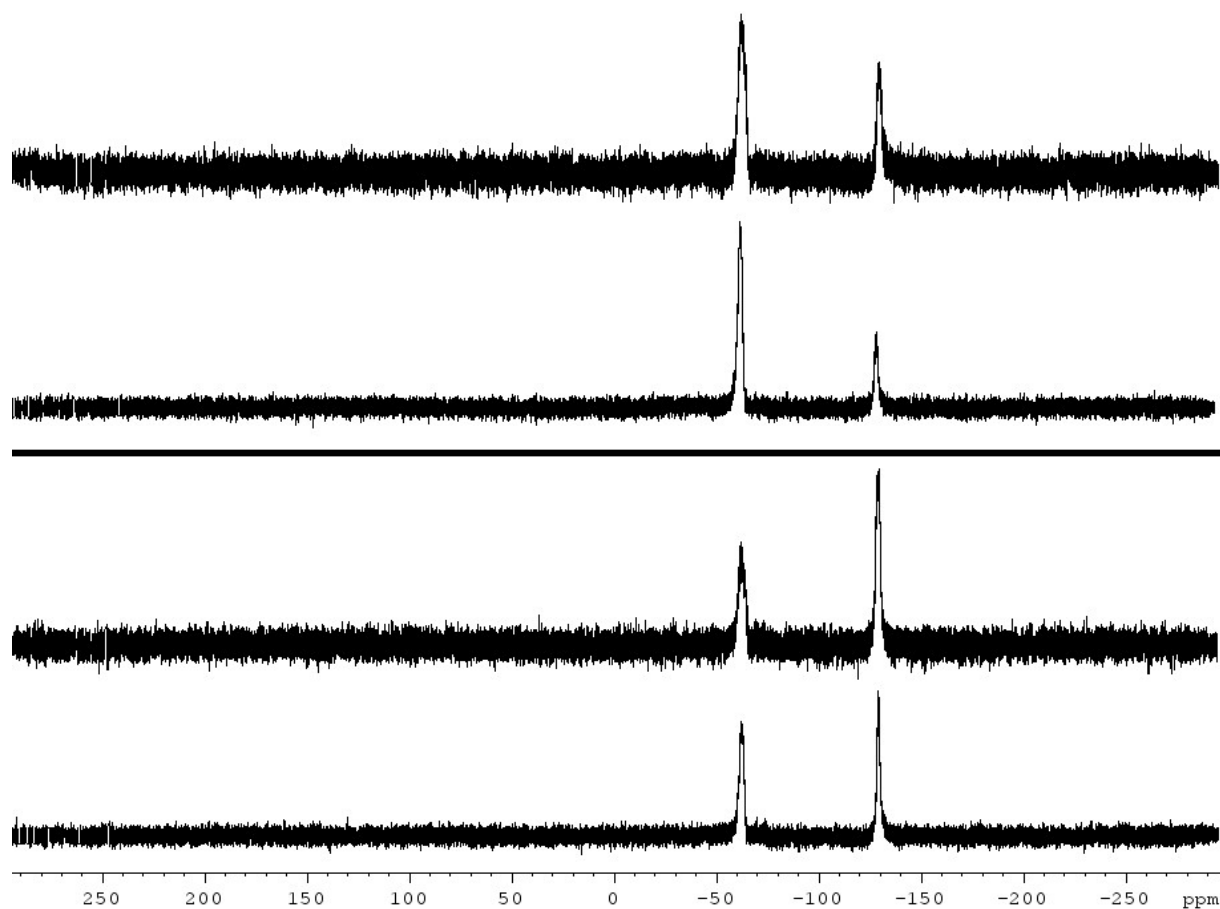


**Figure S17.**  $^{31}\text{P}$  NMR (top) and  $^{31}\text{P}\{^1\text{H}\}$  NMR (bottom) spectra of **1a** ( $c = 0.03$  mol/L) after stirring at r.t. for 210 min (lower half) and 42 h (upper half) in the presence of 10 mol% of  $[(\eta^5\text{-}\eta^1\text{-C}_5\text{H}_4\text{C}_{10}\text{H}_{14})_2\text{Ti}]$ .

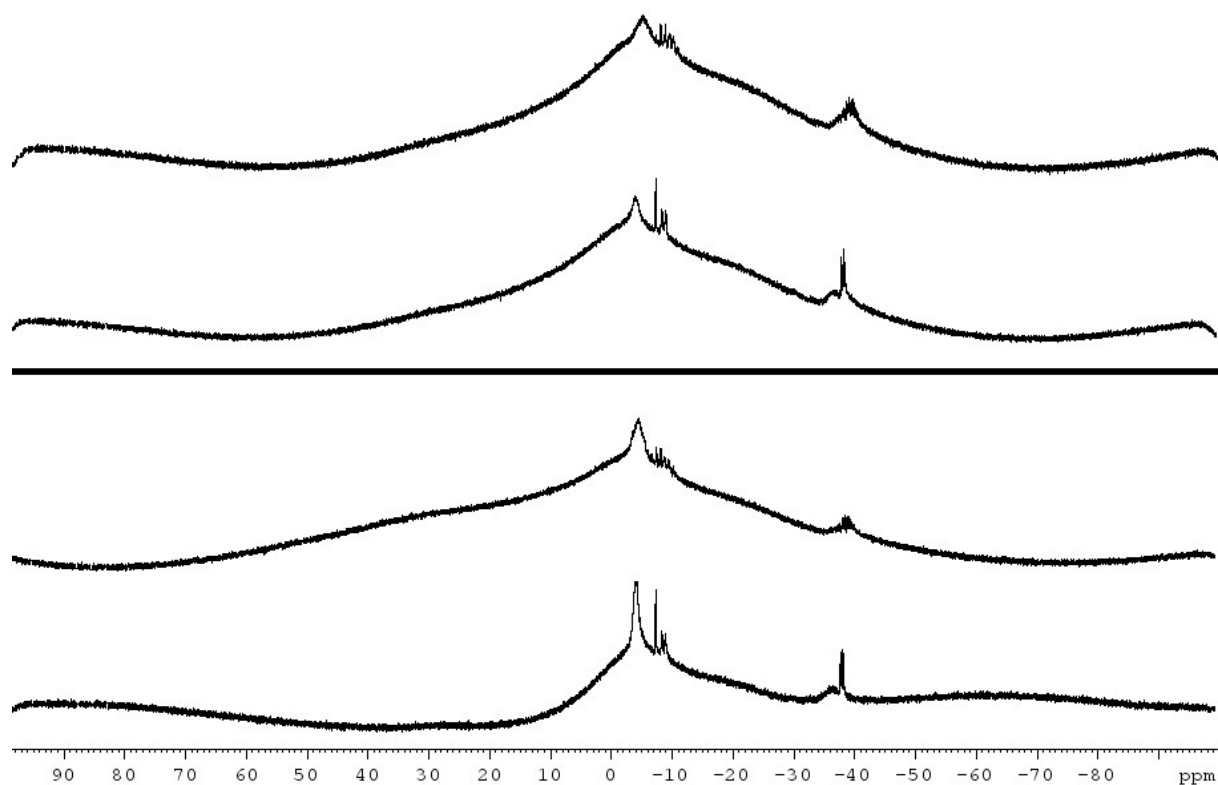


**Figure S18.** <sup>11</sup>B NMR (top) and <sup>11</sup>B{<sup>1</sup>H} NMR (bottom) spectra of **1a** (*c* = 0.03 mol/L) after stirring at r.t. for 210 min (lower half) and 42 h (upper half) in the presence of 10 mol% of [( $\eta^5$ : $\eta^1$ -C<sub>5</sub>H<sub>4</sub>C<sub>10</sub>H<sub>14</sub>)<sub>2</sub>Ti].

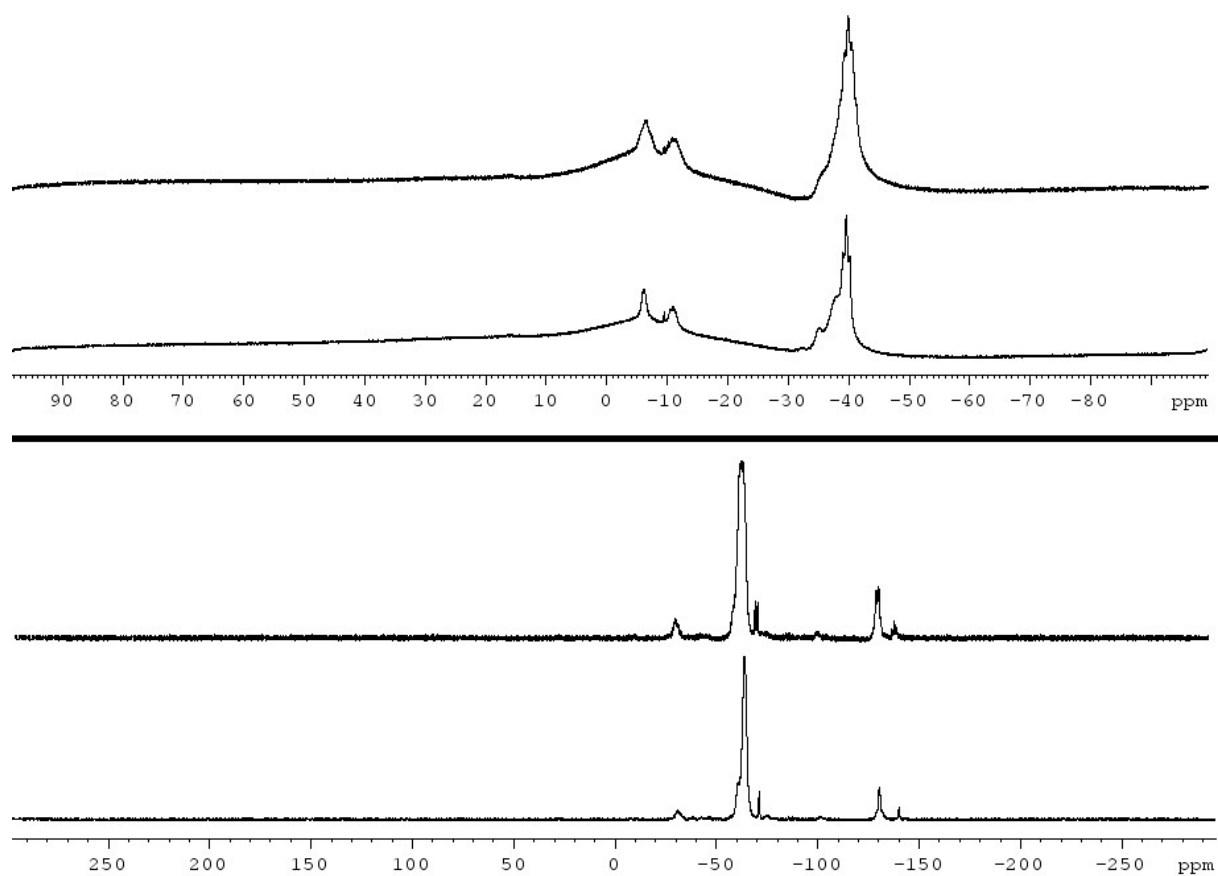


**Figure S19.** <sup>11</sup>B NMR (top, upper half), <sup>11</sup>B{<sup>1</sup>H} NMR (bottom, upper half), <sup>31</sup>P NMR (top, lower half), and <sup>31</sup>P{<sup>1</sup>H} NMR (bottom, lower half) spectra of **1b** (*c* = 0.5 mol/L) after stirring at r.t. for 21 d in the presence of 5 mol% of [( $\eta^5$ : $\eta^1$ -C<sub>5</sub>H<sub>4</sub>C<sub>10</sub>H<sub>14</sub>)<sub>2</sub>Ti].

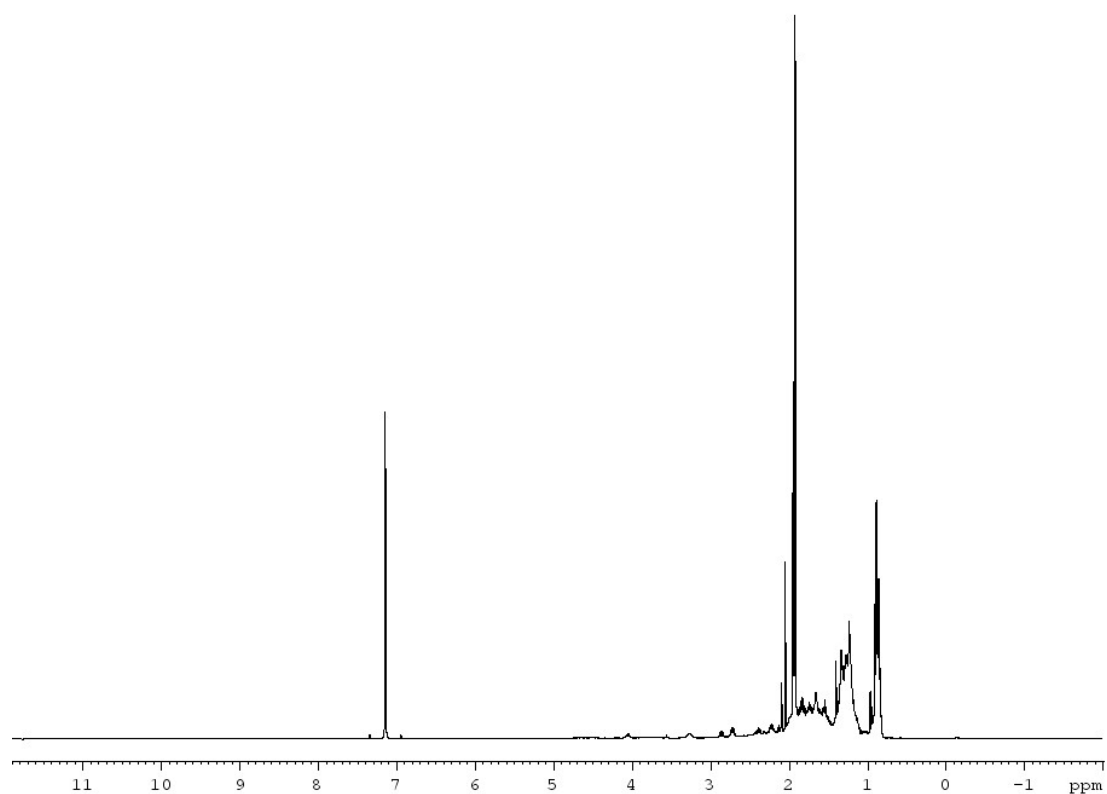


Figure S20.  $^1\text{H}$  NMR spectrum of neat **1c** after stirring at r.t. for 4 d

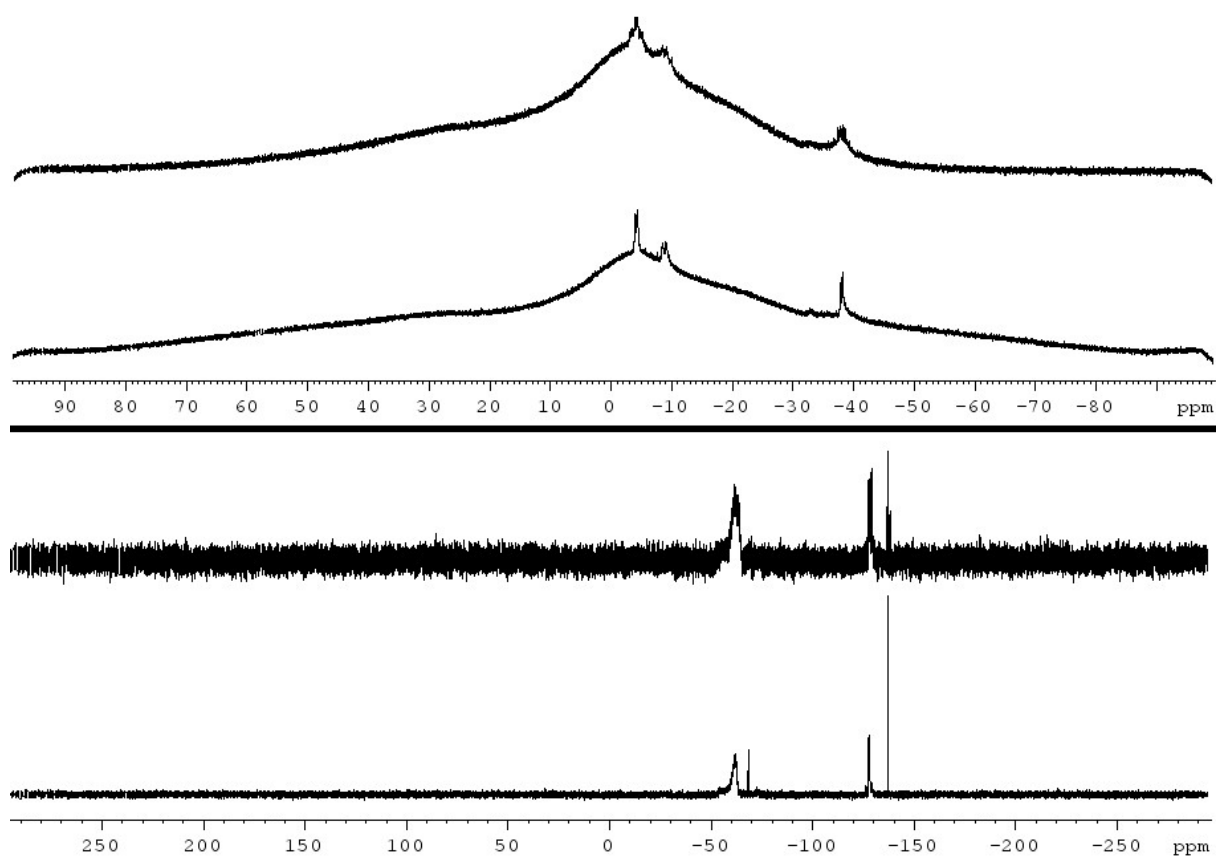


Figure S21.  $^{11}\text{B}$  NMR (top, upper half),  $^{11}\text{B}\{^1\text{H}\}$  NMR (bottom, upper half),  $^{31}\text{P}$  NMR (top, lower half), and  $^{31}\text{P}\{^1\text{H}\}$  NMR (bottom, lower half) spectra of **1c** (neat) after stirring at r.t. for 4 d

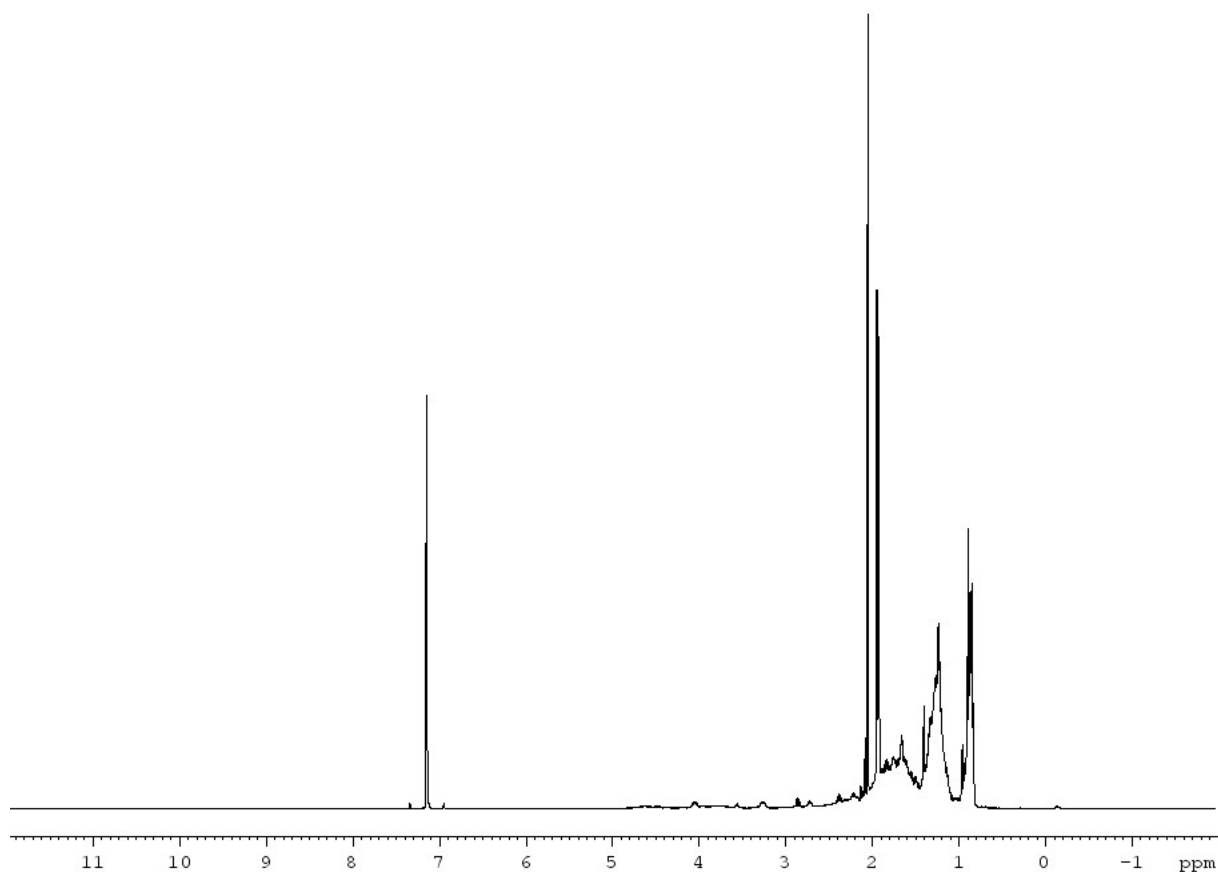


Figure S22. <sup>1</sup>H NMR spectrum of neat **1c** after stirring for 16h at 323 K

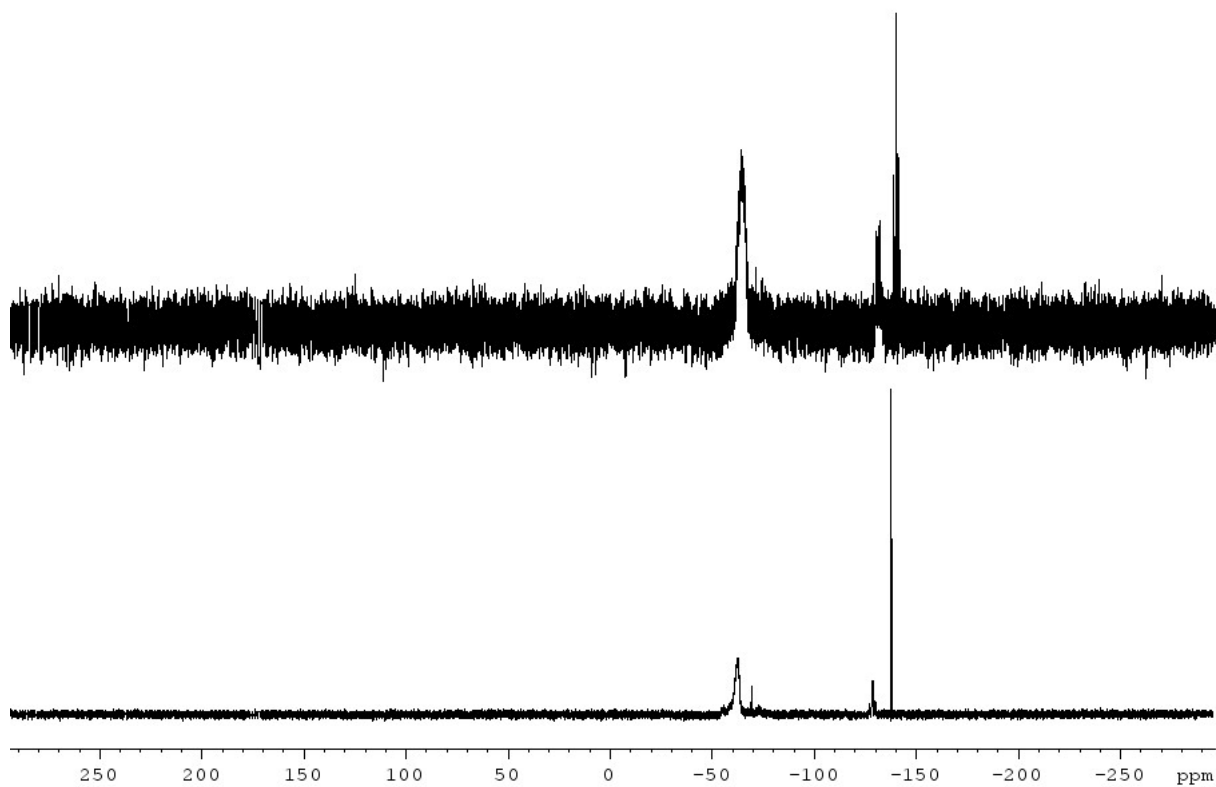
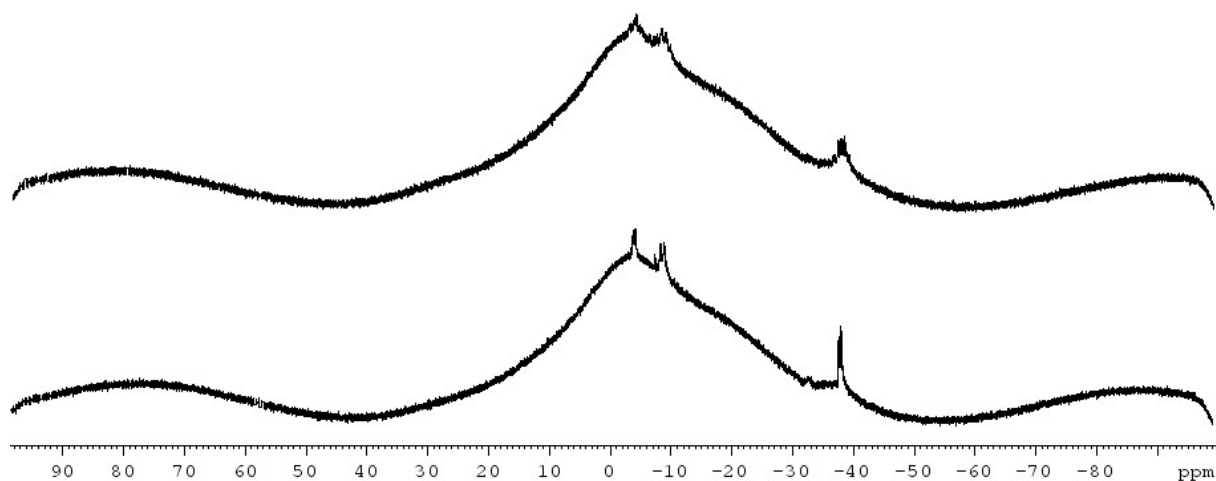
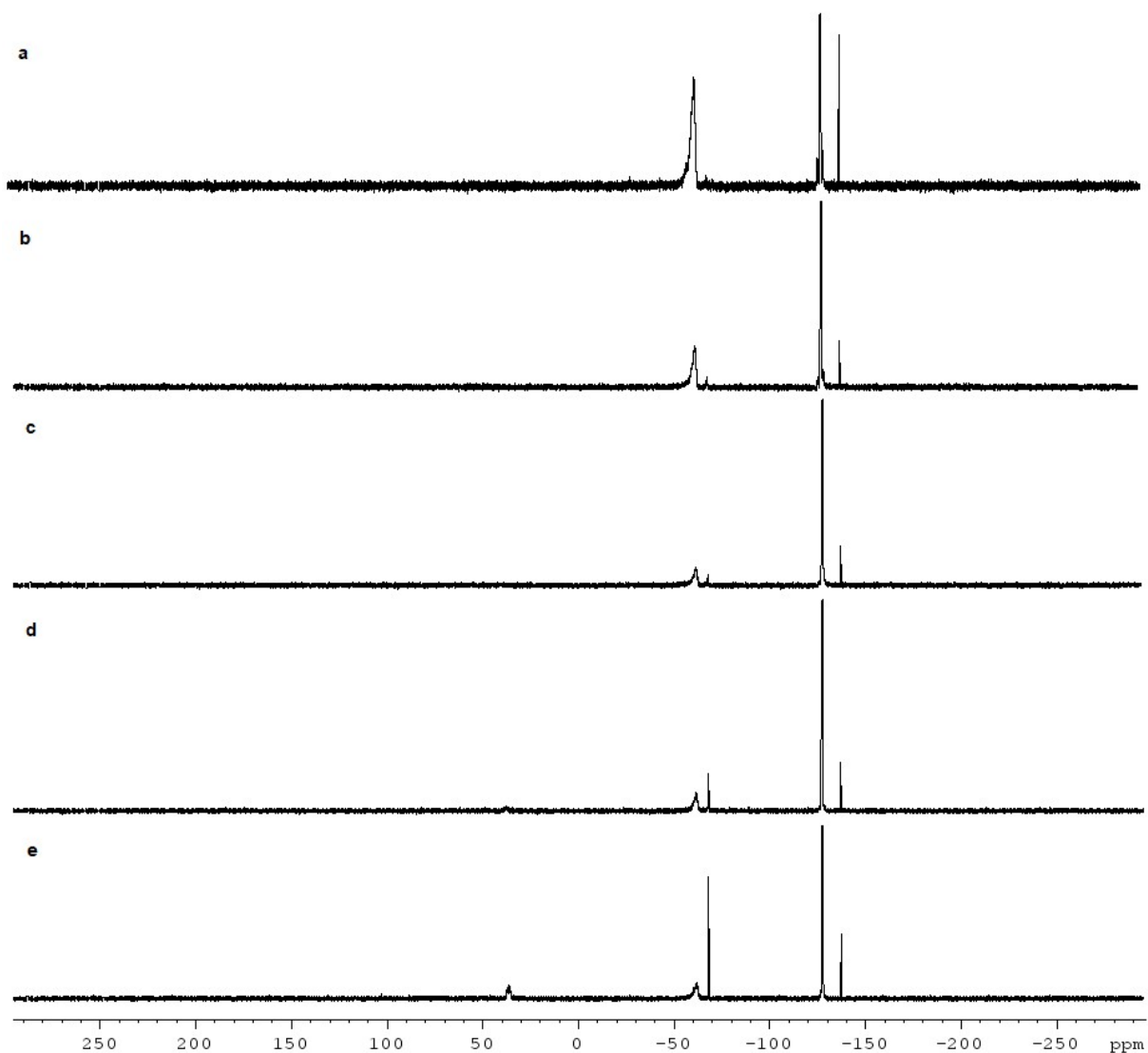


Figure S23. <sup>31</sup>P NMR (top) and <sup>31</sup>P{<sup>1</sup>H} NMR (bottom) spectra of **1c** (neat) after stirring for 16h at 323 K



**Figure S24.**  $^{11}\text{B}$  NMR (top) and  $^{11}\text{B}\{^1\text{H}\}$  NMR (bottom) spectra of **1c** (neat) after stirring for 16h at 323 K



**Figure S25.**  $^{31}\text{P}\{^1\text{H}\}$  NMR spectra of **1c** ( $c = 0.4$  mol/L) after stirring for 21d (a), 7d (b), 16h (c), 90 min (d), 30 min (e) at r.t. in the presence of 4 mol% of  $[(\eta^5\text{-}\eta^1\text{-C}_5\text{H}_4\text{C}_{10}\text{H}_{14})_2\text{Ti}]$ .

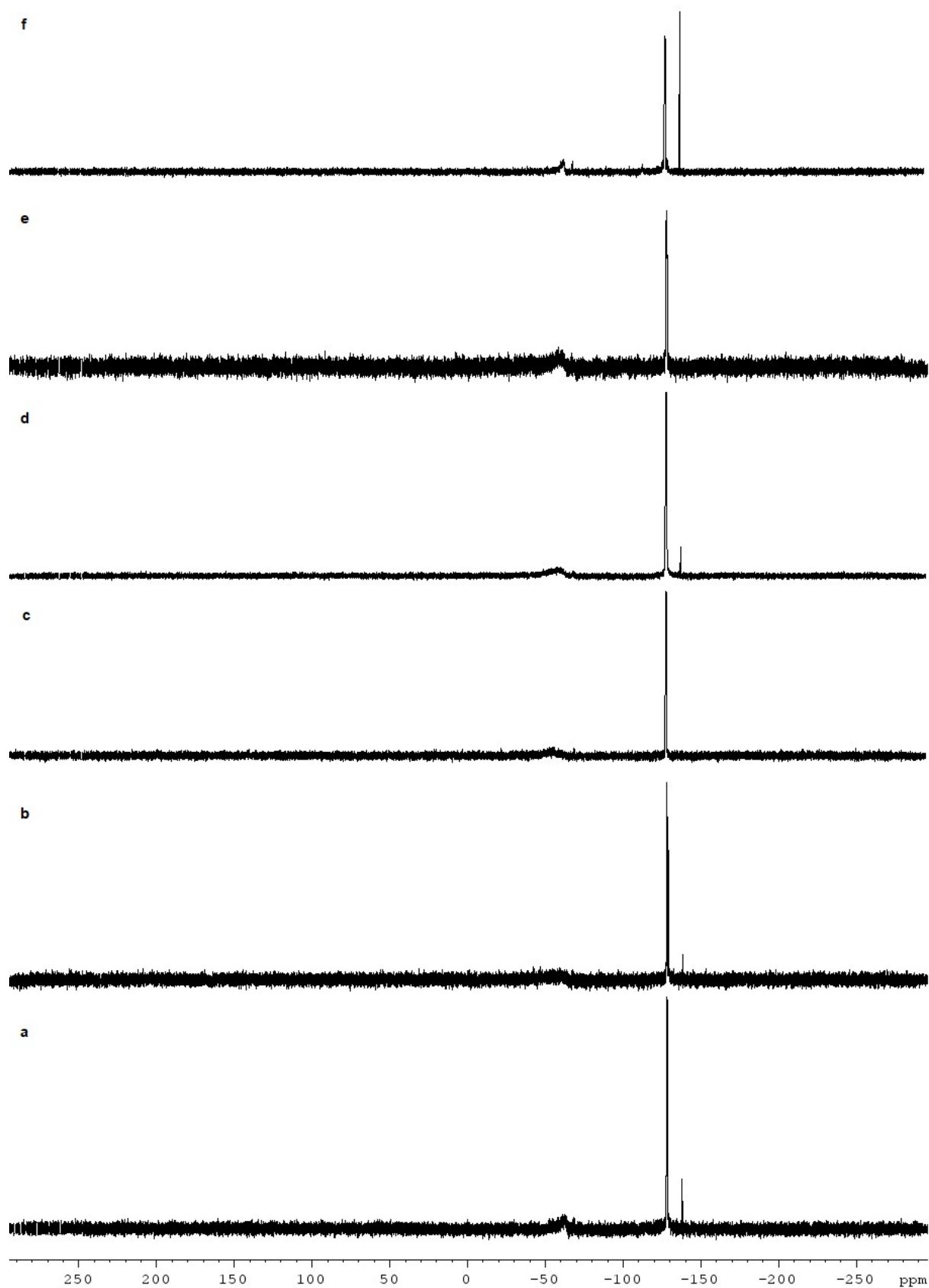


**Figure S26.**  $^{31}\text{P}\{^1\text{H}\}$  NMR spectra of **1c** in toluene at.r.t for 3h under different conditions: a) 5 mol% [Ti], c (**1c**) = 0.1 mol/L; b) 10 mol% [Ti], c (**1c**) = 0.1 mol/L; c) 10 mol% [Ti], c (**1c**) = 0.1 mol/L, in 1:1 mixture of THF and toluene; d) 10 mol% [Ti], c (**1c**) = 0.2 mol/L; e) 25 mol% [Ti], c (**1c**) = 0.1 mol/L; f) in absence of [Ti], c (**1c**) = 0.1 mol/L

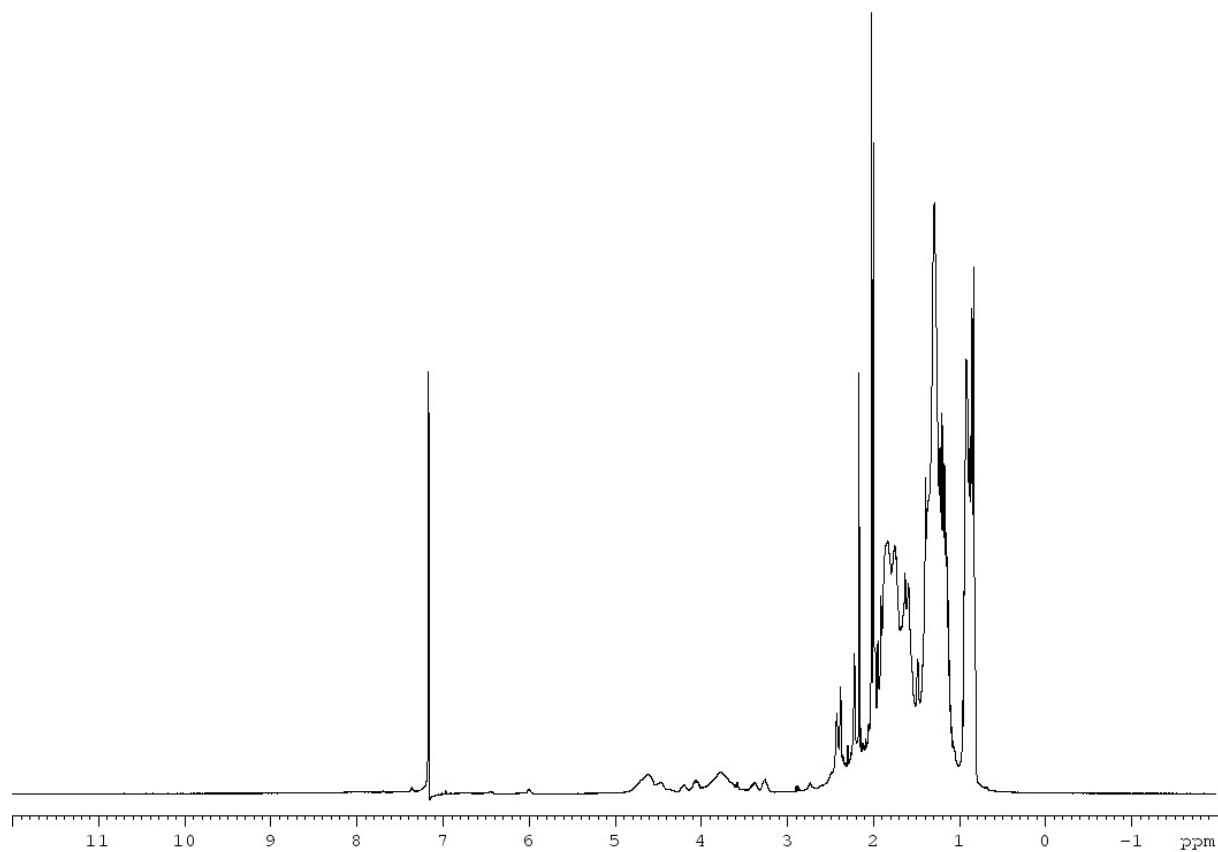


Figure S27.  $^1\text{H}$  NMR spectrum of neat **1c** after stirring for 40h at 323 K

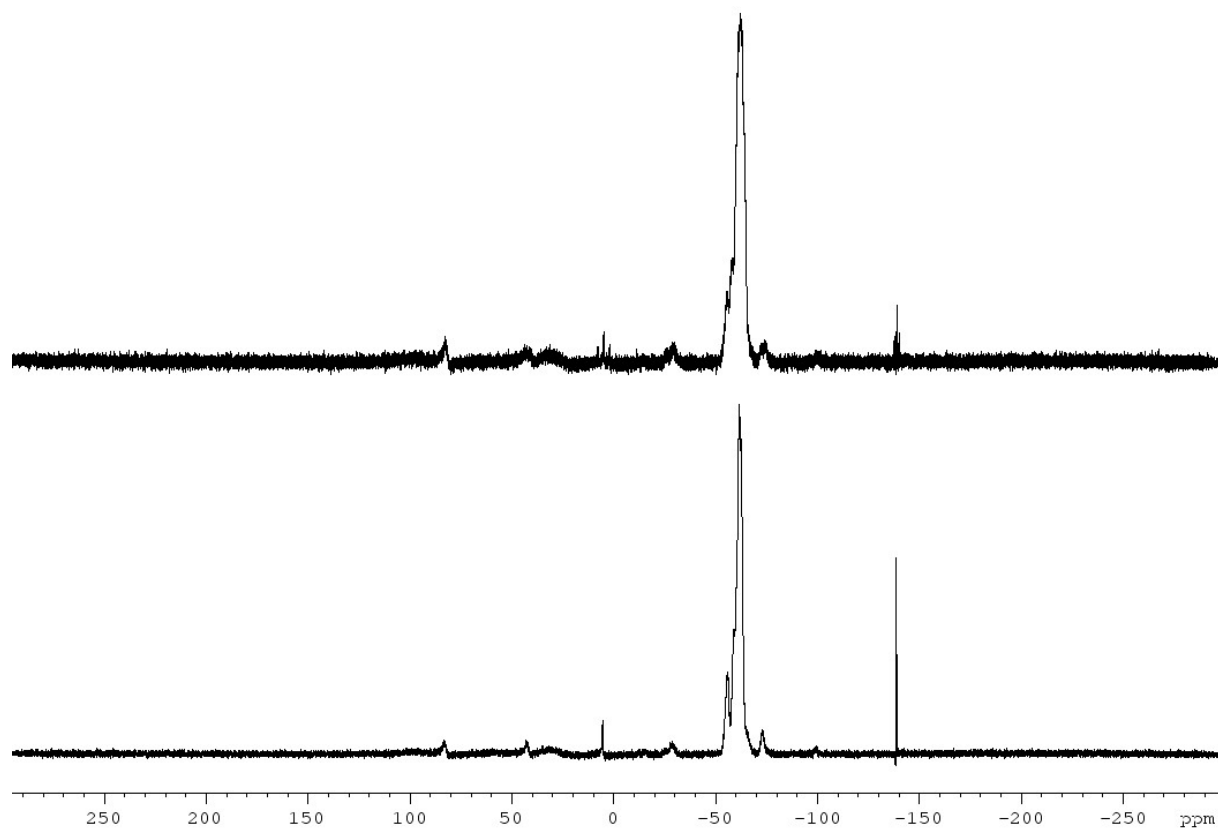


Figure S28.  $^{31}\text{P}$  NMR (top) and  $^{31}\text{P}\{^1\text{H}\}$  NMR (bottom) spectra of **1c** (neat) after stirring for 40h at 323 K

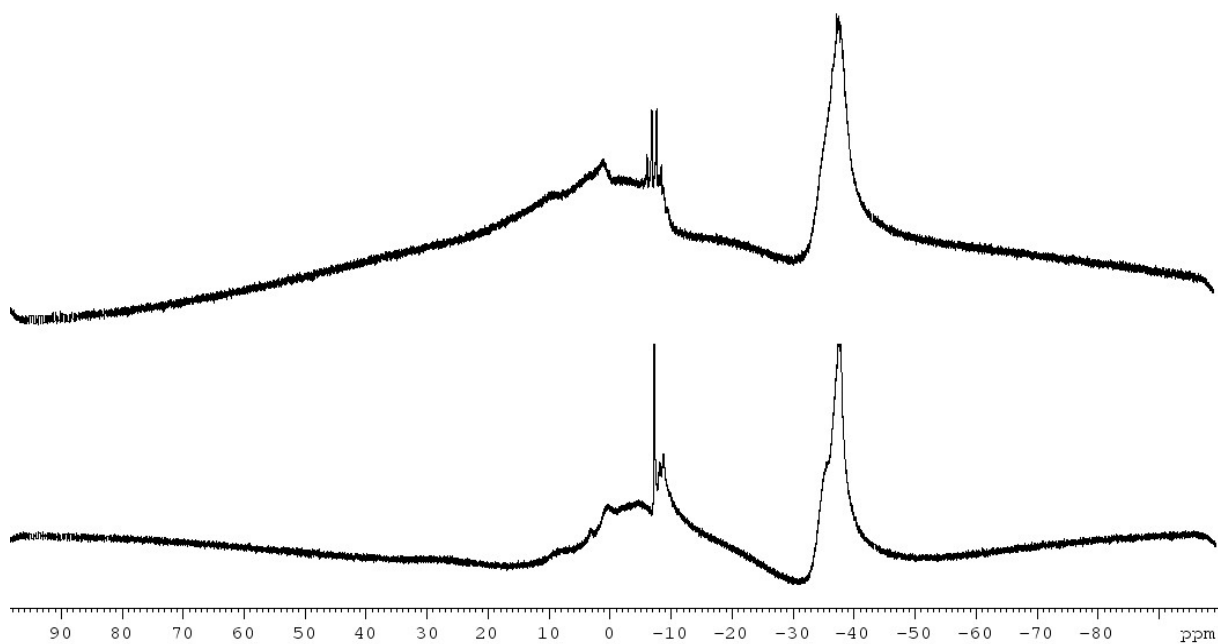


Figure S29. <sup>11</sup>B NMR (top) and <sup>11</sup>B{<sup>1</sup>H} NMR (bottom) spectra of **1c** (neat) after stirring for 40h at 323 K

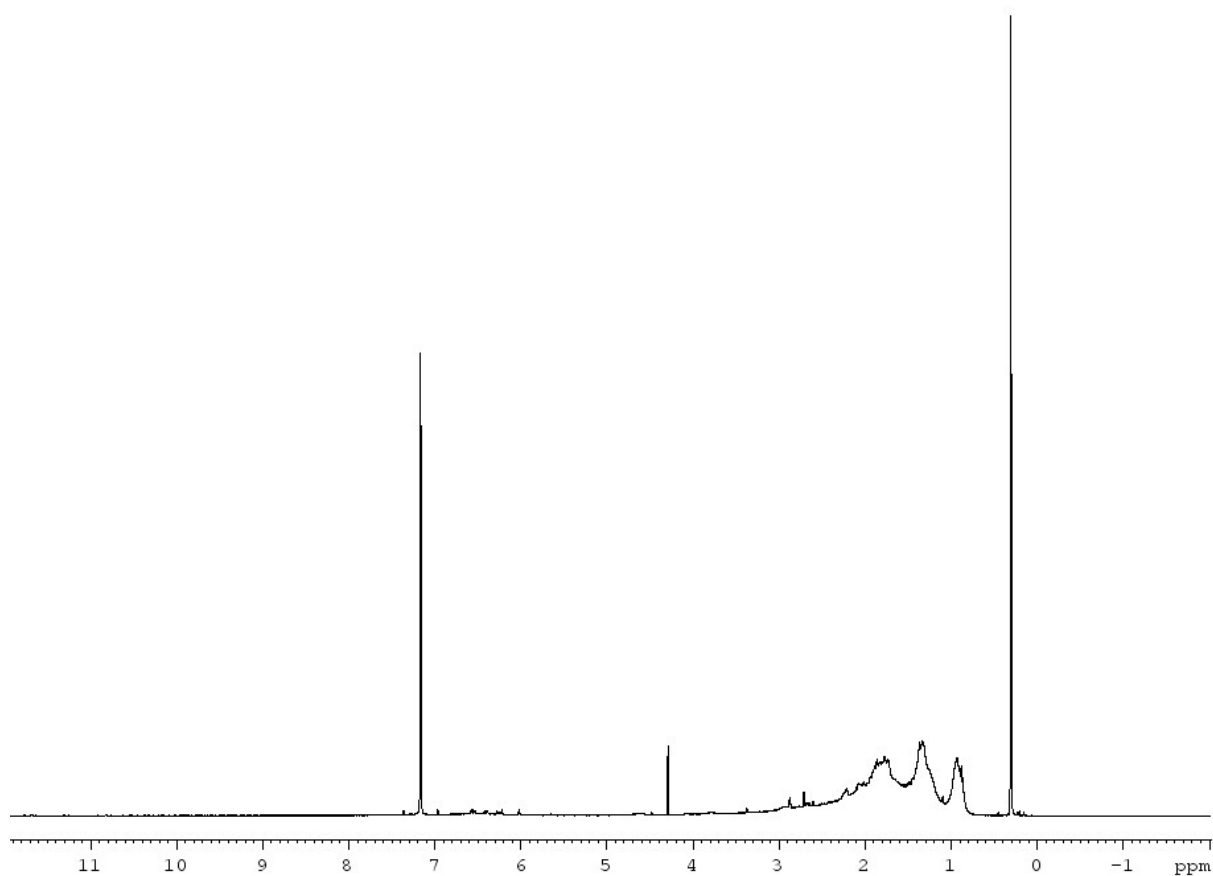
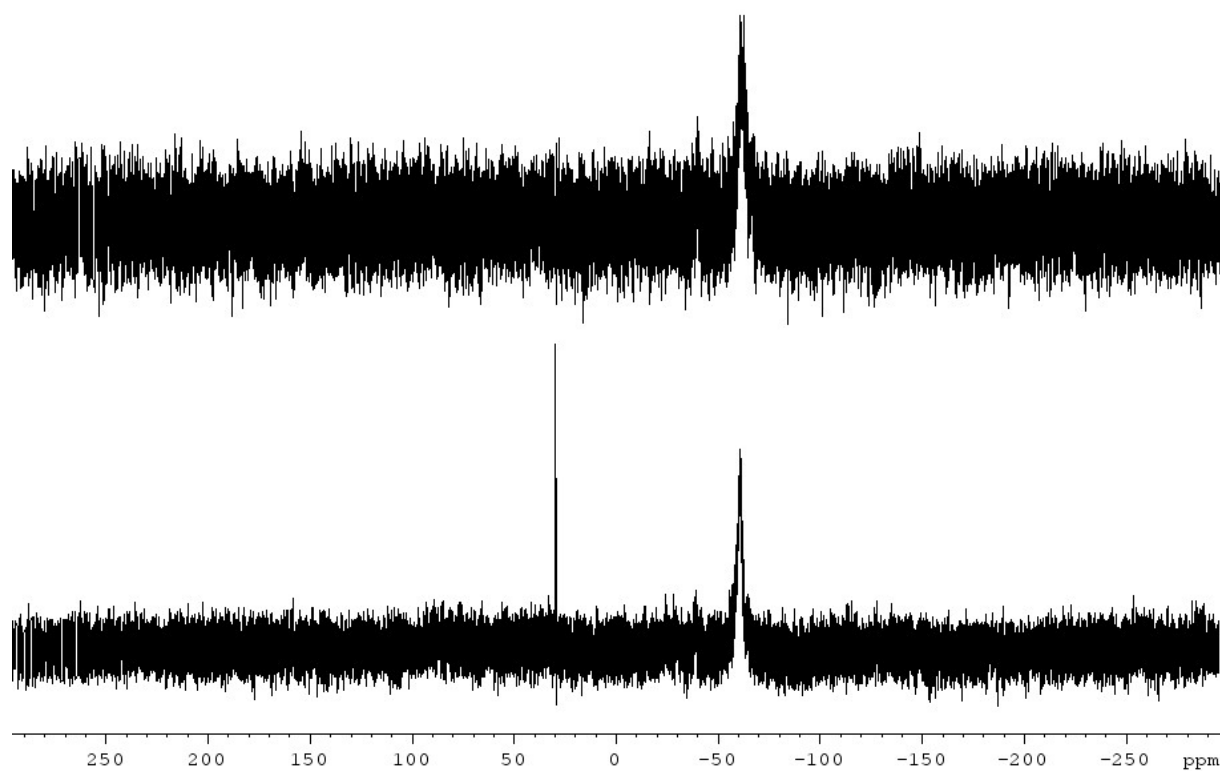
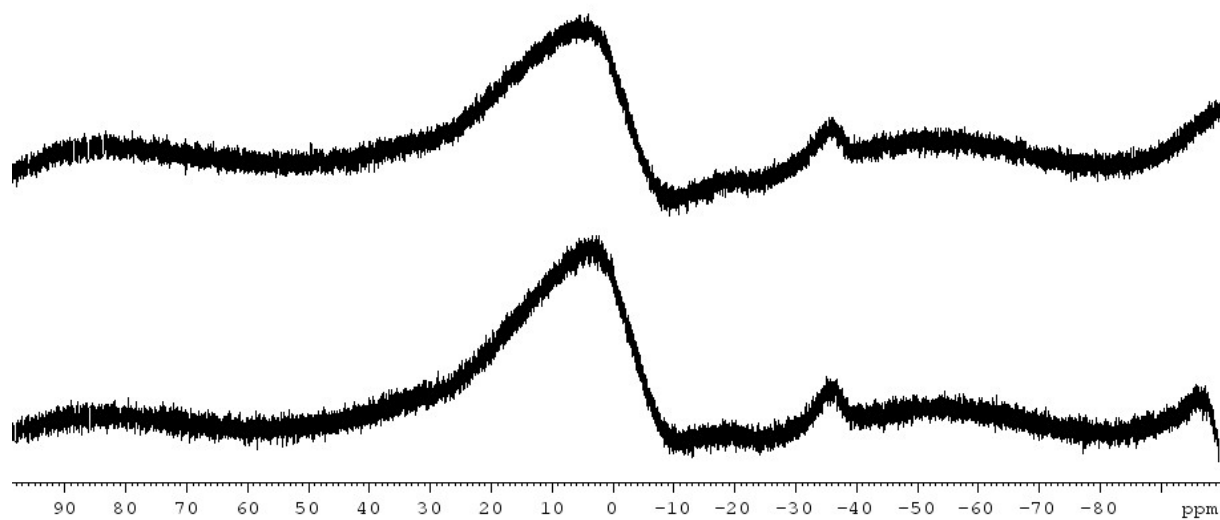


Figure S30. <sup>1</sup>H NMR spectrum of isolated poly-**1c** in C<sub>6</sub>D<sub>6</sub>



**Figure S31.**  $^{31}\text{P}$  NMR (top) and  $^{31}\text{P}\{^1\text{H}\}$  NMR (bottom) spectra of isolated poly-**1c** in  $\text{C}_6\text{D}_6$



**Figure S32.**  $^{11}\text{B}$  NMR (top) and  $^{11}\text{B}\{^1\text{H}\}$  NMR (bottom) spectra of isolated poly-**1c** in  $\text{C}_6\text{D}_6$

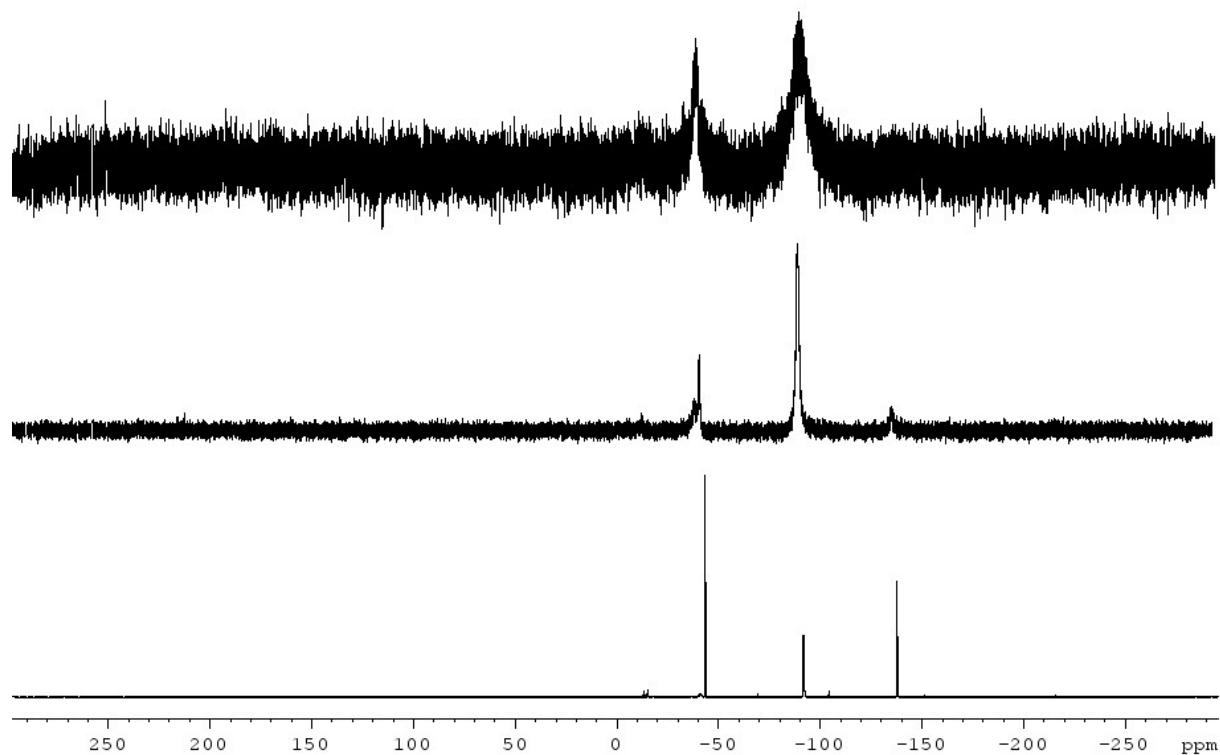


**Figure S33.**  $^{31}\text{P}\{^1\text{H}\}$  NMR spectra of **2** in toluene after 3h at r.t. in the absence of [Ti] (bottom), in the presence of 5mol% [Ti] (middle) and in the presence of 10 mol% [Ti] (top)

## References.

- [1] A. Stauber, T. Jurca, C. Marquardt, M. Fleischmann, M. Seidl, G. R. Whittell, I. Manners, M. Scheer, *Eur. J. Inorg. Chem.* **2016**, 2684-2687.

## 5.6. Author contributions

- The synthesis of compounds **1a-c** by adjusted literature procedures has first been performed by Dr. Jens Braese (in his PhD thesis, Regensburg, **2018**)
- The synthesis of compounds **1a-c** by one-pot reaction starting from NaPH<sub>2</sub> and alkyl halides and the characterization of **1a-c** has been performed by Felix Lehnfeld
- The synthesis and characterization of **2** and **3a-b** has been performed by Felix Lehnfeld
- First polymerization reactions of **1a-c** have been performed by Dr. Jens Braese (in his PhD thesis, Regensburg, **2018**)
- Detailed polymerization studies of **1a-c** and first polymerization studies on **2** have been performed by Felix Lehnfeld
- The manuscript (including supporting information, figures, schemes and graphical abstract) was written by Felix Lehnfeld.



## 6. Thesis treasury: Oxidation of a parent arsanylborane as a route to novel mixed main group element compounds

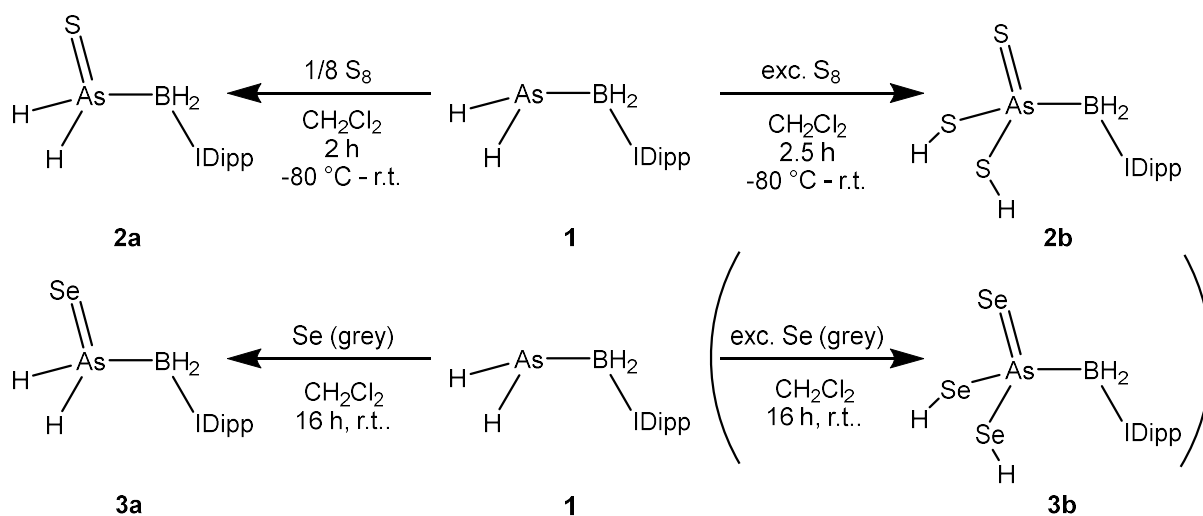
### 6.1. Introduction

Non-carbon-based materials are an important group of compounds due to a vast field of applications. Noteworthy examples include elastomers, lithographic resistant layers, biomaterials, polyelectrolytes, ceramic precursors and for optoelectronics.<sup>[1]</sup> Binary group 13/15 compounds exhibit a broad variety of properties for potential applications such as hydrogen storage or semiconductors.<sup>[2]</sup> The application of N-heterocyclic carbenes (NHCs) has opened up the field of low-valent main group element compounds.<sup>[3]</sup> Important examples for mixed main group element compounds stabilized by NHCs include the first donor/acceptor-stabilized parent germanium(II) dihydride complex IDippGeH<sub>2</sub>BH<sub>3</sub> reported by Rivard *et al.* as well as the only hydrogen substituted stibanylborane H<sub>2</sub>SbBH<sub>2</sub>-IMe reported by our group.<sup>[4]</sup> The further potential of NHCs in the field of Lewis base stabilized pnictogenyltrielanes of the type R<sub>2</sub>EER<sub>2</sub>-LB has been shown by the recent synthesis of novel all-hydrogen-substituted group 13/14/15 chain compounds as well as hydrogen substituted pnictogenyltrielanes with heavier group 13 elements.<sup>[5]</sup> The reactivity of pnictogenylboranes towards chalcogen sources offers an access to mixed group 13/15/16 compounds, as it was reported for various chalcogens in the case of phosphanylboranes RR'PBH<sub>2</sub>NMe<sub>3</sub> (R,R' = H, Ph, *t*Bu) and as part of this work for its organosubstituted arsenic derivative.<sup>[6]</sup> However, the high reactivity of arsanylboranes towards group 16 oxidants has proven to be challenging, as the decomposition of the starting material is always a competing reaction. Therefore, using the recently reported parent arsanylborane stabilized by a NHC AsH<sub>2</sub>BH<sub>2</sub>-IDipp (**1**)<sup>[5b]</sup> for chalcogenation reactions was the next step and leads to selective formation of mixed group 13/15/16 compounds incorporating arsenic and various group 16 elements. First results on this topic are presented in the following.

### 6.2. Results and Discussion

By reacting a solution of **1** in toluene with elemental sulfur and grey selenium at room temperature, either in a stoichiometric reaction or with a 3:1 excess of the

chalcogene, leads to a full conversion after few hours of reaction time according to  $^{11}\text{B}$  NMR spectroscopy (cf. Scheme 1 for details).



**Scheme 1.** Expected reactivity of **1** towards chalcogens in stoichiometric and excess reactions

After 2 h of stirring (193 K to r.t.) and workup, the  $^{11}\text{B}\{^1\text{H}\}$  NMR spectrum of **2a** shows a singlet at  $\delta = -22.6$  ppm, which reveals further splitting into a triplet in the  $^{11}\text{B}$  NMR spectrum with a  $^1J_{\text{B,H}}$  coupling constant of 103 Hz (Figure 1). In addition to signals for the IDipp group the partially overlapped signals corresponding to the  $\text{BH}_2$  group at  $\delta = 2.38 - 2.65$  ppm as a heavily broadened pseudo-quartet and to the  $\text{AsH}_2$  group at  $\delta = 1.29$  ppm as a triplet ( $^3J_{\text{H,H}} = 7$  Hz) can be assigned in the  $^1\text{H}$  NMR spectrum of **2a**. Both signals are shifted to lower field compared to **1**, which is more prominent for the  $\text{AsH}_2$  moiety due to the greater influence of the sulfur atom in its proximity. Additionally, the  $^1\text{H}$  NMR spectrum reveals minor amounts of toluene and negligible amounts of unidentified side products. Any attempts to further purify the compound were not successful up to this point, as any crystallization attempts lead only to precipitation of **2a** as a light yellow solid.

For the reaction of **1** with an excess of  $\text{S}_8$  a heavily broadened singlet is observed at  $\delta = -24.0$  ppm in the  $^{11}\text{B}\{^1\text{H}\}$  NMR spectrum of the reaction mixture, which reveals further broadening in the  $^{11}\text{B}$  NMR spectrum. In the  $^1\text{H}$  NMR spectrum of **2b** heavily overlapped signals corresponding to two species containing IDipp can be observed, but signals for the  $\text{AsH}_2$  and  $\text{BH}_2$  cannot be assigned. As described for **2a**, no crystallization attempts of **2b** up to this point have been successful, but **2b** could be obtained as light-yellow solid. Further crystallization attempts and additional analytics of the powder will be the focus of future research.

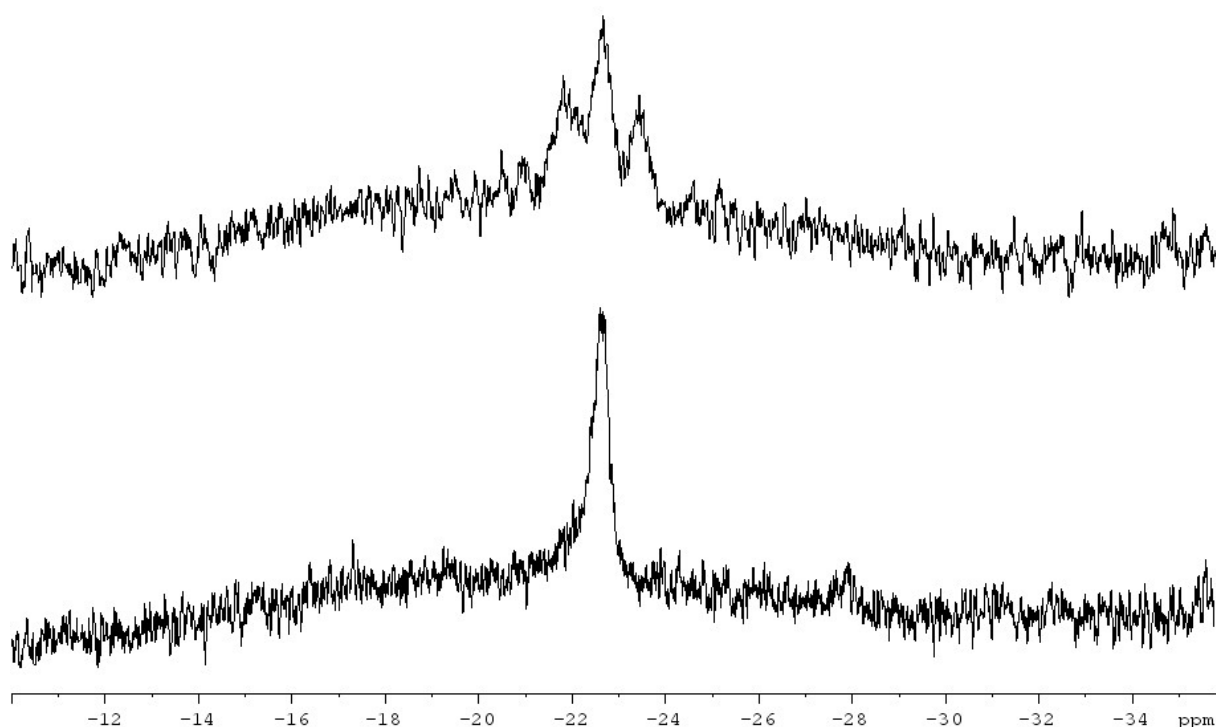


**Figure 1.**  $^{11}\text{B}$  (top) and  $^{11}\text{B}\{^1\text{H}\}$  NMR spectra of **2a** in  $\text{CD}_2\text{Cl}_2$  at r.t.

After the reaction of **1** with one equivalent of grey selenium, similar observations to the reactions with sulfur can be made: A light yellow powder is obtained, which reveals a singlet for **3a** in the  $^{11}\text{B}\{^1\text{H}\}$  NMR spectrum at  $\delta = -36.3$  ppm, which is shifted to higher field compared to the signal corresponding to **2a**. In the  $^{11}\text{B}$  NMR spectrum further splitting into a triplet with a  $^1J_{\text{B,H}}$  of about 90 Hz is observed. In the  $^1\text{H}$  NMR spectrum a mixture of multiple species containing IDipp moieties can be assigned. Therefore, most likely a product mixture of **3a** and compounds, that do not contain boron centers is formed. Any attempts to obtain single crystals of **3a** were not successful up to this point.

In case of the reaction of **1** with a threefold excess of grey selenium, a singlet at  $\delta = -30.9$  ppm can be observed in the  $^{11}\text{B}\{^1\text{H}\}$  NMR spectrum of the reaction mixture. The  $^{11}\text{B}$  NMR spectrum reveals further splitting in a heavily broadened triplet ( $^1J_{\text{B,H}} = 102$  Hz). In the  $^1\text{H}$  NMR the superimposed signals for the  $\text{BH}_2$  and the  $\text{AsH}_2$  group can be observed at  $\delta = 2.67 - 2.18$  ppm and 0.99 ppm, respectively. It was possible to isolate a crystalline product of the reaction as slight yellow blocks by storing a saturated 9:1 mixture methanol/toluene mixture at 279 K. The preliminary structure of this compound via single crystal X-ray diffraction analysis could be obtained. However, the structure

in the solid state did not reveal the formation of **3b**, but instead a cyclic Se<sub>6</sub> unit stabilized by two moieties of **1** (**3c**, Fig. 2).

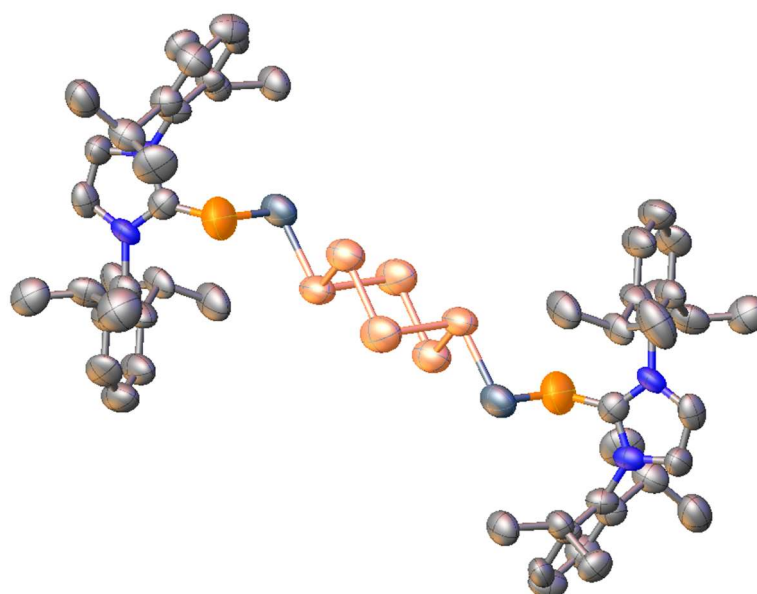
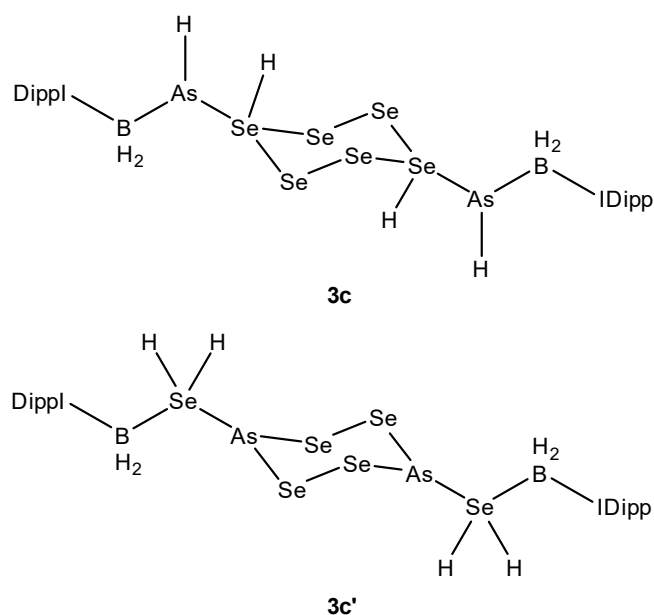


**Figure 2.** Preliminary solid state structure of **3c**. Hydrogen atoms bound to carbon atoms are omitted for clarity.

Due to poor crystal quality, the exact structure of **3c** cannot be clearly determined. In addition, the structure reveals heavy disorder of the six-membered ring and its neighboring atoms. Therefore, the precise location of the hydrogen atoms on the boron and the arsenic atom cannot be identified. Considering the almost identical atomic number of Se and As, two structures are possible (Scheme 2).



**Scheme 2.** Two possible structures of **3c** in the solid state

Structure **3c** is the product of a first-step coordination of a  $\text{Se}_6$  unit by two moieties of **1** followed by a hydrogen transfer from the arsenic atoms to the neighboring selenium atoms. In the case of **3c'**, the potential mechanism leading to this structure is less obvious. Potential formation pathways most likely include the cleavage of the As-B bond and the transfer of two hydrogen atoms from arsenic to selenium, but apart from that, different intermediates are possible. Without further analytical data or a better data set for X-ray crystallography, no final structure can be given.

### 6.3. Experimental section

#### Synthesis of H<sub>2</sub>As(S)BH<sub>2</sub>IDipp (2a)

DippIBH<sub>2</sub>AsH<sub>2</sub> (0.2 mmol, 95.6 mg) and S<sub>8</sub> (0.025 mmol, 6.4 mg) are dissolved in 5 mL of CH<sub>2</sub>Cl<sub>2</sub> at 193 K. After stirring for 60 min at 193 K, the mixture is slowly warmed up to r.t. over 60 min. The solvent is removed under reduced pressure and the remaining light-yellow solid is washed three times with 2 mL of *n*-hexane. By storing a 1:2 mixture of *n*-hexane and toluene at -30°C **2a** is obtained as a light-yellow powder.

Yield: m = 42 mg (41%, 0.08 mmol). <sup>1</sup>H NMR (CD<sub>2</sub>Cl<sub>2</sub>, 293 K) δ [ppm] = 7.66 - 6.93 (m, 6H, IDipp), 2.61 (septet, 4H, <sup>3</sup>J<sub>H,H</sub> = 7 Hz, H<sub>3</sub>C-CH-CH<sub>3</sub>), 2.65 - 2.38 (brm, 2H, <sup>1</sup>J<sub>B,H</sub> = 103 Hz, BH<sub>2</sub>), 1.35 (d, 12H, <sup>1</sup>J<sub>H,H</sub> = 7 Hz, H<sub>3</sub>C-CH-CH<sub>3</sub>), 1.29 (d, 2H, <sup>3</sup>J<sub>H,H</sub> = 7 Hz, AsH<sub>2</sub>), 1.15 (d, 12H, <sup>1</sup>J<sub>H,H</sub> = 7 Hz, H<sub>3</sub>C-CH-CH<sub>3</sub>). <sup>11</sup>B NMR (CD<sub>2</sub>Cl<sub>2</sub>, 293 K) δ [ppm] = -22.7 (t, <sup>1</sup>J<sub>B,H</sub> = 103 Hz). <sup>11</sup>B {<sup>1</sup>H} NMR (CD<sub>2</sub>Cl<sub>2</sub>, 293 K) δ [ppm] = -22.7 (s).

#### Synthesis of (HS)<sub>2</sub>As(S)BH<sub>2</sub>IDipp (2b)

DippIBH<sub>2</sub>AsH<sub>2</sub> (0.2 mmol, 95.6 mg) and S<sub>8</sub> (0.075 mmol, 19.2 mg) are dissolved in 5 mL of CH<sub>2</sub>Cl<sub>2</sub> at 193 K. After stirring for 60 min at 193 K, the mixture is slowly warmed up to r.t. over 90 min. The solvent is removed under reduced pressure and the remaining light-yellow solid is washed three times with 2 mL of *n*-hexane. By storing a 1:2 mixture of *n*-hexane and toluene at -243 K **2b** is obtained as a light-yellow powder.

Yield: m = 35 mg (30%, 0.08 mmol). <sup>1</sup>H NMR (CD<sub>2</sub>Cl<sub>2</sub>, 293 K) δ [ppm] = 7.60 – 7.00 (m, 6H, IDipp), 2.50 (septet, 4H, <sup>3</sup>J<sub>H,H</sub> = 7 Hz, H<sub>3</sub>C-CH-CH<sub>3</sub>), 1.31 (d, 12H, <sup>1</sup>J<sub>H,H</sub> = 7 Hz, H<sub>3</sub>C-CH-CH<sub>3</sub>), 1.17 (d, 12H, <sup>1</sup>J<sub>H,H</sub> = 7 Hz, H<sub>3</sub>C-CH-CH<sub>3</sub>). <sup>11</sup>B NMR (CD<sub>2</sub>Cl<sub>2</sub>, 293 K) δ [ppm] = -24.0 (br). <sup>11</sup>B {<sup>1</sup>H} NMR (CD<sub>2</sub>Cl<sub>2</sub>, 293 K) δ [ppm] = -24.0 (s).

#### Synthesis of H<sub>2</sub>As(Se)BH<sub>2</sub>IDipp (3a)

DippIBH<sub>2</sub>AsH<sub>2</sub> (0.2 mmol, 95.6 mg) and grey selenium (0.2 mmol, 16 mg) are dissolved in 3 mL of toluene at r.t.. After stirring for 16 h at room temperature, the solvent is removed under reduced pressure and the remaining light-yellow solid is washed three times with 2 mL of *n*-hexane. By storing a 1:2 mixture of *n*-hexane and toluene at 243 K **3a** is obtained as a light-yellow solid.

Yield: m = 18 mg (16%, 0.032 mmol). <sup>1</sup>H NMR (CD<sub>2</sub>Cl<sub>2</sub>, 293 K) Product mixture. <sup>11</sup>B NMR (CD<sub>2</sub>Cl<sub>2</sub>, 293 K) δ [ppm] = -36.3 (t, <sup>1</sup>J<sub>B,H</sub> = 90 Hz). <sup>11</sup>B {<sup>1</sup>H} NMR (CD<sub>2</sub>Cl<sub>2</sub>, 293 K) δ [ppm] = -36.3 (s).

**Synthesis of  $\text{Se}_6(\text{H}_2\text{AsBH}_2\text{IDipp})_2$  (**3c**)**

DippIBH<sub>2</sub>AsH<sub>2</sub> (0.2 mmol, 95.6 mg) and grey selenium (0.6 mmol, 47 mg) are dissolved in 4 mL of toluene at r.t.. After stirring for 16 h at room temperature, the solution is decanted off the brown residue. The solvent is removed under reduced pressure and the remaining light-yellow solid is washed three times with 2 mL of *n*-hexane. By storing a 9:1 mixture of methanol and toluene at 243 K **3c** is obtained as light-yellow blocks.

Yield: *m* = 54 mg (37%, 0.037 mmol). <sup>1</sup>H NMR (CD<sub>2</sub>Cl<sub>2</sub>, 293 K) δ [ppm] = 7.38 – 6.78 (m, 6H, IDipp), 2.80 (septet, 4H, <sup>3</sup>J<sub>H,H</sub> = 7 Hz, H<sub>3</sub>C-CH-CH<sub>3</sub>), 2.67 - 2.18 (brm, 2H, <sup>1</sup>J<sub>B,H</sub> = 102 Hz, BH<sub>2</sub>), 1.39 (d, 12H, <sup>1</sup>J<sub>H,H</sub> = 7 Hz, H<sub>3</sub>C-CH-CH<sub>3</sub>), 1.06 (d, 12H, <sup>1</sup>J<sub>H,H</sub> = 7 Hz, H<sub>3</sub>C-CH-CH<sub>3</sub>), 0.99 (t, 2H, <sup>3</sup>J<sub>H,H</sub> = 7 Hz, AsH<sub>2</sub>). <sup>11</sup>B NMR (CD<sub>2</sub>Cl<sub>2</sub>, 293 K) δ [ppm] = -30.9 (t, <sup>1</sup>J<sub>B,H</sub> = 102 Hz). <sup>11</sup>B {<sup>1</sup>H} NMR (CD<sub>2</sub>Cl<sub>2</sub>, 293 K) δ [ppm] = -30.9 (s).

## NMR spectra

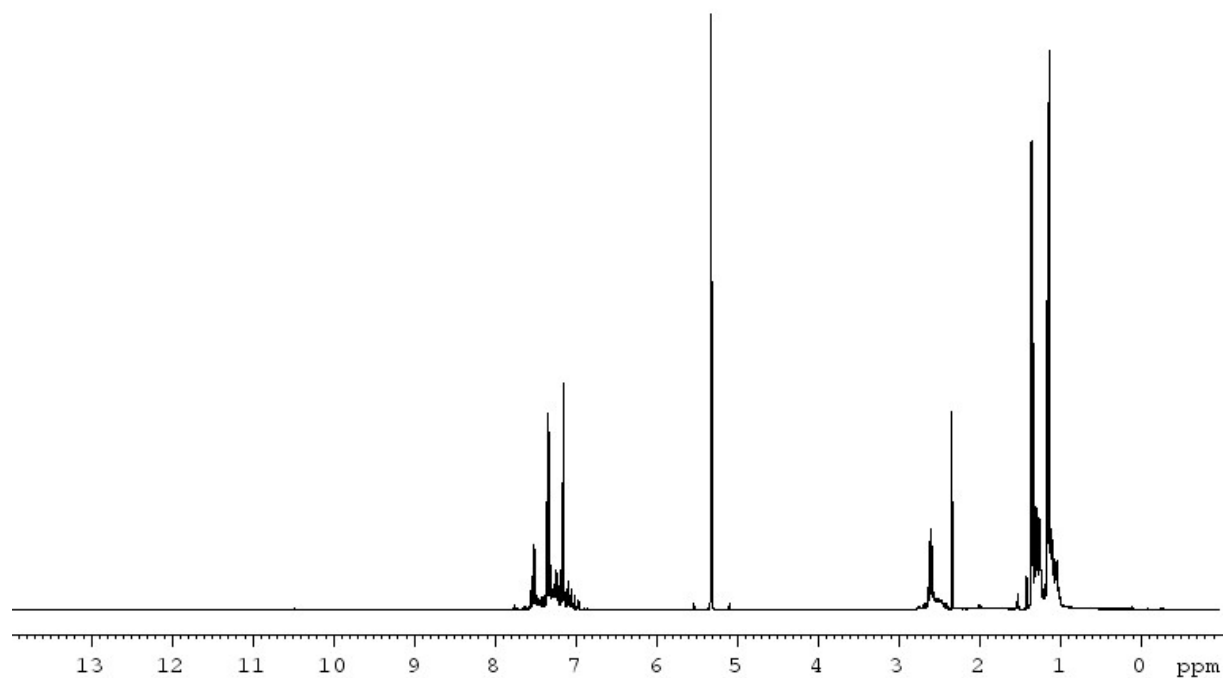
 $\text{H}_2\text{As}(\text{S})\text{BH}_2\text{IDipp}$  (**2a**)

Figure 3.  $^1\text{H}$  NMR spectrum of **2a** in  $\text{CD}_2\text{Cl}_2$  at r.t.

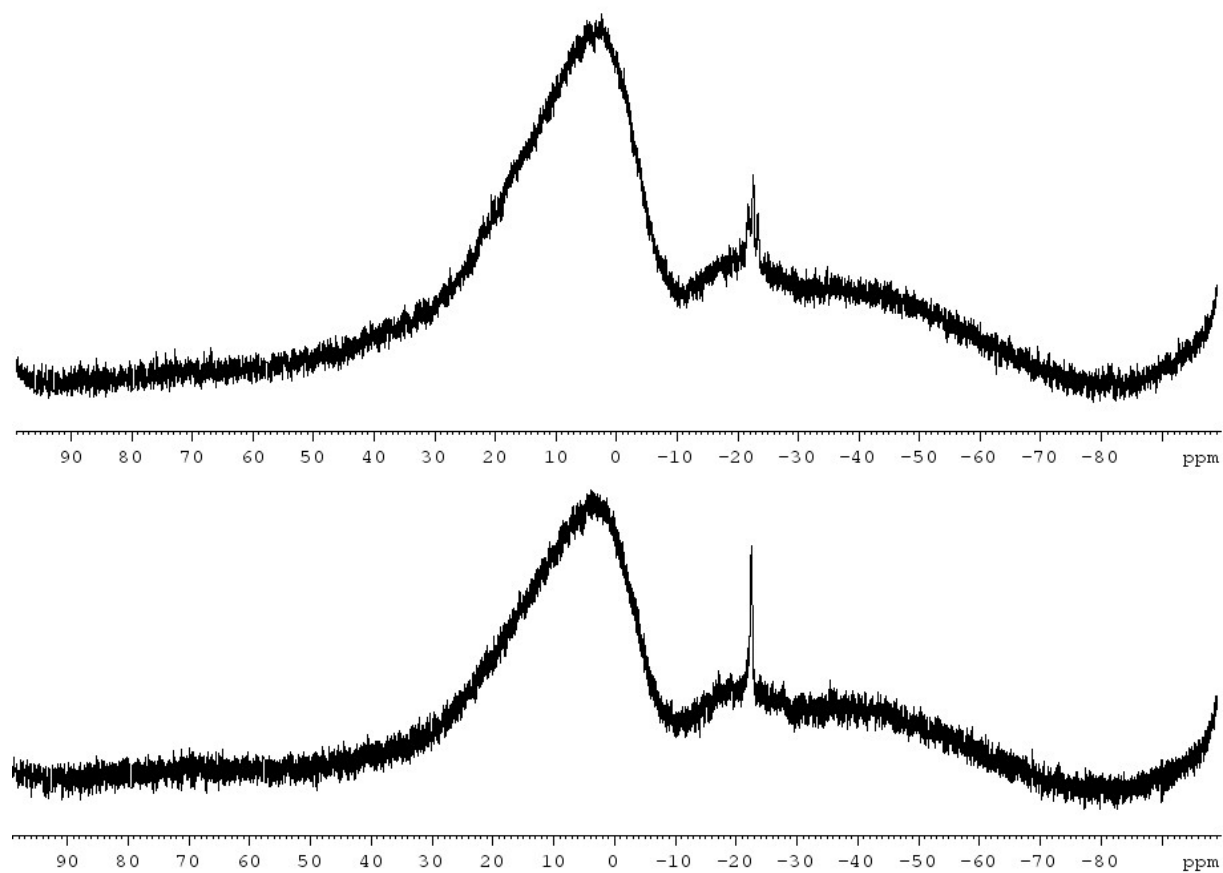
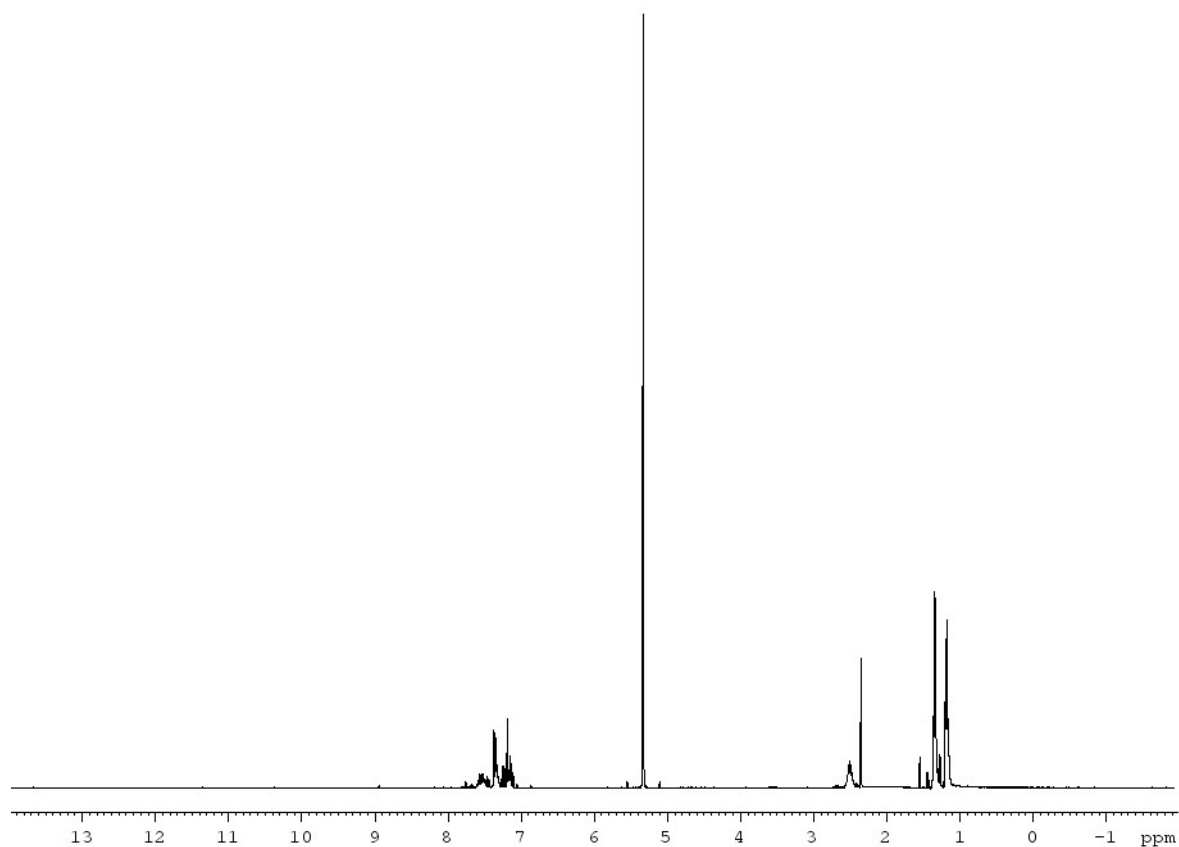
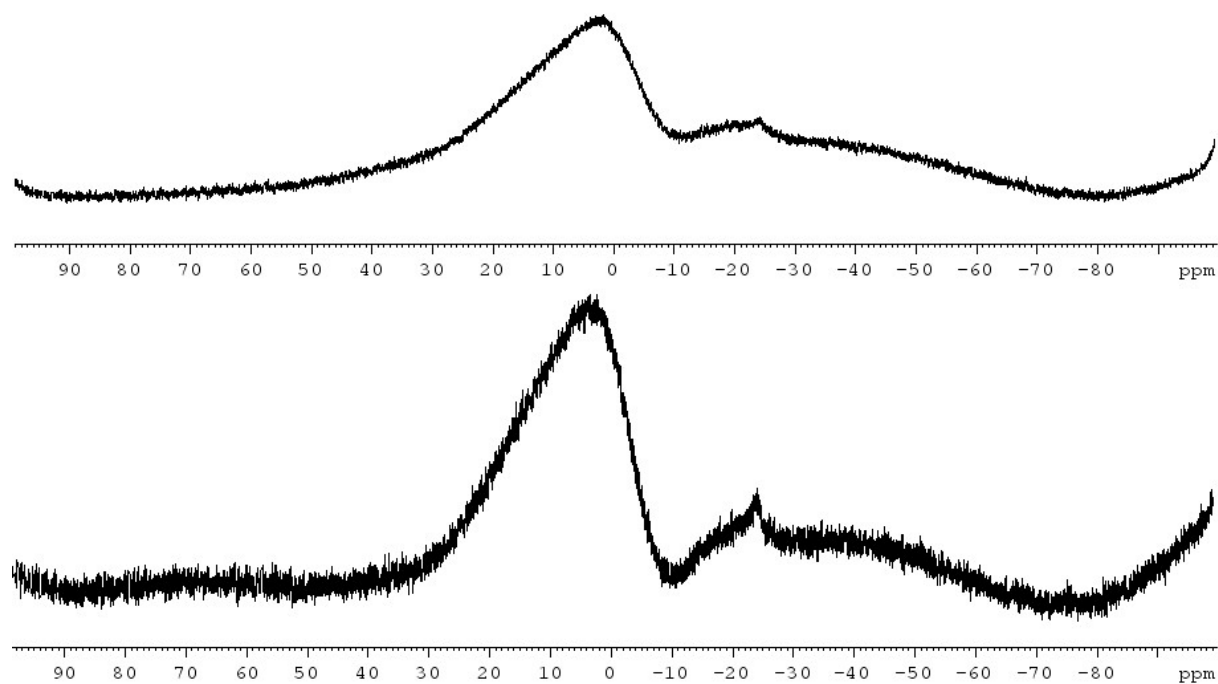
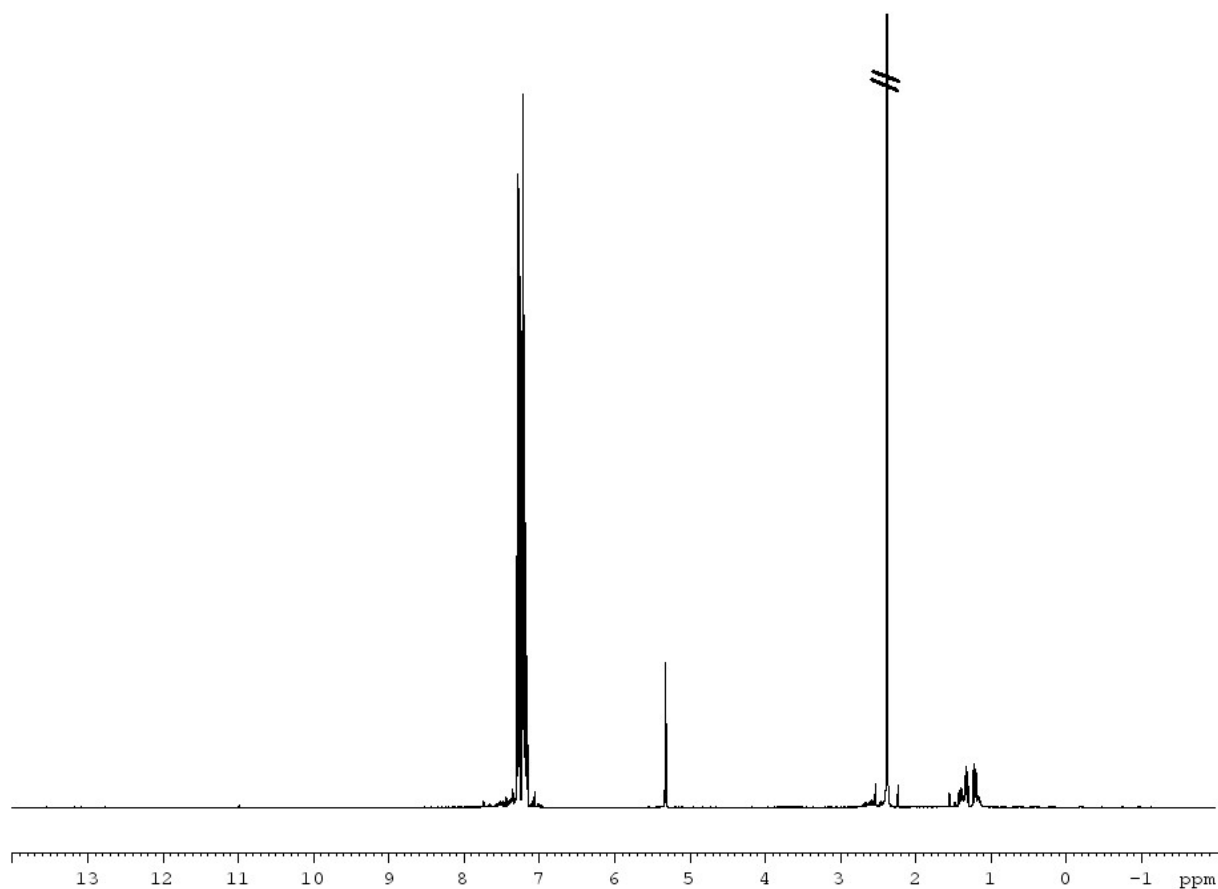
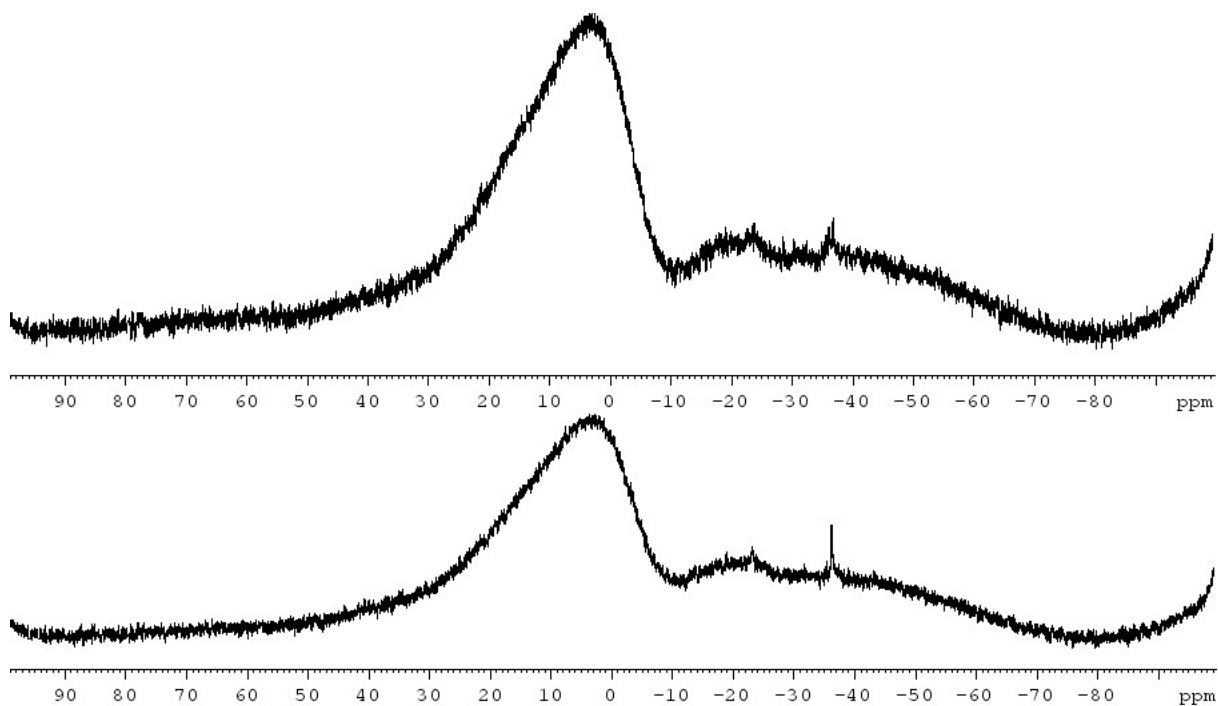
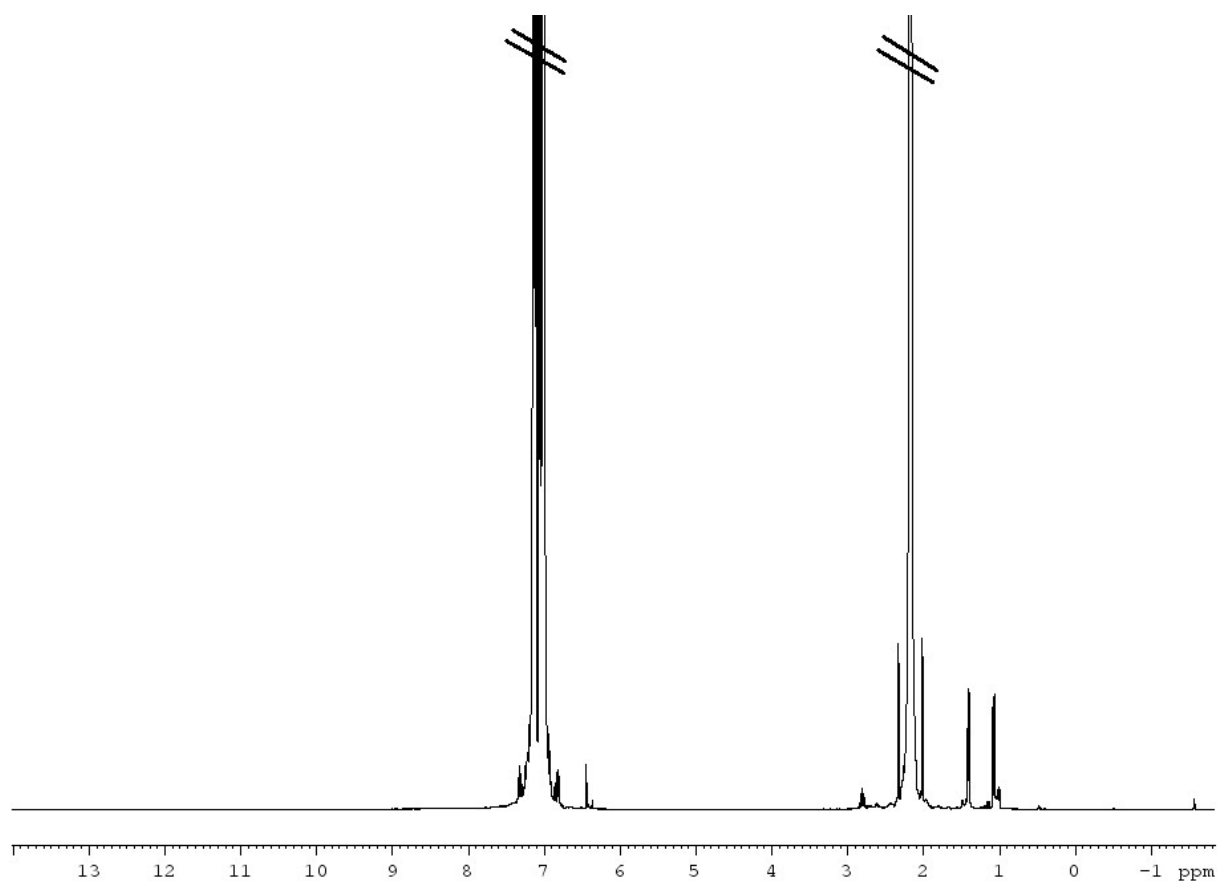
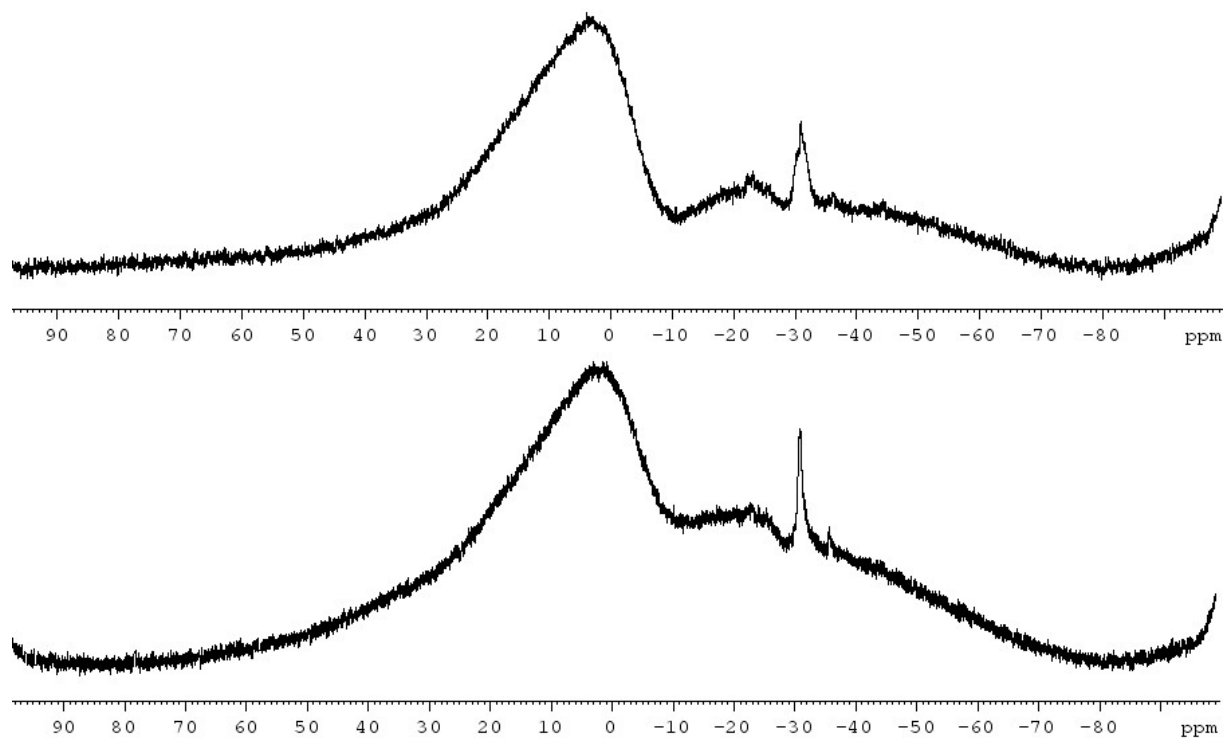


Figure 4.  $^{11}\text{B}$  (top) and  $^{11}\text{B}\{^1\text{H}\}$  NMR spectra of **2a** in  $\text{CD}_2\text{Cl}_2$  at r.t.

**(HS)<sub>2</sub>As(S)BH<sub>2</sub>Dipp (2b)****Figure 5.** <sup>1</sup>H NMR spectrum of **2b** in CD<sub>2</sub>Cl<sub>2</sub> at r.t.**Figure 6** <sup>11</sup>B (top) and <sup>11</sup>B{<sup>1</sup>H} NMR spectra of **2b** in CD<sub>2</sub>Cl<sub>2</sub> at r.t.

**H<sub>2</sub>As(Se)BH<sub>2</sub>IDipp (3a)****Figure 7.** <sup>1</sup>H NMR spectrum of **3a** in CD<sub>2</sub>Cl<sub>2</sub> at r.t.**Figure 8.** <sup>11</sup>B (top) and <sup>11</sup>B{<sup>1</sup>H} NMR spectra of **2a** in CD<sub>2</sub>Cl<sub>2</sub> at r.t.

**Se<sub>6</sub>(H<sub>2</sub>AsBH<sub>2</sub>IDipp)<sub>2</sub> (3c)****Figure 9.** <sup>1</sup>H NMR spectrum of **3c** in toluene with C<sub>6</sub>D<sub>6</sub> capillary at r.t.**Figure 10.** <sup>11</sup>B (top) and <sup>11</sup>B{<sup>1</sup>H} NMR spectra of **3c** in toluene with C<sub>6</sub>D<sub>6</sub> capillary at r.t.

## 6.4. References

- [1] a) M. Liang, I. Manners, *J. Am. Chem. Soc.* **1991**, *113*, 4044-4045; b) H. R. Allcock, *Chem. Mater.* **1994**, *6*, 1476-1491; c) C. H. Honeyman, I. Manners, C. T. Morrissey, H. R. Allcock, *J. Am. Chem. Soc.* **1995**, *117*, 7035-7036; d) R. D. Archer, *Inorganic and Organometallic Polymers*, Wiley VCH, New York, **2001**; e) I. Manners, *Angew. Chem. Int. Ed.* **1996**, *35*, 1602-1621; f) S. J. Clarson, J. A. Semlyen, *Siloxane polymers*, Prentice Hall, **1993**; g) R. H. Neilson, P. Wisian-Neilson, *Chem. Rev.* **1988**, *88*, 541-562; h) R. D. Miller, J. Michl, *Chem. Rev.* **1989**, *89*, 1359-1410; i) R. D. Jaeger, M. Gleria, *Prog. Polym. Sci.* **1998**, *23*, 179-276; j) X. He, T. Baumgartner, *RSC Adv.* **2013**, *3*, 11334-11350; k) S. Wilfert, H. Henke, W. Schoefberger, O. Brüggemann, I. Teasdale, *Macromol. Rapid Commun.* **2014**, *35*, 1135-1141; l) B. W. Rawe, C. P. Chun, D. P. Gates, *Chem. Sci.* **2014**, *5*, 4928-4938; m) P. J. Fazen, J. S. Beck, A. T. Lynch, E. E. Remsen, L. G. Sneddon, *Chem. Mater.* **1990**, *2*, 96-97; n) F. Jäkle, *Chem. Rev.* **2010**, *110*, 3985-4022; o) H. Kutz, F. Cheng, S. Schwedler, L. Böhling, A. Brockhinke, L. Weber, K. Parab, F. Jäkle, *ACS Macro Lett.* **2012**, *1*, 555-559; p) Z. M. Hudson, D. J. Lunn, M. A. Winnik, I. Manners, *Nat. Commun.* **2014**, *5*; q) A. Lorbach, M. Bolte, H. Li, H. W. Lerner, M. C. Holthausen, F. Jäkle, M. Wagner, *Angew. Chem. Int. Ed.* **2009**, *48*, 4584-4588; r) H. R. Allcock, C. Chen, *J. Org. Chem.* **2020**, *85*, 14286-14297; s) F. Vidal, F. Jäkle, *Angew. Chem. Int. Ed.* **2019**, *58*, 5846-5870.
- [2] a) Z. Liu, T. B. Marder, *Angew. Chem. Int. Ed.* **2008**, *47*, 242-244; b) V. Pons, R. T. Baker, *Angew. Chem. Int. Ed.* **2008**, *47*, 9600-9602; c) F. H. Stephens, V. Pons, R. Tom Baker, *Dalton Trans.* **2007**, 2613-2626; d) G. Alcaraz, S. Sabo-Etienne, *Angew. Chem. Int. Ed.* **2010**, *49*, 7170-7179; e) M. E. Sloan, A. Staubitz, T. J. Clark, C. A. Russell, G. C. Lloyd-Jones, I. Manners, *J. Am. Chem. Soc.* **2010**, *132*, 3831-3841; f) A. Staubitz, A. P. Robertson, I. Manners, *Chem. Rev.* **2010**, *110*, 4079-4124; g) J. Linshoeft, E. J. Baum, A. Hussain, P. J. Gates, C. Näther, A. Staubitz, *Angew. Chem. Int. Ed.* **2014**, *53*, 12916-12920; h) A. Hübner, Z.-W. Qu, U. Englert, M. Bolte, H.-W. Lerner, M. C. Holthausen, M. Wagner, *J. Am. Chem. Soc.* **2011**, *133*, 4596-4609; i) R. De Jaeger, M. Gleria, *Prog. Polym. Sci.* **1998**, *23*, 179-276; j) A. M. Prieger, B. W. Rawe, S. C. Serin, D. P. Gates, *Chem. Soc. Rev.* **2016**, *45*, 922-953; k) F. Choffat, S. Käser, P.

- Wolfer, D. Schmid, R. Mezzenga, P. Smith, W. Caseri, *Macromolecules* **2007**, *40*, 7878-7889; l) H. R. Allcock, *Chem. Mater.* **1994**, *6*, 1476-1491; m) G. Zhang, G. M. Palmer, M. W. Dewhurst, C. L. Fraser, *Nat. Mater.* **2009**, *8*, 747-751; n) R. West, *J. Organomet. Chem.* **1986**, *300*, 327-346; o) T. Wideman, P. J. Fazen, K. Su, E. E. Remsen, G. A. Zank, L. G. Sneddon, *Appl. Organomet. Chem.* **1998**, *12*, 681-693.
- [3] a) M. M. Roy, A. A. Omana, A. S. Wilson, M. S. Hill, S. Aldridge, E. Rivard, *Chem. Rev.* **2021**, *121*, 12784-12965; b) A. Doddi, M. Peters, M. Tamm, *Chem. Rev.* **2019**, *119*, 6994-7112; c) V. Nesterov, D. Reiter, P. Bag, P. Frisch, R. Holzner, A. Porzelt, S. Inoue, *Chem. Rev.* **2018**, *118*, 9678-9842; d) G. Prabusankar, A. Sathyanarayana, P. Suresh, C. N. Babu, K. Srinivas, B. P. R. Metla, *Coord. Chem. Rev.* **2014**, *269*, 96-133.
- [4] a) K. C. Thimer, S. I. Al-Rafia, M. J. Ferguson, R. McDonald, E. Rivard, *Chem. Commun.* **2009**, 7119-7121; b) E. Rivard, *Dalton Trans.* **2014**, *43*, 8577-8586; c) C. Marquardt, O. Hegen, M. Hautmann, G. Balázs, M. Bodensteiner, A. V. Virovets, A. Y. Timoshkin, M. Scheer, *Angew. Chem. Int. Ed.* **2015**, *54*, 13122-13125.
- [5] a) M. T. Ackermann, M. Seidl, F. Wen, M. J. Ferguson, A. Y. Timoshkin, E. Rivard, M. Scheer, *Chem. Eur. J.* **2022**, *28*, e202103780; b) M. T. Ackermann, M. Seidl, R. Grande, Y. Zhou, M. J. Ferguson, A. Timoshkin, E. Rivard, M. Scheer, *Chem. Sci.* **2023**; c) M. A. Weinhart, A. S. Lisovenko, A. Y. Timoshkin, M. Scheer, *Angew. Chem. Int. Ed.* **2020**, *59*, 5541-5545; d) M. A. Weinhart, M. Seidl, A. Y. Timoshkin, M. Scheer, *Angew. Chem. Int. Ed.* **2021**, *60*, 3806-3811.
- [6] a) C. Marquardt, O. Hegen, T. Kahoun, M. Scheer, *Chem. Eur. J.* **2017**, *23*, 4397-4404; b) K.-C. Schwan, A. Y. Timoshkin, M. Zabel, M. Scheer, *Chem. Eur. J.* **2006**, *12*, 4900-4908.

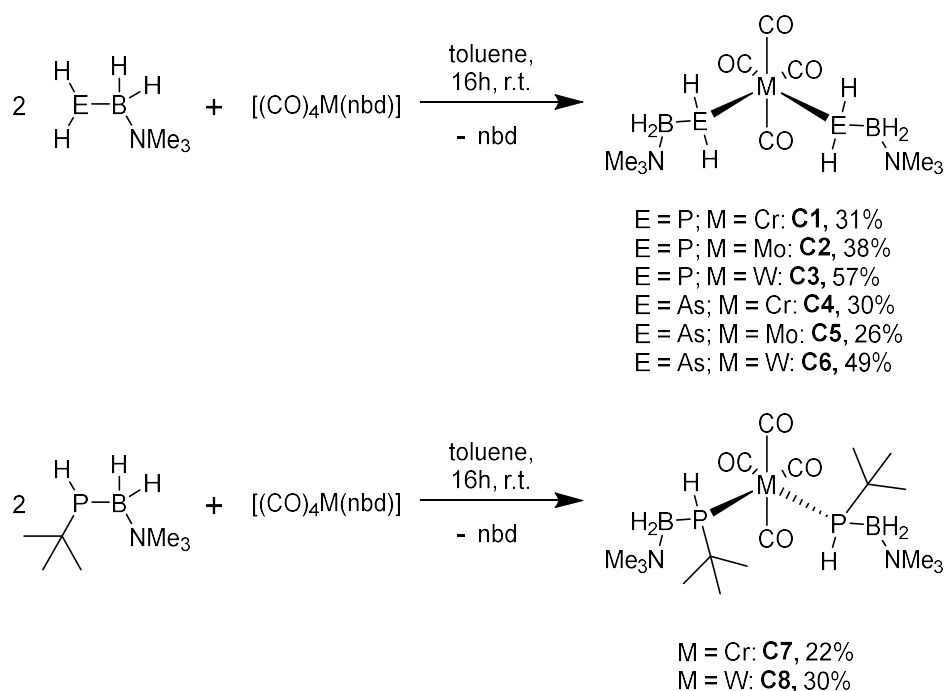
## 6.5. Author contributions

- The synthesis and characterization of **1a-b** and **2a-c** has been performed by Felix Lehnfeld
- X-ray diffraction analysis of **2c** has been performed by Felix Lehnfeld with help from Dr. Michael Bodensteiner
- The manuscript (including supporting information, figures, schemes and graphical abstract) was written by Felix Lehnfeld.

## 7. Conclusion

### 7.1. Coordination of pnictogenylboranes towards group 6 Lewis acids

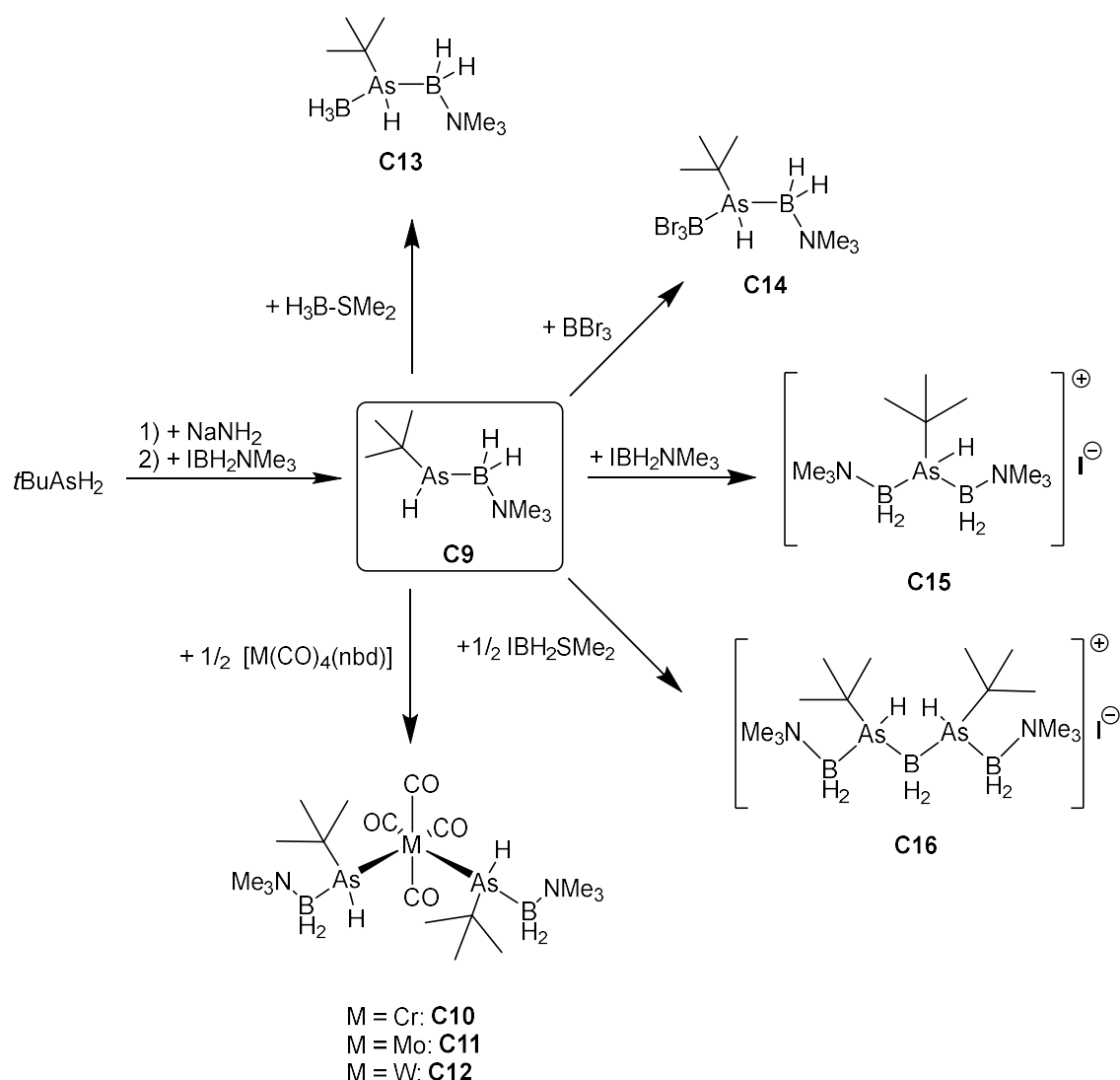
To deepen the knowledge about the versatile coordination chemistry of pnictogenylboranes, a systematic approach was pursued in this work. By reaction of the phosphanylborane  $\text{PH}_2\text{BH}_2\text{NMe}_3$ , arsanylborane  $\text{AsH}_2\text{BH}_2\text{NMe}_3$  and the alkyl substituted phosphanylborane  $t\text{BuPHBH}_2\text{NMe}_3$  with group 6 Lewis acids  $[(\text{CO})_4\text{M}(\text{nb})]$  bearing a labile norbornadiene (= nbd) ligand, several different coordination compounds could be isolated (Scheme 1, **C1-C8**). All reported compounds were fully characterized by multinuclear NMR spectroscopy, single crystal X-ray diffraction analysis, mass spectrometry and infrared spectroscopy. The high purity and good yields of the reported compounds allowed to use them as model system for the coordination behavior of pnictogenylboranes. Through detailed analysis of the obtained analytical data, systematic trends within this compound family could be elaborated. This knowledge allows for a better general understanding of the reactivity in the context of early transition metal coordination chemistry. Especially the impact of the substitution pattern on the pnictogen atom was identified as most important influence, although also the influence of the pnictogen atom and the metal center could be observed. Considering the donor/acceptor strength, a small difference between the arsenic and the phosphorus compounds is observed, which is significantly smaller than the difference between unsubstituted phosphanylborane and its *t*Bu substituted derivative. All findings were additionally supported by DFT calculations.



**Scheme 1.** Synthesis of the group 6 coordination products of different pnictogenylboranes **C1-C8**

## 7.2. Synthesis and reactivity of an alkyl substituted arsanylborane

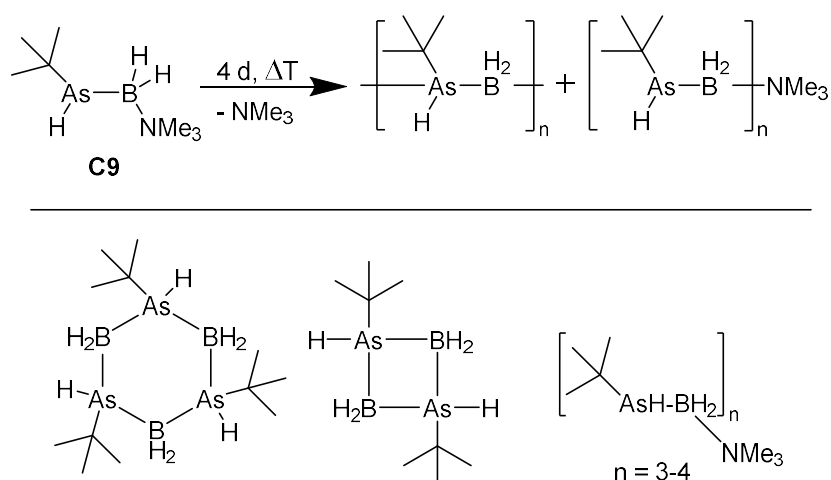
In view of the report on the only LB stabilized parent arsanylborane and the recent report on a diphenyl substituted derivative, the investigation of an alkyl substituted arsanylborane was the consequent next interest. In the case of phosphorus the *t*Bu substituted compound *t*BuPHBH<sub>2</sub>NMe<sub>3</sub> revealed a very rich and versatile reactivity, therefore the synthesis of a similarly substituted arsenic derivative was targeted. By metalation of AsH<sub>2</sub> with NaNH<sub>2</sub> and subsequent salt metathesis with IBH<sub>2</sub>NMe<sub>3</sub> the only LB stabilized alkyl substituted *t*BuPHBH<sub>2</sub>NMe<sub>3</sub> (Scheme 2, **C9**) was synthesized in good yields.



**Scheme 2.** Synthesis and reactivity of the *t*Bu substituted arsanylborane **C9**

Compound **C9** was fully characterized and its reactivity was investigated in a variety of reactions: The coordination chemistry towards group 6 metal centers presented in chapter one of this thesis could be expanded by also reporting the coordination of **C9** towards  $[(\text{CO})_4\text{M}(\text{nbd})]$  (Scheme 2, **C10-C12**). Furthermore, compound **C9** proved to be a valuable starting material for arsenic-boron based mixed *catena* compounds. Neutral three membered chains were obtained by reaction with  $\text{BH}_3\text{SMe}_2$  or  $\text{BBr}_3$  (Scheme 2, **C13-C14**). When reacted with  $\text{IBH}_2\text{LB}$  (LB =  $\text{NMe}_3$ ,  $\text{SMe}_2$ ) a three- and a five-membered cationic chain like compound could be isolated (Scheme 2, **C15-C16**). All compounds were obtained in moderate to good yields and were fully characterized, including the determination of the structure in the solid state by single crystal X-ray diffraction analysis for all compounds except **C14**. All reactions were found to be in agreement with theoretical data obtained through DFT computations. Furthermore, compounds **C9** could also be used as starting material for thermal oligomerization due

to its relatively high thermal stability. The obtained oligomers by this pathway were characterized via NMR spectroscopy, mass spectrometry and DFT calculations and the oligomers most likely formed during this reaction were determined: In addition to linear oligomers build up by three or four arsanylborane repeating units two cyclic four and six membered oligomers were identified as the most probable products. (Scheme 3).

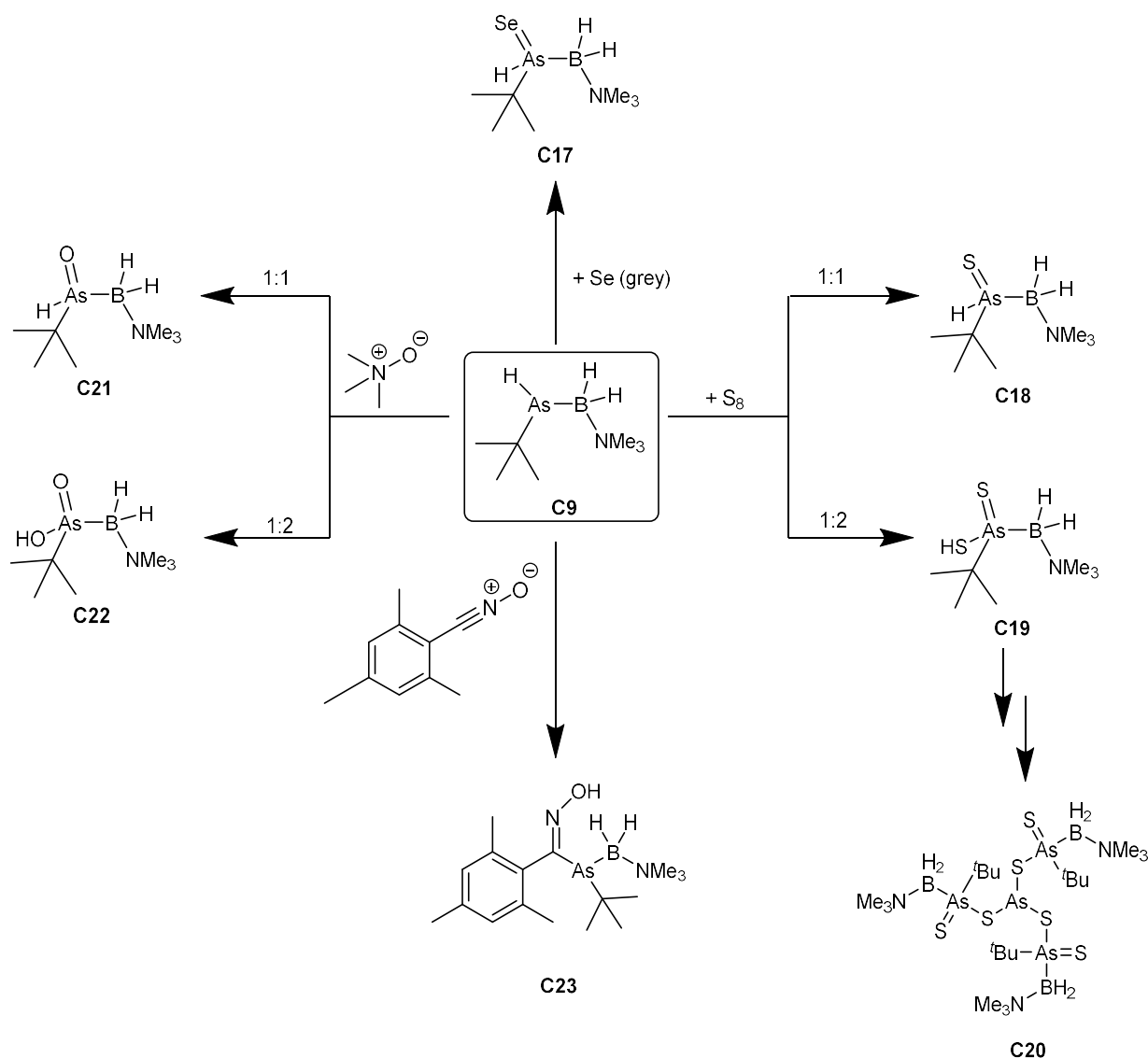


**Scheme 3.** Top: Thermal oligomerization of **C9**; bottom: Most likely structures of thermal generated oligomers according to ESI-MS and DFT calculations.

### 7.3. Controlled oxidation of **tBuAsHBH<sub>2</sub>NMe<sub>3</sub>**

As discussed in chapter two of this work, *t*BuAsHBH<sub>2</sub>NMe<sub>3</sub> (**C9**) is a well suited starting material for a variety of reactions due to its relatively stable As-B bond compared to other arsanylborane derivatives. Therefore, the investigation of the so far only very limited accessible oxidation chemistry of arsanylboranes was investigated by reaction of **C9** towards various chalcogens and chalcogen reagents. The reaction of **C9** towards stoichiometric amounts of grey selenium leads to the formation of *t*BuAsH(Se)BH<sub>2</sub>NMe<sub>3</sub> in a selective reaction (Scheme 4, **C17**). **C17** could be obtained in medium yields and was fully characterized. In case of the reaction towards S<sub>8</sub>, **C9** revealed a more diverse reactivity: it was possible to isolate both the sulfur analogue to **C17**, *t*BuAsH(S)BH<sub>2</sub>NMe<sub>3</sub>, as well as the arsanylborane analogue of a thioarsenic acid *t*BuAsSH(S)BH<sub>2</sub>NMe<sub>3</sub> (Scheme 4, **C18-C19**). Both compounds were fully characterized, but due to their instability in solution, only crystals of an intermediate

product of their decomposition could be characterized by single crystal X-ray diffraction (Scheme 4, **C20**).

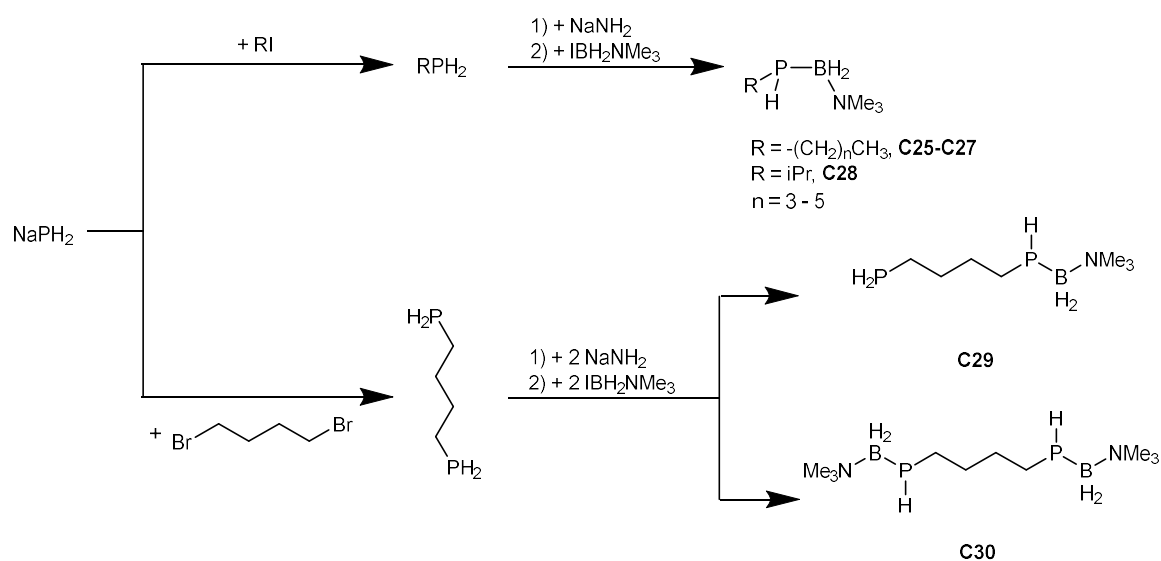


**Scheme 4.** Oxidation chemistry of **C9**

In the case of oxygen, the first isolable oxo-arsanylboranes (Scheme 4, **C21-C22**) could be obtained via the reaction with  $\text{Me}_3\text{NO}$ . As observed for the reaction with elemental sulfur, both the mono-oxygenated species as well as a compound incorporating two oxygen atoms could be isolated. Additionally, by the reaction with mesityl nitrile-N-oxide the formation of a unique and very labile product of an As-H activation could be observed (Scheme 4, **C24**). Despite its rapid decomposition in solution, it was possible to characterize **C24** by single crystal X-ray diffraction.

### 7.4. Improved synthesis of alkyl substituted phosphanylboranes as starting material for poly(alkylphosphinoborane)s

As monoalkyl substituted phosphanylboranes are well suited as precursors for high molecular weight polymers, a more generally applicable synthetic pathway to these monomers is important. Within this work a one pot reaction starting from  $\text{NaPH}_2$  and halogenated alkyl halides for primary and secondary alkyl substituents has been developed. By *in situ* generation of the respective phosphine, consecutive metalation with  $\text{NaNH}_2$  and salt metathesis with  $\text{IBH}_2\text{NMe}_3$  different phosphanylboranes stabilized only by a LB with different primary alkyl substituents, the secondary alkyl substituent *i*Pr and a butyl-bridged diphosphanylborane have been synthesized (Scheme 5, **C25-C30**).



**Scheme 5.** Synthesis of novel mono alkyl substituted phosphanylboranes

Compounds **C25-C27** have been used as starting material in both thermal and bis( $\eta^5$ : $\eta^1$ -adamantylidenepentafulvene)titanium catalyzed polymerization reactions. The influence of various reaction conditions such as reaction time, temperature, catalyst loading or concentration as well as the impact of the substituent on the starting monomer were investigated. Preliminary polymerization studies with **C28** revealed no polymer formation. In the case of polymerization under catalytic conditions, analytical data indicates the formation of a paramagnetic coordination compound.

## 8. Appendices

### 8.1. Alphabetic List of Abbreviations

r	radius
°C	degree Celsius
ATR	attenuated total reflection
br (NMR)	broad
btmsa	bis(trimethylsilyl)acetylene
cod	Cycloocta-1,5-diene
Cp	cyclopentadienyl, C <sub>5</sub> H <sub>5</sub>
δ	chemical shift
d (NMR)	doublet
DFT	Density functional theory
E <sup>0</sup> <sub>0</sub>	Reaction energy
EA	Elemental analysis
EN	electronegativity
ESI	electrospray ionization
Et	ethyl, C <sub>2</sub> H <sub>5</sub>
Et <sub>2</sub> O	diethyl ether
Fig	figure
G <sup>0</sup> <sub>298</sub>	standard gibbs reaction energy
H <sup>0</sup> <sub>298</sub>	standard reaction enthalpy
Hz	Hertz
IDipp	1,3-Bis(2,6-diisopropylphenyl)imidazolin-2-yliden
IMe	1,3,4,5-Tetramethylimidazol-2-yliden
<i>i</i> Pr	iso-propyl, C <sub>3</sub> H <sub>7</sub>
IR	infrared (spectroscopy)
LA	Lewis acid
LB	Lewis base
LIFDI	liquid injection field desorption ionization
m (IR)	medium
m (NMR)	multiplet
Me	methyl, CH <sub>3</sub>

Mes	mesityl, 2,4,6-trimethylphenyl
MHz	Megahertz, $10^6$ Hz
MOCVD	metalorganic chemical vapor deposition
MS	mass spectrometry
Nbd	norbornadiene
<i>n</i> Bu	<i>n</i> -butyl, C <sub>4</sub> H <sub>9</sub>
NHC	N-heterocyclic carbene
<i>n</i> Hex	<i>n</i> -hexyl, C <sub>6</sub> H <sub>13</sub>
NMR	nuclear magnetic resonance
<i>n</i> Pr	<i>n</i> -propyl, C <sub>3</sub> H <sub>7</sub>
OTf	triflate, CF <sub>3</sub> SO <sub>3</sub> <sup>-</sup>
pent (NMR)	pentet
Ph	phenyl, C <sub>6</sub> H <sub>5</sub>
POCOP	[ $\mu$ -1,3-(OP <i>t</i> Bu) <sub>2</sub> C <sub>6</sub> H <sub>3</sub> ]
ppm	parts per million
q (NMR)	quartet
R	organic substituent
r.t.	room temperature
s (IR)	strong
s (NMR)	singlet
S <sup>0</sup> <sub>298</sub>	standard reaction entropy
SI	supporting information
T	temperature
t (NMR)	triplet
<i>t</i> Bu	<i>tert</i> -butyl, C <sub>4</sub> H <sub>9</sub>
THF	tetrahydrofuran
tht	tetrahydrothiophene
Tmeda	tetramethylethylenediamine
TMSO	trimethylsilylperoxide
TOF	time of flight
vw (IR)	very weak
w (IR)	weak

## 8.2. Acknowledgments

Special thanks go to:

- Prof. Dr. Manfred Scheer for giving me the opportunity to work on this very interesting project, providing excellent working conditions and the freedom to pursue my own ideas in the lab
- Dr. Gabór Balázs for all his valuable advice, his great input, his patience and time for even the simplest questions and the accurate proof-reading. Without him, most of this work would not have been possible. Additionally, thanks for always staying light-hearted and ensuring a great working atmosphere.
- Prof. Dr. Alexey Timoshkin for the DFT calculations and their interpretation, as well as for the very interesting and helpful discussions during your stays.
- Dr. Michael Seidl for all his help with X-ray structure problems and for always having an open ear for questions.
- All staff and co-workers of the Central Analytical Services of the University of Regensburg: X-Ray, mass spectrometry, elementary analysis department and the NMR department.
- The staff of the glass blowing, electronic and mechanics facilities of the University of Regensburg
- My current and former lab colleagues (Jens, Olli, Tobi, Matthias) for the very collaborative and friendly atmosphere and for all the awesome moments with you.
- The Stammtisch Scheer and all coworkers that became more than just colleagues for the great time and fun moments during the breaks or outside of work.
- All present and former members of the Scheer group for a pleasant working atmosphere and an unforgettable time.
- Especially to my friends and my family for their enduring support and company during all these years.
- And to Michi for her constant and loving support, which got me through the exhausting last months of the doctoral thesis.